Characterising the palmitoylation and SUMOylation of cardiac myosin binding protein-C in cardiac health and disease

Alice Main

BSc (Hons), MRes

Thesis submitted in fulfilment of the requirements for the degree of Doctor of Philosophy (PhD)

Institute of Cardiovascular and Medical Sciences
College of Medical, Veterinary and Life Sciences
University of Glasgow

August 2022

Abstract

Cardiac myosin binding protein-C (cMyBP-C) is a 12-domain sarcomeric accessory protein that transiently interact with actin, tropomyosin and myosin and regulates the activity of the myofilament to maintain systolic and diastolic function. cMyBP-C is influenced by an increasing list of post-translational modifications (PTMs), including phosphorylation, which occurs predominantly in the N-terminal regions and regulates myofilament force and calcium sensitivity. Whilst the central domains have remained lesser studied, evidence suggests they are may promote different conformations of cMyBP-C, influence myosin binding and are a hot-spot for PTMs. This includes the cysteine modification S-glutathionylation, an increase of which impairs cMyBP-C phosphorylation and increases myofilament calcium sensitivity. In this study, the cysteine modification palmitoylation was investigated, which has not been widely reported for myofilament proteins. Acyl resin assisted capture (Acyl-RAC) was used to purify palmitoylated proteins from cardiac tissue and revealed that actin, myosin and cMyBP-C undergo palmitoylation. Upon investigation of different anatomical regions, cMyBP-C palmitoylation may be highest in the left ventricle and appears reduced when these primary cardiomyocytes are cultured. Furthermore, the palmitoylated form of cMyBP-C may be more resistant to salt extraction from the myofilament lattice. In cardiac pathologies, palmitoylation was reduced in the left ventricle of a rabbit model of heart failure (HF) but increased in ischaemic human HF samples. Site directed mutagenesis revealed C623 and C651, in the C4 and C5 domains respectively, to be candidate palmitoylation sites, which have previously been identified to be modified by S-glutathionylation. Isolated myofilaments treated with palmitoyl CoA, which spontaneously attaches to palmitoylated cysteines, showed significantly increased levels of cMyBP-C palmitoylation and reduced calcium sensitivity of force. Whether this is attributed solely to cMyBP-C palmitoylation remains to be determined, nevertheless this study provides novel evidence that palmitoylation is an important regulatory modification for myofilament function.

Aside from palmitoylation, preliminary data suggests cMyBP-C also undergoes SUMOylation. This was investigated using a cMyBP-C-UBC9 fusion construct (WT) co-expressed with eGFP-SUMO1, which shows a SUMOylated band shift, and a catalytically inactive mutant (C93A) which cannot be SUMOylated. Purification of

the SUMOylated cMyBP-C-UBC9 fusion for mass spectrometry and *in silico* analysis identified several candidate SUMOylation sites, however individual mutation did not result in the loss of the SUMOylated band. Reduced phosphorylation of SUMOylated form of cMyBP-C-UBC9 was observed in HEK293 cells and in virally infected neonatal ventricular cardiomyocytes treated with isoprenaline, which also show a blunted lusitropic response to isoprenaline. This may indicate that SUMOylation of cMyBP-C can regulate cardiac contractility, however experimental limitations, including lack of in-situ evidence that cMyBP-C is SUMOylated, limit the conclusions that can be drawn from this study.

Given the evidence presented here that cMyBP-C palmitoylation is altered in HF, the palmitoylation of other key cardiac substrates was investigated and were found to be altered in animal models and human HF patients in a similar manner. Animal models of cardiac hypertrophy and HF were generally associated with a loss of palmitoylation, whilst human HF showed increased palmitoylation of substrates including NCX1 and Na^+/K^+ ATPase. As NCX1 is a reported substrate, expression and palmitoylation of DHHC5 was evaluated in these samples. Cardiac hypertrophy was associated with an increase in DHHC5 expression as early as 3-days post injury, however HF development was associated with unchanged or reduced levels of DHHC5. Previous work suggests DHHC5 overexpression may not directly impact protein palmitoylation or cardiomyocyte function, therefore DHHC5 palmitoylation was evaluated to investigate whether its activity may be changed. Interestingly, DHHC5 palmitoylation followed a similar pattern in disease to NCX1. This may indicate that there are upstream factors such as fatty acid availability that influence the palmitoylation of all substrates together. This study provides an insight into changes of palmitoylation in cardiac disease, although given that changes in singly palmitoylated proteins are more easily detected by Acyl-RAC, further characterisation using additional methods is required.

Table of Contents

List of Tables

List of Figures

Acknowledgements

Firstly, I would like to sincerely thank the British Heart Foundation and all who support them for the opportunity to carry out this work. Some PhD students are not fortunate enough to have one supportive supervisor in their lives, so I am incredibly grateful to have ended up with three of them. Nikolaj, I will really miss our science chats in your office as you come up with crazy ideas, and I am so thankful for your constant support and encouragement. George, thank you for the opportunity to work on this crazy project with you. I will really miss our honest chats, but not your terrible dad jokes and puns! Will, I know you hate to hear it, but getting to the end of this PhD would not have been possible without you. You have helped me battle every doubt and celebrated every success, and for that I am eternally grateful. You are truly a mentor I am so fortunate to have had, and one, unfortunately for you, I will have for the rest of my (or probably your!) life.

Fortunately, with great supervisors comes amazing, supportive lab groups. Iliyana, Kamila, Badri and Eline, thank you for supporting me or letting me be involved in your projects. To the 535 lab members Joyce, Emma, Chloe, Ellie, Gillian, Angie, Tom, Connor, Jithin, Dilys, Fiona, Jack and Oom; through fire (literally) or flood, you always make the lab a happy place to be. To the Fuller lab members, you made the tough days easier and the best days better. Thank you to Jacquie, for teaching me all the best lab tricks and putting up with our Christmas decorating! Thank you to Krzys and Caglar for adopting me into your exclusive post-doc office and tolerating me making fun of you, and to Sharon for always having the answer to every question and being so supportive. Thank you to my PopMaster buddies Alan, Elaine and anyone else who knows me… and to Olivia for being the most supportive, craziest and entertaining force in my life. Thank you to my all-singing, all-dancing bench buddy Emily - I will miss hating on the neonates with you! Finally, a special mention to my PhD sisters Xing and Samitha. I am so thankful every day that this experience brought you both into my life. It was truly worth every single bad day to have gained you as my friends, and when we are old and have long forgotten what palmitoylation is, I know I will still have you both.

I am very fortunate to have collaborated with some incredible scientists throughout my project. Thank you to the researchers of ICAMS, especially my long-suffering academic friend Simon for being the best deputy-rep. Thank you to

Aileen, Mike, Godfrey, Francis and Sara for beautiful cells and electrophysiology expertise. Thank you to Jolanda and Julien for adopting me into your labs, and to Rajvi for being my best linked-in friend and teaching me how to glue cells to needles! As a newbie in the cMyBP-C field, I am very grateful to Ken, Sakthi and Sam for being so welcoming and answering every question I had without hesitation.

A huge thank you to my ever-supportive friends and family, including the Mains and my adoptive Haley clan, never hesitating to ask me how it was going and always showing an interest in what I was doing. Thank you to my current partner (just kidding, Alex!). You have been such an incredible support throughout my (long) university life, taking care of our normal life whenever I was too PhD-focused to get there, and I am so grateful for you. Thank you for constantly entertaining my number one thesis distraction, Buddy, whose input to this thesis (in the form of dropping his ball on my keyboard) may still remain somewhere…

Author's Declaration

I declare that the work presented in this thesis has been carried out by myself except where otherwise cited or acknowledged. It is entirely of my own composition and has not, in whole or part, been submitted for any other higher degree. This work was supervised by Professor Will Fuller, Professor Nikolaj Gadegaard and Professor George Baillie.

Alice Main, August 2022

Abbreviations

17-ODYA	17-octadecyonic acid
2-BP	2-bromopalmitate
A/R	Anoxia/reperfusion
ABE	Acyl-biotin exchange
ABHD	α/ß hydrolase domain
ACE	Angiotensin converting enzyme
Acyl-RAC	Acyl-resin assisted capture
AMD	Amphiphile mediated degradation
ANOVA	Analysis of variance
AP	Action potential
APT	Acyl protein thioesterase
ATP	Adenosine triphosphate
BH4	Tetrahydrobiopterin
BioID	Proximity biotinylation
BK	Voltage activated potassium channel
BSA	Bovine serum albumin
Ca^{2+}	Calcium ions
CAD	Coronary artery disease
CAMKII	Calcium/calmodulin-dependent kinase II
cAMP	Cyclic adenosine monophosphate
CD50	Contraction duration at 50% of peak
CMA	N-cyanomethyl-N-myracrylamine
cMyBP-C	Cardiac myosin binding protein-C
CoA	Coenzyme A
CypD	Cyclophilin-D
DHHC	Aspartate-histidine-histidine-cysteine
DHHC-PAT	DHHC-palmitoyl acyltransferase
DMEM	Dulbecco's Modified Eagle Medium
DMSO	Dimethyl sulfoxide
Dn90	Time between 90% of upstroke to 90% of downstroke
DOCA	Deoxycorticosterone acetate
DRX	Disordered relaxed state
DTT	Dithiothreitol
ECC	Excitation-contraction coupling
EDP	End-diastolic pressure
EDTA	ethylenediaminetetraacetic acid
EDV	End-diastolic volume
ELC	Essential light chain
eNOS	Endothelial nitric oxide synthase
ER	Endoplasmic reticulum
ESV	End-systolic volume
F_{act}	Active force
FASN	Fatty acid synthase
FBS	Foetal bovine serum
FFR	Force-frequency relationship

F_{max}	Maximal force
$F_{passive}$	Passive force
fps	Frames per second
FRET	Fluorescence resonance energy transfer
fsMyBP-C	Fast skeletal myosin binding protein-C
GAPDH	glyceraldehyde 3-phosphate dehydrogenase
GFP	Green fluorescence protein
GPCR	G-protein coupled receptor
GSK3β	Glycogen synthase kinase 3β
HA	Hydroxylamine
HCM	Hypertrophic cardiomyopathy
HCN	Hyperpolarising activated cyclic nucleotide gated
HDAC	Histone deacetylase
HEK-293	Human embryonic kidney-293 cells
	4-(2-hydroxyethyl)-1-piperazineethanesulfonic acid
HF	Heart failure
HMM	Heavy meromyosin
HFmrEF	Heart failure with mid-range ejection fraction
HFpEF	Heart failure with preserved ejection fraction
HFrEF	Heart failure with reduced ejection fraction
HR	Heart rate
HRP	Horseradish peroxidase
I/R	Ischaemia/reperfusion
ICM	Ischaemic cardiomyopathy
If	"Funny" current
IgG	Immunoglobulin-G
IHD	Ischaemic heart disease
IP	Immunoprecipitation
iPSC-CMs	Induced pluripotent stem cell derived cardiomyocytes
K^+	Potassium ions
kDa	Kilodalton
KO	Knock out
LA	Left atria
LB broth	Luria-Bertani broth
LC-MS/MS	Liquid-chromatography mass spectrometry/mass spectrometry
LDA	Length dependent activation
LMM	Light meromyosin
LTCC	L-type calcium channel
LV	Left ventricle
LVEF	Left ventricular ejection fraction
MCU	Mitochondrial uniporter
MEND	Massive endocytosis
MHC	Myosin heavy chain
MI	Myocardial infarction
miR	Micro-RNA

MLCK	Myosin light chain kinase
MMTS	Methanethiosulfonate
MOI	Multiplicity of infection
MPTP	Mitochondrial permeability transition pore
MR-1	Myofibrillogenesis regulator-1
ms	Milliseconds
MyBP-C	Myosin binding protein-C
Na^+	Sodium ions
NaCl	Sodium chloride
NCS	Newborn calf serum
NCX1	Sodium-calcium exchanger 1
NEB	New England BioLabs
NEM	N-ethylmaleimide
NO	Nitric oxide
NRVM	Neonatal rat ventricular myocytes
ODYA-CoA	Octadecynoic acid-coenzyme A
P/S	Penicillin/streptomycin
P1	1-day old neonatal rat
P2	2-day old neonatal rat
P3	3-day old neonatal rat
P4	4-day old neonatal rat
PBS	Phosphate buffered saline
pCa4.5	Maximally activating calcium (-log[Ca^{2+}])
pCa6.0	Submaximal activating calcium (-log[Ca^{2+}])
PCR	Polymerase chain reaction
PDE	Phosphodiesterase
PKA	Protein kinase A
PKC	Protein kinase C
PKD	Protein kinase D
PLB	Phospholamban
PLM	Phospholemman
PMCA	Plasma membrane calcium ATPase
PNS	Peripheral nervous system
PP	Protein phosphatase
PPT	Palmitoyl-protein thioesterase
PTM	Post-translational modification
RA	Right atrium
RLC	Regulatory light chain
RNS	Reactive nitrogen species
ROS	Reactive oxygen species
rpm	Rotations per minute
RSK	Ribosomal S6 kinase
RV	Right ventricle
RYR	Ryanodine receptor
S1	Myosin subfragment 1
S2	Myosin subfragment 2
S.E.M	Standard error of the mean
SA	Sinoatrial node
SDS-PAGE	Sodium dodecyl sulphate-polyacrylamide gel electrophoresis

SENP	sentrin/SUMO specific protease	**TD50**	Time to 50% of contraction
SERCA	Sarcoplasmic-reticulum calcium ATPase	**Tm**	Tropomyosin
SIM	SUMO interacting motif	**TnC**	Troponin-C
SMN	Sarcomere null	**TnI**	Troponin-I
SNS	Sympathetic nervous system	**TnT**	Troponin-T
SR	Sarcoplasmic reticulum	**T-tubules**	Transverse tubules
SRX	Super relaxed state	**TTP**	Time to peak
ssMyBP-C	Slow skeletal myosin binding protein-C	**UBC9**	E2 conjugating ubiquitin carrier 9
STZ	Streptozotocin	**UF**	Unfractionated
SUMO	Small ubiquitin-like modifier	**Up90**	Time to 90% of contraction
TAC	Thoracic artery constriction	**UPS**	Ubiquitin proteasome system
TBTA	Tris(benzyltrizolylmethyl) amine	**VGSC**	Voltage gated sodium channel
TCEP	Tris(2-carboxyethyl)phosphine	**WT**	Wildtype
		Zn^{2+}	Zinc ions

Presentations, publications and awards

Publications:

- **Main, A.,** Milburn, G. N., Balesar, R., Rankin, A., Smith, G., Campbell, K. S., Baillie, G.S., van der Velden, J. and Fuller, W. (2022). 'Palmitoylation of cardiac myosin binding protein-C is associated with increased myofilament affinity, reduced myofilament calcium sensitivity and is increased in ischaemic heart failure.' biorxiv.org/content/10.1101/2022.06.21.496992v1.

- **Main, A.,** Bogusalvskyii, A., Howie, J., Kuo, C.W., Rankin, A., Burton, F. L, Smith, G. L., Hajjar, R., Baillie, G.S., Shattock, M. J., Campbell, K. S., and Fuller W. (2022). 'zDHHC5 is increased in cardiac hypertrophy and reduced in heart failure but this does not correlate with substrate palmitoylation.' https://www.biorxiv.org/content/10.1101/2022.08.19.504400v1.

- **Main, A.** and Fuller, W. (2021) 'State-of-the-Art Review: Protein S-Palmitoylation: Advances and Challenges in Studying a Therapeutically Important Lipid Modification' The FEBS Journal. https://doi.org/10.111.febs.15781

- **Main, A.,** Fuller, W. and Baillie, G. S. (2020) 'Post-translational regulation of cardiac myosin binding protein-C: A graphical review', Cellular Signalling. Elsevier Inc., p. 109788. https://doi.org/10.1016/j.cellsig.2020.109788

- **Main, A.,** Robertson-Gray. O. and Fuller, W. (2020) 'Cyclophilin D palmitoylation and permeability transition: a new twist in the tale of myocardial ischaemia-perfusion injury', Cardiovascular Research. Oxford University Press (OUP). https://doi.org/10.1093/cvr/cvaa149.

- Gok, C., **Main, A.,** Gao, X., Kerekes, Z., Plain, F., Kuo, C-W., Robertson, A.D., Fraser, N.J and Fuller, W. (2021) 'Insights into the Molecular Basis of the Palmitoylation and Depalmitoylation of NCX1,' Cell Calcium. https://doi.org/10.1016/j.ceca.2021.1.102408

- Gao, X., Kuo, C.W., **Main, A.,** Brown, E., Rios, F., De Lucca Camargo, L., Samji, S., Wypijewski, K.J., Gok, C., Touyz, R. and Fuller, W. (2022). 'Palmitoylation regulates cellular distribution of and transmembrane Ca flux through TrpM7.' Cell Calcium. https://doi.org/10.1016/j.ceca.2022.102639

Oral/Poster Presentation:

Alice Main, Gregory N. Milburn, Rajvi N. M. Balesar, Aileen Rankin, Godfrey L. Smith, Kenneth S. Campbell, George S. Baillie, Jolanda van der Velden and William

Fuller. *Cardiac myosin binding protein-C palmitoylation increases its myofilament affinity, reduces myofilament Ca^{2+} sensitivity and is increased in ischaemic heart failure*.

- FASEB Protein Lipidation Meeting 2022, Vermont, USA

Poster Presentations:

Alice Main, Kenneth S. Campbell, George S. Baillie and William Fuller. *Characterising the palmitoylation of cardiac myosin binding protein-C in cardiac health and disease*.

- The Biophysical Society 66th Annual Meeting 2022, San Francisco, USA
- FASEB Lipidation Meeting 2021, Virtual
- Vascular Summer School 2019, Montreal, Canada
- University of Glasgow Cardiac Theme Meeting 2019, Glasgow, UK
- 27th Northern Cardiovascular Research Group Conference 2018, Leeds, UK

Awards:

- College of Medical Veterinary and Life Sciences Conference Support Award (The Biophysical Society 66th Annual Meeting, San Francisco, USA) - £750
- The Biochemical Society General Travel Grant (The Biophysical Society 66th Annual Meeting, San Francisco, USA) - £500
- College of Medical Veterinary and Life Sciences Training Award (Amsterdam Vumc and University of Copenhagen research visits) - £2000
- Scottish Universities Life Sciences Alliance (SULSA) Emerging Researcher Scheme (Amsterdam Vumc and University of Copenhagen research visits and attendance at the FASEB Protein Lipidation Meeting, Vermont, USA) - £1800

Chapter 1 Introduction

1.1 The cardiac contractile cycle

The cardiac cycle involves the rhythmic action of diastole (heart relaxation and filling of ventricles with oxygenated blood) and systole (heart contractility and ejection of blood into systemic and pulmonary circulatory systems). This facilitates the flow of blood around the body, therefore supplying the organs with oxygen and essential nutrients whilst collecting waste products and carbon dioxide to be expelled through the lungs. This process is tightly regulated, lasting less than 1 second at rest, to allow the heart to consistently meet the body's demands throughout a lifetime, encompassing over 2.5 billion beats (Pollock & Makaryus, 2019).

1.1.1 Excitation-contraction coupling

Although the heart is comprised of several cell types, the mechanical pumping is driven by specialised muscle cells called cardiomyocytes, which comprise 70-80% of the mass of the heart. These cells are influenced by the cycling of calcium (Ca^{2+}) in a mechanism known as excitation-contraction coupling (ECC; Zhou and Pu, 2016). Atrial and ventricular cardiomyocytes have a resting membrane potential of ~-90mV during diastole, predominantly determined by the electrochemical gradient involving the intracellular and extracellular concentration of potassium (K^+) ions. Excitation is initiated by electrical signals from the sinoatrial (SA) node, known as the pacemaker, located in the right atrium (Park & Fishman, 2017). The SA node contains specialised pacemaker cells which have an unstable resting membrane potential due to the presence of hyperpolarising activated cyclic nucleotide gated (HCN) channels. These generate the "funny" current (I_f), allowing slow influx of sodium (Na^+) ions into the cell. Once the membrane potential of these cells reaches -40mV, voltage activated T-type Ca^{2+} channels are opened allowing Ca^{2+} to enter the cell and facilitating rapid depolarisation to +10mV in the upstroke of the action potential. The action potential is propagated through the cardiac conduction system to co-ordinate atrial systole followed by ventricular systole (Figure 1.1; Wei, Yohannan and Richards, 2021)

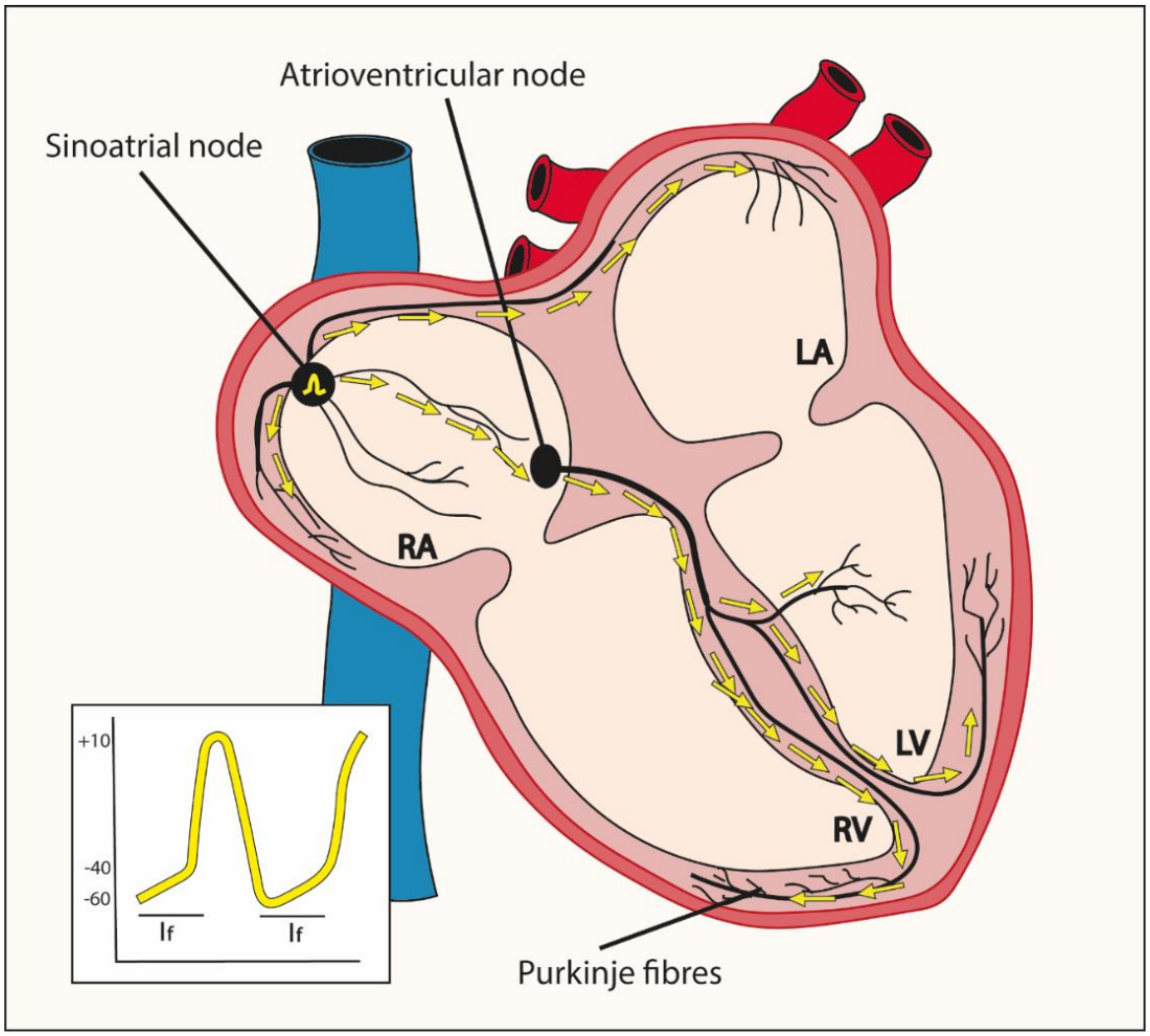

Figure 1.1. The cardiac conduction system.
Action potentials are generated in the sinoatrial node pacemaker cells in the right atrium (RA) of the heart. These cells have unstable membrane potential, with hyperpolarisation activated cyclic nucleotide gated (HCN) channels generating the "funny" current (I_f), leading to slow influx of Na^+ ions and raising the membrane potential from -60mV to -40mV. At -40mV T-type voltage gated calcium channels are activated which triggers the action potential upstroke. The action potential is propagated throughout the heart via bundles of fibres, including purkinje fibres, to the atrioventricular node, left atrium (LA), left ventricle (LV) and right ventricle (RV).

In individual cardiomyocytes, contraction is coupled to excitation by the arrival of the action potential at the sarcolemma leading to the activation of voltage-gated sodium channels (VGSCs) located there. These channels drive an influx of Na^+ which results in the depolarisation of the cardiomyocyte membrane from -90mV to +40mV, and in doing so leads to activation of voltage gated L-type Ca^{2+} channels (LTCC, Ca(v)1.2), which are permeable to Ca^{2+} and allow a small influx of Ca^{2+}. In ventricular cardiomyocytes, LTCCs are localised in specialised membrane invaginations known as transverse-tubules (T-tubules), which propagate signals from action potentials into cardiomyocytes and allow close coupling (~15nm apart) of the LTCCs with cardiac ryanodine receptors (RYR) found on the cardiomyocyte internal Ca^{2+} store, the sarcoplasmic reticulum (SR; Eisner *et al.*, 2017). The Ca^{2+}

influx via LTCCs activates the RYRs leading to a much larger efflux of Ca^{2+} from the SR, up to an intracellular Ca^{2+} ($[Ca]_i$) level of 10 μM from ~100 nM, in a process known as Ca^{2+}-induced Ca^{2+} release. This period is prolonged compared to the initial upstroke of the action potential, as during this plateau Ca^{2+} stimulates the cardiomyocyte contractile machinery which shortens the cell (described in 1.1.2). Cardiomyocytes are electrically linked via gap junctions, and mechanically linked via intercalated discs, allowing ECC to occur simultaneously throughout the tissue, leading to co-ordinated atrial or ventricular systole (Bers, 2002a). Depletion of the SR triggers closure of RYRs and removal of Ca^{2+} to end the contraction and return the cardiomyocyte to a resting state for the cycle to repeat. This occurs predominantly through re-uptake to the SR through the sarcoplasmic reticulum Ca^{2+}-ATPase (SERCA, ~70% of uptake) and removal from the cell in exchange for sodium by the Na^+/Ca^{2+} exchanger 1 (NCX1, ~28% of uptake), closely coupled with the activity of the Na^+/K^+ ATPase. Ca^{2+} removal also occurs through the plasma membrane Ca^{2+} ATPase (PMCA) and the mitochondrial Ca^{2+} uniporter (MCU), to a lesser extent (Figure 1.2; Bers, 2002b; Fearnley, Llewelyn Roderick and Bootman, 2011; Eisner *et al.*, 2017).

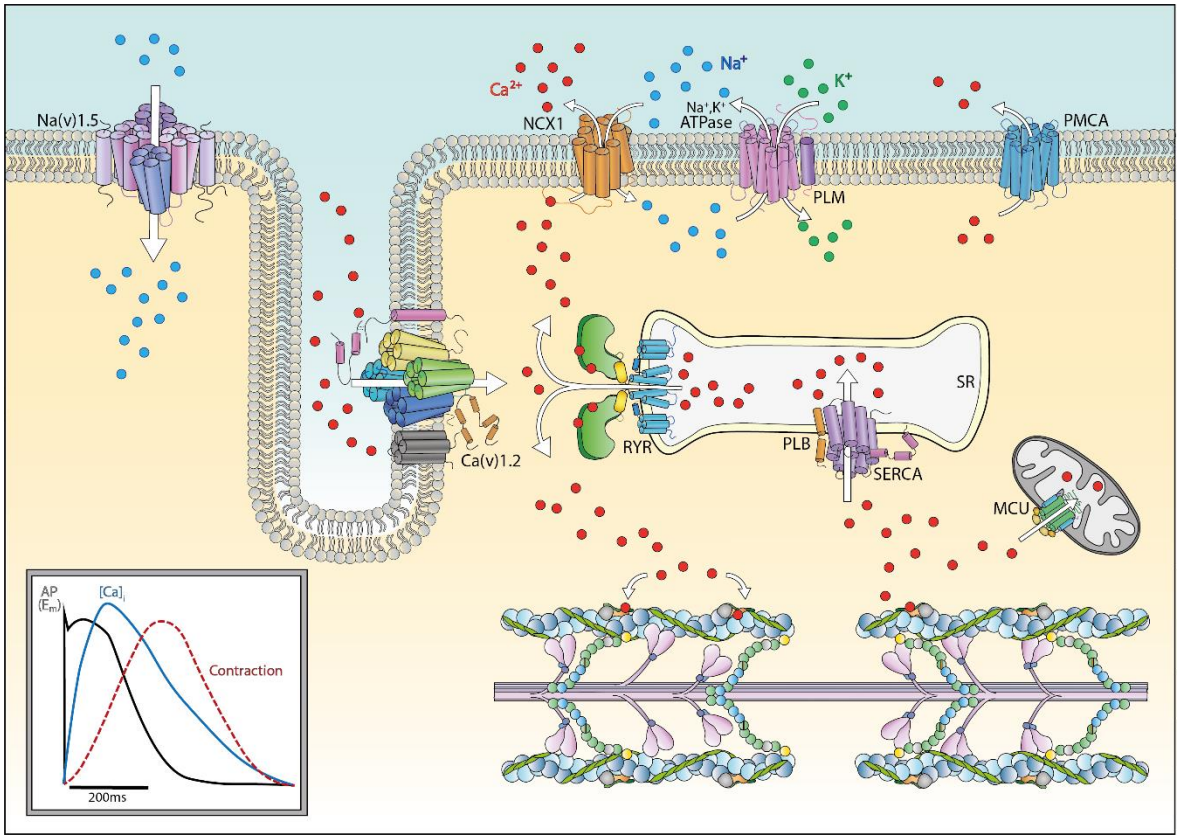

Figure 1.2. Cardiac excitation contraction coupling.
Arrival of an action potential (AP) at the sarcolemma of a cardiomyocyte results in activation of voltage gated sodium channels (Na(v)1.5) located there, allowing sodium (Na^+) to enter the cell, further depolarising the membrane. This depolarisation activates L-type voltage gated calcium channels (LTCC) located in the cardiomyocyte T-tubules, specialised invaginations that allow propagation of signal throughout the cell. LTCCs are permeable to calcium ions (Ca^{2+}) which flow into the cell and bind to closely located ryanodine receptors (RYR) on the sarcoplasmic reticulum (SR), the internal calcium store of the cell. This activation induces a large release of calcium into the cell in the process known as calcium induced calcium release. Calcium then binds to the contractile machinery of the cell and triggers the sequence of events that will result in shortening of the cell and systole. At the end contraction, calcium is removed from the cytoplasm to return it to its resting state, mainly through the sarcoplasmic reticulum Ca^{2+}ATPase, controlled by accessory protein phospholamban (PLB) back into the SR for the next cycle. Calcium is also expelled from the cell via the Na^+/Ca^{2+} exchanger (NCX1) in exchange for sodium (Na^+), the activity of which is closely coupled to the Na^+,K^+ ATPase which maintains the sodium gradient by exchanging it for potassium (K^+), regulated by its accessory protein phospholemman (PLM). Calcium is also removed from the cell by the plasma membrane Ca^{2+} ATPase (PMCA) and the mitochondrial Ca^{2+} uniporter (MCU), to a lesser extent. The inset diagram shows the relationship between AP, intracellular calcium [Ca]i and contraction in a ventricular cardiomyocyte. Adapted from Bers, 2002 and taken from Main and Fuller, 2021.

1.1.2 The cardiac myofilament

During systole, the rise in intracellular Ca^{2+} activates the cardiomyocyte contractile machinery within specialised features of the striated muscle known as sarcomeres. Sarcomeres are repeating units, ~1.7μm to ~2.3μm in diameter (systolic and diastolic lengths in humans), composed of myosin-containing thick filaments, actin-containing thin filaments and a host of accessory proteins that co-ordinate their interaction (collectively known as myofilaments). The sarcomere

is arranged in a lattice structure with overlapping thick and thin filaments in the central A-band, whilst the I-bands contain thin filaments attached to Z-discs to allow the sarcomeres to be linked together. The M-band is the thick filament exclusive region where thick filament tails are wound together to create this region which regulates lattice tension (Agarkova *et al.*, 2003). Accessory proteins include myosin binding protein-C (MyBP-C, discussed in detail in 1.2) located in the C-zone, and the giant protein Titin, which transverses every half sarcomere along the thick filament linking Z-disc and M-band proteins (Figure 1.3; de Tombe and ter Keurs, 2016).

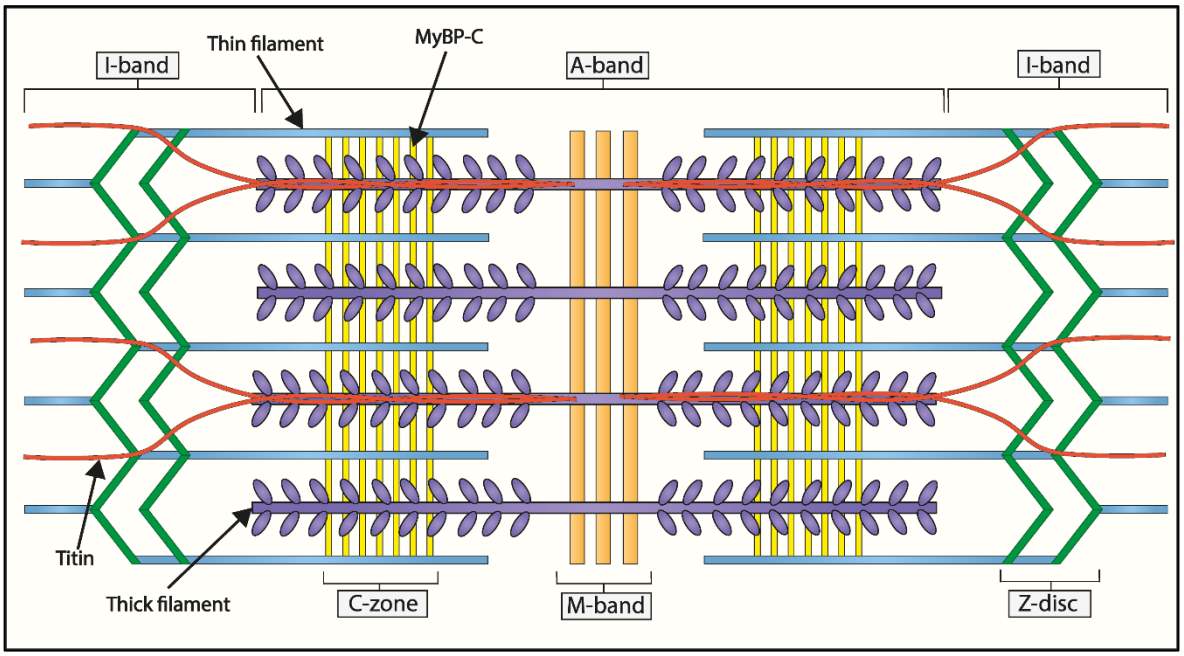

Figure 1.3. The anatomy of a sarcomere.
The sarcomere is primarily composed of myosin thick filaments (purple) and actin thin filaments (blue). The overlapping of actin and myosin in the A-band gives rise to the striated pattern of the skeletal and cardiac tissue where sarcomeres are found. I-bands which contain actin thin filaments are attached to Z-discs which link sarcomeres together. The central M-band of the sarcomere contains thick filaments which provide lattice tension. The C-zone contains the sarcomeric accessory protein myosin binding protein-C (MyBP-C) and the giant sarcomeric protein titin traverses the half sarcomere along the thick filament.

Aside from containing predominantly monomeric actin, which polymerises to form a double stranded helix known as F-actin, thin filaments contain the regulatory troponin-complex on every seventh monomer of actin and the coiled-coil protein tropomyosin (Tm), formed of two polypeptide chains in a super helical strand which runs parallel into the grooves of the actin helix (Figure 1.4; Kobayashi, Jin and de Tombe, 2008). After release from the SR, calcium's interaction with the hetero-dimer troponin complex initiates the contractile process. Troponin-C (TnC) is the Ca^{2+} sensing element of the complex with three Ca^{2+} binding sites. Two of

these are always occupied, and binding of Ca^{2+} to the third, lower affinity site during systole induces the switch peptide of Troponin-I (TnI), the inhibitory component of the complex, to increase its binding to TnC. This interaction produces a conformational change that reduces the interaction between TnI and Troponin-T (TnT), which directly binds to Tm located along the actin thin filament, blocking the binding of myosin to actin. The Ca^{2+}-induced weakening of the troponin complex leads to a conformational shift in Tm's position causing it to move deeper into the actin groove and increases the available binding sites on actin for myosin to attach (de Tombe, 2003).

Structurally, cardiac myosin is composed of two heavy chains (MHC) which can be further divided into "head" (heavy meromyosin, HMM) and "tail" (light meromyosin, LMM) regions, with several LMMs linking together to form the thick filament backbone. The HMM region can be further divided into adenosine triphosphate (ATP)-dependent motor subfragment-1 (S1) region, which contains a nucleotide binding pocket as well as the actin binding interface, and the subfragment2 (S2) neck region. The S2 is thought to play important roles in regulating myosin velocity by imposing a drag on the filaments, and in myosin auto-inhibition and formation of the super-relaxed (SRX) state of myosin (discussed in more detail elsewhere; Barrick *et al.*, 2021). Each chain also has regulatory (RLC) and essential (ELC) light chain unit associated with it, with phosphorylation of the former enhancing contractile function and the latter providing further fine tuning of the motor domain in an isoform dependent manner (Figure 1.4; Hernandez *et al.*, 2007; Toepfer *et al.*, 2013).

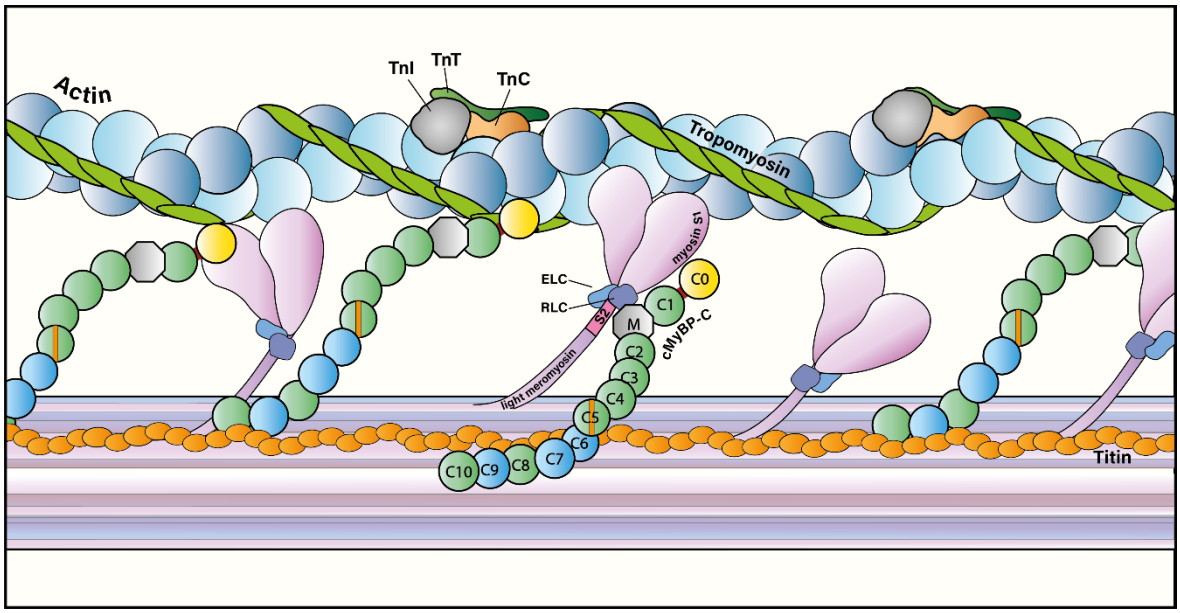

Figure 1.4. Inside the cardiac myofilament.
Cardiac myofilaments are composed of thin filaments, with two strands of woven actin molecules and accessory proteins tropomyosin and the troponin complex (comprising troponin-I (TnI), troponin-T (TnT) and troponin-C (TnC), and myosin thick filaments, including thick filament accessory proteins cardiac myosin binding protein-C (cMyBP-C) and titin. Cardiac myosin has been further structurally defined into the light meromyosin tail, which forms the thick filament backbone, and the heavy meromyosin head unit containing the myosin subfragment2 (S2) neck and the myosin subfragment 1 (S1) motor domain and actin binding sites. There are also essential light chain (ELC) and regulatory light chain (RLC) units in this region of the protein. Taken from Main, Fuller, *et al.*, 2020.

After myosin has bound the newly available sites on actin, the hydrolysis of ATP in the S1 domain leads to the "power stroke", sliding actin along the myosin filaments, shortening the I-bands of the sarcomere and bringing the Z-lines closer together. At the end of contraction, subsequent removal by the processes mentioned induces the release of Ca^{2+} from TnC and results in myosin detachment and relaxation during diastole. This process is known as cross-bridge cycling and when coordinated throughout the cell and tissue, results in contraction of the heart (Bers, 2002a; de Tombe, 2003; Eisner *et al.*, 2017). Overall, myofilaments are essential to cardiac function and as such are involved in both the intrinsic and extrinsic mechanisms that regulate myocardial contractility.

1.1.3 Intrinsic regulation of contractility

Cardiac output, defined as the amount of blood pumped by the heart through the circulatory system per minute, can be adapted by changing heart rate (HR, the number of beats per minute) or stroke volume (SV, amount of blood pumped into the circulatory system, calculated by end-diastolic volume (EDV) minus end-systolic volume (ESV)). Modulating either stroke volume, e.g., through length-dependent activation mechanisms, or heart rate, as observed in the force-

frequency relationship, allows the heart to intrinsically adapt to maintain or alter cardiac output to meet the demands of the body (King & Lowery, 2021).

Cardiac output (CO) = Heart rate (HR) x stroke volume (SV)
(Beats per minute) (EDV-ESV)

1.1.3.1 Length dependent activation

A unique feature of cardiac muscle is its ability to adapt its stroke volume to maintain cardiac output if there are changes in EDV (the volume of blood returning to the heart) and therefore the end-diastolic pressure (pre-load), otherwise known as the Frank-Starling Law of the Heart. This is an important regulatory mechanism as increased venous return, and therefore pre-load in the ventricle, can be caused by a number of factors, including changes in inspiration, the cardiac suction effect or the effect of the skeletal muscle pump. As such, the heart must often adapt its usual stroke volume and end-diastolic pressure (EDP) to expel extra blood. Additionally, any increase in after-load (i.e. the systemic vascular resistance the heart must work against) will have the same effect on increasing pre-load, requiring the stroke volume to be increased to overcome the additional resistance (Tansey *et al.*, 2019).

The fundamental basis of the mechanism is that the stretching of the cardiomyocytes during increased pre-load leads to a phenomenon known as length-dependent activation (LDA) within the stretched sarcomeres, resulting in increased force generation a few milliseconds after stretch (Mateja & de Tombe, 2012). Although a logical explanation would be that increasing sarcomere length increases the extent of overlapping thin and thick filaments and therefore the number of actin-myosin cross-bridges, the length-force relationship is steep and un-uniform and so is likely a more complex phenomenon. It is now understood that the increasing sarcomere length-to-force relationship is governed by changes in thick filament structure, resulting in higher active force, whilst increasing sarcomere length also increases the Ca^{2+} sensitivity of the thin filament, generating more myocardial force at a given Ca^{2+} concentration compared to shorter sarcomere length (Figure 1.5; Claflin, Morgan and Julian, 1998; de Tombe *et al.*, 2010; Zhang *et al.*, 2017).

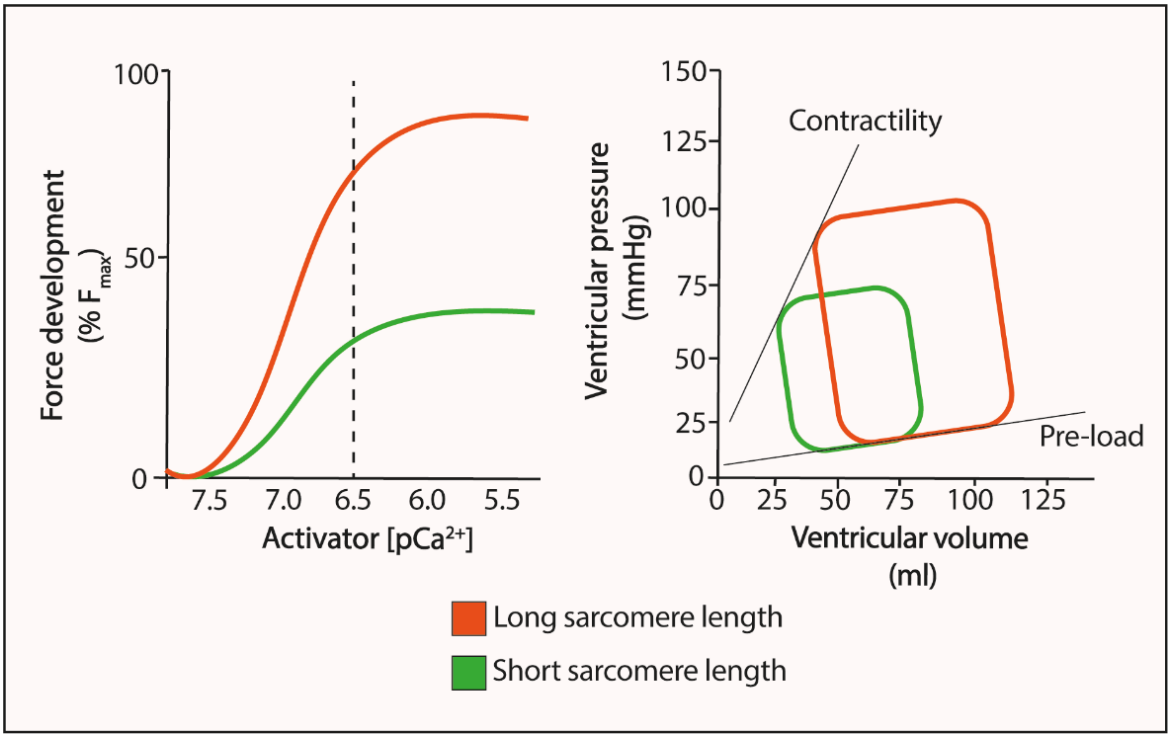

Figure 1.5. Sarcomere length and the Frank-Starling pressure volume system of the heart. The pressure-volume loop of the ventricle demonstrates the Frank-Starling Law of the heart whereby increasing end-diastolic volume and pre-load leads to an adaptation of the ventricle to increase contractility and end-systolic pressure. The underlying mechanisms involves lengthening of cardiac sarcomeres in a mechanism known as length dependent activation, where at a longer sarcomere length, myofilaments are more sensitive to calcium (curve shifts to the left) and can produce a greater force (curve shifts upwards). Adapted from de Tombe *et al.*, 2010.

The exact molecular mechanisms underlying LDA are still being elucidated. At longer sarcomere lengths, the interfilament spacing between the thick and thin filaments is reduced which was hypothesised to drive the increase in myofilament Ca^{2+} sensitivity (Irving *et al.*, 2000). However, when this spacing is replicated using osmotic compression, the same level of sensitivity gained by increasing sarcomere length is not observed, suggesting other mechanisms are involved in LDA (Konhilas *et al.*, 2002). Some more recent work has defined the changing conformation and activity of the troponin complex during LDA. Using X-ray diffraction and fluorescence resonance energy transfer (FRET) based measurements, it has been observed that the TnI/TnC binding relationship, which governs thin filament activation, is altered at increasing sarcomere length in a way that is independent from its change during Ca^{2+} activation or thick filament activity (Zhang *et al.*, 2017).

Whilst increasing thin filament Ca^{2+} sensitivity shifts the force curve to the left at longer sarcomere lengths, the increase in maximum force at a given Ca^{2+} concentration has been shown to involve the thick filament. A change in the

number of force-generating myosin heads or the orientation of these heads before the sarcomere length increases is essential to development of LDA (Caremani *et al.*, 2016; Farman *et al.*, 2011). This involves the ratio of myosin heads in the super relaxed state (SRX, orientated toward the backbone away from actin and hydrolysing ATP at a slow rate) versus the disordered relaxed state (DRX, orientated toward actin but not directly bound, hydrolysing ATP at a fast rate), with stretch of sarcomeres shown to increase the number of myosin heads from the SRX to the DRX state (Kampourakis *et al.*, 2016).

Importantly, the thin and thick filament associated LDA changes have been linked to the giant myofilament accessory protein Titin, which is the main contributor of passive force, defined as the force generated from structural elements of the muscle (Herzog, 2018). Passive force increases at longer sarcomere lengths and removal of titin or altering of its spring elements reduces passive tension, alters inter-filament spacing and reduces Ca^{2+} sensitivity (Ait-Mou *et al.*, 2016). The conformational changes observed in the troponin complex mediating the increase in Ca^{2+} sensitivity have been related to titin, as loss of titin driven passive tension in a transgenic mouse (RBM20) expressing a more compliant form of titin was accompanied by reduction in the sarcomere-length dependent conformational change in TnC, reducing Ca^{2+} sensitivity (Li *et al.*, 2019). X-ray diffraction revealed that in a RBM20 mutation rat model, myosin heads are found closer to the myosin backbone, however the contribution of titin to the SRX:DRX ratio still remains to be investigated (Ait-Mou *et al.*, 2016). Interestingly, MyBP-C has also been implicated in LDA through thick and thin filament regulatory mechanisms, including affecting myofilament Ca^{2+} sensitivity and the SRX:DRX ratio of myosin, which will be discussed in detail in 1.2. Altogether, LDA underlying the Frank-Starling mechanism is largely governed by myofilament protein function, and as such anything that changes myofilament protein behaviour has the potential to alter the fundamental properties of the heart. This is one of the reasons why myofilament proteins are the subject of intense research in cardiac disease, as will be discussed.

1.1.3.2 The force-frequency relationship

As well as through changes in LDA, myocardial force is intrinsically linked to heart rate through the force-frequency relationship (FFR). Bowditch (1871) first made

the observations in an isolated frog heart that rate and rhythm were proportional to contractile force. This is largely because increased heart rate reduces ventricular filling time and EDV, requiring a higher systolic force and velocity in order to maintain cardiac output (Endoh, 2004). Analogous to LDA, Ca^{2+} plays a central role in the FFR as early studies showed that increasing beating frequencies caused an increase in the Ca^{2+} transient amplitude and SR load (Allen & Blinks, 1978; Pieske *et al.*, 1999). The increased intracellular Ca^{2+} is likely due to more Ca^{2+} influx through the LTCC. This, coupled with the fact that increasing frequency increases intracellular Na^{+} levels, leads to a consistently greater intracellular Ca^{2+} concentration during each transient through reduced export by NCX1 and increased uptake by SERCA into the SR (Endoh, 2004; Janssen and Periasamy, 2007). The FFR is species dependent, as whilst most mammalian species including humans, rabbits and pigs, show a positive FFR (increased frequency generates increased force) at frequency rates of 0.5-1Hz, some species, including rats and mice, show a negative FFR. This is likely to do with the physiological HR, as mouse and rat FFR becomes positive at higher frequencies closer to physiological HR. Differences in Ca^{2+} are thought to contribute, as rat and mice cardiomyocytes have a higher SR Ca^{2+} content due to increased activity of SERCA and less extrusion of Ca^{2+} by NCX1 (Bers, 2001; Endoh, 2004).

There has been limited study in myofilament function in FFR compared to the LDA. However, there is increasing interest in studying its role as although human ventricular myocardium has a positive FFR, human heart failure (HF) is associated with a negative or neutral FFR, in a way different to the physiological negative FFR observed in some species, with corresponding blunting in Ca^{2+} transients (Figure 1.6; Endoh, 2004; Lamberts, van der Velden and Stienen, 2008).

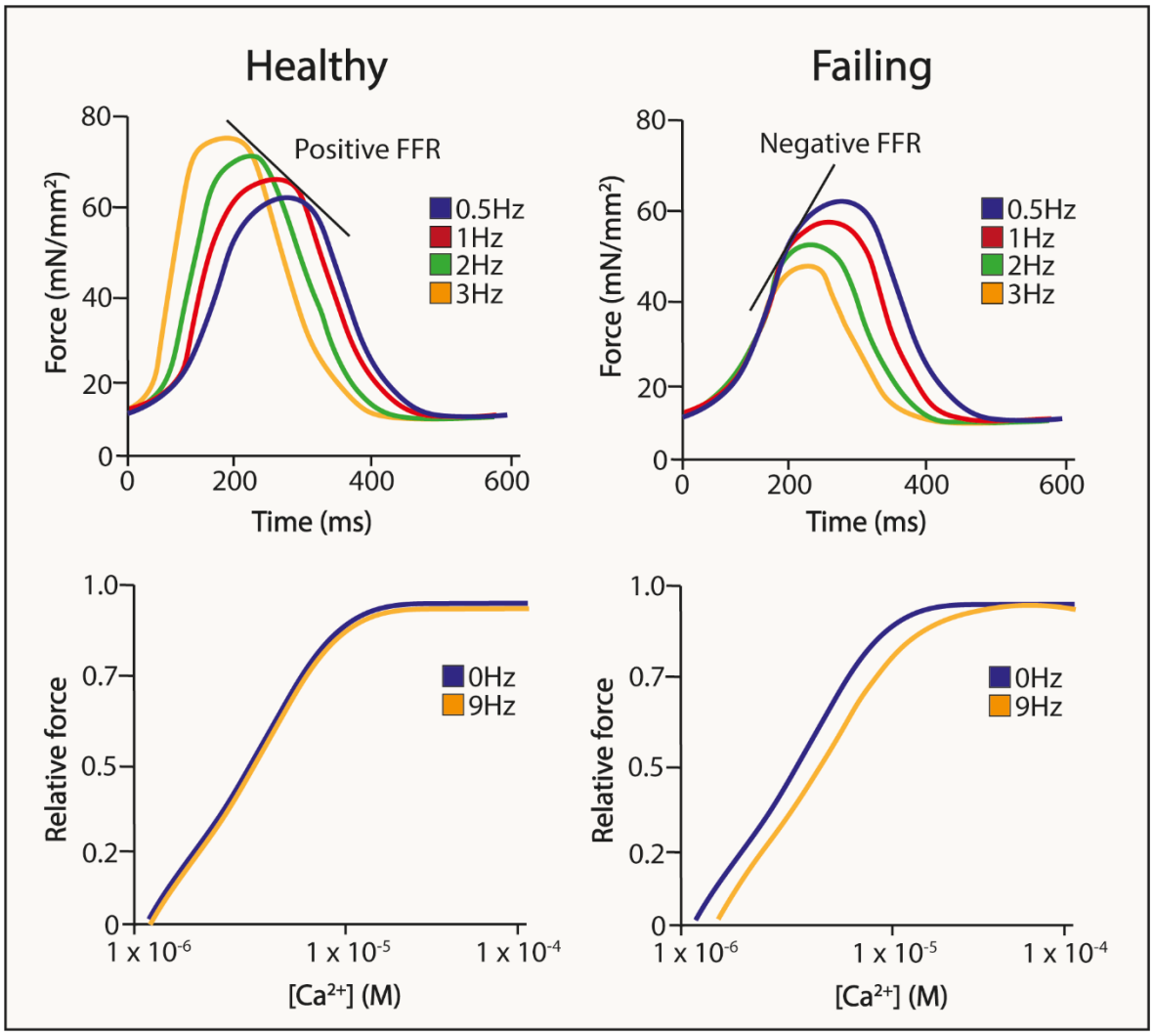

Figure 1.6. The force frequency relationship and myofilament calcium sensitivity in the healthy and failing myocardium.
In the healthy heart, the force frequency relationship (FFR) generates increased force upon increasing frequency (positive FFR), however in the failing heart, increased frequency reduces the force developed (negative FFR). In the healthy myocardium, increasing frequency does not cause a change in Ca^{2+} sensitivity, whilst in the failing heart an increase in frequency is accompanied by a decrease in Ca^{2+} sensitivity (rightward shift of Ca^{2+}-force curve). Adapted from Lamberts, van der Velden and Stienen, 2008.

A study by Lamberts *et al.* showed that whilst increasing frequency generated increased force and Ca^{2+} transients in healthy rat trabeculae, failing hearts showed a decline in force without a change in Ca^{2+} transient amplitude. Similarly, isolated cells from healthy heart had no change in the force-Ca^{2+} relationship curve at increasing frequency, whilst failing heart cells saw a rightward shift. Overall, this indicated that Ca^{2+} sensitivity of the myofilaments does not influence healthy FFR, instead it is the increase in Ca^{2+} transient amplitude which plays a role, whilst in a failing heart, myofilament desensitisation to Ca^{2+} is involved (Lamberts *et al.*, 2008). Interestingly, the exact mechanisms underlying the myofilament role in FFR may involve phosphorylation of myofilament proteins including TnI, with more recent work suggesting that myofilament Ca^{2+} sensitivity may play a role in the

healthy FFR response as well (Ramirez-Correa *et al.*, 2010). Indeed, phosphorylation is without a doubt one of the key extrinsic modulators of cardiac contractility as a whole.

1.1.4 Extrinsic regulation of contractility

Stroke volume, heart rate and subsequently cardiac output can be modulated extrinsically by various neurotransmitter and hormonal pathways. This includes the autonomic nervous system comprising two opposing arms, the sympathetic nervous system (SNS) and the parasympathetic nervous system (PNS). Both are comprised of G-protein coupled receptors (GPCRs) which either activate, i.e. adrenergic GPCRs in the SNS, or inhibit, i.e. cholinergic GPCRs in the PNS, adenylyl cyclase activity and therefore downstream signalling pathways involving cyclic-adenosine monophosphate (cAMP) and activity of protein kinase A (PKA). Whilst anatomically the PNS can innervate all the chambers of the heart, it predominantly regulates contractility via the cardiac conduction system (Ulphani *et al.*, 2010). On the other hand, SNS stimulation has wide ranging affects across the entire heart, generally leading to positive chronotropy, positive inotropy (increased force of contraction) and positive lusitropy (increased rate of relaxation) through activity of noradrenaline on adrenergic receptors (adrenoceptors).

1.1.4.1 The adrenergic system and phosphorylation

Adrenoceptors can be subdivided into α- and ß-, receptors, and whilst α1-adrenoceptors are found in the heart, ß-adrenoceptors are the predominant form (90% of total adrenoceptors, O'Connell *et al.*, 2014). Within the ß-adrenoceptor class there are three isoforms known as ß1, ß2 and ß3, with existence of a fourth isoform ß4 in the cardiac tissue hypothesised but still unconfirmed (Galitzky *et al.*, 1997; Strosberg *et al.*, 1998). The ß1-adrenoceptor constitutes 80% of the ß-adrenoceptor population in cardiac tissue, being present in all cardiomyocytes, whilst the majority of cells lack ß2- and ß3-adrenoceptors, and as such the ß1-adrenoceptor has been the most well characterised in its role in contractile function (de Lucia *et al.*, 2018; Myagmar *et al.*, 2017). As GPCRs, ß1-adrenoceptors are coupled to stimulatory Gαs G-proteins and upon agonist binding, these G-proteins activate adenylyl cyclase which catalyses the conversion

of ATP to cAMP. Unlike a whole cell rise in Ca^{2+} during a contractile transient, activity of cAMP is localised to specific areas to direct its activity, likely driven through compartmentalization of phosphodiesterases (PDEs), which break down cAMP, and anchoring of adenylyl cyclase to distinct membrane regions (Zaccolo, 2009). The main effector of cAMP activity is the enzyme PKA, which contains two regulatory subunits and two catalytic subunits. The binding of cAMP to the regulatory subunits releases the catalytic subunits and allows them to phosphorylate downstream cardiac substrates (Figure 1.7).

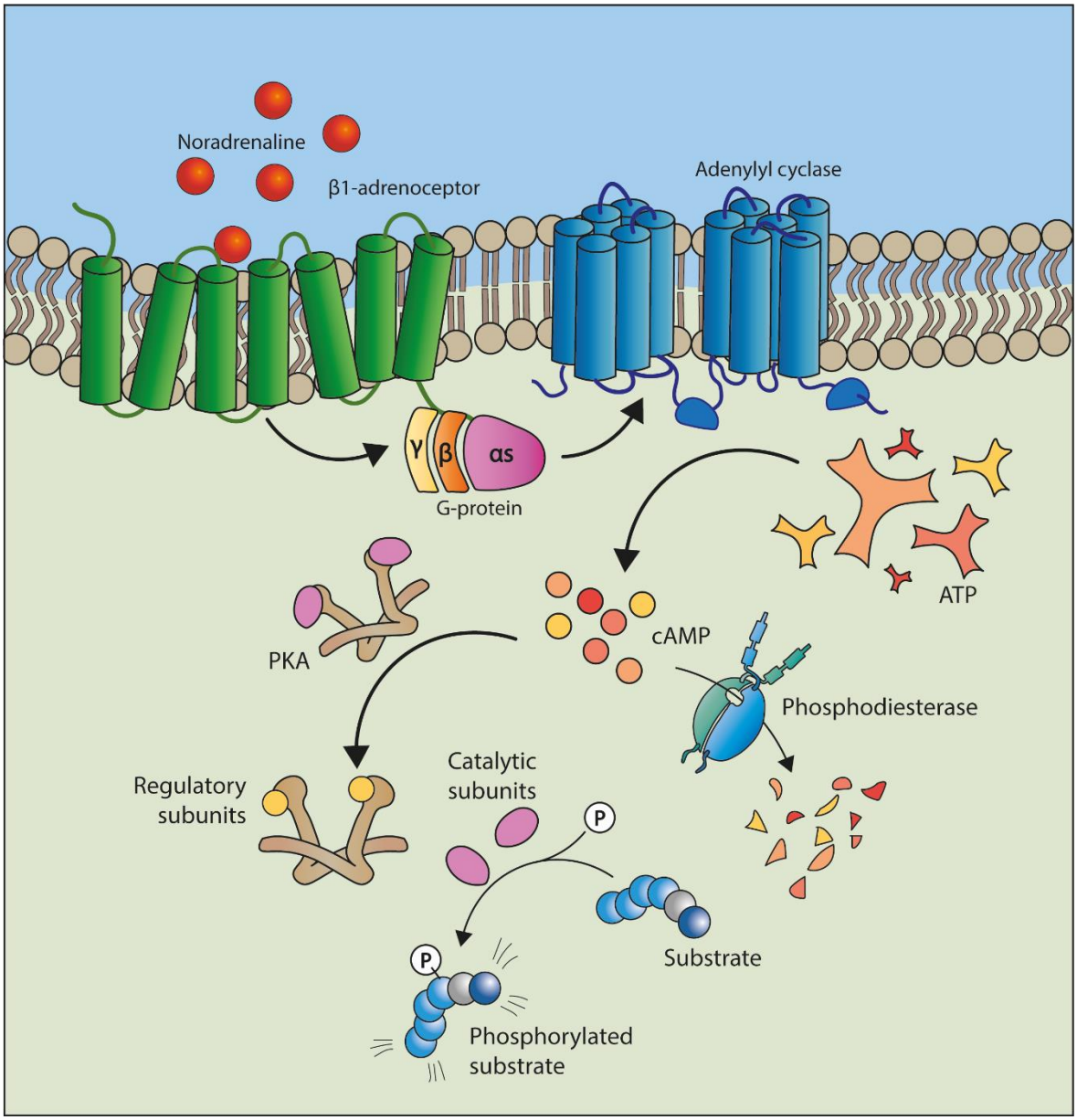

Figure 1.7. β1-adrenoceptor cascade and phosphorylation of downstream substrates. Noradrenaline release from sympathetic nerve fibres acts on β1-adrenoceptors which are coupled to a G-protein. Activation of the receptor causes the Gαs subunit to dissociate from the β and γ subunits and activate adenylyl cyclase. Adenylyl cyclase converts ATP to cAMP which acts upon the enzyme protein kinase A (PKA) and activates it by binding to its regulatory subunits, allowing the catalytic subunits to phosphorylate downstream substrates. Phosphorylation can be limited by the degradation of cAMP by phosphodiesterases. Figure created with components from Baillie, Tejeda and Kelly, 2019.

Phosphorylation, the addition of a phosphate group to an amino acid side chain of a serine, threonine or tyrosine residue, is a post-translational modification that leads to small structural changes within the protein which then induce changes in its biochemical properties. This leads to a wide range of effects including altering ion channel conductance, association of proteins with their binding partners, transcription/translation processes and metabolic function. Phosphorylation is estimated to target at least 30% of the proteome, with more recent mass spectrometry-based analysis suggesting this could be more than 75% (Cohen, 2002;

Sharma *et al.*, 2014). Although PKA mediates the majority of ß1-adrenoceptor driven affects, phosphorylation can occur via other protein kinases including protein kinase C (PKC), protein kinase D (PKD), Ca^{2+}/calmodulin-dependent kinase II (CAMKII) and extracellularly regulated kinases (ERKs; Rapundalo, 1998). Additionally, as phosphorylation has such prominent effects on protein function, it is kept in balance by dephosphorylation driven by protein phosphatases (PP), with PP1, PP2A and PP2B (calcineurin) accounting for 90% of dephosphorylation of cardiac substrates (Weber *et al.*, 2015).

Although an estimation of the percentage of the cardiac proteome that undergoes phosphorylation has not been published, study of individual proteins demonstrates the importance of phosphorylation in mediating SNS driven effects (Lundby *et al.*, 2013). Phosphorylation and dephosphorylation of cardiac myofilament proteins, in particular regulatory proteins associated with actin and myosin, plays a significant role in myofilament Ca^{2+} sensitivity, force generation and relaxation. At the thin filament level, phosphorylation of TnI by PKA at S23/24 (in a cardiac isoform specific region) has been the most well documented, and whilst levels are high in healthy individuals, they are reduced in failing human hearts (Messer *et al.*, 2007). Functionally, phosphorylation of these sites leads to a decrease in myofilament Ca^{2+} sensitivity and increased dissociation of Ca^{2+} causing predominantly lusitropic effects (Zhang, Zhao, & Potter, 1995). This is in part driven by a weakening TnI's binding to TnC in the Ca^{2+} binding site, where it promotes optimal positioning of TnC to bind Ca^{2+}, to an adjacent site (Kachooei *et al.*, 2021). Initially investigation of the role of p-TnI in relaxation provided some conflicting results, with some groups observing this positive lusitropic effect and others observing no effect of increasing PKA on myofilament function (Johns *et al.*, 1997). It is now understood through production of phosphomimetic mutants (serine replaced with aspartic acid) that phosphorylation at both sites, occurring sequentially at S24 followed by slower phosphorylation at S23, is required for these effects (Wijnker *et al.*, 2013). This phenomenon of co-operative phosphorylation of multiple sites is not uncommon, and occurs in MyBP-C, as will be discussed.

Phosphorylation of TnT and TnC is less well characterised, and there is currently no evidence that either is a substrate of PKA. Phosphorylation of Tm at S283 has recently been characterised *in vivo*, where phosphomimetic substitution (S283D)

impaired diastolic function and decreased lusitropy, without affecting Ca^{2+} sensitivity, which contradicted previous *in vitro* work but was supported by *ex vivo* studies (Rajan *et al.*, 2019). Interestingly, unlike TnI phosphorylation, the level of Tm phosphorylation in the mouse heart is high during development but low in the adult (~30%) and levels are increased in cardiomyopathies (Heeley *et al.*, 1982; Schulz *et al.*, 2013). Although the phosphorylating enzyme(s) of Tm have not yet been characterised, it is not surprising then that increasing phosphorylation as a therapeutic strategy has been difficult as it may have contrasting effects on myofilament function depending on the target.

In terms of the thick filament, phosphorylation of the myosin RLC has been well characterised, with early studies showing a positive correlation between phosphorylation and isometric force in skeletal muscle, with similar results then obtained in cardiac tissue (Toepfer *et al.*, 2013). RLC has not been identified as a substrate of PKA and instead is phosphorylated by myosin light chain kinase (MLCK) where the negative charge brought by the phosphate addition repels the myosin heads from RLC toward the thin filament and alters interfilament spacing and therefore promotes cross-bridge activity (Colson *et al.*, 2010). The giant sarcomeric protein Titin is thought to have the most potential phosphorylation sites of the cardiac proteins, but so far few have been characterised. PKA phosphorylation of titin occurs in an area unique to the cardiac isoform and decreases passive tension of cardiomyocytes, with phosphorylation levels reduced in human HF (Krüger & Linke, 2006; Krysiak *et al.*, 2018). One protein for which phosphorylation plays an essential regulatory role, loss of which is implicated in cardiovascular disease, is the sarcomeric accessory protein MyBP-C.

1.2 Cardiac myosin binding protein-C

In 1971, Starr and Offer identified several protein contaminants in a skeletal myosin preparation. These were analysed via gel electrophoresis and annotated in relation to the size of myosin heavy chain (~200kDa, band A) from B to J (Starr & Offer, 1971). Soon after, evidence emerged that the ~140kDa protein found at band C, therefore named “C-protein”, was a new skeletal myofibril protein and follow up electron microscopy revealed its localisation as 7 transverse stripes in each half of the A-band of the sarcomere, in an area known as the C-zone. To date this is one of the best visualisations of the protein in the sarcomere (Craig & Offer,

1976; Offer *et al.*, 1973). C-protein molecules, now more commonly known as myosin binding protein-C (MyBP-C) are spaced precisely 43nm apart in clusters of 2-4 molecules and this localisation in each C-zone is what gives MyBP-C its characteristic "doublet" appearance in immunofluorescence (Figure 1.8; Luther *et al.*, 2011).

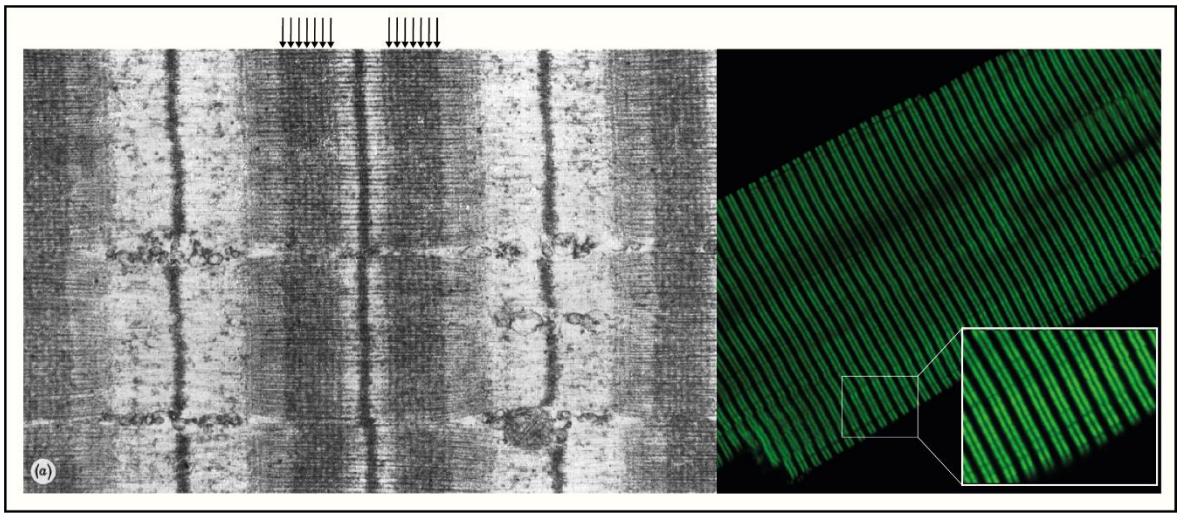

Figure 1.8. Electron and confocal microscopy of MyBP-C.
Early work by Craig and Offer used glycerated rabbit skeletal muscle and an antibody against myosin binding protein-C (MyBP-C) to show its arrangement in the sarcomere with electron microscopy. MyBP-C localised to the A band of the sarcomere and appears in the skeletal muscle as 7 transverse stripes covering what is now known as the C-zone. This localisation means that when visualised with confocal microscopy, MyBP-C (in this example, cardiac MyBP-C stained in adult rabbit cardiomyocytes) shows a distinct "doublet" appearance with each green stripe representing one MyBP-C covered C-zone. Adapted from Craig & Offer, 1976; Winegrad, 1999.

1.2.1 Molecular characterisation

Although much of the early work was conducted in skeletal tissue, MyBP-C was later identified in the myocardium (Yamamoto & Moos, 1983). Following the advances in biochemical sequencing, it was revealed that MyBP-C exists as three paralogues on three different genes; two are found predominantly in the skeletal muscle, known as slow skeletal MyBP-C (ssMyBP-C), encoded by the *MYBPC1* gene, and fast skeletal MyBP-C (fsMyBP-C), encoded by the *MYBPC2* gene. The third isoform, cardiac MyBP-C (cMyBP-C) is encoded by the *MYBPC3* gene and is exclusively expressed in the cardiac tissue during human development (Fougerousse *et al.*, 1998; Weber *et al.*, 1993). The three main isoforms share a similar sequence homology and overall modular structure, with all being comprised of three fibronectin type-III like domains and seven immunoglobulin-like C2-type domains, overall classifying it as a member of the immunoglobulin superfamily of proteins. Additionally, there is a proline/alanine rich linker found

N-terminal to the C1 domain and an "M" domain known as the MyBP-C Motif between C1 and C2. A small homolog, MyBP-H, has also been identified in both skeletal and cardiac tissue, and shares a similar C-terminal domain structure to the other isoforms (Mouton *et al.*, 2015). The cardiac isoform has several unique features including an entire N-terminal immunoglobulin domain, C0, a LAGGGRRIS motif in the M-domain and an additional 28 amino acid loop in the central C5 domain (Gautel *et al.*, 1995; Figure 1.9).

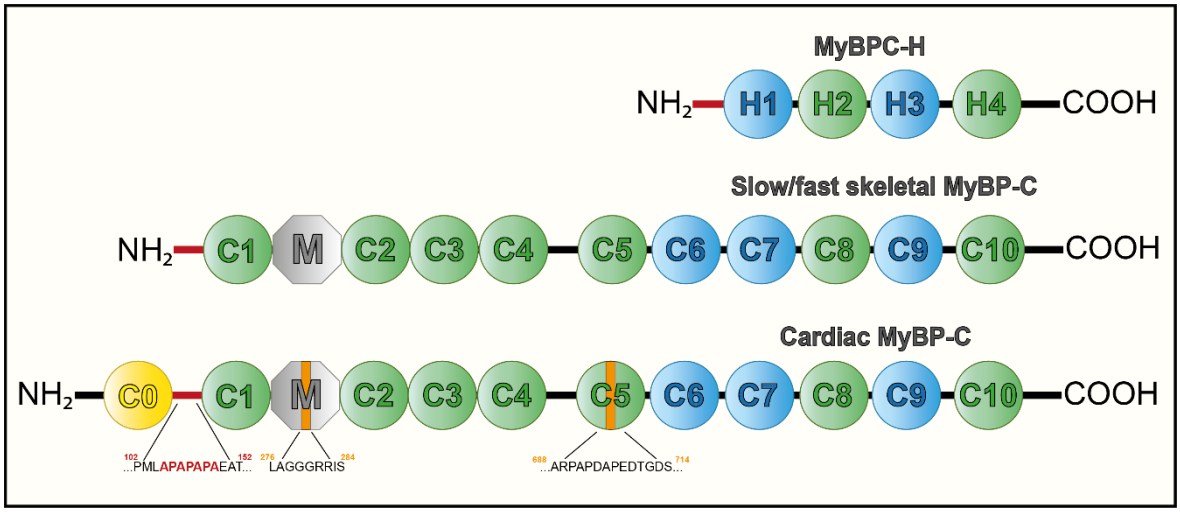

Figure 1.9. Isoforms of MyBP-C.
Myosin binding protein-C (MyBP-C) exists as three paralogues expressed by three different genes. Two are found predominantly in skeletal muscle, slow and fast MyBP-C, and have a similar sequence homology, although there are up to 14 variants of the slow skeletal. Each isoform has seven immunoglobulin-like C2 type domains (green), three fibronectin type-III domains (blue), a proline/alanine rich linker (red) N-terminal from the C1 domain and a MyBP-C Motif domain named the M-domain (grey). cMyBP-C shares a 50-55% homology with the skeletal isoform but has cardiac specific modifications including an entire immunoglobulin domain at the N-terminus (C0, yellow) and cardiac specific sequence insertions in the M domain and the central C5 domains (human sequence). A smaller homolog, MyBP-H, has been identified which shares sequence structure with the C-terminal domains of the MyBP-C isoforms (Main, Fuller, *et al.*, 2020).

As a highly modular protein, there are currently no high-resolution structures of full length cMyBP-C available, which is a major weakness for the field. However, several studies have utilised techniques such as atomic force microscopy, nuclear magnetic resonance and crystallography to elucidate the structure and function of the different domains of cMyBP-C (Finley & Cuperman, 2014). To date, the central domains (C4-C6) remain relatively understudied, but as will be discussed in Chapter 3, may provide an important area of the protein to regulate its stability, PTMs and interactions with myofilament binding partners. By far the most well characterised domains are at the N-terminal (C0-C3) and C-terminal (C7-C10) regions due to their interactions with the thick and thin filaments where cMyBP-C

is an important structural component but most evidently, a regulator of contractility.

1.2.2 cMyBP-C as a structural component of the sarcomere

When it was first discovered, due to its abundance and its precise arrangement in the sarcomere, representing 2% of myofilament mass, MyBP-C was initially thought to play a purely structural role, and several sarcomeric binding partners have been identified. As the name suggests, the first of these was the LMM component of the myosin backbone which is required for its localisation in the sarcomere (Moos *et al.*, 1975; Okagaki *et al.*, 1993; Freiburg and Gautel, 1996; Gilbert *et al.*, 1996). Studies of the binding affinity suggest that whilst there is one predominant myosin binding site in the C10 domain, the final four domains (C7-C10) are required for maximum binding affinity (Flashman *et al.*, 2007). cMyBP-C also interacts with the giant sarcomeric protein Titin, which traverses the sarcomere in super-repeats of IgG and Fn-like domains, 11 of which are found in the C-zone. Transgenic mice lacking two of these repeats show a loss of cMyBP-C localisation to the C-zone and again implicate the C10 domain in binding (Tonino *et al.*, 2019; Zoghbi *et al.*, 2008). Skeletal MyBP-C binds to and is required for FHL1 (four and a half lim protein 1) incorporation into the thick filament, although the relationship in cardiac tissue has not been reported (McGrath *et al.*, 2006). Most recently a strong binding relationship has been reported between cMyBP-C and Fhod3. This protein contributes to actin polymerisation and sarcomere assembly and in the absence of cMyBP-C is mislocalised and dysfunctional (Matsuyama *et al.*, 2018; Taniguchi *et al.*, 2009).

These studies indicate that cMyBP-C plays an essential role in the sarcomere as an anchor for other proteins, particularly with regard to the thick filament. However, in the 1990s two mutations were identified in the *MYBPC3* gene which resulted in familial hypertrophic cardiomyopathy (HCM), a heritable genetic condition which results in hypercontractility and is the leading cause of sudden death in young adults (discussed in detail in 1.2.5.1; Baron *et al.*, 2020). Interestingly, the two mutations identified were in the region reported to be involved in LMM binding (Bonne *et al.*, 1995; Watkins *et al.*, 1995). Whilst the loss of cMyBP-C-LMM binding may account for the sarcomere disarray associated with HCM, emerging studies at the time showed that extraction of the skeletal form of MyBP-C leads to increased

force and velocity, and extraction of the cardiac form altered Ca^{2+} sensitivity analogous to what is observed in HCM (Hofmann, Criss Hartzell, *et al.*, 1991; Hofmann, Greaser, *et al.*, 1991). Importantly, this was observed without changes to sarcomere ultrastructure and began to develop the idea that MyBP-C may play an important functional role in the myofilament. The most compelling evidence in this regard came from the first cMyBP-C knock-out (KO) mouse. These mice were viable but developed a HCM phenotype at 3 months of age, including cardiac hypercontractility with accelerated crossbridge formation and depressed systolic and diastolic function. Observation of the ultrastructure of the sarcomere showed only subtle alterations to thick filament size and definition of M-lines, suggesting that cMyBP-C is modestly important for the development of the sarcomere but not essential for its stability (Harris *et al.*, 2002; Monteiro da Rocha *et al.*, 2016). As such the interest in cMyBP-C as a regulator of cardiac contractility rather than a structural sarcomere component gained traction.

1.2.3 cMyBP-C – a binding partner of myosin and actin

Although still currently debated, the most widely accepted model of cMyBP-C-myosin binding is the trimetric collar model. This depicts the C-terminal domains bound to the backbone of myosin, with potential interaction with other neighbouring cMyBP-C molecules, and the N-terminal domains extended outward (Figure 1.10; Flashman *et al.*, 2008; Moolman-Smook *et al.*, 2002).

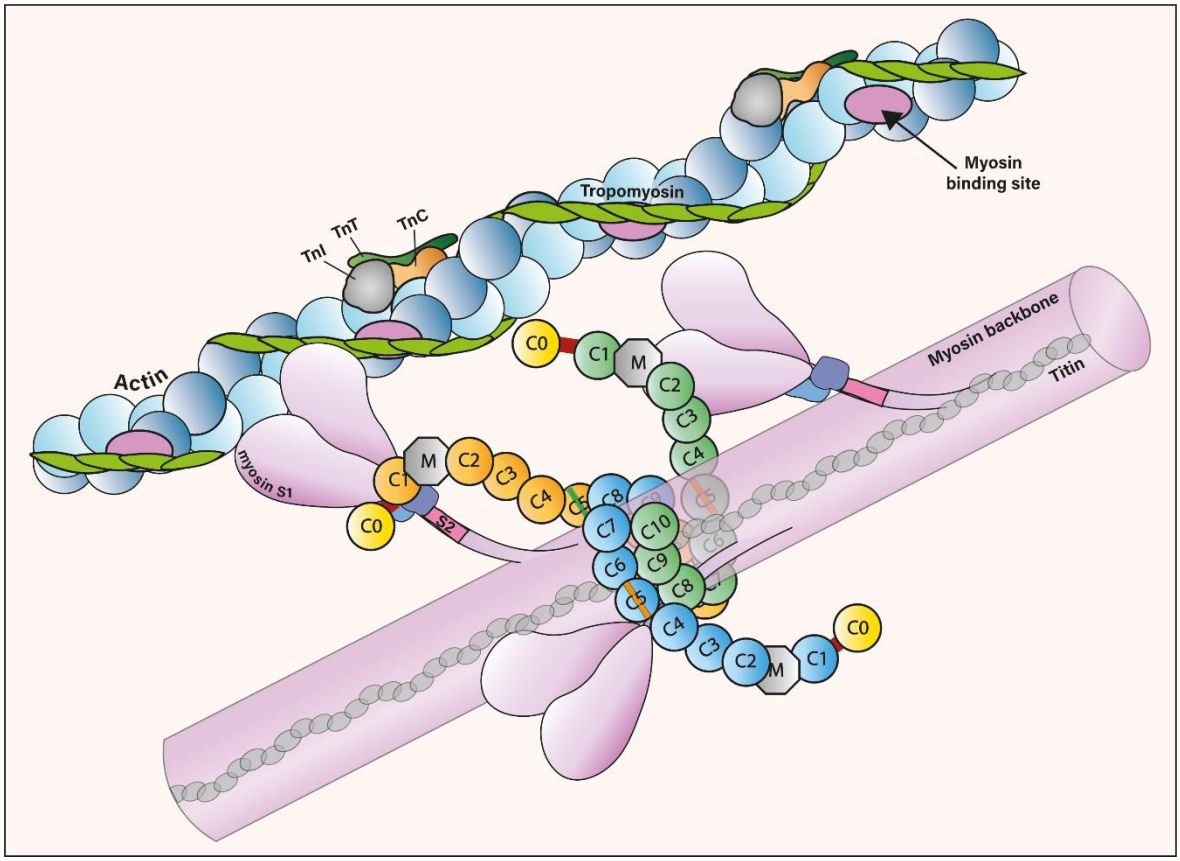

Figure 1.10. Trimetric collar model of cMyBP-C in the myofilament.
The most widely accepted model of cMyBP-C localisation in the myofilament is the trimetric collar model whereby cMyBP-C C-terminal domains (C8-C10) are bound to the myosin backbone and the N-terminal domains C0-C7 are free to extent into the interfilament space. The positioning means cMyBP-C molecules may also interact with each other. Adapted from Oakley *et al.*, 2004.

This model suggests the N-terminal domains are free to interact with proteins in the interfilament space and as such binding of these domains to both myosin and actin has since been described. The first evidence of cMyBP-C binding to myosin in a region outside the LMM came from the observations that HCM-causing mutations in the myosin S2 reduced binding between the S2 and the M-domain of cMyBP-C (Gruen & Gautel, 1999). Whilst the M-domain is particularly important due to the phosphorylation that occurs there (discussed in more detail in 1.2.4.2), the C1 and C2 domains are also required for the interaction, with the C2 containing a HCM-causing mutation (Glu301) and a disulphide bridge between C436 and C443 (human sequence) that may facilitate its binding (Ababou, Gautel and Pfuhl, 2007). Similarly the C1 domain binds to myosin in a region between the S1 and S2, where the RLC and ELC are located (Ababou *et al.*, 2008). Interestingly, the cardiac specific C0 domain has also been implicated in RLC binding, again with evidence that it is disrupted in HCM (Ratti *et al.*, 2011). Most recently, cMyBP-C has been found to interact directly with the force generating myosin heads (S1), potentially via transient binding with myosin arginines. As will be discussed, this

may have important implications for how cMyBP-C regulates myosin in the SRX and DRX states (Nag *et al.*, 2017; Touma *et al.*, 2022).

Whilst the ability of the cMyBP-C N-terminal domains to bind actin was initially seen as controversial, there is a wealth of research available today that supports the interaction. cMyBP-C-actin binding has been observed in intact muscle using electron and super resolution microscopy and many *in vitro* and *in vivo* studies implicate the C0-C2 domains specifically in the interaction (Kensler *et al.*, 2011; Luther *et al.*, 2011; Mun *et al.*, 2011; Rahmanseresht *et al.*, 2021). Although actin binding was first observed in skeletal muscle, interestingly the cardiac specific C0 domain was the first actin binding site to be identified in cMyBP-C (Kulikovskaya *et al.*, 2003; Moos *et al.*, 1978). Since then, more detailed studies have suggested the C1 domain contains the predominant actin binding site, however the C0 domain is required to stabilise this interaction and that this binding occurs sequentially, with C0 binding followed by C1 (Lu *et al.*, 2011). Interestingly, the C1 domain binds in a region closely localised to the low Ca^{2+} binding site of Tm and cMyBP-C has now been shown to directly bind Tm via a positively charged loop, with important consequences for thin filament activation (discussed in 1.2.4.3; Harris *et al.*, 2016; Risi *et al.*, 2018). Additionally, the M-domain has not only been observed to bind myosin, but also actin in a distinct binding site, loss of which prevents proper cMyBP-C localisation (Bhuiyan *et al.*, 2012; Shaffer *et al.*, 2009). Most recently the C2 domain has been shown to bind actin, but does not activate the thin filament in comparison to the C0/C1 and M domain interactions, and therefore its role is currently unknown (Risi *et al.*, 2021). Binding also reportedly exists between the C-terminal domains and actin, however this has not been confirmed by any additional studies and is only considered to occur when cMyBP-C C-terminal domains are not bound to LMM (Rybakova *et al.*, 2011).

The question then arises as to what it is about these binding interactions that allows cMyBP-C to regulate thick and thin filament activity. The fundamental message is that cMyBP-C influences cardiac contractility through altering thin filament activity and Ca^{2+} sensitivity by binding actin/Tm, and alters force generation and rate of force development through interactions with myosin. In general, cMyBP-C is viewed as a negative regulator of contractility, hence why its extraction, loss in KO models and loss in HCM are associated with accelerated

contractility (Harris *et al.*, 2002; Korte *et al.*, 2003). Additionally, this negative regulation facilitates appropriate diastole, so loss is also associated with increased Ca^{2+} sensitivity and impaired relaxation (Pohlmann *et al.*, 2007). However, to complicate matters, these roles are significantly influenced by the PTM state of cMyBP-C, of which several have been identified (discussed in Chapter 3), none more so than phosphorylation, and an understanding of how cMyBP-C functions cannot be gained without considering it.

1.2.4 cMyBP-C phosphorylation

1.2.4.1 cMyBP-C phosphorylation sites and kinases

The first evidence of cMyBP-C phosphorylation came in 1982 when Hartzell and Titus studied the effects of sympathetic and parasympathetic agonists in frog myocardium. Upon identifying a cardiac specific, ~165kDa protein which incorporated radiolabelled phosphorus (^{32}P) upon isoprenaline treatment, they concluded that the C-protein identified 10 years prior undergoes phosphorylation (Hartzell & Titus, 1982). The first phosphorylation site identified was the serine found in the cardiac-specific LAGGGRRIS motif of the M-domain (S282 in rodents, S284 in humans) with two other M-domain serines (S273 and S302, mouse sequence) later identified. Each of these sites is modified by PKA and are highly conserved across species (Gautel *et al.*, 1995; Mohamed *et al.*, 1998).

A breakthrough in our understanding of the importance of these sites came from a series of transgenic mice, where those that were phospho-null for the three M-domain sites (serine (S) to alanine (A)) displaying depressed cardiac function and altered sarcomere structure. Additionally, expression of this form of cMyBP-C could not rescue the HCM phenotype of the cMyBP-C KO mouse, whilst wildtype (WT) and phospho-mimetic (serine (S) to aspartic acid (D)) versions could (Sadayappan *et al.*, 2005). Importantly, phospho-mimetic mice showed enhanced recovery from I/R injury, providing the first indication that phosphorylation was cardioprotective (discussed in 1.2.5.2; Decker *et al.*, 2005; Sadayappan *et al.*, 2006; El-Armouche *et al.*, 2007). However, the M-domain phosphorylation sites are not all equal, with S282 phosphorylation being required for subsequent phosphorylation of the other sites *in vitro* and *in vivo* (Copeland *et al.*, 2010; Sadayappan *et al.*, 2011). Additionally, a series of transgenic animal expressing a

combination of phospho-null, phospho-mimetic and WT versions of the residues revealed that a phospho-mimetic S282D promotes cardioprotection (no development of hypertrophic phenotype) regardless of the presence of the other two sites (Figure 1.11; Gupta *et al.*, 2013).

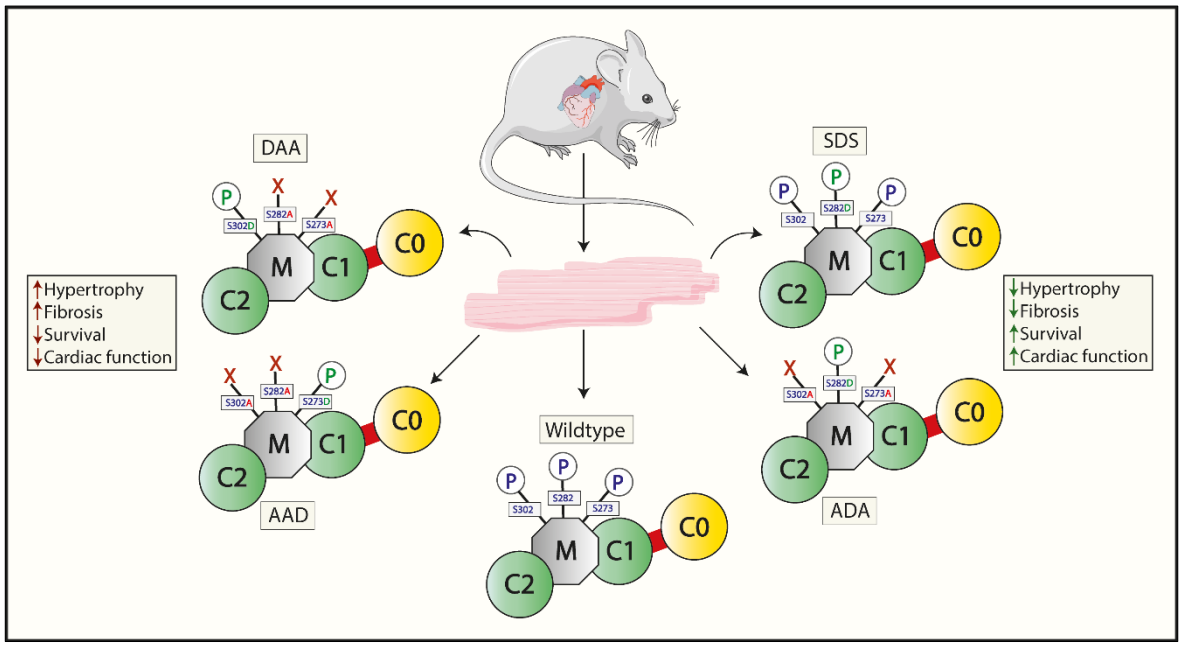

Figure 1.11. The importance of S282 in cMyBP-C phosphorylation mediated cardioprotection.
Three PKA phosphorylated serines were identified in the M-domain of cMyBP-C. A series of transgenic models expressing WT (serine, S), phospho-null (alanine, A) and phospho-mimetic (aspartic acid, D) demonstrated the importance of the sites. Loss of S282 in particular was always associated with cardiac pathophysiology (increased fibrosis, hypertrophy and reduced function and survival) whilst maintaining phosphorylation at this site, either through WT or phospho-mimetic replacement, lead to improved contractile parameters. Figure taken from Main, Fuller, *et al.*, 2020 with information from Gupta and Robbins, 2014.

However, it is worth noting that the phospho-mimetic mutants have been reported to not fully recapitulate the *in vivo* phosphorylation by PKA that occurs at this site, and a transgenic of ASA was not reported in the study for comparison with ADA (Gupta *et al.*, 2013; Kampourakis *et al.*, 2018). Additionally, *in vivo*, whilst both S282 (WT) and D282 (phospho-mimetic) rescue a HCM phenotype, S282 was more effective in restoring the force-Ca^{2+} relationship (Dutsch *et al.*, 2019). However, the importance of S282 as a phosphorylation site is strengthened by the observation that whilst total cMyBP-C phosphorylation is generally reduced in HF, this site is the most impacted (discussed in 1.2.5.2; Copeland *et al.*, 2010).

The non-equivalency of phosphorylation sites may be because of the vast array of kinases involved, identification of which has also uncovered additional phosphorylation sites in the N-terminus, including up to 17 sites *in vivo* (Kooij *et*

al., 2013). Although it has yet to be as well characterised, analysis of cMyBP-C phosphorylation in cardiac tissue from animals and humans indicates there must be one other predominant site aside from the S273, S282 and S302 sites, which could be a S311 site identified in humans (Jia *et al.*, 2010; Copeland *et al.*, 2010). Aside from PKA, PKC can also phosphorylate S273 and S302, PKD can phosphorylate S302 and CAMKII can phosphorylate all four M-domain sites in the mouse (Bardswell *et al.*, 2010, 2012; Dirkx *et al.*, 2012; Lu *et al.*, 2012). More novel kinases have been identified including ribosomal S6 kinase (RSK), which can phosphorylate S282, and glycogen synthase kinase 3β (GSK3β), which can phosphorylate 302 and potentially a novel phosphorylation site (S133) in the P/A linker (Figure 1.12; Cuello *et al.*, 2011; Kuster *et al.*, 2013).

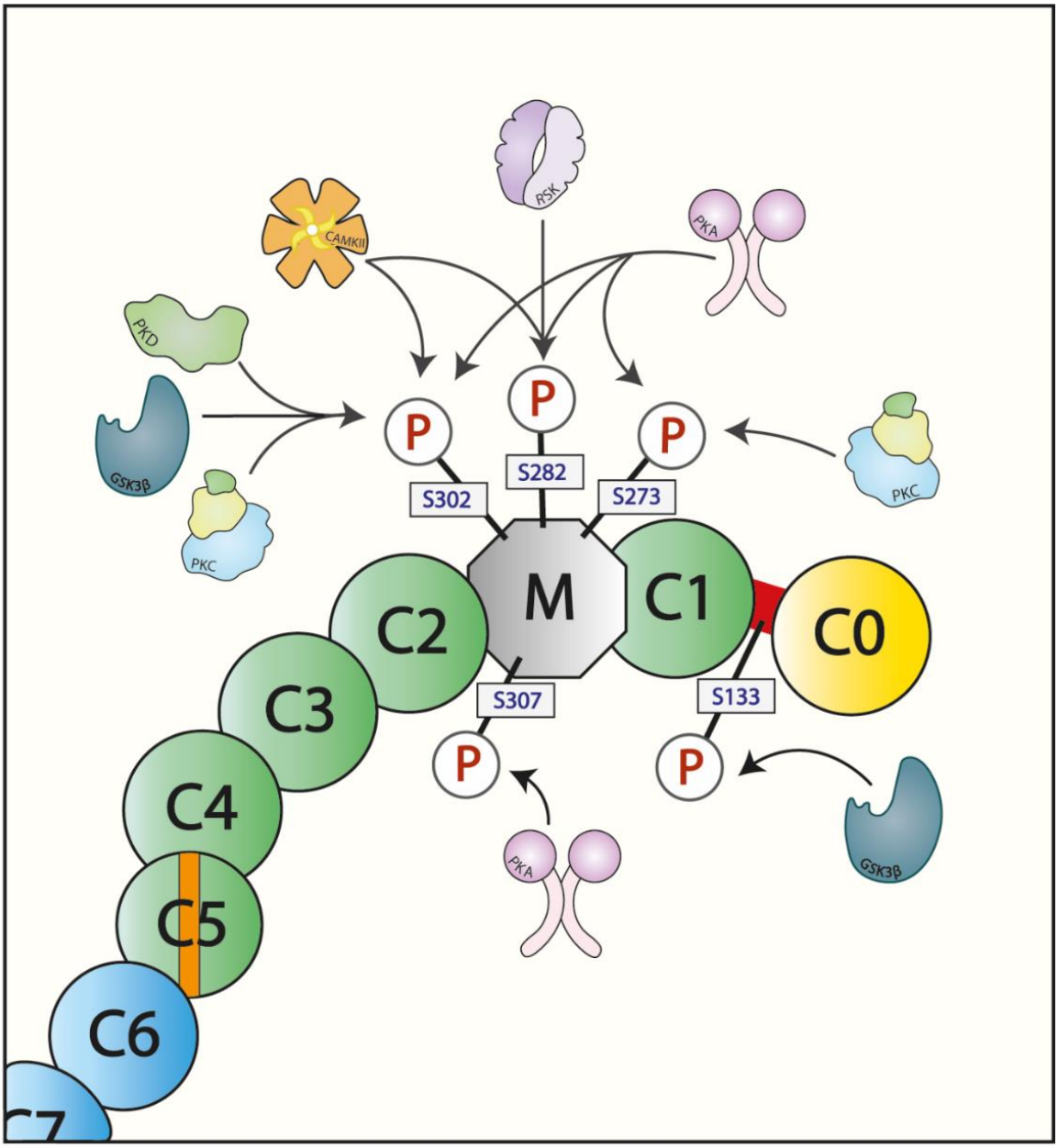

Figure 1.12. Kinases reported to target the cMyBP-C N-terminal domains.
The four predominant phosphorylation sites of the cMyBP-C M-domain (mouse sequence), and a novel reported site in the P/A linker between C0 and C1 can be targeted by a host of different kinases. PKA, the main effector of the β-adrenergic signalling pathway, targets S273, S282 and S302 whilst PKC targets S273 and S302 and PKD targets only S302. Additional kinases have been reported including RSK, which phosphorylates S282 and GSK3β which phosphorylates S302 and S133 in the P/A linker. Adapted from Main, Fuller and Baillie, 2020.

A major weakness in the field is that most of the kinase studies are carried out *in vitro*, so whether these kinases are responsible for *in vivo* phosphorylation remains largely unknown. Nevertheless, the focus in phosphorylation has largely been on PKA-mediated effects and clearly demonstrates, *in vitro* and *in vivo*, that phosphorylation significantly influences cMyBP-C's regulation of both the thick and thin filament and overall myocardial contractility.

1.2.4.2 cMyBP-C phosphorylation and control of contractile function

The cMyBP-C phospho-null mice demonstrate that phosphorylation is fundamental for cardiac physiology. A closer study of the myofilaments mechanics reveals phospho-null mice have reduced cross-bridge formation, and whilst PKA treatment accelerates cross-bridge formation, it is ineffective when cMyBP-C is absent or phospho-ablated (Colson *et al.*, 2010; Tong *et al.*, 2008). Similarly *in vivo*, cMyBP-C KO mice do not respond to ß-adrenergic stimulation and show systolic and diastolic dysfunction (Brickson *et al.*, 2007).

cMyBP-C phosphorylation is fundamental in appropriate LDA as part of the Frank Starling mechanism (discussed in 1.1.3.1). In skinned ventricular myocardium, both cMyBP-C KO and PKA-treated WT myocardium show an accelerated rate of force development and enhanced the LDA. Importantly, PKA had no effect on stretch activation or force development in cMyBP-C KO myofilaments even though TnI was still phosphorylated, and a later study estimated that cMyBP-C phosphorylation contributed ~67% to LDA compared to ~33% from TnI phosphorylation (Kumar *et al.*, 2015; Stelzer *et al.*, 2006). This was supported by a study that utilised the phospho-null (3SA) and phospho-mimetic (3SD) mice and showed that whilst physiological LDA relies on increasing sarcomere length sensitizing the myofilament to Ca^{2+}, this is blunted in phospho-null mice. Additionally, magnitude and rate of force development in response to stretch is also reduced in phospho-null animals (Mamidi *et al.*, 2016). Translation of these observations to whole hearts demonstrated the Frank-Starling relationship of ventricular function was steepest in phospho-mimetic mice, consistent with the myofilament observations (Hanft *et al.*, 2021). It is now understood that cMyBP-C's influence on maximum force and force development is largely through its regulation of the thick filament.

1.2.4.3 cMyBP-C phosphorylation and control of myosin activity

Myosin heads are arranged in axial repeats of 3 heads every 43nm (Craig & Offer, 1976). Given the precise localisation of cMyBP-C in the C-zone, MyBP-C may only influence every third myosin head and as such, only a small number of cross-bridges. Despite this, cMyBP-C appears to have profound effects on myofilament contractility through regulation of the thick filament, mediated by

phosphorylation of its extensible N-terminal domains. Soon after cMyBP-C was identified as a binding partner of the myosin S2, the same group showed that this interaction was abolished upon MyBP-C M-domain phosphorylation (Gruen *et al.*, 1999). Several studies have observed that this phosphorylation-induced loss of cMyBP-C-myosin interaction is associated with increased force production, rate of force development and dissociation of MgADP from myosin facilitating relaxation (Coulton & Stelzer, 2012; Previs *et al.*, 2012; Tanner *et al.*, 2021). This indicates that cMyBP-C is a negative regulator of myosin activity until phosphorylation abolishes it. This is supported by X-ray diffraction studies showing phosphorylation of cMyBP-C shifts myosin heads toward the thin filament (Colson *et al.*, 2012).

For a long time, the negative regulatory effect of cMyBP-C on myosin was thought to involve cMyBP-C acting as a drag or a tether, preventing binding of the myosin heads to actin. However, several studies had observed the phosphorylation-mediated effects on the thick filament in the absence of tethering (Harris *et al.*, 2004; Kunst *et al.*, 2000). Today, the current understanding is that cMyBP-C regulates the number of force generating heads available (i.e. the SRX:DRX ratio, discussed in 1.1.3.1). cMyBP-C KO mice and samples from HCM patients with *MYBPC3* mutations have a reduction in the proportion of myosin heads in the SRX state, and an increase in ATP turnover, suggesting more active myosin heads which is likely contributing to the hypercontractile phenotype (McNamara *et al.*, 2016, 2017). Indeed, the most recent work by McNamara *et al.* utilising the phospho-null (S3A) mice demonstrated they had an increased stabilisation of the SRX, and this was correlated with a reduction in myofilament force production. In contrast, phospho-mimetic (S3D) mice had a destabilised SRX and a corresponding increase in the rate of tension redevelopment and force, with a reduction in the binding of cMyBP-C to myosin. PKA treatment reduced the number of myosin heads in the SRX, but only in myofilaments where cMyBP-C could be phosphorylated, again implicating S282 in particular as the critical phosphorylation site in this interaction (McNamara *et al.*, 2019). This work is supported by evidence that cMyBP-C binds directly to the S1 of myosin, and phosphorylation reduces this binding resulting in a decrease in the SRX state (Sarkar *et al.*, 2020; Spudich, 2015).

Structural studies utilising atomic force spectroscopy and motility assays revealed that the C0-C3 domains of cMyBP-C are freely extensible and phosphorylation of

the M-domain reduces the length of the C0-C3 fragment, allowing it to adopt a more stable structure (Michalek *et al.*, 2013). Whilst this may contribute to its loss of binding to myosin, interestingly a follow up study revealed this adaptation of the stable state is abolished by increasing Ca^{2+}, restoring the cMyBP-C inhibitory effect even in the presence of phosphorylation (Previs *et al.*, 2016). The relationship between cMyBP-C, phosphorylation and Ca^{2+} has come to light in particular through studies of its regulation of the thin filament.

1.2.4.4 cMyBP-C phosphorylation and control of thin filament activity

Initial investigations into phosphorylation-mediated effects on the thick filament attributed the Ca^{2+} sensitivity changes to this interaction. However, today the current understanding is that cMyBP-C's N-terminal domains interact with actin, reducing its rotational flexibility and sliding speed, in part through acting as a drag on actin (Walcott *et al.*, 2015). Phosphorylation of the M-domain regulates this interaction, compacting the terminals and reducing binding of the N-terminal domains to actin, accelerating sliding (Previs *et al.*, 2016). Additionally, phosphorylated cMyBP-C is bound to Tm, maintaining its position in the open/high Ca^{2+} state, reducing its interaction with actin, and therefore increasing myofilament Ca^{2+} sensitivity and prolonging relaxation (Bunch *et al.*, 2019; Mun *et al.*, 2014; C. Risi *et al.*, 2018).

However, phosphorylated cMyBP-C's regulation of the thin filament is highly dependent on cytosolic Ca^{2+} levels, with the phosphorylation mediated effects abolished at the peak of the Ca^{2+} transient. This allows cMyBP-C to perform both inhibitory and activating roles during the Ca^{2+} transient to facilitate appropriate systole and diastole (Previs *et al.*, 2016). For example, the C1 interaction with Tm only occurs at low Ca^{2+} levels at the beginning of contraction, where cMyBP-C shifts it from its blocked state toward its open/high Ca^{2+} state, promoting increased myofilament Ca^{2+} sensitivity and enhanced systole. However, at high Ca^{2+}, cMyBP-C binding to Tm is reduced, increasing its block on actin and reducing Ca^{2+} sensitivity, promoting appropriate relaxation (Harris *et al.*, 2016). In terms of actin, at low Ca^{2+}, cMyBP-C-actin binding is reduced, facilitating faster thin filament sliding, whilst at high Ca^{2+} cMyBP-C slows the sliding of actin to aid relaxation (Figure 1.13; Mun *et al.*, 2014).

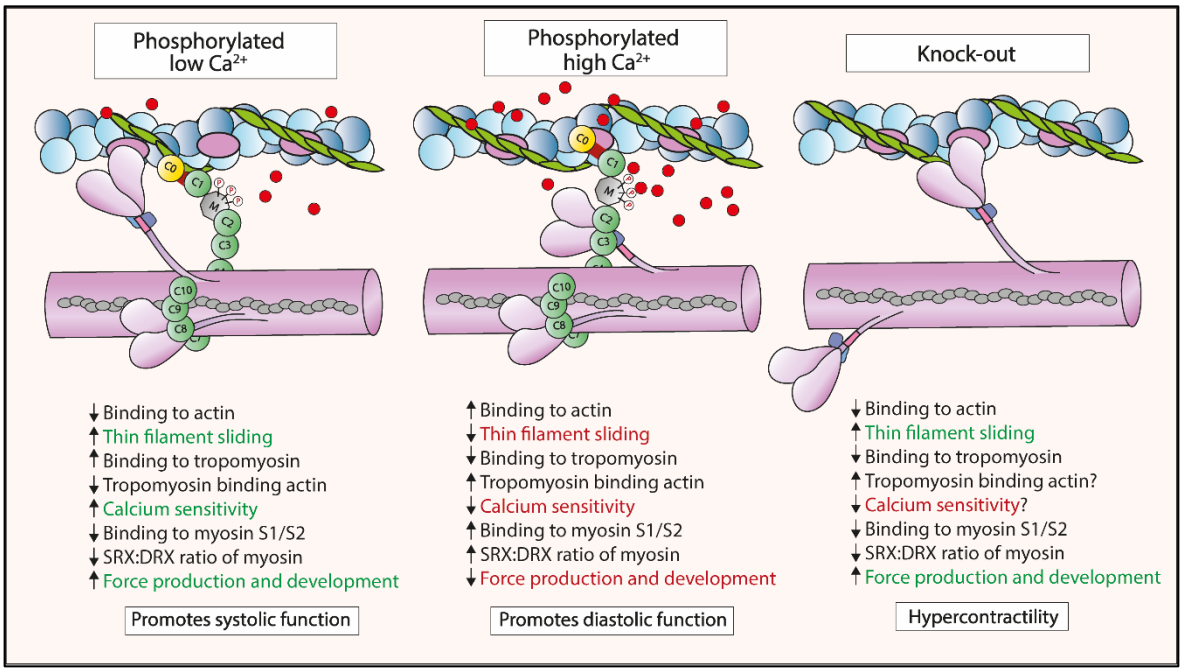

Figure 1.13. The effect of phosphorylation, calcium and knock-out of cMyBP-C on myofilament function.
When Ca^{2+} levels are low at the beginning of contraction, phosphorylated cMyBP-C promotes systolic function by reducing its binding of actin, facilitating thin filament sliding. Additionally, it increases its binding to tropomyosin, moving it into the open/high Ca^{2+} state and reducing its blocking of the myosin binding sites. This allows myosin to bind actin at lower Ca^{2+} therefore enhancing myofilament Ca^{2+} sensitivity and increasing the number of cross-bridges. This is enhanced by a reduction in the binding of cMyBP-C to the S1/S2 of myosin and a reduction in the SRX:DRX ratio, promoting increased force production and rate of force development. However, during high Ca^{2+} at the peak of contraction, Ca^{2+} is antagonistic to these effects to promote diastolic function. This is the same effect as an unphosphorylated cMyBP-C in its inhibitory form. When cMyBP-C is absent, such as in the first cMyBP-C KO mouse, hypercontractility occurs due to loss of myosin and actin binding, resulting in reduced SRX state of myosin, increased actin-myosin binding and increased actin sliding. Additionally, since cMyBP-C binding tropomyosin is lost, tropomyosin may bind actin more, resulting in myofilaments with reduced Ca^{2+} sensitivity, however this element is still unclear as many studies show increased Ca^{2+} sensitivity upon cMyBP-C knock-out. Red spots = Ca^{2+}.

Other studies have shared similar observations, adding that ablation of phosphorylation returns the inhibitory function of cMyBP-C but only at low Ca^{2+} levels (Previs *et al.*, 2016; Tanner *et al.*, 2021). Fluorescent dynamic imaging shows the C0-C3 domains diffuse along the thin filament with weak binding capacity, potentially as a mechanism for sensing its activation state. However, at higher Ca^{2+}, this diffusion is reduced and C0-C3 binds in clusters, preventing myosin binding (Inchingolo *et al.*, 2019; Ponnam & Kampourakis, 2022). The most recent super resolution imaging of cMyBP-C in intact muscle suggests the N-terminal domains are biased toward the thin filament in both relaxed and active muscle. This may indicate that the thin filament interactions may be the predominant mechanism by which cMyBP-C regulates contractility (Rahmanseresht *et al.*, 2021).

However, whilst loss of cMyBP-C inhibitory effect on myosin and actin would explain the hypercontractility phenotype observed in HCM, loss of cMyBP-C and therefore Tm regulation should result in reduced myofilament Ca^{2+} sensitivity. Although this was observed to a modest extent in the first cMyBP-C KO mouse, several groups have since reported increased Ca^{2+} sensitivity in KO samples (Cazorla *et al.*, 2006; Harris *et al.*, 2002; Hofmann, Criss Hartzell, *et al.*, 1991; Pohlmann *et al.*, 2007). Indeed, the majority of HCM studies report increased myofilament Ca^{2+} sensitivity (Jacques *et al.*, 2008; van Dijk *et al.*, 2009). This may be dependent on the type of *MYBPC3* mutation and whether cMyBP-C is truncated, as investigation of point mutation (L348P) demonstrated increased Ca^{2+} sensitivity through enhanced cMyBP-C-Tm binding (Mun *et al.*, 2016). Additionally, TnI phosphorylation is reduced in many *MYBPC3* HCM samples that may contribute to the increased Ca^{2+} sensitivity, with PKA treatment demonstrated to alleviate the Ca^{2+} sensitivity changes in these samples (van Dijk *et al.*, 2009).

Additionally, it is important to note that isolated myofilaments from KO animals that show increased Ca^{2+} sensitivity paradoxically display accelerated relaxation, despite intact cells and *in vivo* results demonstrating slow relaxation (Harris *et al.*, 2002; Pohlmann *et al.*, 2007). The most recent evidence utilising the phospho-null transgenic mice (3SA) suggests this is due to changes in upstream Ca^{2+} kinetics leading to prolonged Ca^{2+} transients, mediated through reduced function and extrusion of Ca^{2+} by NCX1 and reduction in the phosphorylation of Ca^{2+} cycling proteins (Kumar *et al.*, 2020). As such, there are confounding changes in cMyBP-C KO studies that make understanding its role difficult, whilst studies in skinned myofilaments lack the contribution of excess Ca^{2+} that is causing the impaired relaxation in intact cells and *in vivo*. This is a particularly important consideration when evaluating myofilament targeting treatments for cardiovascular diseases.

1.2.5 cMyBP-C and cardiac disease

1.2.5.1 Hypertrophic cardiomyopathy

HCM is heritable, genetic condition that affects 1:500 people worldwide and is a leading cause of sudden death in young adults (Baron *et al.*, 2020; Maron *et al.*, 1995). The disease is characterised by cardiac hypertrophy and associated LV systolic and diastolic dysfunction, resulting in exercise intolerance, angina and

dyspnoea. HCM is a complex disease that currently lacks any effective treatments to correct the cardiac dysfunction (Suay-Corredera *et al.*, 2022). *MYBPC3* was the fourth gene identified to contribute to the disease, following myosin heavy chain (*MYH7*), TnT (*TNNT2*) and Tm (*TPM1*). However, *MYBPC3* is now the most commonly mutated of the at least 10 genes involved, with over 350 individual mutations representing ~40-50% of cases (Carrier *et al.*, 2015). Of these, 70-90% are predicted to produce a truncated form of cMyBP-C with a loss of C-terminal domains, although it has been difficult to detect and characterise these forms of the protein from patient samples (Glazier *et al.*, 2019; Rottbauer *et al.*, 1997). However, *MYBPC3* HCM patients in general, regardless of missense or truncating mutations, show an overall loss of total cMyBP-C which suggests haploinsufficiency is the cause of the observed phenotype (Marston *et al.*, 2009; van Dijk *et al.*, 2009). This may be due to rapid degradation of the mutant form of the protein, such as that observed through the ubiquitin-proteasome system (UPS), nonsense mediated decay of the mutant mRNA, or loss due to the inability of the mutant form to incorporate fully into the sarcomere (Yang *et al.*, 1999; Sarikas *et al.*, 2005; Vignier *et al.*, 2009).

As such, gene therapy is actively being investigated as a therapeutic strategy for HCM (Carrier, 2021). Transfer of the *MYBPC3* gene into newborn KO mouse rescued the HCM phenotype and improved cardiac function, although the therapeutic effect was lost after 2 months suggesting optimisations are required (Gedicke-Hornung *et al.*, 2013). Nevertheless, the relevance of the approach was clearly demonstrated in a transgenic mouse with a tetracycline-inducible cMyBP-C KO, which has normal cardiac function until the cMyBP-C KO is induced, with the reversal of the dysfunction observed when the inducible KO is removed again (Giles *et al.*, 2019). The importance of the N-terminal domains was further highlighted by a study showing replacing the C0-C2 domains was effective in rescuing the HCM phenotype (Li *et al.*, 2020). A previous study supports this finding, however found returning the N-domains only corrected maximal active force, whilst increased Ca^{2+} sensitivity at low Ca^{2+} was still observed compared to WT (Witt *et al.*, 2001). This may explain why *MYBPC3* truncating mutations that lack the LMM-binding C-terminal domains result in HCM, and therefore the therapeutic relevance of just returning the N-terminal domains is questionable. Nevertheless, returning full length cMyBP-C in animal models has proven

efficacious, and gene replacement was also demonstrated in induced pluripotent stem cell derived cardiomyocytes (iPSC-CMs) produced from a HCM patient. This may provide a valuable tool for personalised medicine and validating whether this approach is suitable for all HCM *MYBPC3* mutation types, considering the heterogeneity that exists in the disease (Gedicke-Hornung *et al.*, 2013).

A recent breakthrough was made in the approval of the myosin inhibitor mavacamten for the treatment of symptomatic obstructive HCM (Olivotto *et al.*, 2020). As HCM is associated with hypercontractility and hypertrophy, reducing the activity of myosin alleviates this. Mavacamten was shown to slow the release of ADP from the S1 and is likely mediating an increase in the number of myosin heads in the SRX state (Green *et al.*, 2016; Kawas *et al.*, 2017). As cMyBP-C plays such a crucial regulatory role in myosin activity, including in regulating the SRX and DRX states, it is hoped small molecules targeting this interaction will provide therapeutic benefit in HCM in the next few years. In contrast, ischaemic HF is associated with loss of contractility, with myosin activators actively been considered here, as well as approaches that would enhance the positive regulatory role of cMyBP-C phosphorylation.

1.2.5.2 Ischaemic heart failure

Ischaemic heart disease (IHD), also known as coronary artery disease (CAD), is characterised by the development of atherosclerotic plaques in the coronary vasculature, preventing appropriate blood flow and nutrient delivery to cardiac tissue (Bhandari *et al.*, 2021). As a result, the tissue becomes ischaemic and can develop clinically to ischaemic cardiomyopathy (ICM), defined by the presence of left ventricular (LV) systolic dysfunction (Briceno *et al.*, 2016). In general, CAD is initially stable as revascularisation occurs to maintain appropriate oxygen and nutrient delivery. However, prolonged ischaemia, or an acute ischaemic event such as a myocardial infarction (MI), leads to irreversible cardiac damage and pathophysiological remodelling. Importantly, IHD and associated ICM are the leading cause of mortality and morbidity in the industrialised world, with the latest epidemiological research estimating there are 126 million people suffering from IHD, with 9 million deaths globally as a result, and the prevalence is estimated to rise to over 140 million by 2030 (Khan *et al.*, 2020; Virani *et al.*, 2020). Aside from the impact of mortality, there are significant socioeconomic

pressure that accompanies an aging population living with IHD, with data from the World Heart Federation estimating a global spend of $863 billion in 2010, due to rise to over $1 trillion in 2030 (Khan *et al.*, 2020). This increasing prevalence is in part due to greater survival following acute ischaemic events such as an MI, where thrombolytic and coronary intervention have been advanced and refined in recent years (Briceno *et al.*, 2016). However, as a result of the damage, the majority of IHD and ICM cases involve progression to HF, which itself has a global burden of 26 million with 3.6 million patients diagnosed every year, and is the ultimate cause of the mortality (Ambrosy *et al.*, 2014; Simmonds *et al.*, 2020).

Although HF can be broadly classified as the inability of the heart to meet the systemic demand of the body, via systolic or diastolic left ventricular (LV) dysfunction, it is widely recognised as a complex clinical syndrome with a spectrum of clinical presentations. The current classification strategy is based on symptoms and measured LV ejection fraction (LVEF), with an LVEF of >50% classified as HF with preserved ejection fraction (HFpEF), LVEF of <40% classified as HF with reduced ejection fraction (HFrEF), and LVEF of ~40-50% classified as HF with mid-range LVEF (HFmrEF; Bozkurt *et al.*, 2021). All clinical therapies currently aim to reduce myocardial demand by either reducing peripheral resistance and pre-load (e.g. through angiotensin-converting enzyme inhibitors (ACEi)) or ventricular after-load and remodelling (e.g. through ß-blockers; Shah *et al.*, 2017). This largely helps to compensate for a reduction in ejection fraction and systolic dysfunction and therefore has been effective in HFrEF rather than HFpEF, which currently lacks any selective therapies (Bozkurt *et al.*, 2021). Even though improved therapeutic recommendations for HFrEF significantly reduce morbidity and mortality rates in clinical trials, prognosis is still poor in this group with a trial of 40,000 hospitalised HF patients demonstrating a 5-year mortality rate of 75%, independent of LVEF (McMurray *et al.*, 2014; Shah *et al.*, 2017). As such, there remains a largely unmet clinical need for therapies in all HF categories.

In the early stages of HF, neurohormonal remodelling occurs in response to an increased after-load, cardiac injury or mutation of key cardiac proteins which drives cardiac hypertrophy, as observed in HCM. This is initially compensatory as it allows the heart to maintain systolic force by increasing the left ventricular

thickness. However, it is accompanied by a series of deleterious molecular and biochemical changes that develop over time to cause cardiomyocyte apoptosis, LV dilatation and cardiac dysfunction (Figure 1.14; Tham *et al.*, 2015).

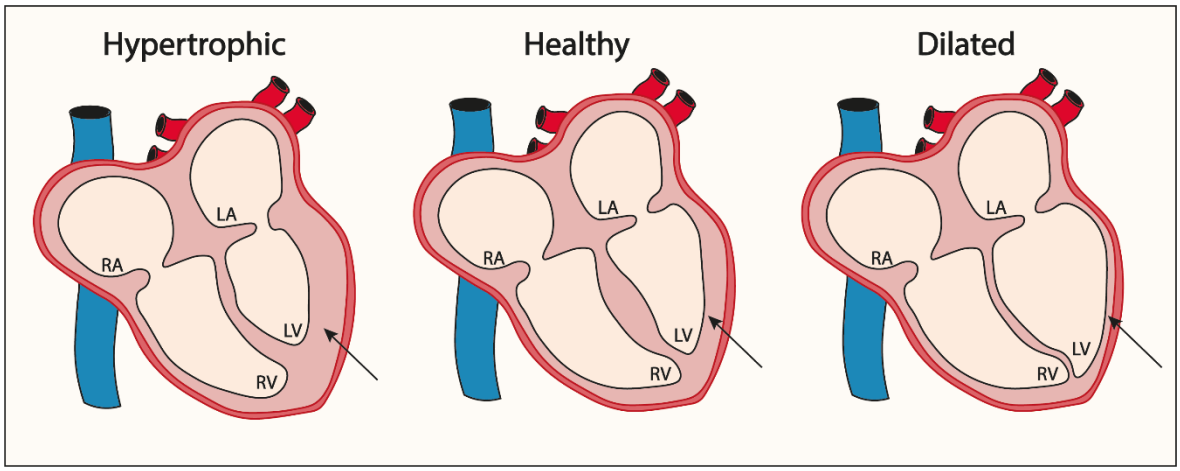

Figure 1.14. Ventricular wall thickness during hypertrophic and dilated heart disease.
An increase in left ventricular wall thickness is associated with cardiac hypertrophy, as seen in hypertrophic cardiomyopathy (HCM) in order to compensate for an increase in after-load to maintain systolic force. In decompensated ischaemic heart failure, loss of cardiomyocyte size and number results in a reduced LV wall thickness and dilated cardiomyopathy.

It is unsurprising therefore, that all the mechanisms mentioned so far, including LDA, FFR and regulation of cardiac proteins via phosphorylation are pathologically altered in chronic HF (Tham *et al.*, 2015). There are an array of mechanisms that contribute to this, including altered metabolism, fibrosis, inflammation, oxidative stress and changes in the expression and modification of Ca^{2+} handling proteins (discussed in more detail in Chapter 5; Konstam *et al.*, 2011). However, given its important regulatory role in myofilament function, loss of cMyBP-C phosphorylation has been frequently observed in cardiac disease states, including HF, post-cardiac stunning, in aortic stenosis and atrial fibrillation (Anand *et al.*, 2018; El-Armouche *et al.*, 2006, 2007; Jacques *et al.*, 2008; Yuan *et al.*, 2006). Preservation of phosphorylation is cardioprotective in animal models subjected to I/R injury and has even been shown to mitigate age-related cardiac dysfunction (Rosas *et al.*, 2019; Sadayappan *et al.*, 2006) Interestingly, S282 shows significantly reduced phosphorylation compared to the other M-domain sites in ischaemic HF, further supporting its role as the key cMyBP-C phosphorylation site (Copeland *et al.*, 2010; Kooij *et al.*, 2013).

Whilst myosin activators may prove effective in ischaemic HF to increase contractile performance without increased oxygen demands, there are also alterations to Ca^{2+} cycling that may not be modified by this approach (Kumar *et*

al., 2020; Malik *et al.*, 2011). As such, improving cMyBP-C phosphorylation or intervening in its interaction with the thick and thin filament may provide a valuable way to modulate cardiac output in HF, targeting both force and Ca^{2+} sensitivity issues. As a proof of concept, peptides designed against the M-domain, thought to disrupt the interaction between cMyBP-C and myosin, improve contractility in disease models, however are limited by poor permeability and the effect on Ca^{2+} sensitivity has not been measured (Hou *et al.*, 2022). Interestingly, cMyBP-C contains a site for calpain-mediated cleavage within the M-domain, and this has been observed very soon after cardiac injury, producing a fragment (C0-C1f) which is actively been investigated as a suitable biomarker for MI diagnosis (Govindan, McElligott, *et al.*, 2012; Kaier *et al.*, 2017). The cleaved product causes its own pathological effects and has been associated with HF progression, likely in part through inducing an inflammatory response, and ablation of the cleavage sites is cardioprotective (Barefield *et al.*, 2019; Razzaque *et al.*, 2013; Yogeswaran *et al.*, 2021). Structural studies also suggest phosphorylation causes compactness of the M-domain which may reduce access to the cleavage site (Colson *et al.*, 2016). Indeed, in the ischaemic heart post-MI, cMyBP-C dephosphorylation was correlated with increased cleavage and release of the fragment (Govindan, McElligott, *et al.*, 2012; Govindan, Sarkey, *et al.*, 2012).

Taken together, preservation of cMyBP-C phosphorylation may protect against cardiac dysfunction and improve contractile performance, benefitting patients with HF. Paradoxically, the inhibition of PKA has been investigated for HF therapy, showing promise in reduced infarct size and improving inotropy and lusitropy. However, in contrast, PKA activation has shown benefit particularly in the setting of I/R injury (Fontes-Sousa *et al.*, 2009; Kwak *et al.*, 2008; Makaula *et al.*, 2005; Sichelschmidt *et al.*, 2003). This is likely due to the wide range of substrates targeted by each kinase, leading to both positive and negative effects on cardiac physiology and therefore limiting the therapeutic use of inhibitors or activators. For cMyBP-C, this may be confounded due to the non-equivalency of the sites and the range of kinases involved in its phosphorylation, many of which have not been characterised *in vivo*. As such, there has been a concerted effort over the last decade to identify novel PTMs of cMyBP-C and determine whether they influence function or phosphorylation in a way that can be therapeutically modulated (discussed in detail in Chapter 3). One such modification that influences several

cardiac substrates with a relevance to HF is the cysteine modification of palmitoylation.

1.3 Palmitoylation

Lipid modifications, in particular the addition of fatty acids as a PTM, are one of the most common types of PTM with an estimated 25-40% of proteins modified by lipids in some way (Levental, Grzybek, *et al.*, 2010). Although first noted in the brain in the 1950s, the incorporation of lipids into proteins was not thought to play any important functional role until a seminal study 40 years later showed lipid incorporation influenced protein trafficking through the secretory pathway (Bankaitis *et al.*, 1990; Folch & Lees, 1951). Although the lipids involved can include cholesterol, phospholipids and isoprenoids, in mammalian cells, addition of fatty acids to proteins in a process known as acylation has shown important clinical relevance in a number of disease areas. These modifications have been named and classified by the reactive group being modified (i.e. S- for the thiol of a cysteine, N- for the amide group of a lysine, glycine or a protein N-terminal) and the hydrocarbon (C) length of the fatty acid (i.e. myristoyl (C14:0), farnesyl (C15:3), palmitoyl (C16:0), geranylgeranyl (C20:4); Figure 1.15).

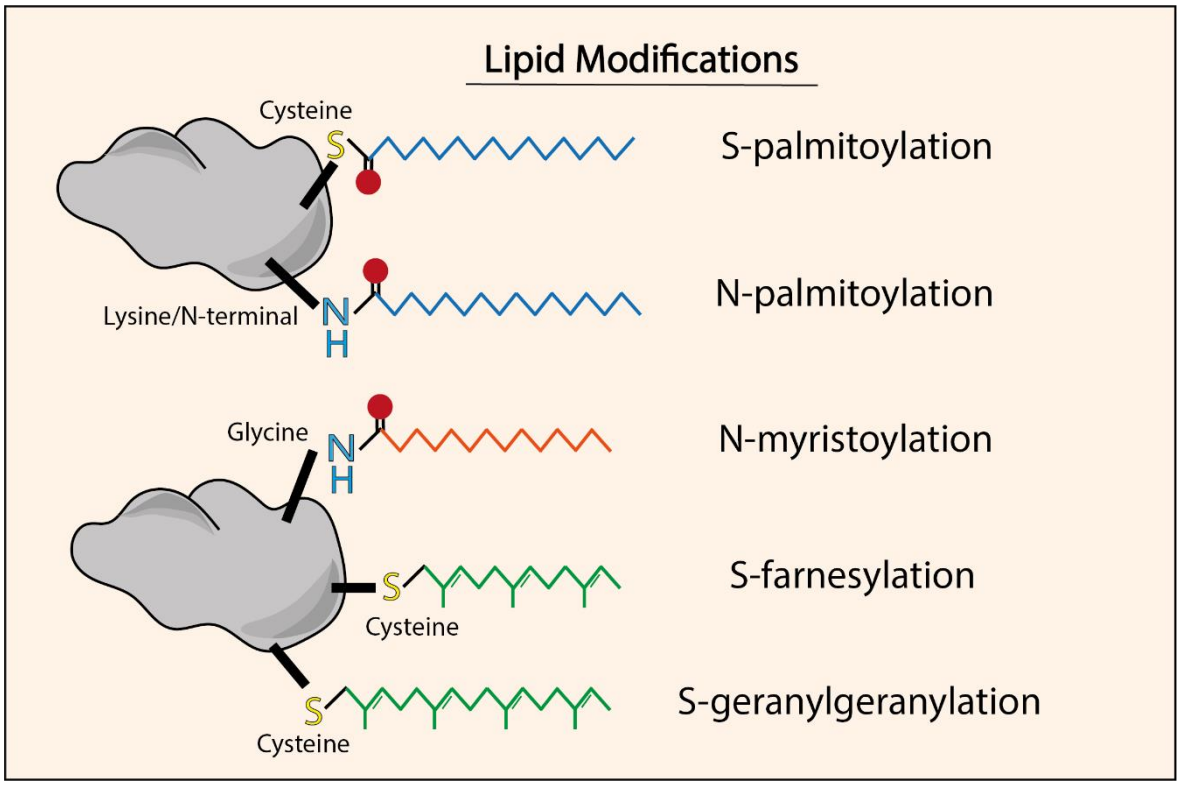

Figure 1.15. Fatty acylation.
Fatty acylation involves the addition of a fatty acid (usually eight to twenty carbons in length) to an amino acid residue or the N/C-terminal groups of a protein. These include S-palmitoylation (C16:0), S-farnesylation (C15:3) and S-geranylgeranylation (C20:4) which all attach to the thiol of a cysteine residue, with the first being reversible and the latter two irreversible. Other irreversible additions include those targeting amide groups of a lysine, glycine or protein N-terminal including N-palmitoylation (C16:0) and N-myristylation (C14:0). The 0 in this scenario denotes that the hydrocarbon does not have any double bonds. Taken from Main and Fuller, 2021.

One of the most well characterised types of acylation is the reversible cysteine modification of palmitoylation, as the 16C palmitate (also known as palmitoyl/palmitic acid, most commonly derived from palmitoyl-Coenzyme A (CoA)) is the most common fatty acid attached to proteins and is estimated to target 10% of the proteome (Blanc *et al.*, 2015; Chamberlain and Shipston, 2015). Although first reported in 1980, study of palmitoylation was initially hampered for several years due to a lack of safe and effective tools to study it (discussed in more detail in 1.3.3; Schlesinger, Magee and Schmidt, 1980). Nevertheless, as the list of substrates regulated by palmitoylation continues to grow, including several crucial cardiac substrates, it is clear it is an essential regulatory modification warranting of investigation.

1.3.1 Palmitoylation enzymology

1.3.1.1 DHHC-palmitoyl acyltransferases

Aside from a lack of available tools, interest in palmitoylation was also slow as one of the first investigated proteins, the G-protein Giα1, was shown to be auto-palmitoylated, a phenomenon involving direct interaction of a protein with palmitoyl-CoA. Although this observation occurred at non-physiological concentrations of palmitoyl-CoA (>100 μM relative to 1-10 μM in in the cell), this study introduced the idea that palmitoylation may be controlled by local fatty acid concentration and therefore modulation would be challenging (Chan *et al.*, 2016; Duncan & Gilman, 1996). This idea was cemented by the fact that attempts to identify palmitoylating enzymes had been so far unsuccessful with more proteins identified as being auto-palmitoylated in the meantime (Dietrich & Ungermann, 2004). However, in 2002 a seminal study in *Saccharomyces cerevisiae* (yeast) used genetic screening to identify a zinc (Zn^{2+})-finger containing enzyme capable of palmitoylating Ras2, already named ERF2 (effector of Ras function) as it had previously been shown to influence Ras2 subcellular localisation (Lobo *et al.*, 2002). This enzyme, along with several others identified in yeast soon after, is a multidomain membrane spanning protein with a conserved ~55 amino acid region containing an aspartate-histidine-histidine-cysteine (DHHC) motif in the enzyme active site. Mutagenic studies revealed this motif was crucial to enzymatic function, initially becoming autopalmitoylated on the cysteine before transferring the palmitoyl to a substrate (Rana, Lee, *et al.*, 2018). As such these enzymes have now been reclassified as DHHC-palmitoyl acyltransferases (DHHC-PATs or zDHHC-PATs for Zn^{2+} binding), with 23 isoforms now identified in humans. A study in HEK293 cells expressing GFP-tagged versions of each enzyme demonstrated that they are located throughout the secretory pathway in the Golgi apparatus, endoplasmic reticulum (ER) and plasma membrane, with some present in more than one compartment (Figure 1.16; Ohno *et al.*, 2006; Aicart-Ramos, Valero and Rodriguez-Crespo, 2011).

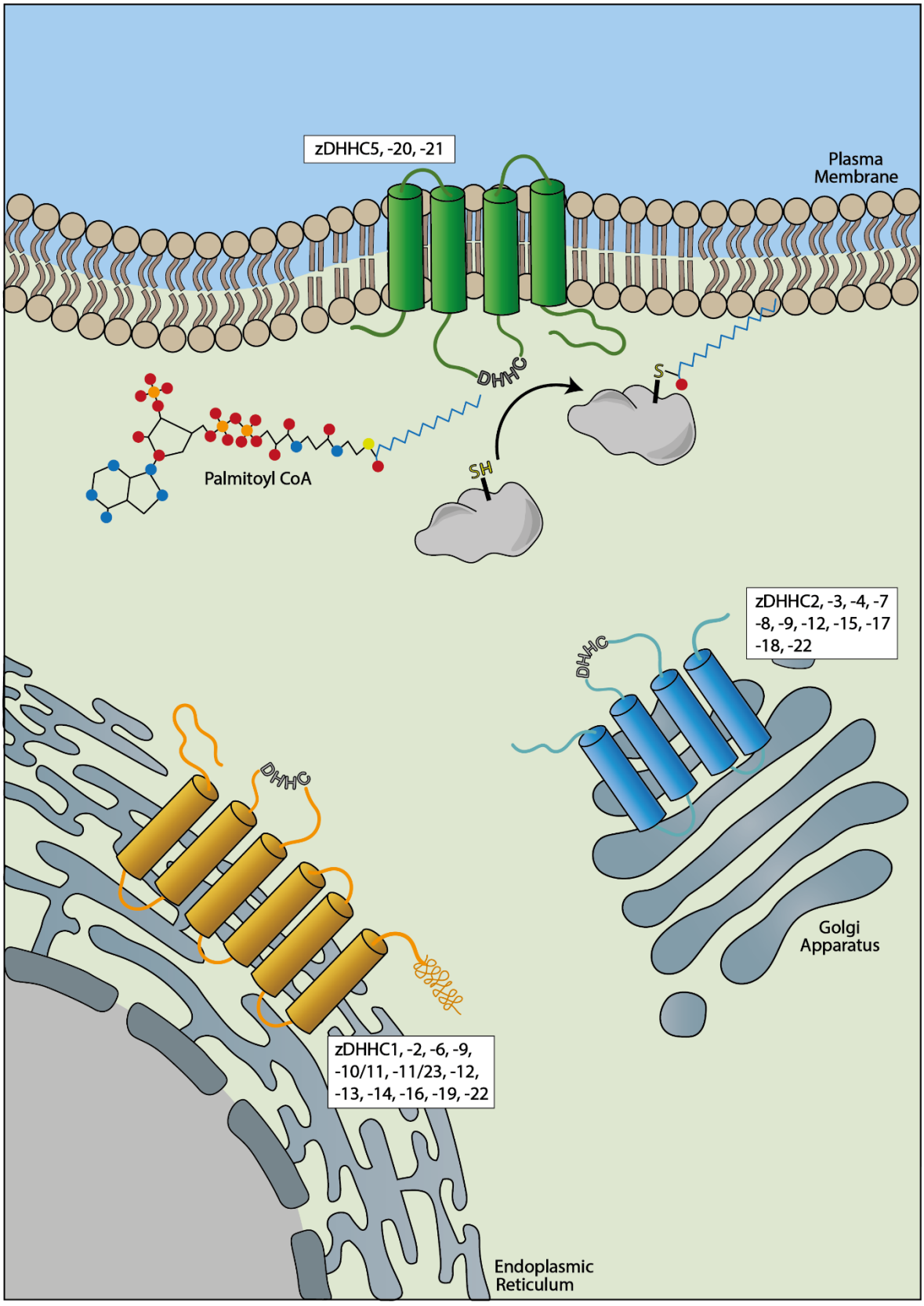

Figure 1.16. Subcellular localisation of DHHC-PATs.
Palmitoylation is the addition of a palmitoyl (C16:0) derived from palmitoyl coenzyme A (CoA) to the sulfhydryl group of a cysteine. The enzymes that catalyse palmitoylation, zinc finger containing DHHC-palmitoyl acyltransferases (zDHHC-PATs), are located throughout the secretory pathway in the Golgi apparatus, endoplasmic reticulum (ER) and cell membrane. Some are exclusively localised in one region i.e. DHHC5 at the cell membrane, or in more than one region i.e. DHHC2 in the Golgi apparatus and the ER. Taken from Main and Fuller, 2021.

1.3.1.2 Acylthioesterases

Palmitoylation is the only reversible form of acylation, and this can occur through slow hydrolysis of the thioester that connects the palmitoyl to the cysteine residue, or through enzyme driven mechanisms involving soluble acyl thioesterases. The first of these enzymes identified are the lysosomal palmitoyl-protein thioesterases (PPTs), with PPT1 first observed as mediating H-Ras depalmitoylation in brain homogenates. Although two isoforms have been discovered, PPT1 is the only one that hydrolyses cysteine thioesters and as such is the most well characterised, particularly in neuronal function where loss of function is associated with a neurological disorder characterised by toxic accumulation of lipidated proteins (Koster & Yoshii, 2019; Soyombo & Hofmann, 1997). However, although initially identified in cytosolic fractions, further study has shown PPTs operate in an acidic environment inside the lysosome to remove fatty acids from proteins prior to their breakdown (Lin & Conibear, 2015). As such they are not thought to be part of the regulation of proteins by palmitoylation as a dynamic PTM and have therefore remained largely unstudied.

The second class, Acyl protein thioesterases (APTs), are the most well characterised thioesterases, with the first (APT1) initially identified through its ability to mediate Gαs depalmitoylation (Duncan & Gilman, 1998). Located predominantly in the cytosol in both yeast and mammalian cells, this soluble protein is a member of the α/ß serine hydrolase family and a catalytic triad in its active site is essential for its enzymatic activity (Davda & Martin, 2014). Soon after its discovery, bioinformatic analysis revealed a homolog sharing 68% sequence similarity, APT2, and both enzymes have since been shown to mediate depalmitoylation by shuttling from the Golgi apparatus to the cytosol to exert their effects, mediated by their own palmitoylation (Vartak *et al.*, 2014). Unlike DHHCs, substrate recruitment and selectivity by APTs has been lesser studied and together they appear to depalmitoylate a wide variety of substrates whilst showing some substrate selectivity (Tian *et al.*, 2012; Tomatis *et al.*, 2010). Additionally, there are some proteins not depalmitoylated by either of them, developing the idea that more thioesterases might exist. Indeed, the neuronal synaptic protein PSD-95 and N-Ras are two proteins not regulated by APTs, and a study of their depalmitoylation identified the most recently classified thioesterases, a family of α/ß hydrolase domain (ABHD) containing enzymes.

These enzymes have long been noted for their role in lipid metabolism, and similarly to APTs contain an α/ß hydrolase fold with a nucleophilic residue mediating their depalmitoylase activity (Lord *et al.*, 2013). In this study, three cytosolic localised ABHD17 enzymes (A, B and C, ~70% sequence homology) were identified as controlling N-Ras depalmitoylation and localisation (David Tse Shen Lin and Conibear, 2015). Additionally, this class may not just operate in the cytosol, as discovery of ABHD10 showed depalmitoylase activity in the mitochondria, particularly regulating the activity of the antioxidant protein peroxiredoxin-5, which may implicate palmitoylation as an important regulator of redox homeostasis (Cao *et al.*, 2019; Martin *et al.*, 2012). Aside from depalmitoylase activity, ABHD proteins also possess an acyltransferase consensus motif, with one study showing ABHD5-mediated transfer of long-chain acyl-CoA derivatives including palmitoyl-CoA to an acceptor lipid, although whether this occurs on protein substrates remains to be determined (Montero-Moran *et al.*, 2010). Nevertheless, with at least 19 proteins in the ABHD superfamily, this is an emerging area of research that will aid in our understanding of how palmitoylation is regulated (Lord *et al.*, 2013). Research into palmitoylating and depalmitoylating enzymes in cardiac tissue has been hampered by lack of experimental tools and attempts to purify them (discussed in 1.3.3). Despite this, palmitoylation is emerging as a central regulatory modification for several important cardiac substrates.

1.3.2 Cellular effects of palmitoylation

1.3.2.1 Palmitoylation regulating protein-membrane localisation

The fundamental consequence of protein palmitoylation is a change in hydrophobicity due to the addition of the fatty acid. Whilst there is a growing appreciation for its role in regulating protein activity, protein-protein interactions and interplay with other PTMs, this has traditionally been viewed as a mechanism of protein localisation and trafficking via directing of the fatty acid and attached substrate to hydrophobic membrane compartments (Blaskovic *et al.*, 2013). Due to the distinct localisation of the DHHC-PATs throughout the secretory pathway, this can include the Golgi, ER and plasma membrane, with signalling molecules including G-proteins and GTPases dynamically palmitoylated, allowing them to quickly cycle between the compartments (Goodwin *et al.*, 2005; Henis *et al.*,

2009; Rocks *et al.*, 2005). Whilst this can occur in any area of the membrane, studies suggest the majority of palmitoylated proteins reside in cholesterol and sphingolipid-enriched microdomains known as lipid rafts. Although their existence was controversial for a long time due to lack of effective tools to study them, recent advances in microscopy and modelling techniques have provided strong evidence for their presence in the plasma membrane (Levental, Grzybek, *et al.*, 2010). These domains are important physiologically for signal transduction, as they selectively recruit receptors, scaffolding molecules and signalling proteins, and the loss of lipid rafts is associated with aberrant signalling from these proteins (George & Wu, 2012).

Although studies in living cells have been limited, lipid rafts have been reported in cardiomyocytes, with a particular focus on a subtype known as caveolae (Norman *et al.*, 2018). Whilst many proteins including transmembrane channels were thought not to incorporate due to the tight lipid packing of the raft, increasing evidence suggests palmitoylation plays a role in regulating their dynamic caveolae and lipid raft affinity (Levental, Lingwood, *et al.*, 2010; Lorent *et al.*, 2017). This includes GPCR localisation, with α1 and ß2 adrenoceptors exclusively found in caveolae and many G-proteins enriched there, and ion channels, including the Na^+/K^+ ATPase which has two caveolin binding sites and is found in caveolae in cardiomyocytes which is important for its stabilisation (Fuller *et al.*, 2013). Additionally, caveolae are associated with scaffolding proteins such as caveolin-3, which is highly expressed and palmitoylated in cardiomyocytes and KO is associated with cardiac hypertrophy, reduced contractility and loss of caveolae (Woodman *et al.*, 2002). Whilst proteomics suggests palmitoylated proteins are predominantly localised in caveolae, not all palmitoylated proteins associate with lipid rafts, including those trafficked to the ER which is low in cholesterol and therefore not likely to form lipid rafts (Blaskovic *et al.*, 2013; Gould *et al.*, 2015). However, the majority of studies do not make the distinction between specific raft localisation, making estimation of the number of proteins for which palmitoylation regulates raft affinity challenging.

Nevertheless, in cardiac tissue palmitoylation regulates the membrane localisation of several important channels and structural proteins. Of note, palmitoylation of the voltage sensing α-subunit of the voltage and Ca^{2+} activated

potassium (BK) channel controls its cell surface localisation, but only when its accessory ß1-subunit is present. When both are present, palmitoylation regulates the coupling between the subunits, disruption of which increases the voltage required to activate the channel (Duncan *et al.*, 2019). Similarly, whilst the palmitoylation status of the potassium channel Kv4.3 remains to be uncovered, palmitoylation of its accessory protein KChIP2 has been reported. Palmitoylation regulates its membrane localisation in cardiac myocytes, potentially through co-localisation with DHHC5 of which KChIP2 is a substrate, with loss of palmitoylation associated with early cardiac injury (discussed in Chapter 5; Murthy *et al.*, 2019). The scaffolding proteins Junctophilins act as tethers between the SR and plasma membrane, helping to form the cardiac dyad in ventricular cardiomyocytes. Palmitoylation of junctophillin-2 occurs at multiple cysteines and either allows targeting to the plasma membrane or to the SR, depending on the proximity of the cysteine to those compartments (Jiang *et al.*, 2019). In terms of vascular function, whilst this remains a relatively underdeveloped field, palmitoylation of endothelial nitric oxide synthase (eNOS) leads to localisation to caveolae in smooth muscle cells and is required for maintenance of vascular function (Fernández-Hernando *et al.*, 2006; Liu *et al.*, 1996; Wei *et al.*, 2011). Altogether, palmitoylation is essential for appropriate targeting of cardiac substrates to membrane compartments, however there are several membrane spanning channels for which palmitoylation is not reported to regulate their localisation, but instead has direct effects on their function, activity and protein-protein interactions.

1.3.2.2 Palmitoylation regulating protein activity and protein-protein interactions

Almost all of proteins involved in ventricular cardiomyocyte Ca^{2+} cycling (Figure 1.2) reportedly undergo palmitoylation, with a wide range of effects on substrate function. The process of ECC is initiated by the activation of the VGSC Nav1.5, the palmitoylation of which prolongs the action potential duration by influencing channel availability and inactivation. This occurs through palmitoylation on at least 4 cysteines in the II-III linker, but mutation of a single site (C981) alters channel function in a similar manner to loss of all four, suggesting a non-equivalency between palmitoylation sites (Pei *et al.*, 2016). Interestingly, this site is mutated in an inherited form of arrythmia, implicating palmitoylation in the

pathogenesis of this process. This is supported by the observation that cardiomyocytes treated with palmitic acid show an increase in early after depolarisations (Kapplinger *et al.*, 2009; Pei *et al.*, 2016). Similar results were observed for the Nav1.6 channel located in the brain, with an additional palmitoylation site unique to this isoform identified that alters channel amplitude, again supporting the idea that palmitoylation on different cysteines has diverse functions (Pan *et al.*, 2020).

Nav1.5 activation triggers an influx of Ca^{2+} via the cardiac LTCC, which contains the pore forming α1c subunit and an accessory ß2a subunit. The ß2a is required to target the α1c to the membrane and promotes channel activation by reducing voltage dependent inactivation (Buraei & Yang, 2010). Palmitoylation of the ß2a subunit has been reported, however loss of palmitoylation did not alter membrane localisation or its ability to bind or direct the α1c to the membrane, but instead were associated with a reduction in current carried by each functional channel (Chien *et al.*, 1996). Our recent work indicates the α1c subunit is also palmitoylated, loss of which was associated with reduced Ca^{2+} transient amplitudes in iPSC-CMs (Kuo, *et al. In revision*). Next in the signalling cascade, whilst palmitoylation of the cardiac RYR2 has not been reported, study of the skeletal isoform RYR1 revealed loss of palmitoylation suppresses channel activity. This study identified up to 18 palmitoylated cysteines, many of which were clustered in an important functional region of the protein, 12 of which are conserved in the cardiac isoform (Chaube *et al.*, 2014). However, this characterisation was achieved using hydroxylamine, which would depalmitoylate several substrates, and promiscuous inhibitor of DHHC-PATs 2-Bromopalmitate (2-BP) which, as will be discussed, has several off-target effects making its use unsuitable overall, therefore RYR palmitoylation requires further characterisation.

Whilst palmitoylation is important for the activity of the channels involved in the production of the Ca^{2+} transient during ECC, it also regulates proteins involved in maintaining the ionic gradient. Whilst the vast majority of Na^{+}/K^{+} ATPase are found in caveolae, relatively little has been reported about the role of palmitoylation. Palmitoylation of the isoform expressed in the brain was reported in 1987, and more recent proteomic evidence suggests all subunits are

palmitoylated (Howie *et al.*, 2018; Schmidt & Catterall, 1987). More is known about the palmitoylation of Na^+/K^+ ATPase accessory protein PLM (FXYD1 in uncardiac tissue), which modulates Na^+/K^+ ATPase localisation by promoting the interaction of the channel with caveolins, and inhibits pump activity, mediated by its own palmitoylation (Howie *et al.*, 2013; Wypijewski *et al.*, 2015). PLM palmitoylation occurs at two sites located near the transmembrane spanning region, however is most often singly palmitoylated in cardiac tissue at C40, with loss of palmitoylation enhancing PLM turnover (Tulloch *et al.*, 2011). Interestingly, whilst the ability of DHHC5 to palmitoylate the Na^+/K^+ ATPase remains unknown, localisation of the Na^+/K^+ ATPase to caveolae is required for its direct interaction with DHHC5, which in turn palmitoylates PLM allowing it to exert its inhibitory effect on the pump (Howie *et al.*, 2014; Plain *et al.*, 2020).

Regulation of the Na^+/K^+ ATPase and PLM by palmitoylation undoubtedly has knock-on effects for the closely linked NCX1, the palmitoylation of which at a single cysteine (C739) has been extensively studied in recent years. Whilst NCX1 palmitoylation occurs in the Golgi, it does not mediate its cell surface localisation but instead regulates its inactivation (Fuller *et al.*, 2016; Reilly *et al.*, 2015). The inactivation process involves the hydrolysis of phospholipid PIP2, releasing the inhibitory XIP peptide which binds to the NCX1 regulatory loop (Plain *et al.*, 2017). When palmitoylation is lost, XIP binding and therefore inactivation is impaired, likely leading to prolonged Ca^{2+} transients and levels of intracellular Ca^{2+}, although this is yet to be demonstrated (Reilly *et al.*, 2015). It will be interesting to determine whether NCX1 palmitoylation is changed at different points in the transient as part of a regulatory mechanisms, similar to Ca^{2+} regulation of cMyBP-C phosphorylation (Previs *et al.*, 2016). Palmitoylation is also thought to promote NCX1 dimerization and XIP engagement, again highlighting its importance in regulating protein-protein interactions (Gök *et al.*, 2020).

Perhaps the best example of the diverse nature of palmitoylation as a PTM is its control of the ß2-adrenoceptor, where it regulates membrane localisation, protein-protein binding, and interplay with other PTMs in cardiac tissue. Agonist-induced ß2-adrenoceptor desensitisation is an important mechanism to prevent aberrant phosphorylation and activation, however palmitoylation at C341 within the cytoplasmic C-terminal tail is required to prevent uncontrolled receptor loss

and stabilises the receptor at the membrane (Loisel *et al.*, 1996; Moffett *et al.*, 1993). This influence on desensitization may also be mediated by palmitoylation-dependent association of ß-arrestin-2 with the channel. This study also demonstrated that palmitoylation is required for the receptor to couple with the Gs protein and activate adenylyl cyclase. Additionally, loss of palmitoylation was associated with reduced binding to PDE4 which regulates the local cAMP gradient around the receptor, increasing PKA mediated phosphorylation and cardiomyocyte contraction rate as a consequence (Liu *et al.*, 2012). In fact, palmitoylation and phosphorylation of the receptor are closely coupled, as agonist stimulation increases palmitoylation and most recently, a novel palmitoylation site (C265) has been described which relies on the phosphorylation of the nearby S262 in order to become palmitoylated (Adachi *et al.*, 2016; Loisel *et al.*, 1999).

1.3.2.3 Palmitoylation regulating post-translational modifications

Aside from the dynamic control of the ß2-adrenoceptor, one of the first studies that reignited interest in palmitoylation was the observation that Gαs palmitoylation could be modulated by isoprenaline stimulation which was later shown to redistribute them from the plasma membrane to internal compartments (Martin & Lambert, 2016; Wedegaertner & Bourne, 1994). As such, the relationship between phosphorylation and palmitoylation has been slowly uncovered over the last few years. Most recently, ß-adrenergic stimulation was shown to mediate DHHC5 dependent palmitoylation, and therefore signalling, of Gα proteins in cardiomyocytes (Chen *et al.*, 2020). This study also identified that the DHHC5 C-terminal tail can be palmitoylated in response to adrenergic stimulation, which as will be discussed in Chapter 5, has important functional consequences for the enzyme's activity. Post-translational crosstalk plays an important role in palmitoylation regulation of BK channels. Palmitoylation at the N-terminus regulates membrane localisation, whereas palmitoylation at the C-terminus regulates the interaction of the channel with PKA and PKC (Shipston, 2014). Loss of palmitoylation by pharmacological or site directed mutagenesis allows PKC to phosphorylate and inhibit channel activity (Zhou *et al.*, 2012). Similarly, whilst palmitoylation allows PLM to inhibit the Na^+/K^+ ATPase this is enhanced by PLM phosphorylation, which paradoxically works to inhibit pump activity (Tulloch *et al.*, 2011). Palmitoylation has also been observed in the accessory protein of SERCA, phospholamban (PLB), loss of which results in reduced interaction with

PKA and hypo-phosphorylation and therefore reduced inactive pentamer formation and increased inhibition of SERCA (Zhou *et al.*, 2015). Overall, it is clear there is an important relationship between palmitoylation and phosphorylation. Given the dysregulation of phosphorylation in diseases such as HF, palmitoylation may be important in controlling the sensitivity of proteins to phospho-regulation.

In cardiac tissue, the relationship between palmitoylation and phosphorylation has been most well characterised, however studies in other systems suggest palmitoylation may influence other PTMs including ubiquitylation, redox modifications and other lipid modifications. Ubiquitylation involves the addition of small ubiquitin proteins to the lysine residues of substrates which targets them for degradation by the UPS. Proteins that are deficient in palmitoylation undergo increased ubiquitinylation both *in vitro* and *in vivo* and the two modifications are generally reported as antagonistic (Valdez-Taubas & Pelham, 2005; Yount *et al.*, 2012). Whilst palmitoylation appears to regulate the turnover of PLM, whether this is mediated by ubiquitylation is unknown. As will be discussed in more detail in Chapter 3, there are several examples of palmitoylation and redox modifications occurring in concert or antagonistically altering protein function. S-glutathionylation often occurs on the same cysteines that are palmitoylated but confers an overall negative charge resulting in functionally different effects (Burgoyne *et al.*, 2012; Howie, Swarbrick, *et al.*, 2013). Similarly, NO donors mediating S-nitrosylation reduce and displace palmitate from several scaffolding and signalling molecules. This includes synaptic protein PSD-95, where S-nitrosylation and reduced palmitoylation was associated with reduced clustering and formation of synapses (Ho *et al.*, 2011; Salaun *et al.*, 2010). Palmitoylation is often observed with other lipid modifications such as farnesylation, where palmitoylation of a farnesylated Ras increases its membrane affinity over 100 times (Ahearn *et al.*, 2012). Similarly, myristoylation or prenylation are thought to occur on proteins to allow weak membrane attachment and localisation to DHHC-PATs which can then palmitoylate and increase membrane affinity (Guan & Fierke, 2011).

1.3.3 Tools to study palmitoylation

1.3.3.1 Detection methods

Given the reversible, dynamic, enzymatic regulation of palmitoylation, there is great interest in developing tools to study and target palmitoylation to regulate the mechanisms discussed above. However, developments in the field have been hampered for many years due to a lack of safe and effective tools to study it. Initially radioactive assays were the gold standard measure, involving incubation of live cells with mCurie amounts of radioactive-palmitate ([^{3}H]-palmitate) followed by electrophoresis and exposure of dried gels to X-ray films for several weeks (Schlesinger *et al.*, 1980). Although fundamental in early palmitoylation discoveries, including the depalmitoylation of H-Ras and introducing the first "pulse-chase" method of measuring protein palmitoylation dynamically, this labour-intensive method has fallen out of use (Baker *et al.*, 2003). There is also potential for the ^{3}H-palmitate to form oxyester linkages with serine/threonine residues as well as cysteines (Pedone *et al.*, 2009).

Affinity purification of palmitoylated proteins is a more widely adopted technique, the two most common being the acyl-biotin exchange (ABE) and the acyl-resin assisted capture (Acyl-RAC). Both approaches can be used in any cells or tissue of interest and involve initial alkylation or methylation of free cysteines under denaturing conditions. This is followed by specific cleavage of the thioester bond between the palmitate and palmitoylated cysteine, most commonly with neutral hydroxylamine, with a negative control of sodium chloride often included. The newly freed, previously palmitoylated cysteine(s) can then be affinity purified using a biotin-streptavidin pulldown method for ABE, or thiopropyl sepharose beads for Acyl-RAC, followed by analysis for protein(s) of interest using electrophoresis (Figure 1.17; Drisdel & Green, 2004; Forrester *et al.*, 2011).

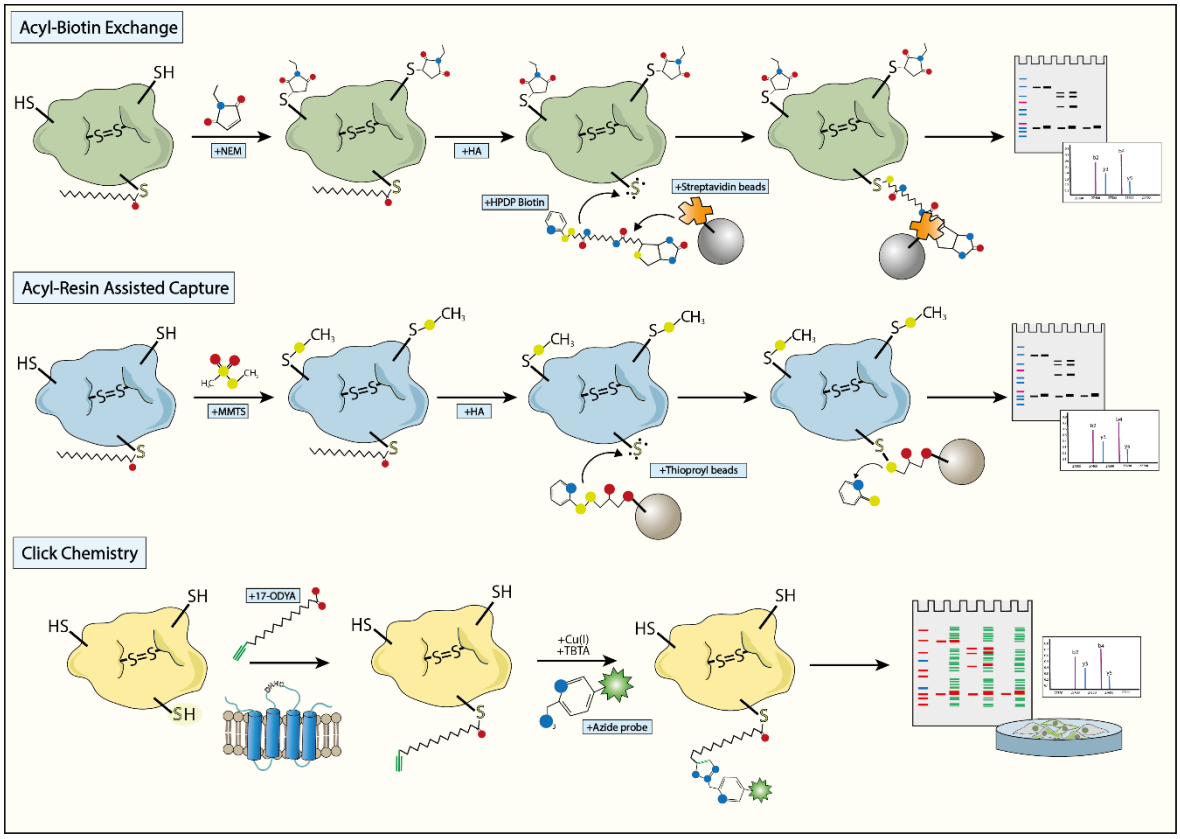

Figure 1.17. Modern methods of detecting protein palmitoylation.
In a move away from radioactive methods, protein palmitoylation is more commonly studied using affinity purification techniques or click chemistry. Acyl-biotin exchange (ABE) involves the initial alkylation of free cysteines with N-ethylmaleimide (NEM) followed by cleavage of the thioester bond between palmitate and cysteine using hydroxylamine (HA). The freed cysteine can then be affinity purified by reacting first with HPDP-biotin and then pulled down using streptavidin beads. Acyl-resin assisted capture follows a similar method, with initial methylation using methanethiosulfonate (MMTS) followed by HA cleavage and capture using thiopropyl-sepharose beads. The output of ABE and Acyl-RAC is most commonly determined by gel electrophoresis for a protein of interest, however can be followed by mass spectrometry analysis of the whole sample. Click chemistry involves incubation of cells with an azide-containing fatty acid molecule (most commonly 17-ODYA for palmitoylation), with incorporation into palmitoylated proteins relying on the enzymatic machinery of the cell. The attachment can then be detected by "clicking" in a Cu(i)-catalysed [3+2] Huisgen cycloaddition reaction to an alkyne-containing fluorescent detection system (most commonly Biotin or a fluorophore). Again, the output can then be measured by electrophoresis, mass spectrometry or specific probes can be used and analysed via fluorescence microscopy. Taken from Main & Fuller, 2021.

As the final sample will have a pool of all the palmitoylated proteins in the cell/tissue of interest, usefully mass spectrometry can be utilised to survey the palmitoylome, which was demonstrated by the global profiling of palmitoylated proteins in yeast, neurons and more recently, cardiac tissue (Kang *et al.*, 2008; Miles *et al.*, 2021; Roth *et al.*, 2006). However, using such a sensitive approach can often lead to false positives, with no indication given as to whether a meaningful fraction of the protein is modified. With affinity purification, comparison of the purified fraction to the initial starting material allows the percentage of the total protein that is modified by palmitoylation to be determined. This does however limit its usefulness in understanding

palmitoylation as a dynamic modification, as they can only provide a "snapshot" of stoichiometry at a given point. As palmitoylation regulates the function of many important cardiac substrates, it is not unreasonable to assume stoichiometry may vary on a beat-by-beat basis *in vivo* that cannot be observed via these techniques. Additionally, these techniques do not detect palmitoylation specifically, only the presence of a thioester on a cysteine, but as palmitate (C16:0) is the predominant fatty acid in the cell, the terms are often used interchangeably (Muszbek *et al.*, 1999).

Click chemistry is another widely adopted method to measure palmitoylation, involving the incubation of cells with azido-containing fatty acids, with 17-octadecyonic acid (17-ODYA) most used for palmitoylation (Martin & Cravatt, 2009). This is followed by "clicking" to a suitable alkyne-containing detection system (biotin or a fluorophore) and analysis using electrophoresis, with newer adaptations allowing fluorescent microscopy observations (Figure 1.17; Gao & Hannoush, 2018; Kostiuk *et al.*, 2008). This technique resulted in significant developments in the field, however there are several limitations including that in contrast to affinity purification electrophoresis, all palmitoylated proteins are fluorescently labelled and detected in one measurement via electrophoresis. As such, proteins with a low palmitoylation stoichiometry may require additional purification steps to be visible in comparison to highly palmitoylated proteins of similar molecular weights. Additionally, investigation of primary cells such as cardiomyocytes and plant cells by click chemistry have reportedly been limited due to lack of uptake and incorporation of the probes, which limits its applicability (reviewed in Main & Fuller, 2021). A great benefit is the ability to engineer probes to study any fatty acid length, however the consequences of the azido/alkyne linkage on fatty acid function and localisation and whether it represents physiological acylation remains to be determined, although fortunately many of these probes have been extensively characterised in this regard (Hannoush & Sun, 2010).

More recently, novel palmitoylated proteins are being identified through identifying interactions with DHHC-PATs. This includes utilising proximity-biotinylation (BioID) which is increasingly being adopted in cardiovascular research and beyond, including two recent studies where DHHC-PAT interactors were

identified for the LTCC and SARS-CoV-2 proteins (Liu *et al.*, 2020; Samavarchi-Tehrani *et al.*, 2020). This technique involves fusing the protein of interest with a biotin ligase (commonly birA, APEX or TurboID) that produces biotin free radicals (bio-adenylate), causing nearby proteins (<20nm) to become biotinylated which can be subsequently purified by streptavidin pulldown (Sears *et al.*, 2019). This can also be achieved using the DHHC-PAT as the "bait". A study of DHHC5 used this technique to identify regulatory pathways involving DHHC20 and an enzyme responsible for the PTM O-GlcNAcylation, both of which were later demonstrated to have knock-on effects for DHHC5 palmitoylation of PLM and control of Na^+/K^+ ATPase function (Plain *et al.*, 2020). This study also utilised the technique of peptide array (discussed in more detail in 3.3.1.1) to identify the specific regions of DHHC5 involved in Na^+/K^+ ATPase binding and had previously been used more broadly to identify interacting partners from cardiac lysate where the Na^+/K^+ ATPase was initially identified (Howie *et al.*, 2014; Plain *et al.*, 2020). Similarly, novel interacting partners of the ankyrin-repeat domain of DHHC17 were identified using this method (Lemonidis *et al.*, 2017).

Both techniques have their limitations, including that BioID identified binding does not necessarily indicate an enzyme-substrate functional relationship, as demonstrated in the example of PSD-95 which, whilst showing close proximity to DHHC5, is only palmitoylated by DHHC2 at the synapse (Li *et al.*, 2010; Noritake *et al.*, 2009). Additionally, this technique most often requires overexpression of an exogenously labelled version of the protein in a non-physiological setting (Roux *et al.*, 2018). For peptide array, the interaction is observed in a non-physiological environment which does not take into account the 3D structure of the proteins, or the protein-membrane interactions which would be particularly applicable to studying palmitoylation. Nevertheless, both provide a starting point which can then be validated further by the above-mentioned methods in a relevant cell or tissue.

1.3.3.2 Pharmacological approaches

Our understanding of the palmitoylating machinery is limited in that KO models of DHHC-PATs and acylthioesterases show functional redundancy. To elucidate their function, both selective and non-selective inhibitors of the enzymes are of interest for development as experimental tools. The development of specific DHHC-PAT

inhibitors has been particularly challenging due to difficulties in crystallisation and therefore a lack of high-resolution structures. By far the most well used inhibitor is 2-bromopalmitate (2-BP), which is known as a broad spectrum, irreversible DHHC-PAT inhibitor which inactivates the catalytic site via cysteine alkylation and nucleophilic displacement (Jennings *et al.*, 2009). Identified over 20 years ago, although 2-BP has aided in crystallizing the structure of DHHC20, which may yield crucial studies on how to develop selective inhibitors, it is highly promiscuous and an estimated ~99% of 2-BP's targets are not DHHC-PATs, including acylthioesterases themselves (Davda *et al.*, 2013; Pedro *et al.*, 2013; Rana, Kumar, *et al.*, 2018). This, coupled with the poor potency and toxicity due to its frequent use at concentrations above its $IC_{50,}$ makes its use in characterising palmitoylation largely unreliable (Jennings *et al.*, 2009).

With a lack of alternatives, 2-BP is understandably still widely used in the field. However, attempts have been made to develop more effective inhibitors including a new broad-spectrum DHHC inhibitor N-cyanomethyl-N-myracrylamine (CMA). This compound shares a similar inhibiting mechanism to 2-BP and was able to inhibit DHHC-PATs, including DHHC20, with limited toxicity and higher potency in comparison (IC_{50} of 1.35 μM vs 5.33 μM for 2-BP; Azizi *et al.*, 2021; Lan *et al.*, 2021). The identification of novel inhibitors has been aided by developments in different screening methods, including a scaffold-ranking library which identified an inhibitor of DHHC9 which was later shown to reduce SARS-Cov2 infectivity, and a recent fluorescence resonance energy transfer (FRET) based high throughput system which identified two novel tetrazole containing compounds that inhibited several DHHC-PATs in HEK293 cells (Hamel *et al.*, 2016; Ramadan *et al.*, 2021; Salaun *et al.*, 2022). Although these novel compounds do not specifically target individual enzymes, they warrant further development as experimental tools to characterise palmitoylation. Additionally, more potent, broad-spectrum inhibitors with less off-target effects may be useful in cancer therapy in particular, as the polypharmacy of currently used kinase inhibitors is a key factor in their efficacy (Ko & Dixon, 2018).

The key to targeting individual DHHC-PATs may lie in disrupting enzyme-substrate interactions using small cell penetrating peptides. Although sharing a high level of homology, DHHC-PATs do vary structurally particularly in their disordered C-

terminal regions which are thought to be important in substrate recruitment. This was recently achieved through targeting the interaction of DHHC5 with the Na^+/K^+ ATPase using a stearate-tagged peptide, which was shown to reduce DHHC5-mediated palmitoylation of PLM and therefore increase pump activity, identifying a potential route by which palmitoylation could be targeted in HF therapy (Plain *et al.*, 2020). Although these peptides have poor pharmacokinetic and pharmacodynamic properties, they provide a starting point through which small molecules may be designed.

On the other hand, maintenance or increasing palmitoylation of certain substrates, particularly those seen as tumour suppressors, may be of interest therapeutically, and therefore inhibitors of depalmitoylation have also been developed. Most recently a novel approach utilising cell penetrating, amphiphilic compounds was employed which reduced H-Ras palmitoylation *in vitro* and *in vivo*. The amphiphilic mediated degradation (AMD) of palmitoylated substrates was effective in redirecting several mis-localised proteins found in a model of PPT1 loss of function and toxic accumulation of fatty acid modified substrates, known as infantile neuronal ceroid lipofuscinosis (Rudd *et al.*, 2018). However, whether the general use of this compound would target additional thioesters, including those involved in active site activity of enzymes such as GAPDH or other post-translational modifications such as SUMOylation remains to be determined (Alberts *et al.*, 2002; Main & Fuller, 2021). Overall, there are several novel pharmacological tools that may provide vital insight into substrate palmitoylation in the next few years and characterising their activity in a variety of cells and tissues will be of importance. Another important cardiac PTM for which advancements in tools to study it have developed in recent years is the regulatory modification of SUMOylation.

1.4 SUMOylation

SUMOylation is a PTM which shares many similarities to ubiquitination in that it involves the covalent attachment of a small protein to a lysine residue and has been shown to regulate substrate degradation, protein-protein interactions and activity. Although traditionally associated with nuclear proteins and transcription, evidence of SUMOylation as an important regulatory PTM of extra-nuclear

substrates, including cardiac ion channels and sarcomeric proteins, has emerged over recent years (Celen & Sahin, 2020).

1.4.1 SUMOylation cascade

SUMOylation involves the ATP-dependent conjugation of a small ubiquitin-like modifier (SUMO) protein onto a lysine residue, mediated by a series of catalytic steps as detailed in Figure 1.18.

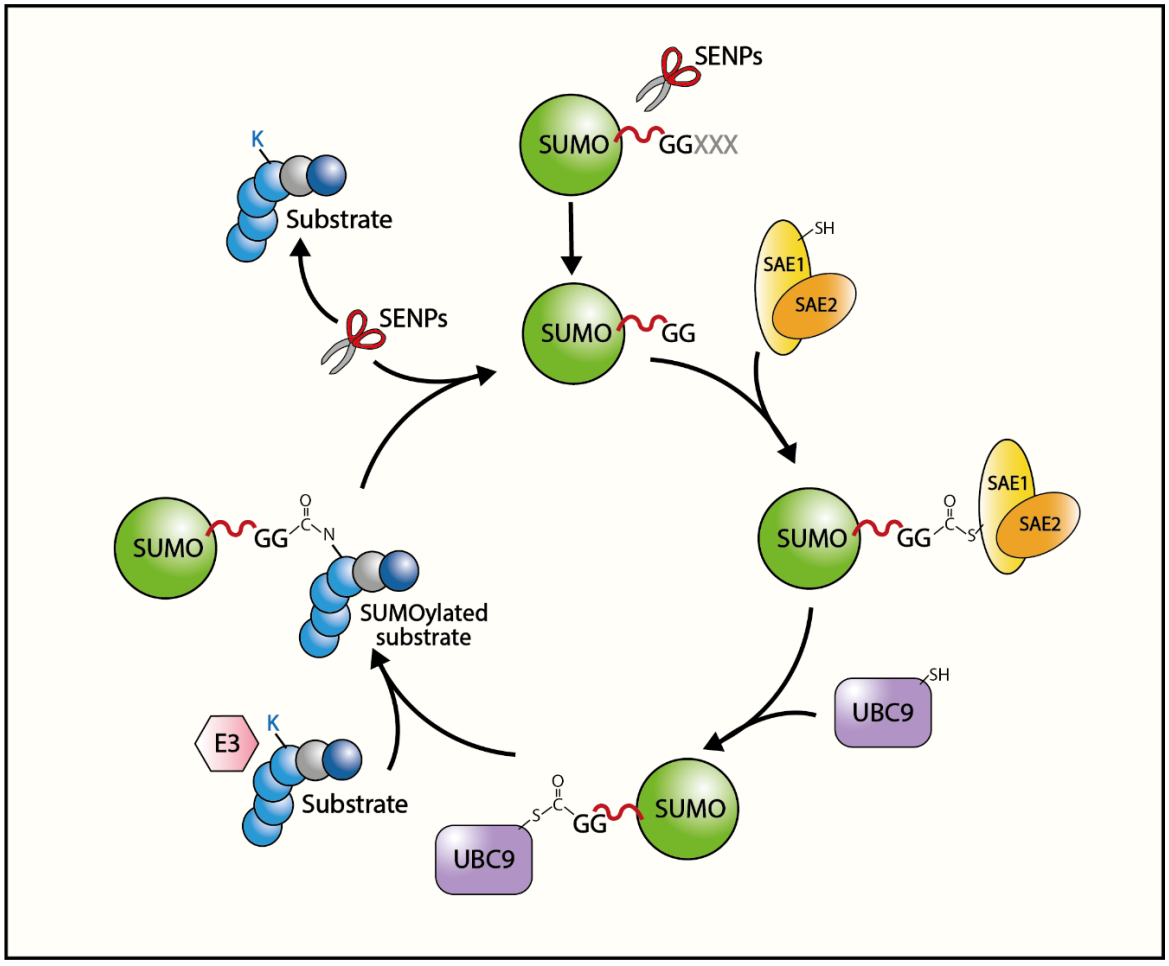

Figure 1.18. The SUMOylation cascade.
In the process of substrate SUMOylation, the SUMO molecule is produced as a pro-peptide and is activated by cleavage of its C-terminal glycine-glycine (GG) motif by sentrin/SUMO specific proteases (SENPs), as this is the site that will eventually conjugate to the substrate lysine residue. The mature form of SUMO is then conjugated to a heterodimer of SUMO activating enzyme subunits 1 and 2 (SAE1 and SAE2) via adenylation of the SUMO C-terminus allowing conjugation via a thioester bond to a cysteine in the dimer. This allows the transfer of the SUMO molecule to the catalytic cysteine of the conjugating enzyme UBC9, again via another thioester bond, which finally transfers the SUMO molecule to the lysine of a substrate via an isopeptide bond, aided by the fine-tuning action of E3 SUMO ligases which provide a scaffold between the UBC9-SUMO complex and the substrate. The process can also be reversed by removal of the SUMO molecule by breaking the isopeptide bond, completed by many enzymes with isopeptidase activity including the SENPs. Adapted from Hendriks and Vertegaal, 2016.

The first SUMO isoform, SUMO1, was identified in the 1990s where similar to ubiquitin it was found covalently conjugated to proteins in a variety of processes

including DNA recombination, cell death and protein targeting (Hay, 2005; Le *et al.*, 2017). A few years later two other isoforms, SUMO2 and SUMO3, were identified in vertebrates which share a ~50% sequence identity to SUMO1, but a ~95% homology to each other (three N-terminal residues difference), and as such are often referred to as SUMO2/3 (Kamitani *et al.*, 1998). Whilst these isoforms exist in all tissues investigated to date, a fourth isoform, SUMO4, has been identified in kidney cells, with later evidence showing expression in the lymph node and spleen but not the heart (Le *et al.*, 2017). Additionally, its functional role has not been determined and a unique C-terminal proline prevents the same maturation as SUMO1-3, so it has remained relatively unstudied (Owerbach *et al.*, 2005). Similarly, and most recently, a fifth isoform was identified, SUMO5, which shows a high sequence homology to SUMO1 but has a distinct tissue specific mRNA expression pattern, being highest in the testes and peripheral blood leukocytes with low or undetectable levels in the heart, although this has yet to be confirmed in terms of protein expression (Liang *et al.*, 2016).

Each SUMO isoform is ~12kDa in size and can attach as a single molecule per lysine, in the case of SUMO1, or in a poly-SUMOylated chain as observed through SUMO2/3 addition (Tatham *et al.*, 2001). The shift in molecular weight means SUMOylation can often be distinguished from the non-SUMOylated version via western blotting, however in the majority of cases, ~1% of the protein is SUMOylated at one time, making detection difficult especially for larger proteins (Geiss-Friedlander & Melchior, 2007). Around ~50% of substrates are SUMOylated at a consensus motif of Ψ-K-x-D/E where Ψ is a hydrophobic residue and X is any amino acid (Impens *et al.*, 2014). SUMO can also interact non-covalently with hydrophobic regions on the protein known as SUMO interaction motifs (SIMs), and covalent SUMOylation to a lysine residue also encourages protein-protein interactions via these sites (Kerscher, 2007; Ullmann *et al.*, 2012). Given the consensus sequences of the SUMO site and of SIMS, prediction software has been developed to aid in SUMO site identification (discussed in detail in Chapter 4).

Although SUMOylation involves several enzymatic steps, conjugation can be directed by SUMO and the E2 conjugating enzyme ubiquitin carrier 9 (UBC9) overexpression alone, and therefore these components are the most well characterised elements of the cascade (Cartier *et al.*, 2019). UBC9 binds SUMO by

a thioester bond on its active site cysteine (C93) before interacting with and conjugating SUMO to the substrate, with the aid of scaffolding E3 ligase proteins such as PIAS (Shetty *et al.*, 2020). UBC9 shares a high sequence homology with other E2 enzymes involved in ubiquitination but is the only E2 enzyme involved in the regulation of SUMOylation (Bernier-Villamor *et al.*, 2002). Interestingly, whilst expressed in high levels in the lung and spleen, only low levels of UBC9 are detected in the heart and skeletal muscle (Gołebiowski *et al.*, 2003). Despite this, SUMOylation plays an essential role in regulating protein stability, protein-protein interactions and influencing other PTMs, particularly in cardiac tissue.

1.4.2 Cellular effects of SUMOylation

Whilst the majority of SUMOylated substrates are found in the nuclear compartment where it regulates DNA replication, transcription and cell cycle progression, there is increasing evidence of SUMOylated cardiac substrates outside the nucleus. Three main functions of SUMOylation are of interest when it comes to cardiac substrate regulation – 1) SUMOylation provides a method to recruit or block protein binding partners to SIMs and regulates protein-protein interactions, 2) SUMOylation regulates substrate stability and activity including by competing for lysines with other PTMs such as ubiquitylation and acetylation, and 3) SUMOylation can induce structural changes in a protein that alters their function (Le *et al.*, 2017). In this regard, in a similar manner to palmitoylation, SUMOylation affects cardiac substrates throughout the contractile cycle and therefore plays a crucial role in cardiac physiology and importantly, pathophysiology.

1.4.2.1 SUMOylation in cardiac physiology

In terms of cardiac channels and transporters, SUMOylation has been most well studied in the regulation of voltage gated potassium channels that control the ventricular re-polarisation phase of the action potential. Co-expression of SUMO1 and SUMO2 with UBC9 decreased the activity of Kv11.1 (hERG1), which controls the Ikr current, leading to a reduction in current amplitude and an increase in inactivation time (Steffensen *et al.*, 2018). Similarly, the KV7.1 (KCNQ1) channel, which controls the Iks current, is formed of four pore forming units, each with an identical SUMOylation site at K424, with each addition of SUMO2 shifting the half-maximal activation voltage by +8mV in neonatal ventricular cardiomyocytes.

Interestingly, when accessory protein KCNE1 is lost, SUMOylation only occurs on two of the four sites, indicating that protein-protein interactions are important for maintenance of SUMOylation (Xiong *et al.*, 2017). Whilst SUMOylation appears to generally limit the activity of potassium channels, it is proposed to activate sodium channels. Increased SUMOylation of Nav1.2 in the brain was associated with larger sodium currents and reduced inactivation, with similar observations made for Nav1.5 in the heart (Plant *et al.*, 2016, 2020). With regards to Ca^{2+} regulation, aside from SERCA2a discussed in detail below, relatively little is known of the role of SUMOylation. Increased SUMOylation of NCX3 (the isoform found in the brain) in a region involved in transporter activity and stability is neuroprotective as part of ischaemic pre-conditioning in the brain (Cuomo *et al.*, 2016). Although this site is not conserved in the cardiac isoform (NCX1 Q590, Clustal Omega alignment), the study provides an important example for the role of SUMOylation in ischaemia, which has been uncovered in cardiac tissue over recent years.

1.4.2.2 SUMOylation in cardiac pathophysiology

The importance of SUMOylation in cardiac development is evident in that UBC9-KO mice are embryonic lethal, and SUMO1 KO mice have cardiac defects and progress to sudden death (Nacerddine *et al.*, 2005; Wang *et al.*, 2011). Interestingly, SUMO2 KO mice have no overt cardiac dysfunction, indicating that SUMO1 may play a more important role in cardiac physiology. This is surprising as SUMO2 mRNA is the most abundant, representing ~80% compared to ~20% SUMO1 expression (Wang, Wansleeben, *et al.*, 2014). However, based on the current evidence, it appears SUMO2 modification is associated with cardiac dysfunction whilst SUMO1 is associated with cardioprotection. This has been displayed in studies of cardiac hypertrophy, where overexpression of SUMO2 resulted in cardiomyopathy leading to premature death, with expression level correlating with severity (Kim *et al.*, 2015). In contrast, micro-RNA induced loss of SUMO1 was associated with the development of cardiac hypertrophy in the rat (Oh *et al.*, 2018). Recent work on the crosstalk between PARylation, the addition of an ADP-ribose polymer to a substrate catalysed by PARP1, and SUMOylation revealed they can occur on the same lysine. Overexpression of PARP1 and increased PARylation of transcription factor C/EBPß results in reduced SUMO1 conjugation which effects its stability, contributing to cardiac hypertrophy (Wang *et al.*, 2022). However,

there are conflicting studies suggesting attenuation of cardiac hypertrophy can occur by indirectly inhibiting SUMO1 of certain substrates, including in diabetic cardiomyopathy where both SUMO1 and SUMO2/3 conjugation to transcription factor XBP1 were associated with cardiac defects (Pai *et al.*, 2018; Wang *et al.*, 2021).

Similarly, conflicting studies on the cardioprotective or detrimental role of SUMOylation has been demonstrated in studies of I/R injury and in HF. SUMO1 expression is decreased in failing human hearts, whilst SUMO1 gene transfer improves cardiac function in a pig model of I/R injury (discussed in more detail in 1.4.2.3; Kho *et al.*, 2011; Tilemann *et al.*, 2013). Additionally, MI and ischaemia are associated with a reduction in substrate acetylation and increased expression of histone deacetylases (HDACs) which results in increased reactive oxygen species (ROS) production and apoptosis in cardiomyocytes (Granger *et al.*, 2008). SUMOylation of HDAC4 at a single lysine by SUMO1 increases ubiquitylation and subsequent degradation and attenuates these pathological effects (Du *et al.*, 2015; Tatham *et al.*, 2001). This provides another example of the interplay between SUMOylation and other PTMs in the regulation of cardiac physiology. In further support of the positive effects of SUMOylation on cardiac function, increased expression of UBC9 has generally been found to be cardioprotective. Knock-down of UBC9 in cardiomyocytes was associated with protein aggregation and decreased proteasomal function, suggesting UBC9 mediated SUMOylation is crucial for protein quality control (Gupta *et al.*, 2014). Follow up work from the group demonstrated that transgenic mice overexpressing UBC9 have enhanced SUMOylation and an upregulation of cardiac autophagy. When these mice are subjected to a cardiac proteotoxicity model, they show reduced protein aggregation, reduced hypertrophy and improved cardiac function (Gupta *et al.*, 2016).

Similar to cardiac hypertrophy, SUMO2/3 has been associated with cardiac pathophysiology, with increased levels observed in human HF, and gain-of-function SUMO2 transgenic mice showing increased apoptosis and cardiomyopathy development (Kim *et al.*, 2015). However conversely, pharmacological intervention leading to the upregulation of SUMO2 has been associated with cardioprotection against I/R injury (Zhao *et al.*, 2021). This is supported by

transgenic mice lacking DJ-1, a protein associated with cardioprotection, where reduced accumulation of SUMO2/3 conjugated proteins has been associated with mitochondrial dysfunction (Shimizu *et al.*, 2016). This likely reflects the different roles SUMO2/3 conjugation plays in the developing heart compared to the adult heart. Additionally, the increase in conjugated SUMO2/3 substrates observed in HF may be occurring as part of a protective mechanism. Indeed, this is observed with SUMO1, where upregulation of SUMO1 targeted proteins is associated with the protective effect of moderate hypothermia prior to I/R conditioning (Chen *et al.*, 2020). Similarly, SUMOylation of PPARγ protects against I/R injury mediated particularly by E3 ligase PIAS1, with a reduction in PIAS1 expression associated with apoptosis and inflammation (Xie *et al.*, 2018). This is supported by work in the brain showing increased SUMOylation mediated by UBC9 overexpression is protective against ischaemic injury (Lee *et al.*, 2011).

Whilst the majority of the evidence points to SUMO1 being protective against hypertrophy and I/R injury, there is evidence to suggest increased SUMO1-mediated SUMOylation is detrimental. Increased SUMOylation by SUMO1 of Nav1.5 occurs during hypoxia and is associated with prolonged channel opening and decreased inactivation, contributing to pro-arrhythmic currents (Plant *et al.*, 2020). Additionally, pharmacological downregulation of SUMO1 expression has been demonstrated to reduce cardiac fibrosis post-MI (Qiu *et al.*, 2018). However, there was no reperfusion element to these models, and studies in the heart have demonstrated initial changes in SUMO1 conjugation during ischaemia that are reversed upon reperfusion depending on the substrate involved, therefore whether inhibiting SUMO1 would be beneficial in a clinical setting is unknown (Hotz *et al.*, 2020). As such, the decision as to whether SUMOylation is truly cardioprotective or detrimental is likely to be highly specific to the substrate, developmental stage and SUMO isoform involved, complicating the picture as to how to target SUMOylation for therapeutic benefit. The most well-developed example of this is the targeting of SERCA2a SUMOylation.

1.4.2.3 Targeting SUMOylation: A case study on SERCA2a

In 2011, a seminal paper was published in Nature investigating the role of SUMOylation in SERCA2a expression and function, both of which are lost in ischaemic HF. SUMOylation of SERCA2a by SUMO1 was detected at two highly

conserved lysines in the nucleotide binding domain, with loss of SUMOylation associated with reduced ATPase activity and reduced half-life, suggesting SUMOylation is indispensable for its activity and stability. Adenoviral gene transfer of SUMO1 increased overall SERCA2a expression levels and was associated with improved cardiac function in mice with cardiac dysfunction induced by pressure-overload (Kho *et al.*, 2011). The same results were later obtained in a pig model of I/R, arguably more clinically relevant (Tilemann *et al.*, 2013). Additionally, SUMO1 transfer decreased the ubiquitinated form of SERCA2a at the same sites, again suggesting SUMO1 mediates its stabilising effects through competing with ubiquitylation (Kho *et al.*, 2011). The group also further elucidated the fluctuating levels of SUMO1 expression during cardiac disease pathogenesis, showing an increase during hypertrophy which was reduced dramatically in the development of HF. Despite increased SUMO1 levels in hypertrophy, SUMO1 gene transfer prior to injury attenuated hypertrophy and development to HF, in particular reducing oxidative stress and its negative effects on SERCA2a activity (Lee *et al.*, 2014). The work has been supported by others, including in an obese rat model which has impaired systolic and diastolic function, where reduced SERCA2a SUMOylation and UBC9 expression were observed, and study of Luetolin, a compound which improves contractility following I/R, was shown to enhance SERCA2a SUMOylation (Hu *et al.*, 2017; Yao *et al.*, 2015). The most recent work from the group shows SERCA2a SUMOylation can be modulated pharmacologically using N106, an activator of the E1 ligase which matures SUMO1 during the SUMOylation cascade, resulting in increased SR Ca^{2+} suggesting increased activity of SERCA2a (Kho *et al.*, 2015). Additionally, a microRNA (miR-149a) that targets SUMO1 has been identified, with an increase in its expression strongly correlated to decreased SUMO1 levels as HF progresses. Inhibition of the miR-146a increased SERCA2a SUMOylation and improved cardiac function (Oh *et al.*, 2018). Given all three of these approaches (gene transfer, pharmacological and miRNA targeting) raise global SUMO1 levels and activity, it will be important to determine whether other cardiac substrates, including those in the myofilament (discussed in Chapter 4), undergo the same level of regulation when it comes to SUMOylation.

1.5 Hypothesis and aims

Cardiac MyBP-C undergoes cysteine PTMs such as S-nitrosylation and S-glutathionylation, and lysine modifications including acetylation and ubiquitinylation, indicating solvent exposed residues within its structure are available for modification. These PTMs have important functional and clinical relevance for HCM, IHD and HF, of which there is a significant unmet clinical need. In terms of HF, understanding how cMyBP-C is regulated by PTMs may identify novel therapeutic avenues to target its activity therapeutically. Preliminary evidence suggests that cMyBP-C undergoes two novel post-translational modifications, palmitoylation and SUMOylation, both of which are implicated in cardiac physiology and disease. I hypothesise that these modifications of cMyBP-C regulate its function in the myofilament and there regulate cardiac contractility. Dysregulation of these modifications may contribute to the pathogenesis of heart failure. The aims of this work are therefore to:

- Investigate cellular control of palmitoylation and SUMOylation of cMyBP-C in cardiac tissue from animals and humans

- Investigate the disease relevance of cMyBP-C palmitoylation in samples from animal models of HF and samples from patients with HCM or ischaemic HF

- Identify experimental tools that can be used to study cMyBP-C palmitoylation and SUMOylation *in vitro* including purification assays, pharmacological inhibitors and over-expression systems including adenoviruses

- Identify the amino acids sites responsible for cMyBP-C palmitoylation and SUMOylation and characterise the functional effect of their loss or gain on cMyBP-C function and cardiac contractility

Chapter 2 Materials and Methods

2.1 General laboratory practice

Equipment and reagents were of a high-quality grade and commercially available from rom Sigma-Aldrich (Dorset, UK), Thermo Fisher Scientific (Paisley, UK), Corning (Birmingham, UK) or Grant Instruments (Cambridgeshire, UK) unless otherwise stated. All glassware was cleaned with detergent and autoclaved before use and sterile, disposable or autoclaved plastic was used throughout experiments. Water used for experiments was either distilled (dH_2O) or ultrapure.

2.2 Cardiomyocyte isolation

2.2.1 Ethical statement

All experimental procedures utilising animals conformed with the United Kingdom Animal Procedures Act (1986); ARRIVE Guidelines (Kilkenny *et al.*, 2010) and the Guide for the Care and Use of Laboratory Animals published by the United States National Institute of Health (NIH publication no.85-23, revised 2001) and were approved by the University of Glasgow's Ethics Review Committee. Where required, all work was carried out at the University of Glasgow by a valid personal licence holder and under the authority of a project license granted by the home office.

2.2.2 Adult rabbit ventricular cardiomyocytes

2.2.2.1 Materials

Table 2.1. Adult rabbit ventricular cardiomyocyte isolation and culture materials

Isolation		
Solution A	**Krafte-Brühe Solution**	**Modified Krebs-Henseleit Solution**
130 mM NaCl 5 mM HEPES 4.5 mM KCl 0.4 mM NaH_2PO_4 3.5 mM $MgCl_2.6H_2O$ 10 mM Glucose (pH to 7.25 with NaOH)	70 mM KOH 40 mM KCl 50 mM L-Glutamic Acid 20 mM Taurine 20 mM KH_2PO_4 3 mM $MgCl_2.6H_2O$ 10 mM HEPES 0.5 mM EGTA (pH to 7.2 with KOH)	120 mM NaCl 20 mM HEPES 5.4 mM KCl 0.52 mM NaH_2PO_4 3.5 mM $MgCl_2.6H_2O$ 20 mM Taurine 10 mM Creatine 11 mM Glucose (pH to 7.4 with NaOH)
Culture		
Myocyte Culture Medium		
Gibco® Medium 199 (M-199) modified with Hank's salts (1.8 mM calcium), L-glutamine, 25 mM HEPES and phenol red: +5 mM Taurine +2 mM Creatine +2 mM Carnitine +1% penicillin/streptomycin		

2.2.2.2 Isolation

Isolation of adult rabbit cardiomyocytes was completed by Mrs Aileen Rankin and Mr Michael Dunne, University of Glasgow. New Zealand White male rabbits (12 weeks old, ~3 kg) were euthanised with a terminal dose of sodium pentobarbital (100 mg/kg) with heparin (500 IU) via ear vein injection, following which the thoracic cavity was opened and the heart and aorta were removed and placed into ice-cold Solution A to arrest the heart and lower oxygen demand (Table 2.1). The heart was cannulated on a Langendorff system maintained at 37°C and retrogradely perfused via a peristaltic pump (20 ml/min) with Solution A to clear the coronary circulation of blood. The heart was then perfused by Solution A supplemented with ethylene glycol tetracetic acid (EGTA, 100 μM) to chelate calcium ions and prevent contraction. Finally, the heart was perfused with Solution A containing protease (0.1 mg/ml, protease type XIV, Sigma) and collagenase (0.6 ml/ml Type 1 collagenase, Worthington Chemical) enzymes for ~15 minutes to dissolve the extracellular matrix of the tissue. The heart was removed from the system and cut into sections (left atria, right atria, right ventricle, left ventricle and septal regions) and each was finely dissected in

Krafte-Brühe solution (KB; Table 2.1). The mixture was then triturated before shaking for 10 minutes following which the solution was filtered into a falcon tube to remove undigested tissue. The remaining cell suspension was centrifuged manually for a minute before the pellet of cells were re-suspended in fresh KB.

Following isolation, cells in the falcon tube were placed in a water bath at 37°C for 10 minutes to allow them to settle to the bottom of the tube following which the KB was removed and the cells were re-suspended in modified Krebs-Henseleit solution (Krebs) containing 100 µM of $CaCl_2$ and left to settle for an additional 10 minutes (Table 2.1). This process was then repeated using 200 µM, 500 µM, 1 mM and 1.8 mM concentrations of $CaCl_2$ in a process known as "stepping up" whereby cells are slowly returned to physiological calcium. Following the addition of 1.8 mM $CaCl_2$ Krebs, cells were either cultured (detailed in 2.2.2.3) or pelleted, snap frozen and stored at -80°C for later use. Quality of cells was determined by observing a small volume under a phase contrast microscope and estimating roughly the number of rod-shaped healthy cells to round dead cells. Populations with >60% rods were used for experiments where possible.

2.2.2.3 Culture

Following addition of the 1.8 mM $CaCl_2$ Krebs, the cells were allowed to settle for an additional 10 minutes before removal of Krebs and resuspension in an appropriate volume of myocyte culture medium (Table 2.1). Cells were plated into 12-well plates for expression analysis or 12-well plates with 16mm glass coverslips (Scientific Laboratory Supplies, No. 1.5) for immunofluorescence. All culture dishes were coated with mouse laminin in dH_2O (15 µg/ml; Sigma-Aldrich, L2020) and incubated at 37°C for one hour before plating. Medium was replaced 4 hours after initial plating to remove dead cells.

2.2.2.4 Rabbit heart failure model

Ventricular cardiomyocytes were also obtained from Male New Zealand White Rabbits (~3 kg, 20 weeks) that had undergone a myocardial infarction (MI) without reperfusion procedure (Kettlewell *et al.*, 2013). Briefly, the left anterior descending coronary artery was ligated in anaesthetised animals at 12-weeks of age to induce an ischaemic area in the left ventricle, with the rabbit maintained

for an additional 8 weeks to allow a heart failure phenotype to develop. The left ventricular dysfunction/heart failure phenotype was confirmed by a reduction in left ventricular ejection fraction (LVEF) to >45%. Sham animals underwent the thoracotomy and maintenance without the coronary artery ligation and had a LVEF of ~60%. Isolation of cardiomyocytes was carried out as described in 2.2.2.2.

2.2.3 Adult rat ventricular cardiomyocytes

2.2.3.1 Wistar kyoto rats

Adult rat cardiac tissue used in this study was from Wistar rats (male, ~250-300 g) and were either provided by Dr Krzysztof Wypijewski prepared at the University of Dundee or by Mrs Aileen Rankin and Mr Michael Dunne at the University of Glasgow. Briefly, hearts were retrogradely perfused on a Langendorff system and the tissue either snap frozen in liquid nitrogen and homogenised before use, or ventricular cardiomyocytes isolated in a similar manner to that described in 2.2.2.2. Isolated ventricular cardiomyocytes were centrifuged (1500 RPM, 5 minutes, 4^{o}C), snap frozen and stored at -80^{o}C until use.

2.2.3.2 Type-2 diabetic rat model

Cardiac tissue was supplied by Professor Lisa Heather (University of Oxford) from a model of type-2 diabetes, along with healthy controls. Briefly, male Wistar rats underwent three weeks of high-fat diet to induce insulin resistance along with an intraperitoneal injection streptozotocin (STZ), a pancreatic ß-cell toxin, to impair ß-cell function and insulin secretion, mimicking the phenotype of late-stage type-2 diabetic humans. Additionally, the low dose of STZ used (<30 mg/kg) induces cardiac metabolic changes including reduced glucose metabolism and increased fatty acid metabolism (Mansor *et al.*, 2013). Cardiac tissue was pulverised before use.

2.2.4 Neonatal rat ventricular cardiomyocytes

2.2.4.1 Materials

Table 2.2 Neonatal rat ventricular cardiomyocyte isolation and culture materials

Isolation	Culture	
10x ADS Solution	**Day One Medium (M1)**	**Post-Day One Medium (M2)**
1.06 M NaCl 200 mM HEPES 8 mM NaH_2PO_4 53 mM KCl 4 mM MgSO4 50 mM Glucose (pH to 7.4 with NaOH) (Stored 4°C)	4:1 ratio of DMEM (high glucose, 25 mM HEPES) to M-199 media: + 10% horse serum + 5% new-born calf serum + 1% L-glutamine + 1% penicillin/streptomycin (Used within one week)	4:1 ratio of DMEM (high glucose, 25 mM HEPES) to M-199 media: + 5% horse serum + 0.5% new-born calf serum + 1% L-glutamine + 1% penicillin/streptomycin (Used within one week)

2.2.4.2 Isolation and culture

Neonatal rat ventricular cardiomyocytes (NRVM) were isolated from Sprague-Dawley rats between 1-4 days old. Rats were euthanised by an intraperitoneal injection of a lethal dose of Euthatal before confirmation of death was carried out by severing the femoral artery or cervical dislocation. The hearts were then removed from the thoracic cavity and placed into 1x ADS solution (from 10x ADS solution, Table 2.2) on ice. The atria were then removed along with any excess tissue or blood and at this point, the ventricular tissue was either snap frozen for whole tissue analysis or use to isolate ventricular cardiomyocytes.

To isolate the cardiomyocytes, the ventricular tissue was dissected into $1mm^3$ pieces before transfer to digestion buffer containing 1x ADS with collagenase (0.05%, w/v) and pancreatin (0.03%, w/v). The tissue was digested for 5 minutes to remove pericardial collagen (supernatant discarded) before a further incubation in digestion buffer for 20 minutes, following which the tissue was triturated and the supernatant added to a falcon tube containing newborn calf serum (NCS) to inactivate the digestion buffer. The supernatant was then centrifuged at 1250 RPM for 5 minutes to produce a pellet of cells which was re-suspended in NCS and kept at 37°C until four further digestions of the remaining tissue were complete.

After the final digestion, all cells were combined in M1 media (Table 2.2) and plated onto a 10cm petri dish for 2 hours to allow fibroblasts and endothelial cells to adhere (pre-culture) before the remaining non-adhered cardiomyocytes were then collected and counted using a haemocytometer. For expression studies, cardiomyocytes were the plated onto bovine gelatin (1%, w/v) coated 6-well (1 million cells per well) and 12-well plates (500,000 cells per well) which were incubated at 37ºC for at least 1 hour before use. For contractility or confocal analysis, cells were plated onto coverslips or 35mmdishes with 14mm No 1.5 coverslip (P35G-1.5-14-C; Mat-tek) containing with 2-well silicone inserts (Thistle Scientific, IB-80209-150) coated with mouse laminin in dH_2O (15 µg/ml; Sigma-Aldrich, L2020) and incubated at 37ºC for at least 1 hour before use. Cells were kept in a humidified incubator (37ºC, 5% CO_2) and medium was changed to M2 medium the next day and every 48 hours subsequently (Table 2.2). Cells were kept in culture for a maximum of 5 days. For adenoviral infection, NRVM were infected (described in 4.3.4.1) at least 2 hours after the first M2 medium change and maintained for 24 hours before use.

2.2.5 Subcellular fractionation of rabbit and neonatal cardiomyocytes

In order to more closely investigate the distribution of endogenous and exogenous proteins present in adult and neonatal cardiomyocytes, a subcellular fractionation protocol was used. Cells were harvested in F60 buffer (60 mM KCl, 30 mM Imidazole, 2 mM $MgCl_2 \bullet 6H_2O$) with 1% Triton X-100 before an analytical sample was taken (unfractionated) and the remaining lysate centrifuged at 14,000 G for 5 minutes at 4ºC. This allows separation of the soluble components of the cell (supernatant) and the myofilaments (pellet). An additional step was taken to resolubilise the myofilament pellet with 500 mM NaCl which would separate myofilament proteins (NaCl supernatant) from insoluble cytoskeletal components (NaCl pellet; Figure 2.1; Kuster *et al.*, 2015).

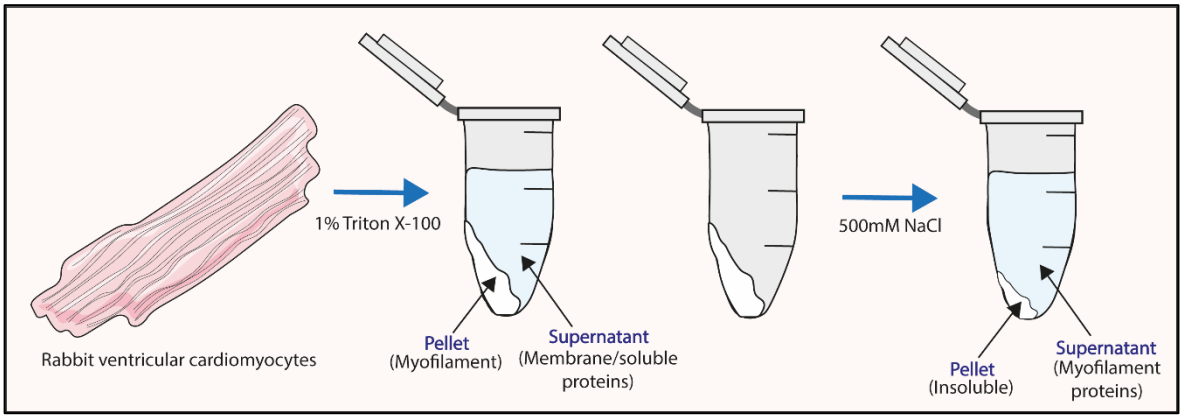

Figure 2.1. Subcellular fraction of rabbit ventricular cardiomyocytes.
Cardiomyocytes were fractionated into myofilament (pellet) and non-filament (supernatant) fraction by extraction with 1% Triton X-100. The myofilament pellet was then solubilised in 500 mM NaCl to produce a supernatant of myofilament proteins, separated from insoluble cytoskeletal components. This method was adapted from (Kuster *et al.*, 2015).

2.3 Mammalian cell lines

All cell culture experiments were performed in a Biological Safety Class II vertical laminar flow cabinet using sterile techniques. Cell culture materials were supplied by Gibco™ (ThermoFisher Scientific, Paisley, UK) unless otherwise stated. A phase contrast inverted microscope was used to examine cultures to confirm the absence of contamination and check the confluence.

2.3.1 Cell line culture

Human embryonic kidney (HEK) 293 cells were maintained between passages 5 and 30 in T75 flasks in a humidified incubator (37°C, 5% CO_2). Cells were passaged between 80-90% confluence to prevent contact inhibition by aspirating the media and washing with pre-warmed sterile phosphate buffered saline (PBS) before incubation for 2-3 minutes with 0.05% Trypsin-EDTA. The flasks were gently tapped to dislodge the cells and the trypsin was neutralised by addition of cell culture medium (Dulbecco's Modified Eagle Medium (DMEM), 10% foetal bovine serum (FBS), 1% penicillin/streptomycin). The cells were then centrifuged for 3 minutes at 1000 RPM following which the medium was aspirated and the pellet suspended in fresh cell culture medium to allow transfer of cells to new flasks or plates. After experimentation, plates were washed with PBS before appropriate lysis buffer for each experiment was added.

2.3.1.1 Transient transfection

Cells were transiently transfected the day after plating using Lipofectamine 2000 Reagent (Invitrogen, #10696153) according to manufacturer's instructions. Briefly, for each well of a 12-well plate 3 µl of Lipofectamine 2000 Reagent was added to 125 µl of Opti-MEM whilst 1µg of plasmid DNA was added to a separate 125 µl of Opti-MEM. These were incubated for 5 minutes before they were combined and incubated for a further 30 minutes. The transfection mixture was then added to the well in a dropwise manner and incubated for 24 hours.

2.4 Polymerase chain reaction

Polymerase chain reaction (PCR) is a technique which allows the amplification of double standard DNA (Wages, 2005). The process requires a master mix containing the template DNA to be replicated, along with free nucleotides, a heat-stable DNA polymerase and sequence specific forward and reverse primers. PCR involves three main stages of denaturation, to separate double stranded DNA, annealing, to anneal the forward and reverse primers to the single strands, and extension, whereby DNA polymerase adds the free nucleotides to make new strands (Figure 2.2).

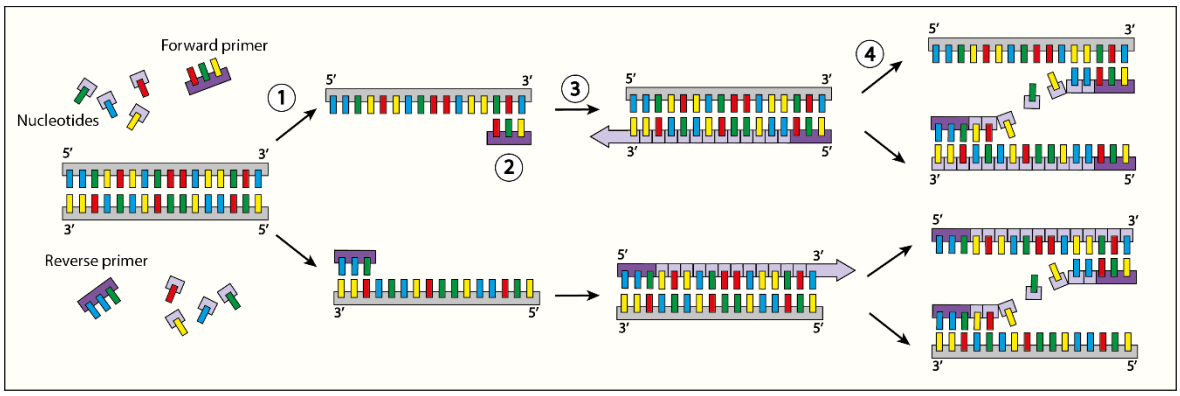

Figure 2.2: An overview of the general principles of polymerase chain reaction (PCR).
PCR involves the replication of double stranded DNA with the use of sequence specific forward and reverse primers, free nucleotides and a heat-stable DNA polymerase. The reaction is set up in thin-walled PCR tubes and placed into a thermocycler. Firstly, double stranded template DNA is denatured at ~95º to separate the strands (1). The primers are allowed to bind the single strands in the annealing phase, the temperature of which depends on the melting temperature (Tm) of the designed primers, often between 55-70ºC (2). Finally, the elongation phase takes place at the optimum temperature for the DNA polymerase (~72ºC specific to the polymerase being used) to allow the polymerase to add new nucleotides to the 3' end of the forward and reverse primers, using base-pair matching rules, and extend out the strand (3). The cycles are then repeated with the original and new strands and continues for 25-35 cycles to amplify the DNA (4).

2.4.1 Primer design

The primers used in a PCR reaction can be designed to introduce specific additions, substitutions or deletions into a sequence whilst they replicate the DNA, and this was utilised throughout this study for the production of protein fusions and site directed mutants (Table 2.3 and Table 2.4). Several commercial PCR kits are available and were used throughout this study. All primers were prepared by Eurofins and resuspend in nuclease free water to a stock concentration of 100 µM.

Table 2.3 Mutagenesis primers for production of FLAG-cMyBP-C and alanine/cysteine point mutants

Primers	Sequences	Ta (°C)	Purpose	PCR Kit
FLAG addition to cMyBP-C	F = 5'GATGATGATAAACCTGAGCCGGGGAAGAAG3' R = 5'ATCTTTATAATCCATCCTGAGAGACGTCACAC3'	65	Introduce a FLAG-tag to the N-terminal of cMyBP-C after initiator methionine	Q5
cMyBP-C C623A	F = 5'CTTCGCCGCCAACCTGTCAGCCAAGCTCCAC3' R = 5'AGGTTGGCGGCGAAGCCCTCGGGCAC3'	66.9	Mutant of cysteine at position 623 to alanine in the human cMyBP-C sequence	Infusion
cMyBP-C C651A	F = 5'CCTGGACGCCCCAGGCCGCATACCAGACACC3' R = 5'CCTGGGGCGTCCAGGTGGATCTTGGGAGG3'	65.9	Mutant of cysteine at position 651 to alanine in the human cMyBP-C sequence	Infusion
cMyBP-C A239C	F = 5'CTATAGATGCGAGGTGTCCACCAAGGACA3' ACCTCGCATCTATAGCTGCCGGTAAAGGCT3'	62.1	Mutant of alanine at position 239 to cysteine in cysless version of human cMyBP-C sequence	Infusion
cMyBP-C A249C	F = 5'GTTCGACTGCTCCAACTTCAACCTGACCG3' R = 5'TTGGAGCAGTCGAACTTGTCCTTGGTGG3'	60.4	Mutant of alanine at position 249 to cysteine in cysless version of human cMyBP-C sequence	Infusion
cMyBP-C A426C	F = 5'TTCTCAGTGCTCCCTGGCCGACGACGCC3' R = 5'AGGGAGCACTGAGAAATTGTCAGGGTCCGCTTG3'	67.7	Mutant of alanine at position 426 to cysteine in cysless version of human cMyBP-C sequence	Infusion
cMyBP-C A436/443CC	F = 5'TTGTTGGCGGAGAGAAGTGCTCCACCGAGCTGTTCGTG3' R = 5'TCTCTCCGCCAACAACGCATTGATAAGCGGCGTCGTCG3'	62.7	Mutant of alanines at position 436/443 to cysteines in cysless version of human cMyBP-C sequence	Infusion
cMyBP-C A475C	F = 5'ATTCGAGTGCGAGGTGTCCGAAGAGGGCG3' R = 5'ACCTCGCACTCGAATTCCACTCTCTGTCCG3'	63.6	Mutant of alanine at position 475 to cysteine in cysless version of human cMyBP-C sequence	Infusion
cMyBP-C A528C	F = 5'CGCCCTTTGCACATCTGGTGGACAGGCCC3' R = 5'GATGTGCAAAGGGCGTAGTGGCCGGC3'	66.0	Mutant of alanine at position 528 to cysteine in cysless version of human cMyBP-C sequence	Infusion
cMyBP-C A566C	F = 5'GTTCAAATGCGAAGTGTCCGACGAGAATGTGC3' R = 5'ACTTCGCATTTGAACACGGCCTGGTC3'	62.1	Mutant of alanine at position 566 to cysteine in cysless version of human cMyBP-C sequence	Infusion
cMyBP-C A623C	F = 5'CTTCGCCTGCAATCTGTCTGCCAAGCTGCAC3' R = 5'AGATTGCAGGCGAAGCCCTCAGGCAC3'	64.8	Mutant of alanine at position 623 to cysteine in cysless version of human cMyBP-C sequence	Infusion
cMyBP-C A651C	F = 5'TCTGGATTGCCCTGGCAGAATCCCCGACA3' R = 5'CCAGGGCAATCCAGATGGATCTTAGGAGGCTCT3'	64.1	Mutant of alanine at position 651 to cysteine in cysless version of human cMyBP-C sequence	Infusion
cMyBP-C A719C	F = 5'GCTGCTGTGCGAGACAGAGGGAAGAGTGCGC3' R = 5'GTCTCGCACAGCAGCTTCTTGTCGAACACC3'	64.6	Mutant of alanine at position 719 to cysteine in cysless version of human cMyBP-C sequence	Infusion
cMyBP-C A788C	F = 5'AGATAGCTGCACCGTGCAGTGGGAACCA3' R = 5'ACGGTGCAGCTATCTTCTCCCACGTTAGAGA3'	62.6	Mutant of alanine at position 788 to cysteine in cysless version of human cMyBP-C sequence	Infusion
cMyBP-C A909/913CC	F = 5'TTGCCCTGAGGGCTGCTCTGAGTGGGTTGCAGCAC3' R = 5'CAGCCCTCAGGGCAATATTCCACGCTGTAGCCATCCAG3'	63.6	Mutant of alanines at position 909/913 to cysteines in cysless version of human cMyBP-C sequence	Infusion
cMyBP-C A1124C	F = 5'GACACACTGCGTGGTGCCAGAGCTGATCATC3' R = 5'ACCACGCAGTGTGTCCGTCTGTAGTGTTCCAG3'	64.1	Mutant of alanine at position 1124 to cysteine in cysless version of human cMyBP-C sequence	Infusion
cMyBP-C A1201/1202CC	F = 5'TGCTGTGCTGCGCTGTCAGAGGCAGCCCC3' R = 5'CAGCGCAGCACAGCATAGCGGTGTAGCCGG3'	65.4	Mutant of alanines at position 1201/1202 to cysteines in cysless version of human cMyBP-C sequence	Infusion
cMyBP-C A1244C	F = 5'AAAGCCCTGCCCTTTCGACGGCGGCATC3' R = 5'AAAGGGCAGGGCTTTCTGATTTCCAGGGTC3'	63.7	Mutant of alanine at position 1244 to cysteine in cysless version of human cMyBP-C sequence	Infusion
cMyBP-C A1253C	F = 5'CTATGTGTGCAGAGCCACCAATCTGCAGGG3' R = 5'GCTCTGCACACATAGATGCCGCCGTCG3'	64.1	Mutant of alanine at position 1253 to cysteine in cysless version of human cMyBP-C sequence	Infusion
cMyBP-C A1264/66CC	F = 5'TAGATGCGAATGCAGACTGGAAGTTCGGGTGCC3' R = 5'CTGCATTCGCATCTAGCTTCGCCCTGCAGATTGG3'	65.6	Mutant of alanines at position 1264/66 to cysteines in cysless version of human cMyBP-C sequence	Infusion

(F, forward primer; R, reverse primer; Ta, average melting temperature)

Table 2.4 Primers for production of FLAG-cMyBP-C-UBC9 fusion and lysine to arginine or cysteine to alanine point mutants

Primers	Sequences	Ta (ºC)	Purpose	PCR Kit
FLAG-cMyBP-C-UBC9 Fusion	cMyBP-C F = 5'GATTATAAAGATGATGATGATAAAC3' cMyBP-C R = 5'CATCCTGAGAGACGTCACACCAG3'	58.3	To produce a fusion protein of FLAG-cMyBP-C and SUMO E2 ligase UBC9 to enhance SUMOylation	Infusion
	UBC9 F = 5'ACGTCTCTCAGGATGTCGGGGATCGCCCTCAGC3' UBC9 R = 5'ATCATCTTTATAATCTGAGGGCGCAAACTTCTTGGC3'	66.4		
UBC9 C93A	F = 5'CACAGTGGCCCTGTCCATCCTGGAGGAAGACAAG3' R = 5'GACAGGGCCACTGTGCCAGAAGGATACACG3'	64.8	Mutant of cysteine 93 to alanine in UBC9 human sequence to produce catalytically inactive version	Infusion
cMyBP-C K89R	F = 5'CAAGGTCCGTTTCGACCTCAAGGTCATAGAGGCA3' R = 5'TCGAAACGGACCTTGGAGGAGCCAGC3'	63.8	Mutant of lysine at position 89 to arginine in the human cMyBP-C sequence	Infusion
cMyBP-C K93R	F = 5'CGACCTCCGTGTCATAGAGGCAGAGAAGGCAGAGC3' R = 5'ATGACACGGAGGTCGAACTTGACCTTGGAGG3'	65.6	Mutant of lysine at position 93 to arginine in the human cMyBP-C sequence	Infusion
cMyBP-C K301R	F = 5'GCTGAAACGTAGAGACAGTTTCCGGACCCC3' R = 5'TCTCTACGTTTCAGCAGTGAGCTGAAGTCC3'	63.2	Mutant of lysine at position 301 to arginine in the human cMyBP-C sequence	Infusion
cMyBP-C K312R	F = 5'GGACTCGAGGCTGGAGGCACCAGCAGAGG3' R = 5'TCCAGCCTCGAGTCCCTCGGGGTCCG3'	65.6	Mutant of lysine at position 312 to arginine in the human cMyBP-C sequence	Infusion
cMyBP-C K367/367RR	F = 5'TTCAGCGCCGCCTGGAGCCGGCCTACCAG3' R = 5'CCAGGCGGCGCTGAAAGGCTGTGCTCTTCTTC3'	63.0	Mutant of lysines at position 367/368 to arginines in the human cMyBP-C sequence	Infusion
cMyBP-C K635R	F = 5'GGAGGTCAGGATTGACTTCGTACCCAGGCAGG3' R = 5'TCAATCCTGACCTCCATGAAGTGGAGCTTGG3'	64.8	Mutant of lysine at position 635 to arginine in the human cMyBP-C sequence	Infusion
cMyBP-C K185R	F = 5'CCTCCTGCGCCCGCCTGTGGTCAAGTGG3' R = 5'GGCGGGCGCAGGAGGCTGGCGCCGGC3'	67.2	Mutant of lysine at position 185 to arginine in the human cMyBP-C sequence	Infusion
cMyBP-C K398R	F = 5'ATGGCTCCGCAATGGCCAGGAGATCCAGATGAG3' R = 5'CCATTGCGGAGCCATTTGACCTCAGCGTC3'	63.8	Mutant of lysine at position 398 to arginine in the human cMyBP-C sequence	Infusion
cMyBP-C K450R	F = 5'CTTTGTGCGCGAGCCCCCTGTGCTCATCAC3' R = 5'GGCTCGCGCACAAAGAGCTCCGTGCTACAC3'	64.5	Mutant of lysine at position 450 to arginine in the human cMyBP-C sequence	Infusion
cMyBP-C K488R	F = 5'ATGGCTGCGCGACGGGGTGGAGCTGACC3' R = 5'CCGTCGCGCAGCCATTTGACTTGCGCC3'	63.7	Mutant of lysine at position 488 to arginine in the human cMyBP-C sequence	Infusion
cMyBP-C K504R	F = 5'GGTTCCGCCGCGACGGGCAGAGACACCACC3' R = 5'CGTCGCGGCGGAACCGGTATTTGAAGGTCTCCTCC3'	64.8	Mutant of lysine at position 504 to arginine in the human cMyBP-C sequence	Infusion
cMyBP-C K542/543RR	F = 5'AGGAACGCCGCCTGGAGGTGTACCAGAGCATCG3' R = 5'CCAGGCGGCGTTCCTGCACAATGAGCTCAGC3'	63.9	Mutant of lysines at position 542/543 to arginines in the human cMyBP-C sequence	Infusion
cMyBP-C K565R	F = 5'GGTGTTCCGCTGTGAGGTCTCAGATGAGAATGTTC3' R = 5'TCACAGCGGAACACCGCCTGGTCCTTTG3'	63.0	Mutant of lysine at position 565 to arginine in the human cMyBP-C sequence	Infusion
cMyBP-C K579R	F = 5'GTGGCTGCGCAATGGGAAGGAGCTGGTGCC3' R = 5'CCATTGCGCAGCCACACACCCCGAAC3'	64.2	Mutant of lysine at position 579 to arginine in the human cMyBP-C sequence	Infusion
cMyBP-C K754R	F = 5'CACAGTGCGCAACCCTGTGGGCGAGGACC3' R = 5'GGGTTGCGCACTGTGACCGTGTAGACGCC3'	66.1	Mutant of lysine at position 754 to arginine in the human cMyBP-C sequence	Infusion
cMyBP-C K1000R	F = 5'CCAGGGCCGCCCCCGGCCTCAGGTGACC3' R = 5'CGGGGGCGGCCCTGGAAAGGGATGAGAAGG3'	65.9	Mutant of lysine at position 1000 to arginine in the human cMyBP-C sequence	Infusion
UBC9 K1216R	F = 5'CTGGTTCCGCAATGGCCTGGACCTGGGAG3' R = 5'CCATTGCGGAACCAGGAAATCTTGGGCTTGG3'	63.9	Mutant of lysine at position 1216 to arginine in the combined human cMyBP-C-UBC9 sequence	Infusion
UBC9 K1351R	F = 5'GCTTTTCCGCGATGATTATCCATCTTCGCCACC3' R = 5'TCATCGCGGAAAAGCATCCGTAGTTTAAACAAG3'	60.3	Mutant of lysine at position 1351 to arginine in the combined human cMyBP-C-UBC9 sequence	Infusion

(F, forward primer; R, reverse primer; Ta, average melting temperature)

2.4.2 Production of FLAG-cMyBP-C with Q5® Site-Directed Mutagenesis

E-coli transformed with the plasmid backbone pCMV Sport6 vector backbone (Clone ID: IRATp970G11139D) containing Homo Sapiens cMyBP-C sequence were purchased from Source BioScience and plasmid DNA was prepared as described in Section 2.5. To identify transfected cMyBP-C over endogenous, a FLAG tag (DYKDDDDK) was added to the N-terminus using custom primers and Q5® Site-Directed Mutagenesis Kit (New England BioLabs (NEB), UK) according to manufacturer's instructions. Briefly, a mix of cMyBP-C plasmid DNA (25-100ng), forward and reverse primers (0.5 µM each) and Q5 Hot Start High-Fidelity Master Mix (containing dNTPs and DNA polymerase) were added to a Thermal Cycler on the following programme:

STEP		TEMPERATURE	TIME
Initial denaturation		98°C	30 seconds
25 Cycles	Denaturation	98°C	10 seconds
	Annealing	65°C	20 seconds
	Extension	72°C	4 minutes
Final extension		72°C	2 minutes
Hold		4°C	∞

After the PCR reaction, the contents were incubated with KLD (kinase, ligase, DpnI) reaction mix at 37°C for 1 hour. This allows the ligation and re-circularisation of the DNA, whilst the DpnI restriction enzyme will recognise and cleave methylated DNA, so any DNA produced in bacteria (i.e. the parental plasmid) will be removed leaving the newly mutated plasmid DNA.

2.4.3 Production of FLAG-cMyBP-C-UBC9 fusion and lysine, cysteine and alanine point mutants using In-fusion® HD

In-Fusion® HD Cloning Kit (Takara Bio, EU) was used to produce the majority of the recombinant proteins throughout this project. This was due to its diversity allowing the production of protein truncations, individual site mutants and the

fusion of two proteins together and its high efficiency in completing these tasks compared to other PCR kits. Briefly, primers were designed using Takara's In-fusion primer design tool which incorporates overlapping ends to the primers to allow the plasmid to be re-linearized or two products to be fused together. (Figure 2.3).

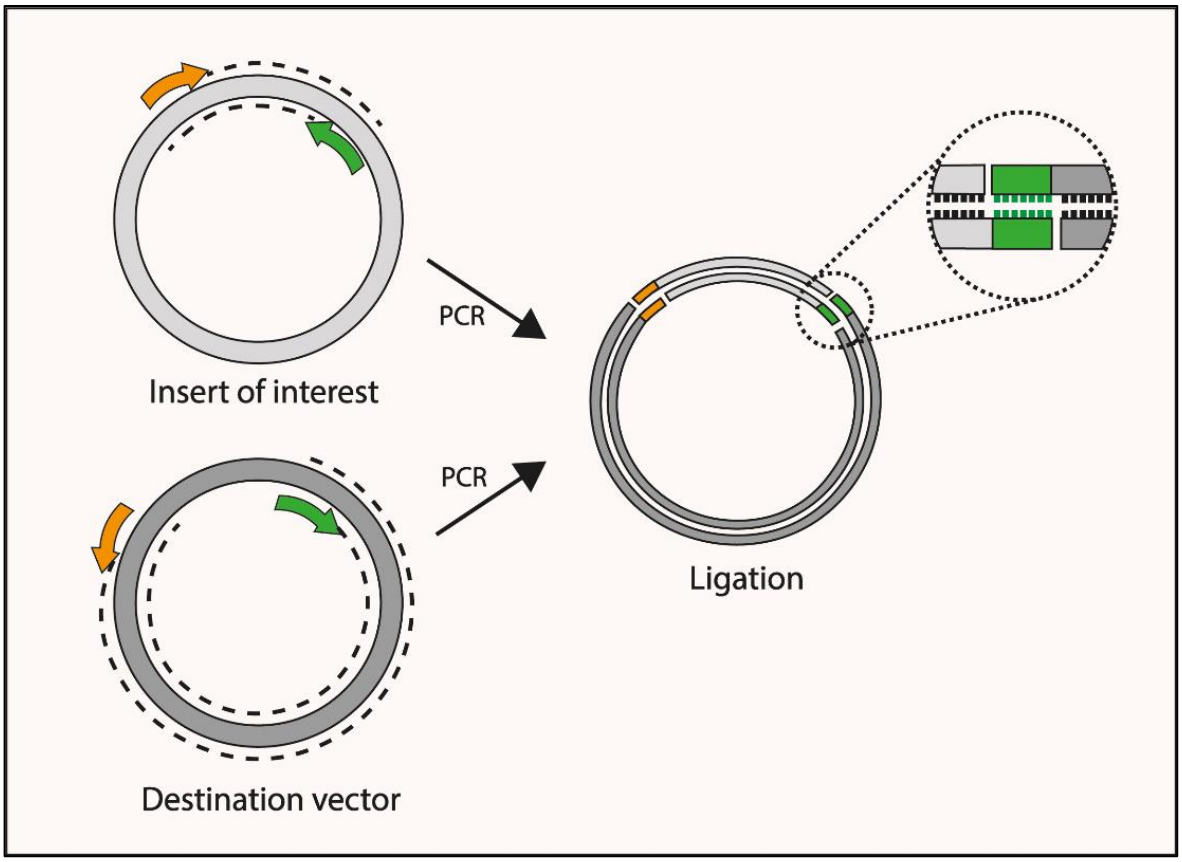

Figure 2.3. In-fusion PCR Cloning.
In-fusion PCR cloning involves amplifying one or more fragments of DNA by standard PCR where the primers (orange and green arrows) used in the synthesis are designed with 15bp extensions complementary to either each end of the plasmid (for re-linearization of a single product) or completely to another product to allow the fusion of the two (as pictured). The fusion is then completed by re-ligation using the In-Fusion enzyme.

To enhance the SUMOylation of cMyBP-C to allow improved detection, a construct expressing a fusion of FLAG-cMyBP-C with the E2 SUMO ligase UBC9 was produced. This has been shown to enhance the detection of the SUMOylated isoform of the protein of interest (Kim *et al.*, 2009). The Infusion® HD reaction was carried out in two separate reactions whereby the UBC9 gene was amplified in one and pCMV Sport6 FLAG-cMyBP-C was amplified in the other. Combination of both PCR products with In-Fusion® HD Enzyme Premix then allowed the fusion of the two products into one linearized plasmid product. Similarly, in order to narrow down the region of cMyBP-C that is palmitoylated or SUMOylated, individual amino acids in pCMV6-FLAG-cMyBP-C or pCMV6-FLAG-cMyBP-C-UBC9 were mutated in a PCR

reaction before re-ligation. In all cases, the plasmid DNA was linearized using mutagenic forward and reverse primers and CloneAmp Hifi PCR Premix (containing dNTPs and DNA polymerase) and added to the Thermal Cycler on the following programme:

STEP		TEMPERATURE	TIME
35 Cycles	Denaturation	98°C	10 seconds
	Annealing	65°C*	15 seconds
	Extension	72°C	5 seconds per kb of plasmid
Hold		4°C	∞

*Temperature varies depending on the primers used (Table 2.3 and Table 2.4).

The PCR reaction mix was then incubated with DpnI enzyme (37°C, >3 hours) to remove parental DNA following which a PCR Clean Up Kit (Monarch® PCR & DNA; NEB, UK) was used to remove excess buffer, enzymes and primers from the reaction mix. The purified, linearized PCR product was then re-circularised to produce a functional plasmid by incubation of 200-300 ng of PCR product with In-Fusion® HD Enzyme Premix at 50°C for 15 minutes before being place on ice prior to transformation.

2.5 Plasmid preparation

All bacterial work was carried out under sterile conditions by keeping items proximal to a Bunsen flame where possible and sterilising all tips, stripettes and spreaders before use. Ampicillin (final concentration 100 µg/ml) and Kanamycin (final concentration 50 µg/ml) were thawed on ice and added when appropriate to Agar for plates and Luria-Bertani (LB) broth for the growing of bacterial cultures. Plates and cultures were stored at 4°C.

2.5.1 Transformation of chemically competent cells

DH5α (NEB), XL-10 gold (Agilent) or Stellar™ (Takara Bio) chemically competent cells (stored at -80°C) were thawed on ice before addition of plasmid DNA or PCR product post-DpnI treatment. The cells and DNA were gently mixed and incubated for 30 minutes on ice, gently agitating every few minutes. Heat shock to allow the

competent cells to uptake the DNA was then carried out at 42°C for 30 seconds, before recovery on ice for 5 minutes. To the transformed cells, the appropriate volume of SOC medium (DH5α and Stellar™) or NZY+ broth (XL-10 gold) was added, and the cells incubated at 37°C with shaking at 200 RPM for 1 hour. After incubation, the transformed cells were spread onto Agar plates with appropriate antibiotics before incubation upside down at 37°C overnight.

Successful transformation was determined by the presence of clear, individual colonies and a number of these were picked with sterile pipette tips and used to inoculate 3-5 mls of LB broth with appropriate antibiotic for 16-20 hours in a shaking incubator (180-200 RPM, 37°C). After inoculation, bacteria were either harvested for mini prep and/or transferred to a larger culture for midi/maxi prep. Glycerol stocks were produced from overnight cultured by mixing 1 ml of culture with 1 ml of 50% glycerol in sterile water and snap frozen for long term storage at -80°C.

2.5.2 Preparation of plasmid DNA

Preparation of plasmid DNA from individual colonies was completed using either QIAGEN® Plasmid Mini/Midi/Maxi Prep Kits (Qiagen, UK) or ZymoPURE Mini/Midi/Maxi Prep Kits (Zymo Research, UK) with the kit used dependent on the volume of culture grown or amount of plasmid DNA to be prepared. Briefly, the bacterial culture was pelleted in a high-speed centrifuge followed by lysis, neutralisation and precipitation with appropriate buffers. The lysate containing the plasmid DNA was then cleared by centrifugation or syringe filter and the supernatant collected and transferred to a resin that binds the plasmid DNA. The bound DNA was subsequently washed via centrifugation or vacuum manifold before it was eluted in Tris-EDTA buffer (TE; 10 mM Tris-Cl, 1 mM EDTA; pH 8.0). The concentration of DNA and the purity was determined by a NanoDrop 2000 spectrophotometer (Denovix) whereby absorbance at 260nm determined the concentration in ng/µl and the A_{260}/A_{280} ratio determined purity. Preparations were stored at -20°C.

2.5.3 Agarose gel electrophoresis

In order to determine the success of mutagenesis, plasmids were run on an agarose gel which allows the separation of DNA products according to their size and compared to the parental plasmid from which they were made. Agarose gels (1%, w/v) was prepared in Tris-acetate-EDTA buffer (TAE, 40 mM Tris Base, 20 mM Acetic Acid, 1 mM EDTA in dH_2O, pH 8.5) and boiled until the agarose had dissolved. SYBR Green I Nucleic Acid Gel Stain was added at a volume of 1 µl/ml to stain the double-stranded DNA for detection. After the gel had set, samples were added at a final concentration of 150-300 ng and gels were run at 100 V for 1 hour before visualisation with a BioRad Imaging System and Quantity One software (BioRad, UK). Plasmids were sequenced using gene specific primers and Eurofins TubeSeq Service to confirm mutagenesis.

2.6 SDS-Polyacrylamide Gel Electrophoresis (SDS-PAGE)

2.6.1 Materials

Table 2.5 Polyacrylamide gradient gel recipes

Polyacrylamide Gradient Gels		
6% (light) fraction	**20% (heavy) fraction**	**Stacking gel**
0.4 M Tris-HCl (pH 8.8) 0.1% SDS 6% Acryl-bisacrylamide mix 0.04% TEMED 0.04% APS	0.4 M Tris-HCl (pH 8.8) 0.1% SDS 20% Acryl-bisacrylamide mix 0.04% TEMED 0.04% APS	0.125 M Tris-HCl (pH 6.8) 0.1% SDS 5% Acryl-bisacrylamide mix 0.1% TEMED 0.1% APS

Table 2.6 SDS-PAGE reagents

SDS-PAGE Reagents			
2X SDS-PAGE Loading Buffer			
100 mM Tris 4% SDS 20% glycerol 0.02% bromophenol blue 5% β-mercaptoethanol			
TBS-T	**PBS-T**	**Running Buffer**	**Transfer Buffer**
20 mM Tris 150 mM NaCl 0.1% Tween-20 (pH to 7.5 with HCl)	137 mM NaCl 2.7 mM KCl 10 mM Na_2HPO_4 1.8 mM KH_2PO_4 0.1% Tween-20 (pH 7.4)	25 mM Tris 192 mM Glycine 0.1% SDS	25 mM Tris 192 mM Glycine 0.01% SDS 20% methanol

Table 2.7 Primary and secondary antibodies

Antibody (Species)	Dilution (Use)	Supplier and Product Number
Anti-cMyBP-C primary antibody (mouse)	1:1000 – 1:2000 (WB) 1:200 (IF) 1 µg (IP)	Santa Cruz Biotechnology, sc-137237
Anti-cMyBP-C primary antibody (rabbit)	1:1000 (WB) 1:200 (IF)	Invitrogen, 703574
Anti-phospho-cMyBP-C [pSer^{282}] primary antibody (rabbit)	1:1000 (WB)	Enzo Life Sciences, ALX-215-057-R050
Anti-FLAG® M2 primary antibody (mouse)	1:2000 (WB) 1:200 (IF)	Sigma-Aldrich, G3165
Anti-Flotillin-2 primary antibody (mouse)	1:2000 (WB)	BD Biosciences, 610383
Anti-Caveolin-3 primary antibody (mouse)	1:4000 (WB)	BD Biosciences, 610420
Anti-DHHC5 primary antibody (rabbit)	1:1000 (WB)	Sigma, HPA014670
Anti-GFP primary antibody (rabbit)	1:5000 (WB)	Abcam, ab6556
Anti-Na^+/K^+ ATPase primary antibody (mouse)	1:200 (WB)	Developmental Studies Hybridoma Bank, α6F
Anti-FXYD1 (PLM) (rabbit)	1:2000 (WB)	Abcam, ab76597
Anti-Gαi primary antibody (rabbit)	1:1000 (WB)	Pierce Antibodies
Anti-NCX1 primary antibody (mouse)	1:1000 (WB)	Swant, R3F1
Anti-Cav1.2 (CACNA1C, LTCC) primary antibody (guinea pig)	1:200 (WB)	Alomone, AGP-001
Anti-UBC9 primary antibody (rabbit)	1:1000 (WB)	Cell Signalling Technology, D26F2
Anti-HA tag primary antibody (rat)	1:1000 (WB)	Roche, 11867423001
Anti-myosin primary antibody (mouse)	1:200 (WB)	Developmental Studies Hybridoma Bank, MF20
Anti-actin primary antibody (rabbit)	1:200 (WB)	Developmental Studies Hybridoma Bank, JLA20
Anti-tropomyosin primary antibody (mouse)	1:200 (WB)	Developmental Studies Hybridoma Bank, CH1
Anti-troponin-T (TNNT2, cardiac/slow) primary antibody (mouse)	1:200 (WB)	Developmental Studies Hybridoma Bank, CT3
Anti-troponin-I primary antibody (cardiac) (mouse)	1:200 (WB)	Developmental Studies Hybridoma Bank, TI-1
Slow skeletal-MyBP-C (MYBPC1) (rabbit)	1:1000 (WB)	Caltag Medsystem (ProSci), PSI-6679
Fast skeletal-MyBP-C (MYBPC2) (rabbit)	1:1000 (WB)	Caltag Medsystem (ProSci), PSI-5651
Anti-GAPDH primary antibody (mouse)	1:1000 (WB)	Sigma, G8795
Anti-SUMO1 primary antibody (rabbit)	1:1000 (WB) 1:200 (IF)	Enzo Life Sciences, BML-PW8330-0025
Anti-rabbit HRP conjugated secondary antibody (goat)	1:2000 - 1:5000 (WB)	Jackson ImmunoResearch, 111-035-144
Anti-mouse HRP conjugated secondary antibody (rabbit)	1:2000 - 1:10000 (WB)	Jackson ImmunoResearch, 315-035-003
Anti-rat HRP conjugated secondary antibody (mouse)	1:2000 (WB)	Jackson ImmunoResearch, 212-035-082
Anti-guinea pig HRP conjugated secondary antibody (donkey)	1:2000 (WB)	Jackson ImmunoResearch, 706-035-148
Anti-mouse IgG H&L AlexaFluor® 488 secondary antibody (goat)	1:500 (IF)	Abcam, ab150113
Anti-rabbit IgG H&L AlexaFluor® 546 secondary antibody (goat)	1:500 (IF)	Thermofisher, A-21085

(IF, immunofluorescence; IP, immunoprecipitation; PA, peptide array; WB, western blot)

2.6.2 Bradford assay

Total protein concentration from cell lysates was determined using a BioRad protein assay utilising a protein concentration dependent colour change for quantification (Bradford, 1976). A standard curve was produced from a known range of bovine serum albumin (BSA) samples to which Bradford Reagent (1:5 dilution in dH_2O; company product) was added. Cell lysates were then prepared in triplicate (1:50 dilution in dH_2O) before addition of Bradford Reagent. Absorbance was measured at 585 nm using an Anthos 2010 plate reader and ADAP software, with unknown samples compared to the standard curve for estimation of protein concentration in ng/µl, which was then adjusted for dilution.

2.6.3 Western immunoblotting

Proteins within a sample were resolved using precast (NuPAGE™ 4-12% Bis-Tris Protein Gels) or prepared gradient gels, in which spacer plates (0.75 mm), short plates and a multicasting chamber (BioRad, UK) were used to prepare the resolving gel before the addition of a stacking gel and 15-well comb (solutions detailed in Table 2.5). SDS-PAGE allows separation of proteins by molecular weight and proteins are identified by their size when compared with a molecular weight marker containing proteins of known size (Dual Color Precision Plus, BioRad). Gels were immersed in running buffer (Table 2.6) and a voltage applied at 100 V until the sample had travelled through the stacking gel before running at up to 200 V through the resolving gel until the dye front had reached the bottom of the gel, or further to separate larger proteins only. Gels were then transferred to Immobilin® PVDF membranes (activated for two minutes in methanol) using a Trans-Blot® Semi-Dry Transfer Apparatus (20 V, 1.0 A, 30 minutes; BioRad, UK) and transfer buffer (Table 2.6). After transfer membranes were incubated in 5% milk in PBS-T or 5% milk in TBS-T for phospho-antibodies for 1 hour to block unspecific binding sites before incubating with desired primary antibody overnight at 4°C (Table 2.7). Membranes were washed three times for 15 minutes with PBS-T or TBS-T before incubation with appropriate horseradish peroxidase (HRP)-conjugated or fluorescent secondary antibody for 1 hour at room temperature (Table 2.7). Membranes were washed with PBS-T or TBS-T for 15 minutes (fluorescence) or 2-3 hours (HRP) before visualization.

2.6.4 Densitometry

For detection of HRP-conjugated secondaries, membranes were incubated with an Immobilon® Western Chemiluminescent HRP Substrate and visualised with a BioRad Imaging System and Quantity One software (BioRad, UK). Quantification of bands was completed using Quantity One software whereby a box was drawn around each band and the background subtracted. Abundance of proteins of interest were normalised to total protein or loading controls where possible.

2.7 *In vitro* palmitoylation

2.7.1 Acyl-resin assisted capture (Acyl-RAC)

The following method has been modified from a protocol from (Forrester *et al.*, 2011) which allows the capture of palmitoylated proteins within a sample. Cultured and pelleted cells or pulverised tissue were lysed using blocking buffer (Table 2.8) and lysates were incubated at 40ºC shaking at 1000 RPM for 4 hours to allow the methyl methanethiosulfonate (MMTS) to methylate all free cysteines. Non-pulverised tissues were treated in the same way except were homogenised in the solution prior to incubation. Proteins were then precipitated using 3 volumes of 100% acetone at -20ºC for 20 minutes and centrifuged at 10,000 G for 2 minutes, with the resulting pellet subsequently washed five times using 70% acetone to remove excess MMTS, before air-drying the resulting pellet to remove excess acetone. The pellets were then re-suspended in binding buffer (Table 2.8) for 1-2 hours at 40ºC with shaking at 1200 RPM. Following pellet redissolving, a portion of the sample was transferred to a separate labelled Eppendorf as a measure of total protein (unfractionated sample) and an equal volume of 2X SDS-PAGE loading buffer with 100 mM DTT was added. A volume of lysate 5 times that of the unfractionated was then incubated with 250 mM NH_2OH (hydroxylamine, HA, pH 7.5), to hydrolyse the thioester bonds between palmitate and palmitoylated cysteine, with the same concentration of sodium chloride (NaCl, pH 7.5) added in its place for negative control samples. The solution was the incubated with thiopropyl sepharose beads hydrated in binding buffer and rotated for 2.5 hours at room temperature to allow the available cysteines to bind to the beads. The samples were then centrifuged at 10,000 G for 3 minutes before the supernatant was aspirated and the beads were subsequently washed with five times binding

buffer, rotating and centrifuging with each wash. After the final wash an equal volume of 2X SDS-PAGE loading buffer with 100 mM DTT was added to the samples, following which the samples were heated to 60ºC for 10 minutes to elute the captured proteins (Figure 2.4). For analysis, the band intensity in the palmitoylated fraction (hydroxylamine dependent, HA) is divided by the band intensity in the unfractionated (UF) starting material to give a ratio of palmitoylation relative to expression. As the palmitoylated fraction was 5 times enriched compared to the UF sample, this ratio can be divided by 5 and multiplied by 100 to give a percentage (%) palmitoylation of each substrate (Figure 2.4).

Table 2.8 Acyl-resin assisted capture (Acyl-RAC) components.

Acyl-RAC Components	
Acyl-RAC blocking buffer	**Acyl-RAC binding buffer**
100 mM HEPES 1 mM EDTA 2.5% SDS 1% MMTS	100 mM HEPES 1 mM EDTA 1% SDS

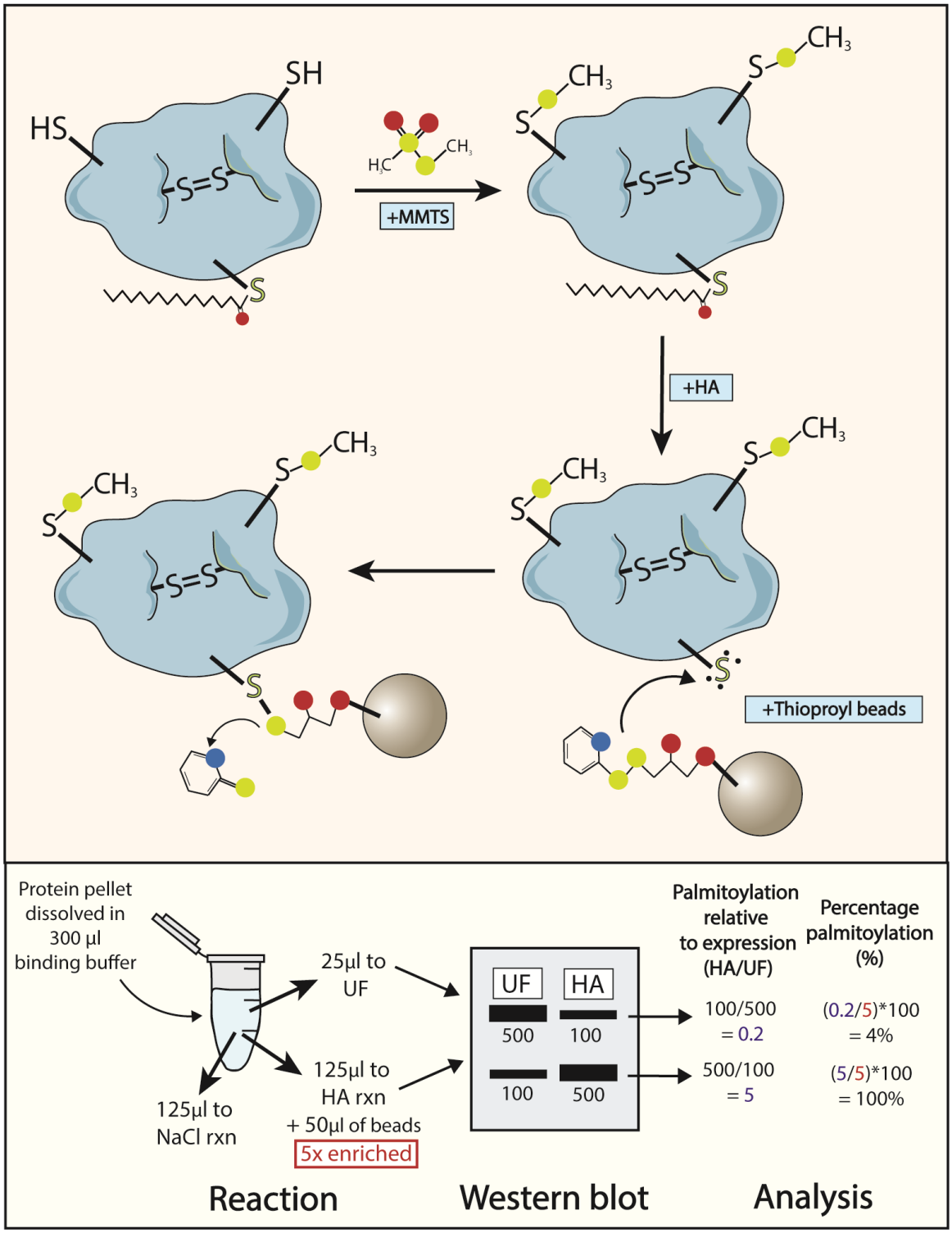

Figure 2.4. Schematic of acyl-resin assisted capture (Acyl-RAC).
Free cysteines within a sample are firstly methylated with methyl methanethiosulfonate (MMTS), followed by incubation with NH_2OH (hydroxylamine) to remove any acyl/palmitoyl groups from palmitoylation sites by hydrolysing the thioester bonds (NaCl can be used at this stage as a negative control). The free cysteine residues are then captured by thiopropyl sepharose beads. Elution of the protein attached to the beads and analysis using SDS-PAGE for protein of interest is then completed. For analysis, the band intensity in the palmitoylated fraction (hydroxylamine dependent, HA) is divided by the band intensity in the unfractionated (UF) starting material to give a ratio of palmitoylation relative to expression. As the palmitoylated fraction was 5 times enriched compared to the UF sample, this ratio can be divided by 5 and multiplied by 100 to give a percentage (%) palmitoylation of each substrate. Rxn = reaction. Adapted from Forrester *et al.*, 2011 and Main and Fuller, 2021.

2.7.2 Acyl-RAC of human heart tissue

Human heart tissue from organ donors and heart failure patients was kindly provided by Dr Niall MacQuaide, University of Strathclyde, collected from Kenneth Campbell, University of Kentucky, as previously described (Blair *et al.*, 2016) with details displayed in Table 2.9. Briefly, portions of the left ventricular endocardium were homogenised in CHAPS buffer by Dr Gillian Borland and Miss Jiayue Ling and the soluble fraction aliquoted and stored at -80ºC for later use. To identify the palmitoylation stoichiometry of several substrates from the samples, 2 mg of protein from each sample was used in an Acyl-RAC with a ratio of 1:2 sample to blocking buffer, with final concentration of 1% MMTS. The protocol was then carried out as described in 2.7.1. All samples were labelled with patient ID's and were not unblinded until after densitometry analysis was completed.

Table 2.9. Human organ donor and heart failure information.

Record ID	Case type	Sex	Primary diagnosis
24713	Organ Donor	Female	N/A
2B487	Organ Donor	Male	N/A
31331	Organ Donor	Female	N/A
4B3FA	Organ Donor	Female	N/A
4D931	Organ Donor	Male	N/A
5155D	Organ Donor	Male	N/A
632FD	Organ Donor	Male	N/A
8CB30	Organ Donor	Female	N/A
B23E3	Organ Donor	Male	N/A
BC90C	Organ Donor	Female	N/A
DOF54	Organ Donor	Male	N/A
D61ZE	Organ Donor	Male	N/A
FC3CB	Organ Donor	Female	N/A
046E	Heart Failure	Male	Ischaemic cardiomyopathy
05FF7	Heart Failure	Female	Ischaemic HFrEF
14C39	Heart Failure	Male	Ischaemic cardiomyopathy
3F6DC	Heart Failure	Male	Ischaemic cardiomyopathy
58545F	Heart Failure	Male	Ischaemic cardiomyopathy s/p MI
6DB85	Heart Failure	Male	HFrEF from Ischemic cardiomyopathy
7CE52	Heart Failure	Female	Ischaemic heart failure
8296A	Heart Failure	Male	Ischaemic cardiomyopathy
8E8D8	Heart Failure	Male	Ischaemic cardiomyopathy
97CDC	Heart Failure	Male	Ischaemic cardiomyopathy
9D7E9	Heart Failure	Male	Ischaemic cardiomyopathy
AF1FF	Heart Failure	Male	Chronic systolic HF
B8BE2	Heart Failure	Male	Ischaemic heart failure
BO644	Heart Failure	Female	Ischaemic cardiomyopathy
C3B57	Heart Failure	Male	Ischaemic cardiomyopathy
CB8A5	Heart Failure	Male	Ischaemic cardiomyopathy
DA820	Heart Failure	Male	Ischaemic cardiomyopathy
EF5CB	Heart Failure	Male	Ischaemic heart failure
FE8E2	Heart Failure	Male	Chronic systolic HF

2.8 Confocal microscopy

For confocal microscopy, cell lines were plated onto poly-l-lysine (0.01% w/v in dH_2O, Sigma-Aldrich) coated coverslips whilst cardiomyocytes were plated onto laminin (15 µg/ml) coated coverslips which had been preincubated at 37°C for 1 hour before plating. Following experimentation, cells were washed with sterile PBS before fixation with 4% paraformaldehyde in PBS for 20 minutes at room temperature, followed by three PBS washes. Cells were then permeabilised in 0.1% Triton-X100 in PBS for 10 minutes at room temperature before three PBS washes and blocking using 1% bovine serum albumin (BSA), 10% horse serum in PBS for 1 hour at room temperature. Coverslips were then incubated in primary antibody diluted in 0.1% BSA, 1% horse serum in PBS for 1 hour at room temperature before three PBS washes and incubation in appropriate fluorescent secondary antibody diluted in 0.1% BSA, 1% horse serum in PBS for an additional hour (Table 2.7). Coverslips were then mounted onto glass slides using Dako Mounting Medium (Agilent, S3023) or NucRed™ Live 647 ReadyProbes™ Reagent (Thermofisher, R37106) and left to dry overnight in the dark. The coverslips were then sealed using clear nail polish and images obtained using a Zeiss LSM Pascale Exciter laser scanning confocal microscope with a 63x/1.4 oil objective. Contrast was adjusted in images for visualisation purposes using ImageJ.

2.9 Statistical analysis

Statistical analysis was completed using GraphPad Prism (Version 7; California, USA) and was completed on groups with 3 biological replicates or more. Data is expressed as mean ± standard error or the mean (S.E.M). For comparisons in data sets with more than two groups, a one-way analysis of variance (ANOVA) with an appropriate *post hoc* test (Tukey (for all groups compared), Sidak (for select groups compared) or Dunnett's (for all groups compared to one control)), with comparisons detailed in the figure legend. For comparisons of two groups, an unpaired student's t-test was used, or in cases where the same samples were measured twice and compared, a paired t-test was used. All data was tested for significant outliers using a Grubb's test. A probability value of $p<0.05$ was considered to be statistically significant.

Chapter 3 Palmitoylation of cMyBP-C

3.1 Introduction

3.1.1 Post-translational modifications of cMyBP-C

Given the importance of cMyBP-C phosphorylation to overall cardiac contractility and its role in ischaemic HF, there has been a concerted effort over the last few decades to identify and characterise additional modifications of cMyBP-C (Figure 3.1; reviewed in Main, Fuller and Baillie, 2020).

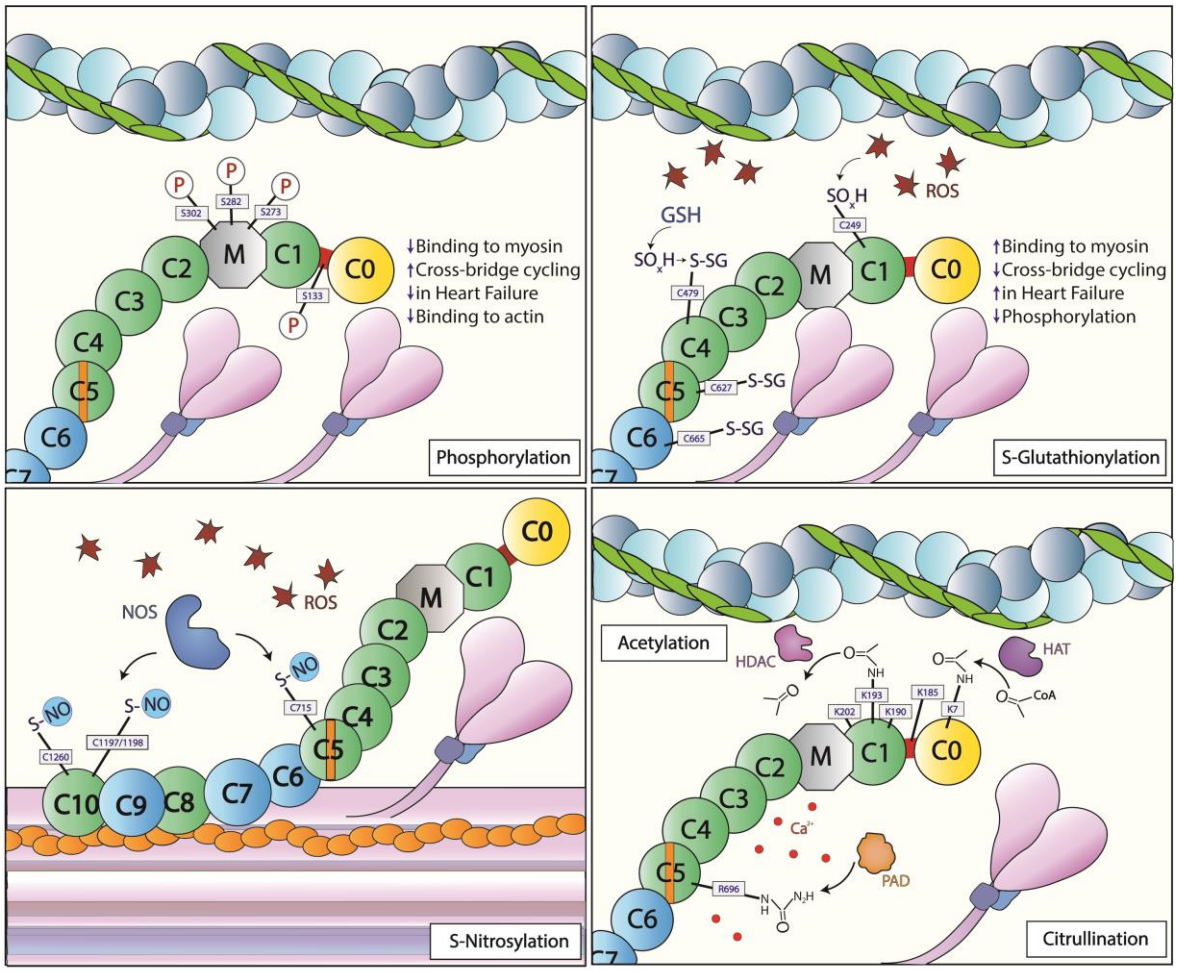

Figure 3.1. An overview of the reported post-translational modifications of cMyBP-C. Cardiac myosin binding protein-C (cMyBP-C) is under the control of several different post-translational modifications, including those more well characterised such as phosphorylation and S-glutathionylation, and those lesser studied including S-nitrosylation, acetylation and citrullination. In all cases some putative modification sites have been identified although most have not been confirmed *in vivo*. Taken from Main, Fuller and Baillie, 2020.

3.1.1.1 Acetylation

Acetylation, the addition of an acetyl group to a lysine residue, targets several cardiac substrates and is important in cardiac physiology and muscle contraction. Of note, an increase in deacetylation by histone deacetylases (HDAC) is associated with ischaemia/reperfusion (I/R) injury and HDAC inhibitors are beneficial in

protecting against I/R in pre-clinical models, with their clinical development currently in progress (Yang *et al.*, 2020). A study aiming to identify sarcomeric acetylation enzymes demonstrated that increased acetylation was associated with enhanced myofilament Ca^{2+} sensitivity and contractility (Gupta *et al.*, 2008). Acetylation of lysine residues in the myosin motor domain may be the main contributor, as an increase in myosin acetylation enhanced actin-myosin crossbridge formation (Samant *et al.*, 2015). Interestingly, the enzymes responsible for myosin acetylation were found localised to the A-band of the sarcomere where cMyBP-C resides. It is perhaps unsurprising therefore that cMyBP-C acetylation was identified soon after, both *in vitro* and *in vivo*, and the same acetylase that targets myosin was also found to target cMyBP-C (Ge *et al.*, 2009; Govindan, Sarkey, *et al.*, 2012). Interestingly, five of the putative cMyBP-C acetylation sites are located in the N-terminal domains and the cleaved cMyBP-C associated with MI and HF is heavily acetylated (Govindan, Sarkey, *et al.*, 2012). However, despite these sites being in a region of the protein of great functional significance, further characterisation has yet to be completed.

3.1.1.2 Citrullination

Citrullination, the enzyme driven conversion of an arginine amino acid to citrulline, is a lesser studied PTM, however is generally associated with loss of protein structure and binding partner interactions (Fert-Bober & Sokolove, 2014). A recent study suggests myofilament proteins including actin, myosin and cMyBP-C undergo citrullination, and that overall, this is associated with decreased myofilament Ca^{2+} sensitivity and cross-bridge cycling activity (Fert-Bober *et al.*, 2015). Despite this, cMyBP-C citrullination remains uncharacterised.

3.1.1.3 Redox modifications

Reactive oxygen species (ROS) are highly reactive signalling molecules produced primarily by NADPH-dependent oxidases and the mitochondria during aerobic metabolism. Although aberrant ROS production is associated with many diseases, including the development of cardiac hypertrophy, physiological ROS production is essential for normal cellular processes including the inflammatory response and the process of aging (Finkel, 2011). Similarly, the physiological production of reactive nitrogen species (RNS), including nitric oxide (NO), is a key mechanism in

the regulation of vascular tone as well as mediating some effects of the adrenergic system on cardiomyocyte function (Balligand *et al.*, 1993; Loscalzo & Welch, 1995). As reactive species can target many regulatory pathways, homeostasis is maintained through the production of antioxidant metabolites such as glutathione (GSH, or the oxidised form GSSG), the most abundant cysteine containing thiol in the cell, depletion of which is associated with exacerbation of ROS damage and disease (Aoyama and Nakaki, 2015). A key way in which ROS/RNS/GSH exert their effects is through driving reduction-oxidation (redox) post-translational modifications of substrates. This includes reversible cysteine modifications such as S-glutathionylation (-S-SG) and S-nitrosylation (-S-NO). Unlike phosphorylation, these modifications are usually driven by reactivity and availability of amino acid side chains, rather than through enzymatic pathways.

S-nitrosylation has been well studied in the context of Ca^{2+} handling and I/R injury, whereby increased S-nitrosylation occurs during I/R to "condition" cardiac substrates, including RYR2 and SERCA2a, which results in a reduction in damage and enhanced functional recovery from injury (Hogg *et al.*, 2007; Tong *et al.*, 2014). In terms of myofilament proteins, almost all have been identified to be S-nitrosylated including Tm, of which S-nitrosylation was upregulated in HF, however functional studies are still lacking (Canton *et al.*, 2011). Of note, myosin ATPase activity was inhibited by S-nitrosylation in skeletal muscle and follow up work in cardiomyocytes showed this again, but at a concentration of nitrothiols more associated with pathophysiology (i.e. in sepsis; Nogueira *et al.*, 2009; Figueiredo-Freitas *et al.*, 2015). Despite this, physiological concentrations of nitrothiols and increased S-nitrosylation of sarcomeric proteins was associated with decrease myofilament maximal force development and decreased Ca^{2+} sensitivity (Figueiredo-Freitas *et al.*, 2015). This may indicate a protective mechanism whereby S-nitrosylation is used to protect against deleterious effects of Ca^{2+} overload, for example during I/R.

S-nitrosylation of both cardiac and skeletal isoforms of cMyBP-C has been detected previously (Balon & Nadler, 1994; Sun *et al.*, 2007). In one study, in vivo upregulation of S-nitrosothiols using lipopolysaccharide allowed the detection of several S-nitrosylated sarcomeric proteins, including one of cMyBP-C length (Figueiredo-Freitas *et al.*, 2015). This was followed up by identification of S-nitrosylated cMyBP-C peptides by mass spectrometry, detecting a cluster of

potential S-nitrosylation sites in the C-terminal domains, with further *in vitro* characterisation identifying cMyBP-C S-nitrosylation at C1260 (mouse sequence) specifically (Sun *et al.*, 2007). Although the functional consequences of this modification have not been established, including if it occurs in normal physiology *in vivo*, the proposed sites lie in an area involved in LMM and titin binding, therefore further investigation is certainly warranted (Flashman *et al.*, 2007; Rybakova *et al.*, 2011; Tonino *et al.*, 2019). However, while S-nitrosylation has been widely implicated as an important PTM, there is increasing evidence to suggest that this modification may be a transient state before disulphide bond formation. This could indicate that disulphide bond formation is the main contributor of the effects observed, and therefore conclusions drawn from S-nitrosylation studies must be treated with caution going forward (Wolhuter *et al.*, 2018).

Similar to S-nitrosylation, increased S-glutathionylation of cardiac substrates, including sarcomeric proteins, is associated with cardiac pathologies including I/R injury and MI, often correlating to loss of protein function (Avner *et al.*, 2012; Eaton *et al.*, 2002). With regards to myofilament proteins, actin, myosin, TnI and cMyBP-C are reported to be S-glutathionylated, however much of the work has pointed to cMyBP-C as the main target in the sarcomere (Cuello *et al.*, 2018). cMyBP-C was one of 11 cardiac substrates identified in a proteomic screen of rat ventricular cardiomyocytes utilising a glutathione-linked biotin purification method (Brennan *et al.*, 2006). Greater interest came when one study showed enhanced S-glutathionylation of cMyBP-C was present in a deoxycorticosterone acetate (DOCA)-salt rat model of hypertension (from ~5% to ~15% of total cMyBP-C; Lovelock *et al.*, 2012). This model is associated with cardiovascular remodelling and hypertrophy, analogous to what is seen in HF (Iyer *et al.*, 2010). DOCA-salt rat cardiomyocytes had impaired diastolic function which was independent of changes in intracellular Ca^{2+}, and isolated myofilament experiments showed they had increased Ca^{2+} sensitivity and maximal tension. Moreover, reversal of the oxidative stress in this model with the anti-ischaemic compound ranolazine was associated with improved contractility and diastolic function, although there was no significant reversal in cMyBP-C S-glutathionylation levels (Lovelock *et al.*, 2012). Nevertheless, a follow up study provided evidence that the NO generating co-factor tetrahydrobiopterin (BH_4) provides its beneficial effects on reversing

diastolic dysfunction through preventing cMyBP-C S-glutathionylation (Jeong *et al.*, 2013).

Interestingly, cMyBP-C phosphorylation appeared unaltered by DOCA-salt induction or ranolazine treatment in the rat model but was significantly decreased at S282 in the DOCA-salt mouse myofilaments, with a further reduction observed following BH_4 treatment, even though diastolic function was improved. This could indicate that any effect of cMyBP-C S-glutathionylation on diastolic function may be occurring independently of phosphoregulatory effects (Jeong *et al.*, 2013; Lovelock *et al.*, 2012). However, others have provided evidence that there is a connection between S-glutathionylation and phosphorylation, as an increase in cMyBP-C S-glutathionylation in dilated and ischaemic cardiomyopathy samples and explanted failing hearts was correlated with a reduction in PKA and PKC mediated phosphorylation (Budde *et al.*, 2021; Stathopoulou *et al.*, 2016). Additionally, increased S-glutathionylation blunted the phosphorylation of cMyBP-C in response to isoprenaline in rat ventricular cardiomyocytes, suggesting an interplay between them.

In support of the phosphorylation-independent effects of S-glutathionylation, the glutathione mediated effects on myofilament cross-bridging cycling kinetics and passive force were only present in cMyBP-C WT and not knock-out myofilaments, although this doesn't rule out that S-glutathionylation requires a phosphorylated form of cMyBP-C in order to exert its effects (Stathopoulou *et al.*, 2016). This study also added more detail as to why S-glutathionylation of cMyBP-C may reduce myofilament cross-bridge cycling, as S-glutathionylation of recombinant C1-M-C2 enhanced its associated with the myosin S2 (Stathopoulou *et al.*, 2016). It will be important to determine whether this contributes to cMyBP-C's role in the SRX state of myosin, especially as the DOCA-salt mouse model was associated with reduced myofibril ATPase activity, which was attenuated upon BH_4 treatment and reduction in cMyBP-C S-glutathionylation (Jeong *et al.*, 2013). Another area of interest may be the contribution of S-glutathionylation of cMyBP-C to LDA, as stretching is associated with increased oxidation, inhibition of which results in diastolic dysfunction in a mouse model (Scotcher *et al.*, 2016). Indeed, the most recent work has shown the positive correlation between S-glutathionylated cMyBP-C and diastolic dysfunction in humans, mice and monkeys, providing evidence for its use as a biomarker in this regard (Zhou *et al.*, 2022).

In terms of S-glutathionylation sites, initial investigation revealed 3 potential sites in the lesser studied C3, C4 and C5 domains of cMyBP-C (C475, C623 and C651, human sequence; Patel, Wilder and John Solaro, 2013). However, a later study identified a total of 15 S-glutathionylated cysteines in human heart samples, with only some of these associated with the increased S-glutathionylation observed in diseased samples (Stathopoulou *et al.*, 2016). *In vitro*, using a recombinant form of the cMyBP-C N-terminal, C249 was found to be the predominant acceptor of S-glutathionylation, although S-glutathionylation at C623 and C651 was associated with increased Ca^{2+} sensitivity and reduced rate of cross-bridge development (Patel *et al.*, 2013; Stathopoulou *et al.*, 2016). For both S-nitrosylation and S-glutathionylation, a major disadvantage is the lack of evidence of cMyBP-C modification and function in-situ without using a pathological or pharmacological approach to increase the extent to which it is modified. One approach that has shown success in characterising cMyBP-C phosphorylation would be site directed mutagenesis of S-glutathionylation/S-nitrosylation cysteines, which could be achieved *in vitro* or *in vivo*. However, this method would be limiting as it would remove any other previously unreported cysteine modifications occurring at the same sites. With the estimation that there are over 400 types of PTMs, and cysteines are targeted by at least 10 of them, including palmitoylation, this is an important point to consider in any mutagenesis studies (Ramazi & Zahiri, 2021).

3.1.2 Palmitoylation and fatty acid accumulation

Aside from pharmacological compounds, the simplest approach to studying increased protein palmitoylation is supplementation with the fatty acid substrate, palmitate/palmitoyl-CoA. This enhances the palmitoylation of some proteins in cell culture, however the applicability of this approach *in vivo* has not been investigated (Gök *et al.*, 2020; Pei *et al.*, 2016). Nevertheless, this approach may have physiological relevance, as whilst fatty acids in the healthy heart are essential for ATP production, excess is associated with high fat diets, diabetes and insulin resistance (Burgoyne *et al.*, 2012; Glatz *et al.*, 2020). Increased myocardial work leads to increased fatty acid uptake and increased surface expression of the fatty acid transporting glycoprotein CD36 (Luiken *et al.*, 2003). CD36-null mice demonstrated that it accounts for ~70% of fatty acid uptake into cardiomyocytes and loss of CD36 is associated with protection against high fat diet induced cardiac dysfunction (Habets *et al.*, 2007; Steinbusch *et al.*, 2011; Sung *et al.*, 2011). At a

cardiomyocyte level, treatment with high concentrations of palmitate results in increased surface expression of CD36, and this was coupled with a reduction in peak sarcomere shortening which could be attenuated by inhibiting CD36 (Angin *et al.*, 2012).

Whilst the mechanisms are still being elucidated, excess fatty acid uptake, including that promoted by CD36, may contribute to a shift in the myocardium from using glucose as energy to using fatty acids, resulting in insulin insensitivity and eventual contractile dysfunction (Glatz *et al.*, 2020). However, despite numerous important cardiac substrates undergoing palmitoylation, the relationship between increased fatty acid uptake and palmitoylation remains relatively unknown. Nevertheless, studies in the brain and skeletal muscle indicate it may play an important role (Schianchi *et al.*, 2020). Of note, a high fat diet led to increased fatty acid uptake and insulin resistance in the brain, including increased palmitoylation of the AMPA glutamate receptor with knock on effects on synaptic plasticity (Spinelli *et al.*, 2017). In skeletal muscle, the protein kinase PKCε regulates TnI and MyBP-C phosphorylation, contributing to overall myofilament Ca^{2+} sensitivity (Kooij *et al.*, 2010). Hyper-palmitoylation and overactivity of PKCε was observed in palmitate-loaded myotubes where it was found to downregulate genes involved in insulin sensitivity, although any contribution to myofilament function was not investigated (Dasgupta *et al.*, 2011). Interestingly, CD36 itself is palmitoylated which induces its translocation to the cell surface, supporting the idea of a positive feedback loop that may be contributing to the disease phenotype, although this has been better studied in the context of non-alcoholic steatohepatitis (NASH; Zhao *et al.*, 2018). Going forward, it will be important to determine whether increased fatty acid availability, and likely increased palmitoylation of cardiac substrates, is involved in the regulation of cardiac contractility.

3.2 Aims

Cardiac MyBP-C is an essential regulator of myocardial contractility and is under the influence of an increasingly expanding profile of PTMs. Changes in cMyBP-C PTM status, particularly that of phosphorylation and the cysteine modification S-glutathionylation, promotes functional changes in the setting of HF (Main *et al.*, 2020). Palmitoylation is another dynamic cysteine modification which can alter the function of key cardiac ion transporters, including NCX1 and the Na^+/K^+ ATPase, and soluble proteins including Ras and G-proteins (Main & Fuller, 2021). Traditionally associated with membrane trafficking and localisation, the presence or function of palmitoylation on myofilament proteins has not been investigated. Previously, Acyl-RAC was used to purify all palmitoylated proteins from rat ventricular tissue, followed by mass spectrometry analysis (Supplementary Table 7.1). cMyBP-C was among the proteins identified as a novel cardiac palmitoylation substrate and follow up preliminary data demonstrated that it was palmitoylated in primary rabbit ventricular cardiomyocytes. The aim of this work is therefore to:

- Characterise the palmitoylation stoichiometry of cMyBP-C in primary cardiac tissues and isolated cells from animal models, including those with disease phenotypes, using Acyl-RAC

- Identify whether the palmitoylation cMyBP-C is altered in cardiac pathologies using samples from organ donors, HCM patients and ischaemic HF patients

- Identify chemical tools that can influence cMyBP-C palmitoylation including novel palmitoylation inhibitors

- Identify the palmitoylated cysteines in cMyBP-C using HEK293 cells and translate this finding to study the functional consequence of their palmitoylation on cMyBP-C function in cardiomyocytes

3.3 Methods

3.3.1 Palmitoylation peptide array

3.3.1.1 General principles and solid phase peptide synthesis

The past 30 years has seen the development of the peptide array technique, which has been widely used as a high throughput method for identifying protein-protein interaction sequences, post-translational modification sites and for antibody validation (Frank, 2002). The technique involves the synthesis of a series of peptides, normally 10-25 amino acids in length, onto a cellulose membrane which can typically hold up to 1000 unique peptide sequences. The sequences are entirely under an experimenter's control, and the process can be largely automated through array machines such as the Autospot Robot ASS 222 (Intavis, Germany) which was used in this case. The general principle involves the addition of an amino acid with an available carboxyl group to a cellulose membrane (Whatman 50 cellulose membrane, Sigma) and a coupling of the next amino acid in the sequence via its amino terminus. During the addition, the amino terminus of the next amino acid and the side changes of each amino acid are protected by an Fmoc (9-fluroenylmethyloxycarbonyl) group to prevent them from interacting spontaneously with the available carboxyl terminus until required. The amino terminus Fmoc is removed before each addition using piperidine in DMF (dimethylformamide) and the side chains are all de-protected in the final stage of the synthesis. Once synthesised, the membrane can be treated as a far-western involving overlaying a protein/chemical/antibody before using a suitable detection system to measure which sequences are involved in the interaction. Importantly, these sequences can be further narrowed down by creating shifted versions of a sequence (i.e. shifted by 5 amino acids at a time), sequentially truncating the peptide, or producing alanine substitutions of every amino acid to identify key residues involved in the interaction.

3.3.1.2 Adaptation of peptide array for detection of palmitoylation sites

A common modern method for detecting palmitoylation is the technique of click chemistry. As well as in living cells, this can also be utilised in cell-free systems using purified proteins. In this case, a novel method was developed combining the techniques of peptide array and click chemistry in an attempt to identify cMyBP-

C palmitoylation sites. After their synthesis as described above, membranes were submerged briefly in 100% ethanol before washing with PBS-T for 10 minutes to remove excess chemicals. Membranes were then blocked in 5% BSA for 1 hour at room temperature before incubation for 1 hour at room temperature in reaction buffer (50 mM Tris pH8.0, 1% Triton X-100 in dH_2O) containing 20 μM ODYA-CoA (9,12-octadecadiynoic acid; Sigma, O5636), a palmitoyl-CoA analogue which can spontaneously attach to available cysteine residues and contains an alkyne group. The hypothesis is that the ODYA-CoA will spontaneously react with cysteines that would be palmitoylated enzymatically, which has previously been shown for proteins, but has not been reported for peptides (Dietrich & Ungermann, 2004; Duncan & Gilman, 1998). The membranes were then washed 3 times for 10 minutes in reaction buffer before incubating for 1 hour at room temperature in click reaction mix (2 mM copper sulphate ($CuSO_4$), 0.2 mM Tris(benzyltrizolylmethyl)amine (TBTA) in dH_2O) containing 4 mM of an azide dye (either Cy5.5 azide (Click chemistry tools, 1059) or CW800 azide (LI-COR, 929-60002)). The membrane was then washed 5 times for 10 minutes using reaction buffer before visualisation on a LI-COR (Figure 3.2).

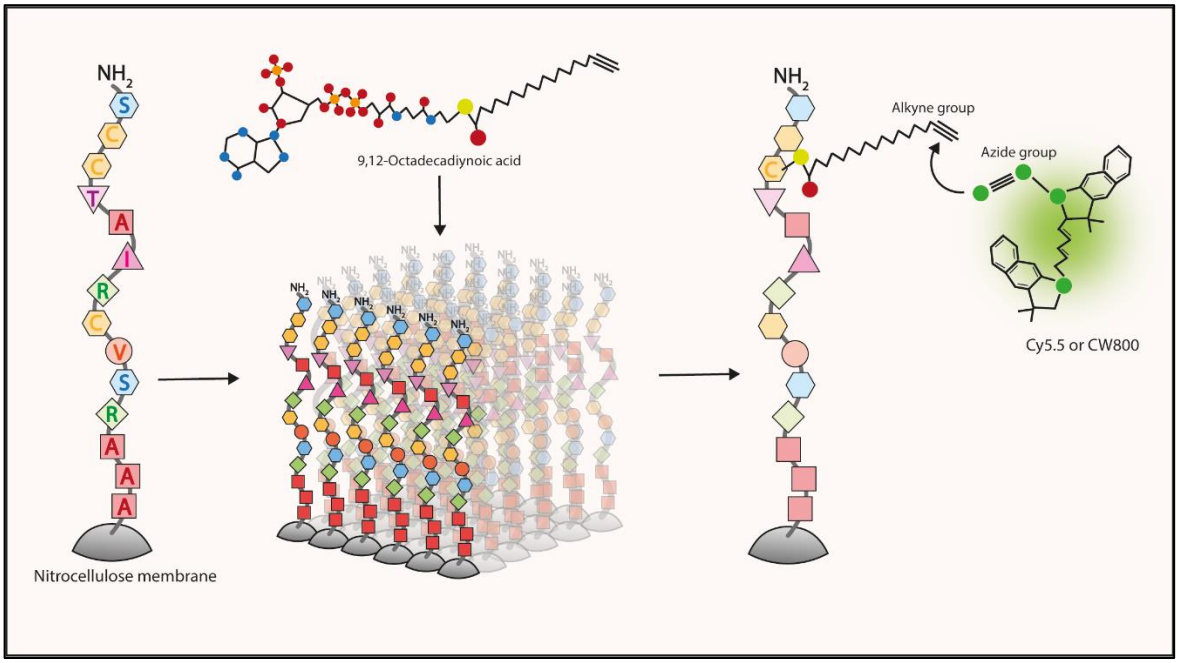

Figure 3.2. Palmitoylation peptide array strategy.
Peptides were designed and synthesised using a peptide array machine and prepared immobilised as spots on cellulose membrane, with multiple copies of the same peptide found per spot. Membranes were then incubated with 9,12-Octadecadiynoic acid (ODYA-CoA), a palmitoyl CoA analogue, which was hypothesised to conjugate to palmitoylatable cysteines within the array. The alkyne group of the ODYA-CoA can be "clicked" to the azide of the fluorescent Cy5.5 or CW800 molecule which can be visualised using a LI-COR imaging system.

3.3.2 Myofilament isolation and functional measurements in primary cardiomyocytes

3.3.2.1 Myofilament isolation and treatment

To determine the effect of pharmacologically palmitoylating myofilament proteins, myofilaments from adult rabbit cardiomyocytes were isolated and treated before analysis via Acyl-RAC or isometric force experiments. Whilst frozen cells could be used for biochemical measurements, for functional experiments fresh cells were used. In both cases cells were incubated with relaxing buffer (Na_2ATP (5.9 mM), $MgCl_2$ (6.04 mM), EGTA (2 mM), KCl (139.6 mM), Imidazole (10 mM) in dH_20, pH 7.4, pCa9.0) containing 0.5% triton and rotated at 4°C for 30 minutes to permeabilise the membrane and reveal the myofilaments. Myofilaments were then centrifuged at 4°C at 1200 RPM for 5 minutes before the supernatant was removed and discarded. The resulting myofilament pellet was then washed in relaxing buffer three times with centrifugation to remove any residual triton. For treatment, myofilaments were resuspended in relaxing buffer containing palmitoyl alkyne-coenzyme A (palmitoyl-CoA; 20 μM; Cambridge Biosciences, CAY15968) and rotated at 4°C for a further 30 minutes before centrifugation. For isometric force experiments, myofilament pellets were

resuspended in a 50% glycerol solution in relaxing buffer and stored at -20 until use.

3.3.2.2 Myofilament passive tension, active force and calcium sensitivity measurements

Mechanical myofilament measurements were performed at Amsterdam University under the supervision of Professor Jolanda van der Velden using a muscle mechanics workstation as previously described (van der Velden *et al.*, 1999). The system was maintained at 15^{o}C using a water bath and myofilaments viewed using an inverted microscope and a 5X (0.12NA) or a 32X (0.4NA) objective. Skinned myofilaments (preparation described in 3.3.2.1) were placed in relaxing buffer on a glass coverslip and individual cells were selected based on size and uniformity of striations. Individual myofilaments were then attached to thin, stainless-steel needles with one attached to a piezoelectric motor (Physike Instrumente, Waldbrunn, Germany) and the other attached to a force transducer (SensoNor, Horten, Norway). Overall cell length, width and sarcomere length was determined by using a CCD video camera and a spatial Fourier transform algorithm. Passive tension of the myofilament ($F_{passive}$) was determined by rapid shortening to 30% of the length of the cell at three different sarcomere lengths ranging from 2 μm to 2.2 μm (±0.005 μm) which has been reported to encompass the working range of the heart (Figure 3.3). The depth of the cell was estimated to be 80% of cell width. Active (F_{act}) and passive force of the myofilaments at a sarcomere length of 2.2 μM was determined in activating solution (pCa4.5, F_{max}), followed by submaximal Ca^{2+} (pCa6.0) and then activating solution again. The run down between the first and second activating solutions could then be determined and those with large rundowns (>25%) indicating potential cell detachment/loss of sarcomere length were excluded from analysis.

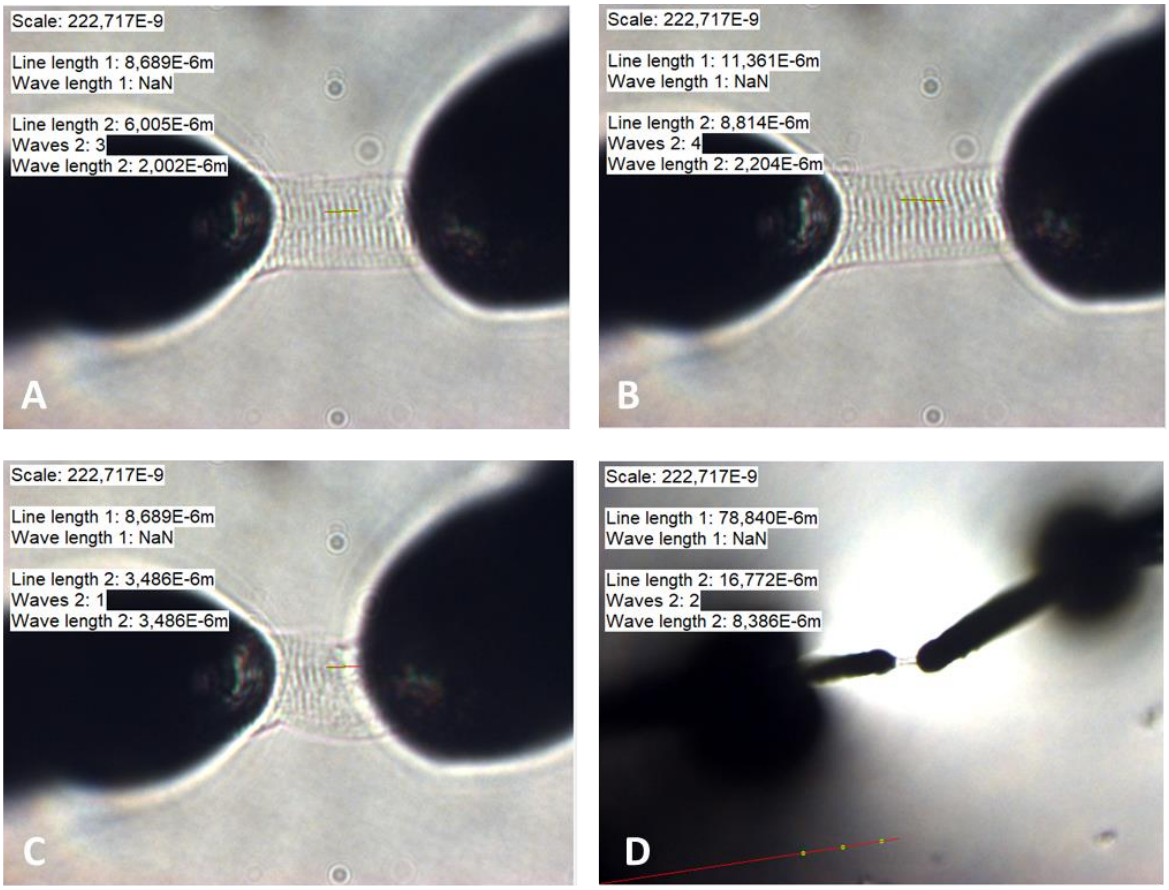

Figure 3.3. An example myofilament mounted to a muscle mechanics set up.
A single myofilament mounted between a force transducer needle (left) and a needle attached to an electric motor (right). The myofilament is then stretched to a desired sarcomere length (i.e. A = 2µm and B = 2.2µm). At the desired sarcomere length, the total length of the cell (needle to needle) can be determined, and the cell slackened by 30% of its length (as shown in C) to measure the passive tension. The cell can then be transferred between wells containing relaxing solutions and different concentrations of Ca^{2+} to measure active force (as shown in D). Images A-C were captured using a 32X (0.4NA) objective and image D using a 5X (0.12NA) objective.

3.3.3 Acyl-RAC of hypertrophic cardiomyopathy samples

Human heart tissue from organ donors and hypertrophic cardiomyopathy samples were kindly provided by Professor Jolanda van der Velden, Amsterdam University, collected as previously described with details displayed in Table 3.1 (Schuldt *et al.*, 2021). For Acyl-RAC, ~20 mg of ventricular tissue was homogenised to a fine powder in a mortar and pestle under liquid nitrogen before proceeding through the assay as described in 2.7.1.

Table 3.1. Human organ donor and hypertrophic cardiomyopathy information.

Record ID	Primary Diagnosis	Mutation type
1838LV	Organ Donor	
1840LV	Organ Donor	
1843LV	Organ Donor	
1850LV	Organ Donor	
D6008	Organ Donor	
D7040	Organ Donor	
D7054	Organ Donor	
HCM 113	Hypertrophic cardiomyopathy	MYBPC3
HCM 120	Hypertrophic cardiomyopathy	MYBPC3
HCM 123	Hypertrophic cardiomyopathy	MYBPC3
HCM 133	Hypertrophic cardiomyopathy	MYBPC3
HCM 169	Hypertrophic cardiomyopathy	MYBPC3
HCM 204	Hypertrophic cardiomyopathy	MYBPC3
HCM 219	Hypertrophic cardiomyopathy	MYBPC3
HCM 231	Hypertrophic cardiomyopathy	MYL2
HCM 233	Hypertrophic cardiomyopathy	SMN
HCM 234	Hypertrophic cardiomyopathy	TNNT2
HCM 236	Hypertrophic cardiomyopathy	MYH7
HCM 239	Hypertrophic cardiomyopathy	SMN
HCM 244	Hypertrophic cardiomyopathy	SMN
HCM 255	Hypertrophic cardiomyopathy	SMN
HCM 256	Hypertrophic cardiomyopathy	MYBPC3
HCM 257	Hypertrophic cardiomyopathy	SMN
HCM 259	Hypertrophic cardiomyopathy	MYH6 (VUS, class 3)
HCM 261	Hypertrophic cardiomyopathy	SMN
HCM 263	Hypertrophic cardiomyopathy	MYBPC3
HCM 265	Hypertrophic cardiomyopathy	MYBPC3
HCM 276	Hypertrophic cardiomyopathy	SMN

3.4 Results

3.4.1 Palmitoylation of cMyBP-C in primary cardiomyocytes

3.4.1.1 Palmitoylation of sarcomeric proteins in cardiac tissue from animal models

Palmitoylation is important for regulating the localisation, function, and protein-protein interactions of several cardiac substrates including ion channels and signalling molecules, however its relevance for myofilament proteins has not been widely reported. As such, acyl-resin assisted capture (Acyl-RAC) was used to purify palmitoylated proteins from ventricular cardiomyocytes isolated from adult rabbit, rat and mouse, whilst the same approach was used on homogenised ventricular tissue from neonatal rat hearts. Acyl-RAC revealed that ~10% of myosin, actin and cMyBP-C are all palmitoylated in these tissues, whilst no measurable palmitoylation was detected for Tm, TnT or TnI. As it is constitutively palmitoylated with a high stoichiometry, Caveolin-3 was included as an assay control (Howie *et al.*, 2014; Figure 3.4 and Supplementary Figure 7.1).

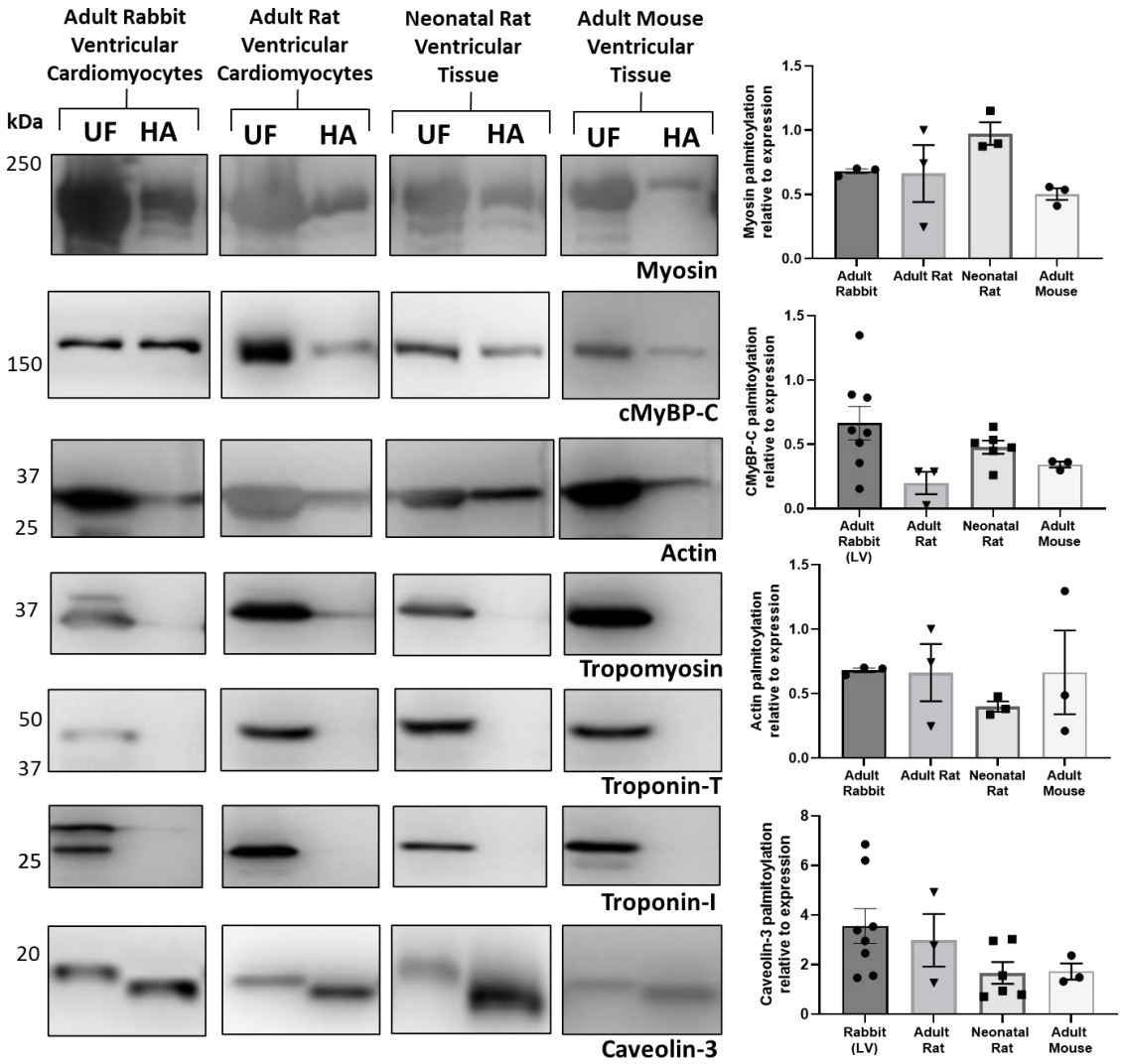

Figure 3.4. Palmitoylation of myofilament proteins in the cardiac tissue of animal models. Acyl-resin assisted capture (Acyl-RAC) was used to purify palmitoylated proteins from rabbit ventricular cardiomyocytes (male, 12-week-old), rat ventricular cardiomyocytes (male, 12-week-old), neonatal rat ventricular tissue (male and female, 1-4 days old) and adult mouse ventricular tissue (male, 20 weeks old). Palmitoylation of myosin, cMyBP-C, actin, tropomyosin, troponin-T troponin-I and assay control Caveolin-3 was determined and palmitoylated fraction (HA, hydroxylamine dependent) normalised to total protein (UF, unfractionated) with percentage palmitoylation versions found in Supplementary Figure 7.1. Acyl-RAC revealed myosin, actin and cMyBP-C are palmitoylated in all animal model tissues. Data is mean ±S.E.M.

3.4.1.2 TCEP and DTT pre-treatment in rabbit cardiomyocytes

As MyBP-C's critical control over myofilament function is fine-tuned by an increasingly developing list of PTMs, the rest of this chapter will focus on characterising the palmitoylation of cMyBP-C. A disadvantage of the Acyl-RAC technique is that the initial methylation of free cysteines may not be efficient for cysteines that are involved in other transient reactions that then become free to capture later in the process, providing false positives (Main & Fuller, 2021). Although the reaction is completed in a 2.5% SDS buffer to reduce this, cysteines 436 and 443 of cMyBP-C reportedly form a disulphide bond which could evade initial methylation and disulfide change with the thiopropryl sepharose beads

(Sadayappan & de Tombe, 2012). As such, prior to Acyl-RAC, samples were treated with 10 mM Tris(2-carboxyethyl)phosphine (TCEP) or dithiothreitol (DTT) to ensure reduction of disulphide bonds. This pre-treatment did not result in a significant change in cMyBP-C palmitoylation, suggesting false positives due to disulphide bond formations are not contributing to cMyBP-C palmitoylation level and therefore Acyl-RAC is an appropriate method to study cMyBP-C palmitoylation (Figure 3.5).

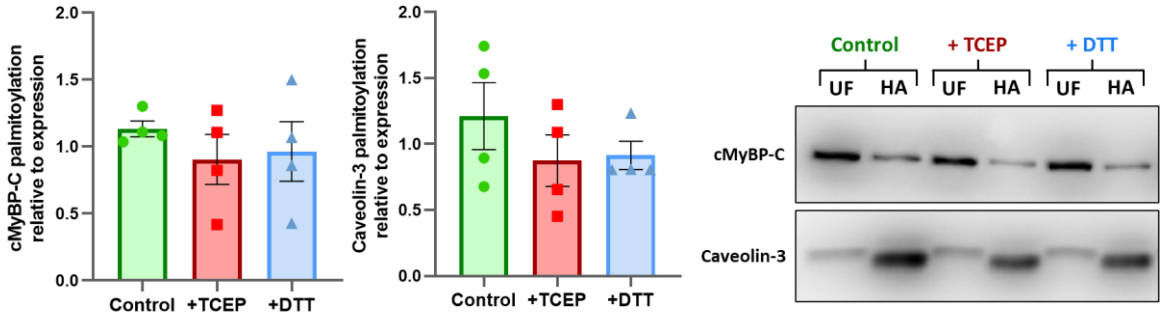

Figure 3.5. Palmitoylation of cMyBP-C in the presence of Tris(2-carboxyethyl)phosphine (TCEP) and Dithiothreitol (DTT).
Prior to detection of palmitoylated cMyBP-C, rabbit ventricular cardiomyocyte lysates were treated for 10 minutes with 10 mM DTT or TCEP to reduce disulphides. Palmitoylation of cMyBP-C and assay control Caveolin-3 was then determined by Acyl-Resin Assisted Capture (Acyl-RAC) and palmitoylated fraction (HA, hydroxylamine dependent) normalised to total protein (UF, unfractionated). There was no significant difference in palmitoylation level with TCEP or DTT addition compared with no pre-treatment (control). N=4-8 per group. Data is mean ±S.E.M normalised to the experimental average and analysed via a one-way ANOVA with a Dunnett's *post hoc* test.

3.4.1.3 Palmitoylation of cMyBP-C in different anatomical regions

The cardiac isoform of MyBP-C is expressed in the cardiac tissue exclusively, but is located in both ventricular, septal (region between left and right ventricles) and atrial tissue (Lin *et al.*, 2013; Sadayappan & de Tombe, 2012). However, regional specific variations in cMyBP-C PTM modification has been unstudied or underreported thus far. Acyl-RAC was used to purify palmitoylated proteins from different anatomical regions of the rabbit heart to determine whether levels of cMyBP-C palmitoylation varied by region. In ventricular tissue, cMyBP-C was palmitoylated in the left, right and septal region, however there may be higher levels in the left ventricle compared to the right. cMyBP-C was also palmitoylated in the left atrium, although to a lesser extent, with no palmitoylation detected in the right atrium (Figure 3.6). As such, ventricular cardiomyocytes were deemed a more suitable system to characterise cMyBP-C palmitoylation further.

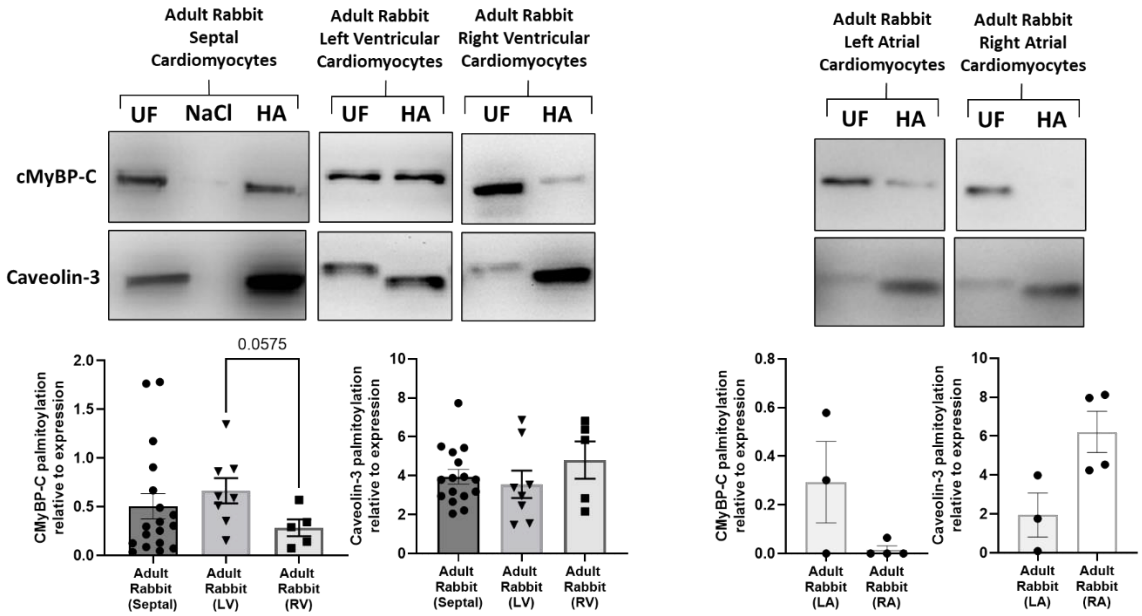

Figure 3.6. Palmitoylation of cMyBP-C in different anatomical regions of the rabbit heart. Cardiomyocytes were isolated from the adult rabbit heart and separated into left ventricular (LV), right ventricular (RV), septal region (between right and left ventricle), left atrium (LA) and right atrium (RA). Palmitoylation of cMyBP-C and assay control Caveolin-3 was then determined by Acyl-Resin Assisted Capture (AcylRAC) and palmitoylated fraction (HA, hydroxylamine dependent) normalised to total protein (UF, unfractionated), with sodium chloride used as a negative control (NaCl). Statistical comparison between left and right ventricle made via an unpaired student's t-test. Data is mean ±S.E.M.

3.4.1.4 Localisation of palmitoylated cMyBP-C in the cardiac myofilament

cMyBP-C is anchored to the myofilament predominantly by electrostatic interactions of its C-terminal domains with the LMM portion of the myosin backbone and titin, and any population of functional cMyBP-C located outside the myofilament has not been reported (Lee *et al.*, 2015). However, as palmitoylation is traditionally associated with subcellular membrane attachment, the question arises as to whether the palmitoylated fraction of cMyBP-C may be attached to a membrane and localised outside the myofilament. To investigate this, myofilament subcellular fractionation was used to separate membrane/soluble proteins from the myofilament lattice and associated proteins by permeabilising cells in 1% Triton X-100. No expression of cMyBP-C was detected in the soluble/membrane fraction of these cells, indicating all of cMyBP-C is localised in the myofilament. Furthermore, the electrostatic interactions that anchor cMyBP-C to the myofilament can be disrupted by treatment with a high concentration of sodium chloride (NaCl; Gaspar *et al.*, 2020) As such, the myofilament pellet was further fractionated into proteins with less affinity for the myofilament lattice, and therefore soluble in 500 mM sodium chloride (soluble), and those with greater affinity for the myofilament lattice, and therefore not solubilised by 500 mM NaCl

(pellet). The majority of cMyBP-C was found to be soluble in NaCl, with a smaller fraction insoluble, however when these fractions were analysed for their level of palmitoylation via Acyl-RAC, this insoluble fraction of cMyBP-C had a higher level of palmitoylation stoichiometry compared to the soluble fraction (Figure 3.7).

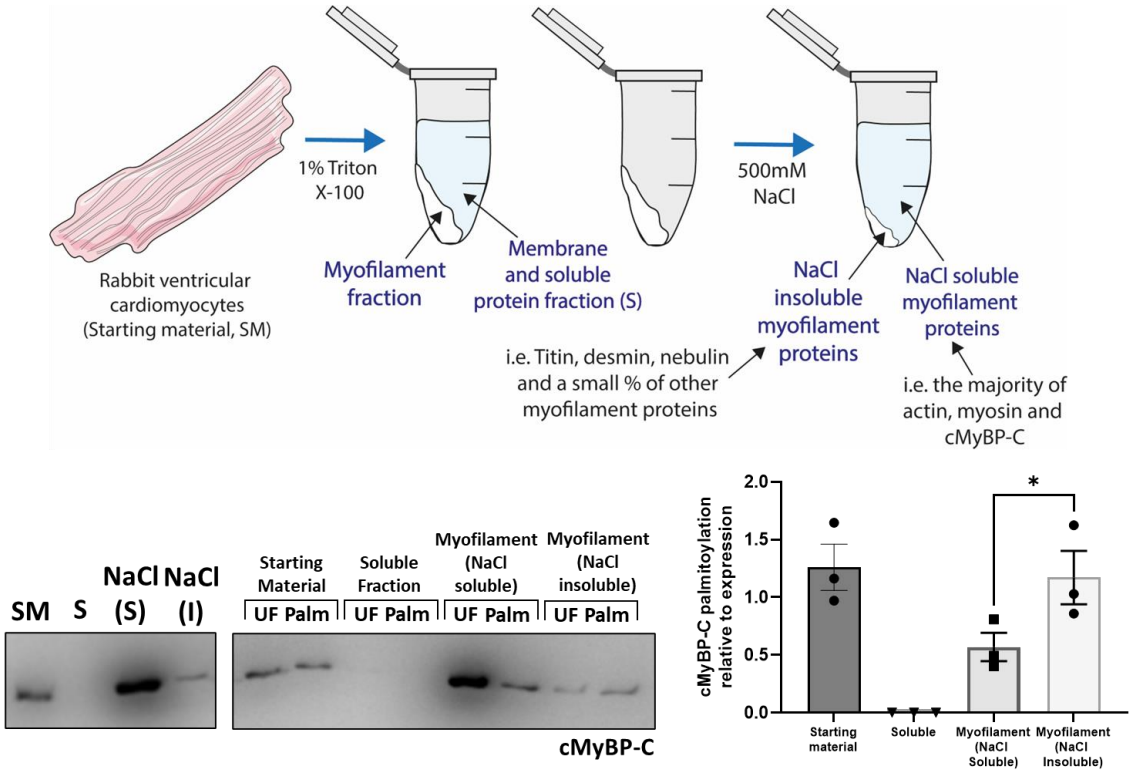

Figure 3.7. Localisation of the palmitoylated fraction of cMyBP-C in rabbit ventricular cardiomyocytes.
Prior to detection of palmitoylated cMyBP-C, a myofilament extraction protocol was performed whereby rabbit septal cardiomyocytes were homogenised in F60 buffer with 1% Triton X-100. A sample was taken for starting material (SM) before fractionation by centrifugation into soluble (S, cytosolic and membrane fraction) and myofilament lattice. The myofilament lattice was further fractionated into myofilament proteins soluble in 500 mM NaCl (NaCl S) and those insoluble in 500 mM NaCl (NaCl I). Palmitoylation of cMyBP-C in each fraction was determined by Acyl-Resin Assisted Capture (Acyl-RAC) with palmitoylation (HA, hydroxylamine dependent) normalised to abundance in that particular fraction (UF, unfractionated). Acyl-RAC revealed that palmitoylated cMyBP-C is found in the myofilament, but most palmitoylated cMyBP-C is insoluble in 500 mM NaCl. Statistical comparison of myofilament (soluble) vs myofilament (insoluble) made by a one-way ANOVA with a Sidak's *post hoc* test. Data is mean ±S.E.M normalised to the experimental average. *p<0.05.

Interest in palmitoylation as a dynamic modification was hampered for several years under the impression it was a non-enzymatic modification that relied on local concentration of palmitoyl CoA. This is due to substrates, including the DHHC-PATs themselves, being able to auto-palmitoylate on cysteines (Rana, Lee, *et al.*, 2018). Whilst enzyme regulation in palmitoylation has since been well established, tools to induce auto-palmitoylation remain a powerful tool to study the effect of increasing substrate palmitoylation. In order to more directly target cMyBP-C palmitoylation, isolated myofilaments were treated with palmitoyl-CoA

and Acyl-RAC revealed this led to a significant increase in overall cMyBP-C palmitoylation (Figure 3.8).

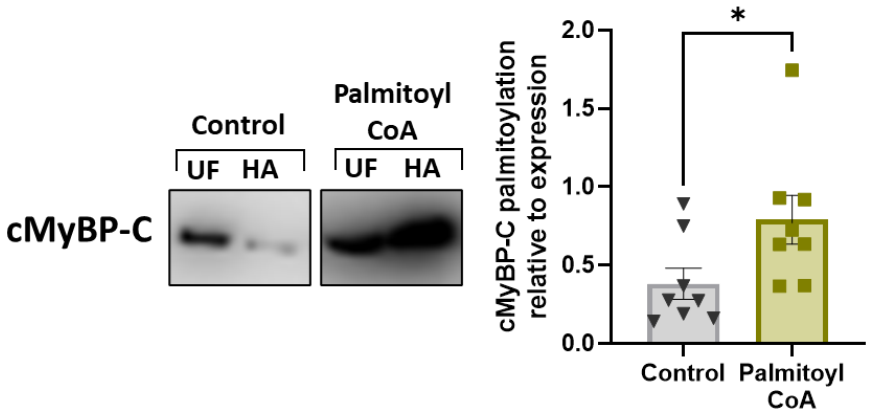

Figure 3.8. Palmitoylation of cMyBP-C in isolated rabbit ventricular myofilaments treated with palmitoyl CoA.
The effect of palmitoyl CoA (20 µM), which can spontaneously palmitoylate solvent exposed cysteines, was tested using myofilaments isolated from rabbit ventricular cardiomyocytes. Myofilaments were treated for 30 minutes with palmitoyl CoA before centrifugation and collecting of the myofilament pellet. Palmitoylation was determined by Acyl-Resin Assisted Capture (Acyl-RAC) and total protein (UF, unfractionated) compared to palmitoylated fraction (hydroxylamine dependent, HA). Palmitoyl CoA significantly increased cMyBP-C palmitoylation in the myofilament. Data is mean ±S.E.M analysed via a student's unpaired t-test. *p<0.05.

3.4.2 Palmitoylation of cMyBP-C in cardiac disease

PTMs of cMyBP-C are not only important for its physiological control of myofilament function, but as also dysregulated in pathological conditions including HCM, post-MI and in HF (Main *et al.*, 2020). This includes phosphorylation, reduced levels of which have been reported in MI, HF, HCM, DCM and ICM (Kuster *et al.*, 2012). Conversely, elevated levels of the cysteine modification S-glutathionylation have associated been associated with DCM and ischaemic HF (Budde *et al.*, 2021; Stathopoulou *et al.*, 2016). Understanding how the cMyBP-C PTM profile varies in disease is essential to understanding how to appropriately target it for cardiac disease therapy.

3.4.2.1 Palmitoylation of cMyBP-C in a rabbit model of heart failure

The rabbit heart remains an excellent model for human cardiac function, as the electrophysiological profile closely resembles that of human in terms of action potential shape and expression pattern of key ion channels (Ellermann *et al.*, 2021). In particular when modelling HF, mouse models have been shown to vary dramatically from humans in changes in Ca^{2+} cycling during contraction and

relaxation, with the rabbit model more accurately reflecting the changes in Ca^{2+} flux during human HF (Bers, 2002b; Sanbe *et al.*, 2005). In order to investigate changes in cMyBP-C palmitoylation in the setting of HF, a rabbit model was subjected to a left anterior descending coronary ligation to induce an MI, followed by maintenance for 8 weeks. The induction of the HF phenotype was confirmed via electrocardiogram measurements of LVEF, which was <45% in the MI group (Kettlewell *et al.*, 2009). Cardiomyocytes were then isolated from the left ventricular and septal region of the rabbit heart, along with control rabbits, and palmitoylation of cMyBP-C was determined by Acyl-RAC. In the left ventricle, cMyBP-C palmitoylation was significantly reduced in the MI model compared to control, whilst no significant difference was observed in the septal region or in assay control Caveolin-3 (Figure 3.9).

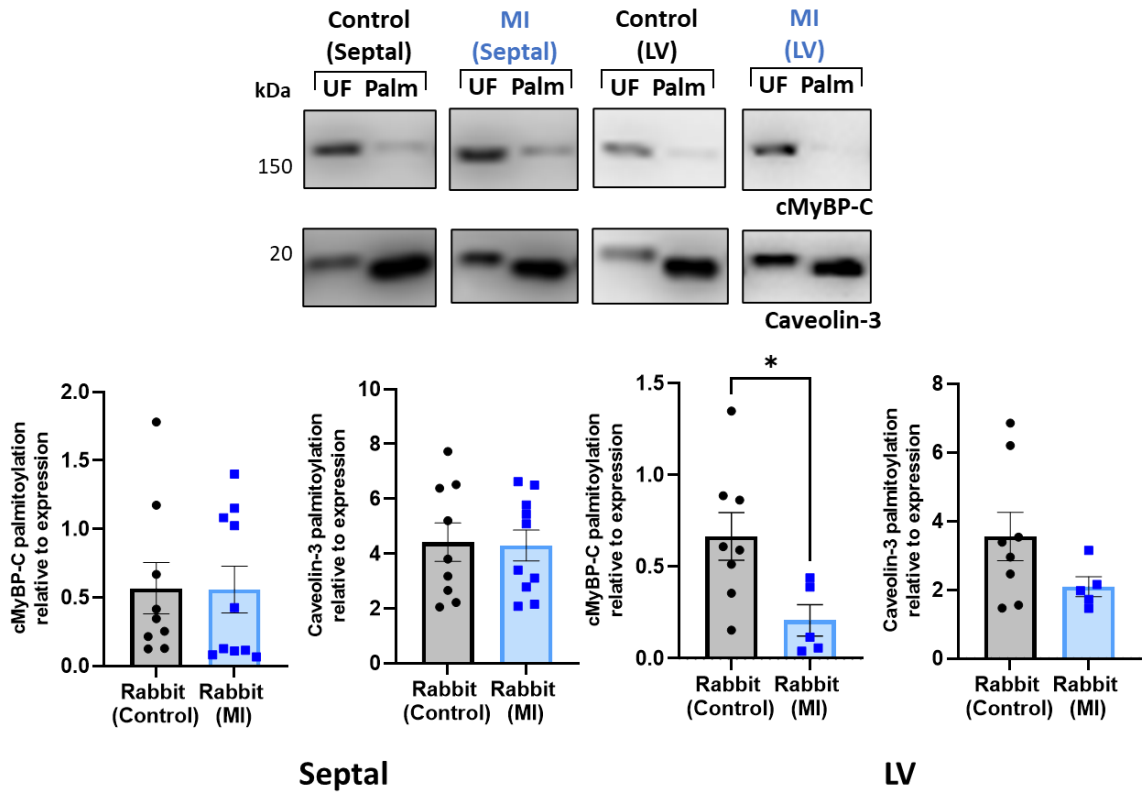

Figure 3.9. Palmitoylation of cMyBP-C is reduced in the left ventricular region of the rabbit heart following myocardial infarction (MI).
Ventricular cardiomyocytes were isolated from septal and left ventricular (LV) regions of the rabbit heart. Rabbits were either stock/sham at 12/20 weeks of age, or a model of myocardial infarction (MI) whereby the rabbits underwent left anterior descending coronary artery ligation at 12 weeks of age before being maintained for a further 8 weeks. Palmitoylation of cMyBP-C and assay control Caveolin-3 was determined by Acyl-Resin Assisted Capture (Acyl-RAC) and palmitoylated fraction (HA, hydroxylamine dependent) normalised to total protein (UF, unfractionated). Palmitoylation of cMyBP-C was reduced in cardiomyocytes from the left ventricle, but not septal, region of the rabbit heart following MI (*p<0.05). Data is mean ±S.E.M analysed by a student's unpaired t-test.

3.4.2.2 Palmitoylation of cMyBP-C in a pig model of heart failure

Similarly, the pig is a useful tool for modelling human cardiac function, with advantages including comparable coronary anatomy, heart rate and heart to body weight size with humans. In terms of HF, the pig has been a useful model for studying post-MI LV remodelling as they show a reproducible, progressive infarct over several weeks with localisation in the mid/sub-endocardium (Dixon & Spinale, 2009). This model also offers the advantage over the rabbit model in that it is a model of ischaemia followed by reperfusion, which may more accurately reflect the human clinical situation (Baehr *et al.*, 2019). Acyl-RAC was used to purify palmitoylated proteins from both sham and post-MI ventricular tissue, obtained from Professor Roger Hajjar, Mount Sinai Research Institute. Although not statistically significant, there may be lower levels of cMyBP-C palmitoylation in the MI ventricular tissue compared to sham control, with no significant change in assay controlled Flotillin-2 (Caveolin-3 not detected in pig tissue, Figure 3.10).

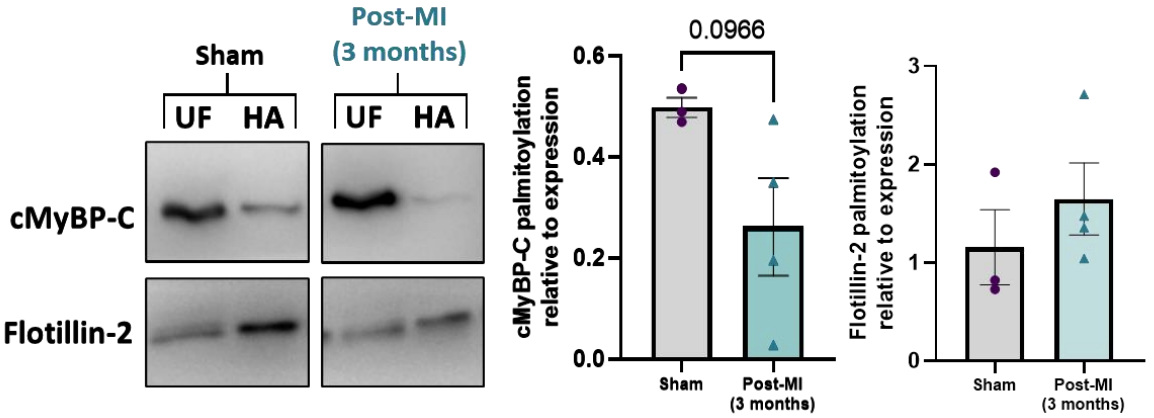

Figure 3.10. Palmitoylation of cMyBP-C may be decreased in a porcine model of HF. Cardiac tissue from pigs was obtained 3 months post-MI myocardial infarction (MI) along with sham controls. Palmitoylation of cMyBP-C and assay control Flotillin-2 (Caveolin-3 not detected in pig tissue) was determined by Acyl-Resin Assisted Capture (Acyl-RAC) and palmitoylated fraction (hydroxylamine dependent, HA) normalised to total protein (UF, unfractionated). Palmitoylation of the of cMyBP-C shows a trend to decrease in MI tissue compared to control (p=0.0966) and no change observed in Flotillin-2. Additionally, levels of p-cMyBP-C (normalised to total cMyBP-C) are not significantly different between groups. Data is mean ±S.E.M analysed via a student's unpaired t-test.

3.4.2.3 Palmitoylation of cMyBP-C in a rat model of type-2 diabetes

As the models of cardiac injury and HF progression suggest cMyBP-C palmitoylation levels may be reduced, the question arises as to whether this is specific to an ischaemic insult on the cardiac tissue, or whether cardiac dysfunction developed by other means show the same changes. Many cases of HF and ischaemic heart disease cases are associated with co-morbidities such as type-2 diabetes and lipid metabolism disorders (Loosen *et al.*, 2022). Type-2 diabetes and obesity are associated with elevated levels of fatty acids and increased palmitoylation of substrates, although studies in a cardiovascular context have been limited (Schianchi *et al.*, 2020). To investigate changes in cMyBP-C palmitoylation in the setting, samples from a rat model of type-2 diabetes were obtained from Professor Lisa Heather, University of Oxford. This model involves a low dose of streptozotocin in combination with a high fat diet which induces changes in cardiac metabolism and an increased in non-esterified fatty acids (Mansor *et al.*, 2013). Acyl-RAC of ventricular tissue from type-2 diabetic rats and controls revealed there was no significant change in cMyBP-C palmitoylation in these samples (Figure 3.11).

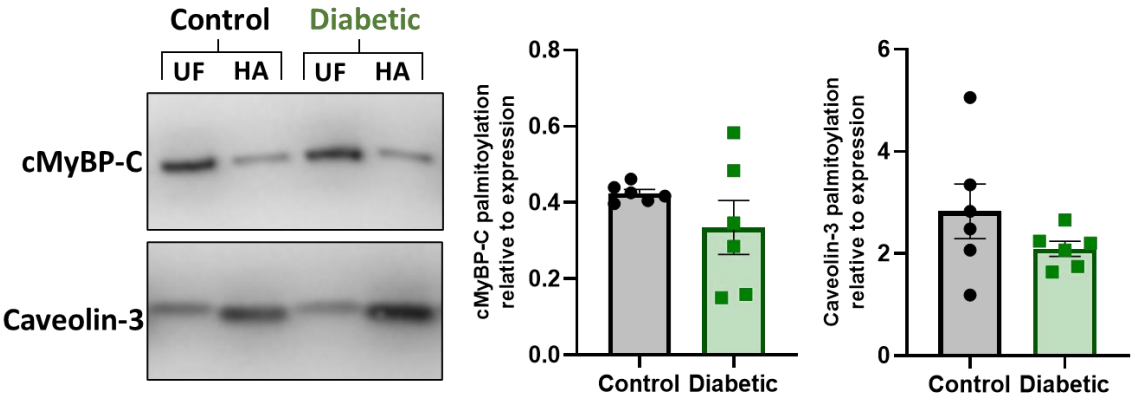

Figure 3.11. Palmitoylation of cMyBP-C is unchanged between control and a rat model of type-2 diabetes.
Samples were obtained from Professor Lisa Heather (University of Oxford) including control and a rat model of type-2 diabetes (high fat diet leading non-esterified fatty acid excess). Palmitoylation of cMyBP-C and assay control Caveolin-3 was determined by Acyl-Resin Assisted Capture (Acyl-RAC) palmitoylated fraction (HA, hydroxylamine dependent) normalised to total protein (UF, unfractionated). There was no significant difference in palmitoylation levels of cMyBP-C or Caveolin-3 between samples. Data is mean ±S.E.M analysed by a student's unpaired t-test.

3.4.2.4 Palmitoylation of cMyBP-C in ischaemic human heart failure

As cMyBP-C appears either reduced or unchanged in animal models of cardiovascular disease, it is important to determine whether this is representative of the human condition. As such, Acyl-RAC was used to purify palmitoylated proteins from ventricular endocardium samples from ischaemic human HF patients and organ donor controls (details in Table 2.10). Analysis of cMyBP-C expression revealed no significant differences, whilst phosphorylation at S282 was reduced although not significantly (p=0.0537). In terms of palmitoylation, there was a significant increase in cMyBP-C palmitoylation in HF samples compared to organ donors (Figure 3.12).

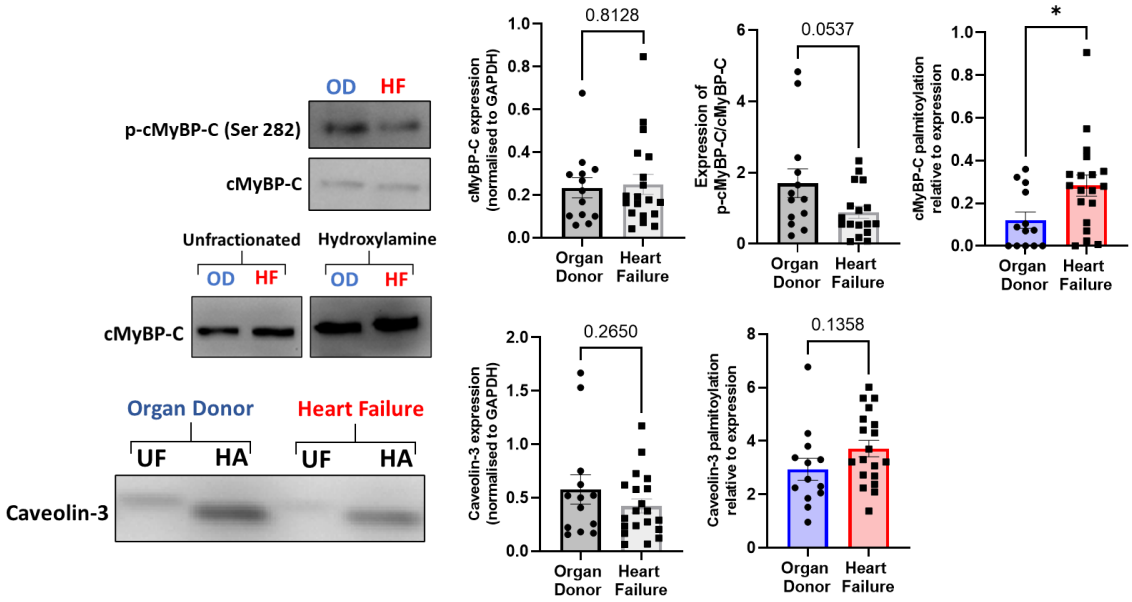

Figure 3.12. Expression, palmitoylation and phosphorylation of cMyBP-C and Caveolin-3 in organ donor and human heart failure ventricular endocardium.
Expression and palmitoylation of cMyBP-C and assay control Caveolin-3 was determined by Acyl-Resin Assisted Capture (Acyl-RAC) in ventricular endocardium from organ donor and ischaemic heart failure samples, represented as palmitoylated protein (HA, hydroxylamine dependent) normalised to total protein (UF, unfractionated). Palmitoylation of cMyBP-C is significantly increased in HF samples compared to organ donor, with no significant change in overall expression and a trending decrease in phosphorylation (p=0.0537). *p<0.05. Data is mean ±S.E.M analysed via an unpaired student's t-test.

The study of transplanted tissue and organ donor controls is very useful for understanding the underlying mechanisms of disease pathogenesis. However, patients are heterogenous and often come with several comorbidities, pharmacological interventions and lifestyle factors that add a great deal of complexity. As such, samples were stratified based on sex, age, BMI, comorbidities and interventions to determine whether there were any additional factors influencing cMyBP-C palmitoylation level in these sample. When divided based on sex, whilst overall cMyBP-C expression did not change between organ donor and HF samples of either sex, cMyBP-C phosphorylation at S282 may be lower in female samples (organ donor vs. HF, p=0.1112) but not male samples (organ donor vs. HF p>0.999). In contrast, cMyBP-C palmitoylation was increased, although not significantly, in male samples (organ donor vs HF, p=0.0623) but not female samples (organ donor vs HF, p=0.3796). Although there may be sex-specific changes when comparing organ donor to HF samples, comparison of female and male organ donor samples showed no significant differences in phosphorylation or palmitoylation (Figure 3.13). Additionally, a follow up study was also completed using neonatal rat ventricular tissue samples from healthy male and female

animals, and revealed no significant difference in palmitoylation between healthy males and females (Figure 3.14).

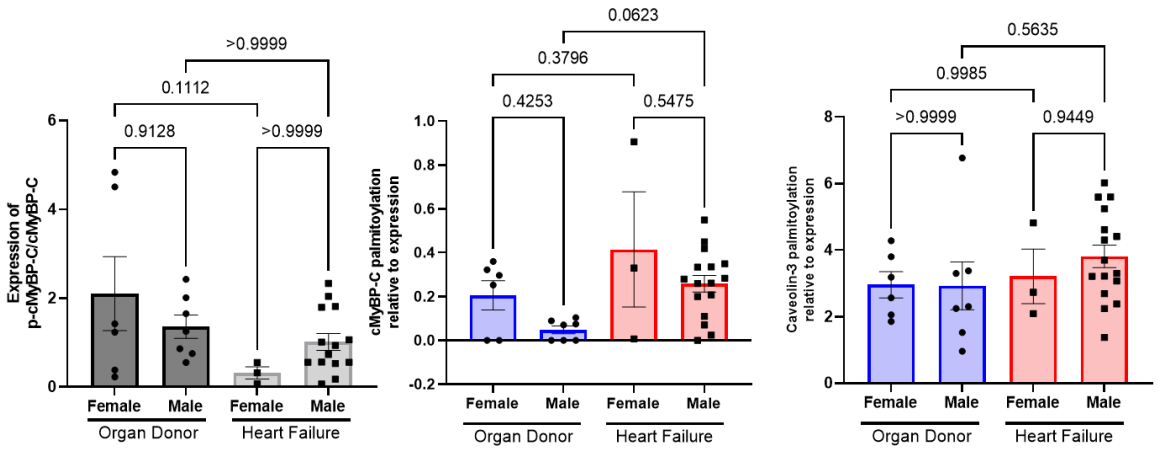

Figure 3.13. Palmitoylation of cMyBP-C in male and female organ donor and heart failure ventricular endocardium.
Palmitoylation of cMyBP-C and Caveolin-3 was determined by Acyl-Resin Assisted Capture (Acyl-RAC) in ventricular endocardium from organ donor and ischaemic heart failure, and split into groups based on sex. Palmitoylation is plotted as palmitoylated protein (HA, hydroxylamine dependent) relative to total protein (UF, unfractionated). Palmitoylation of cMyBP-C is increased in male heart failure samples (ANOVA, $p<0.05$; *post hoc* comparison $p=0.06$) compared to organ donor but the same trend is not observed in females. Additionally female heart failure samples may have the lowest level of p-cMyBP-C. There is no significant difference in palmitoylation of Caveolin-3 between any groups. Statistical comparisons made one-way ANOVA followed by a Dunnett's *post hoc* test. *$p<0.05$. Data is mean ±S.E.M.

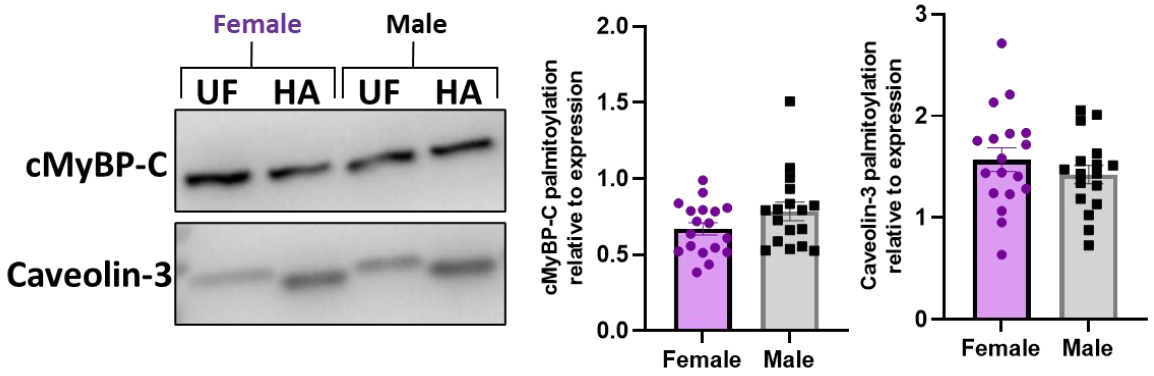

Figure 3.14. Palmitoylation of cMyBP-C in male and female neonatal cardiac tissue.
Palmitoylation of cMyBP-C and Caveolin-3 was determined by Acyl-Resin Assisted Capture (Acyl-RAC) in ventricular cardiac tissue from 1-4 day old male and female neonatal Sprague Dawley rats. Palmitoylation of cMyBP-C or Caveolin-3 is not significantly different between male and female animals. Palmitoylation (HA, hydroxylamine dependent) was normalised to total protein (UF, unfractionated). Data is mean ±S.E.M analysed via an unpaired student's t-test.

3.4.2.5 Palmitoylation of cMyBP-C in hypertrophic cardiomyopathy

Although cMyBP-C has recently been associated with ischaemic HF development, it was initially of interest as the most commonly mutated protein in HCM

(Schlossarek *et al.*, 2011). The majority of mutations result in a loss of total cMyBP-C due to haploinsufficiency (Marston *et al.*, 2009; van Dijk *et al.*, 2009). In order to determine whether changes in cMyBP-C palmitoylation are relevant in HCM, ventricular samples from HCM patients and organ donor controls were homogenised and Acyl-RAC used to purify palmitoylated proteins. HCM samples were grouped by mutation, encompassing those with *MYBPC3* mutations, those with other sarcomeric mutations (*MYH7, MYL2* and *TNNT2*) and those with non-sarcomeric mutations (sarcomere-null, SMN). Total cMyBP-C was significantly less in *MYBPC3* mutation group compared to organ donor control. There was no significant change in cMyBP-C palmitoylation in any HCM group compared to organ donor controls (Figure 3.15).

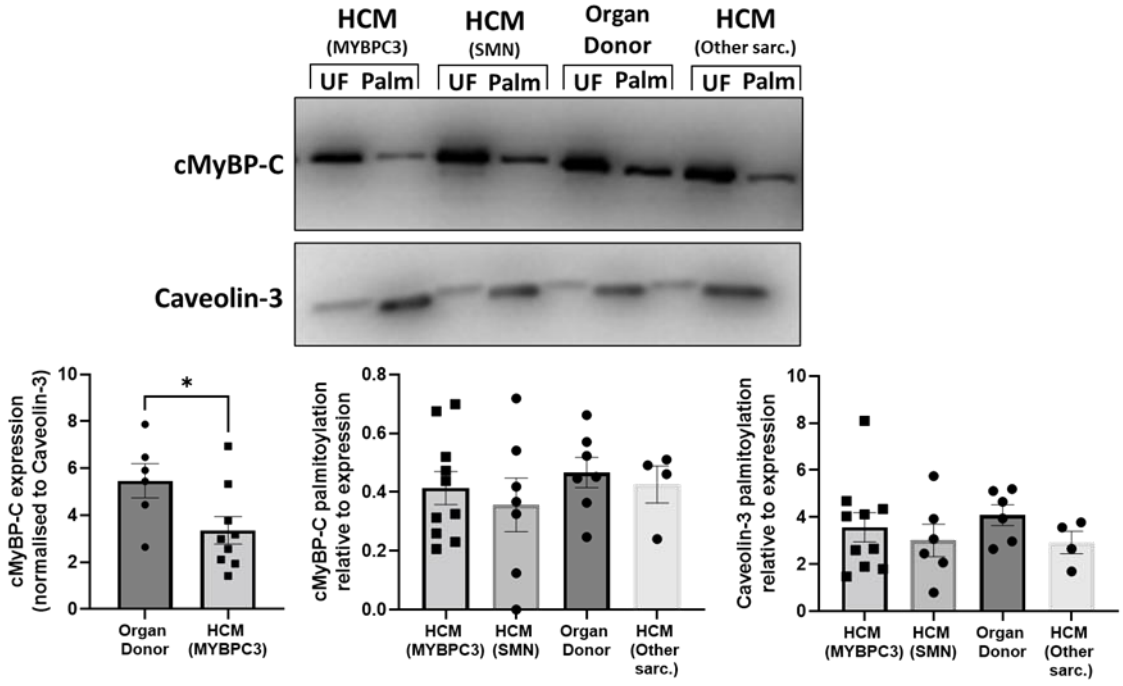

Figure 3.15. Palmitoylation of cMyBP-C in hypertrophic cardiomyopathy samples. Palmitoylation of cMyBP-C and assay control Caveolin-3 was determined by Acyl-Resin Assisted Capture (Acyl-RAC) in ventricular tissue from organ donor and hypertrophic cardiomyopathy (HCM) samples with either *MYBPC3* mutations, non-sarcomeric mutations (SMN) or other sarcomeric mutations (*MYH7, MYL2* and *TNNT2*). Results are represented as palmitoylated protein (HA, hydroxylamine dependent) normalised to total protein (UF, unfractionated). There was no significant difference in cMyBP-C or Caveolin-3 palmitoylation between groups. Data is mean ±S.E.M analysed via a One-way ANOVA with a Tukey *post hoc* test.

3.4.2.6 Palmitoylation of skeletal isoforms of MyBP-C

The findings here that MyBP-C is palmitoylated in cardiac tissue and changes in disease state that may translate to the study the skeletal isoforms of MyBP-C, which as themselves dysregulated in skeletal myopathy and several modifications including phosphorylation, target all three isoforms although not all sites are

shared between them (McNamara & Sadayappan, 2018). As such, Acyl-RAC was used to purify palmitoylated proteins from both mouse and neonatal rat homogenised skeletal tissue (hindlimb biopsy) and revealed both the fast skeletal (fs-MyBP-C) and slow skeletal (ss-MyBP-C) are palmitoylated in these tissues (Figure 3.16 and Supplementary Figure 7.1), suggesting palmitoylation is not a unique modification for cMyBP-C and importantly the findings here may be of interest in skeletal myopathies.

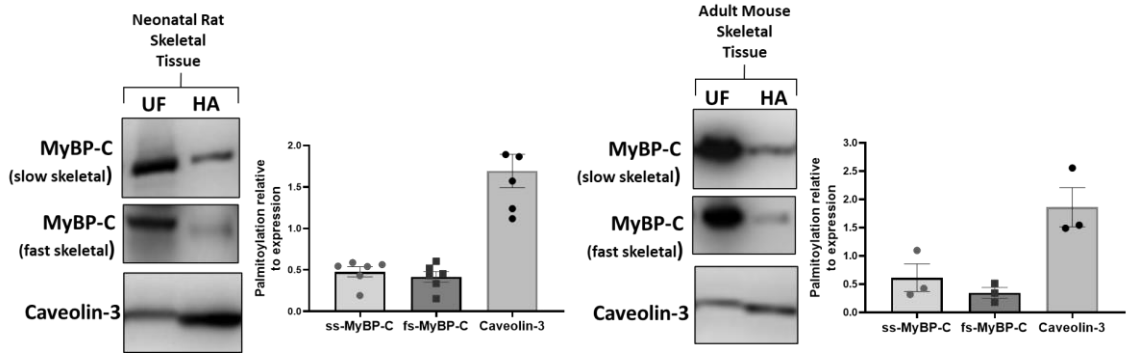

Figure 3.16. Palmitoylation of slow and fast skeletal isoforms of MyBP-C.
Palmitoylation of slow skeletal MyBP-C (ssMyBP-C) and fast skeletal MyBP-C (fs-MyBP-C) along with assay control Caveolin-3 was determined by Acyl-Resin Assisted Capture (Acyl-RAC) in skeletal tissue from 1-4 day old male and female neonatal rats and adult mice (male, 20 weeks). Palmitoylation (HA, hydroxylamine dependent) was normalised to total protein (UF, unfractionated) with percentage palmitoylation versions found in Supplementary Figure 7.1.. Acyl-RAC revealed both ssMyBP-C and fsMyBP-C are palmitoylated in skeletal tissue. Data is mean ±S.E.M.

3.4.3 Characterising tools to study cMyBP-C palmitoylation

3.4.3.1 Palmitoylation of cMyBP-C in cultured cells

HEK293 cells are a well-used model for studying palmitoylation as aside from being easy to use and maintain, they express all the components of the palmitoylation machinery (Tian *et al.*, 2010). HEK293 do not endogenously express any MyBP-C isoforms, and as such these cells were transfected with an exogenous FLAG-tagged cMyBP-C. Palmitoylation of FLAG-cMyBP-C was determined by Acyl-RAC and revealed a fraction is palmitoylated in these cells. Confocal microscopy revealed FLAG-cMyBP-C did not localise to any specific membrane compartment and was largely cytosolic (Figure 3.17)

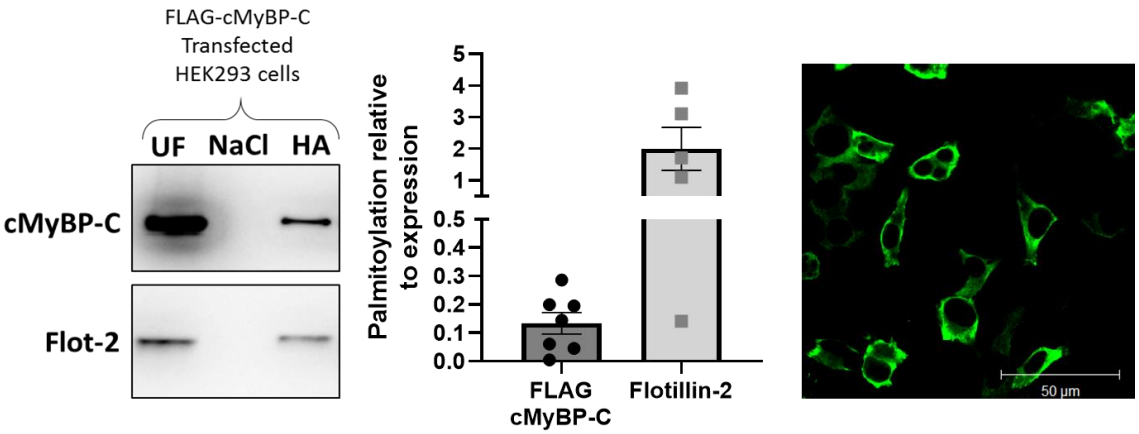

Figure 3.17. FLAG-cMyBP-C can be expressed in HEK293 cells and Acyl-RAC reveals it is palmitoylated in these cells.
Acyl-resin assisted capture (Acyl-RAC) of transiently transfected HEK293 cells with 1 µg of FLAG-cMyBP-C revealed cMyBP-C is palmitoylated in these cells, with Flotillin-2 (Flot-2) used as an assay control. Palmitoylation (HA, hydroxylamine dependent) was normalised to total protein (UF, unfractionated) with percentage palmitoylation versions found in Supplementary Figure 7.1. Sodium chloride (NaCl) is included as a negative control. Confocal microscopy of transfected cells using cMyBP-C and Alexa Fluor 488 secondary antibody revealed that FLAG-cMyBP-C expression is largely cytoplasmic and not clearly localised to any membrane compartment. Scale bar is 50µm. Representative confocal image of n=1.

FLAG-cMyBP-C palmitoylation in cultured HEK293 cells represented ~3% of total protein compared to ~13% in rabbit ventricular cardiomyocytes (Figure 3.4 and Supplementary Figure 7.1). The question then arises as to whether this is due to HEK293 being a non-cardiac cell type and the mis-localisation of cMyBP-C in the cytoplasm, or the prolonged culturing of cells containing cMyBP-C. In order to determine the effect of culture on cMyBP-C palmitoylation, rabbit and neonatal rat ventricular cardiomyocytes were isolated and cultured for 24 hours and compared to non-cultured cells. Following culture, cMyBP-C palmitoylation was significantly reduced in cultured cardiomyocytes, indicating that whilst cMyBP-C can still be detected, cultured ventricular cardiomyocytes may not be a suitable system to characterise the functional effect of cMyBP-C palmitoylation (Figure 3.18).

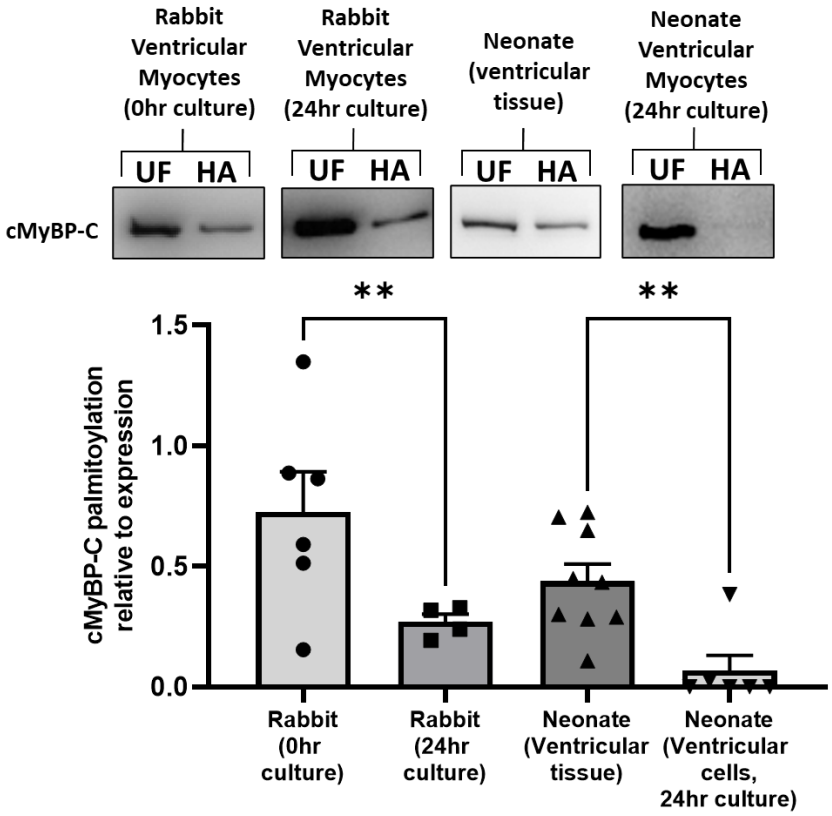

Figure 3.18. Palmitoylation of cMyBP-C in cultured and non-cultured cells.
Acyl-Resin Assisted Capture (Acyl-RAC) was used to detect the palmitoylation of cMyBP-C in rabbit ventricular cardiomyocytes both pre (0hr) and 24-hour post culture, neonatal cardiomyocytes both pre-isolation (ventricular tissue) and 24 hours post culture after isolation. Analysis revealed that in rabbit cardiomyocytes, culture reduced cMyBP-C palmitoylation level and in neonatal cardiomyocytes, isolation or culture reduced palmitoylation. Total protein (UF) was compared to palmitoylated fraction (HA, hydroxylamine dependent). Data is mean ±S.E.M analysed via a one-way ANOVA with a Sidak's *post hoc* test. **p<0.01.

3.4.3.2 Characterising pharmacological compounds that alter protein palmitoylation

Pharmacological tools that either inhibit or activate palmitoylating enzymes, or directly target substrate palmitoylation, are currently lacking. Whilst palmitoylation of cMyBP-C could be characterised using widely used DHHC-PAT inhibitor 2-BP, or acylthioesterase inhibitor palmostatin-B, the off-target effects of these drugs would limit conclusions that can be drawn from their use (Lan *et al.*, 2021; Lin & Conibear, 2015). Recently, a class of compounds known as amphiphiles have been of interest as they were reported to break thioester bonds between palmitate and substrates (Rudd *et al.*, 2018). Three of these compounds (AMD1, AMD7 and AMD14) were supplied by Dr Andrew Rudd, University of California and tested using neonatal rat ventricular cardiomyocytes, followed by Acyl-RAC. As a well characterised cardiac substrate with a single palmitoylation site, NCX1 was chosen to investigate the efficacy of these compounds. Acyl-RAC

revealed that AMD7 was the most effective at reducing NCX1 palmitoylated at concentration of 10 µM and 50 µM (Figure 3.19).

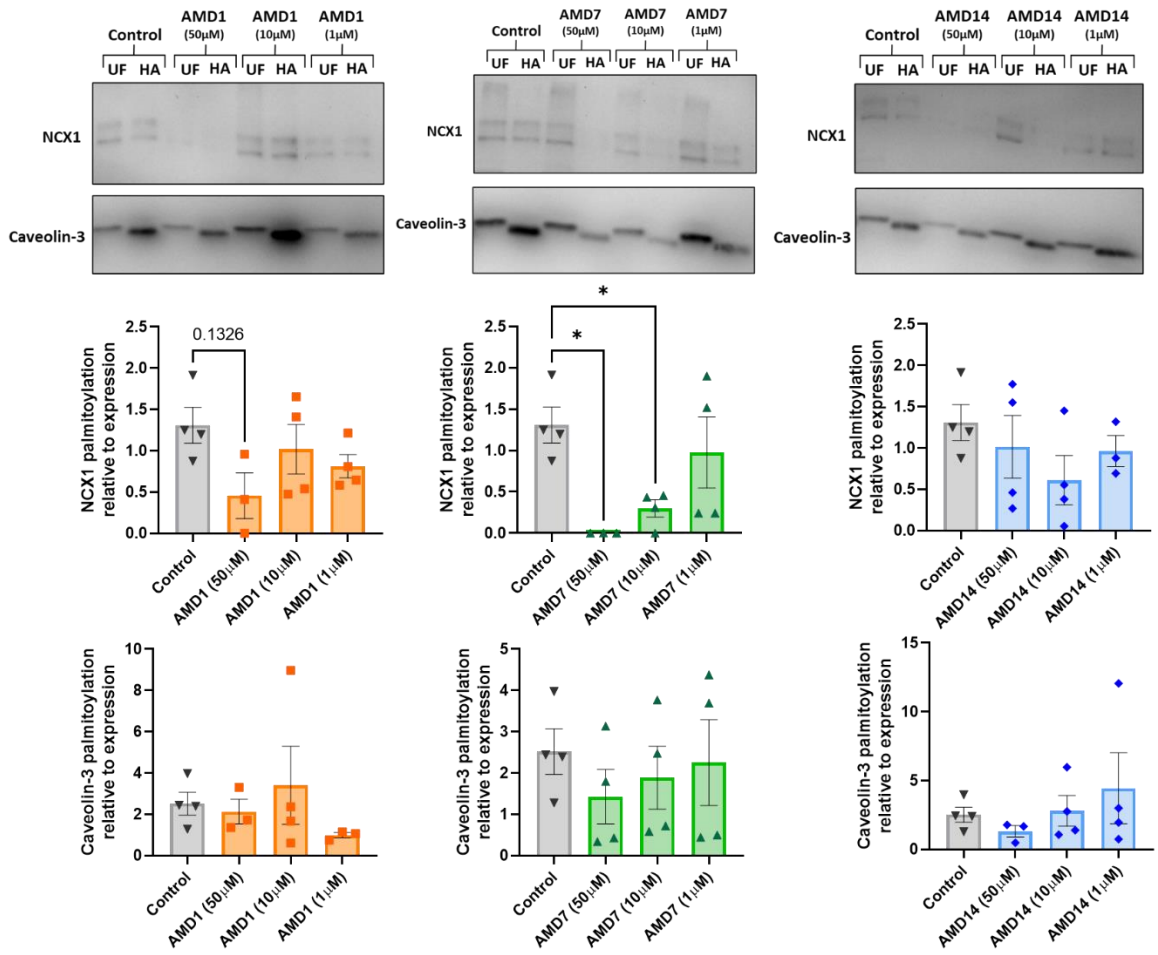

Figure 3.19. Palmitoylation of NCX1 and Caveolin-3 in neonatal rat ventricular cardiomyocytes after 24 hours of treatment with AMD-1, AMD-7 and AMD-14.
The effect of pharmacological amphiphilic compounds (AMD1, AMD7 and AMD14, obtained from Dr Andrew Rudd, University of California) that break thioester bonds between palmitate and palmitoylated cysteines was tested using neonatal rat ventricular cardiomyocytes. Cells were treated for 24 hours before palmitoylation of NCX1 and assay control Caveolin-3 was then determined by Acyl-Resin Assisted Capture (Acyl-RAC) and palmitoylated fraction (hydroxylamine dependent, HA) normalised to total protein (UF, unfractionated). NCX1 was chosen as it is a well characterised palmitoylated substrate in neonatal ventricular cardiomyocytes, whereas cMyBP-C palmitoylation stoichiometry is very low in these cells. AMD-7 was most effective in reducing palmitoylation of NCX1 at 50 µM and 10 µM (*p<0.05). Data is mean ±S.E.M analysed via a one-way ANOVA with a Sidak's *post hoc* test.

Due to a complete loss of palmitoylation of cMyBP-C upon culture, neonatal rat ventricular cardiomyocytes are not a suitable system to study cMyBP-C palmitoylation. As such, further characterisation of AMD7 was completed in cultured rabbit ventricular cardiomyocytes which do retain a level of cMyBP-C palmitoylation upon culture. However, in contrast to neonatal cells, treatment of rabbit cardiomyocytes with 50 µM AMD7 resulted in cell toxicity and death and treatment with 10 µM did not result in a significant difference in NCX1 or cMyBP-C palmitoylation in these cells (Figure 3.20).

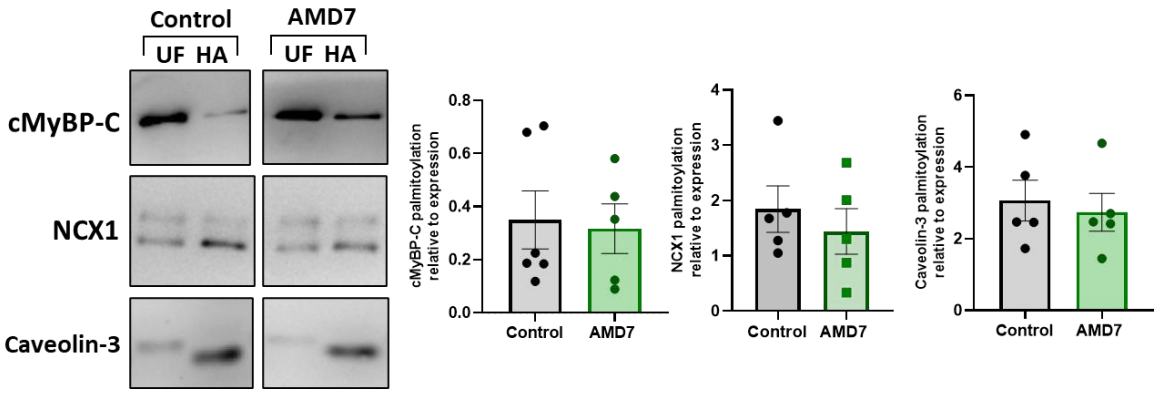

Figure 3.20. Palmitoylation of cMyBP-C, NCX1 and Caveolin-3 in rabbit ventricular cardiomyocytes after 24-hour treatment with AMD7.
The effect of the pharmacological amphiphilic compound AMD7 (10 µM, obtained from Dr Andrew Rudd, University of California) that break thioester bonds between palmitate and palmitoylated cysteines was tested using rabbit ventricular cardiomyocytes. Cells were treated for 24 hours in before palmitoylation of cMyBP-C, NCX1 and assay control Caveolin-3 was then determined by Acyl-Resin Assisted Capture (Acyl-RAC) and palmitoylated fraction (hydroxylamine dependent, HA) normalised to total protein (UF, unfractionated). There was no significant effect of AMD7 treatment on cMyBP-C, NCX1 or Caveolin-3 palmitoylation. Data is mean ±S.E.M analysed via student's unpaired t-test.

3.4.4 Identifying cMyBP-C palmitoylation site

3.4.4.1 Palmitoylation peptide array – cMyBP-C palmitoylation cannot be determined by click chemistry-based peptide array

A common method used to characterise palmitoylation of a substrate is to identify the cysteine upon which palmitoylation is occurring and determine the consequences of its loss (Main & Fuller, 2021). Whilst no consensus sequence currently exists for palmitoylation sites, there are several features of the reportedly palmitoylated cysteines that could inform prediction of future sites. This has been more well established for membrane proteins where proximity to the membrane, the presence of amphipathic helices and the nature of surrounding amino acids all indicate that a cysteine may be a candidate site, but prediction for soluble, non-membrane proteins is more challenging (Salaun *et al.*, 2010). In order to narrow down cMyBP-C palmitoylation site, an experimental technique combining peptide array and palmitoylation click chemistry was utilised. Peptides of 20 amino acids in length of cMyBP-C sequences containing single or multiple cysteines were constructed on a cellulose membrane following which they were incubated with alkyne containing ODYA-CoA before "clicking" to an azide containing Cy5.5 for detection. Analysis revealed several specific peptides were detected in the cMyBP-C sequence, whilst the NCX1 positive control (palmitoylated cysteine) was detected but not the NCX1 negative control (non-palmitoylated cysteine). However, the PLM positive control did not appear on the

array whilst the negative control was recognised. Furthermore, treatment of the membrane with hydroxylamine to cleave the ODYA-CoA-Cy5.5 complex from the cysteines did not result in any loss of signal (Figure 3.21).

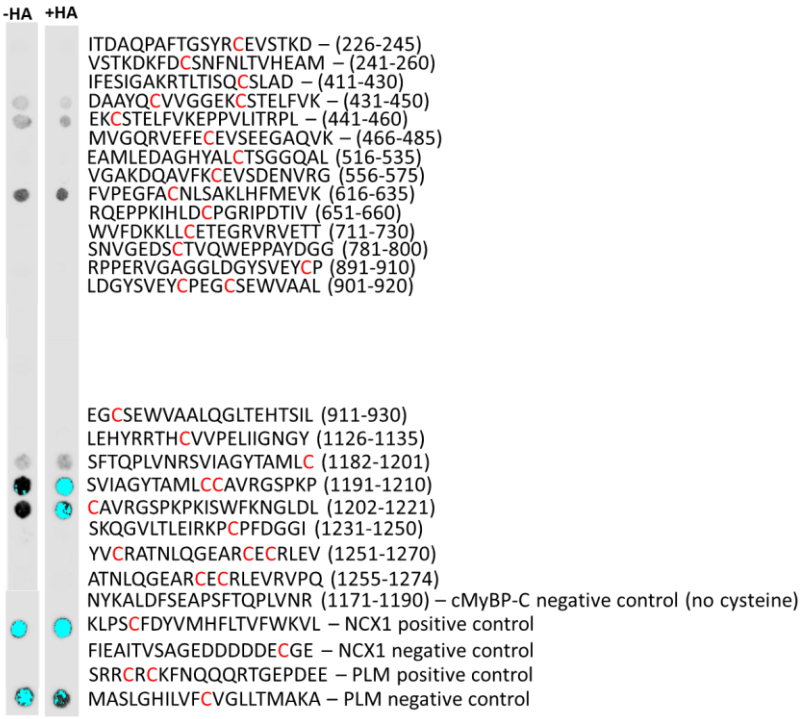

Figure 3.21. Palmitoylation peptide array of cMyBP-C sequences.
Peptides were synthesised using a peptide array synthesiser and immobilised on cellulose membranes. Membranes were incubated with 20 µM ODYA-CoA before incubation with Cy5.5 and visualisation on LICOR imaging system. Visualisation revealed several spots indicating attachment of the ODYA-CoA-Cys5.5 conjugate to a particular peptide, including N and C-terminal localised peptides. Additionally, attachment occurred on a peptide with a palmitoylated cysteine from the sodium-calcium exchanger (NCX1) but not a peptide containing a non-palmitoylated cysteine sequence. However, a peptide with two palmitoylated cysteines in phospholemman (PLM) did not show attachment where the negative control of a non-palmitoylated cysteine did. Additionally, incubation with hydroxylamine (HA) for 1 hour did not result in any reduction in signal, suggesting the conjugation is not via an ODYA-CoA thioester bond with the available cysteine. Representative image of n=2.

In order to further characterise the palmitoylation peptide array technique, an array was constructed around established palmitoylation substrate NCX1. Sequences containing the NCX1 palmitoylated cysteine and a non-palmitoylated cysteine negative control sequence were constructed on the array, including truncated versions of both sequences (removing one C-terminal amino acid per sequence) and alanine replacements of cysteines. No signal was detected post-blocking with BSA or post-ODYA-CoA treatment, however upon incubation with either Cy5.5 or CW800, peptides were detected whether in the presence of ODYA-CoA or not, indicating the Cy5.5 and CW800 are attaching directly to the sequences in a palmitoyl-CoA independent manner (Figure 3.22). As such, the

current technique does not model the modification of palmitoylation and therefore cannot be used reliably to inform on palmitoylation site.

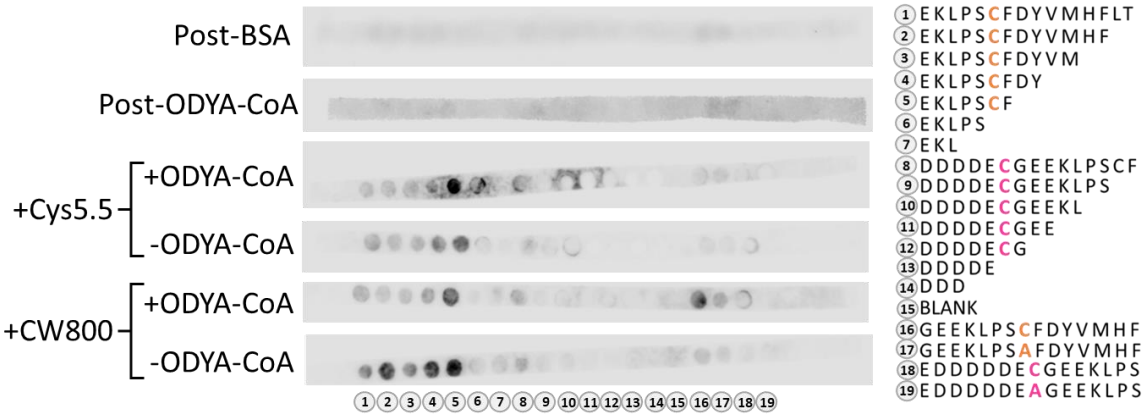

Figure 3.22. Truncation and alanine replacement of NCX1 peptide array sequences.
In order to determine the specificity of the ODYA-CoA-Cy5.5 conjugation to palmitoylation peptide array sequences, peptides were synthesised using a peptide array synthesiser and immobilised on cellulose membranes including truncated version and alanine replacements of an NCX1 palmitoylated sequence (1-7, 16 and 17 - orange C) and non-palmitoylated sequence (8–14, 18 and 19 - pink C). Each array was blocked using 5% BSA and visualised before incubation with ODYA-CoA or PBS as a negative control. Arrays were then incubated in Cy5.5 or LICOR CW800 clickable azide compounds and visualised. Visualisation revealed that although truncation of the palmitoylatable sequence of NCX1 showed the hypothesised loss of signal after the cysteine was truncated and no signal was detected for the unpalmitoylatable sequence, this occurred regardless of the presence of ODYA-CoA suggesting the Cys5.5 and CW800 are attaching to the array without clicking to the ODYA-CoA. N=1.

3.4.4.2 Cysless strategy – removal of all cMyBP-C cysteines eliminates palmitoylation which is not returned upon single cysteine re-incorporation

As the palmitoylation peptide array was identified as an unsuitable system to detect cMyBP-C palmitoylation, an alternative strategy was employed utilising site directed mutagenesis. Although HEK293 cells transfected with FLAG-cMyBP-C show a lower level of palmitoylation compared to primary cells, they provide a simple system in which to monitor the presence of absence of cMyBP-C palmitoylation. As such, a cysless version of FLAG-cMyBP-C was constructed whereby all cysteines were mutated to alanine. As expected, this completely abolished cMyBP-C palmitoylation (Figure 3.23). Site direct mutagenesis was then used to return individual, or two closely located, cysteines to the cysless version of FLAG-cMyBP-C. Acyl-RAC revealed that returning of individual/closely located cysteines did not result in the return of cMyBP-C palmitoylation. This may indicate that cMyBP-C palmitoylation is formed by more than one site, either through cooperation or that a single site palmitoylation is below the detection limits of the assay (Figure 3.24).

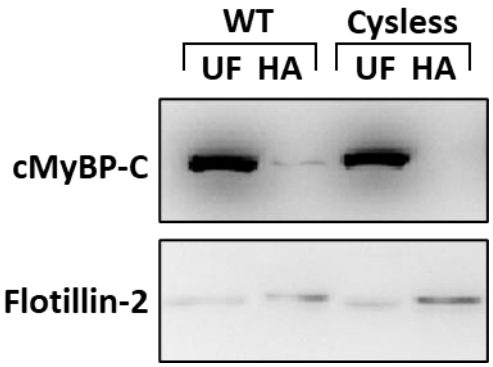

Figure 3.23. Palmitoylation is eliminated in a cysless mutant of cMyBP-C.
Acyl-RAC revealed production of a version of FLAG-cMyBP-C with all cysteines mutated to alanine and expression in HEK293 leads to complete loss of palmitoylation. Palmitoylation (hydroxylamine dependent, HA) was normalised to total protein (UF, unfractionated). Representative image of n=3 experiments.

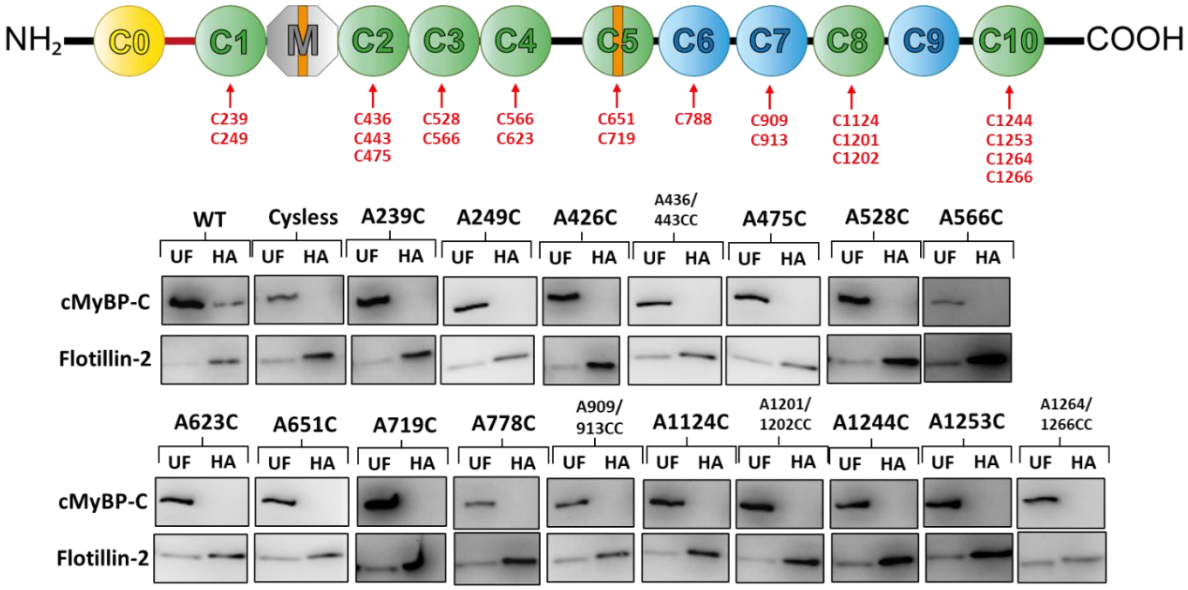

Figure 3.24. Returning individual or closely localised cysteines in a cysless cMyBP-C does not return lost palmitoylation.
Site directed mutagenesis was used to create several constructs from the cysless FLAG-cMyBP-C in which selected alanines were mutated back to cysteines. Acyl-RAC of these constructs transiently transfected into HEK293 cells revealed no single cysteine returned any detectable level of palmitoylation, suggesting that multiple sites contribute to cMyBP-C palmitoylation in these cells. Palmitoylation (hydroxylamine dependent, HA) was normalised to total protein (UF, unfractionated). Representative images of n=3 experiments.

3.4.4.3 Point mutant strategy – cMyBP-C palmitoylation sites are reported S-glutathionylation sites

Cysteines that are solvent exposed are more likely candidates to be palmitoylation sites, and this can be determined by whether they are modified by any other cysteine modifications. S-glutathionylation and other modifications have been reported at several cysteines in cMyBP-C and therefore may be targeted by other modifications such as palmitoylation (Table 3.2).

Table 3.2. Analysis of cysteine isoform comparison, species comparison, established modifications and surface availability.

Domain (cMyBP-C, human)	Cysteine number (cMyBP-C, human)	Sequence	Cysteine isoform conservation	Adjacent area isoform conservation score (Clustal Omega) (max: 27)*	Cysteine species conservation	Adjacent area species conservation score (Clustal Omega) (max: 27)*	Established modifications or mutations (cMyBP-C, any species)	Surface availability based on AlphaFold (human)	Surface availability based on crystallography (human)
1	239	GSYRCEVST	Slow skeletal	16	Mouse, rat and rabbit	25	S-glutathionylation	No	Yes
1	249	DKFDCSNFN	Unique to cMyBP-C	15	Unique to human	23	S-glutathionylation	Yes	
2	426	TISQCSLAD	All	16	Mouse, rat and rabbit	27	S-glutathionylation	Yes	Yes
2	436	AAYQCVVGG	Unique to cMyBP-C	8	Mouse, rat and rabbit	27	Disulphide bond with C443, S-glutathionylation	No	No
2	443	GGEKCSTEL	All	19	Mouse, rat and rabbit	27	Disulphide bond with C436, S-glutathionylation	Yes	Yes
3	475	VEFECEVSE	Slow skeletal	20	Mouse, rat and rabbit	27	S-glutathionylation	No	No
3	528	HYALCTSGG	Unique to cMyBP-C	16	Unique to human	23	S-glutathionylation	Yes	Yes
4	566	AVFKCEVSD	All	16	Mouse, rat and rabbit	27	C566R mutation in HCM	No	
4	623	EGFACNLSA	Unique to cMyBP-C	12	Mouse, rat and rabbit	27	S-glutathionylation	Yes	
5	651	IHLDCPGRI	Fast skeletal	12	Mouse, rat and rabbit	21	S-glutathionylation	Yes	Yes
5	719	KKLLCETEG	Unique to cMyBP-C	9	Mouse, rat and rabbit	27	S-glutathionylation	Yes	Yes
6	788	GEDSCTVQW	Slow skeletal	14	Mouse, rat and rabbit	24	S-glutathionylation	No	
7	909	SVEYCPEGC	All	18	Mouse, rat and rabbit	24	S-glutathionylation	Partially	
7	913	CPEGCSEWV	Unique to cMyBP-C	10	Mouse, rat and rabbit	19	S-glutathionylation	Yes	
9	1124	RRTHCVVPE	Fast skeletal	13	Mouse, rat and rabbit	23		Yes	
10	1201	TAMLCCAVR	Unique to cMyBP-C	18	Mouse, rat and rabbit	22		Yes	
10	1202	AMLCCAVRG	All	20	Mouse, rat and rabbit	24		Partially	
10	1244	IRKPCPFDG	Unique to cMyBP-C	21	Mouse, rat and rabbit	26	S-glutathionylation	Yes	
10	1253	GIYVCRATN	All	18	Mouse, rat and rabbit	26		No	
10	1264	GEARCECRL	Unique to cMyBP-C	15	Mouse, rat and rabbit	26	C1264F in DCM	Yes	
10	1266	ARCECRLEV	All	18	Mouse, rat and rabbit	26		Yes	

Conservation scoring was based on Clustal Omega alignment whereby 4 amino acids either side of lysine were scored - 3 points for perfect alignment (*) with both isoforms, 2 points for an amino acids with a strong similarity (:), 1 point for a weak similarity (.) and 0 points for no similarity

In the cysless construct, returning of multiple reported S-glutathionylation sites returned cMyBP-C palmitoylation to a certain extent. Additionally, site directed mutagenesis was used to mutate C623 and C651 in the WT FLAG-cMyBP-C construct, and Acyl-RAC revealed that palmitoylation was significantly reduced, indicating that as well as being S-glutathionylation sites, these sites are also modified by S-palmitoylation. Importantly, mutation of both sites did not abolish palmitoylation, suggesting other sites are still involved. (Figure 3.25).

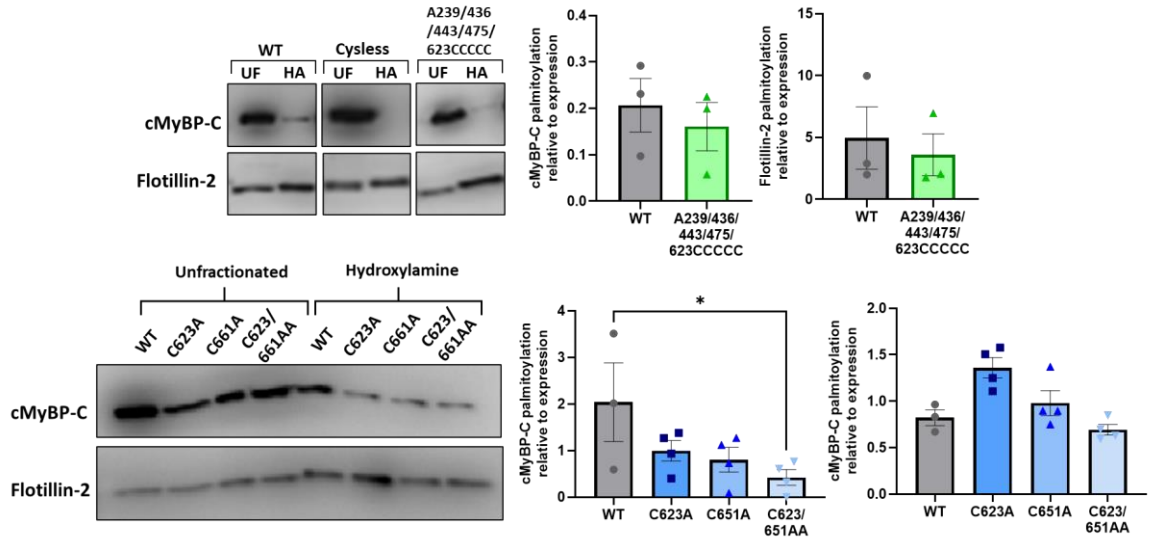

Figure 3.25. cMyBP-C S-glutathionylation sites are also palmitoylated.
Site directed mutagenesis was used to a create version of cysless FLAG-cMyBP-C in which several alanines were mutated back to cysteines. These sites were chosen based on their reported S-glutathionylation. Acyl-RAC of these constructs transiently transfected into HEK293 cells revealed when multiple cysteines are returned palmitoylation of cMyBP-C can be detected, suggesting that multiple sites contribute to cMyBP-C palmitoylation in these cells. This was further confirmed by mutating candidate cysteines C623 and C651 to alanine in wildtype FLAG-cMyBP-C which resulted in a loss of palmitoylation when both sites were mutated (*p<0.05). Palmitoylation (hydroxylamine dependent, HA) was normalised to total protein (UF, unfractionated) and values normalised to the experimental average for cysteine to alanine mutants. Data is mean ±S.E.M analysed via a one-way ANOVA with a Dunnett's *post hoc* test.

3.4.5 Functional characterisation of cMyBP-C palmitoylation

Characterisation of cMyBP-C modification site has been successfully completed using mutant versions of the protein where the site is mutated, particularly in studying the importance of phosphorylation (Sadayappan *et al.*, 2006). However, in this case, the identified sites of cMyBP-C palmitoylation are also reported S-glutathionylation sites, and therefore the functional significance of loss of the site cannot be exclusively attributed to loss of palmitoylation. As an alternative strategy, myofilaments treated with palmitoyl CoA show significantly enhanced cMyBP-C palmitoylation (Figure 3.8), which can be functionally characterised using myofilament assays.

3.4.5.1 Phosphorylation in palmitoyl-CoA treated myofilaments

As palmitoylation was significantly increased in palmitoyl CoA treated myofilaments, expression and phosphorylation of cMyBP-C was investigate in these samples. Compared to total cMyBP-C, there was no significant difference in cMyBP-C phosphorylation compared to untreated controls. Whilst total cMyBP-C palmitoylation is increased following treatment (Figure 3.8), palmitoylation of the phosphorylated form of cMyBP-C is not changed, indicating that the fraction of cMyBP-C whose palmitoylation increased may not be phosphorylated (Figure 3.26).

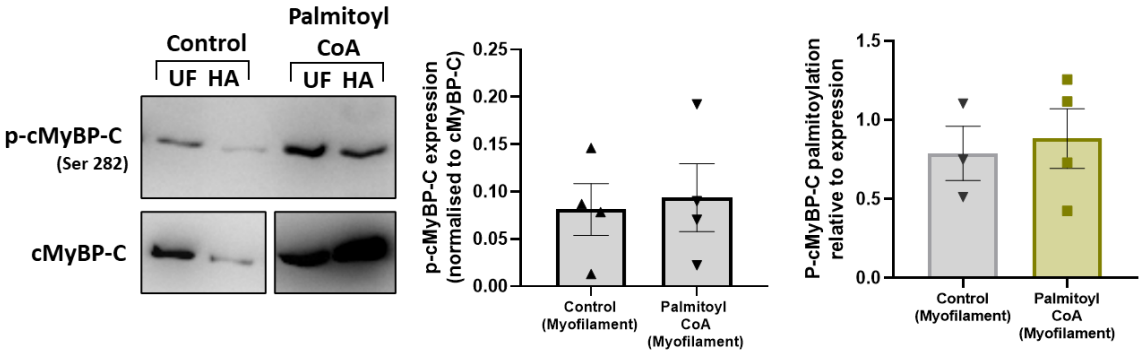

Figure 3.26. Increased palmitoylation of total cMyBP-C by palmitoyl CoA does not affect expression or palmitoylation of phosphorylated cMyBP-C.
The effect of palmitoyl CoA (20 µM), which can spontaneously palmitoylate solvent exposed cysteines, was tested using myofilaments isolated from rabbit ventricular cardiomyocytes. Myofilaments were treated for 30 minutes with palmitoyl CoA before centrifugation and collecting of the myofilament pellet and supernatant. Palmitoylation in each fraction was determined by Acyl-Resin Assisted Capture (Acyl-RAC) and total protein (UF, unfractionated) compared to palmitoylated fraction (hydroxylamine dependent, HA). Palmitoyl CoA did not increase the level of cMyBP-C phosphorylation (pSer282 – pcMyBP-C/cMyBP-C). Whilst total cMyBP-C palmitoylation is increased upon palmitoyl CoA treatment, the palmitoylation of the phosphorylated form of cMyBP-C is not increased. Data is mean ±S.E.M analysed via an unpaired student's t-test.

3.4.5.2 Passive tension in palmitoyl CoA treated rabbit myofilaments

The sarcomere maintains a passive tension when stretched beyond its slack length which is important in maintaining the ventricular wall tension during diastole, providing resistance to stretch without activation, and in determining shortening velocity upon activation (Granzier & Irving, 1995). In isolated myofilament preparations in particular, passive tension is mainly driven by the molecular spring of Titin, elimination of which has been shown to abolish passive force (Herzog, 2018). Reducing the length of a stretched myofilament by 30% removes this tension and therefore determining force pre- and post-slackening can be used to measure the original passive force of a cell at a given sarcomere length. In order to determine whether palmitoyl-CoA treatment affected myofilament passive force, cells were stretched to 3 different sarcomere lengths ranging between 2

μM and 2.2 μM before slackening to 30% of their length for 5 seconds. Pre-treatment with palmitoyl-CoA had no significant effect on passive tension ($F_{passive}$) at any sarcomere length (Figure 3.27).

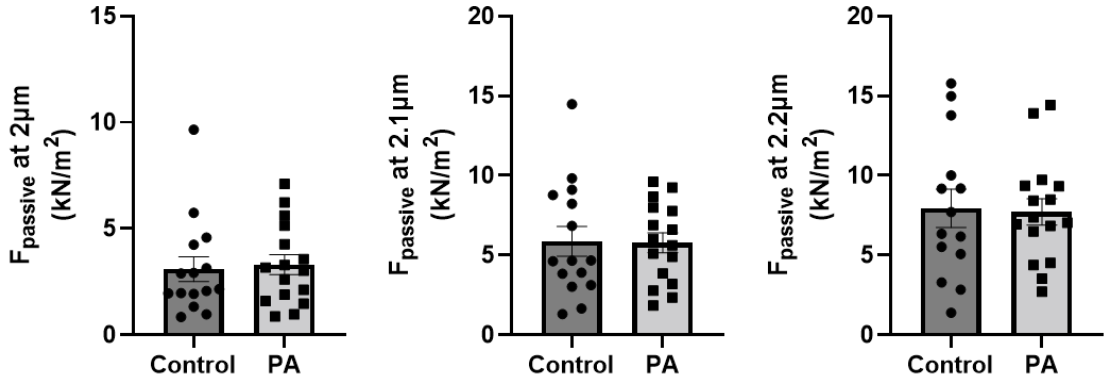

Figure 3.27. The effect of palmitoyl CoA treatment on passive tension in rabbit ventricular myofilaments at increasing sarcomere lengths.
Myofilaments were isolated from rabbit ventricular cardiomyocytes and treated with palmitoyl CoA (20 μM) before mounting to a muscle mechanics set up. Myofilaments were stretched to 3 different sarcomere lengths (2μm, 2.1μm and 2.2μm) and passive tension was determined by slackening cells by 30% of their length and measuring the difference in force pre and post slacking. Treatment with palmitoyl CoA had no significant effect on passive tension at any sarcomere length. N=15-16 cells from 4 animals. Data is mean ±S.E.M analysed via an unpaired student's t-test.

3.4.5.3 Active force and calcium sensitivity in palmitoyl CoA treated rabbit myofilaments

Active force of a myofilament is generated by acto-myosin interactions and is influenced by the sarcomere length (as part of LDA mechanism) and the presence of Ca^{2+}, whereby myofilaments generate increased force in increasing levels of Ca^{2+} and at increasing sarcomere length (de Tombe & ter Keurs, 2016). In order to determine whether palmitoyl-CoA treatment had any effect on active force or Ca^{2+} sensitivity, treated myofilaments were stretched to a sarcomere length of 2.2 μM and active force was determined in submaximal (pCa6.0, F_{act}) and maximal (pCa4.5, F_{max}) Ca^{2+} solutions. Analysis revealed that whilst palmitoyl CoA had no significant effect on active force at maximally activating Ca^{2+} levels (F_{max} at pCa4.5), there was a significant decrease in the force generated at submaximal Ca^{2+} (F_{max} at pCa6.0) in palmitoyl CoA treated myofilaments compared to control, indicating that palmitoyl CoA reduced the Ca^{2+} sensitivity of the myofilaments (Figure 3.28).

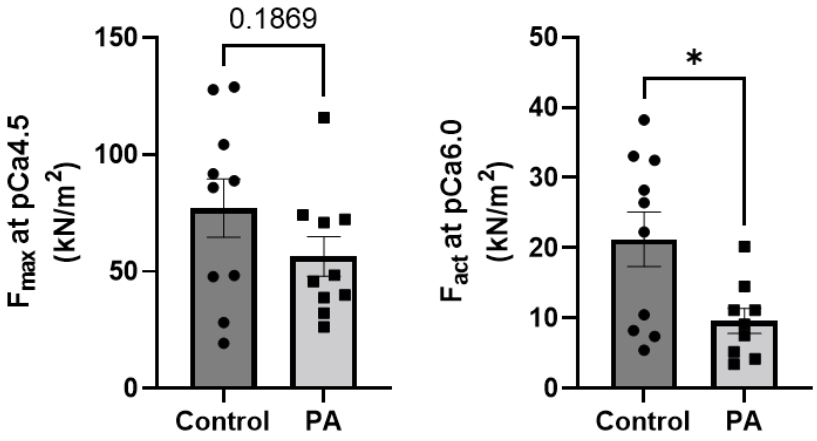

Figure 3.28. The effect of palmitoyl CoA on active force and calcium sensitivity in rabbit ventricular myofilaments at a sarcomere length of 2.2 µM.
Myofilaments were isolated from rabbit ventricular cardiomyocytes and treated with palmitoyl CoA (20 µM) before mounting to a muscle mechanics set up. Myofilaments were stretched to 2.2µm and active force was measured in maximally activating Ca^{2+} ($F_{max,}$ pCa4.5) and submaximal Ca^{2+} ($F_{act,}$ pCa6.0). Treatment with palmitoyl CoA had no effect on maximal active force in activating Ca^{2+} but significantly reduced the force generated in response to submaximal Ca^{2+}. N=9-10 cells from 4 animals. Data is mean ±S.E.M analysed via an unpaired student's t-test. *p<0.05.

3.5 Discussion

The aim of the present study was to characterise the palmitoylation of the essential cardiac regulatory protein cMyBP-C. To achieve this, Acyl-RAC was used to purify palmitoylated cMyBP-C from cardiac tissue, including from different anatomical regions and diseased samples. Isolation of myofilaments from rabbit cardiomyocytes was used to indicate where palmitoylated cMyBP-C was localised. Whilst novel pharmacological tools were ineffective in altering cMyBP-C palmitoylation, treatment of isolated myofilaments with palmitoyl CoA allowed characterisation of their calcium sensitivity, passive and active force when cMyBP-C palmitoylation was increased. Finally, putative cMyBP-C palmitoylation sites were identified by site directed mutagenesis in HEK293 cells.

3.5.1 Palmitoylation is a novel post-translational modification of myofilament proteins

Palmitoylation is an essential regulatory modification that alters protein-protein interactions, protein-membrane interactions and influences other PTMs in order to fine tune a substrate's localisation and function (Essandoh *et al.*, 2020). In the present study, Acyl-RAC was used to identify novel palmitoylation of sarcomeric proteins myosin, actin and cMyBP-C in ventricular tissue from rabbit, rat and mouse. Thin filament-based proteins TnI, TnT and Tm were not found to be palmitoylated in these samples (Figure 3.4).

As well as PTM regulation of cMyBP-C, there has been significant interest in understanding the regulatory modifications of myosin heavy chain, which similarly undergoes phosphorylation and acetylation and shows disease relevant changes (Landim-Vieira *et al.*, 2021). Despite being >230kDa, cardiac myosin only contains 14 cysteines, one of which is mutated in HCM in three different forms (C905F, C905R, C905Y). Although the functional consequence of loss of this cysteine has not been investigated, this residue is part of the proximal S2 domain and several other nearby residues are also associated with cardiac disorders, making it a "HCM hotspot" (Singh *et al.*, 2021; Stenson *et al.*, 2014).

In terms of actin, available information on the structure suggests C374 is the most accessible and is also reportedly modified by S-glutathionylation (Cuello *et al.*, 2018; Gross & Lehman, 2013). Interestingly, several studies utilising FRET to

understand actin dynamics use this site as an anchor for the probe, which could be unintentionally impeding its ability to be modified at this site (Guhathakurta *et al.*, 2015; Xing *et al.*, 2008). However, whilst structural analysis of the relative surface accessibility of amino acids is a useful predictor of PTM modification, crystallography data and AlphaFold analysis of the human cMyBP-C sequence suggests sites including C475 are not solvent exposed and yet have been reported to be modified by S-glutathionylation (Table 3.2). Indeed, a study assessing the accessibility of cysteines in sarcomeric proteins, including actin, demonstrated that contractile state affects cysteine availability, and therefore any of the cysteines of actin or myosin may still be candidate palmitoylation sites (Gross & Lehman, 2013).

Further validation of both actin and myosin palmitoylation in cardiac tissue is required, as due to sample availability a suitable negative control was not included unlike in the study of cMyBP-C in cardiac myocytes and HEK293 (Figure 3.6 and Figure 3.17). As such, non-specific binding in the Acyl-RAC assay cannot be ruled out at this stage. Nevertheless, in line with the data presented, the Tseng group have recently published a study characterising the cardiac palmitoylome using mass spectrometry, identifying more than 400 proteins with cMyBP-C, myosin and actin among them (Miles *et al.*, 2021). Interestingly, the study also identified TnT, TnI and Tm, despite the evidence presented here that they are not palmitoylated in cardiac tissue (Figure 3.4). Whilst TnI and Tm have the capacity to be palmitoylated, TnT does not contain any cysteines so cannot undergo S-palmitoylation and therefore has likely been detected as a false positive. These proteins were also identified in our own mass spectrometry analysis of the rat heart (Supplementary Table 7.1), altogether emphasising the importance of further validation of palmitoylated proteins identified in mass spectrometry studies.

Aside from information on the cardiac palmitoylome, Miles *et al.* also provided some valuable insight into the enzymatic machinery involved in cardiac palmitoylation. The subcellular localisation of DHHC-PATs to the surface, Golgi apparatus and ER is based on exogenous HEK293 studies and an understanding of the distribution of the enzymes in cardiac tissue specifically would be a valuable tool (Ohno *et al.*, 2006). Using custom antibodies, the group identified 11 of the 23 DHHC-PATs as being expressed in the heart, despite another study utilising

global RNA sequencing suggesting mRNA of all 23 can be detected (more detail in Chapter 5; Hahn *et al.*, 2021; Miles *et al.*, 2021). Interestingly, follow up work from published abstracts of the group suggests they have identified DHHCs localised to different areas of the sarcomere, including DHHC2 to the M-lines and DHHC5 to the Z-discs, suggesting there is close membrane association with the sarcomere (Miles *et al.*, 2020). Although our previous work of a virally encoded HA-DHHC5 construct infected into adult rabbit cardiomyocytes observed a striated pattern and intercalated disc localisation, reliable DHHC-PAT antibodies have been challenging to produce in the past and therefore further validation of the enzymes in these regions is warranted (Main *et al.*, 2022). Additionally, sarcolemma proteins including the LTCC produce a striated staining pattern due to their localisation in the T-tubules, so it remains to be determined whether there is close localisation to the sarcomere. Nevertheless, in terms of sarcomeric protein palmitoylation, this may suggest that DHHC-PATs are in the vicinity and able to palmitoylate these proteins.

3.5.2 Location-specific modulation of cMyBP-C palmitoylation

Cardiac MyBP-C is an essential regulator of cardiac inotropy and lusitropy through PTM-dependent modulation of actin-myosin interactions and myofilament Ca^{2+} sensitivity (Barefield & Sadayappan, 2010). In this study, cMyBP-C palmitoylation was detected in ventricular cardiac tissue by Acyl-RAC (Figure 3.4) and any potential false positives through the C436 and C443 reported disulphide bond were ruled out by pre-treatment with reducing agents (Figure 3.5). Whilst cMyBP-C is highly expressed in the ventricles, it is also expressed in the atria, although the relative quantities have not been directly compared (Lin *et al.*, 2013; Sadayappan & de Tombe, 2012). Given the precise arrangement of cMyBP-C molecules in the sarcomere (7-9 molecules per C-zone) there may not be any cell-to-cell variability in cMyBP-C expression in this regard. However, given the importance of cMyBP-C PTMs in regulating cardiac contractility, and the difference in force generation and electrophysiological properties between the atria and the ventricles, it is surprising there is a lack of study on the extent of PTM modification between the anatomical regions (Molina *et al.*, 2016; Pham *et al.*, 2019). Although not directly measuring cMyBP-C, a recent study mapped cardiac protein PTMs in different anatomical regions of the heart. Analysis of the supplementary data presented in the paper revealed that whilst 60 phosphorylated peptides of cMyBP-C were

detected in the LV, only 38 were detected in the RA (Bagwan *et al.*, 2021). In terms of palmitoylation, cMyBP-C was found to be palmitoylated in the left, right and septal region of the adult rabbit ventricle, with potentially higher levels in the LV compared to the RV. cMyBP-C palmitoylation was only minimally detected in the LA and not detected in the RA (Figure 3.6). This may suggest that there is regional specific variability in cMyBP-C PTM modification, however whether this correlates to the overall function of the different regions remains to be determined. Nevertheless, this will be an important consideration when judging the therapeutic potential of targeting a cMyBP-C PTM in left versus right HF for example, particularly as right HF in HFpEF has been associated with increased cMyBP-C phosphorylation (Hegemann *et al.*, 2021).

Cardiac MyBP-C is localised in the C-zone of the sarcomere and no populations outside this region have been described. Given the role palmitoylation plays in membrane attachment and trafficking, it could be hypothesised that the palmitoylated form is localised outside the myofilament. In this study, myofilament extraction was performed in adult rabbit cardiomyocytes and, whilst is under the constraints of western blot detection limits, identified all of cMyBP-C as being localised in the myofilament (Figure 3.7). In the sarcomere, giant structural proteins such as titin, desmin and nebulin are insoluble in concentrated salt solutions, whilst 470 mM to 680 mM is required to solubilise myofilament proteins (myosin, actin, cMyBP-C etc.), but this is highly dependent on the substrate (Li, Wang, *et al.*, 2022; López-Bote, 2017). In this study, salt extraction of the myofilament pellet revealed whilst the majority of cMyBP-C was solubilised upon salt treatment, a small amount remained, and Acyl-RAC revealed this portion has a higher palmitoylation stoichiometry compared to the fraction that is salt-soluble (Figure 3.7). This could indicate that the palmitoylated form of cMyBP-C has greater electrostatic interactions with the myofilament lattice or attachment to closely localised membrane structures, potentially aided by the hydrophobic environment created by adding the palmitoyl group(s) (Li *et al.*, 2022). Going forward, utilising the technique of click chemistry combined with immunofluorescence would give the opportunity to observe the palmitoylated form of cMyBP-C with a greater accuracy in-situ, as has been demonstrated for potassium channel accessory protein KChIP2, although effective tools for

cardiomyocyte click chemistry are still lacking (Gao & Hannoush, 2014; Main & Fuller, 2021; Murthy *et al.*, 2019).

Additional evidence to support the importance of palmitoylation as a modification of myofilament-localised cMyBP-C is that when cMyBP-C is exogenously expressed in non-cardiac HEK293 cells, palmitoylation is reduced to ~3% compared to 13% in primary cardiomyocytes (Figure 3.17 and Supplementary Figure 7.1). Furthermore, whilst cMyBP-C is highly palmitoylated in neonate rat ventricular tissue, upon isolation and culture this palmitoylation is abolished (Figure 3.18). Whilst neonatal cardiomyocytes provide a useful system for cardiac research, they are limited in their physiological relevance as upon culture they undergo rapid dedifferentiation and redifferentiation which induces a more stem cell-like quality with spontaneous beating observed (Ehler *et al.*, 2013). Furthermore, cultured neonatal cells lack defined T-tubules making them more like adult atrial cells than ventricular cells, which as demonstrated have low levels of palmitoylated cMyBP-C (Figure 3.6; Fearnley *et al.*, 2011). cMyBP-C palmitoylation is also lost upon culture of adult ventricular cardiomyocytes, although not to the extent of loss in neonatal cells (Figure 3.18). Adult cardiomyocytes undergo a change in morphology upon culture, including loss of T-tubule definition and myofibrillar structure (Eppenberger *et al.*, 1988; Piper *et al.*, 1982). As recent evidence suggests some DHHCs may be localised in areas of the sarcomere, it will be important to determine whether loss of cardiomyocyte structure upon culture alters enzyme expression pattern or activity which could explain the loss of cMyBP-C palmitoylation (Miles *et al.*, 2020).

3.5.3 Palmitoylation is a therapeutically relevant post-translational modification of cMyBP-C

The disease relevance cMyBP-C PTM regulation, particularly concerning phosphorylation, acetylation and S-glutathionylation, has been demonstrated using animal models of cardiac injury and in samples from patients of HCM and HF (Copeland *et al.*, 2010; Govindan, Sarkey, *et al.*, 2012; Sadayappan *et al.*, 2006; Stathopoulou *et al.*, 2016). In order to determine the therapeutic relevance of cMyBP-C palmitoylation, Acyl-RAC was used to characterise ventricular tissue from animal models and patient samples. In a rabbit model of HF, cMyBP-C palmitoylation is reduced in the remodelled myocardium 8-weeks post-MI in the

LV (infarct, peri-infarct and remote) but not in the adjacent septal regions (remote; Figure 3.9). Similarly, in a pig model of I/R and HF, cMyBP-C palmitoylation is reduced, although not significantly, 3 months post-injury (Figure 3.10). As will be discussed in Chapter 5, the same trends were observed in other non-myofilament cardiac substrates including well characterised NCX1.

The LV is the site of infarct in both these models, whilst the septal region of the rabbit heart is likely involved in secondary remodelling (Konstam *et al.*, 2011). Additionally, the peri-infarct region undergoes the most substantial change in terms of haemodynamic stress and remodelling (Burton *et al.*, 2000). This could indicate that cMyBP-C palmitoylation changes are occurring in the area that is undergoing the most significant remodelling, including that of T-tubules (Setterberg *et al.*, 2021). Indeed, a study investigating the remodelling post-MI in the rabbit heart reported that the fibrotic remodelling and inflammation that drives the development of HF occurred to a greater extent in the vicinity of the MI (Wu *et al.*, 2017). There was no significant change in cMyBP-C palmitoylation in a rat model of type 2 diabetes, which is associated with increased levels of non-esterified fatty acids and some degree of cardiac dysfunction, particularly diastolic (Figure 3.11; Mansor *et al.*, 2013). This could suggest that cMyBP-C palmitoylation may not be driven by fatty acid availability but instead through maladaptive changes in palmitoylation machinery in response to direct cardiac insult. A limitation in this conclusion is that extent of remodelling has been reported to directly correlate with infarct size, which is difficult to control from a methodological point of view (Konstam *et al.*, 2011).

Nevertheless, cMyBP-C appears to show disease related changes in palmitoylation, and the question arises as to whether this accurately models what happens in humans. Analysis of samples obtained from organ donors and ischaemic human HF patients revealed whilst cMyBP-C phosphorylation was reduced, although not significantly, cMyBP-C palmitoylation was significantly increased in HF samples (Figure 3.12). The loss of cMyBP-C phosphorylation in HF has been widely reported, and this is often accompanied by an increase in cMyBP-C released into the blood, with it now being considered as a biomarker for acute MI (Barefield *et al.*, 2019; Govindan, McElligott, *et al.*, 2012; Tong *et al.*, 2017). Given the evidence presented that cMyBP-C palmitoylation increases is affinity for the myofilament, it is perhaps surprising to observe higher levels of palmitoylated cMyBP-C in HF

patients where this may be occurring. However, the cleaved product is in the N-terminal domain (C0-C1f) and as will be discussed, cMyBP-C palmitoylation may be occurring in the central domains (Lynch *et al.*, 2021). Although cMyBP-C phosphorylation is generally found to be reduced in cardiac disease and HF, this is not always the case. A recent study evaluated cMyBP-C-myosin targeting peptides in a rat model of MI reported that whilst cMyBP-C phosphorylation was significantly reduced up to 3 days post-MI, there was no significant change after 1-week and even an increase at 4- and 8-weeks post injury. This may suggest a compensatory mechanism is occurring changing the cMyBP-C PTM profile as HF develops (Hou *et al.*, 2022). As such, the results of these models or human samples may not be representative of the wider population and continuing to build a more complete picture of cMyBP-C palmitoylation changes in disease states will be important going forward.

Interestingly, in contrast to ischaemic HF samples, HCM caused by *MYBPC3* mutations, other sarcomeric mutations or non-sarcomeric mutations did not result in a significant change in cMyBP-C palmitoylation (Figure 3.15). The cMyBP-C PTM profile is complex in HCM, as whilst many mutations result in loss of cMyBP-C phosphorylation, particularly ones found in the vicinity of the M-domain, this is not observed in all cases (Jacques *et al.*, 2008; van Dijk *et al.*, 2009). This may be due to the heterogeneity of mutations and phenotypes within the *MYBPC3* HCM cohort, and therefore an understanding of the role of cMyBP-C palmitoylation may be better gained from focussing on a particular HCM phenotype i.e. the heterozygous mutations that change cMyBP-C location in the sarcomere (Parbhudayal *et al.*, 2018).

Similarly to what was observed in the animal models, the increase in palmitoylation in ischaemic HF samples is not unique to cMyBP-C and was also observed in other cardiac substrates, as will be discussed in Chapter 5. Whilst there may be underlying remodelling of palmitoylating pathways contributing to the observed increase in cMyBP-C palmitoylation, there are many confounding factors that could play a role. Phosphorylation of cMyBP-C was reduced, although not significantly, in female HF patients compared to organ donors but not in males (Figure 3.13). Sex-dependent changes in phosphorylation of cMyBP-C have not been widely reported and those that use male and female animals have not noted any profound impact of sex (Rosas *et al.*, 2019; Wang *et al.*, 2014). In terms of

palmitoylation, the difference associated with HF is predominantly in the male samples but not the females, as the females start with higher, although not significantly, levels of palmitoylation (Figure 3.13). However, in healthy animals, comparison of male and female neonatal rats revealed no significant difference in levels of cMyBP-C palmitoylation (Figure 3.14). As such, a lack of sample numbers, particularly in the female HF cohort, limit the conclusions of the role of sex in cMyBP-C PTM modification. Nevertheless, it is an important point to consider as HF disproportionately affects males and HCM disease progression is different in males than females (Butters *et al.*, 2021; Lam *et al.*, 2019). Other variables in the human samples like the role of an MI, which the animal models may more accurately reflect, the presence of hyperlipidaemia, or comorbidities such as diabetes may influence cMyBP-C PTMs. However, the relatively small sample size make statistically relevant comparisons challenging overall.

3.5.4 Palmitoylation inhibitors and peptide array as tools to study cMyBP-C palmitoylation

There has been a significant lack of selective pharmacological compounds to study palmitoylation. Recently, a class of compounds known as amphiphiles have been of interest as they were reported to break thioester bonds between palmitoyls and substrates (Rudd *et al.*, 2018). In the present study, three AMDs were tested for their ability to reduce NCX1 palmitoylation in NRVM, with AMD7 showing the greatest efficacy at 50 μM and 10 μM (Figure 3.19). However, upon treatment of adult rabbit cardiomyocytes, AMD7 was toxic to the cells at 50 μM and had no significant effect on reducing cMyBP-C or NCX1 palmitoylation at 10 μM, making it an unsuitable compound for investigating the functional consequences of cMyBP-C palmitoylation (Figure 3.20). There are significant differences between neonatal and adult cardiomyocyte structure and morphology, including neonatal cells being more readily manipulated genetically, which may contribute to the selective effectiveness of AMD7 in this case (Lam *et al.*, 2001). Additionally, the non-selective nature of these compounds could mean they are interfering with other thioester interactions, such as those regulating the catalytic activity of enzymes like GAPDH or other post-translational modifications such as SUMOylation (Alberts *et al.*, 2002; Main & Fuller, 2021). This may be contributing to the observed toxicity in these cells.

Aside from pharmacological tools, a common technique for studying the functional consequence of loss of palmitoylation is the identification, and mutation, of substrate palmitoylation site(s) (Main & Fuller, 2021). However, this is challenging as no consensus sequence exists for palmitoylation, and the current "rules" that allude to potential palmitoylation sites are most relevant for membrane proteins (Salaun *et al.*, 2010). As such, the present work attempted to develop a novel technique for palmitoylation site identification utilising the techniques of peptide array and palmitoylation click chemistry, with the theory that the palmitoyl analogue ODYA-CoA would conjugate to available cysteines which could then be detected by clicking with the fluorescently labelled azide. In an array of cMyBP-C peptides, the technique identified distinct peptides including a di-cysteine motif, which is another feature common of palmitoylation sites, and, as will be discussed, a site (C623) that was revealed to be palmitoylated by other methods (Figure 3.21; Linder & Deschenes, 2003). In order to assess further the validity of the technique, a peptide array containing sequences with the sole palmitoylated cysteine of NCX1, and negative control sequence, were developed. Similarly, this resulted in distinct peptides identified, including a loss of signal when the palmitoylation site was truncated or mutated (Figure 3.22). However, these spots could be identified without the presence of ODYA-CoA, suggesting the fluorescent azide probes are directly attaching to the sequences. Cy5.5 has been reported to attach to cysteines, but only with a maleimide attached (Choi *et al.*, 2011). In this case neither the Cy5.5 or the CW800 contain a maleimide, or any group capable of forming a bond with the cysteine, whilst incubation with hydroxylamine had no effect on reducing the signal, suggesting they are not binding via cysteine thioesters. An understanding of where in the sequence the fluorescent probes are attaching could be gained from alanine scans of positive peptides, replacing every amino acid sequentially with alanine (Bolger *et al.*, 2006). In any case, the technique cannot be used reliably to predict palmitoylation sites, but further developments are certainly warranted.

3.5.5 Palmitoylation of cMyBP-C in the central domains

As an alternative strategy to identify cMyBP-C palmitoylation sites, a cysless version of FLAG-cMyBP-C was produced and Acyl-RAC revealed complete loss of palmitoylation (Figure 3.23). Following this, individual or closely localised cysteines were returned, however no single construct showed any return of

palmitoylation (Figure 3.24). This may be because palmitoylation is occurring at a cluster of cysteines, as has been observed for cMyBP-C S-glutathionylation (Stathopoulou *et al.*, 2016). In support of this, returning of multiple cysteines based on their ability to undergo S-glutathionylation and therefore available for modification by palmitoylation, returned palmitoylation to the cysless construct to a certain extent. Two of these sites, C623 and C651 located in the C4 and C5 domains respectively, were later identified to be palmitoylation sites through site directed mutagenesis of the WT cMyBP-C construct (Figure 3.25).

Whilst much research around cMyBP-C has focussed on the actin-myosin binding N-terminal domains, and the myosin-titin binding C-terminal domains, relatively little is known about the central domains in comparison. This is despite containing some unique features, including a cardiac specific loop in the C5 domain and an elongated linker between C4 and C5 domains (Sadayappan & de Tombe, 2012). The loop in particular is largely undefined in structure and has been speculated to function as a scaffold for interactions of other molecules, including as an enzyme docking site (Gautel *et al.*, 1995). Interestingly, cMyBP-C has also been reported to form bent conformations, 40% of the time involving two hinges one of which may be occurring between the C4 and C5 domains (Doh, Bharambe, *et al.*, 2022; Previs *et al.*, 2016). It will be important to determine whether increased palmitoylation, and potentially increased hydrophobicity, in this region influences the hinge motion of cMyBP-C, and whether this may represent a novel mechanism, similar to the SRX/DRX states of myosin, by which cMyBP-C function is regulated (Nag & Trivedi, 2021). Additionally, based on the trimetric collar model of myosin-cMyBP-C binding, these domains may be interacting with the C-terminal domains on other cMyBP-C molecules, another factor which hydrophobicity and palmitoylation may influence (Flashman *et al.*, 2008). In further support of the importance of the central domains, a recent study identified that whilst the N-terminal domains interact with the myosin S1 region as has previously been reported, the highest affinity binding is between the central domains and the S1, even suggesting cMyBP-C may be involved in cross-linking different myosin molecules together through these interactions (Ponnam & Kampourakis, 2022). Interestingly, phosphorylation of the M-domain did not influence this central domain interaction, however this region may have its own PTM profile, as aside from S-glutathionylation, a recent study identified 13 novel phosphorylation sites

in this region, along with new acetylation and novel ubiquitination sites (Doh *et al.*, 2022; Ponnam & Kampourakis, 2022; Stathopoulou *et al.*, 2016).

Interestingly, whilst palmitoylation was also identified in both skeletal isoforms of MyBP-C to a similar extent of the cardiac isoform, C623 is a site unique to cMyBP-C, whilst C651 is only shared with the fast skeletal isoform (Figure 3.16 and Table 3.2) Adjacent amino acids around both the sites are also poorly conserved between isoforms, but well conserved between species (Table 3.2). This is not uncommon for cMyBP-C modifications, as of the three M-domain phosphorylation sites, only one site exists in the slow skeletal isoform and none in the fast skeletal isoform, although a direct comparison of total phosphorylated cMyBP-C between skeletal and cardiac tissue has not been reported (McNamara & Sadayappan, 2018). Whilst C623 and C651 may be the predominant sites of cMyBP-C palmitoylation, several of the cysteines within cMyBP-C are poorly conserved between isoforms, indicating that the skeletal isoforms may have their own sites that could contribute to the overall similar level of palmitoylation. Loss of both C623 and C651 did not abolish palmitoylation, indicating there are other sites in cMyBP-C that have not been identified and should be investigated further (Figure 3.25).

A limitation of detecting palmitoylation sites in HEK293 cells is that whilst they can provide a useful system to detect the presence or absence of palmitoylation, they show low levels of palmitoylated cMyBP-C and lack of proper cellular location. Furthermore, limits of the assay sensitivity could lead to falsely undetectable quantities of cMyBP-C palmitoylation. Additionally, a study has shown that cysteine availability may be dependent on contractile state, and therefore palmitoylated cysteines detected in HEK293 cells may not be as important for endogenous MyBP-C in cardiomyocytes or skeletal muscle cells (Gross & Lehman, 2013). This has previously been observed for phosphorylation of cMyBP-C, where higher levels were observed *in vivo*, including the identification of 9 new sites, compared to *in vitro* and *ex vivo* studies (Kooij *et al.*, 2013). Nevertheless, the ability of a cysteine to undergo both S-glutathionylation and S-palmitoylation has previously been observed for cardiac substrates, including in our own work where S-glutathionylation antagonises the palmitoylation of PLM, with potential knock-on consequences for Na^+/K^+ ATPase function (Howie *et al.*, 2013; Tulloch *et al.*, 2011). Furthermore, high sucrose/glucose treatment in mice and endothelial cells leads to oxidation of HRas palmitoylated cysteines, and

reduced palmitoylation as a result (Burgoyne *et al.*, 2012). It will be important to characterise the relationship between cMyBP-C S-glutathionylation and palmitoylation going forward.

3.5.6 Increased cMyBP-C palmitoylation negatively regulates myofilament function

Whilst it is interesting that the cysteines identified undergo both S-glutathionylation and S-palmitoylation, as a result, characterisation of palmitoylation by mutating the sites, as has been frequently utilised in the study of phosphorylation, cannot be completed in this way (Sadayappan *et al.*, 2006). To elucidate the potential functional role of cMyBP-C palmitoylation, myofilaments treated with palmitoyl CoA (which show increased cMyBP-C palmitoylation; Figure 3.8) were investigated for changes in passive and active force. Palmitoyl CoA had no significant effect on passive force at three different sarcomere lengths, which is primarily driven by the molecular spring of Titin, the palmitoylation status of which is unknown (Figure 3.27; Herzog, 2018). Similarly, there was no significant effect on the ability of the myofilaments to generate maximal force in saturating Ca^{2+} (pCa4.5), however, there was a significant decreased in the force generated in submaximal Ca^{2+} (pCa6.0) in the palmitoyl CoA treated myofilaments compared to control, suggesting a loss of Ca^{2+} sensitivity (Figure 3.28).

In permeabilised ventricular trabeculae and ventricular cardiomyocytes, pCa5.5-6.0 is the typical range for the pCa_{50} (the Ca^{2+} concentration required to give half maximal force). As such, pCa6.0 measurements provide important information on Ca^{2+} sensitivity, compared to pCa4.5 where the maximal force will likely have already been reached and plateaued at lower concentrations (Cazorla *et al.*, 2009; Sun & Irving, 2010). However, it is important to note that the $F_{passive,}$ F_{max} and F_{act} values observed here are much higher, with an F_{max} of ~75Kn/m^2 compared to 20-30Kn/m^2 reported in other studies (Bito *et al.*, 2007; Kovács *et al.*, 2017). This is likely due to technical issues in the software measurements, which takes the raw voltage values detected by the force transducer and determines the corresponding Kn/m^2 force based on cell area and magnification. Nevertheless, as all measurements were obtained on one setup a comparison between palmitoyl CoA treated myofilaments and controls is still meaningful.

In line with what is presented here, a study treating rat cardiomyocytes with a mixture of fatty acids including palmitic acid, although at a higher concentration, reported changes in Ca^{2+} dynamics, including increased Ca^{2+} transients and influx through the LTCC, but counterintuitively, a reduction in myofilament Ca^{2+} sensitivity (Zhao *et al.*, 2016). This may be because dysfunction at a myofilament level has been demonstrated to feedback to the Ca^{2+} cycling machinery and alter Ca^{2+} transients (Huke & Knollmann, 2010; Robinson *et al.*, 2007; Schober *et al.*, 2012). This includes a contribution of cMyBP-C phosphorylation, loss of which negatively regulates Ca^{2+} extrusion by NCX1 (Kumar *et al.*, 2020). Increased cardiomyocyte fatty acid availability does have physiological and pathophysiological relevance and it will be interesting to determine in particular whether the observed effects of increased fatty acid availability on sarcomere shortening are driven by myofilament-palmitoylation mechanisms (Angin *et al.*, 2012).

Interestingly, in contrast to what is observed here, increased S-glutathionylation at the two sites identified in this study, C623 and C651, is correlated with increased myofilament Ca^{2+} sensitivity and slower cross-bridge kinetics (Patel *et al.*, 2013). Whilst rate of crossbridge development was not measured in this study, it will be important to determine whether this too has an opposing effect to S-glutathionylation. S-glutathionylation has a reported effect on antagonising cMyBP-C phosphorylation, which may be contributing to its pathological effects. However, the relationship between cMyBP-C palmitoylation and phosphorylation requires further investigation as whilst total cMyBP-C palmitoylation is increased in response to palmitoyl CoA treatment, there is no effect on the overall level of p-cMyBP-C as a result. However, in contrast to total cMyBP-C, the portion of cMyBP-C that is phosphorylated did not show increased palmitoylation (Figure 3.26). This may indicate that the non-phosphorylated form of cMyBP-C is preferentially palmitoylated, which may partially explain the detrimental effect on myofilament Ca^{2+} sensitivity, of which phosphorylation of cMyBP-C enhances (Mamidi *et al.*, 2016). Additionally, as demonstrated, HF samples with reduced cMyBP-C phosphorylation show increased palmitoylation (Figure 3.12). However, the biological replicates in the p-cMyBP-C myofilament experiment were lower in comparison to the total cMyBP-C study, and therefore further repetition is needed before conclusions can be drawn.

The functional evidence presented here does not allow an understanding of the exact role of cMyBP-C palmitoylation, as the sarcomere contains at least 28 different proteins, any of which could be targeted by palmitoylation and contribute to the loss of Ca^{2+} sensitivity (Huxley, 1957). An alternative strategy would be to repeat the experiment in myofilaments from WT and cMyBP-C KO mice, a comparison of which would allow the contribution of cMyBP-C palmitoylation to be determined. This has previously been achieved in the study of cMyBP-C S-glutathionylation, however the limitation is that cMyBP-C KO mice already have significant functional changes that may confound the results (Cuello *et al.*, 2018; Stathopoulou *et al.*, 2016). Recently, a novel method has been developed by the Harris lab involving a transgenic mouse in which the C0-C7 domains of cMyBP-C can be "cut" away from isolated myofilaments and replaced rapidly by "pasting" a recombinant version in its place. Using this method, they were able to elegantly show the contribution of the C0-C7 domains on actin-myosin cross-bridge kinetics and Ca^{2+} sensitivity as well as identify a novel role for cMyBP-C in spontaneous oscillations (Napierski *et al.*, 2020). Using this method, a recombinant form of C0-C7 with increased palmitoylation could be introduced and the effect on myofilament function determined, with the opportunity for *in vivo* study.

3.6 Conclusion

Overall, this work has provided new evidence that palmitoylation is an important regulatory modification for myofilament proteins in the cardiac tissue, and that increased palmitoylation at a myofilament level is associated with reduced myofilament Ca^{2+} sensitivity. Importantly, this may be driven through palmitoylation of cMyBP-C, levels of which are reduced in animal models of disease but increased in samples from human HF patients. There are several factors that influence cMyBP-C palmitoylation level, including anatomical region and the effect of culture on primary cells. Whilst all the sites responsible for total cMyBP-C palmitoylation could not be identified by a novel method of peptide array or by returning cysteines to a cysless version of cMyBP-C, two previously reported S-glutathionylation sites have been demonstrated to be palmitoylated in HEK293 cells. Understanding the functional consequence of cMyBP-C palmitoylation in this central domain region, including its influence on S-glutathionylation and

phosphorylation, will be important in understanding why palmitoylated cMyBP-C is altered in cardiac disease and whether it represents a novel therapeutic target.

Chapter 4 SUMOylation of cMyBP-C

4.1 Introduction

4.1.1 SUMOylation as a regulator of the sarcomere

Given that the majority of SUMOylated proteins are involved in nuclear activities, SUMOylation has been most well studied in the context of sarcomere assembly and maintenance (Nayak *et al.*, 2020). Myogenesis in muscle cells involves the transition of precursor cells (myoblasts) to multinucleated myotubes that have irreversibly exited the cell cycle. SUMOylation appears to be key to the process, as loss of UBC9 is associated with reduced myotube formation in skeletal muscle cells (Riquelme *et al.*, 2006). This may be through the important interplay between SUMOylation and acetylation, which has been investigated in the study of MyoD, a transcription factor which initiates myoblast differentiation. In skeletal myotubes, de-acetylation of MyoD by HDAC1 represses its activity, and SUMOylation of HDAC1 alleviates this inhibition, allowing myogenesis to occur (Joung *et al.*, 2018).

In the myofilament, TnI SUMOylation has been observed in drosophila, occurring predominantly at a lysine near the C-terminus (V**K**EE), where SUMOylation is required for its nuclear translocation during development (Sahota *et al.*, 2009). Interestingly, although the drosophila form of TnI is larger and only shares a 22% homology, the site identified is conserved in skeletal and cardiac isoforms. Indeed, our recent work identified SUMOylation of cardiac TnI (cTnI) at K177 (V**K**KE), however this was studied in the context of the developed sarcomere (discussed below) therefore it is unknown whether this site contributes to TnI regulation during development (Fertig *et al.*, 2022). Nevertheless, a HCM mutation in cTnI (I172T) is located near to the site, which is thought to increase cTnI nuclear localisation, therefore it will be interesting to determine whether this is because of altered SUMOylation (van Driest *et al.*, 2003). Indeed, many HCM mutations in Tm increase the likelihood that a region would become SUMOylated by developing a new SUMOylation consensus site. SUMOylated α-Tm is associated with greater nuclear localisation in HEK293 cells, although this remains to be characterised in a cardiac setting (Chase *et al.*, 2013; Manza *et al.*, 2004).

Sarcomere turnover and assembly are tightly regulated to maintain cardiac function, and SUMOylation has been implicated in this process. Study of the

myofibrillogenesis regulator 1 (MR-1), overexpression of which is associated with cardiac hypertrophy, demonstrated that it drives SUMOylation and translocation from the nucleus of myomesin, the main structural component of the M-line, therefore facilitating sarcomere assembly (Wang *et al.*, 2012). As increased sarcomere assembly is observed in the early stages of hypertrophy, this may suggest a potential consequence of SUMOylation upregulation in early cardiac hypertrophy.

The most recent work from our group has uncovered the role of SUMOylation for cTnI and the ß2-adrenoceptor, indicating that SUMOylation plays an important regulatory role in the adult cardiomyocyte. SUMOylation of the ß2-adrenoceptor reduces isoprenaline stimulated activity of PKA, including of its own phosphorylation site, which in turn maintains ß2-adrenoceptor expression and reduces receptor internalisation (Wills, 2017). However, the consequences of this on cardiomyocyte contractility are currently unclear (Ling, 2021). In contrast, SUMOylation of cTnI has been studied in virally infected adult cardiomyocytes where it indirectly alters myofilament Ca^{2+} sensitivity by potentially "scavenging" SUMO1 molecules away from other substrates, as this effect is blocked when the SUMOylation site is mutated (Fertig *et al.*, 2022). This indicates that SUMOylation may play an important role in the function of other myofilament proteins. Interestingly, in contrast to SERCA2a, ß2-adrenoceptor and cTnI SUMOylation is upregulated in a pig model of HF, with increased cTnI SUMOylation also observed in human HF samples. Protein levels of each are often reduced in this setting, however SUMOylation does not appear to contribute to ß2-adrenoceptor or cTnI turnover by the UPS, indicating SUMOylation may be regulating the proteins functionally in pathological conditions ((Fertig *et al.*, 2022; Ling, 2021; Wills, 2017). As such, there is a great interest in characterising the SUMOylation of additional cardiac substrates.

4.1.2 Tools to study SUMOylation

As SUMOylation is a dynamic modification that occurs in ~1% of a protein at a given point, it has been very difficult to detect endogenously and therefore characterise (Nayak *et al.*, 2020). To address this, several novel methods have been developed to detect SUMOylation in both *in vitro* and *in vivo* settings. *In vitro* SUMOylation assays have been developed which contain active components of the SUMOylation

cascade and can be used to enhance SUMOylation of proteins from cell lysates, which has been successfully demonstrated in several settings (Cilenti *et al.*, 2020; Li *et al.*, 2020; Sarge & Park-Sarge, 2009). Although SUMOylation occurs in a cascade involving several enzymes, over-expression of SUMO and UBC9 is sufficient to catalyse SUMOylation of a substrate (Cartier *et al.*, 2019). As such, fusion of a substrate of interest to UBC9 has been shown to enhance SUMOylation levels from undetectable to almost 40% in the case of SUMO1 substrates p53 and STAT1. Additionally, this UBC9-driven SUMOylation is lost upon SUMOylation site mutation or fusion with an inactive UBC9 (Jakobs *et al.*, 2007). However, this method is limited in that it represents an enhanced/non-physiological form of SUMOylation and cannot inform on SUMOylation dynamics *in vivo*. Endogenous SUMOylation can be detected by purifying the protein of interest from a relevant cell or tissue and probing with SUMO1 or SUMO2/3 antibodies (Sarge & Park-Sarge, 2009; C. Tong *et al.*, 2013). However, this may require high levels of protein to observe the SUMOylated form and as such, SUMO site-specific antibodies for substrates have also been developed, including for SERCA2a and cTnI which importantly allowed characterisation of SUMOylation levels in healthy and diseased myocardium (Fertig *et al.*, 2022; Kho *et al.*, 2011).

In terms of SUMOylation site discovery, the knowledge of the SUMOylation consensus motif that occurs in ~50% of SUMOylated substrates has led to the development of several SUMOylation prediction algorithms, providing an accessible starting point for the discovery of SUMOylation sites (Beauclair *et al.*, 2015; C. C. Chang *et al.*, 2018; Impens *et al.*, 2014; Zhao Q, Xie Y, 2014). However, it is important to note that ~38% of SUMOylated substrates are not SUMOylated at these motifs, and ~12% are SUMOylated at inverted consensus motifs, meaning many SUMOylation sites cannot be detected by this method (Lamoliatte *et al.*, 2014). As discussed in Chapter 3, peptide array is a powerful tool for characterisation of protein-protein interactions and has been utilised to study potential post-translational modification sites, including SUMOylation. Lysine containing sequences incubated with *in vitro* SUMOylation reagents results in detection of SUMO conjugation, and the flexibility of peptide arrays means the importance of the adjacent amino acids can also be investigated (Schwamborn *et al.*, 2008; Zhu *et al.*, 2016). In our previous work, this method resulted in identification of putative SUMOylation sites in the β2-adrenoceptor, cTnI, the

LTCC and cMyBP-C (Fertig *et al.*, 2022; Wills, 2017). Finally, a more specific but technically challenging technique that would allow identification of endogenous SUMOylation levels and sites is the use of mass spectrometry. Indeed, recently this method was reported to identify over 6000 SUMOylated substrates and 40,000 SUMO acceptor sites (Hendriks *et al.*, 2018). Although low quantities of SUMOylation proteins still challenge mass spectrometry measurements, combining purification techniques to enrich a substrate of interest with mass spectrometry has been successful in identifying SUMOylation sites for several substrates (Rosas-Acosta *et al.*, 2005; Sheng *et al.*, 2019).

4.2 Aims

Cardiac MyBP-C undergoes regulation by PTMs including phosphorylation, redox modifications and palmitoylation. These all have important disease relevance and may alter cMyBP-C function in the myofilament. SUMOylation is an essential regulator of cardiac contractility through modification of substrates including ion channels, signalling molecules and myofilament proteins, however the SUMOylation status of cMyBP-C is unknown. Previously, a peptide array screen was carried out and identified cMyBP-C as a SUMOylation substrate, as well as the ß2-adrenoceptor, the LTCC and cTnI, the SUMOylation of which has recently been characterised (Fertig *et al.*, 2022; Wills, 2017). The aim of this work is therefore to:

- Determine whether SUMOylation of cMyBP-C occurs in cardiac tissue
- Identify the sites of SUMOylation in cMyBP-C in HEK293 cells using co-transfection of SUMOylation substrates, UBC9-fusion and mass spectrometry
- Characterise the effect of loss of SUMOylation on cMyBP-C phosphorylation and overall cardiomyocyte contractility

4.3 Methods

4.3.1 Co-immunoprecipitation of endogenous cMyBP-C

In order to validate the protein-protein interaction of cMyBP-C with components of SUMOylation pathway, co-immunoprecipitation was used to pull down cMyBP-C and transient interacting partners. All steps were carried out at 4°C. Cardiomyocytes were lysed in 2 mg/ml C12E10 (decaethylene glycol monododecyl ether, Sigma) buffer with protease inhibitor cocktail III (Calbiochem) and equalised to the desired protein quantity (750 µg for endogenous protein). Protein G Sepharose™ 4 Fast Flow beads (GE Healthcare, Fisher Scientific) were used to capture antibody complexes and were equilibrated in the C12E10 buffer. Lysates were split into two reactions: one containing 1 µg of target primary antibody and one containing 1 µg of IgG antibody of the same species as the target protein primary antibody (detailed in Table 2.8). Both contained 30 µl of beads and the volume was made up to 500 µl before samples were rotated overnight. The next day the beads were centrifuged at 500 G for 3 minutes before the supernatant was removed and the beads washed 5 times in 0.5 mg/ml C12E10 buffer with protease inhibitor cocktail. After the final wash the supernatant was removed and the 2X SDS-PAGE loading buffer with 100 mM dithiothreitol (DTT) was added. Samples were then boiled at 60°C for 10 minutes to elute the captured proteins and ensure sufficient denaturation of the antibody within the sample.

4.3.2 Immunoprecipitation of SUMOylated FLAG-cMyBP-C-UBC9 fusion

To aid in the identification of SUMOylated sites on cMyBP-C, SUMOylated FLAG-cMyBP-C-UBC9 (production detailed in 2.4.3) was purified from HEK293 cells to be used for mass spectrometry performed by Dr Sheon Samji (University of Glasgow). HEK293 cells were transfected with FLAG-cMyBP-C-UBC9 fusion and eGFP-SUMO1. Cells were then lysed in purification buffer (50 mM Tris-HCl, 1% Triton X-100 and protease inhibitor cocktail III (Calbiochem), pH 8.0) and centrifuged at 4°C for 10 minutes at 13,000 G to separate supernatant and pellet. A sample of the supernatant was collected (unfractionated) and the remaining lysate was incubated for one hour with ANTI-FLAG® M2 Affinity Agarose Gel (Sigma Aldrich). An unbound sample was obtained and the beads were then washed five times with purification buffer before incubation with 100 µg/ml 3X FLAG® Peptide (Sigma

Aldrich) to elute the captured FLAG-tagged complex from the beads. This was repeated twice to ensure maximal elution and samples taken at each stage for analysis. The eluted lysate was then incubated for 1 hour with GFP-Trap Agarose (Chromotek) before an unbound fraction was taken and beads washed five times with purification buffer before eluting in 2XSDS with 100 mM DTT (Figure 4.1).

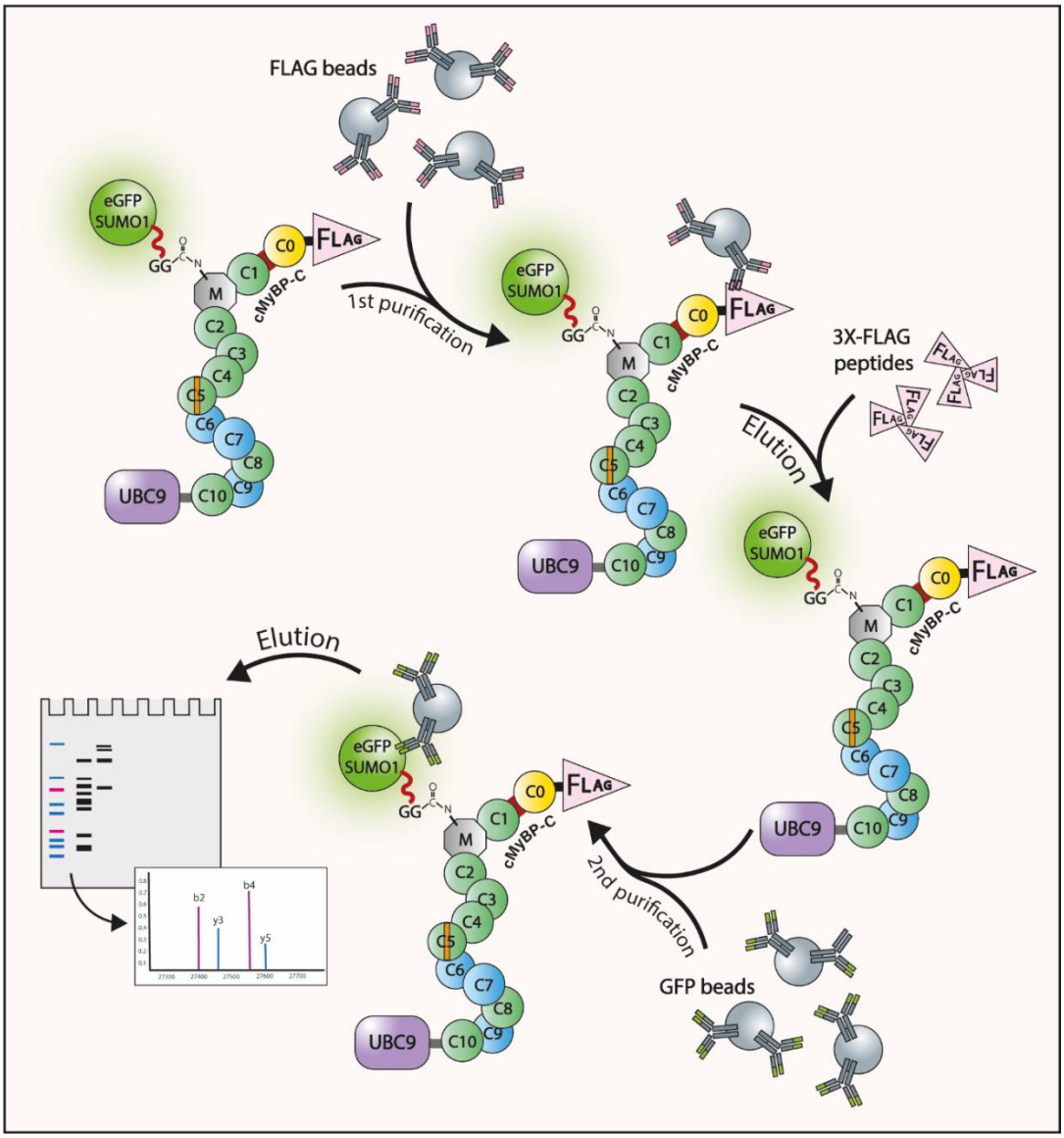

Figure 4.1. Purification of SUMOylated FLAG-cMyBP-C-UBC9.
When co-transfected into HEK293 cells, FLAG-cMyBP-C-UBC9 and eGFP-SUMO1 form a complex. This complex was purified from the lysate by first incubation with FLAG beads to capture the FLAG-tagged complex, followed by elution from the beads from a 3X FLAG peptide. The eluted solution was then incubated with GFP beads to capture the eGFP-SUMO1 attached to the FLAG-cMyBP-C complex. This can then be eluted, and the appropriate bands excised from an acrylamide gel for analysis via mass spectrometry.

4.3.2.1 Liquid chromatography mass spectrometry

Liquid chromatography mass spectrometry (LC-MS/MS) was performed by Dr Sheon Samji at the University of Glasgow. Briefly, following purification, samples eluted following incubation with GFP-Trap Agarose were separated on a polyacrylamide

gel through the stacker until they had reached the resolving gel. A clean, sterile scalpel was then used to excise the area of interest containing the protein to be analysed and kept in ultrapure nuclease free water. Samples were then analysed using an UltiMate3000 nano-flower system (Dionex/LC Packings) connected to an LTQ Orbitrap hybrid mass spectrometer Velos FTMAS (Thermo Fisher Scientific, Germany) equipped with a nano-electrospray ion source, as has been described previously (Mary *et al.*, 2021).

4.3.3 SUMOylation prediction software

Unlike many post-translational modifications, the modification of SUMOylation, the attachment of a small ubiquitin-like modifier (SUMO) protein to a lysine residue, is often found at a site with a specific consensus sequence surrounding the SUMOylated lysine. The motif, ψ-K-x-E, where ψ is any hydrophobic amino acid (A, I, L, M, P or V) and X is any amino acid, was shown to be present in 50% of known SUMOylation sites (Zhao *et al.*, 2014). As such there are still many examples of SUMOylated lysines that don't fall into the traditional motif, or examples of an ψ-K-x-E/D sequence that is not a SUMOylation site, making SUMOylation site prediction more complex. This fact has been considered in more recently developed SUMOylation software predictors such as SUMOsp, and newer version SUMO-GPS, which uses leave-one-out validation and 5-fold cross validation originally designed for phosphorylation site prediction, and also considering the presence of SUMO protein interactor domains as well as sites (Xue *et al.*, 2006; Zhao *et al.*, 2014). For this study, three freely available SUMOylation site prediction software's (SUMOgo (Chang *et al.*, 2018), SUMOplot (Abcepta, 2022) and GPS SUMO (Zhao *et al.*, 2014)) were utilised to analyse the cMyBP-C human sequence (Uniprot ID: Q14896). Each software predicted a SUMOylation site with a confidence between 0-1 based on a number of factors including presence of the SUMOylation motif, as well as comparison to similar sequences within other SUMOylated proteins. For analysis, an average confidence interval score from the different prediction software was generated for each lysine in cMyBP-C.

4.3.4 Adenoviral infection

4.3.4.1 Infection of neonatal rat ventricular cardiomyocytes

Adenoviruses were purchased from Welgen, inc. (Massachusetts, USA) for which the plaque-forming unit (PFU) per ml was calculated by the manufacturer. Viruses were and aliquoted on arrival and stored at -80 until use. For infection of neonatal rat ventricular cardiomyocytes, viruses were thawed on ice and added to cells in culture media at the desired multiplicity of infection (MOI, calculate from the viral PFU/ml as described below) which determines the number of viral particles per cell. Cell number was determined by seeding density at time of isolation (as detailed in 2.2.4.2).

$$Multiplicity\ of\ Infection\ (MOI) = \frac{Titre\ of\ Virus\ (\frac{pfu}{ml})}{Total\ number\ of\ cells}$$

4.3.4.2 Amplification of adenoviruses

To amplify a larger quantity of crude virus for infection of primary cardiomyocytes, adenoviruses were amplified using Adeno-X-293 cells (Takara Bioscience, 632271) were used to package and multiply the virus. Briefly, 25-30 T150 flasks at 80% confluence were infected with $2x10^4$ PFU/ml of adenovirus and maintained in culture (approximately 7 days) until a cytopathic effect had occurred (cells round and detached; Figure 4.2).

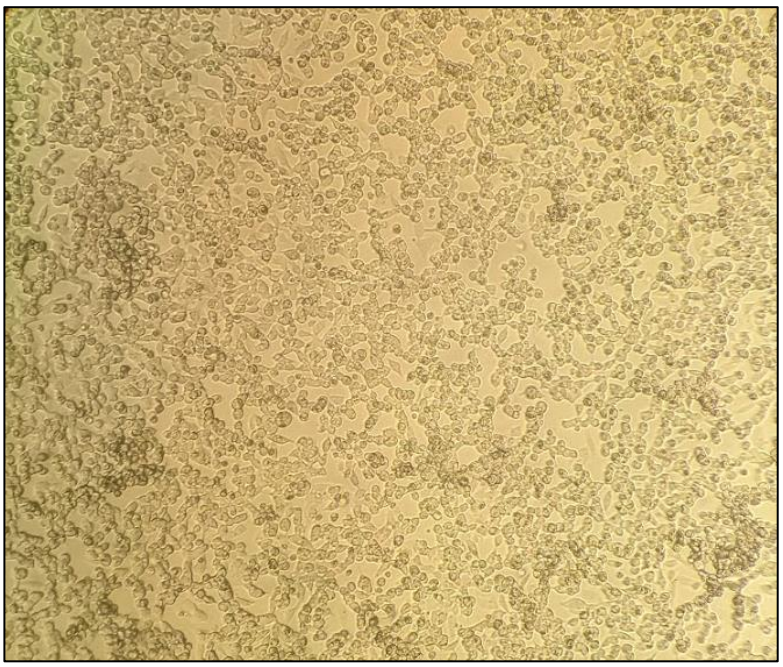

Figure 4.2. Cytopathic effect during amplification of adenovirus particles in AD-293 cells. Adenoviral particles were amplified to produce a crude virus in AD-293 cells. 25-30 T150 of 80% confluent AD-293 cells were infected with with $2x10^4$ PFU/ml and maintained until a cytopathic effect had occurred (cells round and beginning to detach) before cells were collected and virus purified. Image taken using a standard phase contrast microscope with a 10X objective (0.25NA).

Cells were then incubated with trypsin and centrifuged at 1000 RPM for 3 minutes before the remaining pellet of cells was resuspended in 10-15 ml of PBS and stored at -80ºC. A freeze-thaw protocol was used to release the virus from the cells. Cells were thawed at 32ºC followed by vortexing three times in 15 second-on, 15 second-off intervals and snap frozen for 2 minutes. This process was repeated three times before centrifuging at 4ºC for 10 minutes at 2500 G. The supernatant containing the viral particles was then collected, aliquoted and stored at -80ºC until use.

4.3.5 Analysis of neonatal ventricular cardiomyocyte contractility

4.3.5.1 CellOPTIQ™ and Contractility Tool

In order to determine the functional effect of cMyBP-C SUMOylation, contractility of neonatal rat ventricular cardiomyocytes infected with FLAG-cMyBP-C-UBC9 fusion adenoviruses, alone or co-infected with eGFP-SUMO1 virus, was investigated using a CellOPTIQ™ system (Clyde Biosciences, Ltd). Analysis was performed using an ImageJ Macro written by Dr Francis Burton, University of Glasgow.

Briefly, neonatal rat ventricular cardiomyocytes were isolated as described in 2.2.4.2. and plated onto Mat-tek dishes with inserts at a density of 75,000 cells per half insert. The remainder of the dish was filled with media to maintain the humidity. The following day cells were infected with adenoviruses for 1 hour before the medium was replaced and cells were maintained for 24 hours before recording. On the day of recording the insert was removed and Tyrode's buffer (120 mM NaCl, 5 mM KCl, 1 mM $MgCl_2$, 1.8 mM $CaCl_2$ and 10 mM HEPES, 5.5 mM Glucose, pH 7.4) warmed to 37ºC was added. Cells were maintained throughout the experiment in a heated incubator (37 ± 1ºC, 5% CO_2) which could be controlled by a motorised stage. Cells were paced using stimulating field electrodes and an ION Optix C-Pace Cell Stimulator at 1Hz frequency, 2ms pulse duration and 40V. Ten second recordings (capturing 8-10 contractile cycles) were obtained using Inverted Olympus microscope with a Hamamatsu camera and a 60X objective (0.6NA) at 100 frames per second (fps), with 10-15 recordings/areas obtained per dish. Cell recordings were then analysed using the ImageJ Macro which analyses the changes in sarcomere length as a measurement of cardiomyocyte contractility by determining the spatial frequency of the intensity profile of sarcomere bands over time. This can therefore be used to calculate several characteristics of the contractile transient including time to peak (TTP), contraction duration and up-stroke and down-stroke times (Figure 4.3; Rocchetti *et al.*, 2014)

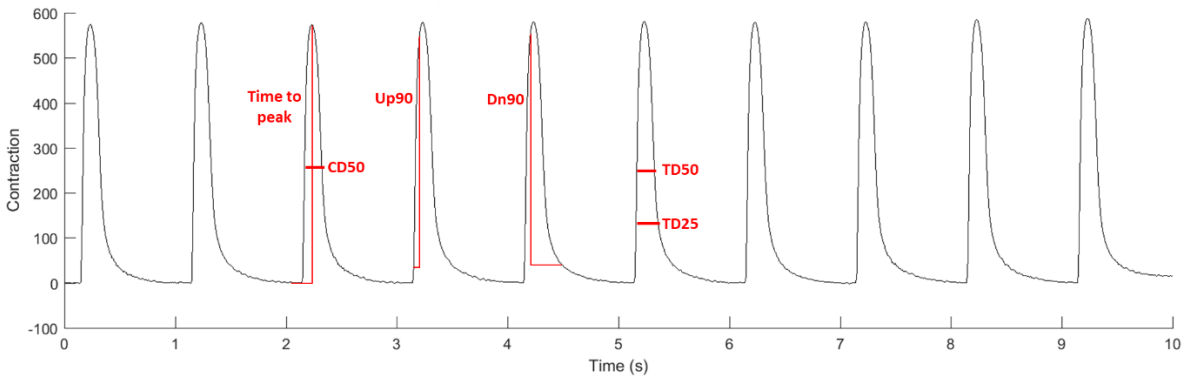

Figure 4.3. Example of neonatal ventricular cardiomyocyte contractile transients and parameters of contractility that can be determined from recordings analysed via Contractility Tool.

Transients recorded from paced neonatal ventricular cardiomyocytes can be analysed using Contractility Tool, designed by Dr Francis Burton, which takes an average of the 10 transients per recording and produces an average contractile transient that can give parameters such as time to peak (TTP), contraction duration at 50% of peak (CD50), time from 10% to 90% of contraction (Up90), time from 90% of contraction to 90% of relaxation (Dn90) as well as time to 50% of contraction (TD50) and time to 75% of relaxation (TD25, also known as time to 25% of remaining relaxation).

4.4 Results

4.4.1 Methods to detect endogenous SUMOylation of cMyBP-C

4.4.1.1 cMyBP-C-SUMO1 co-immunoprecipitation in rabbit cardiomyocytes

Given the importance of cMyBP-C regulation by PTMs, including newly discovered ubiquitylation and the preliminary evidence from peptide arrays, cMyBP-C may undergo SUMOylation (Wills, 2017). A common method to detect SUMOylation is purifying the protein of interest and probing for the covalently attached SUMO1 (Sarge & Park-Sarge, 2009; C. Tong *et al.*, 2013). This was completed in rabbit ventricular cardiomyocytes and purification of cMyBP-C led to detection of SUMO1 specific bands between 150kDa and 250kDa. However, this was only detected in one sample of six, and suggested a high level of purified cMyBP-C is required in order to view these bands (Figure 4.4).

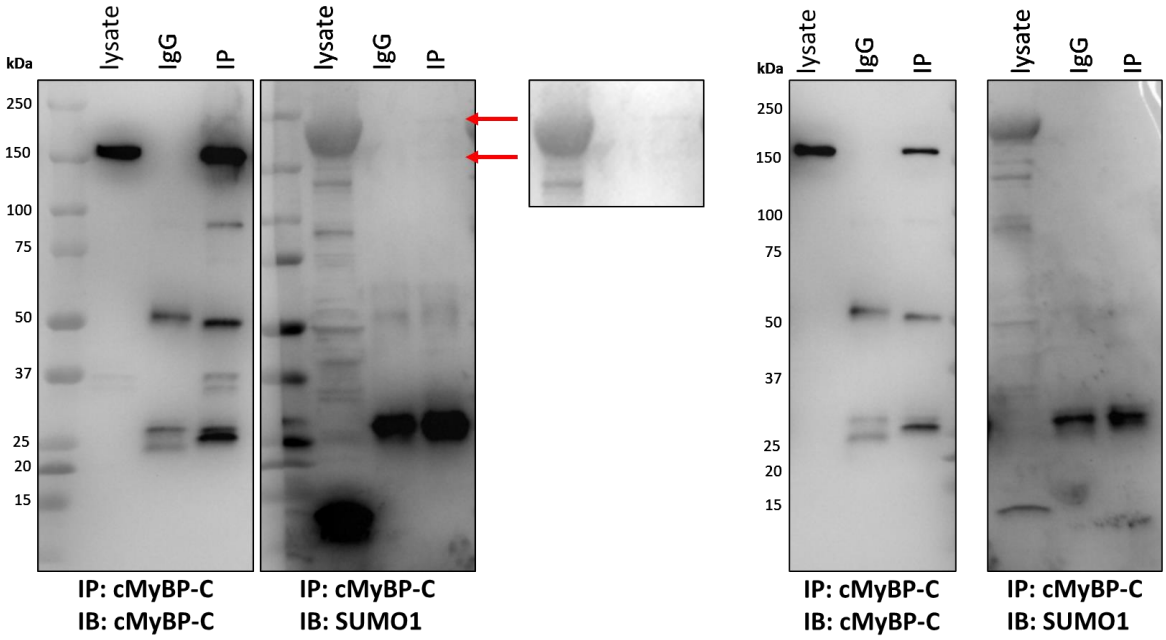

Figure 4.4. cMyBP-C-SUMO1 complex is rarely detected in rabbit ventricular cardiomyocytes.
Lysate prepared from adult rabbit septal cardiomyocytes was incubated with Protein-G sepharose beads with a cMyBP-C primary antibody (IP) along with a non-specific antibody control (IgG). cMyBP-C was specifically purified in the IP compared to the IgG sample (cMyBP-C antibody). In IP samples, faint bands were detected at ~160kDa and ~190kDa when probed with SUMO1 antibody. However, this was only present in n=1 one sample (left example) and an additional 5 repeats did not reproduce this result (right example). IP = immunoprecipitation, IB = immunoblot.

4.4.1.2 cMyBP-C co-expression with SUMOylation components

Purification of cMyBP-C-SUMO1 suggests it is present in a very low quantity, which is consistent with the observation that SUMOylated substrates are rapidly turned

over and often represent only 1% of the total protein. However, co-expression with components of the SUMOylation cascade including E2 conjugating enzyme UBC9 and E3 ligases PIAS-1, PIAS-3 and PIAS-γ, can enhance SUMOylation leading to the detection of a band shift due to the addition of the ~12kDa SUMO molecule. This approach was investigated using FLAG-cMyBP-C transfected HEK293 cells, however no band shift was detected in any case (Figure 4.5).

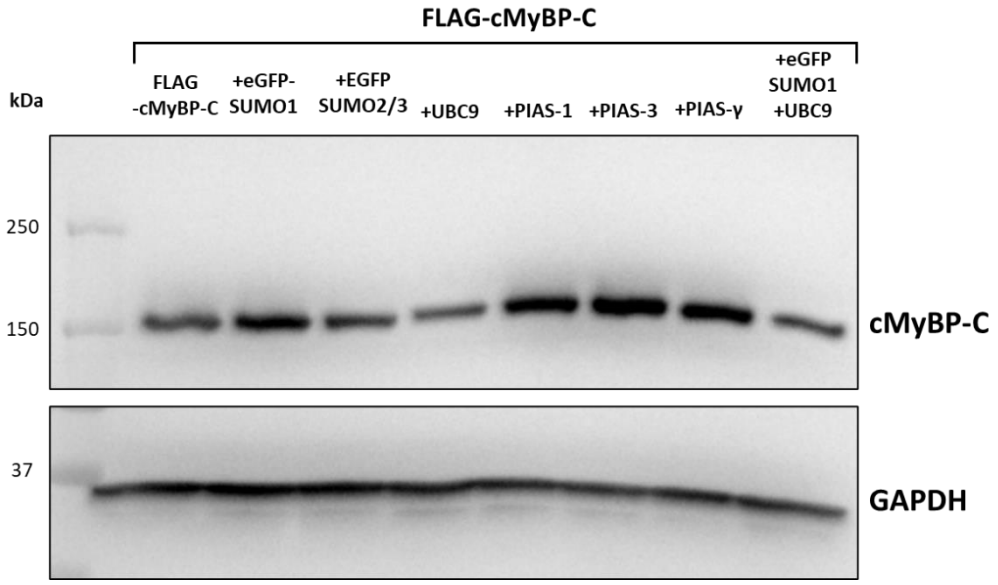

Figure 4.5. FLAG-cMyBP-C co-transfection with SUMOylation components does not result in detectable SUMOylated cMyBP-C.
FLAG-cMyBP-C was co-transfected in HEK293 cells with components of the SUMOylation cascade including eGFP-tagged SUMO1 and SUMO2/3, E2 conjugating enzyme UBC9 and E3 ligases PIAS-1, PIAS-3 and PIAS-Ч. Co-transfection did not result in any detectable SUMOylation in cMyBP-C as evidenced by a band at a higher weight. Representative blot of n=3-4 experiments.

4.4.1.3 UBC9-fusion directed SUMOylation of cMyBP-C

The difficulty in detecting SUMOylation of a substrate has significantly impeded study of its regulation of protein function. As such, investigation of substrate SUMOylation has been achieved by enhancing SUMOylation by fusing the E2 ligase UBC9 to the substrate of interest (Jakobs *et al.*, 2007). UBC9 binding a substrate is a crucial step in the process of SUMOylation. As such, a FLAG-cMyBP-C-UBC9 fusion construct was created and co-transfected in HEK293 cells with eGFP-SUMO1. This led to a detectable band shift that was dependent on eGFP-SUMO1 co-expression. Analysis of the SUMOylated band compared to the unSUMOylated band indicated it represents ~20% of total FLAG-cMyBP-C-UBC9 (Figure 4.6).

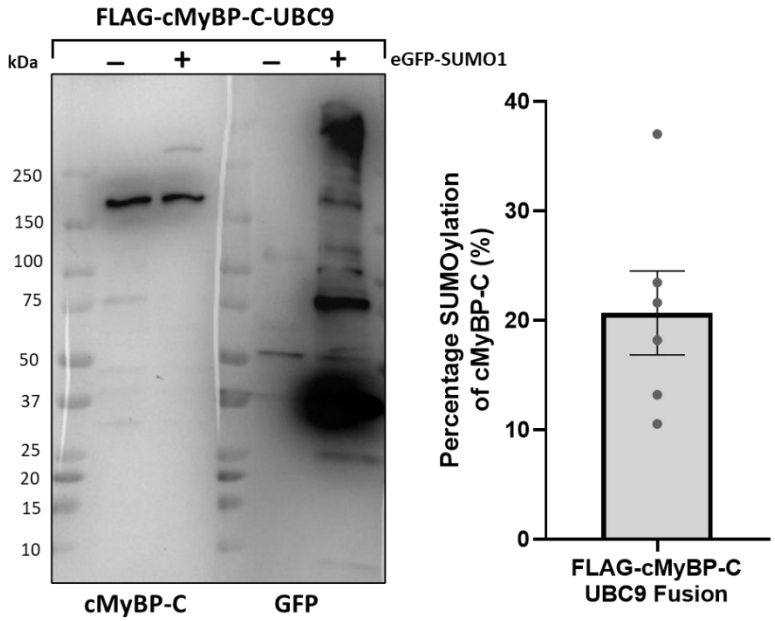

Figure 4.6. FLAG-cMyBP-C-UBC9 fusion co-transfection with SUMO-GFP results in detectable band shift.
Production of a fusion construct of FLAG-cMyBP-C and E2 conjugating enzyme UBC9 results in a detectable band shift when co-expressed with eGFP-SUMO1 in HEK293 cells. The eGFP-SUMO1 specific band represents ~20% of the total construct (shifted band/shift + non-shifted band total). Data is mean ±S.E.M normalised to total cMyBP-C (SUMOylated + non-SUMOylated bands).

This suggests the increased proximity of FLAG-cMyBP-C and UBC9 enhances its ability to become SUMOylated. Furthermore, this was demonstrated to be dependent on a catalytically active UBC9, as mutation of the active site cysteine to alanine (C93A) resulted in loss of the SUMOylated band (Figure 4.7). However, SUMO1 attaches to UBC9 via this cysteine before conjugation to the substrate of interest, and therefore the band-shift may be as a result of SUMO1 binding UBC9 in the complex. To rule this out, samples were treated with 250 mM hydroxylamine which would cleave the thioester bond between the SUMO1 and UBC9. This did not result in a loss of the SUMOylated band shift, indicating the SUMOylated band shift is due to SUMO1 attaching to FLAG-cMyBP-C (Figure 4.7). This is supported by work showing UBC9-fusion to other substrates does not always induce a band shift (data not shown).

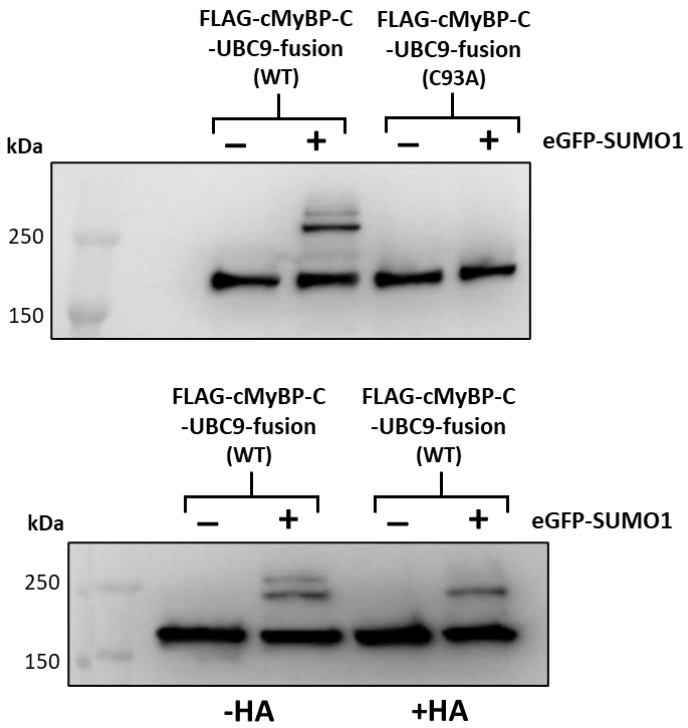

Figure 4.7. Catalytically inactive UBC9 removes FLAG-cMyBP-C-UBC9 fusion band shift and disruption of any thioester-dependent interaction between UBC9 and SUMO1-GFP with hydroxylamine does not eliminate band shift.
In order to facilitate SUMOylation, SUMO1 first attaches to UBC9 at its catalytic cysteine (C93) before conjugation to the target protein. Production of a catalytically inactive FLAG-cMyBP-C-UBC9 construct (UBC9 C93A) results in a complete loss of eGFP-SUMO1 specific band shift. Additionally, treatment with hydroxylamine (HA, 250 mM, 30 minutes) which would hydrolyse any thioester bonds between eGFP-SUMO1 and UBC9. The band shift is still maintained following treatment with hydroxylamine. Representative of n=3 experiments.

4.4.2 Identifying cMyBP-C SUMOylation site

SUMOylation has been implicated in cardiac hypertrophy, ischaemia and HF through increased or reduced SUMOylation of a substrate. However, with the exception of SERCA2a, cTnI and Nav1.5, there are very few studies indicating how SUMOylation functionally regulates individual cardiac substrates (Fertig *et al.*, 2022; Kho *et al.*, 2011; Plant *et al.*, 2020). A common method to characterise SUMOylation is to identify the lysines being SUMOylated in order to characterise the functional effect of their loss (Fertig *et al.*, 2022). As such, identification of cMyBP-C candidate lysines was attempted using *in silico* analysis and purification of SUMOylated FLAG-cMyBP-C-UBC9 fusion followed by mass spectrometry.

4.4.2.1 *In silico* analysis of cMyBP-C lysine conversation

As ~50% of substrates are SUMOylated at a specific consensus motif, several SUMOylation prediction algorithms have been created to allow sequence analysis

based on established SUMOylated substrates (Beauclair *et al.*, 2015; C. C. Chang *et al.*, 2018; Impens *et al.*, 2014; Zhao Q, Xie Y, 2014). This was completed for the human cMyBP-C sequence (Uniprot ID: Q14896), with a confidence score generated from an average of four different prediction softwares, with a value closer to 1 indicating high confidence. The top 20 sites based on confidence are represented in Table 4.1, along with information about conservation within isoforms, species, surface availability of sites and whether they have been identified in other PTM studies. This revealed there are several candidate lysines for cMyBP-C SUMOylation.

Table 4.1. cMyBP-C lysine conservation and SUMOylation site prediction analysis.

Domain (cMyBP-C, human)	Lysine number (cMyBP-C, human)	Average confidence score (Max: 1)	Lysine isoform conservation	Adjacent area isoform conservation score (Clustal Omega) (max: 27)	Lysine species conservation	Adjacent area species conservation score (Clustal Omega) (max: 27)	Established modifications or mutations (cMyBP-C, any species)	Surface availability based on AlphaFold (human)	Surface availability based on crystallography (human)
0	14	0.477	Unique to cMyBP-C	0	Mouse, rat and rabbit	25		Yes	Yes
0	89	0.699	Unique to cMyBP-C	0	Mouse, rat and rabbit	27		Yes	Yes
0	93	0.79	Unique to cMyBP-C	0	Mouse, rat and rabbit	21		Yes	Yes
0-1	99	0.585	Unique to cMyBP-C	0	Unique to human	6	Ubiquitylation	Yes	
1	185	0.49	Unique to cMyBP-C	0	Mouse, rat and rabbit	27	Ubiquitylation, Acetylation	Yes	Yes
1	190	0.424	Fast skeletal	21	Mouse, rat and rabbit	27	Acetylation	Yes	
1	246	0.408	Slow skeletal	13	Mouse, rat and rabbit	23		Yes	
1-2	301	0.713	Fast skeletal	17	Mouse, rat and rabbit	23		Yes	
1-2	312	0.605	Fast skeletal	1	Mouse, rat and rabbit	23	Ubiquitylation	Yes	
1-2	367	0.553	All	19	Mouse, rat and rabbit	27		Yes	Yes
1-2	368	0.402	Fast skeletal	20	Mouse, rat and rabbit	27		Yes	
2	395	0.391	All	15	Mouse, rat and rabbit	27		Yes	
2	398	0.387	All	23	Mouse, rat and rabbit	27	Ubiquitylation	Yes	
2-3	450	0.487	Fast skeletal	25	Mouse, rat and rabbit	27	Ubiquitylation	Yes	Yes
3	488	0.472	All	19	Unique to human	27	Ubiquitylation	Yes	Yes
3	504	0.524	Fast skeletal	20	Mouse, rat and rabbit	26		Yes	
3-4	543	0.555	All	15	Mouse, rat and rabbit	27	Ubiquitylation	Yes	Yes
3-4	544	0.492	Unique to cMyBP-C	15	Mouse, rat and rabbit	27	Ubiquitylation	Yes	
4	559	0.571	Unique to cMyBP-C	6	Mouse, rat and rabbit	24		Yes	
4	565	0.584	All	18	Mouse, rat and rabbit	27	Ubiquitylation	Yes	
4	579	0.418	All	15	Mouse, rat and rabbit	27		Yes	
4	582	0.512	Unique to cMyBP-C	11	Mouse, rat and rabbit	27		Yes	
4-5	635	0.778	Fast skeletal	3	Mouse, rat and rabbit	27		Yes	
5	716	0.366	Slow skeletal	6	Mouse, rat and rabbit	27	Ubiquitylation	Yes	
5	731	0.433	Unique to cMyBP-C	10	Mouse, rat and rabbit	25		Yes	
5	743	0.451	Unique to cMyBP-C	18	Mouse, rat and rabbit	27		Yes	Yes
5	754	0.525	Slow skeletal	13	Mouse, rat and rabbit	26		Yes	Yes
9	1087	0.543	Unique to cMyBP-C	13	Mouse, rat and rabbit	26		Yes	
9	1104	0.36	All	23	Mouse, rat and rabbit	27		Yes	
9-10	1155	0.495	All	8	Mouse, rat and rabbit	25	Ubiquitylation	Yes	
10	1216	0.468	All	15	Mouse, rat and rabbit	27	Ubiquitylation	Yes	

SUMOylation prediction softwares SUMOgo, GPS SUMO and Abgent were used to analysis the cMyBP-C sequence. The table shows sites for which the average confidence score was above the group average of 0.350 (green = highest, red = lowest). Conservation scoring was based on Clustal Omega alignment whereby 4 amino acids either side of lysine were scored - 3 points for perfect alignment (*) with both isoforms, 2 points for an amino acids with a strong similarity (:), 1 point for a weak similarity (.) and 0 points for no similarity

4.4.2.2 cMyBP-C-UBC9 fusion purification and mass spectrometry

In combination with the information gained from cMyBP-C sequence analysis, a mass spectrometry approach was taken to identify SUMOylated lysines. As co-transfection of FLAG-cMyBP-C-UBC9 fusion with eGFP-SUMO1 drives the attachment of SUMO to cMyBP-C, this complex was purified from HEK293 cells for analysis via mass spectrometry. This was completed using a two-step purification process, with FLAG-beads, followed by elution with a 3X-flag peptide, and further purification using GFP beads (detailed in 4.3.1). This resulted in the concentrated, purification of the FLAG-cMyBP-C-UBC9-eGFP-SUMO1 complex (SUMOylated) for analysis, but interestingly the non-SUMOylated form of the complex was still detected, which may indicate that non-SUMOylated and SUMOylated cMyBP-C are interacting. However, this may also be as a result of cross-contamination with FLAG-beads during the purification, which would explain the heavy and light chain antibody bands (~25kDa and ~50kDa) in this sample, which should not be present using the GFP-nanobody (Figure 4.8).

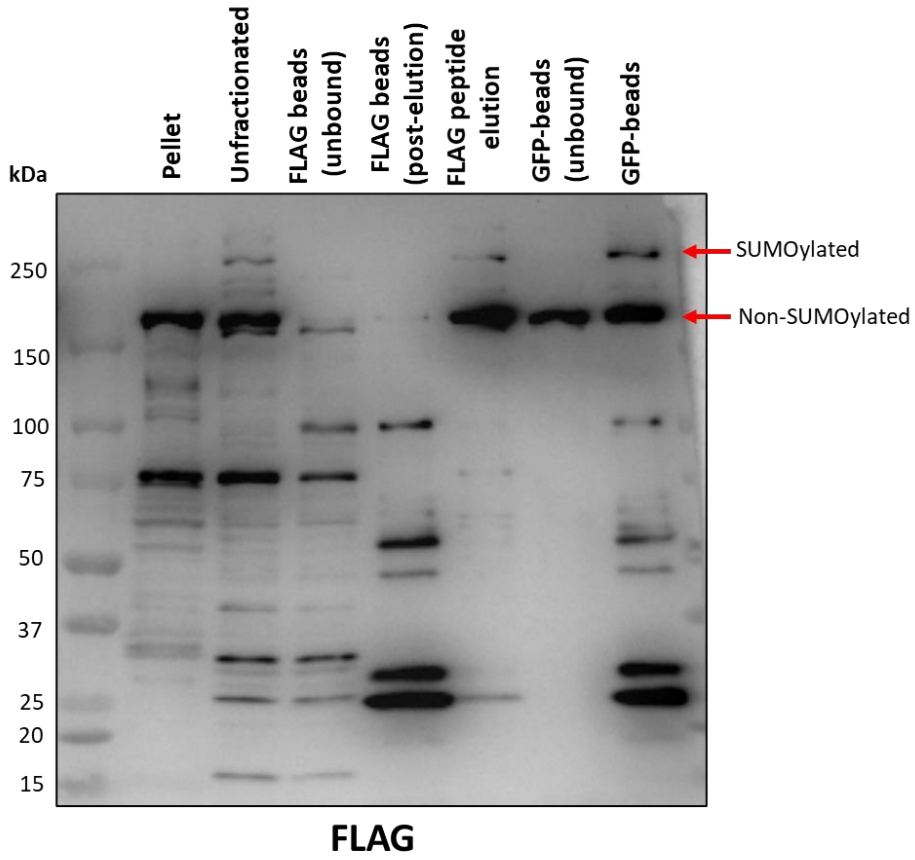

Figure 4.8. SUMOylated cMyBP-C-UBC9 fusion can be purified from transfected HEK293 for analysis via mass spectrometry.
In order to analyse the FLAG-cMyBP-C-UBC9-eGFP-SUMO1 complex via mass spectrometry analysis, a two-step purification protocol was applied to cells co-transfected with FLAG-cMyBP-C-UBC9 and eGFP-SUMO1. Lysates were first incubated with ANTI-FLAG M2 affinity gel before elution using a 3X-FLAG peptide. The resulting eluant was then further incubation with GFP-Trap agarose. Samples were taken at all stages for analysis via western blot. Representative image of n=4 experiments.

Nevertheless, SUMOylated FLAG-cMyBP-C-UBC9 fusion was present in a large enough quantity to perform mass spectrometry, completed by Dr Sheon Samji, University of Glasgow, which resulted in a 74.3% sequence coverage for FLAG-cMyBP-C-UBC9 fusion. This identified several candidate lysines for SUMOylation, all which were identified during *in silico* analysis except for K1351 which would fall in the UBC9 part of the complex (Figure 4.9).

LC/MS of FLAG-cMyBP-C-UBC9 fusion
Sequence Coverage: 74.3%

mdykddddkp epgkkpvsaf **SKKPRSVEVA AGSPAVFEAE TER**agvkvrw
QRGGSDISAS NKYGLATEGT RHTLTVREVG PADQGSYAVI AGSSKVKFdl
kvieaekaep mlapapapae atgapgeapa paaelgesap spkgsssaal
ngptpgapdd piglfvmrpq dgevtvggsi tfsar**VAGAS LLKPPVVKW**f
k**GKWVDLSSK VGQHLQLHDS YDR**askvylf **ELHITDAQPA FTGSYRCEVS**
TKDKFDCSNF nltvheamgt gdldllsafr rtslagggr**R ISDSHEDTGI**
LDFSSLLKKr dsfrtpr**DSK LEAPAEEDVW EILRQAPPSE YERIAFQYGV**
TDLRGMLKRl kgmrr**DEKKS TTFQKKLEPA YQVSKGHK**ir **LTVELADHDA**
EVKWLKNGQE IQMSGSKYIF ESIGAKRTLT ISQCSLADDA AYQCVVGGEK
CSTELFVKEP PVLITRPLED QLVMVGQRVE FECEVSEEGA QVKWLKDGVE
LTREETFKYR fkkdggrhhl iineamleda ghy**ALCTSGG QALAELIVQE**
KKLEVYQSIA DLMVGAKDQA VFKCEVSDEN VRGVWLKNGK ELVPDSRIKV
SHIGRvhk**LT IDDVTPADEA DY**sfvpegfa cnlsak**LHFM EVKIDFVPRQ**
EPPKIHLDCP GRIPDTIVVV AGNKLRLDVP ISGDPAPTVI WQKaitqgnk
APARPAPDAP EDTGDSDEWV FDKKLLCETE GRvrvettkd r**SIFTVEGAE**
KEDEGVYTVT VKNPVGEDQV NLTVKVIDVP DAPAAPKISN VGEDSCTVQW
EPPAYDGGQP ILGYilerkk kksyrwmr**LN FDLIQELSHE ARr**MIEGVVY
EMRVYAVNAI GMSRpspasq pfmpigppse pthl**AVEDVS DTTVSLKWRP**
PERVGAGGLD GYSVEYcpeg csew**VAALQG LTEHTSILVK DLPTGAR**llf
rvr**AHNMAGP GAPVTTTEPV TVQEILQRPR** lqlprhlrqt iqk**KVGEPVN**
LLIPFQGKPR PQVTWTKEGQ PLAGEEVSIR NSPTDTILFI Raar**RVHSGT**
YQVTVRienm edk**ATLVLQV VDKPSPPQDL R**vtdawglnv alew**KPPQDV**
GNTELWGYTV QKADKKtmew f**TVLEHYR**rT **HCVVPELIIG NGYYFRVFSQ**
NMVGFSDRAA TTKEPVFIPR PGITYEPPNY KALDFSEAPS FTQPLVNRSV
IAGYTAMLCC AVRgspkpki swf**KNGLDLG EDAR**frmf**SK QGVLTLEIRK**
PCPFDGGIYV CRATNLQGEA Rcecr**LEVRV PQEFGGGSGI ALSR**laqerk
awr**KDHPFGF VAVPTKNPDG TMNLMNWECA IPGKKGTPWE GGLFK**lr**MLF**
KDDYPSSPPK CKf**EPPLFHP NVYPSGTVCL SILEEDKDWR PAITIK**qill
giqel**LNEPN IQDPAQAEAY** tiy**CQNRVEY** ekrvraqakk faps

Position	Group	Comments	Number of Unique Peptides
K643	LHFME VKID FVPRQ	Peptides are present but no duplicates	
K97	AGSSK VKFD LKVIE	Peptides are present but no duplicates	
K1351	KLRML FKDD YPSSP	14 peptides - FKDD, KDD	8 unique peptides
K573	KDQAV FKCE VSDEN	4 peptides - FKCE, KCE	2 unique peptides
K512	TFKYR FKKD GQRHH	78 peptides - FKKD,KKD	11 unique peptides
K762	VYTVT VKNP VGEDQ	12 peptide - VKNP	3 unique peptides
K458	STELF VKEP PVLIT	2 peptides - VKEP	1 unique peptides
K193	AGASL LKPP VVKWF	15 peptides - LKKP, KKP	6 unique peptides
K587	VRGVW LKNG KELVP	45 peptides - LKNG,KNG	11 unique peptides
K496	AQVKW LKDG VELTR	7 peptides - LKDG, KDG	3 unique peptides
K406	AEVKW LKNG QEIQM	5 peptides - LKNG	2 unique peptides
K1224	PKISW FKNG LDLGE	18 peptides - FKNG	5 unique peptides

Figure 4.9. Mass spectrometry of FLAG-cMyBP-C-UBC9-eGFP-SUMO1 complex.
Mass spectrometry of purified FLAG-cMyBP-C-UBC9 fusion sample results in a 74.3% coverage of FLAG cMyBP-C-UBC9 fusion with several lysines identified as being conjugated by SUMO1-GFP. Representative of n=1 experiment. Sites identified are +8 amino acids from human cMyBP-C sequence due to the FLAG-tag. Mass spectrometry performed by Dr Sheon Samji.

4.4.2.3 Mutation of cMyBP-C mass predicted by *in silico* analysis, mass spectrometry or peptide array does not remove cMyBP-C SUMOylation

Following the information from both sequence analysis and mass spectrometry, sites that were shared between them were mutated to arginine (K>R) in the FLAG-cMyBP-C-UBC9 fusion complex. Additionally, K93, K301, K312, K367/368 and K398 not identified in mass spectrometry had high confidence scores in sequence analysis, and therefore were included. Aside from this, three additional sites were included. Preliminary work from the Baillie group identified candidate lysine K543 as a cMyBP-C SUMOylation site using peptide array (Wills, 2017). Recent SUMO proteomic work identified K1000 as a SUMOylation site in skeletal MyBP-C, a site which is conserved in the cardiac form (Hendriks *et al.*, 2018). Finally, the lysine identified in mass spectrometry that lies in UBC9 (K1351) was also included. Site directed mutagenesis mutation of every site individually in the FLAG-cMyBP-C-UBC9 complex did not result in complete loss of the SUMOylated band shift, indicating these are not the predominant sites of SUMO1 attachment in cMyBP-C (Figure 4.10).

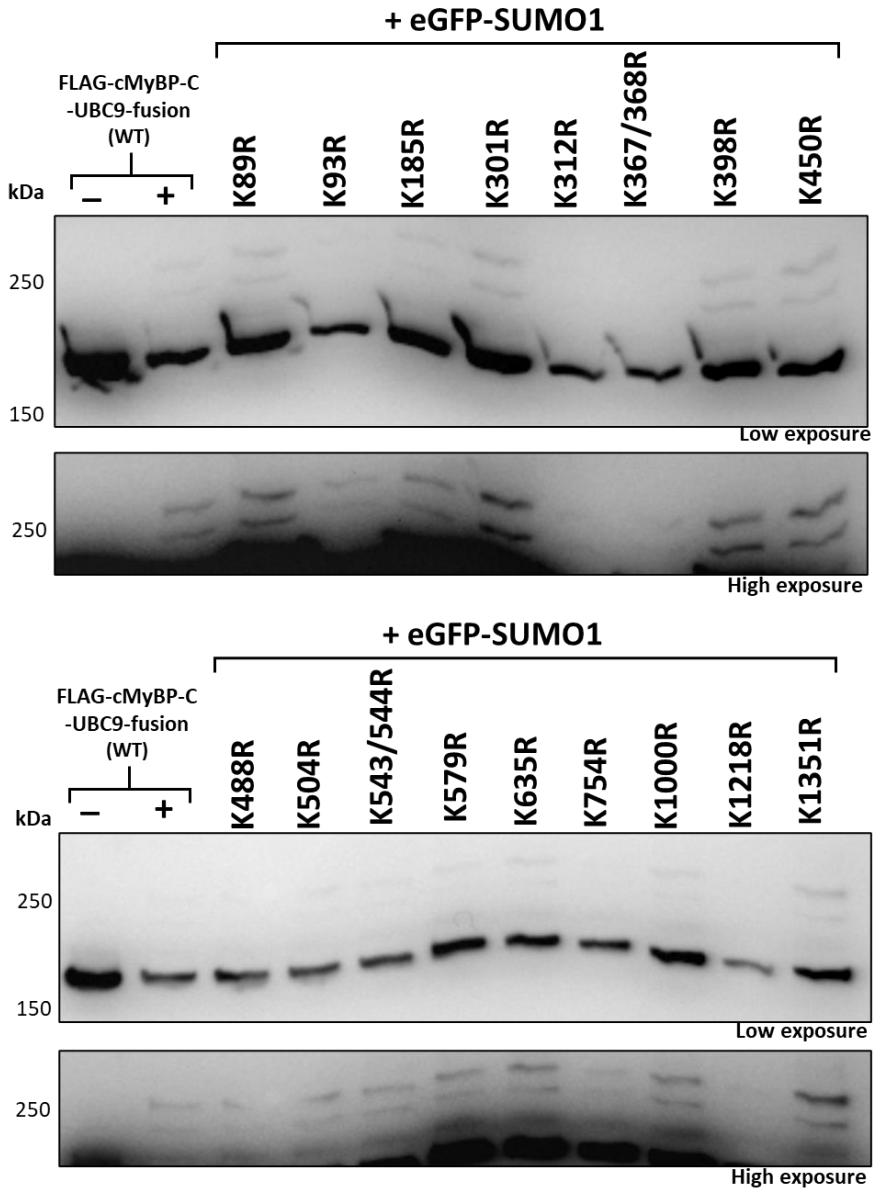

Figure 4.10. Mutation of predicted sites of cMyBP-C SUMOylation does not remove FLAG-cMyBP-C-UBC9 SUMOylated band shift.
SUMOylation prediction algorithms identified several candidate lysines in cMyBP-C as being SUMOylation sites. These were ranked according to confidence and the top five, K89, K93, K301, K312 and K635 mutated (K>R), however this did not remove the SUMOylated band shift. Mass spectrometry revealed additional lysines, K185, K367/368, K398, K450, K504, K579 and K754 to be candidate sites for conjugation of eGFP-SUMO1. Production of arginine mutants did not result in the removal of the SUMOylated band shift. Additionally, mass spectrometry of skeletal MyBP-C identified K1000 as a potential SUMOylation site, but mutation of this site did not remove SUMOylation in cMyBP-C. Peptide array completed by Dr Lauren Wills also identified K543/544 to be a candidate site but mutation did not result in a loss of the band shift. Additionally, one site identified by mass spectrometry in the UBC9 portion of the fusion protein (K1351) was also investigated but did not result in removal of the band-shift. Representative image of n=2-4 experiments.

4.4.3 Determining the functional effect of cMyBP-C-UBC9 fusion directed SUMOylation

Although cMyBP-C SUMOylation site(s) could not be detected in this study, characterisation of the FLAG-cMyBP-C-UBC9 fusion (WT) with eGFP-SUMO1 co-expression, alongside its negative control (C93A; (Figure 4.7), would provide information on the effect of enhanced SUMOylation of cMyBP-C. In HEK293 cells, the FLAG-cMyBP-C-UBC9-eGFP-SUMO1 complex could be detected by the phospho-cMyBP-C (Ser282) antibody, however comparison of the SUMOylated and non-SUMOylated fractions demonstrated SUMOylated form was hypophosphorylated compared to the non-SUMOylated form (Figure 4.11).

4.4.3.1 UBC9 fusion driven SUMOylation of cMyBP-C and the effect on phosphorylation in HEK293 cells

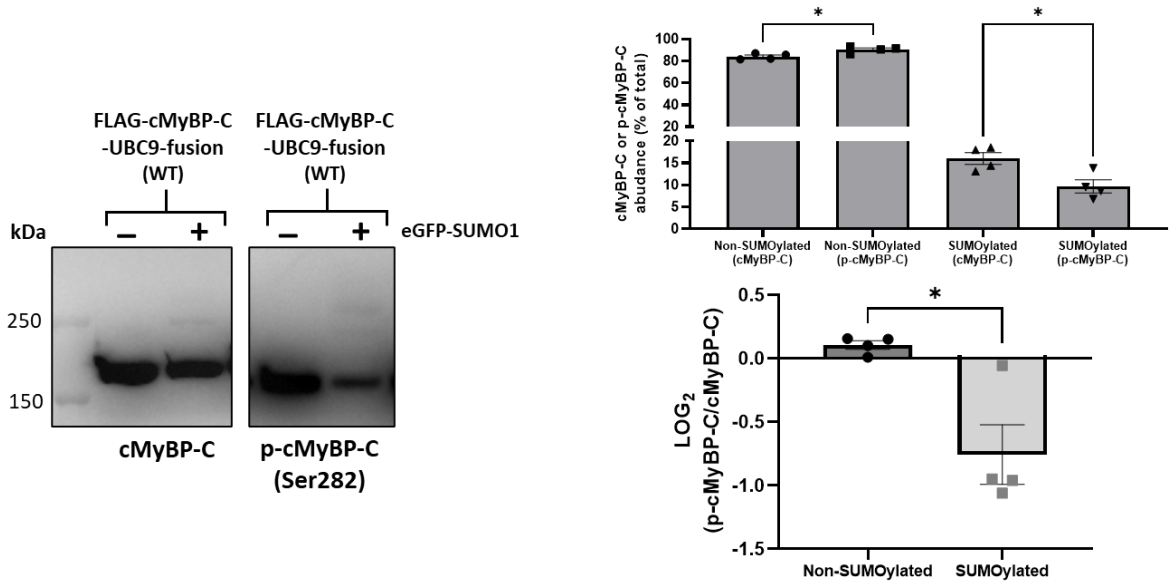

Figure 4.11. The non-SUMOylated form of FLAG-cMyBP-C-UBC9 fusion shows preferential phosphorylation in HEK293.
In order to investigate the relationship between SUMOylation and phosphorylation of cMyBP-C, HEK293 cells were transfected with FLAG-cMyBP-C-UBC9 fusion -/+ eGFP-SUMO1. Samples were probed for cMyBP-C and p-cMyBP-C (Ser282) the quantity of SUMOylated and non-SUMOylated protein was determined and normalised to total (SUMOylated + non-SUMOylated). Analysis revealed that whilst the non-SUMOylated form represents ~84% of total cMyBP-C, it represents ~90% of p-cMyBP-C. Similarly, the SUMOylated form represents ~16% of total cMyBP-C but only ~10% of p-cMyBP-C (*p<0.05). P-cMyBP-C levels were then normalised to total cMyBP-C and calculate at LOG_2 to be able to directly compare non-SUMOylated and SUMOylated p-cMyBP-C levels and show any change between them. Analysis revealed that compared to the non-SUMOylated form, there is a 2-fold reduction in p-cMyBP-C in the SUMOylated form. Data is mean ±S.E.M analysed via an unpaired student's t-test. *p<0.05.

4.4.3.2 Viral expression of WT and C93A cMyBP-C-UBC9 fusion constructs in neonatal rat ventricular cardiomyocytes

In order to characterise the WT and C93A cMyBP-C-UBC9 fusion constructs in a more physiologically relevant system, adenoviruses were produced and used to infect neonatal ventricular cardiomyocytes. Expression of WT and C93A cMyBP-C-UBC9 fusion was detected by western blot and revealed the viral form constituted ~80% of the total cMyBP-C in the samples. Additionally, confocal microscopy revealed viral constructs were expressed in the sarcomere, demonstrated by the striated staining pattern, and myofilament extraction also identified viral cMyBP-C in the myofilament. However, viral cMyBP-C was also expressed outwith the sarcomere, as evidenced by confocal microscopy in comparison to endogenous and the presence of a band in the soluble/membrane fraction following myofilament extraction (Figure 4.12).

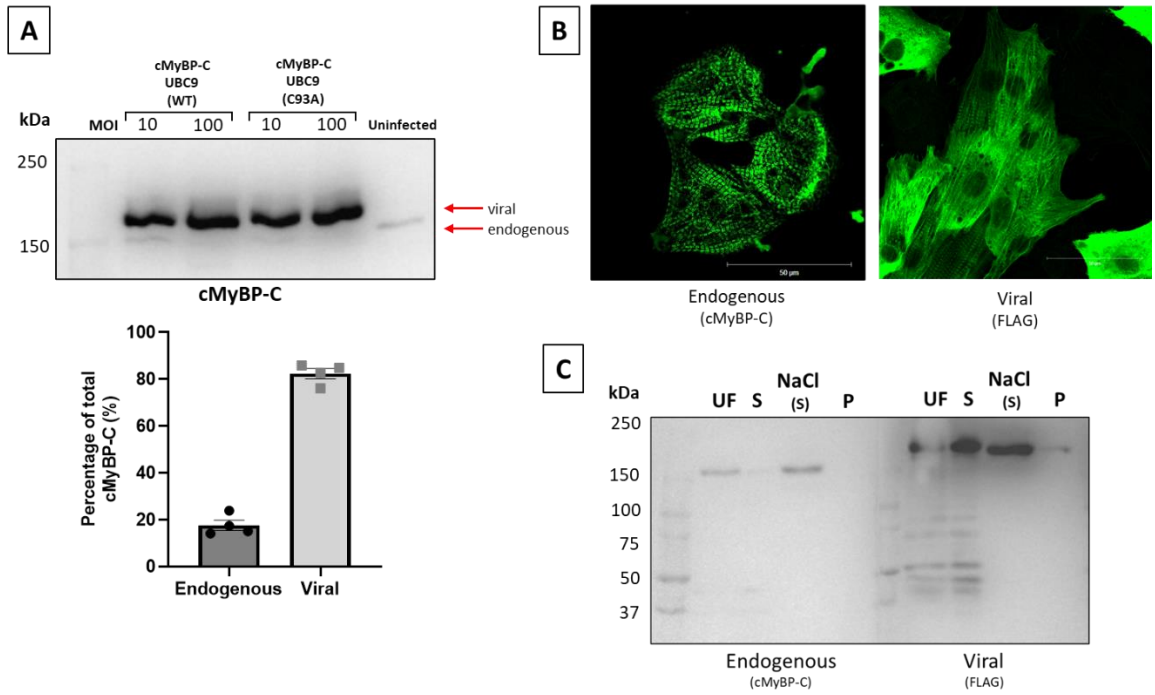

Figure 4.12. Expression profile of FLAG-cMyBP-C-UBC9 fusion constructs in neonatal ventricular cardiomyocytes.
A) Application of FLAG-cMyBP-C-UBC9 fusion adenoviruses (WT and C93A) at MOI 10 or 100 results in overexpression compared to endogenous cMyBP-C in neonatal ventricular cardiomyocytes, with roughly 80% of total cMyBP-C being the viral version. Data is mean ±S.E.M. **B)** Confocal microscopy imaging of cMyBP-C (endogenous) and FLAG (WT 100, viral) revealed myofilament localisation of viral WT FLAG-cMYBP-C-UBC9 fusion with additional staining throughout the cells. Representative of n=1 experiment. Scale bar is 50µm**. C)** Localisation of the viral WT FLAG-cMyBP-C-UBC9 fusion construct was determined in neonatal ventricular cardiomyocytes by myofilament extraction whereby uninfected (endogenous) and infected (viral, WT MOI 100) cells were homogenised in F60 buffer with 1% Triton X-100. A sample was taken for unfractionated (total protein) before fractionation by centrifugation into soluble (cytosolic and membrane fraction) and myofilament lattice. The myofilament lattice was further fractionated into myofilament proteins soluble in 500 mM NaCl (NaCl soluble) and those insoluble in 500 mM NaCl (pellet). Analysis revealed that although endogenous cMyBP-C is mainly localised in the myofilament fraction (NaCL (S)), WT FLAG-cMyBP-C-UBC9 fusion adenovirus localises in the myofilament (NaCl (S) and P fractions) with some localised in the membrane and soluble fraction. Representative image of n=3 experiments.

As well as WT and C93A viral constructs, an adenovirus expressing eGFP-SUMO1 was also produced. Co-infection of this virus in neonatal ventricular cardiomyocytes with the WT construct resulted in a detectable band shift which was lost when co-infecting with the C93A virus, replicating the result from the HEK293 experiments. However, the eGFP-SUMO1 virus expression was low compared to the FLAG-cMyBP-C-UBC9 constructs despite a higher MOI used (2000 vs 100) and did not result in as much SUMOylated cMyBP-C as in the HEK293 cells, as shown in the positive control (Figure 4.13).

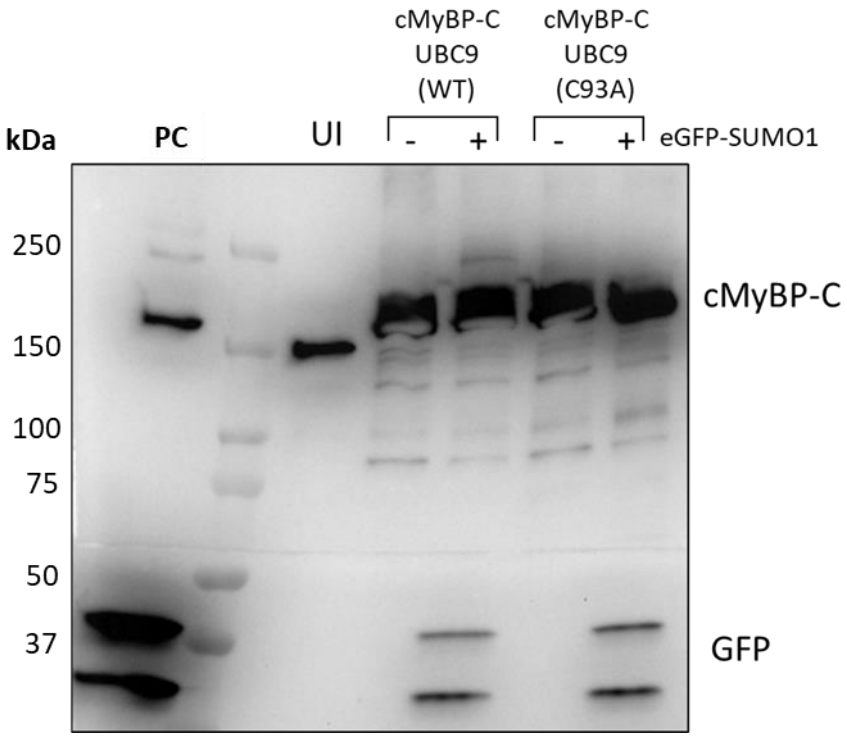

Figure 4.13. Co-infection of FLAG-cMyBP-C-UBC9 fusion constructs (WT and C93A) with an eGFP-SUMO1 adenovirus.
Viral FLAG-cMyBP-C-UBC9 fusion constructs (WT and C93A, MOI 100) were co-infected in neonatal ventricular cardiomyocytes with an eGFP-SUMO1 adenovirus. Whilst the co-infection did result in a detectable band shift in the WT, but not C93A, infected cells, the eGFP-SUMO1 adenovirus, used at MOI 2000, is poorly expressed compared to WT, C93A and positive control (PC, HEK293 co-transfected cells). Representative image of n=3. UI = uninfected.

To improve the eGFP-SUMO1 viral expression, an additional round of amplification and purification was completed in AD293 cells. The resulting virus expressed after 24 hours, and co-infected with WT-cMyBP-C-UBC9 fusion lead to a detectable band shift detected at a similar intensity at an MOI of 10 and 30 (Figure 4.14). As such, this purified virus was used for further characterisation.

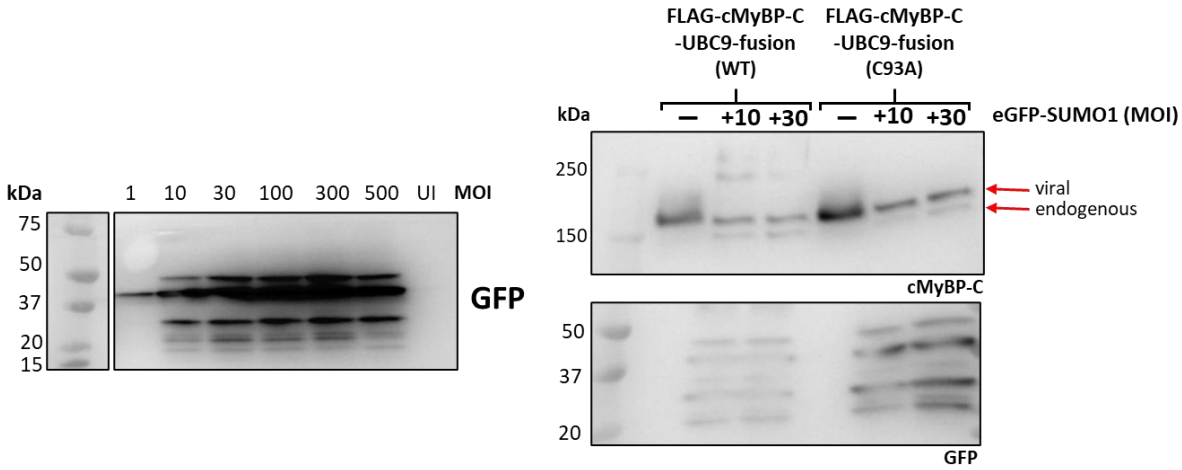

Figure 4.14. Amplification of eGFP-SUMO1 in AD293 cells results in a greater infection efficiency in neonatal ventricular cardiomyocytes.
To improve infectivity of the eGFP-SUMO1 adenovirus, viral particles were amplified using AD293 cells and isolated to produce a crude virus. The virus was tested on neonatal ventricular cardiomyocytes at different multiplicities of infection (MOI) for 24 hours. Each MOI led to expression of eGFP-SUMO1. Additionally, co-infection of FLAG-cMyBP-C-UBC9 fusion adenoviruses (WT and C93A, MOI 100) with the newly purified eGFP-SUMO1 (MOI 10 and 30) lead to a detectable band shift in the WT, but not C93A, infected cells. UI = uninfected. Representative images of n=1.

4.4.3.3 UBC9 fusion driven SUMOylation of cMyBP-C and the effect on phosphorylation in neonatal rat ventricular cardiomyocytes

Given that the SUMOylated form of the FLAG-cMyBP-C-UBC9 fusion construct is under-phosphorylated compared to the non-SUMOylated form in HEK293 cells (Figure 4.11), the same experiment was completed in virally infected neonatal ventricular cardiomyocytes. Whilst at baseline the quantity of phosphorylated cMyBP-C was not different between the SUMOylated and unSUMOylated forms, upon isoprenaline treatment which increases cMyBP-C phosphorylation, the SUMOylated form was hypophosphorylated compared to the non-SUMOylated form (Figure 4.15).

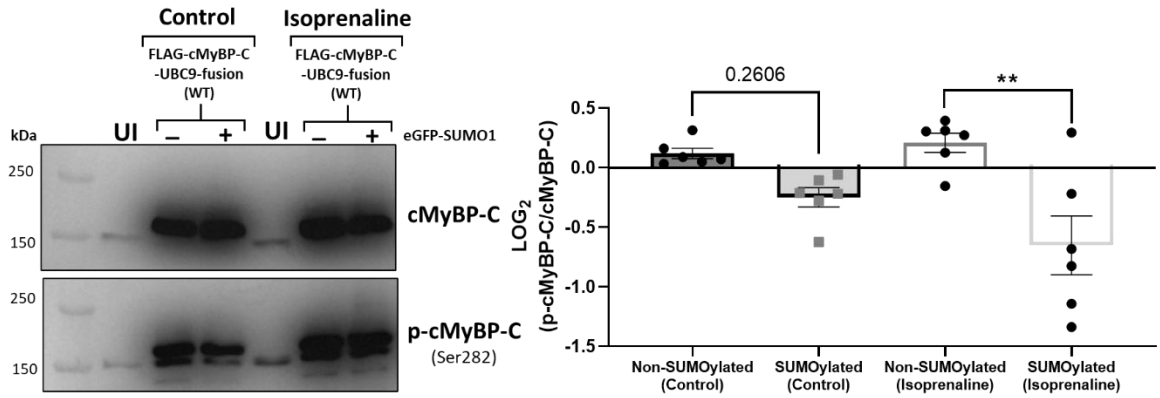

Figure 4.15. The non-SUMOylated form of cMyBP-C-UBC9 fusion does not show preferential phosphorylation in neonatal ventricular cardiomyocytes unless phosphorylation is enhanced by isoprenaline treatment.
In order to determine the interplay between cMyBP-C phosphorylation and SUMOylation, neonatal ventricular cardiomyocytes co-infected with WT FLAG-cMyBP-C-UBC9 fusion and eGFP-SUMO1 adenoviruses were treated with isoprenaline (10 minutes, 100 nM) and levels total and phospho-cMyBP-C in SUMOylated and non-SUMOylated bands were measured. Data is represented as a LOG_2 of p-cMyBP-C/total cMyBP-C to directly compare SUMOylated and unSUMOylated fractions. Analysis reveals that whilst there is no significant difference between levels of phosphorylation in non-SUMOylated and SUMOylated forms of cMyBP-C in these cells (p=0.2606), following isoprenaline treatment the non-SUMOylated form of cMyBP-C is preferentially phosphorylated compared to the SUMOylated form. Data is mean ±S.E.M analysed by a one-way ANOVA with a Sidak's *post hoc* test. **p<0.01. UI = uninfected.

4.4.4 Analysis of the contractile properties of neonatal ventricular cardiomyocytes

4.4.4.1 Characterising neonatal ventricular cardiomyocyte contractility using CellOPTIQ™

Neonatal ventricular cardiomyocytes are a useful system for studying cardiac contractility, as they can be easily isolated, genetically manipulated and spontaneously beat in culture, and have been previously used to characterise both TnI and ß2-adrenoceptor SUMOylation (Fertig *et al.*, 2022; Ling, 2021). As such, virally infected cells were used to investigate the consequence of enhanced SUMOylation of cMyBP-C. Given the importance of the FFR in cell contractility, cells were paced consistently at 1Hz to eliminate any effect of variability beating rate on contractility measurements. As cells are isolated from neonatal rats aged between 1 to 4 days, and kept in culture for 2 to 3 days, the effect of culture and aged of animals was investigated. Cardiomyocytes in culture for 3 days compared to 2 days had significantly slower relaxation time with no change in the speed of the upstroke (Figure 4.16). In contrast, cardiomyocytes cultured for 3 days but isolated from 4-day old animals compared to 1-day old animals had significantly reduced relaxation time, as well as reduced time to peak contraction, overall shortening the contractile duration (Figure 4.17).

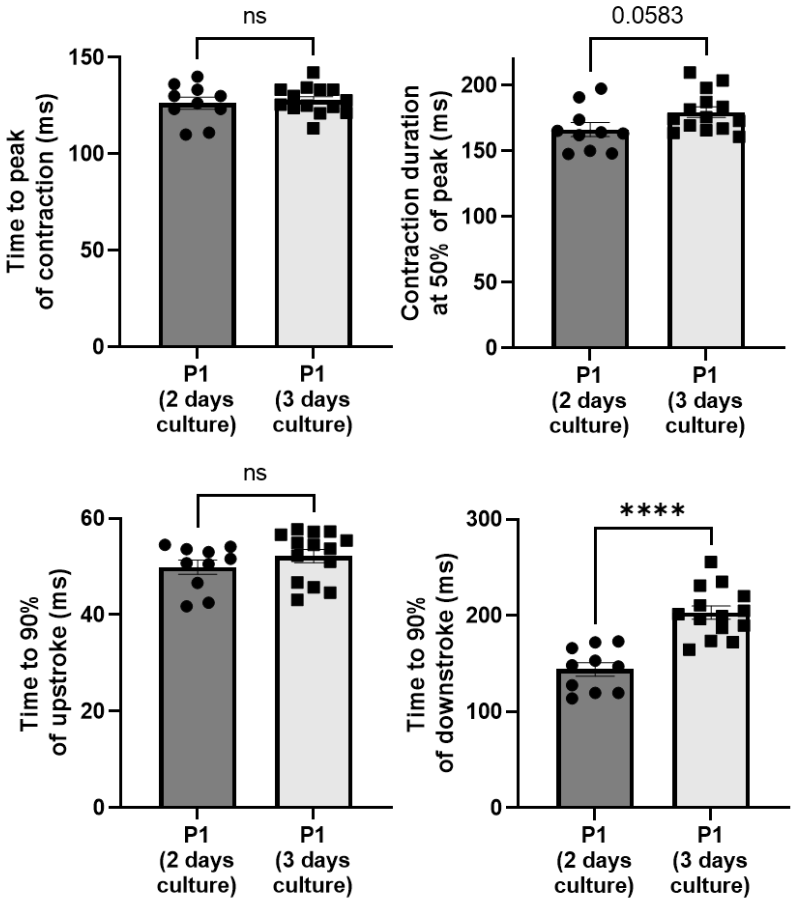

Figure 4.16. The lusitropy of neonatal ventricular cardiomyocytes may be affected by days in culture, whilst other contractility parameters remain unchanged.
Contractile transients were recorded in neonatal ventricular cardiomyocytes paced at 1Hz, 2ms and 40V for 10 seconds. Recordings were taken using a 60X objective with a 0.6NA and recorded at 120fps before analysis using custom-built CellOPTIQ™ analysis software which gave an average transient of the 8-10 transients in each recording. Contractile parameters such as time to peak of contraction, contraction duration at 50% of transient, time to from 10% to 90% of contraction and time from 90% of contraction to 90% of relaxation, all measured in milliseconds (ms), were analysed. In order to determine the effect of prolonged culture of isolated cells on overall contractile parameters, cells were isolated from 1-day old (P1) animals but cultured for 2 and 3 days respectively were compared. Analysis revealed that whilst time to peak and time to 90% of contraction remained unchanged, time to 90% of relaxation were significantly increased in cells isolated for 3 days. This led to a trending increase in overall contraction duration in these cells ($p=0.0583$). Data is mean ± S.E.M. N=1 biological replicate, 10-14 cells per replicate. Analysis was completed using a student's unpaired t-test. ****$p<0.0001$.

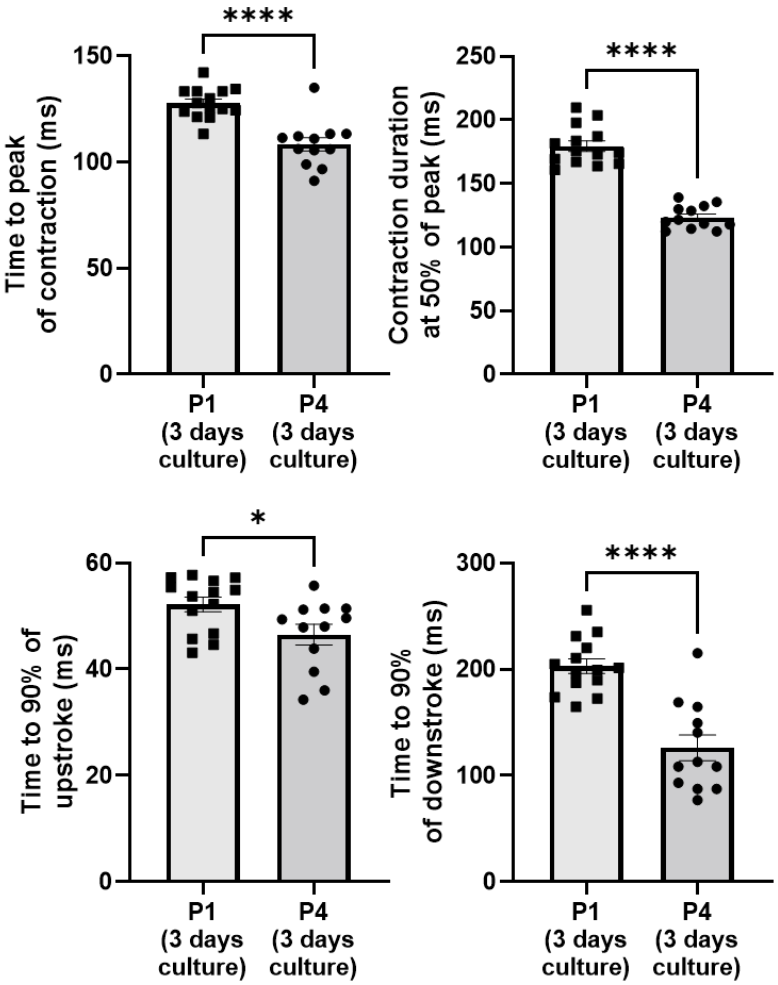

Figure 4.17. Cardiomyocytes isolated from 4-day old neonatal rats may have faster contractility parameters compared to cells isolated from 1-day old animals.
Contractile transients were recorded in neonatal ventricular cardiomyocytes paced at 1Hz, 2ms and 40V for 10 seconds. Recordings were taken using a 60X objective with a 0.6NA and recorded at 120fps before analysis using custom-built CellOPTIQ™ analysis software which gave an average transient of the 8-10 transients in each recording. Contractile parameters such as time to peak of contraction, contraction duration at 50% of transient, time to from 10% to 90% of contraction and time from 90% of contraction to 90% of relaxation, all measured in milliseconds (ms), were analysed. In order to determine the effect of age of animals on overall contractile parameters, cells isolated from 1-day old (P1) or 4-day old (P4) were cultured for 3 days and compared. Analysis revealed that cells isolated from older animals had significantly reduced time to peak, time to 90% of contraction and relaxation and overall contraction duration at 50% of peak, compared to 1-day old animals. Data is mean ± S.E.M. N=1 biological replicate, 12-14 cells per replicate. Analysis was completed using a student's unpaired t-test. ****p<0.0001, *p<0.05.

4.4.4.2 Treatment with isoprenaline enhances contractility parameters in neonatal ventricular cardiomyocytes

Given the potentially altered contractile parameters caused by culture time and age of animals, 1-2-day old animals cultured for 2 days were used for subsequent experiments. In these cells, isoprenaline treatment significantly enhanced contractile performance, reducing time to peak contraction, time to 50% and 75% of relaxation, but not 90%, with an overall shortening contractile duration (Figure 4.18).

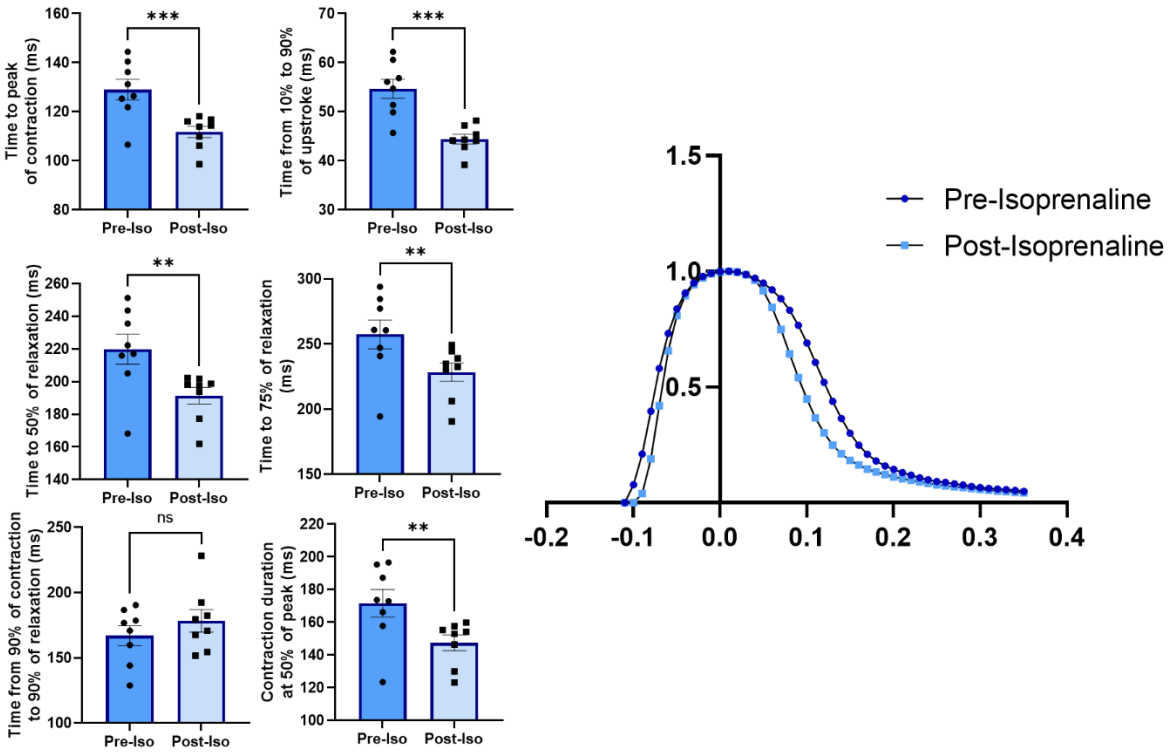

Figure 4.18. The effect of isoprenaline on neonatal cardiomyocyte contractile parameters. Contractile transients were recorded in neonatal ventricular cardiomyocytes paced at 1Hz, 2ms and 40V for 10 seconds. Recordings were taken using a 60X objective with a 0.6NA and recorded at 120fps before analysis using custom-built CellOPTIQ™ analysis software which gave an average transient of the 8-10 transients in each recording. Contractile parameters such as time to peak of contraction, contraction duration at 50% of transient, time to from 10% to 90% of contraction, time to 50% and 75% of relaxation and time from 90% of contraction to 90% of relaxation, all measured in milliseconds (ms), were analysed. In order to determine the effect of incubation of cardiomyocytes with 100 nM isoprenaline, cells were recorded both pre and 10 minutes-post isoprenaline addition. Isoprenaline caused a significant decrease in time to peak of contraction, time to 90% of upstroke and time to 50% and 70% of relaxation, as well as overall contraction duration at 50% of peak, but had no effect on time to 90% of relaxation. An example trace of the average transient from one recording (8-10 individual transients) is shown with maximal peaks aligned. Data is mean ± S.E.M. N=8 biological replicates, 10-15 cells per replicate. Analysis was completed using a student's paired t-test. **p<0.001, **p<0.01.

4.4.5 Analysis of contractility in virally infected cardiomyocytes

4.4.5.1 The effect of cMyBP-C SUMOylation viruses on neonatal ventricular cardiomyocyte contractile parameters

In order to determine the functional effect of cMyBP-C SUMOylation on neonatal ventricular cardiomyocyte contractile parameters, both WT and C93A constructs were infected alone or co-infected with eGFP-SUMO1. Analysis of contractile parameters revealed no significant differences between groups at baseline (Figure 4.19). Treatment with isoprenaline significantly accelerated contractile parameters in each group (data not shown), however comparison between the groups showed no significant differences in response to isoprenaline between the groups (Figure 4.20).

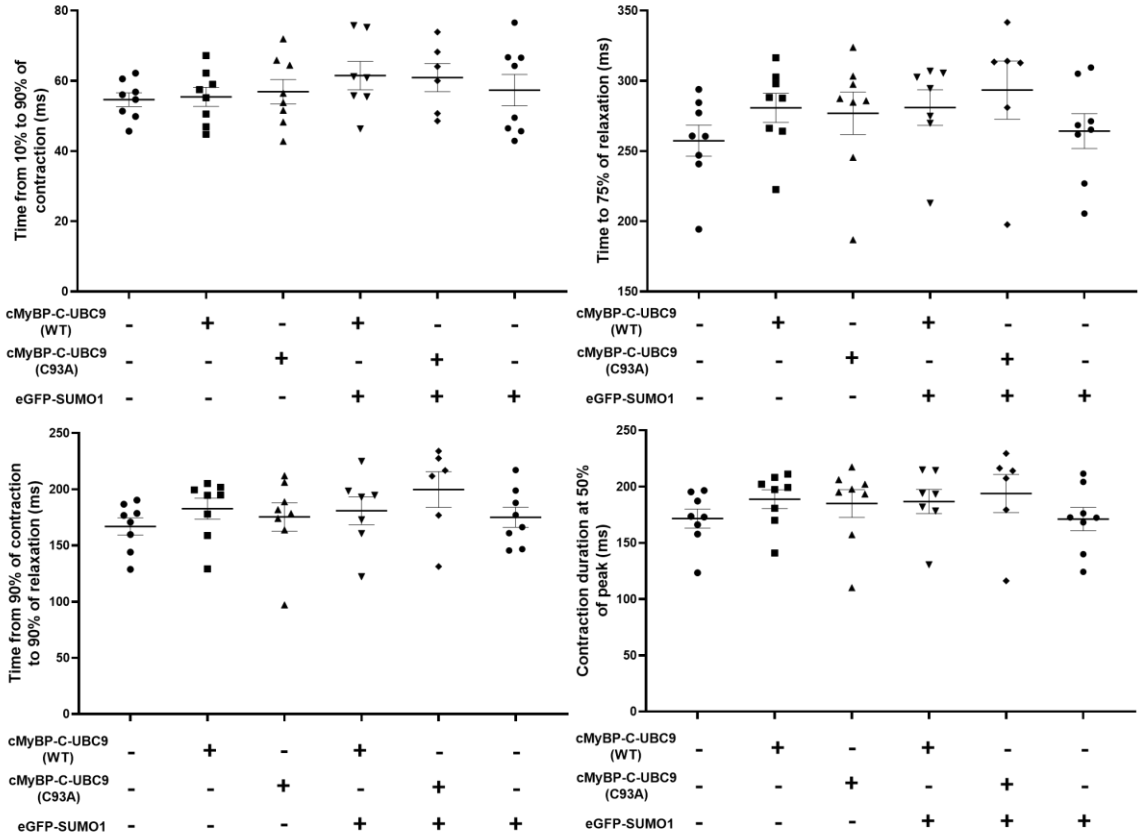

Figure 4.19. Contractile parameters in virally infected neonatal ventricular cardiomyocytes. To determine the functional effect of cMyBP-C SUMOylation on neonatal ventricular cardiomyocyte contractile parameters, both WT and C93A constructs were infected alone or co-infected with eGFP-SUMO1. Contractile transients were recorded in cells paced at 1Hz, 2ms and 40V for 10 seconds with analysis using custom-built CellOPTIQ™ analysis software which gave an average transient from the 8-10 transients in each recording. Contractile parameters including, time to from 10% to 90% of contraction, time to 75% of relaxation, time from 90% of contraction to 90% of relaxation and contraction duration at 50% of transient were analysed, all measured in milliseconds (ms). There were no significant differences in contractile parameters between groups. N=5-8 biological replicates with 8-10 cells per replicate. Data is mean ± S.E.M analysed via a one-way ANOVA with a Tukey *post hoc* test.

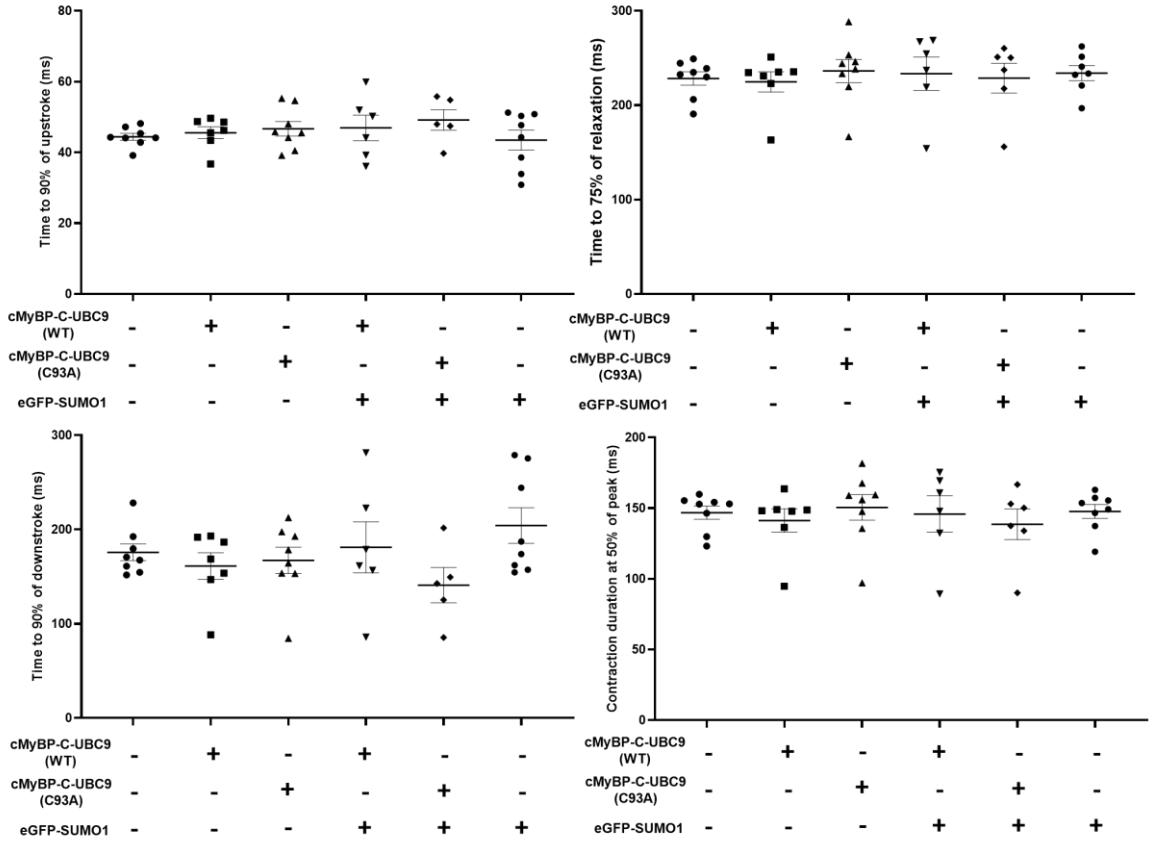

Figure 4.20. The effect of isoprenaline on contractile parameters in virally infected neonatal ventricular cardiomyocytes.
To determine whether WT or C93A viruses alone or co-infected with eGFP-SUMO1 altered response to isoprenaline, infected neonatal ventricular cardiomyocytes were treated with 100 nM isoprenaline for 10 minutes before recordings were taken. Contractile transients were recorded in cells paced at 1Hz, 2ms and 40V for 10 seconds with analysis using custom-built CellOPTIQ™ analysis software which gave an average transient from the 8-10 transients in each recording. Contractile parameters including, time to from 10% to 90% of contraction, time to 75% of relaxation, time from 90% of contraction to 90% of relaxation and contraction duration at 50% of transient were analysed, all measured in milliseconds (ms). There were no significant differences in contractile parameters in response to isoprenaline between groups. N=5-8 biological replicates with 8-10 cells per replicate. Data is mean ± S.E.M analysed via a one-way ANOVA with a Tukey *post hoc* test.

In order to more closely compare the effect of eGFP-SUMO1 addition and conjugation (or not) to cMyBP-C, WT and C93A co-infections with eGFP-SUMO1 were normalised to the singly infected counterparts and the logs plotted. Using this approach, if a parameter is unchanged between two groups, the normalised response is equal to 1, and the log normalised response is zero. If a parameter is larger in a group infected with one virus than a group infected with 2 viruses, the normalised response is greater than 1, and the log normalised response is a positive integer. If a parameter is small in a group infected with one virus than a group infected with 2 viruses, the normalised response is less than one, and the log normalised response is a negative integer.

At baseline, there was no significant difference between WT and C93A co-infected with eGFP-SUMO1 in time to peak contraction, however C93A infected cells, which

would not have SUMO1 conjugated to cMyBP-C, show significantly increased time to relaxation. However, upon addition of isoprenaline, both WT and C93A show similar response in shortened time to peak contraction, but C93A cells have significantly shorter time to relaxation, indicating that isoprenaline is less effective at reducing relaxation time in cells with SUMOylated cMyBP-C-UBC9 (Figure 4.21).

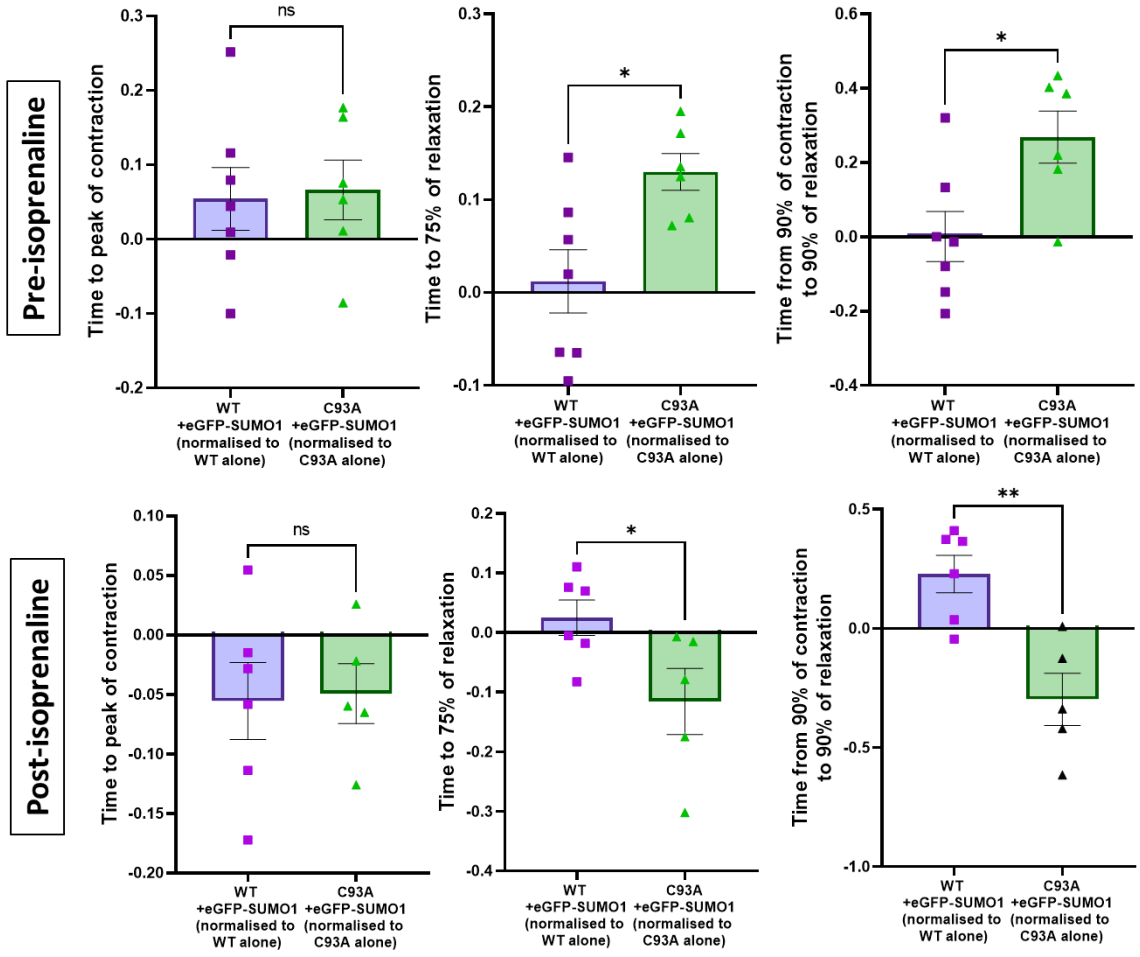

Figure 4.21. Comparison of contractile parameters from cMyBP-C-UBC9 (WT and C93A) and eGFP-SUMO1 co-infected neonatal ventricular cardiomyocytes pre- and post-isoprenaline treatment.
To compare the effect of the presence (WT) or absence (C93A) of eGFP-SUMO1 conjugation to cMyBP-C, WT and C93A co-infections with eGFP-SUMO1 were normalised to the singly infected counterparts. Contractile transients were recorded in cells paced at 1Hz, 2ms and 40V for 10 seconds with analysis using custom-built CellOPTIQ™ analysis software which gave an average transient from the 8-10 transients in each recording. Contractile parameters including, time to from 10% to 90% of contraction, time to 75% of relaxation and time from 90% of contraction to 90% of relaxation were analysed. At baseline, there was no significant difference between WT and C93A co-infected with eGFP-SUMO1 in time to peak contraction, however C93A infected cells show significantly increased time to relaxation. Upon addition of isoprenaline (100 nM, 10 minutes), both WT and C93A show similar response in shortened time to peak contraction, but C93A cells have significantly shorter time to relaxation, indicating that isoprenaline is less effective at reducing relaxation time in cells with SUMOylated cMyBP-C-UBC9. N=5-6 biological replicates with 8-10 cells per replicate. Data is mean ± S.E.M analysed via unpaired student's t-test. *p<0.05, **p<0.01.

4.5 Discussion

The aim of the present study was to identify and characterise the SUMOylation of cMyBP-C, in a manner similar to what has recently been achieved for cTnI and ß2-adrenoceptor SUMOylation (Fertig *et al.*, 2022; Wills, 2017). Primary ventricular cardiomyocytes were used to attempt to purify and identify SUMOylated cMyBP-C, whilst co-expression in HEK293 cells with components of the SUMOylation cascade or fusion to UBC9 was used to enhance cMyBP-C SUMOylation for detection. Candidate SUMOylation sites were identified using *in silico* analysis, peptide array and mass spectrometry and evaluated using site directed mutagenesis. Finally, the functional effect of increased SUMOylation of cMyBP-C phosphorylation and cardiac contractility was characterised in virally infected neonatal ventricular cardiomyocytes.

4.5.1 Fusion of UBC9 to cMyBP-C enhances SUMOylation

Given the dynamic activity of the SUMOylation and deSUMOylation enzymatic machinery, SUMOylation levels of substrates are often very low and difficult to detect (Nayak *et al.*, 2020). SUMOylation can be driven by overexpression of SUMO and UBC9 alone, although this was insufficient to detect a SUMOylated form of cMyBP-C (Figure 4.5; Cartier *et al.*, 2019). However, direct fusion of UBC9 to SUMO1 substrates p53 and STAT1 resulted in an increase from undetectable levels to 40% detection (Jakobs *et al.*, 2007). In the present study, this approach was taken by fusing the C-terminal of cMyBP-C to UBC9 which, when co-expressed with eGFP-SUMO1, resulted in the detection of a band shift that represented ~15-20% of total protein in both HEK293 and neonatal ventricular cardiomyocytes (Figure 4.6 and Figure 4.13). Additionally, as demonstrated for STAT1 and p53, this is dependent on a catalytically active UBC9 (Figure 4.7). The possibility that SUMO1 was attaching to the catalytic cysteine of UBC9 as the reason for the band shift was ruled out as it was not lost upon cleavage of any thioester bond between them (Figure 4.13; Jakobs *et al.*, 2007). Although a powerful technique to enhance, and therefore study, SUMOylation of a substrate, it is limited in it does not provide information as to whether such a modification would naturally occur in an *in vivo* setting.

4.5.2 cMyBP-C SUMOylation sites could not be detected using *in silico* analysis, mass spectrometry or peptide array

SUMOylation site prediction software has been refined over recent years, taking into consideration that not all SUMOylated lysines fall within the traditional consensus sequence. As such, three SUMOylation algorithms were used to analyse the human cMyBP-C sequence and suggest there are several candidate lysines with a high confidence of being SUMOylated (Table 4.1). Many of these top candidates were identified in mass spectrometry analysis of the FLAG-cMyBP-C-UBC9-eGFP-SUMO1 complex (Figure 4.8 and Figure 4.9). Interestingly, the top candidates were either unique to cardiac MyBP-C or only conserved in the fast skeletal isoform, with very few lysines surrounded by highly conserved amino acids. This is in contrast to the observations in cTnI, where the SUMOylated lysine is conserved within species and across all skeletal and cardiac isoforms (Fertig *et al.*, 2022; Sahota *et al.*, 2009). However, mutation of these sites, along with those detected in skeletal MyBP-C studies and peptide array, did not result in a loss of the SUMOylated band (Figure 4.10; Hendriks *et al.*, 2018). As SUMO1 is being investigated in this study, it cannot form poly-SUMOylated chains like SUMO2/3 (Tatham *et al.*, 2001). This may suggest there is more than one site being targeted, as loss of one would still lead to detection of the other at the same size. Analysis of SUMOylated band density following mutagenesis may indicate whether this is the case, which was not completed due to low replicate numbers in this study. Additionally, it is possible that eGFP-SUMO1 may be attaching to UBC9, as SUMOylation has previously been detected at K14 which either enhanced or reduced SUMOylation of proteins in a substrate-specific manner (Knipscheer *et al.*, 2008). However, this site was not detected in the mass spectrometry analysis, whilst K1351R (representing K65 in human UBC9) was. Interestingly this site is reported to be acetylated, which has knock-on consequences for substrate SUMOylation, however whether this site is SUMOylated has not been reported (Hsieh *et al.*, 2013). Additionally, it did not result in a loss of the band shift upon mutation in this study (Figure 4.10). In support of cMyBP-C SUMOylation, UBC9 fused to the LTCC pore-forming subunit did not result in a detected band shift (data not shown), overall indicating that the band is caused by SUMOylated cMyBP-C. In order to aid in further identification of SUMOylation sites, removal of entire regions of cMyBP-C, including the C0-C1 domains which contains several high probability sites (Table 4.1), may be a possible strategy. Additionally, a mass

spectrometry approach could be taken to identify SUMOylated lysines or SUMO interactions site of cMyBP-C in cardiac tissue, however as demonstrated in Figure 4.4, detection of the endogenously SUMOylated form of cMyBP-C in primary cardiomyocytes is challenging.

4.5.3 Enhanced SUMOylation of cMyBP-C may alter phosphorylation

Increased SUMOylation of cTnI and the ß2-adrenoceptor has been reported in a pig model of I/R and HF development 3-months post-injury, with increased cTnI SUMOylation also observed in ischaemic human HF samples. This analysis was achieved using SUMOylation specific antibodies for each, whilst one is not currently available for cMyBP-C (Fertig *et al.*, 2022; Ling, 2021; Wills, 2017). In the present study, using the cMyBP-C-UBC9 fusion and catalytically inactive mutant, it is possible to investigate the functional consequences of enhanced cMyBP-C SUMOylation.

In HEK293 cells, whilst the SUMOylated band represents ~15% of the total cMyBP-C-UBC9 complex, it only represents ~10% of the phospho-cMyBP-C (S282), suggesting the non-SUMOylated form is preferentially phosphorylated (Figure 4.11). As such, the addition of SUMO1 may be occurring on a lysine within the vicinity of this site, blocking the ability of cMyBP-C to become phosphorylated at this crucial residue or blocking a PKA kinase binding site, which is yet to be mapped for cMyBP-C. Alternatively, although it remains a relatively unstudied field, cMyBP-C is dephosphorylated by protein phosphatase PP1 (Copeland *et al.*, 2010; Schlender *et al.*, 1987). As such, the addition of SUMO1 may be creating a binding site for a phosphatase to attach to the SUMOylated form, leading to the hypophosphorylation observed. The former suggestion may be more likely, as when repeating the experiment in virally infected neonatal cardiomyocytes, the preferential phosphorylation of the non-SUMOylated form was not apparent until isoprenaline treatment (Figure 4.15). The addition of SUMO to a lysine has been frequently shown to regulate recognition by a binding partner at SIMs, and nearby phosphorylated threonine and serine residues are often observed in these regions facilitating these interactions (Stehmeier & Muller, 2009; Ullmann *et al.*, 2012).

In our sequence analysis, the closest located lysines to S282 (S284 in humans) are K300, K301 and K312 (human sequence). Both K301 and K312, with confidence scores 0.713 and 0.605 respectively, are conserved with the fast skeletal isoform but not thought to be surface accessible according to crystal structure analysis (Table 4.1). Additionally, individual mutation of both sites in this study did not result in a loss of SUMOylation (Figure 4.10). Due to its low confidence score (0.248), K300 was not investigated in this study and should be ruled out in future studies. It will be important to determine whether this hypophosphorylation is specific to S282, or occurs on phosphorylation sites S275, S304 and S311 (human sequence) for which phospho-antibodies have been developed (Copeland *et al.*, 2010). However, it is important to consider that the hypophosphorylation of the SUMOylated form may be as a consequence of the SUMO attachment blocking the recognition of the phospho-antibody, therefore conclusions on the effect of SUMOylation on cMyBP-C phosphorylation in this study are limited. Nevertheless, this may still indicate that a nearby lysine is being SUMOylated, which may narrow down site identification for more appropriate characterisation.

4.5.4 Enhanced SUMOylation of cMyBP-C may alter diastolic function in isolated cardiomyocytes

Given the potential consequence of SUMOylation on cMyBP-C phosphorylation, neonatal ventricular cardiomyocytes were used to investigate the contractile profile of cMyBP-C-UBC9 (WT)-eGFP-SUMO1 conjugated infected cells and cMyBP-C-UBC9 (C93A) non-SUMOylated control cells. As these cells beat spontaneously in culture, they were paced at a consistent frequency to limit variability, although this did not allow for a measure of enhanced cMyBP-C SUMOylation on contractile rate (Ehler *et al.*, 2013). These cells provide a useful *in vitro* model as they are easily accessible and can be readily cultured for up to one-week. However, in this study, comparison of cells cultured for 3 days compared to 2 suggests prolonged culture may lead to slower relaxation properties (Figure 4.16). Culture affects the cytoskeletal arrangement of adult cardiomyocytes, and an increase in relaxation time has been observed in adult rat cardiomyocytes between 1.5 and 3 days of culture (Mitcheson *et al.*, 1998). However, this has not been reported in neonatal cardiomyocytes. In contrast, cells isolated from older animals (day 4 compared to day 1) have overall significantly faster contractile profiles independent of culture time (Figure 4.17). This phenomenon has also not been reported previously,

however study of the developing cardiac muscle shows a transitional increase in activation and relaxation kinetics during development in myofibrils, although this was at a foetal stage (Racca *et al.*, 2016). Although conclusions based on this study are limited due to low biological replicate numbers, neonatal cardiomyocytes of consistent age and culture time were used for further characterisation.

Characterisation of cardiac contractility, including upstroke, relaxation and overall contractile duration, revealed no significant effect of infection of the SUMOylated or non-SUMOylated cMyBP-C-UBC9 constructs (Figure 4.19). Additionally, all cells responded to isoprenaline in a manner observed in control cells (Figure 4.18), with no significant difference in response to isoprenaline between groups (Figure 4.20). Although viral cMyBP-C-UBC9 constructs localise to the myofilaments, there is still significant expression outwith the myofilament (Figure 4.12). Several groups have shown that given the precise arrangement of cMyBP-C as 7-9 transverse stripes in the C-zone of the sarcomere, it cannot be expressed beyond native levels (Li *et al.*, 2020; Merkulov *et al.*, 2012; Razzaque *et al.*, 2013). As such, the excess cMyBP-C may have unintended consequences on sarcomere function and contractility. In order to rule this out as a confounding variable, and to more closely determine the effect of SUMO conjugation, or not, to cMyBP-C, the measurements from co-infected WT/C93A with eGFP-SUMO1 cells were normalised to their singly infected counterparts. At baseline cardiomyocytes with a non-SUMOylated form of cMyBP-C had significantly slower relaxation kinetics compared to cells where eGFP-SUMO1 was conjugated to cMyBP-C. Interestingly, upon isoprenaline treatment, whilst both showed similar increases in upstroke kinetics, cardiomyocytes with non-SUMOylated cMyBP-C cells were more responsive to isoprenaline in terms of relaxation, showing a greater reduction in relaxation time compared to SUMOylated cells (Figure 4.21).

Given that the SUMOylated form of cMyBP-C may show reduced phosphorylation in response to isoprenaline treatment compared to the non-SUMOylated, this may explain why these cells do not respond as well to isoprenaline in terms of relaxation time. Indeed, phospho-null (3SD) mice show markedly impaired diastolic function due to slower relaxation kinetics, indicating that phosphorylation of cMyBP-C is key to facilitating appropriate relaxation (Tong *et al.*, 2014). However, upstroke contractile parameters were not different between groups. Phosphorylation of cMyBP-C has not been demonstrated to only affect

diastolic function, and most commonly is associated with increased force of contraction and time for force development, although studies in intact cells are limited in comparison to isolated myofilaments (Barefield & Sadayappan, 2010).

However, it is interesting that whilst there is no significant difference in the phosphorylation of SUMOylated cMyBP-C before isoprenaline treatment (Figure 4.15), the cells without SUMOylated cMyBP-C have slower relaxation kinetics at this point (Figure 4.21). This may imply that without the cMyBP-C present to conjugate to the SUMO1, it is causing slow contractile kinetics by methods elsewhere. Indeed, a study reported that virtually all of SUMO1 is conjugated to a substrate at a given point (Hay, 2007). Interestingly, a similar observation has been demonstrated for cTnI SUMOylation, where increased SUMOylation by N106 treatment increased myofilament Ca^{2+} sensitivity, but only when TnI SUMOylation sites were mutated (Fertig *et al.*, 2022). This overall implies that myofilament proteins "scavenge" excess SUMO1 molecules and may have implications for cases where SUMO1 expression is upregulated, such as during hypoxia (Shao *et al.*, 2004). However, in both cases, the functional consequences for their SUMOylation when SUMO1 is not in excess still remains to be elucidated.

4.5.5 Methodological considerations and future work

As discussed throughout, there are several methodological considerations that limit the conclusions that can be drawn from this study. Firstly, endogenous cMyBP-C SUMOylation could not be reliably detected by purification of cMyBP-C from rabbit cardiomyocytes and probing for SUMO1 (Figure 4.4). This approach is also limited as it assumes cMyBP-C is a substrate for SUMO1. This may be likely as cTnI, SERCA2a and ß2-adrenoceptor are, however SUMO1 is most commonly associated with nuclear targets whilst SUMO2/3 is expressed more in the cytosol, and so SUMO2/3 SUMOylation of cMyBP-C should be investigated in more detail (Fertig *et al.*, 2022; Kho *et al.*, 2011; Le *et al.*, 2017).

Additionally, whilst the UBC9-fusion method allows clear detection of a SUMOylated form of cMyBP-C, it is at extreme/non-physiological levels (undetectable to ~15-20% SUMOylated) which may be detrimental to other roles and modifications of cMyBP-C. This may also be compounded by the fact that excess cMyBP-C-UBC9 fusion is being expressed outwith the myofilament (Figure

4.12). This is important, as in the absence of proper localisation to the C-zone via binding to LMM and titin, cMyBP-C C-terminal domains have been shown to inhibit actin, which may contribute to the changes in relaxation kinetics observed in this study (Bunch *et al.*, 2019). Additionally, although direct comparison of WT/eGFP-SUMO1 and C93A/eGFP-SUMO1 cells allows comparison of SUMOylated and non-SUMOylated cMyBP-C, it cannot be distinguished between the study of an active and an inactive UBC9 expressed in these cells. Similarly, whilst the SUMOylation status of the majority of myofilament proteins remains unknown, having an active UBC9 in the vicinity may drive their SUMOylation. Indeed, although mostly observed in nuclear substrates, a feature of SUMOylation is the "protein group modification" concept whereby functionally related proteins are targeted as a group by SUMOylation (Psakhye & Jentsch, 2012). However, the role of UBC9 expression or activity in modulating contractility is currently unknown. Gain-of-function UBC9 in transgenic mice leads to increased autophagy in neonatal cardiomyocytes with important cardioprotective effects, however contractile parameters did not appear to be different in the transgenic whole heart (Gupta *et al.*, 2016). Whilst applicability of the UBC9-fusion approach is limited, in contrast to site direct mutagenesis of SUMOylation site, it has the advantage of allowing SUMOylation to occur without removing the ability of the site to be targeted by other modifications such as ubiquitylation or acetylation, with which SUMOylation has a dynamic relationship (Blakeslee *et al.*, 2014; Rougier *et al.*, 2010).

In this study, infection of neonatal ventricular cardiomyocytes with eGFP-SUMO1 led to no overt changes in cardiac contractility. In contrast, in adult cardiomyocytes, infection of SUMO1 leads to increased amplitude and faster decay of Ca^{2+} transients, although the effect on contractile or relaxation properties of these cells was not directly measured (Kho *et al.*, 2011).Whilst neonatal cardiomyocytes provide an accessible, cost-effective system to study contractile dynamics, their relevance to human cardiac contractility is limited. Adult cardiomyocytes rely more heavily on SERCA for Ca^{2+} extrusion than NCX1, whilst neonatal cells have lower SERCA2a expression and less reliance on the SR which may explain the lack of effect on cardiomyocyte contractility (Ziman *et al.*, 2010). Applying this approach to adult cardiomyocytes, with a viral infection level that

matches the endogenous cMyBP-C, may provide a more accurate analysis of cMyBP-C SUMOylation in this setting.

4.6 Conclusion

In conclusion, cMyBP-C SUMOylation was investigated in both HEK293 cells and primary cardiomyocytes. Identification of SUMOylated cMyBP-C was achieved by fusion to E2 ligase UBC9 and co-expression with eGFP-SUMO1. This form could be purified for mass spectrometry to identify the SUMOylated lysine(s), however although the suggested sites closely match *in silico* sequence analysis, an individually SUMOylated lysine could not be detected. Characterisation of the cMyBP-C-UBC9-SUMO1 complex in neonatal ventricular cardiomyocytes suggests that the SUMOylated form is hypophosphorylated upon isoprenaline treatment and this may result in impaired diastolic function. However, endogenously SUMOylated cMyBP-C could not be detected consistently in primary cardiac tissue and confounding variables, such as extra-sarcomere expression of cMyBP-C, limit the conclusions that can be drawn from this study.

Chapter 5 Palmitoylation in cardiac disease

5.1 Introduction

5.1.1 Ion transporter regulation in heart failure

Ischaemic HF represents a major socioeconomic burden and is the leading cause of death and disability worldwide. With a lack of effective, targeted therapies there is an increasing need to understand the molecular changes underlying HF, in both animal models and humans. In the failing heart, cardiac remodelling progresses from initial compensatory hypertrophy to ventricular dilatation and HF (Tham *et al.*, 2015). Molecular and cellular changes intensify throughout the process, and whilst myofilament dysfunction is an important parameter, this is often coupled to dysregulation of the upstream processes that regulate ion transport and determine the amplitude and cycling kinetics of Ca^{2+} (Njegic *et al.*, 2020). Indeed, a large component is the dysfunction of SR proteins, including leaky RYR2 channels and hypophosphorylation of PLB leading to increased inhibition and eventual downregulation of SERCA2a. These events result respectively in diastolic Ca^{2+} leak, which prolongs the Ca^{2+} transient duration and can trigger fatal arrythmias, and reduced SR content, leading to smaller Ca^{2+} transients and therefore reduced contractile performance (Arai *et al.*, 1993; Morgan *et al.*, 1990).

Importantly, the plasma membrane regulators of ion transport play an important role in the process. Leaky RYR2s are reported to occur in part due to increased Ca^{2+} entry into the cell through an overactive LTCC, driven in part through increased surface availability and phosphorylation (Goonasekera *et al.*, 2012; Schröder *et al.*, 1998). Similarly, increased NCX1 expression and activity are often observed, and whilst thought to occur as part of a protective mechanism to prevent toxic Ca^{2+} overload, contribute to the reduced SR store and therefore Ca^{2+} transients (Hasenfuss *et al.*, 1999). More importantly, NCX1 activity is associated with diastolic function, where it is closely linked to intracellular Na^+, levels of which are increased early in ischaemic injury, hypertrophy and in chronic HF. This leads to Na^+ dependent inactivation of NCX1, limiting Ca^{2+} extrusion, which may have systolic benefits, but overall contributes to the diastolic dysfunction observed in HF (Kass *et al.*, 2004). The increased Na^+ may in part be due to a reduction in the activity and expression of the Na^+/K^+ ATPase, which works to extrude Na^+ from the cell and to which NCX1 is functionally coupled (Dostanic *et*

al., 2004; Pieske & Houser, 2003). Loss of expression and activity of the Na^+/K^+ ATPase is particularly important in the development of the negative FFR seen in HF, with KO of PLM and alleviation of Na^+/K^+ ATPase inhibition associated with an improvement to a positive FFR (Kennington, Fuller and Shattock, 2006).

As such, inhibition of the LTCC, NCX1 and PLM may be of benefit therapeutically, whilst activating the Na^+/K^+ ATPase would improve extrusion of Na^+. NCX1 inhibitors would be beneficial in several regards, including preventing toxic Ca^{2+} overload associated with I/R, preventing Ca^{2+} influx as a consequence of increased sodium and preventing Ca^{2+} efflux improving diastolic and systolic function. Despite this, first generation inhibitors, showing positive inotropic and anti-arrhythmic properties in pre-clinical studies, have been slow to develop, although more promising selective inhibitors have recently been described (Otsomaa *et al.*, 2020; Pelat *et al.*, 2021). However importantly, inhibiting NCX1 can lead to Ca^{2+} accumulation and trigger SR-overload arrythmias (Chang *et al.*, 2018). Similarly, LTCC antagonists have been demonstrated to inhibit remodelling following pressure overload as well as having beneficial effects in the vasculature, improving compliance (Liao *et al.*, 2005; Richard *et al.*, 1998). However, clinical trials found inhibitors to be largely ineffective or even detrimental in improving morbidity and mortality in HF, with many having negative inotropic effects (Mahé *et al.*, 2003).

The complex picture of transporter inhibition is clearly evidenced by the use of Na^+/K^+ ATPase inhibitors which whilst increasing intracellular Na^+, act as positive inotropes predominantly by indirectly promoting NCX1 activity in the reverse mode (Askari, 2019). Whilst this increase in intracellular Ca^{2+} improves contractile performance, their use is limited due to arrythmias triggered by SR overload (Goldhaber & Hamilton, 2010). In contrast, activation of the Na^+/K^+ ATPase may be more promising to alleviate increased intracellular Na^+, as although it may not improve inotropy, it would have many positive benefits including improving FFR, mitochondrial function and metabolism, although investigations are still preliminary (Aksentijević *et al.*, 2020). One mechanism to activate the pump would be through antagonism of the pump inhibitor PLM, however PLM expression and phosphorylation, which activates the pump, is reduced in HF, therefore global inhibition may not be effective in improving pump activity (Bossuyt *et al.*, 2005). Taken together, global inhibitors of Ca^{2+} handling proteins may not be an effective

strategy and akin to cMyBP-C, modulation of their PTM profile may represent a novel therapeutic approach.

5.1.2 Palmitoylation in cardiac pathophysiology

Palmitoylation regulates almost all proteins involved in ECC (discussed in 1.3.2) and therefore it is unsurprising that it has been implicated in cardiac dysfunction. In terms of electrical excitability, loss of a key palmitoylation residue in Nav1.5 is associated with arrhythmogenesis (Pei *et al.*, 2016). Additionally, cardiac arrest and subsequent resuscitation was associated with a loss of membrane association of KChIP2 in a manner similar to its depalmitoylation, however loss of palmitoylation was not confirmed in this model (Murthy *et al.*, 2019).

Given the putative link between fatty acid availability and substrate palmitoylation, the modification has been implicated in the pathogenesis of the diabetic heart and in insulin resistance. In particular, palmitoylation may be involved in the mitochondrial dysfunction associated with both diabetic and cardiac damage, as the former is associated with increased long chain fatty acids (Schianchi *et al.*, 2020). However more recent work suggests this may be due to palmitoyl CoA exerting a protective, inhibitory effect on the mitochondria, the process of which is blunted in the diabetic heart, although a survey of palmitoylated proteins was not completed (Kerr *et al.*, 2021). Nevertheless, in a study of the regulator of the mitochondrial permeability transition pore (MPTP), Cyclophillin-D (CypD), mutation of the sole palmitoylation site was associated with reduced infarct size and higher mitochondrial Ca^{2+} retention. Whilst, in a similar manner to cMyBP-C, it cannot be ruled out that multiple PTMs occur at this site, both ischaemia and mitochondrial Ca^{2+} overload was associated with CypD depalmitoylation at this site (Amanakis *et al.*, 2021; Main, Robertson-Gray, *et al.*, 2020). Palmitoylation has also been implicated in cardiac ischaemia through study of the autoinflammatory protein STING (stimulator of interferon genes). Previously characterised small molecule inhibitors were shown to target STING cysteine palmitoylation which is required for its assembly and activation of the downstream signalling pathway implicated in autoimmune and inflammatory diseases (Haag *et al.*, 2018). In the setting of MI, whilst the inhibitors did not reduce mortality or immediate infarct size, three weeks of administration resulted in marked reduction in infarct expansion, scarring and show improved systolic

function (Rech *et al.*, 2022). This provides novel evidence that modulating individual protein substrate palmitoylation has therapeutic potential in the setting of cardiac injury. Importantly, palmitoylation regulates the membrane transporters implicated in HF pathology discussed above. This includes the LTCC, where palmitoylation influence the size of Ca^{2+} transients, NCX1, where palmitoylation is required for inactivation, PLM, where palmitoylation is required for its inhibition of the Na^{+}/K^{+} ATPase, and the Na^{+}/K^{+} ATPase itself, although the functional consequences are still unknown (Tulloch *et al.*, 2011; Reilly *et al.*, 2015; Howie *et al.*, 2018; Kuo, *et al*. In revision).

In terms of palmitoylating enzymes, DHHC16 KO mice develop cardiomyopathy and bradycardia, which may be through a loss of PLB palmitoylation and increased inhibition of SERCA2a, as PLB KO alleviated these effects (Zhou *et al.*, 2015). By far the most well studied of the palmitoylating enzymes is the cell surface localised DHHC5. DHHC5, the second most abundantly expressed DHHC-PAT in rat ventricular tissue, co-localises with Caveolin-3 in the caveolae (Howie *et al.*, 2014). Although Caveloin-3 has not been described as a substrate, DHHC5 does palmitoylate lipid raft protein Flotillin-2 (Li *et al.*, 2012; Rybin *et al.*, 2003). Additionally, PLM is a substrate of DHHC5, therefore DHHC5 may indirectly mediate pump activity through PLM palmitoylation (Howie *et al.*, 2014; Plain *et al.*, 2020; Tulloch *et al.*, 2011). DHHC5 also binds and palmitoylates NCX1 and loss of palmitoylation affects the dimerization of NCX1 in the presence of Ca^{2+}, suggesting DHHC5 dynamically regulates NCX1 activity (Gök *et al.*, 2020). Most recently DHHC5 has been implicated in the regulation of ß-adrenergic signalling by mediating rapid palmitoylation of Gαs and Gαi, potentially involving its own C-terminal palmitoylation (Chen *et al.*, 2020).

With regards to cardiac pathophysiology, DHHC5 is a crucial mediator of damage associated with anoxia/reperfusion (A/R). In both fibroblasts and cardiomyocytes, Ca^{2} overload during reperfusion leads to MPTP opening and release of Coenzyme A into the cytoplasm, which is immediately acylated into acyl-CoA, a substrate for DHHC5. DHHC5 palmitoylates plasma membrane proteins, including PLM and Flotillin-2, leading to clustering of palmitoylated proteins in lipid rafts. This triggers the process of massive endocytosis (MEND), in which up to 70% of the cell is internalised and likely crucial to the damage caused during reperfusion (Figure 5.1; Hilgmann *et al.*, 2013; Lin *et al.*, 2013). DHHC5 and PLM KO hearts show

reduced MEND and enhanced functional recovery following A/R, strongly implicating DHHC5 as a key mediator in this process. Interestingly, DHHC5-KO cardiomyocytes also show increased surface availability of PLM, suggesting that increased palmitoylation may drive removal of substrates from the cell membrane via endocytosis (M. J. Lin *et al.*, 2013).

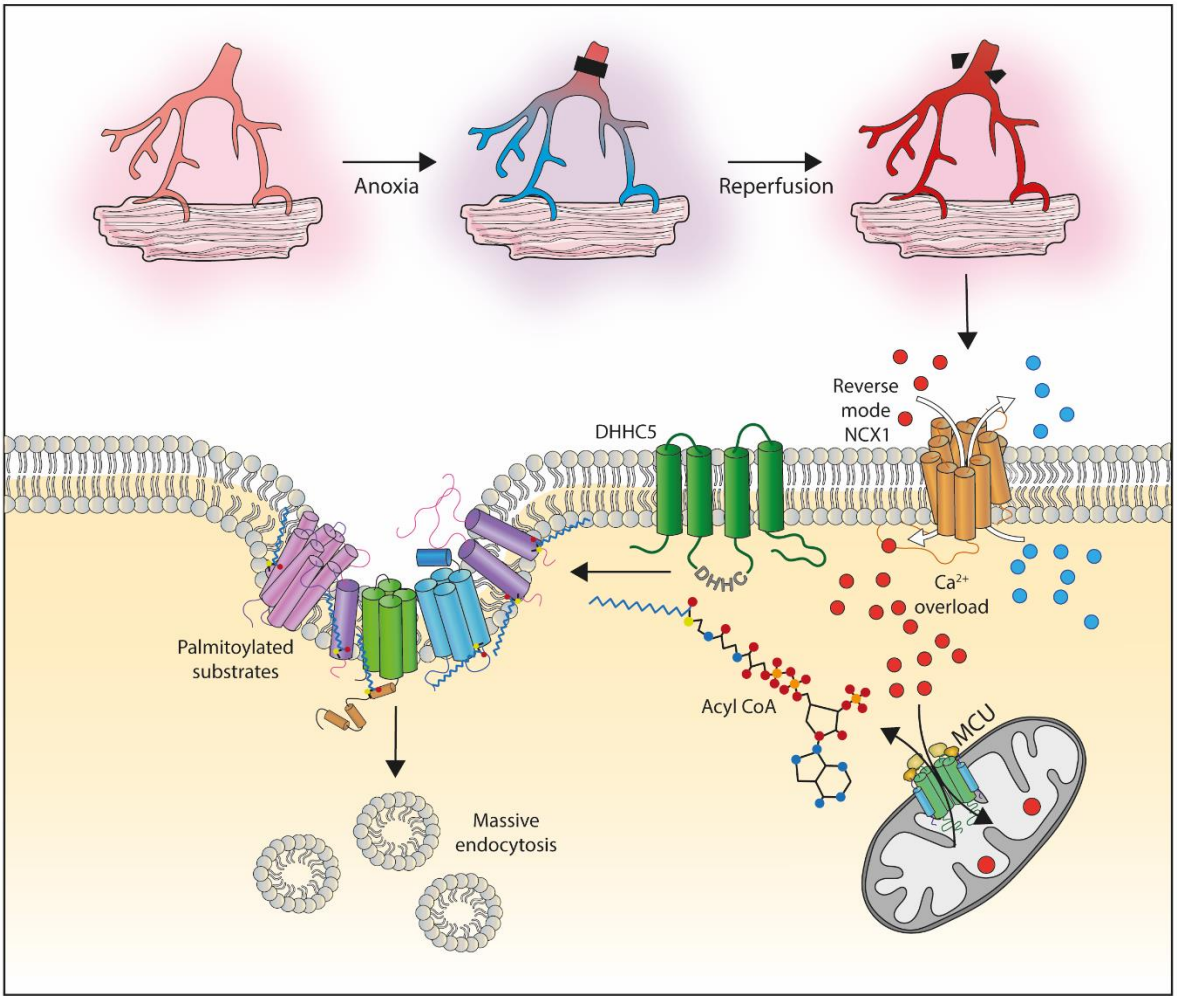

Figure 5.1. DHHC5 mediated massive endocytosis follow anoxia/reperfusion.
During reperfusion following anoxia-reperfusion (A/R) of cardiac tissue, calcium overload occurs and causes mitochondrial permeability transition pore opening (MPTP) opening and release of Coenzyme A into the sarcoplasm which is immediately acylated to Acyl-CoA. DHHC5 palmitoylates surface membrane proteins, including the sodium pump inhibitor phospholemman (FXYD1), which cluster in lipid ordered domains. This triggers the process of massive endocytosis (MEND), in which up to 70% of the cell membrane is internalised and is a key cause of damage following A/R. DHHC5 and PLM knock-out hearts show enhanced functional recovery from A/R and reduced MEND, highlighting their importance in the process.

Overall, loss of palmitoylation is most often detrimental for individual protein function, whilst paradoxically increased DHHC5 activity and fatty acid availability are associated with cardiac pathogenesis. Despite its clear regulatory role in cardiac physiology, there is currently a lack of direct evidence of the extent of palmitoylation or the activity and expression of palmitoylating or de-palmitoylating enzymes in human HF pathology. Recently, a pivotal study used

RNA-sequencing to evaluate mRNA changes in HFrEF and HFpEF with an aim to distinguish unique pathways between them to better target therapies to either group. Many DHHC-PATs and depalmitoylating enzymes (ABHDs, PPTs and LYPLAs) were identified in the study and some show significant dysregulation in HFrEF and HFpEF, with several changes being unique to one HF subtype (Figure 5.2; Hahn *et al.*, 2021). Whilst follow up protein expression studies are required to confirm the presence of these enzymes in the heart, the results suggest significant remodelling of palmitoylation machinery which may result in changes in substrate palmitoylation in HF.

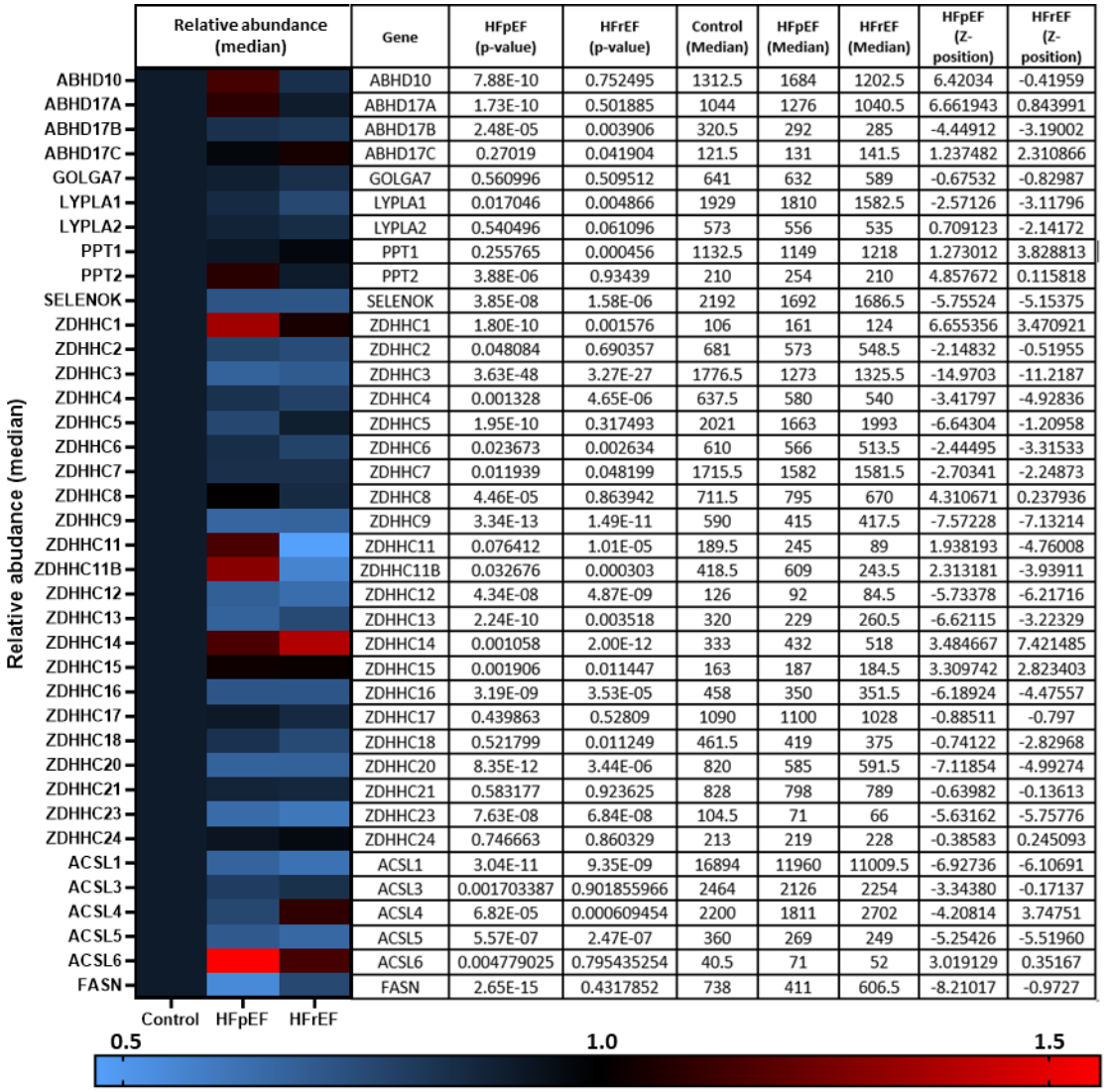

Relative abundance (median)	Gene	HFpEF (p-value)	HFrEF (p-value)	Control (Median)	HFpEF (Median)	HFrEF (Median)	HFpEF (Z-position)	HFrEF (Z-position)
ABHD10	ABHD10	7.88E-10	0.752495	1312.5	1684	1202.5	6.42034	-0.41959
ABHD17A	ABHD17A	1.73E-10	0.501885	1044	1276	1040.5	6.661943	0.843991
ABHD17B	ABHD17B	2.48E-05	0.003906	320.5	292	285	-4.44912	-3.19002
ABHD17C	ABHD17C	0.27019	0.041904	121.5	131	141.5	1.237482	2.310866
GOLGA7	GOLGA7	0.560996	0.509512	641	632	589	-0.67532	-0.82987
LYPLA1	LYPLA1	0.017046	0.004866	1929	1810	1582.5	-2.57126	-3.11796
LYPLA2	LYPLA2	0.540496	0.061096	573	556	535	0.709123	-2.14172
PPT1	PPT1	0.255765	0.000456	1132.5	1149	1218	1.273012	3.828813
PPT2	PPT2	3.88E-06	0.93439	210	254	210	4.857672	0.115818
SELENOK	SELENOK	3.85E-08	1.58E-06	2192	1692	1686.5	-5.75524	-5.15375
ZDHHC1	ZDHHC1	1.80E-10	0.001576	106	161	124	6.655356	3.470921
ZDHHC2	ZDHHC2	0.048084	0.690357	681	573	548.5	-2.14832	-0.51955
ZDHHC3	ZDHHC3	3.63E-48	3.27E-27	1776.5	1273	1325.5	-14.9703	-11.2187
ZDHHC4	ZDHHC4	0.001328	4.65E-06	637.5	580	540	-3.41797	-4.92836
ZDHHC5	ZDHHC5	1.95E-10	0.317493	2021	1663	1993	-6.64304	-1.20958
ZDHHC6	ZDHHC6	0.023673	0.002634	610	566	513.5	-2.44495	-3.31533
ZDHHC7	ZDHHC7	0.011939	0.048199	1715.5	1582	1581.5	-2.70341	-2.24873
ZDHHC8	ZDHHC8	4.46E-05	0.863942	711.5	795	670	4.310671	0.237936
ZDHHC9	ZDHHC9	3.34E-13	1.49E-11	590	415	417.5	-7.57228	-7.13214
ZDHHC11	ZDHHC11	0.076412	1.01E-05	189.5	245	89	1.938193	-4.76008
ZDHHC11B	ZDHHC11B	0.032676	0.000303	418.5	609	243.5	2.313181	-3.93911
ZDHHC12	ZDHHC12	4.34E-08	4.87E-09	126	92	84.5	-5.73378	-6.21716
ZDHHC13	ZDHHC13	2.24E-10	0.003518	320	229	260.5	-6.62115	-3.22329
ZDHHC14	ZDHHC14	0.001058	2.00E-12	333	432	518	3.484667	7.421485
ZDHHC15	ZDHHC15	0.001906	0.011447	163	187	184.5	3.309742	2.823403
ZDHHC16	ZDHHC16	3.19E-09	3.53E-05	458	350	351.5	-6.18924	-4.47557
ZDHHC17	ZDHHC17	0.439863	0.52809	1090	1100	1028	-0.88511	-0.797
ZDHHC18	ZDHHC18	0.521799	0.011249	461.5	419	375	-0.74122	-2.82968
ZDHHC20	ZDHHC20	8.35E-12	3.44E-06	820	585	591.5	-7.11854	-4.99274
ZDHHC21	ZDHHC21	0.583177	0.923625	828	798	789	-0.63982	-0.13613
ZDHHC23	ZDHHC23	7.63E-08	6.84E-08	104.5	71	66	-5.63162	-5.75776
ZDHHC24	ZDHHC24	0.746663	0.860329	213	219	228	-0.38583	0.245093
ACSL1	ACSL1	3.04E-11	9.35E-09	16894	11960	11009.5	-6.92736	-6.10691
ACSL3	ACSL3	0.001703387	0.901855966	2464	2126	2254	-3.34380	-0.17137
ACSL4	ACSL4	6.82E-05	0.000609454	2200	1811	2702	-4.20814	3.74751
ACSL5	ACSL5	5.57E-07	2.47E-07	360	269	249	-5.25426	-5.51960
ACSL6	ACSL6	0.004779025	0.795435254	40.5	71	52	3.019129	0.35167
FASN	FASN	2.65E-15	0.4317852	738	411	606.5	-8.21017	-0.9727

Figure 5.2. RNA transcript changes of palmitoylating enzymes, depalmitoylating enzymes, accessory proteins and in heart failure.
RNA sequencing of biopsies from heart failure patients with preserved ejection fraction (HFpEF, n=41) and reduced ejection fraction (HFrEF, n=30) and donor controls (n=24). Abundance of transcripts of palmitoylating enzymes, depalmitoylating enzymes, accessory proteins and proteins involved in fatty acid synthesis were investigated. The change in HFpEF and HFrEF relative to control (normalised to 1) are depicted in the heat map with of relative abundance and p-values detailed in the accompanying table (produced using the data repository from Hahn and Knutsdottir, *et al.* 2020).

5.2 Aims

Palmitoylation is an important regulatory modification for several cardiac substrates, fine-tuning their localisation, function and protein-protein interactions. Despite this, the role of palmitoylation in cardiac pathophysiology has remained relatively unknown, with the exception of DHHC5 which is an important contributor to MEND following A/R injury. More recently, changes in the mRNA expression of palmitoylating enzymes has been reported in HF, suggesting substrate palmitoylation may be changed. As investigation of cMyBP-C palmitoylation showed disease relevant changes in both human and animal models in the setting of HF, it was hypothesised that there would be changes in the palmitoylation of other key cardiac substrates. The aim of this work is therefore to:

- Evaluate the palmitoylation of key cardiac substrates in tissue from animal models of cardiac disease

- Evaluate the palmitoylation of key cardiac substrates in tissue from ischaemic human HF patients and determine whether the animal models accurately model the end-stage failing heart

- Identify whether any changes in substrate palmitoylation in cardiac disease are associated with changes in expression or palmitoylation of DHHC5

5.3 Results

5.3.1 Palmitoylation of substrates in animal models of cardiac disease

5.3.1.1 Mouse model of left ventricular hypertrophy induced by pressure overload

The use of animal models of cardiac disease and HF is essential to understand the value or targeting individual proteins, pathways and processes therapeutically. However, there are a wide variety available, each better at modelling a different aspect of cardiac hypertrophy and ischaemic HF. To investigate whether palmitoylation changes occur in ventricular hypertrophy, Acyl-RAC was used to purify palmitoylated proteins from a pressure overload mouse model. Ventricular hypertrophy, accompanied by systolic and diastolic dysfunction, was induced via transverse aortic constriction (TAC) in 6-week-old C57BL/6J mice (Boguslavskyi *et al.*, 2014). This model is limited in that TAC extent and position can vary between labs, giving inconsistent cardiac phenotypes (Zi *et al.*, 2019). This is especially important as some labs report the development of concentric hypertrophy, which is associated with the majority of HFrEF cases, whilst others report eccentric hypertrophy (Barrick *et al.*, 2007; Garcia-Menendez *et al.*, 2013; Nauta *et al.*, 2020). Nevertheless, this model provides a valuable tool to understand molecular changes that occurs early in cardiac disease. As such, palmitoylation of key cardiac substrates including NCX1, Na^+/K^+ ATPase and accessory protein PLM, Gαi and two constitutively palmitoylated proteins Caveolin-3 and Flotillin-2 were assessed in the samples 8 weeks post-injury. Palmitoylation of NCX1 and GαI were significantly reduced in hypertrophy samples compared to sham controls (Figure 5.3).

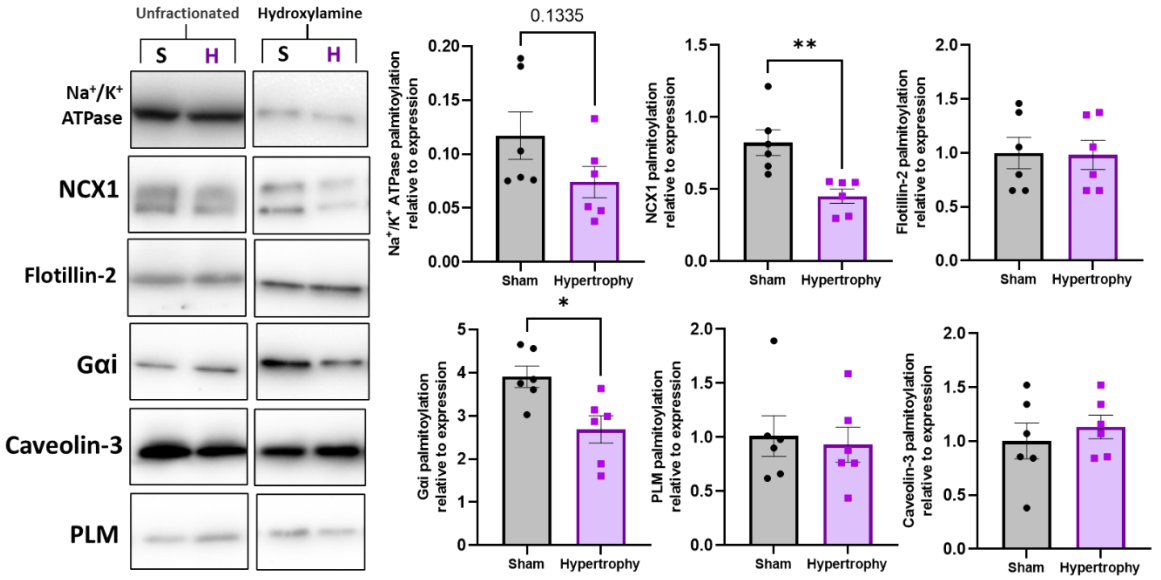

Figure 5.3. Palmitoylation of excitation contraction coupling proteins is decreased or unchanged in a mouse model of left ventricular hypertrophy.
Acyl-Resin Assisted Capture (Acyl-RAC) was used to purify all palmitoylated proteins from ventricular tissue of mice that had left ventricular hypertrophy induced pressure overload (H) and sham controls (S). Palmitoylated fraction (hydroxylamine-dependent) was normalised to total protein (unfractionated, UF) for the sodium-calcium exchanger (NCX1), the Na^+/K^+ ATPase α1 subunit and accessory protein phospholemman (PLM), the G-protein Gαi, Flotillin-2 and Caveolin-3. Palmitoylation of NCX1 and Gαi were significantly decreased in hypertrophy samples (*p<0.05, **p<0.01). Statistical comparisons made by unpaired student's t-test. Data is mean ±S.E.M. Samples were prepared and western blot performed by Dr Jacqueline Howie (University of Dundee).

5.3.1.2 Rat model of heart failure induced by aortic banding

In rats, TAC induces hypertrophy with eventual progression to LV dilatation and HF after 3 months. In contrast to the mouse model, this model is reported to more closely the progression from concentric hypertrophy, to eccentric hypertrophy, to LV dilatation and eventual systolic HF (Hasenfuss, 1998). Whilst this is clinically relevant, the degree of stenosis directly influences the time from hypertrophy to HF, which again can vary between experimenters, with a subset of animals often not developing the HF phenotype at all (Feldman *et al.*, 1993). Nevertheless, this model allows an understanding of the progression from hypertrophy to HF where therapeutic intervention would be beneficial. Acyl-RAC was used to purify palmitoylated proteins from rat model of TAC-induced HF in which ejection fraction was confirmed to be <50%. Palmitoylation of GαI was significantly reduced in banded samples compared to sham controls with no significant change in palmitoylation of NCX1, Na^+/K^+ ATPase, PLM, Caveolin-3 or Flotillin-2 (Figure 5.4).

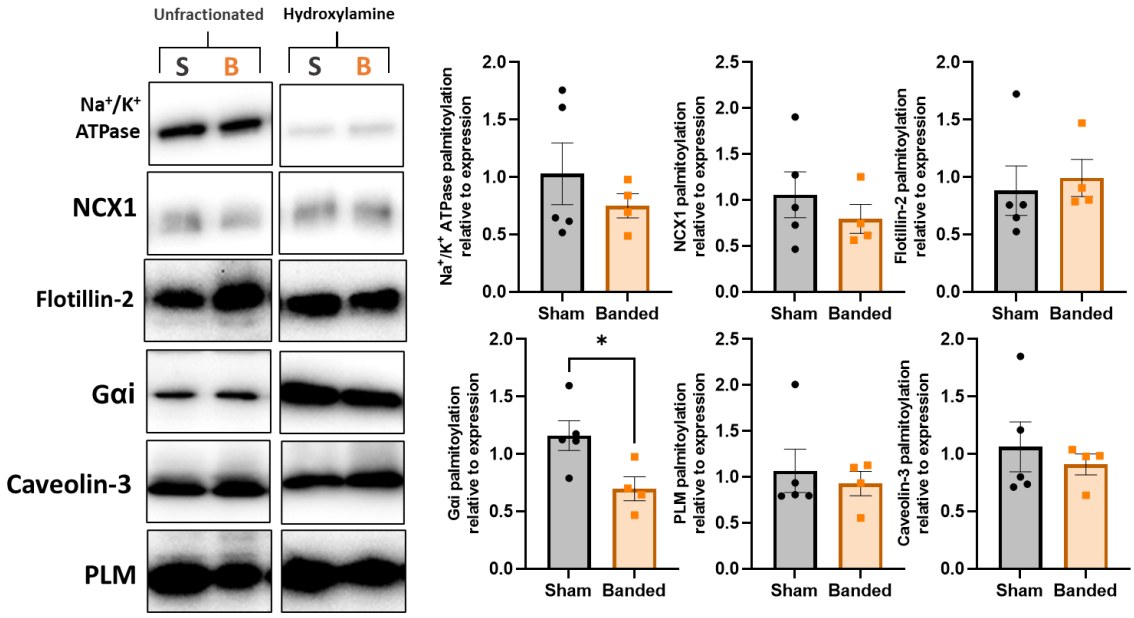

Figure 5.4. Palmitoylation of excitation contraction coupling proteins is decreased or unchanged in a rat model of heart failure.
Acyl-Resin Assisted Capture (Acyl-RAC) was used to purify all palmitoylated proteins from ventricular tissue of rats that had developed heart failure induced by aortic banding (B) and sham controls (S). Palmitoylated fraction (hydroxylamine-dependent) was normalised to total protein (unfractionated, UF) for the sodium-calcium exchanger (NCX1), the Na^+/K^+ ATPase α1 subunit and accessory protein phospholemman (PLM), the G-protein Gαi, Flotillin-2 and Caveolin-3. Palmitoylation Gαi was significantly decreased in hypertrophy samples (*$p<0.05$) and there was no significant difference or trend in Na^+/K^+ ATPase, NCX1, PLM, Caveolin-3 or Flotillin-2 palmitoylation. Statistical comparisons made by unpaired student's t-test. Data is mean ±S.E.M**.** Samples were prepared and western blot performed by Dr Jacqueline Howie (University of Dundee).

5.3.1.3 Rabbit model of heart failure induced by myocardial infarction

The rabbit heart is highly valuable model for human cardiac function, as the electrophysiological profile closely resembles that of human in terms of action potential dynamics and expression ion transporters (Ellermann *et al.*, 2021). In particular when modelling HF, the MI-induced cardiac remodelling in the rabbit more accurately reflects the changes in Ca^{2+} flux during human HF (Bers, 2002b; Sanbe *et al.*, 2005). In this model, rabbits were subjected to a left anterior descending coronary ligation to induce an MI, followed by maintenance for 8 weeks. The induction of the HF phenotype was confirmed via electrocardiogram measurements of LVEF, which was <45% in the MI group (Kettlewell *et al.*, 2009). Acyl-RAC was used to determine the palmitoylation of the LTCC, NCX1, Na^+/K^+ ATPase and accessory protein PLM, Gαi and Caveolin-3 in the left ventricular region. Palmitoylation of NCX1 was significantly reduced in HF samples compared to control with a modest reduction in Gαi ($p=0.095$; Figure 5.5).

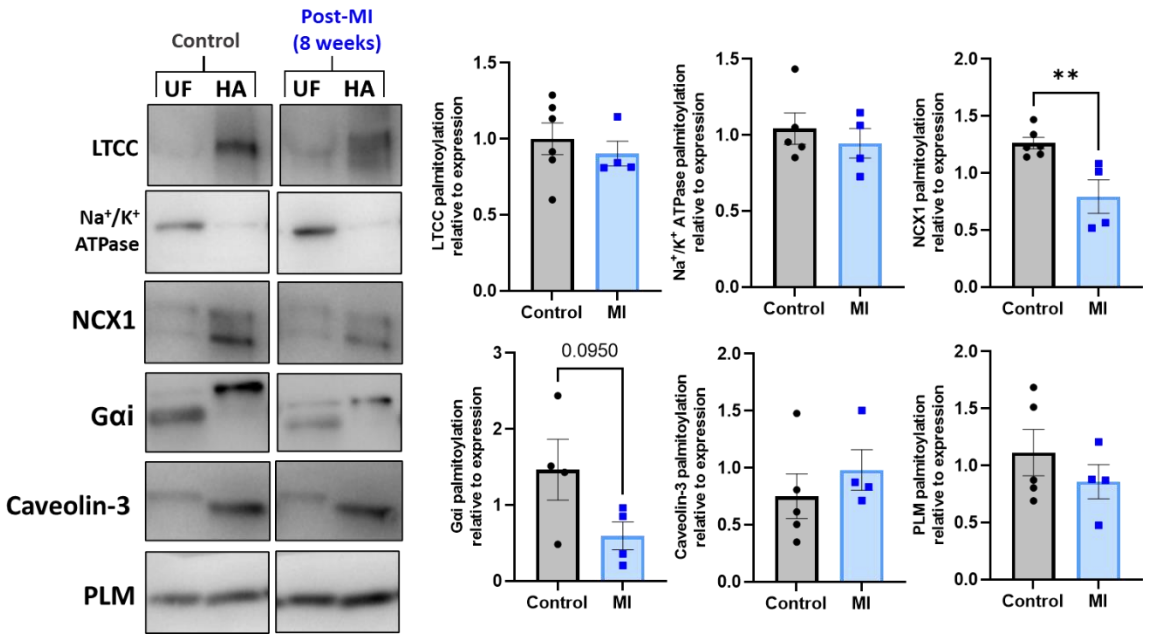

Figure 5.5. Palmitoylation of cardiac substrates in the left ventricular region of the rabbit heart following myocardial infarction (MI).
Ventricular cardiomyocytes were isolated from the left ventricular (LV) region from male rabbits that had undergone myocardial infarction (MI) via left anterior descending coronary artery ligation at 12 weeks of age before being maintained for a further 8 weeks. Palmitoylation of the α1c subunit of the L-type calcium channel (LTCC), the sodium calcium exchanger (NCX1), the Na^+/K^+ ATPase α1 subunit and accessory protein phospholemman (PLM), the G-protein Gαi and assay control Caveolin-3 was determined by Acyl-Resin Assisted Capture (Acyl-RAC) and palmitoylated fraction (hydroxylamine dependent, HA) normalised to total protein (UF). Palmitoylation of NCX1 is decreased in MI tissue compared to control (*p<0.05) with a modest decrease in Gαi (p=0.0950) and no change observed change in the Na^+/K^+ ATPase, PLM, LTCC or Caveolin-3. Data is mean ±S.E.M analysed via a student's unpaired t-test.

5.3.1.4 Pig model of heart failure induced by myocardial infarction

Acyl-RAC was used to purify palmitoylated proteins from a pig model of MI-induced HF (and sham controls) in which pigs were subjected to left anterior descending artery balloon occlusion to induce a MI, followed by reperfusion and maintenance for 3 months (Tilemann *et al.*, 2013). Akin to the rabbit, the pig is a more useful tool for modelling human cardiac function over rodents, with advantages including comparable heart rate and heart to body weight size to humans. The limitations of their use mainly lie in the advanced surgical skills required and time and cost associated with their maintenance. Additionally, they are prone to tachyarrhythmias making mortality rates high (Spannbauer *et al.*, 2019). Nevertheless, in terms of HF modelling, the pathological changes in the LV post-MI are largely reproducible, with a progressive infarct occurring over several weeks in the endocardial region of the heart (Dixon & Spinale, 2009). This model also offers the advantage over the rabbit model in that it is a model of ischaemia followed by reperfusion, which may more accurately reflect the human clinical situation (Baehr *et al.*, 2019). Palmitoylation was assessed for the LTCC, NCX1,

Na^+/K^+ ATPase and accessory protein PLM, Gαi and Flotillin-2. There was a significant reduction in LTCC and NCX1 palmitoylation in post-MI samples, with a modest decrease in Na^+/K^+ ATPase (p=0.1311; Figure 5.6).

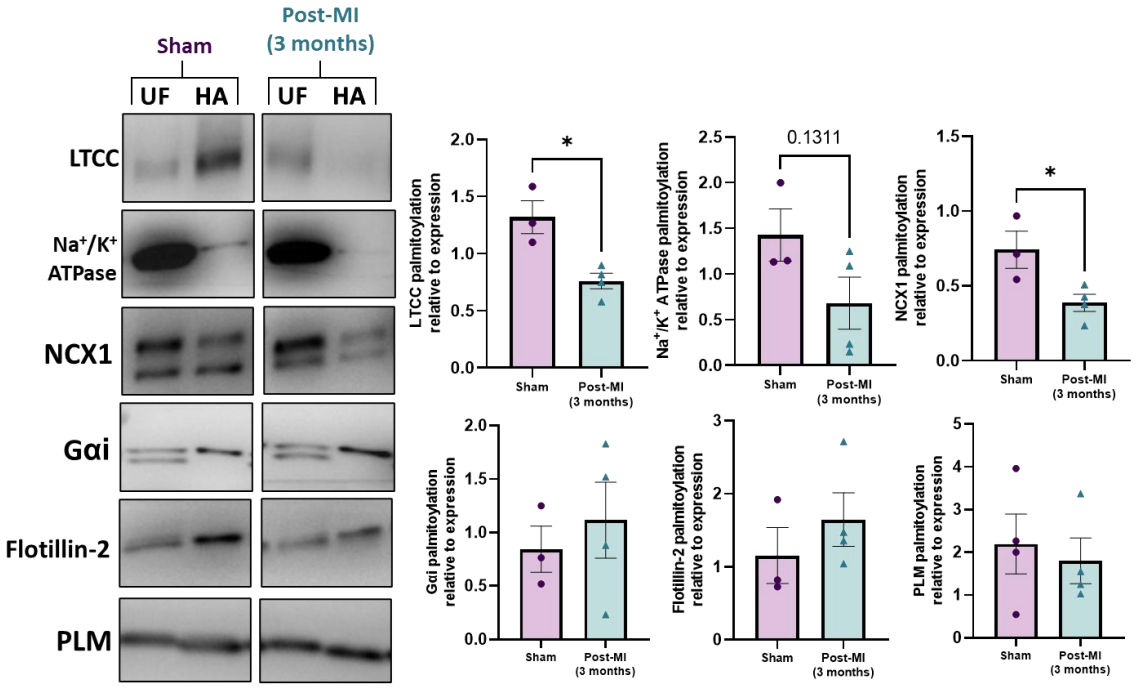

Figure 5.6. Palmitoylation of cardiac substrates in a porcine model of heart failure 3 months post myocardial infarction (MI).
Cardiac tissue from pigs was obtained 3 months post-MI myocardial infarction (MI) along with sham controls. Palmitoylation of the α1c subunit of the L-type calcium channel (LTCC), the sodium calcium exchanger (NCX1), the Na^+/K^+ ATPase α1 subunit and accessory protein phospholemman (PLM), the G-protein Gαi and assay control Flotillin-2 (Caveolin-3 not detected in pig tissue) was determined by Acyl-Resin Assisted Capture (Acyl-RAC) and palmitoylated fraction (hydroxylamine dependent, HA) normalised to total protein (UF). Palmitoylation of the LTCC and NCX1 is decreased in MI tissue compared to control (*p<0.05) with a modest decrease in the Na^+/K^+ ATPase (p=0.1311) and no change observed change in Gαi, Flotillin-2 and PLM. N=3-4 per group. Data is mean ±S.E.M analysed via a student's unpaired t-test.

5.3.2 Palmitoylation of substrates in human heart failure

Although it has been widely reported that HF leads to altered expression and PTM regulation of several cardiac proteins, and despite the extensive remodelling of palmitoylating and depalmitoylation enzymes (Figure 5.2), there is currently no evidence of the extent of substrate palmitoylation in human HF. In order to determine whether expression or palmitoylation of cardiac proteins are changed in ischaemic HF, samples from the endocardium of human ischaemic HF patients and organ donors (details in Table 2.10) were analysed for key cardiac substrates including the LTCC, NCX1, Na^+/K^+ ATPase and accessory protein PLM, Gαi, Caveolin-3 and Flotillin-2. Despite variability between investigations, most often expression of the LTCC, the α1 subunit of the Na^+/K^+ ATPase, PLM and Caveolin-3

are found reduced in HF samples, whilst expression of NCX1, Flotillin2 and Gαi and are mostly found upregulated (Bossuyt *et al.*, 2005; Feiner *et al.*, 2011; Feldman *et al.*, 1991; Hasenfuss *et al.*, 1999; Schwinger, Hoischen, *et al.*, 1999; Schwinger, Wang, *et al.*, 1999; Soni *et al.*, 2016; Takahashi *et al.*, 1992). In these samples, only a significant reduction in the Na^+/K^+ ATPase was observed, with a modest reduction in LTCC expression (p=0.1202; Figure 5.7). Analysis of palmitoylation revealed a significant increase in Na^+/K^+ ATPase and NCX1 palmitoylation in HF samples (Figure 5.8).

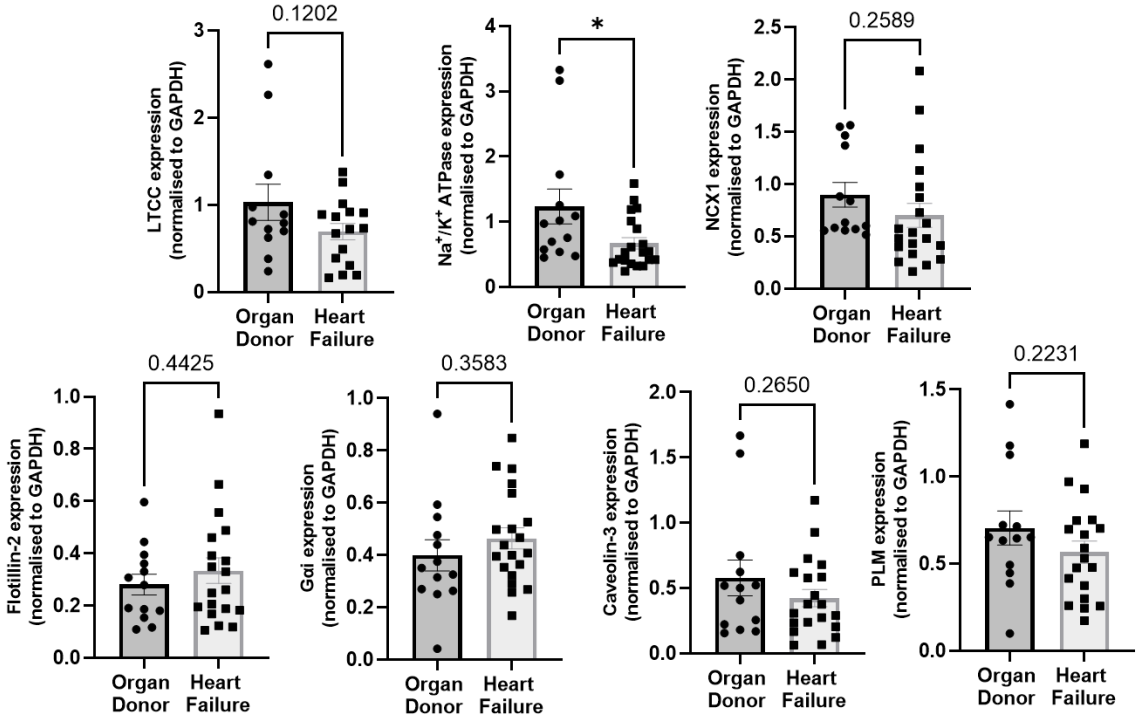

Figure 5.7. Expression of cardiac substrates in organ donor and heart failure ventricular endocardium.
Expression of the L-type calcium channel (LTCC), the Na^+/K^+ ATPase alpha1 subunit, the sodium-calcium exchanger (NCX1), Flotillin-2, the G-protein Gαi, Caveolin-3 and the Na^+/K^+ ATPase accessory protein phospholemman (PLM) was determined from ventricular endocardium of organ donor and ischaemic heart failure patients and normalised to GAPDH. Expression of the Na^+/K^+ ATPase (*p<0.05) was significantly reduced in heart failure samples compared to organ donor. There was no significant difference in the LTCC, NCX1, Flotillin-2, Gαi, Caveolin-3 or PLM expression. Statistical comparisons made by unpaired student's t-test. Data is mean ±S.E.M.

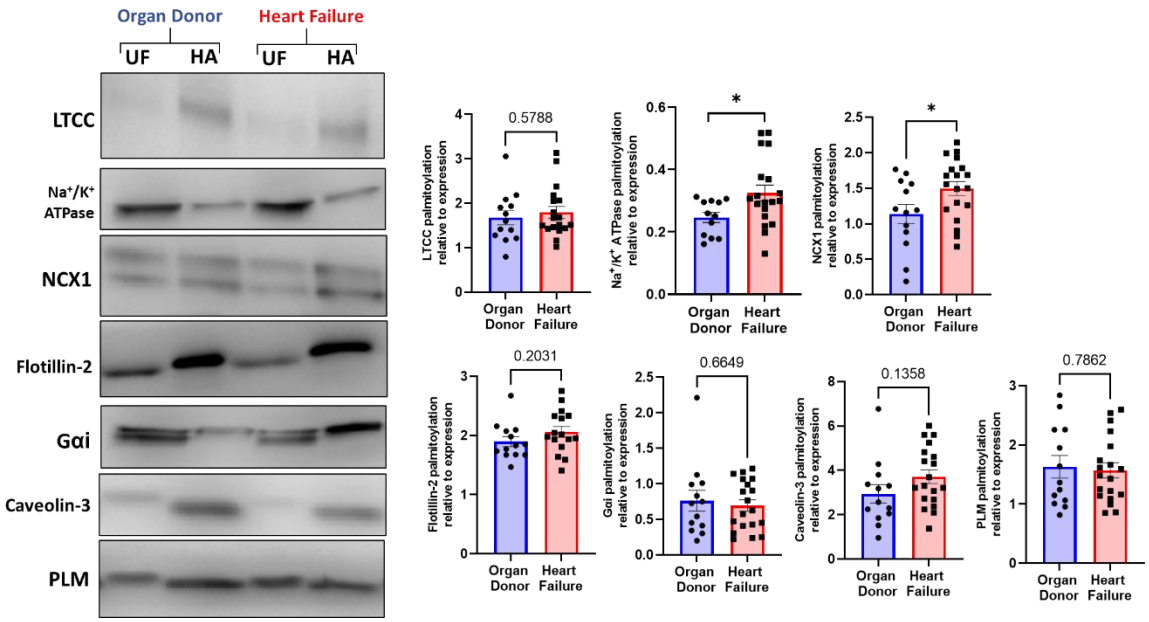

Figure 5.8. Palmitoylation of cardiac substrates in organ donor and heart failure ventricular endocardium.
Acyl-Resin Assisted Capture (Acyl-RAC) was used to determine the palmitoylation of the α1c subunit of the L-type calcium channel (LTCC), the Na^+/K^+ ATPase alpha1 subunit, the sodium-calcium exchanger (NCX1) and), Flotillin-2, the G-protein (Gαi), Caveolin-3 and the Na^+/K^+ ATPase accessory protein phospholemman (PLM) in ventricular endocardium from organ donor and ischaemic heart failure patients. Palmitoylated protein (HA) was normalised to total protein (UF). Palmitoylation of NCX1 and Na^+/K^+ ATPase was significantly increased in heart failure samples compared to organ donor (*p<0.05). There was no significance difference or trend in LTCC, Gαi, Flotillin-2 Caveolin-3 or PLM palmitoylation. Statistical comparisons made by unpaired student's t-test. Data is mean ±S.E.M.

5.3.3 DHHC5 expression and palmitoylation in cardiac disease

Analysis of cardiac substrate palmitoylation in animal models of cardiac hypertrophy and HF revealed disease was either association with unchanged or reduced levels of palmitoylation. In contrast, samples from human HF patients were unchanged or increased in levels of substrate palmitoylation. This may be driven by changes in fatty acid availability or changes in palmitoylation/depalmitoylation enzymatic regulation, especially since several of these enzymes are changed in expression in HF (Hahn *et al.*, 2021). DHHC5 is one of the most highly expressed DHHC-PATs in the myocardium, where it has been reported to regulate the palmitoylation of PLM, NCX1, Gαi and Flotillin-2 (Gök *et al.*, 2020; Howie *et al.*, 2014; Li *et al.*, 2012; Tulloch *et al.*, 2011). DHHC5 is key to mediating ß-adrenergic signalling and upregulated DHHC5 activity is associated with reperfusion injury, and therefore it was hypothesised that DHHC5 expression may be altered in animal models of cardiac disease and human HF (Chen *et al.*, 2020; Lin *et al.*, 2013).

5.3.3.1 DHHC5 expression in animal models of cardiac hypertrophy

In a mouse model of left ventricular hypertrophy that was associated with loss of NCX1 and Gαi palmitoylation (Figure 5.3), DHHC5 expression was significantly increased 2-weeks and 8-weeks after onset of hypertrophy, with a trend to increase after only 3 days (p=0.1056; Figure 5.9).

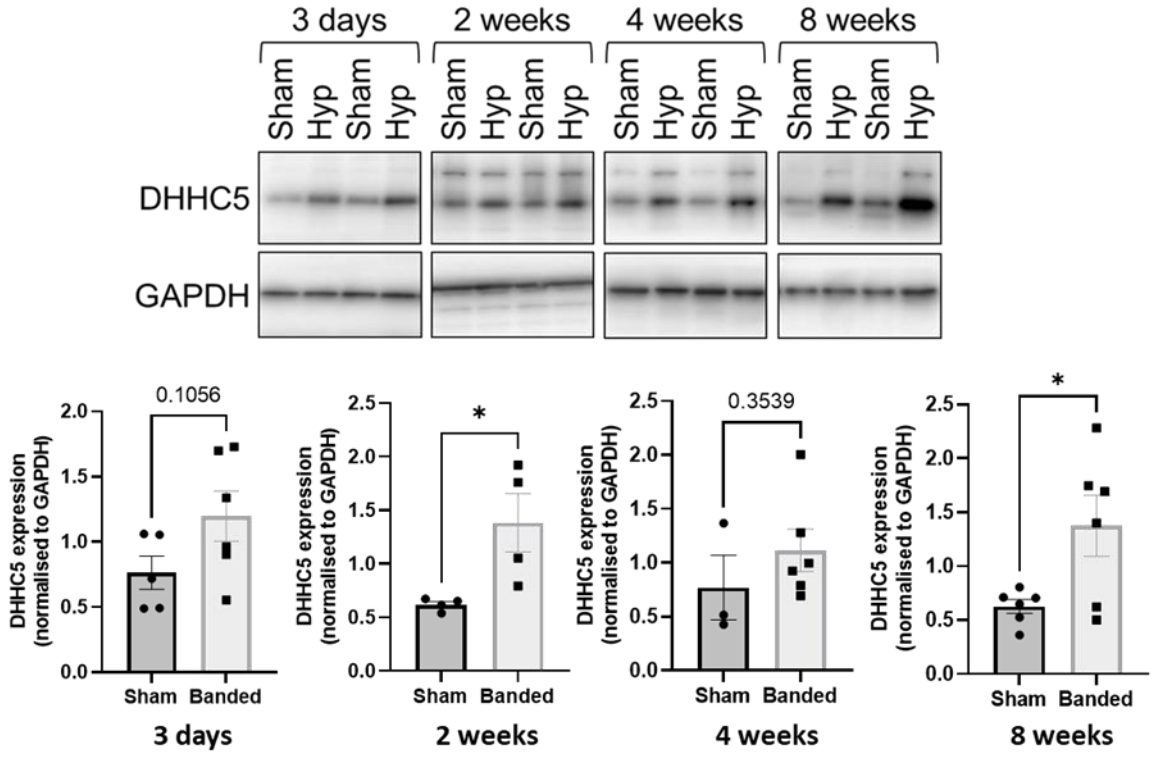

Figure 5.9. Expression of DHHC5 is increased in mice with left ventricular hypertrophy at 2 weeks and 8 weeks post-onset.
Ventricular samples from mice that underwent left ventricular hypertrophy induced by pressure overload and sham controls were taken at 3 days, 2 weeks, 4 weeks, and 8 weeks post-onset. Expression of DHHC5 (normalised to loading control GAPDH) was significantly increased in hypertrophy samples compared to control at 2 weeks and 8 weeks post-onset (*p<0.05). Statistical comparisons made by unpaired student's t-test. Data is mean ±S.E.M**.** Samples were prepared and western blot performed by Dr Jacqueline Howie (University of Dundee).

5.3.3.2 DHHC5 expression and palmitoylation in animal models of heart failure

Following the observation of increased DHHC5 expression associated with cardiac injury and hypertrophy, occurring as early as 2 weeks post-injury, analysis of expression in models of more developed ischaemic HF was completed. In contrast to hypertrophy models, in a rat model of HF associated with a loss of Gαi palmitoylation only, DHHC5 expression was unchanged (Figure 5.10). Similarly, in the rabbit model of MI-induced HF associated with loss of NCX1 palmitoylation, DHHC5 expression was unchanged (Figure 5.11). Additionally, Acyl-RAC was used to assess the palmitoylation status of DHHC5 which may give an indication of its

activity through either palmitate loading on the catalytic cysteine, or its own C-terminal palmitoylation which has been shown to enhance its association with the Na^+/K^+ ATPase and play a role in its regulation of G-protein palmitoylation (Chen *et al.*, 2020; Plain *et al.*, 2020). In the rabbit model, DHHC5 palmitoylation was unchanged, however in the pig model, associated with reduced NCX1 and LTCC palmitoylation, DHHC5 palmitoylation was significantly reduced with a modest reduction in expression (p=0.0684; Figure 5.12).

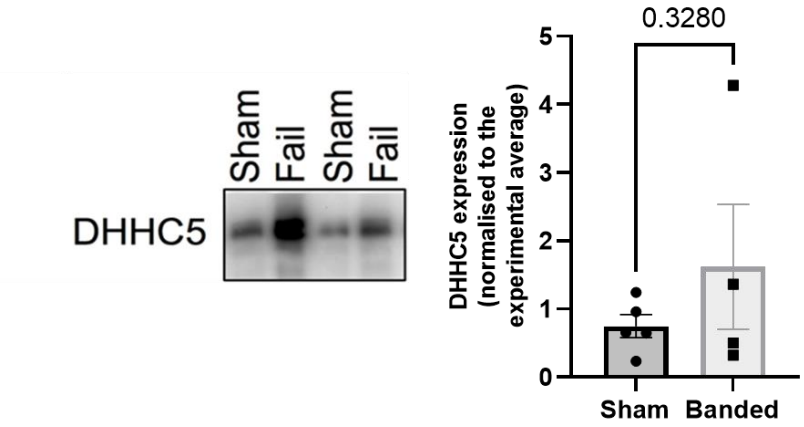

Figure 5.10. Expression of cell surface localised DHHC5 is unchanged in rats with cardiac hypertrophy and heart failure induced by aortic banding.
Expression of DHHC5 was determined from ventricular tissue of rats that had developed heart failure induced by aortic banding and sham controls. Expression of DHHC5 (normalised to the experimental average) was not significantly increased in banded samples. Statistical comparisons made by unpaired student's t-test. Data is mean ±S.E.M**.** Samples were prepared and western blot performed by Dr Jacqueline Howie (University of Dundee).

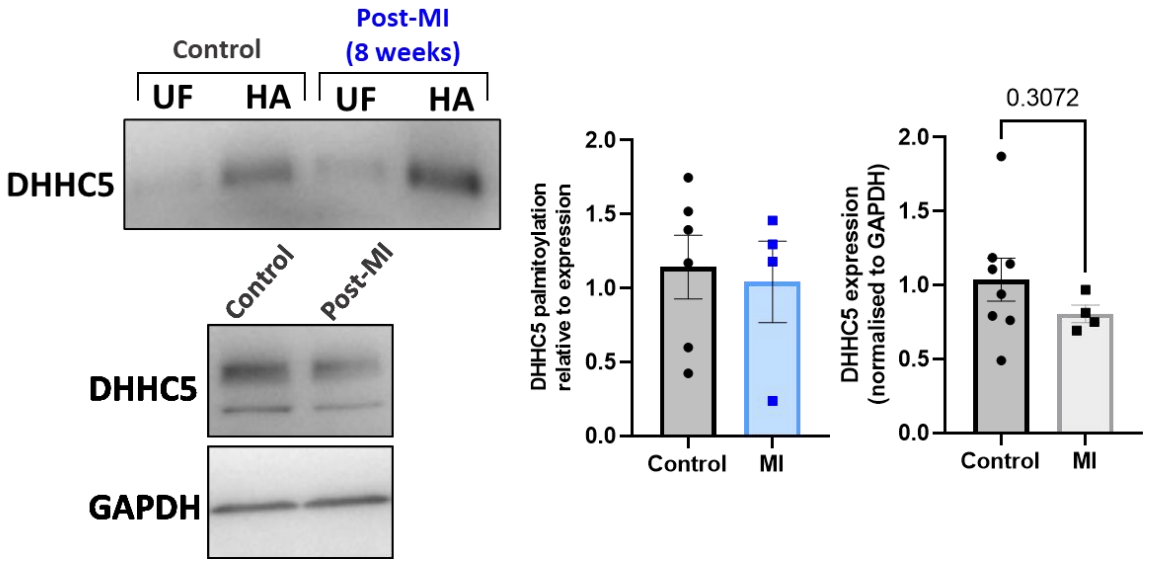

Figure 5.11. Expression and palmitoylation of DHHC5 are unchanged in the left ventricle of a rabbit model of heart failure.
Samples were obtained from ventricular tissue of rabbits that has undergone a myocardial infarction and maintained for 8 weeks and stock/sham controls. Expression of DHHC5 (normalised to loading control GAPDH) were not significantly different between control and post-MI samples whilst palmitoylation DHHC5 was also unchanged. Statistical comparisons made by unpaired student's t-test. Data is mean ±S.E.M.

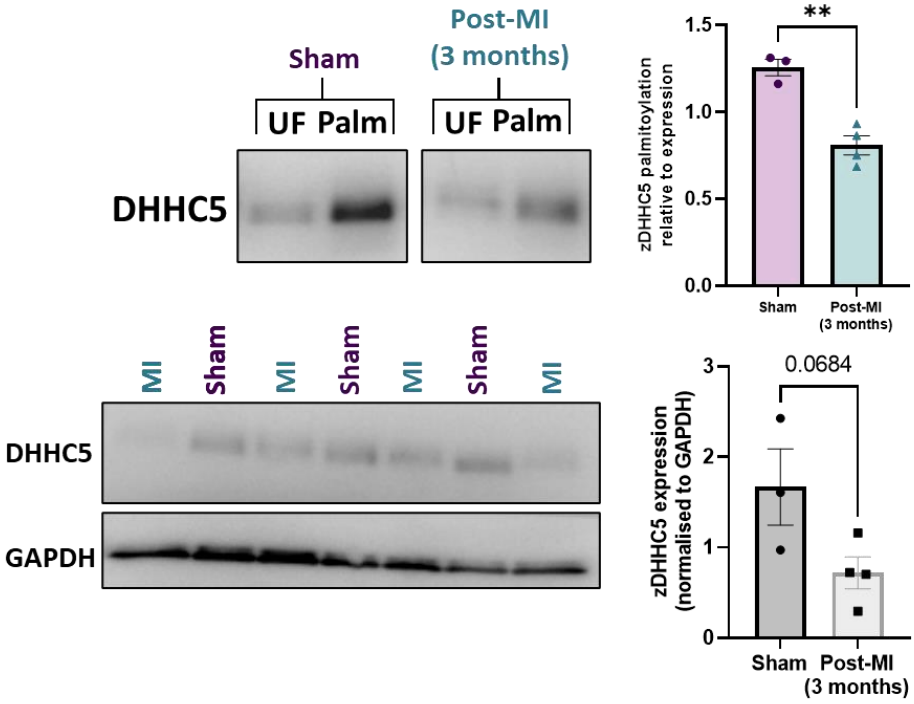

Figure 5.12. S-palmitoylation and expression of DHHC5 are decreased in a pig model of heart failure whilst APT1 remains unchanged.
Acyl-Resin Assisted Capture (Acyl-RAC) was used to purify all palmitoylated proteins from ventricular tissue of pigs 3 months post myocardial infarction (n=4) and sham controls (n=3). Palmitoylated fraction (hydroxylamine-dependent, HA) was normalised to total protein (unfractionated, UF). Palmitoylation of DHHC5 was significantly decreased in MI samples compared to sham (**p<0.01) with a modest reduction in expression (p=0.0684, normalised to loading control GAPDH). Expression of APT1 was unchanged and palmitoylation could not be detected/measured in the samples. Statistical comparisons made by unpaired student's t-test. Data is mean ±S.E.M.

5.3.3.3 DHHC5 expression and palmitoylation in human heart failure

Analysis of DHHC5 in cardiac tissue from animal models of disease revealed hypertrophy was associated with elevated DHHC5, whilst HF was associated with unchanged or reduced levels. Recent RNA sequencing analysis suggests DHHC5 mRNA is significantly reduced in HFpEF, but not HFrEF. In contrast, in ischaemic human HF samples which classify as HFrEF, reduced levels of DHHC5 protein expression were observed. Additionally in these samples which were associated with an increase in NCX1 and Na^+/K^+ ATPase palmitoylation, a modest increase in DHHC5 palmitoylation was detected (p=0.1133; Figure 5.13).

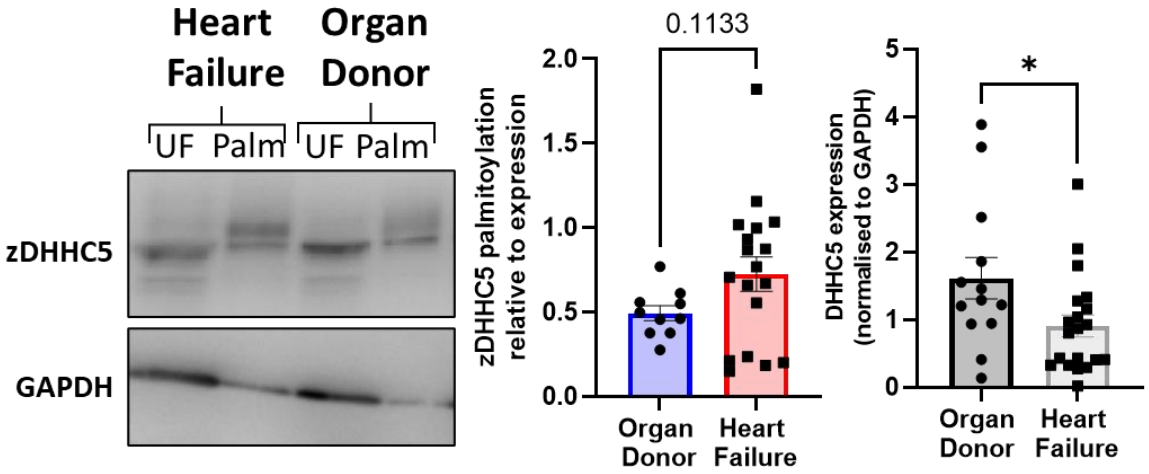

Figure 5.13. Expression of DHHC5 is decreased in human heart failure samples whilst DHHC5 palmitoylation is modestly increased.
Acyl-Resin Assisted Capture (Acyl-RAC) was used to purify all palmitoylated proteins from ventricular endocardium of ischaemic heart failure patients and organ donors. Palmitoylated fraction (hydroxylamine-dependent, HA) was normalised to total protein (unfractionated, UF) for DHHC5 and revealed a modest increase in palmitoylation (p=0.1133). There was a significant decrease in DHHC5 expression (normalised to GAPDH, *p<0.05) in heart failure samples compared to organ donor. Statistical comparisons made by unpaired student's t-test. Data is mean ±S.E.M.

5.4 Discussion

The overall aim of the present study was to identify changes in substrate palmitoylation in the setting of human HF, with further information gained from studying animal models of cardiac hypertrophy and HF. Using Acyl-RAC, palmitoylation of the LTCC, NCX1, Na^+/K^+ ATPase, PLM and Gαi was measured in healthy and diseased samples, and expression and palmitoylation of DHHC5 was characterised to elucidate on the mechanisms involved.

5.4.1 Substrate palmitoylation is reduced in animal models of cardiac hypertrophy and heart failure

Cardiac hypertrophy is associated with initial compensatory changes in LV wall thickness to maintain systolic force against an increased after-load. Whilst this often occurs in the setting of aortic stenosis or hypertension in the human disease, it can be modelled by constricting the transverse aorta in the rodent (Rame & Dries, 2007). In these samples, NCX1 and Gαi palmitoylation was significantly reduced 8-weeks post-injury, with a modest reduction in Na^+/K^+ ATPase palmitoylation (Figure 5.3). The progression from hypertrophy to systolic HF, as observed in the TAC rat model and MI-induced models in the rabbit and pig, was generally associated with a reduction in the palmitoylation of Gαi, NCX1, LTCC and Na^+/K^+ ATPase, although this varied significantly between models (Figure 5.4Figure 5.5Figure 5.6). In all cases, palmitoylation of PLM, Caveolin-3 and Flotillin-2 remained unchanged.

NCX1 palmitoylation was the most consistently downregulated in all apart from the rat model. This may reflect the fact the rat relies less on NCX1 activity and more on SERCA2a for Ca^{2+} removal compared to the human and other animals (Hasenfuss, 1998). Loss of NCX1 palmitoylation is associated with reduced inactivation which would result in increased extrusion of Ca^{2+} in cardiomyocytes, although this has yet to be demonstrated in a cardiac setting (Gök *et al.*, 2020; Reilly *et al.*, 2015). Nevertheless, this reduction in response to hypertrophy may be as part of the protective mechanism to prevent toxic Ca^{2+} overload, however when maintained as HF progresses, would result in systolic and diastolic dysfunction (Kass *et al.*, 2004).

Gαi was the only substrate whose palmitoylation was reduced in the rat model, with reduction also observed in the LV hypertrophy mouse model and a modest reduction in the rabbit MI model. Gαi mediates the inhibitory effects of the ß-adrenoceptors leading to reduced activation of adenylyl cyclase, PKA and downstream phosphorylation, and is also involved in pro-survival by buffering toxic effects of overactive Gs and cAMP (Daaka *et al.*, 1997; O'Hayre *et al.*, 2014). Palmitoylation is required for Gαi membrane attachment and therefore association with the ß-adrenoceptor (Linder *et al.*, 1993; Parenti *et al.*, 1993). Loss of palmitoylation may suggest this association is reduced and may contribute to the chronic adrenergic desensitisation observed in HF pathogenesis (Lymperopoulos *et al.*, 2013). However, interestingly, Gαi is most often reported to be increased in expression and activity in HF samples, although this may be as a pro-survival mechanism through activation of Akt rather than pathogenic (Kawamoto *et al.*, 1994; O'Hayre *et al.*, 2014). In this case, loss of palmitoylation may impede membrane localisation and activation of these mechanisms, contributing to the hypertrophic phenotype.

Na^+/K^+ ATPase palmitoylation was modestly reduced in response to hypertrophy, but only significant reduced in the pig model. Despite limited studies on Na^+/K^+ ATPase palmitoylation, the majority of the transporters are associated with caveolae which is essential for their stabilisation. As palmitoylation often mediates caveolae localisation, it could be hypothesised that palmitoylation of Na^+/K^+ ATPase plays a role in its membrane availability (Fuller *et al.*, 2013; Levental, Lingwood, *et al.*, 2010). As such, it will be important to determine whether the observed loss of palmitoylation is associated with the loss of Na^+/K^+ ATPase expression and activity observed in HF (Pieske & Houser, 2003). However, our work suggests the only α1-subunit palmitoylation site is located immediately adjacent to the catalytic aspartate and therefore highly likely to be involved in regulating pump inhibition, although this remains to be fully characterised (Howie *et al.*, 2018).

Similarly, LTCC palmitoylation, whilst not investigated in the mouse and rat models, only showed significant reduction in the pig model with no change in the rabbit model. Despite being implicated in human HF pathology, a previous study utilising a similar rabbit model showed that whilst infarcted hearts had reduced LTCC current density, suggesting a reduction in expression at the surface, there

was no change in the current-voltage relationship or Ca^{2+} kinetics of the channel (Litwin & Bridge, 1997). Our unpublished work suggests loss of LTCC palmitoylation induces a shift in the voltage activation curve of the channel which results in reduced Ca^{2+} transient amplitude without direct effects on inactivation mechanisms (Kuo, *et al. In revision*). This may suggest that suppression of LTCC palmitoylation is occurring as a compensatory mechanism to protect against the hypertrophy associated with LTCC overactivity in HF (Keung, 1989). However, paradoxically reduction of LTCC current and reduced Ca^{2+} transients are associated with a compensatory neuroendocrine stimulation leading to hypertrophy by additional pathways (Goonasekera *et al.*, 2012). Further work would elucidate whether reduced palmitoylation of cardiac substrates is occurring pathologically or as a compensatory mechanism. Interestingly, recent modelling suggests the pig and human ventricular cells have similar LTCC and NCX1 electrophysiological profiles and therefore this may be the most suitable model to study changes in their palmitoylation in a disease state going forward (Gaur *et al.*, 2021).

5.4.2 Substrate palmitoylation is increased in human heart failure

End-stage ischaemic HF samples are valuable tools to understand the pathological pathways involved in the disease. As such, substrate expression has been widely reported including the LTCC, Na^+/K^+ ATPase, PLM and Caveolin-3, which are most often found reduced, whilst expression of NCX1, Flotillin2 and Gαi and are mostly found upregulated (Bossuyt *et al.*, 2005; Feiner *et al.*, 2011; Feldman *et al.*, 1991; Hasenfuss *et al.*, 1999; Schwinger, Hoischen, *et al.*, 1999; Schwinger, Wang, *et al.*, 1999; Soni *et al.*, 2016; Takahashi *et al.*, 1992). Analysis of HF samples in this study revealed only a significant reduction in Na^+/K^+ ATPase expression and a modest reduction in LTCC expression (Figure 5.7). This may be unsurprising, as studies of human samples frequently report contrasting results when it comes to expression. For example, NCX1 is often increased in HF, however a recent analysis of pre-clinical studies showed of 29 studies, only 14 showed an increased, 10 showed a decrease and 5 showed no change in NCX1 expression (Sipido *et al.*, 2002). This may be due to differences in sampling area, as changes in NCX1 protein levels are reportedly different in the area close to the infarct compared to more remote areas of the myocardium (Yoshiyama *et al.*, 1997). However, despite studies showing no change in NCX1 expression, they still observe change in activity

(Sipido *et al.*, 2002). Additionally, one study suggested NCX1 expression correlates directly with diastolic function which may be different across HF patients (Hasenfuss *et al.*, 1999). This may explain the spread of data observed in this study which has been observed by others (C. Piper *et al.*, 2000). Additionally, the lack of expression changes may be due to the use of GAPDH as a loading control which itself is reportedly varied in transcript expression in response to hypertrophic stimuli and as such, normalisation to total protein may have been a more suitable approach (Winer *et al.*, 1999).

Nevertheless, despite no change in protein expression, NCX1 palmitoylation was significantly increased in HF samples, along with Na^+/K^+ ATPase palmitoylation (Figure 5.8). This was surprising considering all animal models showed reduced palmitoylation, although this did vary significantly between models. This may indicate that the increased palmitoylation in the human is a result of more developed decompensation compared to the animal models, or as a result of pharmacological intervention. Indeed, this is a major limitation of current animal models for HF research, as they rarely include study of novel therapeutic interventions in combination for current optimal clinical care, making translational potential challenging. With regards to the samples in this study, functionally increased NCX1 palmitoylation would enhance inactivation and reduce Ca^{2+} efflux which, whilst improving systolic function, would contribute to diastolic impairment for which NCX1 is a key mediator (Kass *et al.*, 2004). In terms of the Na^+/K^+ ATPase, increased palmitoylation of integral membrane proteins is often associated with increased stability (Salaun *et al.*, 2010; van Dolah *et al.*, 2011). However, as palmitoylation is calculated as palmitoylated fraction divided by total protein, which is reduced, it implies that the amount of palmitoylated Na^+/K^+ ATPase has not changed whilst the non-palmitoylated form is reduced. Therefore, palmitoylation of Na^+/K^+ ATPase may not be pathologically increased by any regulatory mechanism, rather that the palmitoylated form is less prone to loss as it is more stable in the membrane. This may suggest preserved palmitoylation may be beneficial when it comes to the Na^+/K^+ ATPase, however further work on characterisation of Na^+/K^+ ATPase palmitoylation functionally are required to inform on the therapeutic benefit.

However, this decrease in expression, increase in palmitoylation is not the case for cMyBP-C (Chapter 3, Figure 3.12) or NCX1. As such, this may be reflective of

increased fatty acid availability or increased activity of DHHC-PATs such as DHHC5 (discussed below). Additionally, analogous to the study of cMyBP-C, there are many confounding factors such as sex, history of MI, hyperlipidaemia and co-morbidities that may influence the expression and palmitoylation of cardiac substrates. However due to limited sample sizes, statistically meaningful comparisons are challenging. Nevertheless, sex-dependent activity of NCX1 has been reported in pig cardiomyocytes, where no differences were detected at baseline, however upon HF development NCX1 current was greatly increased in males compared to females (Wei *et al.*, 2007).

5.4.3 DHHC5 expression is altered in hypertrophy and heart failure

In an effort to investigate the mechanisms responsible for changes in substrate palmitoylation in HF, analysis of cell surface palmitoyltransferase DHHC5 was investigated in samples. Despite mRNA analysis suggesting DHHC5 expression would not be reduced in HFrEF (Figure 5.2), a significant reduction in DHHC5 expression in these samples was observed (Figure 5.13). Interestingly, the pig model, arguably the most clinically relevant of those investigated, also showed a modest, although not significant, decrease in DHHC5 expression (Figure 5.12). In contrast, no change in DHHC5 expression was observed in the rat (Figure 5.10) or rabbit model (Figure 5.11), whilst LV hypertrophy in the mouse model was associated with a striking increase in DHHC5 from as early as 3-days post injury which was maintained over 8-weeks (Figure 5.9).

In line with hypertrophy but conversely to the ischaemic human HF results, Miles *et al.* report significantly increased levels of DHHC5 in human HF. However, the samples investigated represent a mixture of ischaemic and non-ischaemic samples, limiting the comparison to the ischaemic samples used in this study (Miles *et al.*, 2021). Additionally, our work investigating DHHC5 over-expression in rabbit cardiomyocytes revealed this does not lead to a direct change in substrate palmitoylation or in changes in contractile phenotype of ventricular cells (Main *et al.*, 2022). This may suggest that long-term remodelling and changes in DHHC5 activity, rather than solely expression, are more important in cardiac disease pathogenesis. However, this study represents only 24 hours of overexpression in a non-ischaemic setting so is limited in its comparability. Nevertheless, it will be

important to determine whether DHHC5 expression is changed in diseases of chronic hypertrophy such as HCM which are associated with hypertrophy and an increase LV wall thickness, in contrast to the ischaemic HF models and samples investigated here.

5.4.4 DHHC5 palmitoylation may be altered in heart failure

Interestingly, as well as changes in expression, a significant reduction in DHHC5 palmitoylation in the pig model was observed, with a modest, although not significant, increase observed in human HF samples (Figure 5.13). This follows a similar pattern to NCX1 and the Na^+/K^+ ATPase suggesting palmitoylation or expression of all three may be being regulated by the same upstream mechanisms. DHHC-PATs have been frequently reported to palmitoylate each other, and a proximity biotinylation screen identified DHHC20 as an interactor and palmitoylating enzyme of DHHC5. Palmitoylation of DHHC5 C-terminal tail in response to adrenergic stimulation is required for its own stabilisation at the plasma membrane (Chen *et al.*, 2020; Woodley & Collins, 2021). Additionally, the site lies in an amphipathic helix containing a binding site for DHHC5 accessory protein GOLGA7, which mediates its membrane localisation, and the Na^+/K^+ ATPase (Plain *et al.*, 2020; Woodley & Collins, 2019). Increased DHHC5 palmitoylation as observed in human HF, or reduced palmitoylation as observed in the pig model, may suggest increased or decreased activity of DHHC5 either through a change in palmitate loading into the active site or a change in DHHC20-mediated palmitoylation.

Additionally, other PTMs of DHHC5 may be important to consider, as phosphorylation of DHHC3 was associated with reduced autopalmitoylation and similarly phosphorylation of DHHC5 inactivates it (Hao *et al.*, 2020; Schianchi *et al.*, 2020). In contrast, O-GlycNAcylation of DHHC5 enhanced PLM association and palmitoylation (Plain *et al.*, 2020; Schianchi *et al.*, 2020). However, as the most well characterised partner of DHHC5 is PLM, the palmitoylation of which did not change in any model of in human HF samples, this may imply that DHHC5 activity is not increased. Additionally, like Na^+/K^+ ATPase, DHHC5 expression was reduced meaning there may be no increase in palmitoylation, rather a loss of non-palmitoylated DHHC5, overall increasing the ratio of palmitoylated to

unpalmitoylated substrate. Whether this has direct functional consequences has not been investigated but is important to consider.

5.4.5 Methodological considerations and future work

A major limitation of this study is the lack of consistent results between different animal models making conclusions as to the importance of palmitoylation in cardiac disease challenging. As SERCA2a downregulation is consistently altered in both animal models and human HF samples, confirming the extent of the HF phenotype via this method may help account for the differences between the models. Additionally, proteomic characterisation of palmitoylated fractions from HF and organ donors would give a more unbiased overview on the extent of palmitoylation remodelling in HF. However, as discussed in Chapter 3, whether the fraction of palmitoylation detected is biologically meaningful is difficult to distinguish in mass spectrometry results and often requires additional validation (Main & Fuller, 2021).

The most consistently altered substrate was NCX1, which plays a crucial role in the diastolic dysfunction associated with HF. Whilst small molecule inhibitors are being developed, an approach targeting the XIP domain whose ability to inactivate NCX1 is regulated by palmitoylation or the interaction between NCX1 and DHHC5 may provide a more selective way to regulate NCX1 function in HF therapy (Otsomaa *et al.*, 2020; Pelat *et al.*, 2021). Interestingly, although PLM palmitoylation did not change, this may make it a more suitable target as it is stably palmitoylated consistently across animal models and in humans. Inhibiting palmitoylation of PLM would increase the activity of the Na^+/K^+ ATPase, and recently a novel cell penetrating peptide has been designed that disrupts the interaction between DHHC5 and PLM to achieve this (Plain *et al.*, 2020). However, if DHHC5 expression or activity are dysregulated in HF this approach may not be suitable. Additionally, whilst increased DHHC5 expression, although associated with hypertrophy, does not appear to mediate changes in substrate palmitoylation or cardiomyocyte contractility, assessing the consequences of loss of non-palmitoylated DHHC5 to model what is observed in human HF will be important going forward.

Finally, it is important to consider the limitation of the use of Acyl-RAC solely in the characterisation of substrate palmitoylation in these samples. Whilst providing a robust mechanism to detect protein palmitoylation, changes in substrate palmitoylation in singly palmitoylated proteins are most likely to be observed using this capture method, as opposed to substrates with multiple palmitoylation sites, where the substrate will still be capture even if only one site remains palmitoylated. Indeed, this may be why NCX1 and Na^+/K^+ ATPase are most consistently changed, whilst PLM containing two palmitoylation sites did not vary in any disease state (Howie *et al.*, 2018; Reilly *et al.*, 2015; Tulloch *et al.*, 2011). As such, substrate palmitoylation could be characterised by PEGylation, an adaptation of Acyl-RAC in which a 5-10kA PEG maleimide is conjugated to previously palmitoylated cysteine (Howie *et al.*, 2014; Plain *et al.*, 2020). This method may allow further characterisation of substrates with multiple sites such as PLM, however, is often limited to lower molecular weight proteins.

5.5 Conclusion

Overall, the results of this study indicate that cardiac disease is associated with changes in substrate palmitoylation, particularly that of NCX1, which is reduced in most animal models but increased in human HF samples, but not others, including PLM which is not changed in any samples investigated. Investigation of DHHC5 expression revealed it is markedly upregulated early in hypertrophy, however development of HF in both pigs and humans, but not rabbits or rats, is associated with a loss of DHHC5 expression. In pig and human samples, DHHC5 palmitoylation is also reduced or increased, respectively, however whether this correlates to altered activity of DHHC5 remains to be determined.

Chapter 6 General Discussion

6.1 Palmitoylation in myofilament function

Palmitoylation has been most well characterised (and is traditionally viewed) as a regulatory modification for transmembrane and membrane associated proteins. The addition of the hydrophobic fatty acid often targets parts or the whole substrate to different intracellular compartments (Blaskovic *et al.*, 2013). In this study, novel evidence is presented that key myofilament proteins actin, myosin and cMyBP-C are palmitoylated in primary cardiomyocytes, but could palmitoylation be involved in anchoring them to nearby membranes? The interaction of the myofilament with the membranes is an undiscovered field, particularly in cardiac tissue. Most work which has come from the study of simple model systems such as *Caenorhabditis elegans* (C. elegans) and zebrafish. C. elegans have a limited muscle system of thick filament M-lines and thin filament Z-discs, the latter of which are attached to membranes through cytoskeletal components such as integrins (Benian & Qadota, 2010). Interestingly, C. elegans express 15 DHHC-PAT orthologues and two thioesterases, with several palmitoylated substrates identified that have been previously characterised in brain tissue (Edmonds & Morgan, 2014). In a more physiologically relevant system, study of striated muscle development in zebrafish also indicates the cytoskeletal network plays an important role in connecting the myofilament to the membrane. The Z-disc protein spectrin interacts with membrane localised ankyrin proteins which is hypothesised to stabilise the cardiac muscle membrane relative to the sarcomere, in particular supporting T-tubule structure (Bennett *et al.*, 2004; Raeker *et al.*, 2014). Given that palmitoylated cMyBP-C is resistant to salt extraction, it may well be in the vicinity of, and interacting more with, the insoluble structural components noted above. Additionally, loss of cMyBP-C is associated with cultured cardiomyocytes which undergo remodelling and loss of T-tubule structure (Eppenberger *et al.*, 1994; Fearnley *et al.*, 2011; Piper *et al.*, 1982).

Considering the relatively low palmitoylation stoichiometry of myosin, actin and cMyBP-C (~10%) it could be hypothesised that the modification is occurring in a specific region of the sarcomere, such as molecules closest to the T-tubules or SR. Indeed, cMyBP-C has been reported to directly interact with RYR2, suggesting there is a population in the proximity of the SR. However, this study largely characterised the interaction in non-muscle cells and indicated the interaction

involves the C-terminus, which is usually anchored to the sarcomere, so further characterisation is required (Stanczyk *et al.*, 2018). The likelihood of membrane attachment may be investigated by identifying other lipid modifications, such as prenylation and myristylation. These covalent modifications often precede palmitoylation, allowing weak membrane attachment and proximity to DHHC-PATs before palmitoylation occurs. Identifying whether these modifications occur in palmitoylated myofilament proteins may also elucidate whether this is an enzymatically regulated event (Guan & Fierke, 2011).

Another suggestion as to the function of palmitoylation on sarcomeric proteins is that it is occurring as part of a trafficking mechanism involved in sarcomere assembly, with impaired sarcomere protein turnover associated with HF (Martin *et al.*, 2021). Whilst degradation is more well understood, the process of replacement is lesser studied. Sarcomeric proteins have been shown to be quickly incorporated into the working myofilament, including actin as demonstrated by injection of a fluorescently labelled version which incorporated within 30 seconds (LoRusso *et al.*, 1992). The process may be substrate dependent, as study of Tm showed regional specific replacement at the ends of the thin filament, whilst new TnI incorporated throughout (Michele *et al.*, 1999; Willis *et al.*, 2009). However, if palmitoylation was essential to myofilament protein trafficking, it raises the question as to why all sarcomeric proteins would not be palmitoylated and trafficked in this way. Additionally, the sarcomeric proteins identified in this study have a low palmitoylation stoichiometry, whilst substrates such as CD36 and H-Ras, in which palmitoylation plays an important role in trafficking, typically have a high palmitoylation stoichiometry (Forrester *et al.*, 2011; Hao *et al.*, 2020). However, proteins with a high palmitoylation stoichiometry are not necessarily candidates for palmitoylation-dependent trafficking, as NCX1 is ~60% palmitoylated in cardiac myocytes but palmitoylation does not mediate its movement through the secretory pathway (Gök *et al.*, 2020). Nevertheless, the functional impact of palmitoyl CoA treatment on myofilament Ca^{2+} sensitivity occurs in skinned preparations without the presence of membranes, so membrane trafficking or attachment may not be the primary mechanism by which palmitoylation exerts its effects. It will be important to determine whether these effects are replicated with an intact membrane present, as could be achieved in the “cut and paste” cMyBP-C mouse model (Napierski *et al.*, 2020).

This spontaneous reactivity of palmitoyl CoA and direct functional effects raises the question as to whether cMyBP-C palmitoylation is occurring non-enzymatically and therefore would be difficult to modulate therapeutically (Smotrys & Linder, 2004). Several substrates, including the DHHC-PATs themselves, are reported to undergo autopalmitoylation based on local acyl-CoA concentrations (Duncan & Gilman, 1996; Kümmel *et al.*, 2006; Rana, Lee, *et al.*, 2018). However, the vast majority of studies investigating autopalmitoylation use non-physiological concentrations of palmitoyl CoA, whilst the free cytosolic concentration is likely not in sufficient quantities for palmitoylation to occur spontaneously (Blaskovic *et al.*, 2013). Even study of purified DHHC-PATs themselves only demonstrated their autopalmitoylation using μM concentrations of palmitoyl CoA (Rana, Lee, *et al.*, 2018). For cMyBP-C palmitoylation, there are many factors that altered its palmitoylation that may not be explained by spontaneous palmitoylation, including changes during culture of primary cardiomyocytes and expression in non-muscle cells. Furthermore, in a type-2 diabetic model associated with increased fatty acid availability, cMyBP-C palmitoylation levels were unchanged, whilst they were significantly altered in hypertrophy and HF in a manner similar to enzymatically regulated NCX1 and Na^+/K^+ ATPase. Nevertheless, generation of acyl-CoA and export via the MPTP is associated with cardiovascular diseases and may be affecting all substrates in this setting, and the use of MPTP blockers may indicate whether local acyl-CoA concentrations control cMyBP-C palmitoylation (Zhou & Tian, 2018).

There is no doubt that identification of DHHC-PATs and thioesterases within the sarcoplasmic reticulum and T-tubules, and their proximity to myofilament proteins, will provide a valuable resource to understand the role of palmitoylation in myofilament regulation. This may be achieved by techniques such as proximity biotinylation, proximity ligation analysis (PLA) via microscopy or siRNA of DHHC-PATs (Liu *et al.*, 2020). Importantly, identifying whether this is an enzymatic process will allow the question to be addressed as to whether myofilament palmitoylation can be targeted therapeutically.

6.2 Targeting cMyBP-C PTMs as a therapeutic strategy in HF

Given the overwhelming evidence that loss of cMyBP-C phosphorylation is detrimental to cardiac function, and preservation is cardioprotective, it may be surprising the lack of phosphorylation enhancing therapeutics currently in development (Barefield *et al.*, 2019; Kuster *et al.*, 2012; Sadayappan *et al.*, 2006). This is largely due to the complexity in targeting individual protein phosphorylation sites, as kinases such as PKA target a wide variety of substrates with both detrimental and cardioprotective effects (Fontes-Sousa *et al.*, 2009; Kwak *et al.*, 2008; Makaula *et al.*, 2005; Sichelschmidt *et al.*, 2003). As such, the focus has largely been on developing peptides and inhibitors of the actin/myosin-cMyBP-C interactions to reduce or improve contractility (Hou *et al.*, 2022; Mamidi *et al.*, 2021). However, these may only target one function of cMyBP-C, such as regulation of SRX:DRX ratio of myosin and not the changes in myofilament calcium sensitivity (Kumar *et al.*, 2020). As such, there is still a great interest in harnessing our understanding of cMyBP-C PTM control for therapeutic benefit. This may be where palmitoylation may present more opportunities, with 23 palmitoylating enzymes and an ever-increasing number of thioesterases shown to regulate the modification. However, attempts to purify, crystalize and design selective inhibitors against DHHC-PATs have been largely unsuccessful until recently, and toxicity and promiscuity of inhibitors still remains an issue (Lan *et al.*, 2021). What may be a more direct approach is to understand the recruitment relationship between a DHHC-PAT and a substrate and design a small cell-penetrating peptide to disrupt the interaction. This was recently achieved between the interaction of DHHC5 and PLM, although whether a more clinical approach can be achieved is still unknown (Plain *et al.*, 2020).

In terms of cMyBP-C, increasing its palmitoylation may be associated with reduced Ca^{2+} sensitivity of force, and therefore the question remains as to whether exacerbating or inhibiting cMyBP-C palmitoylation would be useful therapeutically. Increased myofilament Ca^{2+} sensitivity would contribute to diastolic dysfunction at high Ca^{2+}, but at low Ca^{2+} could facilitate better systole. End-stage ischaemic HF is generally associated with increased myofilament Ca^{2+} sensitivity likely driven through changes in the phosphorylation of MLC, TnI and cMyBP-C, which may contribute to diastolic dysfunction and slower relaxation

(Schillinger & Kögler, 2003; van der Velden *et al.*, 2003). Indeed, whilst diastolic dysfunction is more associated with HFpEF, it is observed in HFrEF although is more difficult to evaluate (Tobushi *et al.*, 2017). Interestingly, phosphorylation of cMyBP-C is antagonised by high Ca^{2+} and it will be important to determine whether a similar mechanism regulates cMyBP-C palmitoylation to elucidate whether it may facilitate better diastolic or systolic function (Kumar *et al.*, 2020; Previs *et al.*, 2016). This may also explain why the levels of cMyBP-C palmitoylation vary significantly in isolated rabbit cardiomyocytes, where the contractile state of the tissue and exposure to Ca^{2+} before analysis were not controlled. Understanding the palmitoylation levels on a beat-by-beat basis in both systole and diastole would provide valuable insight, however tools to achieve this are limited. Additionally, in the broader picture of palmitoylation in HF, considering that cMyBP-C, NCX1, Na^+/K^+ ATPase and DHHC5 all show a similar palmitoylation profile in HF, it will be important to consider what factors may be influencing them all. This may include expression and activity of fatty acid synthase (FASN), the predominant source of palmitic acid, levels of which are increased in cancer (Ali *et al.*, 2018; Fiorentino *et al.*, 2008). Although lesser studied, in cardiac tissue impaired fatty acid metabolism is associated with end-stage heart failure. FASN over-expressing cardiomyocytes develop a HF-phenotype, although whether this is coupled to increased palmitoylation of cardiac substrates remains to be determined (Alla *et al.*, 2016).

The same question arises for cMyBP-C SUMOylation - if enhanced SUMOylation in the presence of adrenergic stimulation results in reduced phosphorylation and reduced relaxation time, would this be beneficial or detrimental? TnI phosphorylation is associated with reduced myofilament Ca^{2+} sensitivity and positive lusitropic effects, with levels often reduced in end-stage human HF (Messer *et al.*, 2007; Wijnker *et al.*, 2013; Zhang, Zhao, Mandveno, *et al.*, 1995). Similarly, SUMOylation of TnI may indirectly reduce myofilament Ca^{2+} sensitivity, but surprisingly increased levels are observed in end-stage HF samples, although whether this is in combination with changes in phosphorylation is unknown (Fertig *et al.*, 2022). Additionally, general SUMO1 gene transfer or increasing SUMOylation levels with N106 provides therapeutic benefits. Interestingly, both of these were associated with enhanced relaxation in a similar manner to re-expression of SERCA2a, suggesting the positive effects are predominantly through regulating

SERCA2a SUMOylation (Kho *et al.*, 2011, 2015; Tilemann *et al.*, 2013). This may indicate that SUMOylation of other proteins such as cMyBP-C and TnI does not play a major role in regulating relaxation. Finding a more nuanced way to target cMyBP-C SUMOylation specifically would help to answer that question.

6.3 Final conclusions

This study provides novel evidence that a new class of proteins involved in sarcomeric function undergo palmitoylation. Importantly, this modification appears to be regulatory in terms of cMyBP-C, being associated with increased myofilament affinity, reduced myofilament calcium sensitivity and changes in cardiomyocyte structure as cells are cultured. Additionally, palmitoylation of cMyBP-C, and other cardiac substrates including NCX1 and DHHC5, are altered in ischaemic HF, although whether this contributes to the cardiac dysfunction remains to be determined. This study also provides a prime example of the limitation of mutagenesis experiments in understanding PTM modifications, as glutathionylation and palmitoylation potentially occur on the same cysteines in cMyBP-C. Understanding the relationship between the two in the control of myofilament activity will be important going forward. Whilst SUMOylation of cMyBP-C was investigated in this study, revealing potentially antagonistic effects on phosphorylation and changes in cardiomyocyte relaxation, further characterisation is required to understand its relevance in the heart.

Chapter 7 Appendix

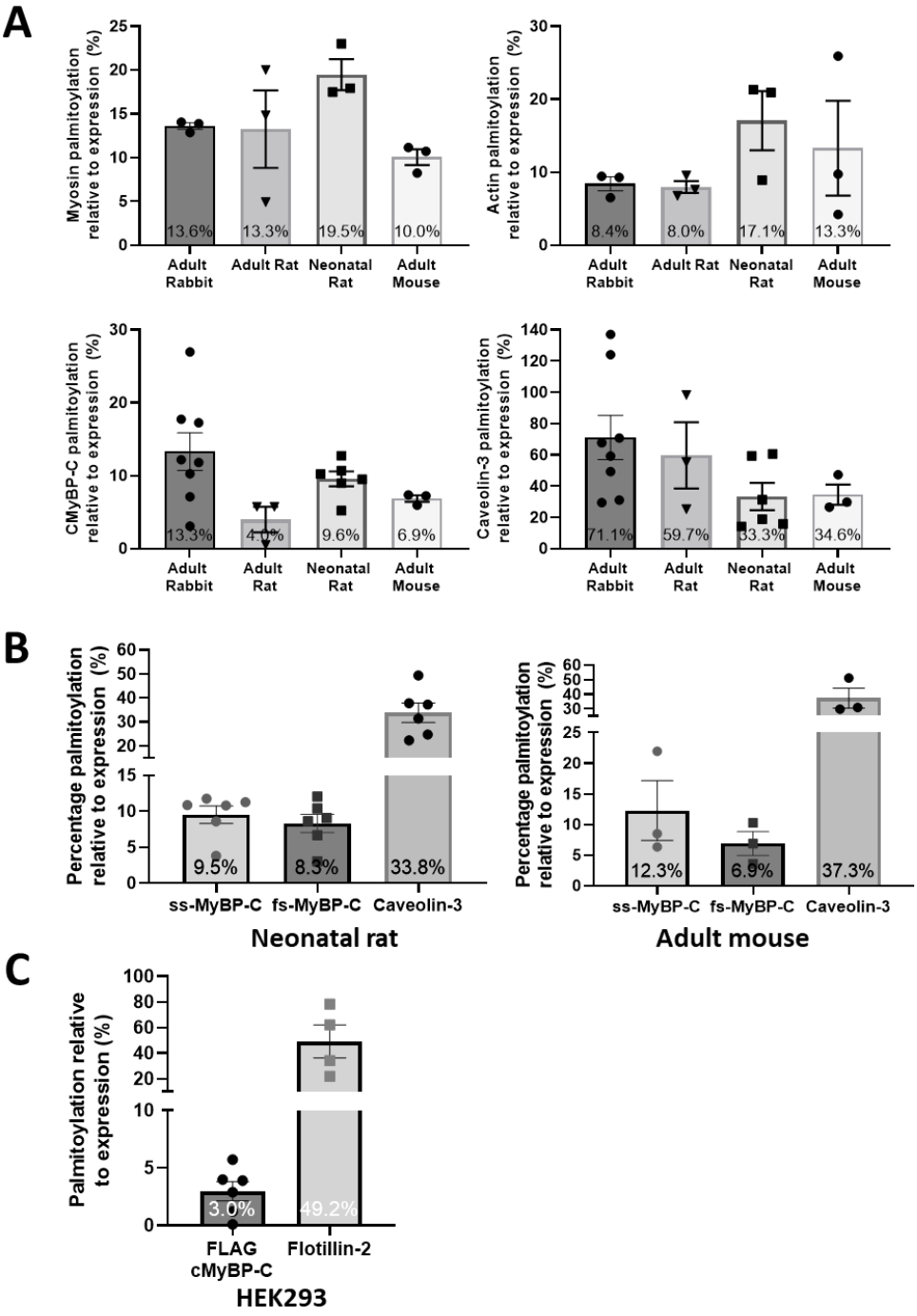

Supplementary Figure 7.1. Percentage palmitoylation (%) examples.
Percentage palmitoylation was calculated from palmitoylation relative to expression values as described in Figure 2.4. A) myosin, actin, cMyBP-C and caveolin-3 in different animal cardiac tissue (from Figure 3.4), B) skeletal versions of MyBP-C in neonatal rat and adult mouse skeletal tissue (from Figure 3.16) and C) FLAG-CMyBP-C and flotillin-2 in HEK293 cells (from Figure 3.17). Mean values are plotted on each bar. Data is mean ±S.E.M.

Supplementary Table 7.1. Myofilament proteins identified by mass spectrometry of purified palmitoylated proteins (Acyl-RAC) from rat ventricular tissue.

Protein IDs and FASTA identifiers	Species	Peptides identified (n=1, 2, 3)	Mol. weight [kDa]	Sequence coverage (n=1, 2, 3 [%])
>sp|P56741|MYPC_RAT Myosin-binding protein C, cardiac-type	Rattus novegicus	95, 97, 94	140.76	75.2, 78.9, 73.3
>tr|G3V8B0|G3V8B0_RAT Myosin-7	Rattus novegicus	171, 178, 182	222.9	65.1, 67, 68
>sp|P04692|TPM1_RAT Tropomyosin alpha-1 chain	Rattus novegicus	20, 17, 18	32.68	58.8, 54.2, 52.1
>tr|Q4PP99|Q4PP99_RAT Cardiac troponin C	Rattus novegicus	9, 9, 10	18.42	62.7, 62.7, 62.7
>tr|F1LQ95|F1LQ95_RAT Troponin T, cardiac muscle	Rattus novegicus	10, 11, 10	35.371	37.5, 36.8, 36.8
>sp|P23693|TNNI3_RAT Troponin I, cardiac muscle	Rattus novegicus	7, 7, 7	24.159	37, 37, 37
>sp|P68035|ACTC_RAT Actin, alpha cardiac muscle	Rattus novegicus	22, 22, 22	42.019	71.1, 70.8, 71.6

References

Ababou, A., Gautel, M., & Pfuhl, M. (2007). Dissecting the N-terminal myosin binding site of human cardiac myosin-binding protein C: Structure and myosin binding of domain C2. *Journal of Biological Chemistry*, *282*(12), 9204–9215. https://doi.org/10.1074/jbc.M610899200

Ababou, A., Rostkova, E., Mistry, S., Masurier, C. le, Gautel, M., & Pfuhl, M. (2008). Myosin binding protein C positioned to play a key role in regulation of muscle contraction: structure and interactions of domain C1. *Journal of Molecular Biology*, *384*(3), 615–630. https://doi.org/10.1016/J.JMB.2008.09.065

Adachi, N., Hess, D. T., McLaughlin, P., & Stamler, J. S. (2016). S-Palmitoylation of a Novel Site in the ß2-Adrenergic Receptor Associated with a Novel Intracellular Itinerary. *The Journal of Biological Chemistry*, *291*(38), 20232. https://doi.org/10.1074/JBC.M116.725762

Agarkova, I., Ehler, E., Lange, S., Schoenauer, R., & Perriard, J. C. (2003). M-band: a safeguard for sarcomere stability? *Journal of Muscle Research and Cell Motility*, *24*(2–3), 191–203. https://doi.org/10.1023/A:1026094924677

Ahearn, I. M., Haigis, K., Bar-Sagi, D., & Philips, M. R. (2012). Regulating the Regulator: Post-Translational Modification of Ras. *Nature Reviews. Molecular Cell Biology*, *13*(1), 39–51. https://doi.org/10.1038/NRM3255

Aicart-Ramos, C., Valero, R. A., & Rodriguez-Crespo, I. (2011). Protein palmitoylation and subcellular trafficking. *Biochimica et Biophysica Acta (BBA) - Biomembranes*, *1808*(12), 2981–2994. https://doi.org/10.1016/J.BBAMEM.2011.07.009

Ait-Mou, Y., Hsu, K., Farman, G. P., Kumar, M., Greaser, M. L., Irving, T. C., & de Tombe, P. P. (2016). Titin strain contributes to the frank-starling law of the heart by structural rearrangements of both thin- and thick-filament proteins. *Proceedings of the National Academy of Sciences of the United States of America*, *113*(8), 2306–2311. https://doi.org/10.1073/PNAS.1516732113/-/DCSUPPLEMENTAL

Aksentijević, D., Karlstaedt, A., Basalay, M. v., O'Brien, B. A., Sanchez-Tatay, D., Eminaga, S., Thakker, A., Tennant, D. A., Fuller, W., Eykyn, T. R., Taegtmeyer, H., & Shattock, M. J. (2020). Intracellular sodium elevation reprograms cardiac metabolism. *Nature Communications 2020 11:1*, *11*(1), 1–14. https://doi.org/10.1038/s41467-020-18160-x

Alberts, B., Johnson, A., Lewis, J., Raff, M., Roberts, K., & Walter, P. (2002). *How Cells Obtain Energy from Food*. https://www.ncbi.nlm.nih.gov/books/NBK26882/

Ali, A., Levantini, E., Teo, J. T., Goggi, J., Clohessy, J. G., Wu, C. S., Chen, L., Yang, H., Krishnan, I., Kocher, O., Zhang, J., Soo, R. A., Bhakoo, K., Chin, T. M., & Tenen, D. G. (2018). Fatty acid synthase mediates EGFR palmitoylation in EGFR mutated non-small cell lung cancer. *EMBO Molecular Medicine*, *10*(3), 8313. https://doi.org/10.15252/EMMM.201708313

Alla, J. A., Graemer, M., Fu, X., & Quitterer, U. (2016). Inhibition of G-protein-coupled Receptor Kinase 2 Prevents the Dysfunctional Cardiac Substrate Metabolism in Fatty Acid Synthase Transgenic Mice. *Journal of Biological Chemistry*, *291*(6), 2583–2600. https://doi.org/10.1074/JBC.M115.702688

Allen, D. G., & Blinks, J. R. (1978). Calcium transients in aequorin-injected frog cardiac muscle. *Nature*, *273*(5663), 509–513. https://doi.org/10.1038/273509A0

Amanakis, G., Sun, J., Fergusson, M. M., McGinty, S., Liu, C., Molkentin, J. D., & Murphy, E. (2021). Cysteine 202 of cyclophilin D is a site of multiple post-translational modifications and plays a role in cardioprotection. *Cardiovascular Research*, *117*(1), 212–223. https://doi.org/10.1093/CVR/CVAA053

Ambrosy, A. P., Fonarow, G. C., Butler, J., Chioncel, O., Greene, S. J., Vaduganathan, M., Nodari, S., Lam, C. S. P., Sato, N., Shah, A. N., & Gheorghiade, M. (2014). The Global Health and Economic Burden of Hospitalizations for Heart Failure: Lessons Learned From Hospitalized Heart Failure Registries. *Journal of the American College of Cardiology*, *63*(12), 1123–1133. https://doi.org/10.1016/J.JACC.2013.11.053

Anand, A., Chin, C., Shah, A. S. V., Kwiecinski, J., Vesey, A., Cowell, J., Weber, E., Kaier, T., Newby, D. E., Dweck, M., Marber, M. S., & Mills, N. L. (2018). Cardiac myosin-binding protein C is a novel marker of myocardial injury and fibrosis in aortic stenosis. *Heart (British Cardiac Society)*, *104*(13), 1101–1108. https://doi.org/10.1136/HEARTJNL-2017-312257

Angin, Y., Steinbusch, L. K. M., Simons, P. J., Greulich, S., Hoebers, N. T. H., Douma, K., van Zandvoort, M. A. M. J., Coumans, W. A., Wijnen, W., Diamant, M., Ouwens, D. M., Glatz, J. F. C., & Luiken, J. J. F. P. (2012). CD36 inhibition prevents lipid accumulation and contractile dysfunction in rat cardiomyocytes. *The Biochemical Journal*, *448*(1), 43–53. https://doi.org/10.1042/BJ20120060

Aoyama, K., & Nakaki, T. (2015). Glutathione in Cellular Redox Homeostasis: Association with the Excitatory Amino Acid Carrier 1 (EAAC1). *Molecules*, *20*(5), 8742. https://doi.org/10.3390/MOLECULES20058742

Arai, M., Alpert, N. R., MacLennan, D. H., Barton, P., & Periasamy, M. (1993). Alterations in sarcoplasmic reticulum gene expression in human heart failure. A possible mechanism for alterations in systolic and diastolic properties of the failing myocardium. *Circulation Research*, *72*(2), 463–469. https://doi.org/10.1161/01.RES.72.2.463

Askari, A. (2019). The sodium pump and digitalis drugs: Dogmas and fallacies. *Pharmacology Research & Perspectives*, *7*(4). https://doi.org/10.1002/PRP2.505

Avner, B. S., Shioura, K. M., Scruggs, S. B., Grachoff, M., Geenen, D. L., Helseth, D. L., Farjah, M., Goldspink, P. H., & Solaro, R. J. (2012). Myocardial Infarction in Mice Alters Sarcomeric Function Via Post-Translational Protein Modification. *Molecular and Cellular Biochemistry*, *363*(0), 203. https://doi.org/10.1007/S11010-011-1172-Z

Azizi, S. A., Lan, T., Delalande, C., Kathayat, R. S., Banales Mejia, F., Qin, A., Brookes, N., Sandoval, P. J., & Dickinson, B. C. (2021). Development of an Acrylamide-Based Inhibitor of Protein S-Acylation. *ACS Chemical Biology*, *16*(8), 1546–1556. https://doi.org/10.1021/ACSCHEMBIO.1C00405/SUPPL_FILE/CB1C00405_SI_002.XLSX

Baehr, A., Klymiuk, N., & Kupatt, C. (2019). Evaluating Novel Targets of Ischemia Reperfusion Injury in Pig Models. *International Journal of Molecular Sciences*, *20*(19). https://doi.org/10.3390/IJMS20194749

Bagwan, N., el Ali, H. H., & Lundby, A. (2021). Proteome-wide profiling and mapping of post translational modifications in human hearts. *Scientific Reports 2021 11:1*, *11*(1), 1–10. https://doi.org/10.1038/s41598-021-81986-y

Baillie, G. S., Tejeda, G. S., & Kelly, M. P. (2019). Therapeutic targeting of 3',5'-cyclic nucleotide phosphodiesterases: inhibition and beyond. *Nature*

Reviews. Drug Discovery, *18*(10), 770–796. https://doi.org/10.1038/S41573-019-0033-4

Baker, T. L., Zheng, H., Walker, J., Coloff, J. L., & Buss, J. E. (2003). Distinct rates of palmitate turnover on membrane-bound cellular and oncogenic H-Ras. *Journal of Biological Chemistry*, *278*(21), 19292–19300. https://doi.org/10.1074/jbc.M206956200

Balligand, J. L., Kelly, R. A., Marsden, P. A., Smith, T. W., & Michel, T. (1993). Control of cardiac muscle cell function by an endogenous nitric oxide signaling system. *Proceedings of the National Academy of Sciences of the United States of America*, *90*(1), 347–351. https://doi.org/10.1073/PNAS.90.1.347

Balon, T. W., & Nadler, J. L. (1994). Nitric oxide release is present from incubated skeletal muscle preparations. *Journal of Applied Physiology (Bethesda, Md. : 1985)*, *77*(6), 2519–2521. https://doi.org/10.1152/JAPPL.1994.77.6.2519

Bankaitis, V. A., Aitken, J. R., Cleves, A. E., & Dowhan, W. (1990). An essential role for a phospholipid transfer protein in yeast Golgi function. *Nature*, *347*(6293), 561–562. https://doi.org/10.1038/347561A0

Bardswell, S. C., Cuello, F., Kentish, J. C., & Avkiran, M. (2012). CMyBP-C as a promiscuous substrate: Phosphorylation by non-PKA kinases and its potential significance. *Journal of Muscle Research and Cell Motility*, *33*(1), 53–60. https://doi.org/10.1007/s10974-011-9276-3

Bardswell, S. C., Cuello, F., Rowland, A. J., Sadayappan, S., Robbins, J., Gautel, M., Walker, J. W., Kentish, J. C., & Avkiran, M. (2010). Distinct sarcomeric substrates are responsible for protein kinase D-mediated regulation of cardiac myofilament Ca2+ sensitivity and cross-bridge cycling. *The Journal of Biological Chemistry*, *285*(8), 5674–5682. https://doi.org/10.1074/JBC.M109.066456

Barefield, D., & Sadayappan, S. (2010). Phosphorylation and function of cardiac myosin binding protein-C in health and disease. *Journal of Molecular and Cellular Cardiology*, *48*(5), 866–875. https://doi.org/10.1016/J.YJMCC.2009.11.014

Barefield, D. Y., McNamara, J. W., Lynch, T. L., Kuster, D. W. D., Govindan, S., Haar, L., Wang, Y., Taylor, E. N., Lorenz, J. N., Nieman, M. L., Zhu, G., Luther, P. K., Varró, A., Dobrev, D., Ai, X., Janssen, P. M. L., Kass, D. A., Jones, W. K., Gilbert, R. J., & Sadayappan, S. (2019). Ablation of the calpain-targeted site in cardiac myosin binding protein-C is cardioprotective during ischemia-reperfusion injury. *Journal of Molecular and Cellular Cardiology*, *129*, 236–246. https://doi.org/10.1016/j.yjmcc.2019.03.006

Baron, E., Karam, N., Puscas, T., Mirabel, M., Bacher, A., Wahbi, K., Mazzella, J. M., Jeunemaitre, X., Donal, E., Reant, P., & Hagège, A. (2020). Hypertrophic cardiomyopathy (HCM) in the young adult: Data from the REMY register of the French Society of Cardiology. *Archives of Cardiovascular Diseases Supplements*, *12*(1), 32. https://doi.org/10.1016/J.ACVDSP.2019.09.066

Barrick, C. J., Rojas, M., Schoonhoven, R., Smyth, S. S., & Threadgill, D. W. (2007). Cardiac response to pressure overload in 129S1/SvImJ and C57BL/6J mice: temporal- and background-dependent development of concentric left ventricular hypertrophy. *American Journal of Physiology. Heart and Circulatory Physiology*, *292*(5). https://doi.org/10.1152/AJPHEART.00816.2006

Barrick, S. K., Greenberg, M. J., De, E., & Cruz, L. (2021). Cardiac myosin contraction and mechanotransduction in health and disease. *Journal of Biological Chemistry*, *297*(5). https://doi.org/10.1016/J.JBC.2021.101297

Beauclair, G., Bridier-Nahmias, A., Zagury, J.-F., Saïb, A., & Zamborlini, A. (2015). JASSA: a comprehensive tool for prediction of SUMOylation sites and SIMs. *Bioinformatics*, *31*(21), 3483–3491.

Benian, G. M., & Qadota, H. (2010). Molecular Structure of Sarcomere-to-Membrane Attachment at M-Lines in C. elegans Muscle. *Journal of Biomedicine and Biotechnology*, *2010*. https://doi.org/10.1155/2010/864749

Bennett, P. M., Baines, A. J., Lecomte, M. C., Maggs, A. M., & Pinder, J. C. (2004). Not Just a Plasma Membrane Protein: in Cardiac Muscle Cells Alpha-II Spectrin also Shows a Close Association with Myofibrils. *Journal of Muscle Research & Cell Motility 2004 25:2*, *25*(2), 119–126. https://doi.org/10.1023/B:JURE.0000035892.77399.51

Bernier-Villamor, V., Sampson, D. A., Matunis, M. J., & Lima, C. D. (2002). Structural Basis for E2-Mediated SUMO Conjugation Revealed by a Complex between Ubiquitin-Conjugating Enzyme Ubc9 and RanGAP1. *Cell*, *108*(3), 345–356. https://doi.org/10.1016/S0092-8674(02)00630-X

Bers, D. M. (2001). *Excitation-Contraction Coupling and Cardiac Contractile Force*. *237*. https://doi.org/10.1007/978-94-010-0658-3

Bers, D. M. (2002a). Cardiac excitation–contraction coupling. *Nature 2002 415:6868*.

Bers, D. M. (2002b). Cardiac Na/Ca Exchange Function in Rabbit, Mouse and Man: What's the Difference? *Journal of Molecular and Cellular Cardiology*, *34*(4), 369–373. https://doi.org/10.1006/JMCC.2002.1530

Bhandari, B., Rodriguez, B. S. Q., & Masood, W. (2021). Ischemic Cardiomyopathy. *Congestive Heart Failure and Cardiac Transplantation: Clinical, Pathology, Imaging and Molecular Profiles*, 119–133. https://doi.org/10.1007/978-3-319-44577-9_8

Bhuiyan, Md. S., Gulick, J., Osinska, H., Gupta, M., & Robbins, J. (2012). Determination of the critical residues responsible for cardiac myosin binding protein C's interactions. *Journal of Molecular and Cellular Cardiology*, *53*(6), 838–847. https://doi.org/10.1016/j.yjmcc.2012.08.028

Bito, V., van der Velden, J., Claus, P., Dommke, C., van Lommel, A., Mortelmans, L., Verbeken, E., Bijnens, B., Stienen, G., & Sipido, K. R. (2007). Reduced force generating capacity in myocytes from chronically ischemic, hibernating myocardium. *Circulation Research*, *100*(2), 229–237. https://doi.org/10.1161/01.RES.0000257829.07721.57

Blair, C. A., Haynes, P., Campbell, S. G., Chung, C., Mitov, M. I., Dennis, D., Bonnell, M. R., Hoopes, C. W., Guglin, M., & Campbell, K. S. (2016). A Protocol for Collecting Human Cardiac Tissue for Research. *The VAD Journal : The Journal of Mechanical Assisted Circulation and Heart Failure*, *2*(1). https://doi.org/10.13023/VAD.2016.12

Blakeslee, W. W., Wysoczynski, C. L., Fritz, K. S., Nyborg, J. K., Churchill, M. E. A., & McKinsey, T. A. (2014). Class I HDAC inhibition stimulates cardiac protein SUMOylation through a post-translational mechanism. *Cellular Signalling*, *26*(12), 2912–2920. https://doi.org/10.1016/J.CELLSIG.2014.09.005

Blanc, M., David, F., Abrami, L., Migliozzi, D., Armand, F., Bürgi, J., & van der Goot, F. G. (2015). SwissPalm: Protein Palmitoylation database. *F1000Research*, *4*. https://doi.org/10.12688/f1000research.6464.1

Blaskovic, S., Blanc, M., & van der Goot, F. G. (2013). What does S-palmitoylation do to membrane proteins? *The FEBS Journal*, *280*(12), 2766–2774. https://doi.org/10.1111/FEBS.12263

Boguslavskyi, A., Pavlovic, D., Aughton, K., Clark, J. E., Howie, J., Fuller, W., & Shattock, M. J. (2014). Cardiac hypertrophy in mice expressing unphosphorylatable phospholemman. *Cardiovascular Research*, *104*(1), 72–82. https://doi.org/10.1093/CVR/CVU182

Bolger, G. B., Baillie, G. S., Li, X., Lynch, M. J., Herzyk, P., Mohamed, A., High Mitchell, L., McCahill, A., Hundsrucker, C., Klussmann, E., Adams, D. R., & Houslay, M. D. (2006). Scanning peptide array analyses identify overlapping binding sites for the signalling scaffold proteins, β-arrestin and RACK1, in cAMP-specific phosphodiesterase PDE4D5. *Biochemical Journal*, *398*(Pt 1), 23. https://doi.org/10.1042/BJ20060423

Bonne, G., Carrier, L., Bercovici, J., Cruaud, C., Richard, P., Hainque, B., Gautel, M., Labeit, S., James, M., Beckmann, J., Weissenbach, J., Vosberg, H. P., Fiszman, M., Komajda, M., & Schwartz, K. (1995). Cardiac myosin binding protein-C gene splice acceptor site mutation is associated with familial hypertrophic cardiomyopathy. *Nature Genetics*, *11*(4), 438–440. https://doi.org/10.1038/NG1295-438

Bossuyt, J., Ai, X., Moorman, J. R., Pogwizd, S. M., & Bers, D. M. (2005). Expression and phosphorylation of the na-pump regulatory subunit phospholemman in heart failure. *Circulation Research*, *97*(6), 558–565. https://doi.org/10.1161/01.RES.0000181172.27931.C3

Bozkurt, B., Coats, A. J. S., Tsutsui, H., Abdelhamid, C. M., Adamopoulos, S., Albert, N., Anker, S. D., Atherton, J., Böhm, M., Butler, J., Drazner, M. H., Michael Felker, G., Filippatos, G., Fiuzat, M., Fonarow, G. C., Gomez-Mesa, J. E., Heidenreich, P., Imamura, T., Jankowska, E. A., … Zieroth, S. (2021). Universal definition and classification of heart failure: a report of the Heart Failure Society of America, Heart Failure Association of the European Society of Cardiology, Japanese Heart Failure Society and Writing Committee of the Universal Definition of Heart Failure. *European Journal of Heart Failure*, *23*(3), 352–380. https://doi.org/10.1002/EJHF.2115

Bradford, M. (1976). A Rapid and Sensitive Method for the Quantitation of Microgram Quantities of Protein Utilizing the Principle of Protein-Dye Binding. *Analytical Biochemistry*, *72*(1–2), 248–254. https://doi.org/10.1006/abio.1976.9999

Brennan, J. P., Miller, J. I. A., Fuller, W., Wait, R., Begum, S., Dunn, M. J., & Eaton, P. (2006). The utility of N,N-biotinyl glutathione disulfide in the study of protein S-glutathiolation. *Molecular and Cellular Proteomics*, *5*(2), 215–225. https://doi.org/10.1074/MCP.M500212-MCP200/ATTACHMENT/6165B6FE-49EF-4308-8F66-1DC71FBD53C7/MMC1.PDF

Briceno, N., Schuster, A., Lumley, M., & Perera, D. (2016). Ischaemic cardiomyopathy: pathophysiology, assessment and the role of revascularisation. *Heart*, *102*(5), 397–406. https://doi.org/10.1136/HEARTJNL-2015-308037

Brickson, S., Fitzsimons, D. P., Pereira, L., Hacker, T., Valdivia, H., & Moss, R. L. (2007). In vivo left ventricular functional capacity is compromised in cMyBP-C null mice. *American Journal of Physiology. Heart and Circulatory Physiology*, *292*(4). https://doi.org/10.1152/AJPHEART.01037.2006

Budde, H., Hassoun, R., Tangos, M., Zhazykbayeva, S., Herwig, M., Varatnitskaya, M., Sieme, M., Delalat, S., Sultana, I., Kolijn, D., Gömöri, K., Jarkas, M., Lódi, M., Jaquet, K., Kovács, Á., Mannherz, H. G., Sequeira, V., Mügge, A., Leichert, L. I., … Hamdani, N. (2021). The interplay between s-

glutathionylation and phosphorylation of cardiac troponin i and myosin binding protein c in end-stage human failing hearts. *Antioxidants*, *10*(7), 1134. https://doi.org/10.3390/ANTIOX10071134/S1

Bunch, T. A., Kanassatega, R. S., Lepak, V. C., & Colson, B. A. (2019). Human cardiac myosin- binding protein C restricts actin structural dynamics in a cooperative and phosphorylation-sensitive manner. *Journal of Biological Chemistry*, *294*(44), 16228–16240. https://doi.org/10.1074/jbc.RA119.009543

Buraei, Z., & Yang, J. (2010). The ß Subunit of Voltage-Gated Ca2+ Channels. *Physiological Reviews*, *90*(4), 1461. https://doi.org/10.1152/PHYSREV.00057.2009

Burgoyne, J. R., Haeussler, D. J., Kumar, V., Ji, Y., Pimental, D. R., Zee, R. S., Costello, C. E., Lin, C., McComb, M. E., Cohen, R. A., & Bachschmid, M. M. (2012). Oxidation of HRas cysteine thiols by metabolic stress prevents palmitoylation in vivo and contributes to endothelial cell apoptosis. *The FASEB Journal*, *26*(2), 832–841. https://doi.org/10.1096/FJ.11-189415

Burton, F. L., Mcphaden, A. R., Cobbe, S. M., Burton, F. L., Cobbe, S. M., & Mcphaden, A. R. (2000). Ventricular fibrillation threshold and local dispersion of refractoriness in isolated rabbit hearts with left ventricular dysfunction. *Basic Research in Cardiology 2000 95:5*, *95*(5), 359–367. https://doi.org/10.1007/S003950070034

Butters, A., Lakdawala, N. K., & Ingles, J. (2021). Sex Differences in Hypertrophic Cardiomyopathy: Interaction With Genetics and Environment. *Current Heart Failure Reports*, *18*(5), 264–273. https://doi.org/10.1007/S11897-021-00526-X/FIGURES/3

Canton, M., Menazza, S., Sheeran, F. L., Polverino De Laureto, P., di Lisa, F., & Pepe, S. (2011). Oxidation of Myofibrillar Proteins in Human Heart Failure. *Journal of the American College of Cardiology*, *57*(3), 300–309. https://doi.org/10.1016/J.JACC.2010.06.058

Cao, Y., Qiu, T., Kathayat, R. S., Azizi, S. A., Thorne, A. K., Ahn, D., Fukata, Y., Fukata, M., Rice, P. A., & Dickinson, B. C. (2019). ABHD10 is an S-depalmitoylase affecting redox homeostasis through peroxiredoxin-5. *Nature Chemical Biology*, *15*(12), 1232–1240. https://doi.org/10.1038/s41589-019-0399-y

Caremani, M., Pinzauti, F., Reconditi, M., Piazzesi, G., Stienen, G. J. M., Lombardi, V., Linari, M., & Spudich, J. A. (2016). Size and speed of the working stroke of cardiac myosin in situ. *Proceedings of the National Academy of Sciences of the United States of America*, *113*(13), 3675–3680. https://doi.org/10.1073/PNAS.1525057113

Carrier, L. (2021). Targeting the population for gene therapy with MYBPC3. *Journal of Molecular and Cellular Cardiology*, *150*, 101–108. https://doi.org/10.1016/J.YJMCC.2020.10.003

Carrier, L., Mearini, G., Stathopoulou, K., & Cuello, F. (2015). Cardiac myosin-binding protein C (MYBPC3) in cardiac pathophysiology. *Gene*, *573*(2), 188–197. https://doi.org/10.1016/j.gene.2015.09.008

Cartier, E., Garcia-Olivares, J., Janezic, E., Viana, J., Moore, M., Lin, M. L., Caplan, J. L., Torres, G., & Kim, Y. H. (2019). The SUMO-conjugase Ubc9 prevents the degradation of the dopamine transporter, enhancing its cell surface level and dopamine uptake. *Frontiers in Cellular Neuroscience*, *13*. https://doi.org/10.3389/FNCEL.2019.00035/FULL

Cazorla, O., Lucas, A., Poirier, F., Lacampagne, A., & Lezoualc'h, F. (2009). The cAMP binding protein Epac regulates cardiac myofilament function.

Proceedings of the National Academy of Sciences of the United States of America, *106*(33), 14144. https://doi.org/10.1073/PNAS.0812536106

Cazorla, O., Szilagyi, S., Vignier, N., Salazar, G., Krämer, E., Vassort, G., Carrier, L., & Lacampagne, A. (2006). Length and protein kinase A modulations of myocytes in cardiac myosin binding protein C-deficient mice. *Cardiovascular Research*, *69*(2), 370–380. https://doi.org/10.1016/J.CARDIORES.2005.11.009/2/69-2-370-FIG6.GIF

Celen, A. B., & Sahin, U. (2020). Sumoylation on its 25th anniversary: mechanisms, pathology, and emerging concepts. *The FEBS Journal*, *287*(15), 3110–3140. https://doi.org/10.1111/FEBS.15319

Chamberlain, L. H., & Shipston, M. J. (2015). The Physiology of Protein S-acylation. *Physiological Reviews*, *95*(2), 341. https://doi.org/10.1152/PHYSREV.00032.2014

Chan, P., Han, X., Zheng, B., Deran, M., Yu, J., Jarugumilli, G. K., Deng, H., Pan, D., Luo, X., & Wu, X. (2016). Autopalmitoylation of TEAD Proteins Regulates Transcriptional Output of Hippo Pathway. *Nature Chemical Biology*, *12*(4), 282. https://doi.org/10.1038/NCHEMBIO.2036

Chang, C. C., Tung, C. H., Chen, C. W., Tu, C. H., & Chu, Y. W. (2018). SUMOgo: Prediction of sumoylation sites on lysines by motif screening models and the effects of various post-translational modifications. *Scientific Reports 2018 8:1*, *8*(1), 1–10. https://doi.org/10.1038/s41598-018-33951-5

Chang, P. C., Lu, Y. Y., Lee, H. L., Lin, S. F., Chu, Y., Wen, M. S., & Chou, C. C. (2018). Paradoxical Effects of Sodium–Calcium Exchanger Inhibition on Torsade de Pointes and Early Afterdepolarization in a Heart Failure Rabbit Model. *Journal of Cardiovascular Pharmacology*, *72*(2), 97–105. https://doi.org/10.1097/FJC.0000000000000598

Chase, P. B., Szczypinski, M. P., & Soto, E. P. (2013). Nuclear tropomyosin and troponin in striated muscle: New roles in a new locale? *Journal of Muscle Research and Cell Motility*, *34*(3–4), 275–284. https://doi.org/10.1007/S10974-013-9356-7/TABLES/4

Chaube, R., Hess, D. T., Wang, Y. J., Plummer, B., Sun, Q. A., Laurita, K., & Stamler, J. S. (2014). Regulation of the skeletal muscle ryanodine receptor/Ca2+- release channel RyR1 by S-palmitoylation. *Journal of Biological Chemistry*, *289*(12), 8612–8619. https://doi.org/10.1074/jbc.M114.548925

Chen, J., Bian, X., Li, Y., Xiao, X., Yin, Y. Y. G., Du, X., Wang, C., Li, L., Bai, Y. W., & Liu, X. Z. (2020). Moderate hypothermia induces protection against hypoxia/reoxygenation injury by enhancing SUMOylation in cardiomyocytes. *Molecular Medicine Reports*, *22*(4), 2617–2626. https://doi.org/10.3892/MMR.2020.11374

Chen, J. J., Marsden, A. N., Scott, C. A., Akimzhanov, A. M., & Boehning, D. (2020). DHHC5 Mediates β-Adrenergic Signaling in Cardiomyocytes by Targeting Gα Proteins. *Biophysical Journal*, *118*(4), 826. https://doi.org/10.1016/J.BPJ.2019.08.018

Chien, A. J., Carr, K. M., Shirokov, R. E., Rios, E., & Marlene Hosey, M. (1996). Identification of Palmitoylation Sites within the L-type Calcium Channel β2a Subunit and Effects on Channel Function *. *Journal of Biological Chemistry*, *271*(43), 26465–26468. https://doi.org/10.1074/JBC.271.43.26465

Choi, S. H., Kwon, I. C., Hwang, K. Y., Kim, I. S., & Ahn, H. J. (2011). Small heat shock protein as a multifunctional scaffold: Integrated tumor targeting and caspase imaging within a single cage. *Biomacromolecules*, *12*(8), 3099–3106. https://doi.org/10.1021/BM200743G/ASSET/IMAGES/LARGE/BM-2011-00743G_0007.JPEG

Cilenti, L., di Gregorio, J., Ambivero, C. T., Andl, T., Liao, R., & Zervos, A. S. (2020). Mitochondrial MUL1 E3 ubiquitin ligase regulates Hypoxia Inducible Factor (HIF-1α) and metabolic reprogramming by modulating the UBXN7 cofactor protein. *Scientific Reports 2020 10:1*, *10*(1), 1–15. https://doi.org/10.1038/s41598-020-58484-8

Claflin, D. R., Morgan, D. L., & Julian, F. J. (1998). The effect of length on the relationship between tension and intracellular [Ca2+] in intact frog skeletal muscle fibres. *The Journal of Physiology*, *508*(Pt 1), 179. https://doi.org/10.1111/J.1469-7793.1998.179BR.X

Cohen, P. (2002). The origins of protein phosphorylation. *Nature Cell Biology 2002 4:5*, *4*(5), E127–E130. https://doi.org/10.1038/ncb0502-e127

Colson, B. A., Locher, M. R., Bekyarova, T., Patel, J. R., Fitzsimons, D. P., Irving, T. C., & Moss, R. L. (2010). Differential roles of regulatory light chain and myosin binding protein-C phosphorylations in the modulation of cardiac force development. *The Journal of Physiology*, *588*(Pt 6), 981–993. https://doi.org/10.1113/JPHYSIOL.2009.183897

Colson, B. A., Patel, J. R., Chen, P. P., Bekyarova, T., Abdalla, M. I., Tong, C. W., Fitzsimons, D. P., Irving, T. C., & Moss, R. L. (2012). Myosin binding protein-C phosphorylation is the principal mediator of protein kinase A effects on thick filament structure in myocardium. *Journal of Molecular and Cellular Cardiology*, *53*(5), 609–616. https://doi.org/10.1016/j.yjmcc.2012.07.012

Colson, B. A., Thompson, A. R., Espinoza-Fonseca, L. M., & Thomas, D. D. (2016). Site-directed spectroscopy of cardiac myosin-binding protein C reveals effects of phosphorylation on protein structural dynamics. *Proceedings of the National Academy of Sciences of the United States of America*, *113*(12), 3233–3238. https://doi.org/10.1073/PNAS.1521281113

Copeland, O., Sadayappan, S., Messer, A. E., Steinen, G. J. M., van der Velden, J., & Marston, S. B. (2010). Analysis of cardiac myosin binding protein-C phosphorylation in human heart muscle. *Journal of Molecular and Cellular Cardiology*, *49*(6), 1003–1011. https://doi.org/10.1016/j.yjmcc.2010.09.007

Coulton, A. T., & Stelzer, J. E. (2012). Cardiac Myosin Binding Protein C and Its Phosphorylation Regulate Multiple Steps in the Cross-Bridge Cycle of Muscle Contraction. *Biochemistry*, *51*(15), 3292. https://doi.org/10.1021/BI300085X

Craig, R., & Offer, G. (1976). The location of C protein in rabbit skeletal muscle. *Proceedings of the Royal Society of London - Biological Sciences*, *192*(1109), 451–461. https://doi.org/10.1098/rspb.1976.0023

Cuello, F., Bardswell, S. C., Haworth, R. S., Ehler, E., Sadayappan, S., Kentish, J. C., & Avkiran, M. (2011). Novel Role for p90 Ribosomal S6 Kinase in the Regulation of Cardiac Myofilament Phosphorylation. *Journal of Biological Chemistry*, *286*(7), 5300–5310. https://doi.org/10.1074/jbc.M110.202713

Cuello, F., Wittig, I., Lorenz, K., & Eaton, P. (2018). Oxidation of cardiac myofilament proteins: Priming for dysfunction? *Molecular Aspects of Medicine*, *63*, 47–58. https://doi.org/10.1016/J.MAM.2018.08.003

Cuomo, O., Pignataro, G., Sirabella, R., Molinaro, P., Anzilotti, S., Scorziello, A., Sisalli, M. J., di Renzo, G., & Annunziato, L. (2016). Sumoylation of LYS590 of NCX3 f-Loop by SUMO1 participates in brain neuroprotection induced by ischemic preconditioning. *Stroke*, *47*(4), 1085–1093. https://doi.org/10.1161/STROKEAHA.115.012514

D. Hamel, L., J. Lenhart, B., A. Mitchell, D., G. Santos, R., A. Giulianotti, M., & J. Deschenes, R. (2016). Identification of Protein Palmitoylation Inhibitors from a Scaffold Ranking Library. *Combinatorial Chemistry & High*

Throughput Screening, *19*(4), 262–274. https://doi.org/10.2174/1386207319666160324123844

Daaka, Y., Luttrell, L. M., & Lefkowitz, R. J. (1997). Switching of the coupling of the beta2-adrenergic receptor to different G proteins by protein kinase A. *Nature*, *390*(6655), 88–91. https://doi.org/10.1038/36362

Dasgupta, S., Bhattacharya, S., Maitra, S., Pal, D., Majumdar, S. S., Datta, A., & Bhattacharya, S. (2011). Mechanism of lipid induced insulin resistance: activated PKCε is a key regulator. *Biochimica et Biophysica Acta*, *1812*(4), 495–506. https://doi.org/10.1016/J.BBADIS.2011.01.001

Davda, D., el Azzouny, M. A., Tom, C. T. M. B., Hernandez, J. L., Majmudar, J. D., Kennedy, R. T., & Martin, B. R. (2013). Profiling targets of the irreversible palmitoylation inhibitor 2-bromopalmitate. *ACS Chemical Biology*, *8*(9), 1912–1917. https://doi.org/10.1021/cb400380s

Davda, D., & Martin, B. R. (2014). Acyl protein thioesterase inhibitors as probes of dynamic S-palmitoylation. In *MedChemComm* (Vol. 5, Issue 3, pp. 268–276). Royal Society of Chemistry. https://doi.org/10.1039/c3md00333g

de Lucia, C., Eguchi, A., & Koch, W. J. (2018). New insights in cardiac β-Adrenergic signaling during heart failure and aging. *Frontiers in Pharmacology*, *9*(AUG), 904. https://doi.org/10.3389/FPHAR.2018.00904/BIBTEX

de Tombe, P. P. (2003). Cardiac myofilaments: mechanics and regulation. *Journal of Biomechanics*, *36*(5), 721–730. https://doi.org/10.1016/S0021-9290(02)00450-5

de Tombe, P. P., Mateja, R. D., Tachampa, K., Mou, Y. A., Farman, G. P., & Irving, T. C. (2010). Myofilament Length Dependent Activation. *Journal of Molecular and Cellular Cardiology*, *48*(5), 851. https://doi.org/10.1016/J.YJMCC.2009.12.017

de Tombe, P. P., & ter Keurs, H. E. D. J. (2016). Cardiac muscle mechanics: Sarcomere length matters. *Journal of Molecular and Cellular Cardiology*, *91*, 148. https://doi.org/10.1016/J.YJMCC.2015.12.006

Decker, R. S., Decker, M. L., Kulikovskaya, I., Nakamura, S., Lee, D. C., Harris, K., Klocke, F. J., & Winegrad, S. (2005). Myosin-binding protein C phosphorylation, myofibril structure, and contractile function during low-flow ischemia. *Circulation*, *111*(7), 906–912. https://doi.org/10.1161/01.CIR.0000155609.95618.75

Dietrich, L. E. P., & Ungermann, C. (2004). On the mechanism of protein palmitoylation. *EMBO Reports*, *5*(11), 1053. https://doi.org/10.1038/SJ.EMBOR.7400277

Dirkx, E., Cazorla, O., Schwenk, R. W., Lorenzen-Schmidt, I., Sadayappan, S., van Lint, J., Carrier, L., van Eys, G. J. J. M., Glatz, J. F. C., & Luiken, J. J. F. P. (2012). Protein kinase D increases maximal Ca2+-activated tension of cardiomyocyte contraction by phosphorylation of cMyBP-C-Ser315. *American Journal of Physiology. Heart and Circulatory Physiology*, *303*(3), 323–331. https://doi.org/10.1152/AJPHEART.00749.2011

Dixon, J. A., & Spinale, F. G. (2009). LARGE ANIMAL MODELS OF HEART FAILURE: A CRITICAL LINK IN THE TRANSLATION OF BASIC SCIENCE TO CLINICAL PRACTICE. *Circulation. Heart Failure*, *2*(3), 262. https://doi.org/10.1161/CIRCHEARTFAILURE.108.814459

Doh, C. Y., Bharambe, N., Holmes, J. B., Dominic, K. L., Swanberg, C. E., Mamidi, R., Chen, Y., Bandyopadhyay, S., Ramachandran, R., & Stelzer, J. E. (2022). Molecular characterization of linker and loop-mediated structural modulation and hinge motion in the C4-C5 domains of cMyBPC. *Journal of Structural Biology*, *214*(2). https://doi.org/10.1016/J.JSB.2022.107856

Doh, C. Y., Dominic, K. L., Swanberg, C. E., Bharambe, N., Willard, B. B., Li, L., Ramachandran, R., & Stelzer, J. E. (2022). Identification of Phosphorylation and Other Post-Translational Modifications in the Central C4C5 Domains of Murine Cardiac Myosin Binding Protein C. *ACS Omega*, *7*(16), 14189–14202. https://doi.org/10.1021/ACSOMEGA.2C00799

Dostanic, I., Schultz, J. E. J., Lorenz, J. N., & Lingrel, J. B. (2004). The alpha 1 isoform of Na,K-ATPase regulates cardiac contractility and functionally interacts and co-localizes with the Na/Ca exchanger in heart. *The Journal of Biological Chemistry*, *279*(52), 54053–54061. https://doi.org/10.1074/JBC.M410737200

Drisdel, R. C., & Green, W. N. (2004). Labeling and quantifying sites of protein palmitoylation. *BioTechniques*, *36*(2), 276–285. https://doi.org/10.2144/04362rr02

Du, J., Zhang, L., Zhuang, S., Qin, G. J., & Zhao, T. C. (2015). HDAC4 degradation mediates HDAC inhibition-induced protective effects against hypoxia/reoxygenation injury. *Journal of Cellular Physiology*, *230*(6), 1321–1331. https://doi.org/10.1002/JCP.24871

Duncan, J. A., & Gilman, A. G. (1996). Autoacylation of G protein α subunits. *Journal of Biological Chemistry*, *271*(38), 23594–23600. https://doi.org/10.1074/jbc.271.38.23594

Duncan, J. A., & Gilman, A. G. (1998). A cytoplasmic acyl-protein thioesterase that removes palmitate from G protein α subunits and p21(RAS). *Journal of Biological Chemistry*, *273*(25), 15830–15837. https://doi.org/10.1074/jbc.273.25.15830

Duncan, P. J., Bi, D., McClafferty, H., Chen, L., Tian, L., & Shipston, M. J. (2019). S-Acylation controls functional coupling of BK channel pore-forming α-subunits and ß1-subunits. *The Journal of Biological Chemistry*, *294*(32), 12066. https://doi.org/10.1074/JBC.RA119.009065

Dutsch, A., Wijnker, P. J. M., Schlossarek, S., Friedrich, F. W., Krämer, E., Braren, I., Hirt, M. N., Brenière-Letuffe, D., Rhoden, A., Mannhardt, I., Eschenhagen, T., Carrier, L., & Mearini, G. (2019). Phosphomimetic cardiac myosin-binding protein C partially rescues a cardiomyopathy phenotype in murine engineered heart tissue. *Scientific Reports*, *9*(1). https://doi.org/10.1038/S41598-019-54665-2

Eaton, P., Wright, N., Hearse, D. J., & Shattock, M. J. (2002). Glyceraldehyde phosphate dehydrogenase oxidation during cardiac ischemia and reperfusion. *Journal of Molecular and Cellular Cardiology*, *34*(11), 1549–1560. https://doi.org/10.1006/JMCC.2002.2108

Edmonds, M. J., & Morgan, A. (2014). A systematic analysis of protein palmitoylation in Caenorhabditis elegans. *BMC Genomics*, *15*(1). https://doi.org/10.1186/1471-2164-15-841

Ehler, E., Moore-Morris, T., & Lange, S. (2013). Isolation and Culture of Neonatal Mouse Cardiomyocytes. *Journal of Visualized Experiments : JoVE*, *79*, 50154. https://doi.org/10.3791/50154

Eisner, D. A., Caldwell, J. L., Kistamás, K., & Trafford, A. W. (2017). Calcium and Excitation-Contraction Coupling in the Heart. In *Circulation Research* (Vol. 121, Issue 2, pp. 181–195). Lippincott Williams and Wilkins. https://doi.org/10.1161/CIRCRESAHA.117.310230

El-Armouche, A., Boknik, P., Eschenhagen, T., Carrier, L., Knaut, M., Ravens, U., & Dobrev, D. (2006). Molecular determinants of altered Ca2+ handling in human chronic atrial fibrillation. *Circulation*, *114*(7), 670–680. https://doi.org/10.1161/CIRCULATIONAHA.106.636845

El-Armouche, A., Pohlmann, L., Schlossarek, S., Starbatty, J., Yeh, Y.-H., Nattel, S., Dobrev, D., Eschenhagen, T., & Carrier, L. (2007). Decreased phosphorylation levels of cardiac myosin-binding protein-C in human and experimental heart failure. *Journal of Molecular and Cellular Cardiology*, *43*(2), 223–229. https://doi.org/10.1016/j.yjmcc.2007.05.003

Ellermann, C., Wolfes, J., Eckardt, L., & Frommeyer, G. (2021). Role of the rabbit whole-heart model for electrophysiologic safety pharmacology of non-cardiovascular drugs. *EP Europace*, *23*(6), 828–836. https://doi.org/10.1093/EUROPACE/EUAA288

Endoh, M. (2004). Force–frequency relationship in intact mammalian ventricular myocardium: physiological and pathophysiological relevance. *European Journal of Pharmacology*, *500*(1–3), 73–86. https://doi.org/10.1016/J.EJPHAR.2004.07.013

Eppenberger, H. M., Hertig, C., & Eppenberger-Eberhardt, M. (1994). Adult rat cardiomyocytes in culture A model system to study the plasticity of the differentiated cardiac phenotype at the molecular and cellular levels. *Trends in Cardiovascular Medicine*, *4*(4), 187–193. https://doi.org/10.1016/1050-1738(94)90056-6

Eppenberger, M. E., Hauser, I., Baechi, T., Schaub, M. C., Brunner, U. T., Dechesne, C. A., & Eppenberger, H. M. (1988). Immunocytochemical analysis of the regeneration of myofibrils in long-term cultures of adult cardiomyocytes of the rat. *Developmental Biology*, *130*(1), 1–15. https://doi.org/10.1016/0012-1606(88)90408-3

Essandoh, K., Philippe, J. M., Jenkins, P. M., & Brody, M. J. (2020). Palmitoylation: A Fatty Regulator of Myocardial Electrophysiology. In *Frontiers in Physiology* (Vol. 11). Frontiers Media S.A. https://doi.org/10.3389/fphys.2020.00108

Farman, G. P., Gore, D., Allen, E., Schoenfelt, K., Irving, T. C., & de Tombe, P. P. (2011). Myosin head orientation: a structural determinant for the Frank-Starling relationship. *American Journal of Physiology. Heart and Circulatory Physiology*, *300*(6). https://doi.org/10.1152/AJPHEART.01221.2010

Fearnley, C. J., Llewelyn Roderick, H., & Bootman, M. D. (2011). Calcium Signaling in Cardiac Myocytes. *Cold Spring Harbor Perspectives in Biology*, *3*(11). https://doi.org/10.1101/CSHPERSPECT.A004242

Feiner, E. C., Chung, P., Jasmin, J. F., Zhang, J., Whitaker-Menezes, D., Myers, V., Song, J., Feldman, E. W., Funakoshi, H., Degeorge, B. R., Yelamarty, R. v., Koch, W. J., Lisanti, M. P., McTiernan, C. F., Cheung, J. Y., Bristow, M. R., Chan, T. O., & Feldman, A. M. (2011). Left ventricular dysfunction in murine models of heart failure and in failing human heart is associated with a selective decrease in the expression of caveolin-3. *Journal of Cardiac Failure*, *17*(3), 253–263. https://doi.org/10.1016/J.CARDFAIL.2010.10.008

Feldman, A. M., Ray, P. E., & Bristow, M. R. (1991). Expression of alpha-subunits of G proteins in failing human heart: a reappraisal utilizing quantitative polymerase chain reaction. *Journal of Molecular and Cellular Cardiology*, *23*(12), 1355–1358. https://doi.org/10.1016/0022-2828(91)90182-L

Feldman, A. M., Weinberg, E. O., Ray, P. E., & Lorell, B. H. (1993). Selective changes in cardiac gene expression during compensated hypertrophy and the transition to cardiac decompensation in rats with chronic aortic banding. *Circulation Research*, *73*(1), 184–192. https://doi.org/10.1161/01.RES.73.1.184

Fernández-Hernando, C., Fukata, M., Bernatchez, P. N., Fukata, Y., Lin, M. I., Bredt, D. S., & Sessa, W. C. (2006). Identification of Golgi-localized acyl transferases that palmitoylate and regulate endothelial nitric oxide

synthase. *Journal of Cell Biology*, *174*(3), 369–377. https://doi.org/10.1083/jcb.200601051

Fert-Bober, J., Giles, J. T., Holewinski, R. J., Kirk, J. A., Uhrigshardt, H., Crowgey, E. L., Andrade, F., Bingham, C. O., Park, J. K., Halushka, M. K., Kass, D. A., Bathon, J. M., & van Eyk, J. E. (2015). Citrullination of myofilament proteins in heart failure. *Cardiovascular Research*, *108*(2), 232–242. https://doi.org/10.1093/CVR/CVV185

Fert-Bober, J., & Sokolove, J. (2014). Proteomics of citrullination in cardiovascular disease. *Proteomics. Clinical Applications*, *8*(7–8), 522–533. https://doi.org/10.1002/PRCA.201400013

Fertig, B., Ling, J., Nollet, E. E., Dobi, S., Busiau, T., Ishikawa, K., Yamada, K., Lee, A., Kho, C., Wills, L., Tibbo, A. J., Scott, M., Grant, K., Campbell, K. S., Birks, E. J., MacQuaide, N., Hajjar, R., Smith, G. L., Velden, J. van der, & Baillie, G. S. (2022). SUMOylation does not affect cardiac troponin I stability but alters indirectly the development of force in response to Ca2+. *The FEBS Journal*. https://doi.org/10.1111/FEBS.16537

Figueiredo-Freitas, C., Dulce, R. A., Foster, M. W., Liang, J., Yamashita, A. M. S., Lima-Rosa, F. L., Thompson, J. W., Moseley, M. A., Hare, J. M., Nogueira, L., Sorenson, M. M., & Pinto, J. R. (2015). S-Nitrosylation of Sarcomeric Proteins Depresses Myofilament Ca2+ Sensitivity in Intact Cardiomyocytes. *Antioxidants & Redox Signaling*, *23*(13), 1017. https://doi.org/10.1089/ARS.2015.6275

Finkel, T. (2011). Signal transduction by reactive oxygen species. *The Journal of Cell Biology*, *194*(1), 7. https://doi.org/10.1083/JCB.201102095

Finley, N. L., & Cuperman, T. I. (2014). Cardiac myosin binding protein-C: A structurally dynamic regulator of myocardial contractility. *Pflugers Archiv European Journal of Physiology*, *466*(3), 433–438. https://doi.org/10.1007/S00424-014-1451-0/FIGURES/2

Fiorentino, M., Zadra, G., Palescandolo, E., Fedele, G., Bailey, D., Fiore, C., Nguyen, P. L., Migita, T., Zamponi, R., di Vizio, D., Priolo, C., Sharma, C., Xie, W., Hemler, M. E., Mucci, L., Giovannucci, E., Finn, S., & Loda, M. (2008). Overexpression of fatty acid synthase is associated with palmitoylation of Wnt1 and cytoplasmic stabilization of β-catenin in prostate cancer. *Laboratory Investigation 2008 88:12*, *88*(12), 1340–1348. https://doi.org/10.1038/labinvest.2008.97

Flashman, E., Korkie, L., Watkins, H., Redwood, C., & Moolman-Smook, J. C. (2008). Support for a trimeric collar of myosin binding protein C in cardiac and fast skeletal muscle, but not in slow skeletal muscle. *FEBS Letters*, *582*(3), 434–438. https://doi.org/10.1016/J.FEBSLET.2008.01.004

Flashman, E., Watkins, H., & Redwood, C. (2007). Localization of the binding site of the C-terminal domain of cardiac myosin-binding protein-C on the myosin rod. *The Biochemical Journal*, *401*(1), 97–102. https://doi.org/10.1042/BJ20060500

Folch, J., & Lees, M. (1951). Proteolipides, a new type of tissue lipoproteins; their isolation from brain. *J Biol Chem*, *191*(2), 807–817.

Fontes-Sousa, A. P., Pires, A. L., Carneiro, C. S., Brás-Silva, C., & Leite-Moreira, A. F. (2009). Effects of adrenomedullin on systolic and diastolic myocardial function. *Peptides*, *30*(4), 796–802. https://doi.org/10.1016/J.PEPTIDES.2008.12.011

Forrester, M. T., Hess, D. T., Thompson, J. W., Hultman, R., Moseley, M. A., Stamler, J. S., & Casey, P. J. (2011). Site-specific analysis of protein S-acylation by resin-assisted capture. *Journal of Lipid Research*, *52*(2), 393–398. https://doi.org/10.1194/jlr.D011106

Fougerousse, F., Delezoide, A. L., Fiszman, M. Y., Schwartz, K., Beckmann, J. S., & Carrier, L. (1998). Cardiac myosin binding protein C gene is specifically expressed in heart during murine and human development. *Circulation Research*, *82*(1), 130–133. https://doi.org/10.1161/01.RES.82.1.130

Frank, R. (2002). The SPOT-synthesis technique. Synthetic peptide arrays on membrane supports--principles and applications. *Journal of Immunological Methods*, *267*(1), 13–26. https://doi.org/10.1016/S0022-1759(02)00137-0

Fuller, W., Reilly, L., & Hilgemann, D. W. (2016). S-palmitoylation and the regulation of NCX1. *Channels*, *10*(2), 75–77. https://doi.org/10.1080/19336950.2015.1099329

Fuller, W., Tulloch, L. B., Shattock, M. J., Calaghan, S. C., Howie, J., & Wypijewski, K. J. (2013). Regulation of the cardiac sodium pump. *Cellular and Molecular Life Sciences*, *70*(8), 1357. https://doi.org/10.1007/S00018-012-1134-Y

Galitzky, J., Langin, D., Verwaerde, P., Montastruc, J. L., Lafontan, M., & Berlan, M. (1997). Lipolytic effects of conventional beta 3-adrenoceptor agonists and of CGP 12,177 in rat and human fat cells: preliminary pharmacological evidence for a putative beta 4-adrenoceptor. *British Journal of Pharmacology*, *122*(6), 1244–1250. https://doi.org/10.1038/SJ.BJP.0701523

Gao, X., & Hannoush, R. N. (2014). Method for cellular imaging of palmitoylated proteins with clickable probes and proximity ligation applied to hedgehog, tubulin, and ras. *Journal of the American Chemical Society*, *136*(12), 4544–4550. https://doi.org/10.1021/ja410068g

Gao, X., & Hannoush, R. N. (2018). A Decade of Click Chemistry in Protein Palmitoylation: Impact on Discovery and New Biology. *Cell Chemical Biology*, *25*(3), 236–246. https://doi.org/10.1016/j.chembiol.2017.12.002

Garcia-Menendez, L., Karamanlidis, G., Kolwicz, S., & Tian, R. (2013). Substrain specific response to cardiac pressure overload in C57BL/6 mice. *American Journal of Physiology - Heart and Circulatory Physiology*, *305*(3), H397. https://doi.org/10.1152/AJPHEART.00088.2013

Gaspar, R., Lund, M., Sparr, E., & Linse, S. (2020). Anomalous Salt Dependence Reveals an Interplay of Attractive and Repulsive Electrostatic Interactions in α-synuclein Fibril Formation. *QRB Discovery*, *1*. https://doi.org/10.1017/QRD.2020.7

Gaur, N., Qi, X. Y., Benoist, D., Bernus, O., Coronel, R., Nattel, S., & Vigmond, E. J. (2021). A computational model of pig ventricular cardiomyocyte electrophysiology and calcium handling: Translation from pig to human electrophysiology. *PLOS Computational Biology*, *17*(6), e1009137. https://doi.org/10.1371/JOURNAL.PCBI.1009137

Gautel, M., Zuffardi, O., Freiburg, A., & Labeit, S. (1995). Phosphorylation switches specific for the cardiac isoform of myosin binding protein-C: a modulator of cardiac contraction? *The EMBO Journal*, *14*(9), 1952–1960. https://doi.org/10.1002/j.1460-2075.1995.tb07187.x

Ge, Y., Rybakova, I. N., Xu, Q., & Moss, R. L. (2009). Top-down high-resolution mass spectrometry of cardiac myosin binding protein C revealed that truncation alters protein phosphorylation state. *Proceedings of the National Academy of Sciences of the United States of America*, *106*(31), 12658–12663. https://doi.org/10.1073/PNAS.0813369106/SUPPL_FILE/0813369106SI.PDF

Gedicke-Hornung, C., Behrens-Gawlik, V., Reischmann, S., Geertz, B., Stimpel, D., Weinberger, F., Schlossarek, S., Précigout, G., Braren, I., Eschenhagen, T., Mearini, G., Lorain, S., Voit, T., Dreyfus, P. A., Garcia, L., & Carrier, L.

(2013). Rescue of cardiomyopathy through U7snRNA-mediated exon skipping in Mybpc3-targeted knock-in mice. *EMBO Molecular Medicine*, *5*(7), 1060. https://doi.org/10.1002/EMMM.201202168

Geiss-Friedlander, R., & Melchior, F. (2007). Concepts in sumoylation: a decade on. *Nature Reviews Molecular Cell Biology 2007 8:12*, *8*(12), 947–956. https://doi.org/10.1038/nrm2293

George, K. S., & Wu, S. (2012). Lipid Raft: A Floating Island Of Death or Survival. *Toxicology and Applied Pharmacology*, *259*(3), 311. https://doi.org/10.1016/J.TAAP.2012.01.007

Giles, J., Patel, J. R., Miller, A., Iverson, E., Fitzsimons, D., & Moss, R. L. (2019). Recovery of left ventricular function following in vivo reexpression of cardiac myosin binding protein C. *Journal of General Physiology*, *151*(1), 77–89. https://doi.org/10.1085/jgp.201812238

Glatz, J. F. C., Luiken, J. J. F. P., & Nabben, M. (2020). CD36 (SR-B2) as a Target to Treat Lipid Overload-Induced Cardiac Dysfunction. *Journal of Lipid and Atherosclerosis*, *9*(1), 66–78. https://doi.org/10.12997/JLA.2020.9.1.66

Glazier, A. A., Thompson, A., & Day, S. M. (2019). Allelic imbalance and haploinsufficiency in MYBPC3-linked hypertrophic cardiomyopathy. *Pflugers Archiv European Journal of Physiology*, *471*(5), 781–793. https://doi.org/10.1007/s00424-018-2226-9

Gök, C., Plain, F., Robertson, A. D., Howie, J., Baillie, G. S., Fraser, N. J., & Fuller, W. (2020). Dynamic Palmitoylation of the Sodium-Calcium Exchanger Modulates Its Structure, Affinity for Lipid-Ordered Domains, and Inhibition by XIP Palmitoylation modifies NCX1 XIP affinity and hence regulates intracellular Ca Dynamic Palmitoylation of the Sodium-C. *CellReports*, *31*, 107697. https://doi.org/10.1016/j.celrep.2020.107697

Goldhaber, J. I., & Hamilton, M. A. (2010). The Role of Inotropic Agents in the Treatment of Heart Failure. *Circulation*, *121*(14), 1655. https://doi.org/10.1161/CIRCULATIONAHA.109.899294

Gołebiowski, F., Szulc, A., Sakowicz, M., Szutowicz, A., & Pawełczyk, T. (2003). Expression level of Ubc9 protein in rat tissues. *Acta Biochimica Polonica*, *50*(4), 1065–1073. https://doi.org/0350041065

Goodwin, J. S., Drake, K. R., Rogers, C., Wright, L., Lippincott-Schwartz, J., Philips, M. R., & Kenworthy, A. K. (2005). Depalmitoylated Ras traffics to and from the Golgi complex via a nonvesicular pathway. *The Journal of Cell Biology*, *170*(2), 261. https://doi.org/10.1083/JCB.200502063

Goonasekera, S. A., Hammer, K., Auger-Messier, M., Bodi, I., Chen, X., Zhang, H., Reiken, S., Elrod, J. W., Correll, R. N., York, A. J., Sargent, M. A., Hofmann, F., Moosmang, S., Marks, A. R., Houser, S. R., Bers, D. M., & Molkentin, J. D. (2012). Decreased cardiac L-type Ca^{2+} channel activity induces hypertrophy and heart failure in mice. *The Journal of Clinical Investigation*, *122*(1), 280–290. https://doi.org/10.1172/JCI58227

Gould, N. S., Evans, P., Martínez-Acedo, P., Marino, S. M., Gladyshev, V. N., Carroll, K. S., & Ischiropoulos, H. (2015). Site-Specific Proteomic Mapping Identifies Selectively Modified Regulatory Cysteine Residues in Functionally Distinct Protein Networks. *Chemistry & Biology*, *22*(7), 965–975. https://doi.org/10.1016/J.CHEMBIOL.2015.06.010

Govindan, S., McElligott, A., Muthusamy, S., Nair, N., Barefield, D., Martin, J. L., Gongora, E., Greis, K. D., Luther, P. K., Winegrad, S., Henderson, K. K., & Sadayappan, S. (2012). Cardiac myosin binding protein-C is a potential diagnostic biomarker for myocardial infarction. *Journal of Molecular and*

Cellular Cardiology, *52*(1), 154–164. https://doi.org/10.1016/j.yjmcc.2011.09.011

Govindan, S., Sarkey, J., Ji, X., Sundaresan, N. R., Gupta, M. P., de Tombe, P. P., & Sadayappan, S. (2012). Pathogenic properties of the N-terminal region of cardiac myosin binding protein-C in vitro. *Journal of Muscle Research and Cell Motility*, *33*(1), 17–30. https://doi.org/10.1007/S10974-012-9292-Y

Granger, A., Abdullah, I., Huebner, F., Stout, A., Wang, T., Huebner, T., Epstein, J. A., & Gruber, P. J. (2008). Histone deacetylase inhibition reduces myocardial ischemia-reperfusion injury in mice. *FASEB Journal : Official Publication of the Federation of American Societies for Experimental Biology*, *22*(10), 3549–3560. https://doi.org/10.1096/FJ.08-108548

Granzier, H. L., & Irving, T. C. (1995). Passive tension in cardiac muscle: contribution of collagen, titin, microtubules, and intermediate filaments. *Biophysical Journal*, *68*(3), 1027. https://doi.org/10.1016/S0006-3495(95)80278-X

Green, E. M., Wakimoto, H., Anderson, R. L., Evanchik, M. J., Gorham, J. M., Harrison, B. C., Henze, M., Kawas, R., Oslob, J. D., Rodriguez, H. M., Song, Y., Wan, W., Leinwand, L. A., Spudich, J. A., McDowell, R. S., Seidman, J. G., & Seidman, C. E. (2016). A small-molecule inhibitor of sarcomere contractility suppresses hypertrophic cardiomyopathy in mice. *Science (New York, N.Y.)*, *351*(6273), 617. https://doi.org/10.1126/SCIENCE.AAD3456

Gross, S. M., & Lehman, S. L. (2013). Accessibility of Myofilament Cysteines and Effects on ATPase Depend on the Activation State during Exposure to Oxidants. *PLOS ONE*, *8*(7), e69110. https://doi.org/10.1371/JOURNAL.PONE.0069110

Gruen, M., & Gautel, M. (1999). Mutations in β-myosin S2 that cause familial hypertrophic cardiomyopathy (FHC) abolish the interaction with the regulatory domain of myosin-binding protein-C. *Journal of Molecular Biology*, *286*(3), 933–949. https://doi.org/10.1006/jmbi.1998.2522

Gruen, M., Prinz, H., & Gautel, M. (1999). cAPK-phosphorylation controls the interaction of the regulatory domain of cardiac myosin binding protein C with myosin-S2 in an on-off fashion. *FEBS Letters*, *453*(3), 254–259. https://doi.org/10.1016/S0014-5793(99)00727-9

Guan, X., & Fierke, C. A. (2011). Understanding Protein Palmitoylation: Biological Significance and Enzymology. *Science China. Chemistry*, *54*(12), 1888. https://doi.org/10.1007/S11426-011-4428-2

Guhathakurta, P., Prochniewicz, E., & Thomas, D. D. (2015). Amplitude of the actomyosin power stroke depends strongly on the isoform of the myosin essential light chain. *Proceedings of the National Academy of Sciences of the United States of America*, *112*(15), 4660–4665. https://doi.org/10.1073/PNAS.1420101112/SUPPL_FILE/PNAS.201420101SI.PDF

Gupta, M. K., Gulick, J., James, J., Osinska, H., Lorenz, J. N., & Robbins, J. (2013). Functional dissection of myosin binding protein C phosphorylation. *Journal of Molecular and Cellular Cardiology*, *64*, 39–50. https://doi.org/10.1016/j.yjmcc.2013.08.006

Gupta, M. K., Gulick, J., Liu, R., Wang, X., Molkentin, J. D., & Robbins, J. (2014). Sumo E2 enzyme UBC9 is required for efficient protein quality control in cardiomyocytes. *Circulation Research*, *115*(8), 721–729. https://doi.org/10.1161/CIRCRESAHA.115.304760

Gupta, M. K., McLendon, P. M., Gulick, J., James, J., Khalili, K., & Robbins, J. (2016). UBC9-Mediated Sumoylation Favorably Impacts Cardiac Function in

Compromised Hearts. *Circulation Research*, *118*(12), 1894–1905. https://doi.org/10.1161/CIRCRESAHA.115.308268

Gupta, M. K., & Robbins, J. (2014). Post-translational control of cardiac hemodynamics through myosin binding protein C. In *Pflugers Archiv European Journal of Physiology* (Vol. 466, Issue 2, pp. 231–236). Pflugers Arch. https://doi.org/10.1007/s00424-013-1377-y

Gupta, M. P., Samant, S. A., Smith, S. H., & Shroff, S. G. (2008). HDAC4 and PCAF bind to cardiac sarcomeres and play a role in regulating myofilament contractile activity. *The Journal of Biological Chemistry*, *283*(15), 10135–10146. https://doi.org/10.1074/JBC.M710277200

Haag, S. M., Gulen, M. F., Reymond, L., Gibelin, A., Abrami, L., Decout, A., Heymann, M., Goot, F. G. van der, Turcatti, G., Behrendt, R., & Ablasser, A. (2018). Targeting STING with covalent small-molecule inhibitors. *Nature 2018 559:7713*, *559*(7713), 269–273. https://doi.org/10.1038/s41586-018-0287-8

Hahn, V. S., Knutsdottir, H., Luo, X., Bedi, K., Margulies, K. B., Haldar, S. M., Stolina, M., Yin, J., Khakoo, A. Y., Vaishnav, J., Bader, J. S., Kass, D. A., & Sharma, K. (2021). Myocardial Gene Expression Signatures in Human Heart Failure with Preserved Ejection Fraction. *Circulation*, 120–134. https://doi.org/10.1161/CIRCULATIONAHA.120.050498

Hanft, L. M., Fitzsimons, D. P., Hacker, T. A., Moss, R. L., & McDonald, K. S. (2021). Cardiac MyBP-C phosphorylation regulates the Frank-Starling relationship in murine hearts. *The Journal of General Physiology*, *153*(7). https://doi.org/10.1085/JGP.202012770

Hannoush, R. N., & Sun, J. (2010). The chemical toolbox for monitoring protein fatty acylation and prenylation. In *Nature Chemical Biology* (Vol. 6, Issue 7, pp. 498–506). Nature Publishing Group. https://doi.org/10.1038/nchembio.388

Hao, J. W., Wang, J., Guo, H., Zhao, Y. Y., Sun, H. H., Li, Y. F., Lai, X. Y., Zhao, N., Wang, X., Xie, C., Hong, L., Huang, X., Wang, H. R., Li, C. bin, Liang, B., Chen, S., & Zhao, T. J. (2020). CD36 facilitates fatty acid uptake by dynamic palmitoylation-regulated endocytosis. *Nature Communications 2020 11:1*, *11*(1), 1–16. https://doi.org/10.1038/s41467-020-18565-8

Harris, S. P., Bartley, C. R., Hacker, T. A., McDonald, K. S., Douglas, P. S., Greaser, M. L., Powers, P. A., & Moss, R. L. (2002). Hypertrophic cardiomyopathy in cardiac myosin binding protein-C knockout mice. *Circulation Research*, *90*(5), 594–601. http://www.ncbi.nlm.nih.gov/pubmed/11909824

Harris, S. P., Belknap, B., van Sciver, R. E., White, H. D., & Galkin, V. E. (2016). C0 and C1 N-terminal Ig domains of myosin binding protein C exert different effects on thin filament activation. *Proceedings of the National Academy of Sciences of the United States of America*, *113*(6), 1558–1563. https://doi.org/10.1073/PNAS.1518891113

Harris, S. P., Rostkova, E., Gautel, M., & Moss, R. L. (2004). Binding of myosin binding protein-C to myosin subfragment S2 affects contractility independent of a tether mechanism. *Circulation Research*, *95*(9), 930–936. https://doi.org/10.1161/01.RES.0000147312.02673.56

Hartzell, H. C., & Titus, L. (1982). Effects of cholinergic and adrenergic agonists on phosphorylation of a 165,000-dalton myofibrillar protein in intact cardiac muscle. *Journal of Biological Chemistry*, *257*(4), 2111–2120.

Hasenfuss, G. (1998). Animal models of human cardiovascular disease, heart failure and hypertrophy. *Cardiovascular Research*, *39*(1), 60–76. https://doi.org/10.1016/S0008-6363(98)00110-2

Hasenfuss, G., Schillinger, W., Lehnart, S. E., Preuss, M., Pieske, B., Maier, L. S., Prestle, J., Minami, K., & Just, H. (1999). Relationship Between Na+-Ca2+–Exchanger Protein Levels and Diastolic Function of Failing Human Myocardium. *Circulation*, *99*(5), 641–648. https://doi.org/10.1161/01.CIR.99.5.641

Hay, R. T. (2005). Review SUMO: A History of Modification. *Molecular Cell*, *18*, 1–12. https://doi.org/10.1016/j.molcel.2005.03.012

Hay, R. T. (2007). SUMO-specific proteases: a twist in the tail. *Trends in Cell Biology*, *17*(8), 370–376. https://doi.org/10.1016/J.TCB.2007.08.002

Heeley, D. A., Moir, A. J. G., & Perry, S. v. (1982). Phosphorylation of tropomyosin during development in mammalian striated muscle. *FEBS Letters*, *146*(1), 115–118. https://doi.org/10.1016/0014-5793(82)80716-3

Hegemann, N., Primessnig, U., Bode, D., Wakula, P., Beindorff, N., Klopfleisch, R., Michalick, L., Grune, J., Hohendanner, F., Messroghli, D., Pieske, B., Kuebler, W. M., & Heinzel, F. R. (2021). Right-ventricular dysfunction in HFpEF is linked to altered cardiomyocyte Ca 2+ homeostasis and myofilament sensitivity. *ESC Heart Failure*, *8*(4), 3130–3144. https://doi.org/10.1002/EHF2.13419

Hendriks, I. A., Lyon, D., Su, D., Skotte, N. H., Daniel, J. A., Jensen, L. J., & Nielsen, M. L. (2018). Site-specific characterization of endogenous SUMOylation across species and organs. *Nature Communications*, *9*(1). https://doi.org/10.1038/s41467-018-04957-4

Hendriks, I. A., & Vertegaal, A. C. O. (2016). A comprehensive compilation of SUMO proteomics. *Nature Reviews Molecular Cell Biology*, *17*(9), 581–595. https://doi.org/10.1038/nrm.2016.81

Henis, Y. I., Hancock, J. F., & Prior, I. A. (2009). Ras acylation, compartmentalization and signaling nanoclusters (Review). *Molecular Membrane Biology*, *26*(1), 80–92. https://doi.org/10.1080/09687680802649582

Hernandez, O. M., Jones, M., Guzman, G., & Szczesna-Cordary, D. (2007). Myosin essential light chain in health and disease. *American Journal of Physiology - Heart and Circulatory Physiology*, *292*(4), 1643–1654. https://doi.org/10.1152/AJPHEART.00931.2006/ASSET/IMAGES/LARGE/ZH40030773280006.JPEG

Herzog, W. (2018). The multiple roles of titin in muscle contraction and force production. *Biophysical Reviews*, *10*(4), 1187. https://doi.org/10.1007/S12551-017-0395-Y

Hilgmann, D. W., Fine, M., Linder, M. E., Jennings, B. C., Lin, M.-J. J., Hilgemann, D. W., Fine, M., Linder, M. E., Jennings, B. C., & Lin, M.-J. J. (2013). Massive endocytosis triggered by surface membrane palmitoylation under mitochondrial control in BHK fibroblasts. *ELife*, *2013*(2), e01293. https://doi.org/10.7554/eLife.01293

Ho, G. P. H., Selvakumar, B., Mukai, J., Hester, L. D., Wang, Y., Gogos, J. A., & Snyder, S. H. (2011). S-Nitrosylation and S-Palmitoylation Reciprocally Regulate Synaptic Targeting of PSD-95. *Neuron*, *71*(1), 131. https://doi.org/10.1016/J.NEURON.2011.05.033

Hofmann, P. A., Criss Hartzell, H., & Moss, R. L. (1991). Alterations in Ca2+ sensitive tension due to partial extraction of C-protein from rat skinned cardiac myocytes and rabbit skeletal muscle fibers. *The Journal of General Physiology*, *97*(6), 1141–1163. https://doi.org/10.1085/JGP.97.6.1141

Hofmann, P. A., Greaser, M. L., & Moss, R. L. (1991). C-protein limits shortening velocity of rabbit skeletal muscle fibres at low levels of Ca2+ activation.

The Journal of Physiology, *439*, 701–715. http://www.ncbi.nlm.nih.gov/pubmed/1895247

Hogg, N., Broniowska, K. A., Novalija, J., Kettenhofen, N. J., & Novalija, E. (2007). Role of S-nitrosothiol transport in the cardioprotective effects of S-nitrosocysteine in rat hearts. *Free Radical Biology & Medicine*, *43*(7), 1086–1094. https://doi.org/10.1016/J.FREERADBIOMED.2007.06.016

Hotz, P. W., Wiesnet, M., Tascher, G., Braun, T., Müller, S., & Mendler, L. (2020). Profiling the Murine SUMO Proteome in Response to Cardiac Ischemia and Reperfusion Injury. *Molecules (Basel, Switzerland)*, *25*(23). https://doi.org/10.3390/MOLECULES25235571

Hou, L., Kumar, M., Anand, P., Chen, Y., El-Bizri, N., Pickens, C. J., Seganish, W. M., Sadayappan, S., & Swaminath, G. (2022). Modulation of myosin by cardiac myosin binding protein-C peptides improves cardiac contractility in ex-vivo experimental heart failure models. *Scientific Reports 2022 12:1*, *12*(1), 1–14. https://doi.org/10.1038/s41598-022-08169-1

Howie, J., Reilly, L., Fraser, N. J., Walker, J. M. V., Wypijewski, K. J., Ashford, M. L. J., Calaghan, S. C., McClafferty, H., Tian, L., Shipston, M. J., Boguslavskyi, A., Shattock, M. J., & Fuller, W. (2014). Substrate recognition by the cell surface palmitoyl transferase DHHC5. *Proceedings of the National Academy of Sciences of the United States of America*, *111*(49), 17534–17539. https://doi.org/10.1073/pnas.1413627111

Howie, J., Swarbrick, J., Shattock, M., & Fuller, W. (2013). *Metabolic stress alters the balance between palmitoylation and glutathionylation of the Na pump regulatory protein phospholemman - The Physiological Society (2013)*.

Howie, J., Tulloch, L. B., Shattock, M. J., & Fuller, W. (2013). Regulation of the cardiac Na(+) pump by palmitoylation of its catalytic and regulatory subunits. *Biochemical Society Transactions*, *41*(1), 95–100. https://doi.org/10.1042/BST20120269

Howie, J., Wypijewski, K. J., Plain, F., Tulloch, L. B., Fraser, N. J., & Fuller, W. (2018). Greasing the wheels or a spanner in the works? Regulation of the cardiac sodium pump by palmitoylation. *Critical Reviews in Biochemistry and Molecular Biology*, *53*(2), 175–191. https://doi.org/10.1080/10409238.2018.1432560

Hsieh, Y. L., Kuo, H. Y., Chang, C. C., Naik, M. T., Liao, P. H., Ho, C. C., Huang, T. C., Jeng, J. C., Hsu, P. H., Tsai, M. D., Huang, T. H., & Shih, H. M. (2013). Ubc9 acetylation modulates distinct SUMO target modification and hypoxia response. *The EMBO Journal*, *32*(6), 791. https://doi.org/10.1038/EMBOJ.2013.5

Hu, W., Xu, T., Wu, P., Pan, D., Chen, J., Chen, J., Zhang, B., Zhu, H., & Li, D. (2017). Luteolin improves cardiac dysfunction in heart failure rats by regulating sarcoplasmic reticulum Ca 2+-ATPase 2a. *Scientific Reports*, *7*. https://doi.org/10.1038/SREP41017

Huke, S., & Knollmann, B. C. (2010). Increased Myofilament Ca2+-Sensitivity and Arrhythmia Susceptibility. *Journal of Molecular and Cellular Cardiology*, *48*(5), 824. https://doi.org/10.1016/J.YJMCC.2010.01.011

Impens, F., Radoshevich, L., Cossart, P., & Ribet, D. (2014). Mapping of SUMO sites and analysis of SUMOylation changes induced by external stimuli. *Proceedings of the National Academy of Sciences of the United States of America*, *111*(34), 12432–12437. https://doi.org/10.1073/PNAS.1413825111/SUPPL_FILE/PNAS.1413825111.SD04.XLS

Inchingolo, A. v, Previs, S. B., Previs, M. J., Warshaw, D. M., & Kad, N. M. (2019). Revealing the mechanism of how cardiac myosin-binding protein C

N-terminal fragments sensitize thin filaments for myosin binding. *Proceedings of the National Academy of Sciences of the United States of America*, *116*(14), 6828–6835. https://doi.org/10.1073/pnas.1816480116

Irving, T. C., Konhilas, J., Perry, D., Fischetti, R., & de Tombe, P. P. (2000). Myofilament lattice spacing as a function of sarcomere length in isolated rat myocardium. *American Journal of Physiology. Heart and Circulatory Physiology*, *279*(5). https://doi.org/10.1152/AJPHEART.2000.279.5.H2568

Iyer, A., Chan, V., & Brown, L. (2010). The DOCA-Salt Hypertensive Rat as a Model of Cardiovascular Oxidative and Inflammatory Stress. *Current Cardiology Reviews*, *6*(4), 291. https://doi.org/10.2174/157340310793566109

Jacques, A. M., Copeland, O., Messer, A. E., Gallon, C. E., King, K., McKenna, W. J., Tsang, V. T., & Marston, S. B. (2008). Myosin binding protein C phosphorylation in normal, hypertrophic and failing human heart muscle. *Journal of Molecular and Cellular Cardiology*, *45*(2), 209–216. https://doi.org/10.1016/J.YJMCC.2008.05.020

Jakobs, A., Himstedt, F., Funk, M., Korn, B., Gaestel, M., & Niedenthal, R. (2007). Ubc9 fusion-directed SUMOylation identifies constitutive and inducible SUMOylation. *Nucleic Acids Research*, *35*(17), 1–8. https://doi.org/10.1093/nar/gkm617

Janssen, P. M. L., & Periasamy, M. (2007). Determinants of Frequency Dependent Contraction and Relaxation of Mammalian Myocardium. *Journal of Molecular and Cellular Cardiology*, *43*(5), 523. https://doi.org/10.1016/J.YJMCC.2007.08.012

Jennings, B. C., Nadolski, M. J., Ling, Y., Baker, M. B., Harrison, M. L., Deschenes, R. J., & Linder, M. E. (2009). 2-bromopalmitate and 2-(2-hydroxy-5-nitro-benzylidene)-benzo[b] thiophen-3-one inhibit DHHC-mediated palmitoylation in vitro. *Journal of Lipid Research*, *50*(2), 233–242. https://doi.org/10.1194/jlr.M800270-JLR200

Jeong, E. M., Monasky, M. M., Gu, L., Taglieri, D. M., Patel, B. G., Liu, H., Wang, Q., Greener, I., Dudley, S. C., & Solaro, R. J. (2013). Tetrahydrobiopterin improves diastolic dysfunction by reversing changes in myofilament properties. *Journal of Molecular and Cellular Cardiology*, *56*(1), 44. https://doi.org/10.1016/J.YJMCC.2012.12.003

Jiang, M., Hu, J., White, F. K. H., Williamson, J., Klymchenko, A. S., Murthy, A., Workman, S. W., & Tseng, G. N. (2019). S-Palmitoylation of junctophilin-2 is critical for its role in tethering the sarcoplasmic reticulum to the plasma membrane. *The Journal of Biological Chemistry*, *294*(36), 13487–13501. https://doi.org/10.1074/JBC.RA118.006772

Johns, E. C., Simnett, S. J., Mulligan, I. P., & Ashley, C. C. (1997). Troponin I phosphorylation does not increase the rate of relaxation following laser flash photolysis of diazo-2 in guinea-pig skinned trabeculae. *Pflügers Archiv 1997 433:6*, *433*(6), 842–844. https://doi.org/10.1007/S004240050353

Joung, H., Kwon, S., Kim, K. H., Lee, Y. G., Shin, S., Kwon, D. H., Lee, Y. U., Kook, T., Choe, N., Kim, J. C., Kim, Y. K., Eom, G. H., & Kook, H. (2018). Sumoylation of histone deacetylase 1 regulates MyoD signaling during myogenesis. *Experimental & Molecular Medicine*, *50*(1), e427. https://doi.org/10.1038/EMM.2017.236

Kachooei, E., Cordina, N. M., Potluri, P. R., Guse, J. A., McCamey, D., & Brown, L. J. (2021). Phosphorylation of Troponin I finely controls the positioning of Troponin for the optimal regulation of cardiac muscle contraction. *Journal of Molecular and Cellular Cardiology*, *150*, 44–53. https://doi.org/10.1016/J.YJMCC.2020.10.007

Kaier, T. E., Twerenbold, R., Puelacher, C., Marjot, J., Imambaccus, N., Boeddinghaus, J., Nestelberger, T., Badertscher, P., Sabti, Z., Giménez, M. R., Wildi, K., Hillinger, P., Grimm, K., Loeffel, S., Shrestha, S., Widmer, D. F., Cupa, J., Kozhuharov, N., Miró, Ò., … Mueller, C. (2017). Direct Comparison of Cardiac Myosin-Binding Protein C With Cardiac Troponins for the Early Diagnosis of Acute Myocardial Infarction. *Circulation*, *136*(16), 1495–1508. https://doi.org/10.1161/CIRCULATIONAHA.117.028084

Kamitani, T., Kito, K., Nguyen, H. P., Fukuda-Kamitani, T., & Yeh, E. T. H. (1998). Characterization of a Second Member of the Sentrin Family of Ubiquitin-like Proteins. *Journal of Biological Chemistry*, *273*(18), 11349–11353. https://doi.org/10.1074/JBC.273.18.11349

Kampourakis, T., Ponnam, S., Sun, Y. B., Sevrieva, I., & Irving, M. (2018). Structural and functional effects of myosin-binding protein-C phosphorylation in heart muscle are not mimicked by serine-to-aspartate substitutions. *Journal of Biological Chemistry*, *293*(37), 14270–14275. https://doi.org/10.1074/jbc.AC118.004816

Kampourakis, T., Sun, Y. B., & Irving, M. (2016). Myosin light chain phosphorylation enhances contraction of heart muscle via structural changes in both thick and thin filaments. *Proceedings of the National Academy of Sciences of the United States of America*, *113*(21), E3039–E3047. https://doi.org/10.1073/PNAS.1602776113

Kang, R., Wan, J., Arstikaitis, P., Takahashi, H., Huang, K., Bailey, A. O., Thompson, J. X., Roth, A. F., Drisdel, R. C., Mastro, R., Green, W. N., Yates, J. R., Davis, N. G., & El-Husseini, A. (2008). Neural palmitoyl-proteomics reveals dynamic synaptic palmitoylation. In *Nature* (Vol. 456, Issue 7224, pp. 904–909). Nature Publishing Group. https://doi.org/10.1038/nature07605

Kapplinger, J. D., Tester, D. J., Salisbury, B. A., Carr, J. L., Harris-Kerr, C., Pollevick, G. D., Wilde, A. A. M., & Ackerman, M. J. (2009). Spectrum and prevalence of mutations from the first 2,500 consecutive unrelated patients referred for the FAMILION® long QT syndrome genetic test. *Heart Rhythm : The Official Journal of the Heart Rhythm Society*, *6*(9), 1297. https://doi.org/10.1016/J.HRTHM.2009.05.021

Kass, D. A., Bronzwaer, J. G. F., & Paulus, W. J. (2004). What mechanisms underlie diastolic dysfunction in heart failure? *Circulation Research*, *94*(12), 1533–1542. https://doi.org/10.1161/01.RES.0000129254.25507.d6

Kawamoto, H., Nakamura, K., Yamamoto, J., Iwasaki, T., & Ohyanagi, M. (1994). Increased levels of inhibitory G protein in myocardium with heart failure. *Japanese Circulation Journal*, *58*(12), 913–924. https://doi.org/10.1253/JCJ.58.913

Kawas, R. F., Anderson, R. L., Bartholomew Ingle, S. R., Song, Y., Sran, A. S., & Rodriguez, H. M. (2017). A small-molecule modulator of cardiac myosin acts on multiple stages of the myosin chemomechanical cycle. *The Journal of Biological Chemistry*, *292*(40), 16571–16577. https://doi.org/10.1074/JBC.M117.776815

Kennington, E. J., Fuller, W., & Shattock, M. J. (2006). Characterisation of the Langendorff-perfused phospholemman knockout mouse heart: Effects of calcium concentration and pacing rate on contractility. *Journal of Molecular and Cellular Cardiology*, *40*(6), 996. https://doi.org/10.1016/J.YJMCC.2006.03.224

Kensler, R. W., Shaffer, J. F., & Harris, S. P. (2011). Binding of the N-terminal fragment C0-C2 of cardiac MyBP-C to cardiac F-actin. *Journal of Structural Biology*, *174*(1), 44–51. https://doi.org/10.1016/j.jsb.2010.12.003

Kerr, M., Dennis, K. M. J. H., Carr, C. A., Fuller, W., Berridge, G., Rohling, S., Aitken, C. L., Lopez, C., Fischer, R., Miller, J. J., Clarke, K., Tyler, D. J., & Heather, L. C. (2021). Diabetic mitochondria are resistant to palmitoyl CoA inhibition of respiration, which is detrimental during ischemia. *FASEB Journal : Official Publication of the Federation of American Societies for Experimental Biology*, *35*(8). https://doi.org/10.1096/FJ.202100394R

Kerscher, O. (2007). SUMO junction—what's your function? New insights through SUMO-interacting motifs. *EMBO Reports*, *8*(6), 550. https://doi.org/10.1038/SJ.EMBOR.7400980

Kettlewell, S., Burton, F. L., Smith, G. L., & Workman, A. J. (2013). Chronic myocardial infarction promotes atrial action potential alternans, afterdepolarizations, and fibrillation. *Cardiovascular Research*, *99*(1), 215–224. https://doi.org/10.1093/cvr/cvt087

Kettlewell, S., Seidler, T., & Smith, G. L. (2009). The effects of over-expression of the FK506-binding protein FKBP12.6 on K(+) currents in adult rabbit ventricular myocytes. *Pflugers Archiv : European Journal of Physiology*, *458*(4), 653–660. https://doi.org/10.1007/s00424-009-0666-y

Keung, E. C. (1989). Calcium current is increased in isolated adult myocytes from hypertrophied rat myocardium. *Circulation Research*, *64*(4), 753–763. https://doi.org/10.1161/01.RES.64.4.753

Khan, M. A., Hashim, M. J., Mustafa, H., Baniyas, M. Y., Suwaidi, S. K. B. M. al, AlKatheeri, R., Alblooshi, F. M. K., Almatrooshi, M. E. A. H., Alzaabi, M. E. H., Darmaki, R. S. al, & Lootah, S. N. A. H. (2020). Global Epidemiology of Ischemic Heart Disease: Results from the Global Burden of Disease Study. *Cureus*, *12*(7). https://doi.org/10.7759/CUREUS.9349

Kho, C., Lee, A., Jeong, D., Oh, J. G., Chaanine, A. H., Kizana, E., Park, W. J., & Hajjar, R. J. (2011). SUMO1-dependent modulation of SERCA2a in heart failure. *Nature*, *477*(7366), 601–605. https://doi.org/10.1038/nature10407

Kho, C., Lee, A., Jeong, D., Oh, J. G., Gorski, P. A., Fish, K., Sanchez, R., Devita, R. J., Christensen, G., Dahl, R., & Hajjar, R. J. (2015). Small-molecule activation of SERCA2a SUMOylation for the treatment of heart failure. *Nature Communications*, *6*(1), 1–11. https://doi.org/10.1038/ncomms8229

Kilkenny, C., Browne, W. J., Cuthill, I. C., Emerson, M., & Altman, D. G. (2010). Improving Bioscience Research Reporting: The ARRIVE Guidelines for Reporting Animal Research. *PLoS Biology*, *8*(6), e1000412. https://doi.org/10.1371/journal.pbio.1000412

Kim, E. T., Kim, K. K., Matunis, M. J., & Ahn, J. H. (2009). Enhanced SUMOylation of proteins containing a SUMO-interacting motif by SUMO-Ubc9 fusion. *Biochemical and Biophysical Research Communications*, *388*(1), 41–45. https://doi.org/10.1016/j.bbrc.2009.07.103

Kim, E. Y., Zhang, Y., Ye, B., Segura, A. M., Beketaev, I., Xi, Y., Yu, W., Chang, J., Li, F., & Wang, J. (2015). Involvement of activated SUMO-2 conjugation in cardiomyopathy. *Biochimica et Biophysica Acta*, *1852*(7), 1388–1399. https://doi.org/10.1016/J.BBADIS.2015.03.013

King, J., & Lowery, D. R. (2021). Physiology, Cardiac Output. *StatPearls*. https://www.ncbi.nlm.nih.gov/books/NBK470455/

Knipscheer, P., Flotho, A., Klug, H., Olsen, J. v., van Dijk, W. J., Fish, A., Johnson, E. S., Mann, M., Sixma, T. K., & Pichler, A. (2008). Ubc9 sumoylation regulates SUMO target discrimination. *Molecular Cell*, *31*(3), 371–382. https://doi.org/10.1016/J.MOLCEL.2008.05.022

Ko, P., & Dixon, S. J. (2018). Protein palmitoylation and cancer. *EMBO Reports*, *19*(10). https://doi.org/10.15252/EMBR.201846666

Kobayashi, T., Jin, L., & de Tombe, P. P. (2008). Cardiac thin filament regulation. *Pflugers Archiv : European Journal of Physiology*, *457*(1), 37. https://doi.org/10.1007/S00424-008-0511-8

Konhilas, J. P., Irving, T. C., & de Tombe, P. P. (2002). Myofilament Calcium Sensitivity in Skinned Rat Cardiac Trabeculae. *Circulation Research*, *90*(1), 59–65. https://doi.org/10.1161/HH0102.102269

Konstam, M. A., Kramer, D. G., Patel, A. R., Maron, M. S., & Udelson, J. E. (2011). Left Ventricular Remodeling in Heart Failure. *JACC: Cardiovascular Imaging*, *4*(1), 98–108. https://doi.org/10.1016/j.jcmg.2010.10.008

Kooij, V., Boontje, N., Zaremba, R., Jaquet, K., Remedios, C. dos, Stienen, G. J. M., & van der Velden, J. (2010). Protein kinase C α and ε phosphorylation of troponin and myosin binding protein C reduce Ca2+ sensitivity in human myocardium. *Basic Research in Cardiology*, *105*(2), 289–300. https://doi.org/10.1007/S00395-009-0053-Z/FIGURES/6

Kooij, V., Holewinski, R. J., Murphy, A. M., & van Eyk, J. E. (2013). Characterization of the cardiac myosin binding protein-C phosphoproteome in healthy and failing human hearts. *Journal of Molecular and Cellular Cardiology*, *60*, 116–120. https://doi.org/10.1016/j.yjmcc.2013.04.012

Korte, F. S., McDonald, K. S., Harris, S. P., & Moss, R. L. (2003). Loaded Shortening, Power Output, and Rate of Force Redevelopment Are Increased With Knockout of Cardiac Myosin Binding Protein-C. *Circulation Research*, *93*(8), 752–758. https://doi.org/10.1161/01.RES.0000096363.85588.9A

Koster, K. P., & Yoshii, A. (2019). Depalmitoylation by Palmitoyl-Protein Thioesterase 1 in Neuronal Health and Degeneration. *Frontiers in Synaptic Neuroscience*, *11*(AUG), 25. https://doi.org/10.3389/FNSYN.2019.00025

Kostiuk, M. A., Corvi, M. M., Keller, B. O., Plummer, G., Prescher, J. A., Hangauer, M. J., Bertozzi, C. R., Rajaiah, G., Falck, J. R., & Berthiaume, L. G. (2008). Identification of palmitoylated mitochondrial proteins using a bio-orthogonal azido-palmitate analogue. *The FASEB Journal*, *22*(3), 721–732. https://doi.org/10.1096/fj.07-9199com

Kovács, Á., Kalász, J., Pásztor, E. T., Tóth, A., Papp, Z., Dhalla, N. S., & Barta, J. (2017). Myosin heavy chain and cardiac troponin T damage is associated with impaired myofibrillar ATPase activity contributing to sarcomeric dysfunction in Ca2+-paradox rat hearts. *Molecular and Cellular Biochemistry*, *430*(1–2), 57–68. https://doi.org/10.1007/S11010-017-2954-8/FIGURES/6

Krüger, M., & Linke, W. A. (2006). Protein kinase-A phosphorylates titin in human heart muscle and reduces myofibrillar passive tension. *Journal of Muscle Research and Cell Motility*, *27*(5–7), 435–444. https://doi.org/10.1007/S10974-006-9090-5

Krysiak, J., Unger, A., Beckendorf, L., Hamdani, N., von Frieling-Salewsky, M., Redfield, M. M., dos Remedios, C. G., Sheikh, F., Gergs, U., Boknik, P., & Linke, W. A. (2018). Protein phosphatase 5 regulates titin phosphorylation and function at a sarcomere-associated mechanosensor complex in cardiomyocytes. *Nature Communications 2018 9:1*, *9*(1), 1–14. https://doi.org/10.1038/s41467-017-02483-3

Kulikovskaya, I., McClellan, G., Flavigny, J., Carrier, L., & Winegrad, S. (2003). Effect of MyBP-C Binding to Actin on Contractility in Heart Muscle. *The Journal of General Physiology*, *122*(6), 761. https://doi.org/10.1085/JGP.200308941

Kumar, M., Govindan, S., Zhang, M., Khairallah, R. J., Martin, J. L., Sadayappan, S., & de Tombe, P. P. (2015). Cardiac Myosin-binding Protein C and Troponin-I Phosphorylation Independently Modulate Myofilament Length-

dependent Activation. *The Journal of Biological Chemistry*, *290*(49), 29241–29249. https://doi.org/10.1074/JBC.M115.686790

Kumar, M., Haghighi, K., Kranias, E. G., & Sadayappan, S. (2020). Phosphorylation of cardiac myosin–binding protein-C contributes to calcium homeostasis. *Journal of Biological Chemistry*, *295*(32), 11275–11291. https://doi.org/10.1074/JBC.RA120.013296

Kümmel, D., Heinemann, U., & Veit, M. (2006). Unique self-palmitoylation activity of the transport protein particle component Bet3: A mechanism required for protein stability. *Proceedings of the National Academy of Sciences of the United States of America*, *103*(34), 12701–12706. https://doi.org/10.1073/pnas.0603513103

Kunst, G., Kress, K. R., Gruen, M., Uttenweiler, D., Gautel, M., & Fink, R. H. A. (2000). Myosin binding protein C, a phosphorylation-dependent force regulator in muscle that controls the attachment of myosin heads by its interaction with myosin S2. *Circulation Research*, *86*(1), 51–58. https://doi.org/10.1161/01.RES.86.1.51

Kuster, D. W. D., Bawazeer, A. C., Zaremba, R., Goebel, M., Boontje, N. M., & van der Velden, J. (2012). Cardiac myosin binding protein C phosphorylation in cardiac disease. *Journal of Muscle Research and Cell Motility*, *33*(1), 43–52. https://doi.org/10.1007/s10974-011-9280-7

Kuster, D. W. D., Govindan, S., Springer, T. I., Martin, J. L., Finley, N. L., & Sadayappan, S. (2015). A hypertrophic cardiomyopathy-associated MYBPC3 mutation common in populations of South Asian descent causes contractile dysfunction. *Journal of Biological Chemistry*, *290*(9), 5855–5867. https://doi.org/10.1074/jbc.M114.607911

Kuster, D. W. D., Sequeira, V., Najafi, A., Boontje, N. M., Wijnker, P. J. M., Rosalie Witjas-Paalberends, E., Marston, S. B., dos Remedios, C. G., Carrier, L., Demmers, J. A. A., Redwood, C., Sadayappan, S., & van der Velden, J. (2013). GSK3ß phosphorylates newly identified site in the proline-alanine-rich region of cardiac myosin-binding protein C and alters cross-bridge cycling kinetics in human: Short communication. *Circulation Research*, *112*(4), 633–639. https://doi.org/10.1161/CIRCRESAHA.112.275602

Kwak, H. J., Park, K. M., Choi, H. E., Chung, K. S., Lim, H. J., & Park, H. Y. (2008). PDE4 inhibitor, roflumilast protects cardiomyocytes against NO-induced apoptosis via activation of PKA and Epac dual pathways. *Cellular Signalling*, *20*(5), 803–814. https://doi.org/10.1016/J.CELLSIG.2007.12.011

Lam, C. S. P., Arnott, C., Beale, A. L., Chandramouli, C., Hilfiker-Kleiner, D., Kaye, D. M., Ky, B., Santema, B. T., Sliwa, K., & Voors, A. A. (2019). Sex differences in heart failure. *European Heart Journal*, *40*(47), 3859–3868c. https://doi.org/10.1093/EURHEARTJ/EHZ835

Lam, M. L., Bartoli, M., & Claycomb, W. C. (2001). The 21-day postnatal rat ventricular cardiac muscle cell in culture as an experimental model to study adult cardiomyocyte gene expression. *Molecular and Cellular Biochemistry*, *000*, 0–000.

Lamberts, R., van der Velden, J., & Stienen, G. (2008). Force-frequency relation and myofilament Ca2+ sensitivity. *Physiology News*, *Summer 2008*, 39–41. https://doi.org/10.36866/PN.71.39

Lamoliatte, F., Caron, D., Durette, C., Mahrouche, L., Maroui, M. A., Caron-Lizotte, O., Bonneil, E., Chelbi-Alix, M. K., & Thibault, P. (2014). Large-scale analysis of lysine SUMOylation by SUMO remnant immunoaffinity profiling. *Nature Communications 2014 5:1*, *5*(1), 1–11. https://doi.org/10.1038/ncomms6409

Lan, T., Delalande, C., & Dickinson, B. C. (2021). Inhibitors of DHHC family proteins. *Current Opinion in Chemical Biology*, *65*, 118–125. https://doi.org/10.1016/J.CBPA.2021.07.002

Landim-Vieira, M., Childers, M. C., Wacker, A. L., Garcia, M. R., He, H., Singh, R., Brundage, E. A., Johnston, J. R., Whitson, B. A., Chase, P. B., Janssen, P. M. L., Regnier, M., Biesiadecki, B. J., Pinto, J. R., & Parvatiyar, M. S. (2021). Post-translational modification patterns on β-myosin heavy chain are altered in ischemic and non-ischemic human hearts. *BioRxiv*, 2021.11.21.469462. https://doi.org/10.1101/2021.11.21.469462

Le, N. T., Martin, J. F., Fujiwara, K., & Abe, J. ichi. (2017). Sub-cellular localization specific SUMOylation in the heart☆. *Biochimica et Biophysica Acta*, *1863*(8), 2041. https://doi.org/10.1016/J.BBADIS.2017.01.018

Lee, A., Jeong, D., Mitsuyama, S., Oh, J. G., Liang, L., Ikeda, Y., Sadoshima, J., Hajjar, R. J., & Kho, C. (2014). The Role of SUMO-1 in Cardiac Oxidative Stress and Hypertrophy. *Antioxidants & Redox Signaling*, *21*(14), 1986. https://doi.org/10.1089/ARS.2014.5983

Lee, K., Harris, S. P., Sadayappan, S., & Craig, R. (2015). Orientation of Myosin Binding Protein C in the Cardiac Muscle Sarcomere Determined by Domain-Specific Immuno-EM. *Journal of Molecular Biology*, *427*(2), 274. https://doi.org/10.1016/J.JMB.2014.10.023

Lee, Y. ja, Mou, Y., Maric, D., Klimanis, D., Auh, S., & Hallenbeck, J. M. (2011). Elevated Global SUMOylation in Ubc9 Transgenic Mice Protects Their Brains against Focal Cerebral Ischemic Damage. *PLOS ONE*, *6*(10), e25852. https://doi.org/10.1371/JOURNAL.PONE.0025852

Lemonidis, K., MacLeod, R., Baillie, G. S., & Chamberlain, L. H. (2017). Peptide array-based screening reveals a large number of proteins interacting with the ankyrin-repeat domain of the zDHHC17 S-acyltransferase. *Journal of Biological Chemistry*, *292*(42), 17190–17202. https://doi.org/10.1074/JBC.M117.799650/ATTACHMENT/4517BD20-B805-43D7-9F43-AD23693FC679/MMC1.ZIP

Levental, I., Grzybek, M., & Simons, K. (2010). Greasing their way: Lipid modifications determine protein association with membrane rafts. In *Biochemistry* (Vol. 49, Issue 30, pp. 6305–6316). UTC. https://doi.org/10.1021/bi100882y

Levental, I., Lingwood, D., Grzybek, M., Coskun, Ü., & Simons, K. (2010). Palmitoylation regulates raft affinity for the majority of integral raft proteins. *Proceedings of the National Academy of Sciences of the United States of America*, *107*(51), 22050–22054. https://doi.org/10.1073/PNAS.1016184107/SUPPL_FILE/PNAS.1016184107_SI.PDF

Li, J., Mamidi, R., Doh, C. Y., Holmes, J. B., Bharambe, N., Ramachandran, R., & Stelzer, J. E. (2020). AAV9 gene transfer of cMyBPC N-terminal domains ameliorates cardiomyopathy in cMyBPC-deficient mice. *JCI Insight*, *5*(17). https://doi.org/10.1172/JCI.INSIGHT.130182

Li, K. L., Methawasin, M., Tanner, B. C. W., Granzier, H. L., Solaro, R. J., & Dong, W. J. (2019). Sarcomere length–dependent effects on Ca2+-troponin regulation in myocardium expressing compliant titin. *Journal of General Physiology*, *151*(1), 30–41. https://doi.org/10.1085/JGP.201812218

Li, M., Xu, X., Chang, C. W., & Liu, Y. (2020). TRIM28 functions as the SUMO E3 ligase for PCNA in prevention of transcription induced DNA breaks. *Proceedings of the National Academy of Sciences of the United States of America*, *117*(38), 23588–23596.

https://doi.org/10.1073/PNAS.2004122117/SUPPL_FILE/PNAS.2004122117.SAPP.PDF

Li, X., Shen, L., Xu, Z., Liu, W., Li, A., & Xu, J. (2022). Protein Palmitoylation Modification During Viral Infection and Detection Methods of Palmitoylated Proteins. *Frontiers in Cellular and Infection Microbiology*, *12*, 45. https://doi.org/10.3389/FCIMB.2022.821596/BIBTEX

Li, X., Wang, W., Wang, S., Shen, Y., Pan, J., Dong, X., & Li, S. (2022). The Solubility and Structures of Porcine Myofibrillar Proteins under Low-Salt Processing Conditions as Affected by the Presence of L-Lysine. *Foods (Basel, Switzerland)*, *11*(6). https://doi.org/10.3390/FOODS11060855

Li, Y., Hu, J., Höfer, K., Wong, A. M. S., Cooper, J. D., Birnbaum, S. G., Hammer, R. E., & Hofmann, S. L. (2010). DHHC5 interacts with PDZ domain 3 of post-synaptic density-95 (PSD-95) protein and plays a role in learning and memory. *Journal of Biological Chemistry*, *285*(17), 13022–13031. https://doi.org/10.1074/jbc.M109.079426

Li, Y., Martin, B. R., Cravatt, B. F., & Hofmann, S. L. (2012). DHHC5 Protein Palmitoylates Flotillin-2 and Is Rapidly Degraded on Induction of Neuronal Differentiation in Cultured Cells. *The Journal of Biological Chemistry*, *287*(1), 523. https://doi.org/10.1074/JBC.M111.306183

Liang, Y. C., Lee, C. C., Yao, Y. L., Lai, C. C., Schmitz, M. L., & Yang, W. M. (2016). SUMO5, a Novel Poly-SUMO Isoform, Regulates PML Nuclear Bodies. *Scientific Reports*, *6*. https://doi.org/10.1038/SREP26509

Liao, Y., Asakura, M., Takashima, S., Ogai, A., Asano, Y., Asanuma, H., Minamino, T., Tomoike, H., Hori, M., & Kitakaze, M. (2005). Benidipine, a long-acting calcium channel blocker, inhibits cardiac remodeling in pressure-overloaded mice. *Cardiovascular Research*, *65*(4), 879–888. https://doi.org/10.1016/J.CARDIORES.2004.11.006

Lin, B., Govindan, S., Lee, K., Zhao, P., Han, R., Runte, K. E., Craig, R., Palmer, B. M., & Sadayappan, S. (2013). Cardiac Myosin Binding Protein-C Plays No Regulatory Role in Skeletal Muscle Structure and Function. *PLoS ONE*, *8*(7), e69671. https://doi.org/10.1371/journal.pone.0069671

Lin, D. T. S., & Conibear, E. (2015). Enzymatic protein depalmitoylation by acyl protein thioesterases. *Biochemical Society Transactions*, *43*(2), 193–198. https://doi.org/10.1042/BST20140235

Lin, M. J., Fine, M., Lu, J. Y., Hofmann, S. L., Frazier, G., & Hilgemann, D. W. (2013). Massive palmitoylation-dependent endocytosis during reoxygenation of anoxic cardiac muscle. *ELife*, *2013*(2), 1295. https://doi.org/10.7554/eLife.01295

Linder, M. E., & Deschenes, R. J. (2003). New insights into the mechanisms of protein palmitoylation. *Biochemistry*, *42*(15), 4317–4320. https://doi.org/10.1021/BI034159A

Linder, M. E., Middleton, P., Hepler, J. R., Taussig, R., Gilman, A. G., & Mumby, S. M. (1993). Lipid modifications of G proteins: alpha subunits are palmitoylated. *Proceedings of the National Academy of Sciences of the United States of America*, *90*(8), 3675. https://doi.org/10.1073/PNAS.90.8.3675

Ling, J. (2021). *Can SUMOylation of the Beta-2-Adrenergic receptor influence cell signalling and cardiac myocyte physiology?* [University of Glasgow]. https://doi.org/10.5525/GLA.THESIS.82652

Litwin, S. E., & Bridge, J. H. B. (1997). Enhanced Na+-Ca2+ Exchange in the Infarcted Heart. *Circulation Research*, *81*(6), 1083–1093. https://doi.org/10.1161/01.RES.81.6.1083

Liu, G., Papa, A., Katchman, A. N., Zakharov, S. I., Roybal, D., Hennessey, J. A., Kushner, J., Yang, L., Chen, B. X., Kushnir, A., Dangas, K., Gygi, S. P., Pitt, G. S., Colecraft, H. M., Ben-Johny, M., Kalocsay, M., & Marx, S. O. (2020). Mechanism of adrenergic CaV1.2 stimulation revealed by proximity proteomics. *Nature*, *577*(7792), 695. https://doi.org/10.1038/S41586-020-1947-Z

Liu, J., García-Cardeña, G., & Sessa, W. C. (1996). Palmitoylation of endothelial nitric oxide synthase is necessary for optimal stimulated release of nitric oxide: Implications for caveolae localization. *Biochemistry*, *35*(41), 13277–13281. https://doi.org/10.1021/bi961720e

Liu, R., Wang, D., Shi, Q., Fu, Q., Hizon, S., & Xiang, Y. K. (2012). Palmitoylation Regulates Intracellular Trafficking of β2 Adrenergic Receptor/Arrestin/Phosphodiesterase 4D Complexes in Cardiomyocytes. *PLoS ONE*, *7*(8). https://doi.org/10.1371/JOURNAL.PONE.0042658

Lobo, S., Greentree, W. K., Linder, M. E., & Deschenes, R. J. (2002). Identification of a Ras palmitoyltransferase in Saccharomyces cerevisiae. *The Journal of Biological Chemistry*, *277*(43), 41268–41273. https://doi.org/10.1074/jbc.M206573200

Loisel, T. P., Adam, L., Hebert, T. E., & Bouvier, M. (1996). Agonist stimulation increases the turnover rate of beta 2AR-bound palmitate and promotes receptor depalmitoylation. *Biochemistry*, *35*(49), 15923–15932. https://doi.org/10.1021/BI9611321

Loisel, T. P., Ansanay, H., Adam, L., Marullo, S., Seifert, R., Lagacé, M., & Bouvier, M. (1999). Activation of the beta(2)-adrenergic receptor-Galpha(s) complex leads to rapid depalmitoylation and inhibition of repalmitoylation of both the receptor and Galpha(s). *The Journal of Biological Chemistry*, *274*(43), 31014–31019. https://doi.org/10.1074/JBC.274.43.31014

Loosen, S. H., Roderburg, C., Curth, O., Gaensbacher, J., Joerdens, M., Luedde, T., Konrad, M., Kostev, K., & Luedde, M. (2022). The spectrum of comorbidities at the initial diagnosis of heart failure a case control study. *Scientific Reports 2022 12:1*, *12*(1), 1–8. https://doi.org/10.1038/s41598-022-06618-5

López-Bote, C. (2017). Chemical and Biochemical Constitution of Muscle. *Lawrie's Meat Science: Eighth Edition*, 99–158. https://doi.org/10.1016/B978-0-08-100694-8.00004-2

Lord, C. C., Thomas, G., & Brown, J. M. (2013). Mammalian alpha beta hydrolase domain (ABHD) proteins: lipid metabolizing enzymes at the interface of cell signaling and energy metabolism. *Biochimica et Biophysica Acta*, *1831*(4), 792. https://doi.org/10.1016/J.BBALIP.2013.01.002

Lorent, J. H., Diaz-Rohrer, B., Lin, X., Spring, K., Gorfe, A. A., Levental, K. R., & Levental, I. (2017). Structural determinants and functional consequences of protein affinity for membrane rafts. *Nature Communications 2017 8:1*, *8*(1), 1–10. https://doi.org/10.1038/s41467-017-01328-3

LoRusso, S. M., Imanaka-Yoshida, K., Shuman, H., Sanger, J. M., & Sanger, J. W. (1992). Incorporation of fluorescently labeled contractile proteins into freshly isolated living adult cardiac myocytes. *Cell Motility and the Cytoskeleton*, *21*(2), 111–122. https://doi.org/10.1002/CM.970210204

Loscalzo, J., & Welch, G. (1995). Nitric oxide and its role in the cardiovascular system. *Progress in Cardiovascular Diseases*, *38*(2), 87–104. https://doi.org/10.1016/S0033-0620(05)80001-5

Lovelock, J. D., Monasky, M. M., Jeong, E. M., Lardin, H. A., Liu, H., Patel, B. G., Taglieri, D. M., Gu, L., Kumar, P., Pokhrel, N., Zeng, D., Belardinelli, L., Sorescu, D., Solaro, R. J., & Dudley, S. C. (2012). Ranolazine improves

cardiac diastolic dysfunction through modulation of myofilament calcium sensitivity. *Circulation Research*, *110*(6), 841. https://doi.org/10.1161/CIRCRESAHA.111.258251

Lu, Y., Kwan, A. H., Jeffries, C. M., Guss, J. M., & Trewhella, J. (2012). The motif of human cardiac myosin-binding protein C is required for its Ca2+-dependent interaction with calmodulin. *Journal of Biological Chemistry*, *287*(37), 31596–31607. https://doi.org/10.1074/jbc.M112.383299

Lu, Y., Kwan, A. H., Trewhella, J., & Jeffries, C. M. (2011). The C0C1 fragment of human cardiac myosin binding protein C has common binding determinants for both actin and myosin. *Journal of Molecular Biology*, *413*(5), 908–913. https://doi.org/10.1016/J.JMB.2011.09.026

Luiken, J. J. F. P., Coort, S. L. M., Willems, J., Coumans, W. A., Bonen, A., van der Vusse, G. J., & Glatz, J. F. C. (2003). Contraction-induced fatty acid translocase/CD36 translocation in rat cardiac myocytes is mediated through AMP-activated protein kinase signaling. *Diabetes*, *52*(7), 1627–1634. https://doi.org/10.2337/DIABETES.52.7.1627

Lundby, A., Andersen, M. N., Steffensen, A. B., Horn, H., Kelstrup, C. D., Francavilla, C., Jensen, L. J., Schmitt, N., Thomsen, M. B., & Olsen, J. v. (2013). In vivo phosphoproteomics analysis reveals the cardiac targets of β-adrenergic receptor signaling. *Science Signaling*, *6*(278). https://doi.org/10.1126/SCISIGNAL.2003506

Luther, P. K., Winkler, H., Taylor, K., Zoghbic, M. E., Craig, R., Padrón, R., Squire, J. M., & Liu, J. (2011). Direct visualization of myosin-binding protein C bridging myosin and actin filaments in intact muscle. *Proceedings of the National Academy of Sciences of the United States of America*, *108*(28), 11423–11428. https://doi.org/10.1073/pnas.1103216108

Lymperopoulos, A., Rengo, G., & Koch, W. J. (2013). The Adrenergic Nervous System in Heart Failure: Pathophysiology and Therapy. *Circulation Research*, *113*(6), 739–753. https://doi.org/10.1161/CIRCRESAHA.113.300308

Lynch, T. L., Kumar, M., McNamara, J. W., Kuster, D. W. D., Sivaguru, M., Singh, R. R., Previs, M. J., Lee, K. H., Kuffel, G., Zilliox, M. J., Lin, B. L., Ma, W., Gibson, A. M., Blaxall, B. C., Nieman, M. L., Lorenz, J. N., Leichter, D. M., Leary, O. P., Janssen, P. M. L., … Sadayappan, S. (2021). Amino terminus of cardiac myosin binding protein-C regulates cardiac contractility. *Journal of Molecular and Cellular Cardiology*, *156*, 33–44. https://doi.org/10.1016/J.YJMCC.2021.03.009

Mahé, I., Chassany, O., Grenard, A. S., Caulin, C., & Bergmann, J. F. (2003). Defining the role of calcium channel antagonists in heart failure due to systolic dysfunction. *American Journal of Cardiovascular Drugs : Drugs, Devices, and Other Interventions*, *3*(1), 33–41. https://doi.org/10.2165/00129784-200303010-00004

Main, A., Bogusalvskyii, A., Howie, J., Kuo, C., Rankin, A., Burton, F. L., Smith, G. L., Hajjar, R., Baillie, G. S., Campbell, K. S., Shattock, M. J., & Fuller, W. (2022). zDHHC5 expression is increased in cardiac hypertrophy and reduced in heart failure but this does not correlate with changes in substrate palmitoylation. *BioRxiv*, 2022.08.19.504400. https://doi.org/10.1101/2022.08.19.504400

Main, A., & Fuller, W. (2021). Protein S-Palmitoylation: advances and challenges in studying a therapeutically important lipid modification. *The FEBS Journal*. https://doi.org/10.1111/FEBS.15781

Main, A., Fuller, W., & Baillie, G. S. (2020). Post-translational regulation of cardiac myosin binding protein-C: A graphical review. In *Cellular Signalling*

(Vol. 76, p. 109788). Elsevier Inc. https://doi.org/10.1016/j.cellsig.2020.109788

Main, A., Robertson-Gray, O., & Fuller, W. (2020). Cyclophilin D palmitoylation and permeability transition: a new twist in the tale of myocardial ischaemia–reperfusion injury. *Cardiovascular Research*. https://doi.org/10.1093/cvr/cvaa149

Makaula, S., Lochner, A., Genade, S., Sack, M. N., Awan, M. M., & Opie, L. H. (2005). H-89, a non-specific inhibitor of protein kinase A, promotes post-ischemic cardiac contractile recovery and reduces infarct size. *Journal of Cardiovascular Pharmacology*, *45*(4), 341–347. https://doi.org/10.1097/01.FJC.0000156825.80951.14

Malik, F. I., Hartman, J. J., Elias, K. A., Morgan, B. P., Rodriguez, H., Brejc, K., Anderson, R. L., Sueoka, S. H., Lee, K. H., Finer, J. T., Sakowicz, R., Baliga, R., Cox, D. R., Garard, M., Godinez, G., Kawas, R., Kraynack, E., Lenzi, D., Lu, P. P., … Morgans, D. J. (2011). Cardiac Myosin Activation: A Potential Therapeutic Approach for Systolic Heart Failure. *Science (New York, N.Y.)*, *331*(6023), 1439. https://doi.org/10.1126/SCIENCE.1200113

Mamidi, R., Gresham, K. S., Verma, S., & Stelzer, J. E. (2016). Cardiac Myosin Binding Protein-C Phosphorylation Modulates Myofilament Length-Dependent Activation. *Frontiers in Physiology*, *7*(FEB). https://doi.org/10.3389/FPHYS.2016.00038

Mamidi, R., Holmes, J. B., Doh, C. Y., Dominic, K. L., Madugula, N., & Stelzer, J. E. (2021). cMyBPC phosphorylation modulates the effect of omecamtiv mecarbil on myocardial force generation. *The Journal of General Physiology*, *153*(7). https://doi.org/10.1085/JGP.202012816

Mansor, L. S., Gonzalez, E. R., Cole, M. A., Tyler, D. J., Beeson, J. H., Clarke, K., Carr, C. A., & Heather, L. C. (2013). Cardiac metabolism in a new rat model of type 2 diabetes using high-fat diet with low dose streptozotocin. *Cardiovascular Diabetology*, *12*(1), 136. https://doi.org/10.1186/1475-2840-12-136

Manza, L. L., Codreanu, S. G., Stamer, S. L., Smith, D. L., Wells, K. S., Roberts, R. L., & Liebler, D. C. (2004). Global shifts in protein sumoylation in response to electrophile and oxidative stress. *Chemical Research in Toxicology*, *17*(12), 1706–1715. https://doi.org/10.1021/TX049767L

Maron, B. J., Gardin, J. M., Flack, J. M., Gidding, S. S., Kurosaki, T. T., & Bild, D. E. (1995). Prevalence of hypertrophic cardiomyopathy in a general population of young adults: Echocardiographic analysis of 4111 subjects in the CARDIA study. *Circulation*, *92*(4), 785–789. https://doi.org/10.1161/01.CIR.92.4.785

Marston, S., Copeland, O., Jacques, A., Livesey, K., Tsang, V., McKenna, W. J., Jalilzadeh, S., Carballo, S., Redwood, C., & Watkins, H. (2009). Evidence from human myectomy samples that MYBPC3 mutations cause hypertrophic cardiomyopathy through haploinsufficiency. *Circulation Research*, *105*(3), 219–222. https://doi.org/10.1161/CIRCRESAHA.109.202440

Martin, B. R., & Cravatt, B. F. (2009). Large-scale profiling of protein palmitoylation in mammalian cells. *Nature Methods*, *6*(2), 135–138. https://doi.org/10.1038/nmeth.1293

Martin, B. R., & Lambert, N. A. (2016). Activated G Protein Gαs Samples Multiple Endomembrane Compartments. *The Journal of Biological Chemistry*, *291*(39), 20295. https://doi.org/10.1074/JBC.M116.729731

Martin, B. R., Wang, C., Adibekian, A., Tully, S. E., & Cravatt, B. F. (2012). Global profiling of dynamic protein palmitoylation. *Nature Methods*, *9*(1), 84–89. https://doi.org/10.1038/nmeth.1769

Martin, T. G., Myers, V. D., Dubey, P., Dubey, S., Perez, E., Moravec, C. S., Willis, M. S., Feldman, A. M., & Kirk, J. A. (2021). Cardiomyocyte contractile impairment in heart failure results from reduced BAG3-mediated sarcomeric protein turnover. *Nature Communications 2021 12:1*, *12*(1), 1–16. https://doi.org/10.1038/s41467-021-23272-z

Mary, S., Small, H., Herse, F., Carrick, E., Flynn, A., Mullen, W., Dechend, R., & Delles, C. (2021). Preexisting hypertension and pregnancy-induced hypertension reveal molecular differences in placental proteome in rodents. *Physiological Genomics*, *53*(6), 259. https://doi.org/10.1152/PHYSIOLGENOMICS.00160.2020

Mateja, R. D., & de Tombe, P. P. (2012). Myofilament length-dependent activation develops within 5 ms in guinea-pig myocardium. *Biophysical Journal*, *103*(1). https://doi.org/10.1016/J.BPJ.2012.05.034

Matsuyama, S., Kage, Y., Fujimoto, N., Ushijima, T., Tsuruda, T., Kitamura, K., Shiose, A., Asada, Y., Sumimoto, H., & Takeya, R. (2018). Interaction between cardiac myosin-binding protein C and formin Fhod3. *Proceedings of the National Academy of Sciences of the United States of America*, *115*(19), E4386–E4395. https://doi.org/10.1073/PNAS.1716498115/-/DCSUPPLEMENTAL

McGrath, M. J., Cottle, D. L., Nguyen, M. A., Dyson, J. M., Coghill, I. D., Robinson, P. A., Holdsworth, M., Cowling, B. S., Hardeman, E. C., Mitchell, C. A., & Brown, S. (2006). Four and a half LIM protein 1 binds myosin-binding protein C and regulates myosin filament formation and sarcomere assembly. *The Journal of Biological Chemistry*, *281*(11), 7666–7683. https://doi.org/10.1074/JBC.M512552200

McMurray, J., Packer, M., Desai, A., Gong, J., Lefkowitz, M., Rizkala, A., Rouleau, J., Shi, V., Solomon, S., Swedberg, K., & Zile, M. (2014). Angiotensin-neprilysin inhibition versus enalapril in heart failure. *The New England Journal of Medicine*, *371*(11), 132–133. https://doi.org/10.1056/NEJMOA1409077

McNamara, J. W., Li, A., Lal, S., Bos, J. M., Harris, S. P., van der Velden, J., Ackerman, M. J., Cooke, R., & dos Remedios, C. G. (2017). MYBPC3 mutations are associated with a reduced super-relaxed state in patients with hypertrophic cardiomyopathy. *PloS One*, *12*(6). https://doi.org/10.1371/JOURNAL.PONE.0180064

McNamara, J. W., Li, A., Smith, N. J., Lal, S., Graham, R. M., Kooiker, K. B., van Dijk, S. J., Remedios, C. G. dos, Harris, S. P., & Cooke, R. (2016). Ablation of cardiac myosin binding protein-C disrupts the super-relaxed state of myosin in murine cardiomyocytes. *Journal of Molecular and Cellular Cardiology*, *94*, 65–71. https://doi.org/10.1016/J.YJMCC.2016.03.009

McNamara, J. W., & Sadayappan, S. (2018). Skeletal myosin binding protein-C: an increasingly important regulator of striated muscle physiology. *Archives of Biochemistry and Biophysics*, *660*, 121. https://doi.org/10.1016/J.ABB.2018.10.007

McNamara, J. W., Singh, R. R., & Sadayappan, S. (2019). Cardiac myosin binding protein-C phosphorylation regulates the super-relaxed state of myosin. *Proceedings of the National Academy of Sciences of the United States of America*, *116*(24), 11731–11736. https://doi.org/10.1073/PNAS.1821660116/-/DCSUPPLEMENTAL

Merkulov, S., Chen, X., Chandler, M. P., & Stelzer, J. E. (2012). In vivo cardiac myosin binding protein C gene transfer rescues myofilament contractile dysfiunction in cardiac myosin binding protein C null mice. *Circulation:*

Heart Failure, *5*(5), 635–644. https://doi.org/10.1161/CIRCHEARTFAILURE.112.968941

Messer, A. E., Jacques, A. M., & Marston, S. B. (2007). Troponin phosphorylation and regulatory function in human heart muscle: dephosphorylation of Ser23/24 on troponin I could account for the contractile defect in end-stage heart failure. *Journal of Molecular and Cellular Cardiology*, *42*(1), 247–259. https://doi.org/10.1016/J.YJMCC.2006.08.017

Michalek, A. J., Howarth, J. W., Gulick, J., Previs, M. J., Robbins, J., Rosevear, P. R., & Warshaw, D. M. (2013). Phosphorylation modulates the mechanical stability of the cardiac myosin-binding protein C motif. *Biophysical Journal*, *104*(2), 442–452. https://doi.org/10.1016/J.BPJ.2012.12.021

Michele, D. E., Albayya, P. P., & Metzger, J. M. (1999). Thin Filament Protein Dynamics in Fully Differentiated Adult Cardiac Myocytes: Toward A Model of Sarcomere Maintenance. *The Journal of Cell Biology*, *145*(7), 1483. https://doi.org/10.1083/JCB.145.7.1483

Miles, M. R., Seo, J., Jiang, M., Wilson, Z. T., Little, J., Hao, J., Andrade, J., Ueberheide, B., & Tseng, G. N. (2021). Global identification of S-palmitoylated proteins and detection of palmitoylating (DHHC) enzymes in heart. *Journal of Molecular and Cellular Cardiology*, *155*, 1–9. https://doi.org/10.1016/J.YJMCC.2021.02.007

Miles, M. R., Seo, J., Wilson, Z., Jiang, M., & Tseng, G. (2020). Abstract 15523: Dynamic Protein S-palmitoylation Contributes to Cardiac Remodeling During Aging With Chronic Hypertension. *Circulation*, *142*(Suppl_3). https://doi.org/10.1161/CIRC.142.SUPPL_3.15523

Mitcheson, J. S., Hancox, J. C., & Levi, A. J. (1998). Cultured adult cardiac myocytes: Future applications, culture methods, morphological and electrophysiological properties. *Cardiovascular Research*, *39*(2), 280–300. https://doi.org/10.1016/S0008-6363(98)00128-X/2/39-2-280-FIG10.GIF

Moffett, S., Mouillac, B., Bonin, H., & Bouvier, M. (1993). Altered phosphorylation and desensitization patterns of a human beta 2-adrenergic receptor lacking the palmitoylated Cys341. *The EMBO Journal*, *12*(1), 349–356. https://doi.org/10.1002/J.1460-2075.1993.TB05663.X

Mohamed, A. S., Dignam, J. D., & Schlender, K. K. (1998). Cardiac Myosin-Binding Protein C (MyBP-C): Identification of Protein Kinase A and Protein Kinase C Phosphorylation Sites. *Archives of Biochemistry and Biophysics*, *358*(2), 313–319. https://doi.org/10.1006/abbi.1998.0857

Molina, C. E., Heijman, J., & Dobrev, D. (2016). Differences in Left Versus Right Ventricular Electrophysiological Properties in Cardiac Dysfunction and Arrhythmogenesis. *Arrhythmia & Electrophysiology Review*, *5*(1), 14. https://doi.org/10.15420/AER.2016.8.2

Monteiro da Rocha, A., Guerrero-Serna, G., Helms, A., Luzod, C., Mironov, S., Russell, M., Jalife, J., Day, S. M., Smith, G. D., & Herron, T. J. (2016). Deficient cMyBP-C protein expression during cardiomyocyte differentiation underlies human hypertrophic cardiomyopathy cellular phenotypes in disease specific human ES cell derived cardiomyocytes. *Journal of Molecular and Cellular Cardiology*, *99*, 197–206. https://doi.org/10.1016/J.YJMCC.2016.09.004

Montero-Moran, G., Caviglia, J. M., McMahon, D., Rothenberg, A., Subramanian, V., Xu, Z., Lara-Gonzalez, S., Storch, J., Carman, G. M., & Brasaemle, D. L. (2010). CGI-58/ABHD5 is a coenzyme A-dependent lysophosphatidic acid acyltransferase. *Journal of Lipid Research*, *51*(4), 709. https://doi.org/10.1194/JLR.M001917

Moolman-Smook, J., Flashman, E., de Lange, W., Li, Z., Corfield, V., Redwood, C., & Watkins, H. (2002). Identification of novel interactions between domains of myosin binding protein-C that are modulated by hypertrophic cardiomyopathy missense mutations. *Circulation Research*, *91*(8), 704–711. https://doi.org/10.1161/01.RES.0000036750.81083.83

Moos, C., Mason, C. M., Besterman, J. M., Feng, I. N. M., & Dubin, J. H. (1978). The binding of skeletal muscle C-protein to F-actin, and its relation to the interaction of actin with myosin subfragment-1. *Journal of Molecular Biology*, *124*(4), 571–586. https://doi.org/10.1016/0022-2836(78)90172-9

Moos, C., Offer, G., Starr, R., & Bennett, P. (1975). Interaction of C-protein with myosin, myosin rod and light meromyosin. *Journal of Molecular Biology*, *97*(1). https://doi.org/10.1016/S0022-2836(75)80017-9

Morgan, J. P., Erny, R. E., Allen, P. D., Grossman, W., & Gwathmey, J. K. (1990). Abnormal intracellular calcium handling, a major cause of systolic and diastolic dysfunction in ventricular myocardium from patients with heart failure. *Circulation*, *81*(2 Suppl), III21-32.

Mouton, J., Loos, B., Moolman-Smook, J. C., & Kinnear, C. J. (2015). Ascribing novel functions to the sarcomeric protein, myosin binding protein H (MyBPH) in cardiac sarcomere contraction. *Experimental Cell Research*, *331*(2), 338–351. https://doi.org/10.1016/j.yexcr.2014.11.006

Mun, J. Y., Gulick, J., Robbins, J., Woodhead, J., Lehman, W., & Craig, R. (2011). Electron microscopy and 3D reconstruction of F-actin decorated with cardiac myosin-binding protein C (cMyBP-C). *Journal of Molecular Biology*, *410*(2), 214–225. https://doi.org/10.1016/J.JMB.2011.05.010

Mun, J. Y., Kensler, R. W., Harris, S. P., & Craig, R. (2016). The cMyBP-C HCM variant L348P enhances thin filament activation through an increased shift in tropomyosin position. *Journal of Molecular and Cellular Cardiology*, *91*, 141. https://doi.org/10.1016/J.YJMCC.2015.12.014

Mun, J. Y., Previs, M. J., Yu, H. Y., Gulick, J., Tobacman, L. S., Previs, S. B., Robbins, J., Warshaw, D. M., & Craig, R. (2014). Myosin-binding protein C displaces tropomyosin to activate cardiac thin filaments and governs their speed by an independent mechanism. *Proceedings of the National Academy of Sciences of the United States of America*, *111*(6), 2170–2175. https://doi.org/10.1073/pnas.1316001111

Murthy, A., Workman, S. W., Jiang, M., Hu, J., Sifa, I., Bernas, T., Tang, W., Deschenes, I., & Tseng, G. N. (2019). Dynamic Palmitoylation Regulates Trafficking of K Channel Interacting Protein 2 (KChIP2) across Multiple Subcellular Compartments in Cardiac Myocytes. *Journal of Molecular and Cellular Cardiology*, *135*, 1. https://doi.org/10.1016/J.YJMCC.2019.07.013

Muszbek, L., Haramura, G., Cluette-Brown, J. E., van Cott, E. M., & Laposata, M. (1999). The pool of fatty acids covalently bound to platelet proteins by thioester linkages can be altered by exogenously supplied fatty acids. *Lipids*, *34 Suppl*(1). https://doi.org/10.1007/BF02562334

Myagmar, B. E., Flynn, J. M., Cowley, P. M., Swigart, P. M., Montgomery, M. D., Thai, K., Nair, D., Gupta, R., Deng, D. X., Hosoda, C., Melov, S., Baker, A. J., & Simpson, P. C. (2017). Adrenergic receptors in individual ventricular myocytes: the beta-1 and alpha-1B are in all cells, the alpha-1A is in a subpopulation, and the beta-2 and beta-3 are mostly absent. *Circulation Research*, *120*(7), 1103–1115. https://doi.org/10.1161/CIRCRESAHA.117.310520

Nacerddine, K., Lehembre, F., Bhaumik, M., Artus, J., Cohen-Tannoudji, M., Babinet, C., Pandolfi, P. P., & Dejean, A. (2005). The SUMO pathway is essential for nuclear integrity and chromosome segregation in mice.

Developmental Cell, *9*(6), 769–779. https://doi.org/10.1016/J.DEVCEL.2005.10.007

Nag, S., & Trivedi, D. v. (2021). To lie or not to lie: Super-relaxing with myosins. *ELife*, *10*, 1–21. https://doi.org/10.7554/ELIFE.63703

Nag, S., Trivedi, D. v., Sarkar, S. S., Adhikari, A. S., Sunitha, M. S., Sutton, S., Ruppel, K. M., & Spudich, J. A. (2017). The myosin mesa and the basis of hypercontractility caused by hypertrophic cardiomyopathy mutations. *Nature Structural and Molecular Biology*, *24*(6), 525–533. https://doi.org/10.1038/nsmb.3408

Napierski, N. C., Granger, K., Langlais, P. R., Moran, H. R., Strom, J., Touma, K., & Harris, S. P. (2020). A novel "cut and paste" method for in situ replacement of cMYBP-C reveals a new role for cMYBP-C in the regulation of contractile oscillations. *Circulation Research*, 737–749. https://doi.org/10.1161/CIRCRESAHA.119.315760

Nauta, J. F., Hummel, Y. M., Tromp, J., Ouwerkerk, W., van der Meer, P., Jin, X., Lam, C. S. P., Bax, J. J., Metra, M., Samani, N. J., Ponikowski, P., Dickstein, K., Anker, S. D., Lang, C. C., Ng, L. L., Zannad, F., Filippatos, G. S., van Veldhuisen, D. J., van Melle, J. P., & Voors, A. A. (2020). Concentric vs. eccentric remodelling in heart failure with reduced ejection fraction: clinical characteristics, pathophysiology and response to treatment. *European Journal of Heart Failure*, *22*(7), 1147–1155. https://doi.org/10.1002/EJHF.1632

Nayak, A., Amrute-Nayak, M., Nayak, C. A., & Amrute-Nayak, M. (2020). SUMO system – a key regulator in sarcomere organization. *The FEBS Journal*, *287*(11), 2176–2190. https://doi.org/10.1111/FEBS.15263

Njegic, A., Wilson, C., & Cartwright, E. J. (2020). Targeting Ca2 + Handling Proteins for the Treatment of Heart Failure and Arrhythmias. *Frontiers in Physiology*, *11*, 1068. https://doi.org/10.3389/FPHYS.2020.01068/BIBTEX

Nogueira, L., Figueiredo-Freitas, C., Casimiro-Lopes, G., Magdesian, M. H., Assreuy, J., & Sorenson, M. M. (2009). Myosin is reversibly inhibited by S-nitrosylation. *The Biochemical Journal*, *424*(2), 221–231. https://doi.org/10.1042/BJ20091144

Noritake, J., Fukata, Y., Iwanaga, T., Hosomi, N., Tsutsumi, R., Matsuda, N., Tani, H., Iwanari, H., Mochizuki, Y., Kodama, T., Matsuura, Y., Bredt, D. S., Hamakubo, T., & Fukata, M. (2009). Mobile DHHC palmitoylating enzyme mediates activity-sensitive synaptic targeting of PSD-95. *Journal of Cell Biology*, *186*(1), 147–160. https://doi.org/10.1083/jcb.200903101

Norman, R., Fuller, W., & Calaghan, S. (2018). Caveolae and the cardiac myocyte. *Current Opinion in Physiology*, *1*, 59–67. https://doi.org/10.1016/J.COPHYS.2017.08.005

Oakley, C. E., Hambly, B. D., Curmi, P. M. G., & Brown, L. J. (2004). Myosin binding protein C: structural abnormalities in familial hypertrophic cardiomyopathy. *Cell Research*, *14*(2), 95–110. https://doi.org/10.1038/SJ.CR.7290208

O'Connell, T. D., Jensen, B. C., Baker, A. J., & Simpson, P. C. (2014). Cardiac Alpha1-Adrenergic Receptors: Novel Aspects of Expression, Signaling Mechanisms, Physiologic Function, and Clinical Importance. *Pharmacological Reviews*, *66*(1), 308. https://doi.org/10.1124/PR.112.007203

Offer, G., Moos, C., & Starr, R. (1973). A new protein of the thick filaments of vertebrate skeletal myofibrils. Extraction, purification and characterization. *Journal of Molecular Biology*, *74*(4), 653–676. https://doi.org/10.1016/0022-2836(73)90055-7

Oh, J. G., Watanabe, S., Lee, A., Gorski, P. A., Lee, P., Jeong, D., Liang, L., Liang, Y., Baccarini, A., Sahoo, S., Brown, B. D., Hajjar, R. J., & Kho, C. (2018). miR-146a Suppresses SUMO1 Expression and Induces Cardiac Dysfunction in Maladaptive Hypertrophy. *Circulation Research*, *123*(6), 673–685. https://doi.org/10.1161/CIRCRESAHA.118.312751

O'Hayre, M., Degese, M. S., & Gutkind, J. S. (2014). Novel insights into G protein and G protein-coupled receptor signaling in cancer. *Current Opinion in Cell Biology*, *27*(1), 126. https://doi.org/10.1016/J.CEB.2014.01.005

Ohno, Y., Kihara, A., Sano, T., & Igarashi, Y. (2006). Intracellular localization and tissue-specific distribution of human and yeast DHHC cysteine-rich domain-containing proteins. *Biochimica et Biophysica Acta - Molecular and Cell Biology of Lipids*, *1761*(4), 474–483. https://doi.org/10.1016/j.bbalip.2006.03.010

Olivotto, I., Oreziak, A., Barriales-Villa, R., Abraham, T. P., Masri, A., Garcia-Pavia, P., Saberi, S., Lakdawala, N. K., Wheeler, M. T., Owens, A., Kubanek, M., Wojakowski, W., Jensen, M. K., Gimeno-Blanes, J., Afshar, K., Myers, J., Hegde, S. M., Solomon, S. D., Sehnert, A. J., … Yamani, M. (2020). Mavacamten for treatment of symptomatic obstructive hypertrophic cardiomyopathy (EXPLORER-HCM): a randomised, double-blind, placebo-controlled, phase 3 trial. *The Lancet*, *396*(10253), 759–769. https://doi.org/10.1016/S0140-6736(20)31792-X

Otsomaa, L., Levijoki, J., Wohlfahrt, G., Chapman, H., Koivisto, A. P., Syrjänen, K., Koskelainen, T., Peltokorpi, S. E., Finckenberg, P., Heikkilä, A., Abi-Gerges, N., Ghetti, A., Miller, P. E., Page, G., Mervaala, E., Nagy, N., Kohajda, Z., Jost, N., Virág, L., … Papp, J. G. (2020). Discovery and characterization of ORM-11372, a novel inhibitor of the sodium-calcium exchanger with positive inotropic activity. *British Journal of Pharmacology*, *177*(24), 5534. https://doi.org/10.1111/BPH.15257

Owerbach, D., McKay, E. M., Yeh, E. T. H., Gabbay, K. H., & Bohren, K. M. (2005). A proline-90 residue unique to SUMO-4 prevents maturation and sumoylation. *Biochemical and Biophysical Research Communications*, *337*(2), 517–520. https://doi.org/10.1016/J.BBRC.2005.09.090

Pai, P., Shibu, M. A., Chang, R. L., Yang, J. J., Su, C. chi, Lai, C. H., Liao, H. E., Viswanadha, V. P., Kuo, W. W., & Huang, C. Y. (2018). ERβ targets ZAK and attenuates cellular hypertrophy via SUMO-1 modification in H9c2 cells. *Journal of Cellular Biochemistry*, *119*(9), 7855–7864. https://doi.org/10.1002/JCB.27199

Pan, Y., Xiao, Y., Pei, Z., & Cummins, T. R. (2020). S-Palmitoylation of the sodium channel Nav1.6 regulates its activity and neuronal excitability. *The Journal of Biological Chemistry*, *295*(18), 6151–6164. https://doi.org/10.1074/JBC.RA119.012423

Parbhudayal, R. Y., Garra, A. R., Götte, M. J. W., Michels, M., Pei, J., Harakalova, M., Asselbergs, F. W., van Rossum, A. C., van der Velden, J., & Kuster, D. W. D. (2018). Variable cardiac myosin binding protein-C expression in the myofilaments due to MYBPC3 mutations in hypertrophic cardiomyopathy. *Journal of Molecular and Cellular Cardiology*, *123*, 59–63. https://doi.org/10.1016/J.YJMCC.2018.08.023

Parenti, M., Vigano, M. A., Newman, C. M. H., Milligan, G., & Magee, A. I. (1993). A novel N-terminal motif for palmitoylation of G-protein alpha subunits. *Biochemical Journal*, *291*(Pt 2), 349. https://doi.org/10.1042/BJ2910349

Park, D. S., & Fishman, G. I. (2017). Development and Function of the Cardiac Conduction System in Health and Disease. *Journal of Cardiovascular Development and Disease*, *4*(4), 7. https://doi.org/10.3390/jcdd4020007

Patel, B. G., Wilder, T., & John Solaro, R. (2013). Novel control of cardiac myofilament response to calcium by S-glutathionylation at specific sites of myosin binding protein C. *Frontiers in Physiology*, *4*. https://doi.org/10.3389/FPHYS.2013.00336

Pedone, K. H., Bernstein, L. S., Linder, M. E., & Hepler, J. R. (2009). *Analysis of Protein Palmitoylation by Metabolic Radiolabeling Methods* (pp. 1623–1636). Humana Press, Totowa, NJ. https://doi.org/10.1007/978-1-59745-198-7_166

Pedro, M. P., Vilcaes, A. A., Tomatis, V. M., Oliveira, R. G., Gomez, G. A., & Daniotti, J. L. (2013). 2-Bromopalmitate Reduces Protein Deacylation by Inhibition of Acyl-Protein Thioesterase Enzymatic Activities. *PLoS ONE*, *8*(10). https://doi.org/10.1371/journal.pone.0075232

Pei, Z., Xiao, Y., Meng, J., Hudmon, A., & Cummins, T. R. (2016). Cardiac sodium channel palmitoylation regulates channel availability and myocyte excitability with implications for arrhythmia generation. *Nature Communications*, *7*(May). https://doi.org/10.1038/ncomms12035

Pelat, M., Barbe, F., Daveu, C., Ly-Nguyen, L., Lartigue, T., Marque, S., Tavares, G., Ballet, V., Guillon, J. M., Steinmeyer, K., Wirth, K., Gögelein, H., Arndt, P., Rackelmann, N., Weston, J., Bellevergue, P., McCort, G., Trellu, M., Lucats, L., … Chézalviel-Guilbert, F. (2021). SAR340835, a Novel Selective Na +/Ca 2+ Exchanger Inhibitor, Improves Cardiac Function and Restores Sympathovagal Balance in Heart Failure. *The Journal of Pharmacology and Experimental Therapeutics*, *377*(2), 293–304. https://doi.org/10.1124/JPET.120.000238

Pham, T., Zgierski-Johnston, C. M., Tran, K., Taberner, A. J., Loiselle, D. S., & Han, J. C. (2019). Energy expenditure for isometric contractions of right and left ventricular trabeculae over a wide range of frequencies at body temperature. *Scientific Reports*, *9*(1). https://doi.org/10.1038/S41598-019-45273-1

Pieske, B., & Houser, S. R. (2003). [Na+]i handling in the failing human heart. *Cardiovascular Research*, *57*(4), 874–886. https://doi.org/10.1016/S0008-6363(02)00841-6

Pieske, B., Maier, L. S., Bers, D. M., & Hasenfuss, G. (1999). Ca2+ handling and sarcoplasmic reticulum Ca2+ content in isolated failing and nonfailing human myocardium. *Circulation Research*, *85*(1), 38–46. https://doi.org/10.1161/01.RES.85.1.38

Piper, C., Bilger, J., Henrichs, E. M., Schultheiss, H. P., Horstkotte, D., & Doerner, A. (2000). Is myocardial Na+/Ca2+ exchanger transcription a marker for different stages of myocardial dysfunction? Quantitative polymerase chain reaction of the messenger RNA in endomyocardial biopsies of patients with heart failure. *Journal of the American College of Cardiology*, *36*(1), 233–241. https://doi.org/10.1016/S0735-1097(00)00703-8

Piper, H. M., Probst, I., Schwartz, P., Hütter, F. J., & Spieckermann, P. G. (1982). Culturing of calcium stable adult cardiac myocytes. *Journal of Molecular and Cellular Cardiology*, *14*(7), 397–412. https://doi.org/10.1016/0022-2828(82)90171-7

Plain, F., Congreve, S. D., Yee, R. S. Z., Kennedy, J., Howie, J., Kuo, C. W., Fraser, N. J., & Fuller, W. (2017). An amphipathic -helix directs palmitoylation of the large intracellular loop of the sodium/calcium exchanger. *Journal of Biological Chemistry*, *292*(25), 10745–10752. https://doi.org/10.1074/jbc.M116.773945

Plain, F., Howie, J., Kennedy, J., Brown, E., Shattock, M. J., Fraser, N. J., & Fuller, W. (2020). Control of protein palmitoylation by regulating substrate recruitment to a zDHHC-protein acyltransferase. *Communications Biology*, *3*(1). https://doi.org/10.1038/s42003-020-01145-3

Plant, L. D., Marks, J. D., & Goldstein, S. A. (2016). SUMOylation of NaV1.2 channels mediates the early response to acute hypoxia in central neurons. *ELife*, *5*. https://doi.org/10.7554/ELIFE.20054

Plant, L. D., Xiong, D., Romero, J., Dai, H., & Goldstein, S. A. N. (2020). Hypoxia Produces Pro-arrhythmic Late Sodium Current in Cardiac Myocytes by SUMOylation of NaV1.5 Channels. *Cell Reports*, *30*(7), 2225. https://doi.org/10.1016/J.CELREP.2020.01.025

Pohlmann, L., Kröger, I., Vignier, N., Schlossarek, S., Krämer, E., Coirault, C., Sultan, K. R., El-Armouche, A., Winegrad, S., Eschenhagen, T., & Carrier, L. (2007). Cardiac myosin-binding protein C is required for complete relaxation in intact myocytes. *Circulation Research*, *101*(9), 928–938. https://doi.org/10.1161/CIRCRESAHA.107.158774

Pollock, J. D., & Makaryus, A. N. (2019). Physiology, Cardiac Cycle. In *StatPearls*. StatPearls Publishing. http://www.ncbi.nlm.nih.gov/pubmed/29083687

Ponnam, S., & Kampourakis, T. (2022). Microscale thermophoresis suggests a new model of regulation of cardiac myosin function via interaction with cardiac myosin-binding protein C. *The Journal of Biological Chemistry*, *298*(1). https://doi.org/10.1016/J.JBC.2021.101485

Previs, M. J., Beck Previs, S., Gulick, J., Robbins, J., & Warshaw, D. M. (2012). Molecular mechanics of cardiac myosin-binding protein C in native thick filaments. *Science*, *337*(6099), 1215–1218. https://doi.org/10.1126/science.1223602

Previs, M. J., Mun, J. Y., Michalek, A. J., Previs, S. B., Gulick, J., Robbins, J., Warshaw, D. M., & Craig, R. (2016). Phosphorylation and Calcium Antagonistically Tune Myosin-Binding Protein C's Molecular Structure and Function. *Biophysical Journal*, *110*(3), 293a. https://doi.org/10.1016/J.BPJ.2015.11.1583

Psakhye, I., & Jentsch, S. (2012). Protein group modification and synergy in the SUMO pathway as exemplified in DNA repair. *Cell*, *151*(4), 807–820. https://doi.org/10.1016/J.CELL.2012.10.021

Qiu, F., Dong, C., Liu, Y., Shao, X., Huang, D., Han, Y., Wang, B., Liu, Y., Huo, R., Paulo, P., Zhang, Z. R., Zhao, D., & Chu, W. F. (2018). Pharmacological inhibition of SUMO-1 with ginkgolic acid alleviates cardiac fibrosis induced by myocardial infarction in mice. *Toxicology and Applied Pharmacology*, *345*, 1–9. https://doi.org/10.1016/J.TAAP.2018.03.006

Racca, A. W., Klaiman, J. M., Pioner, J. M., Cheng, Y., Beck, A. E., Moussavi-Harami, F., Bamshad, M. J., & Regnier, M. (2016). Contractile properties of developing human fetal cardiac muscle. *The Journal of Physiology*, *594*(2), 437. https://doi.org/10.1113/JP271290

Raeker, M. O., Shavit, J. A., Dowling, J. J., Michele, D. E., & Russell, M. W. (2014). Membrane-myofibril cross-talk in myofibrillogenesis and in muscular dystrophy pathogenesis: lessons from the zebrafish. *Frontiers in Physiology*, *5*. https://doi.org/10.3389/FPHYS.2014.00014

Rahmanseresht, S., Lee, K. H., O'Leary, T. S., McNamara, J. W., Sadayappan, S., Robbins, J., Warshaw, D. M., Craig, R., & Previs, M. J. (2021). The N terminus of myosin-binding protein C extends toward actin filaments in intact cardiac muscle. *The Journal of General Physiology*, *153*(3). https://doi.org/10.1085/JGP.202012726

Rajan, S., Jagatheesan, G., Petrashevskaya, N., Biesiadecki, B. J., Warren, C. M., Riddle, T., Liggett, S., Wolska, B. M., Solaro, R. J., & Wieczorek, D. F. (2019). Tropomyosin pseudo-phosphorylation results in dilated cardiomyopathy. *Journal of Biological Chemistry*, *294*(8), 2913–2923. https://doi.org/10.1074/JBC.RA118.004879/ATTACHMENT/C5B50A81-2572-46E1-98B7-2C0F29351E21/MMC1.ZIP

Ramadan, A. A., Mayilsamy, K., McGill, A. R., Ghosh, A., Giulianotti, M. A., Donow, H. M., Mohapatra, S. S., Mohapatra, S., Chandran, B., Deschenes, R. J., & Roy, A. (2021). Inhibition of SARS-CoV-2 spike protein palmitoylation reduces virus infectivity. *BioRxiv*, 2021.10.07.463402. https://doi.org/10.1101/2021.10.07.463402

Ramazi, S., & Zahiri, J. (2021). Post-translational modifications in proteins: resources, tools and prediction methods. *Database: The Journal of Biological Databases and Curation*, *2021*. https://doi.org/10.1093/DATABASE/BAAB012

Rame, J. E., & Dries, D. L. (2007). Heart failure and cardiac hypertrophy. *Current Treatment Options in Cardiovascular Medicine*, *9*(4), 289–301. https://doi.org/10.1007/S11936-007-0024-3

Ramirez-Correa, G. A., Cortassa, S., Stanley, B., Gao, W. D., & Murphy, A. M. (2010). Calcium Sensitivity, Force Frequency Relationship and Cardiac Troponin I: Critical Role of PKA and PKC Phosphorylation Sites. *Journal of Molecular and Cellular Cardiology*, *48*(5), 943. https://doi.org/10.1016/J.YJMCC.2010.01.004

Rana, M. S., Kumar, P., Lee, C.-J., Verardi, R., Rajashankar, K. R., & Banerjee, A. (2018). Fatty acyl recognition and transfer by an integral membraneS-acyltransferase. *Science (New York, N.Y.)*, *359*(6372), eaao6326. https://doi.org/10.1126/science.aao6326

Rana, M. S., Lee, C. J., & Banerjee, A. (2018). The molecular mechanism of DHHC protein acyltransferases. *Biochemical Society Transactions*, *47*(1), 157–167. https://doi.org/10.1042/BST20180429

Rapundalo, S. T. (1998). Cardiac protein phosphorylation: functional and pathophysiological correlates. *Cardiovascular Research*, *38*(3), 559–588. https://doi.org/10.1016/S0008-6363(98)00063-7

Ratti, J., Rostkova, E., Gautel, M., & Pfuhl, M. (2011). Structure and interactions of myosin-binding protein C domain C0: Cardiac-specific regulation of myosin at its neck? *Journal of Biological Chemistry*, *286*(14), 12650–12658. https://doi.org/10.1074/jbc.M110.156646

Razzaque, M. A., Gupta, M., Osinska, H., Gulick, J., Blaxall, B. C., & Robbins, J. (2013). An Endogenously Produced Fragment of Cardiac Myosin Binding Protein C is Pathogenic and Can Lead to Heart Failure. *Circulation Research*, *113*(5), 553–561. https://doi.org/10.1161/CIRCRESAHA.113.301225

Rech, L., Abdellatif, M., Pöttler, M., Stangl, V., Mabotuwana, N., Hardy, S., & Rainer, P. P. (2022). Small molecule STING inhibition improves myocardial infarction remodeling. *Life Sciences*, *291*, 120263. https://doi.org/10.1016/J.LFS.2021.120263

Reilly, L., Howie, J., Wypijewski, K., Ashford, M. L. J., Hilgemann, D. W., & Fuller, W. (2015). Palmitoylation of the Na/Ca exchanger cytoplasmic loop controls its inactivation and internalization during stress signaling. *FASEB Journal*, *29*(11), 4532–4543. https://doi.org/10.1096/fj.15-276493

Richard, S., Leclercq, F., Lemaire, S., Piot, C., & Nargeot, J. (1998). Ca2+ currents in compensated hypertrophy and heart failure. *Cardiovascular Research*, *37*(2), 300–311. https://doi.org/10.1016/S0008-6363(97)00273-3

Riquelme, C., Barthel, K. K. B., Qin, X. F., & Liu, X. (2006). Ubc9 expression is essential for myotube formation in C2C12. *Experimental Cell Research*, *312*(11), 2132–2141. https://doi.org/10.1016/J.YEXCR.2006.03.016

Risi, C., Belknap, B., Forgacs-Lonart, E., Harris, S. P., Schröder, G. F., White, H. D., & Galkin, V. E. (2018). N-Terminal Domains of Cardiac Myosin Binding Protein C Cooperatively Activate the Thin Filament. *Structure (London, England : 1993)*, *26*(12), 1604-1611.e4. https://doi.org/10.1016/J.STR.2018.08.007

Risi, C. M., Patra, M., Belknap, B., Harris, S. P., White, H. D., & Galkin, V. E. (2021). Interaction of the C2 Ig-like Domain of Cardiac Myosin Binding Protein-C with F-actin. *Journal of Molecular Biology*, *433*(19), 167178. https://doi.org/10.1016/J.JMB.2021.167178

Robinson, P., Griffiths, P. J., Watkins, H., & Redwood, C. S. (2007). Dilated and hypertrophic cardiomyopathy mutations in troponin and alpha-tropomyosin have opposing effects on the calcium affinity of cardiac thin filaments. *Circulation Research*, *101*(12), 1266–1273. https://doi.org/10.1161/CIRCRESAHA.107.156380

Rocks, O., Peyker, A., Kahms, M., Verveer, P. J., Koerner, C., Lumbierres, M., Kuhlmann, J., Waldmann, H., Wittinghofer, A., & Bastiaens, P. I. H. (2005). An acylation cycle regulates localization and activity of palmitoylated Ras isoforms. *Science (New York, N.Y.)*, *307*(5716), 1746–1752. https://doi.org/10.1126/SCIENCE.1105654

Rosas, P. C., Warren, C. M., Creed, H. A., Trzeciakowski, J. P., Solaro, R. J., & Tong, C. W. (2019). Cardiac Myosin Binding Protein-C Phosphorylation Mitigates Age-Related Cardiac Dysfunction: Hope for Better Aging? *JACC: Basic to Translational Science*, *4*(7), 817. https://doi.org/10.1016/J.JACBTS.2019.06.003

Rosas-Acosta, G., Russell, W. K., Deyrieux, A., Russell, D. H., & Wilson, V. G. (2005). A universal strategy for proteomic studies of SUMO and other ubiquitin-like modifiers. *Molecular & Cellular Proteomics : MCP*, *4*(1), 56. https://doi.org/10.1074/MCP.M400149-MCP200

Roth, A. F., Wan, J., Bailey, A. O., Sun, B., Kuchar, J. A., Green, W. N., Phinney, B. S., Yates, J. R., & Davis, N. G. (2006). Global Analysis of Protein Palmitoylation in Yeast. *Cell*, *125*(5), 1003–1013. https://doi.org/10.1016/j.cell.2006.03.042

Rottbauer, W., Gautel, M., Zehelein, J., Labeit, S., Franz, W. M., Fischer, C., Vollrath, B., Mall, G., Dietz, R., Kübler, W., & Katus, H. A. (1997). Novel splice donor site mutation in the cardiac myosin-binding protein-C gene in familial hypertrophic cardiomyopathy. Characterization Of cardiac transcript and protein. *Journal of Clinical Investigation*, *100*(2), 475. https://doi.org/10.1172/JCI119555

Rougier, J. S., Albesa, M., & Abriel, H. (2010). Ubiquitylation and SUMOylation of cardiac ion channels. *Journal of Cardiovascular Pharmacology*, *56*(1), 22–28. https://doi.org/10.1097/FJC.0B013E3181DAAFF9

Roux, K. J., Kim, D. I., Burke, B., & May, D. G. (2018). BioID: A Screen for Protein-Protein Interactions. *Current Protocols in Protein Science*, *91*(1), 19.23.1. https://doi.org/10.1002/CPPS.51

Rudd, A. K., Brea, R. J., & Devaraj, N. K. (2018). Amphiphile-Mediated Depalmitoylation of Proteins in Living Cells. *Journal of the American Chemical Society*, *140*(50), 17374–17378. https://doi.org/10.1021/JACS.8B10806/SUPPL_FILE/JA8B10806_SI_002.AVI

Rybakova, I. N., Greaser, M. L., & Moss, R. L. (2011). Myosin binding protein C interaction with actin: characterization and mapping of the binding site.

The Journal of Biological Chemistry, *286*(3), 2008–2016. https://doi.org/10.1074/JBC.M110.170605

Rybin, V. O., Grabham, P. W., Elouardighi, H., Steinberg, S. F., & Elouar-Dighi, H. (2003). Caveolae-associated proteins in cardiomyocytes: caveolin-2 expression and interactions with caveolin-3. *Am J Physiol Heart Circ Physiol*, *285*, 325–332. https://doi.org/10.1152/ajpheart.00946.2002

Sadayappan, S., & de Tombe, P. P. (2012). Cardiac myosin binding protein-C: redefining its structure and function. *Biophysical Reviews*, *4*(2), 93–106. https://doi.org/10.1007/s12551-012-0067-x

Sadayappan, S., Gulick, J., Osinska, H., Barefield, D., Cuello, F., Avkiran, M., Lasko, V. M., Lorenz, J. N., Maillet, M., Martin, J. L., Brown, J. H., Bers, D. M., Molkentin, J. D., James, J., & Robbins, J. (2011). A Critical Function for Ser-282 in Cardiac Myosin Binding Protein-C Phosphorylation and Cardiac Function. *Circulation Research*, *109*(2), 141–150. https://doi.org/10.1161/CIRCRESAHA.111.242560

Sadayappan, S., Gulick, J., Osinska, H., Martin, L. A., Hahn, H. S., Dorn, G. W., Klevitsky, R., Seidman, C. E., Seidman, J. G., & Robbins, J. (2005). Cardiac Myosin-Binding Protein-C Phosphorylation and Cardiac Function. *Circulation Research*, *97*(11), 1156–1163. https://doi.org/10.1161/01.RES.0000190605.79013.4d

Sadayappan, S., Osinska, H., Klevitsky, R., Lorenz, J. N., Sargent, M., Molkentin, J. D., Seidman, C. E., Seidman, J. G., & Robbins, J. (2006). Cardiac myosin binding protein C phosphorylation is cardioprotective. *Proceedings of the National Academy of Sciences of the United States of America*, *103*(45), 16918–16923. https://doi.org/10.1073/pnas.0607069103

Sahota, V. K., Grau, B. F., Mansilla, A., & Ferrús, A. (2009). Troponin I and Tropomyosin regulate chromosomal stability and cell polarity. *Journal of Cell Science*, *122*(15), 2623–2631. https://doi.org/10.1242/JCS.050880

Salaun, C., Greaves, J., & Chamberlain, L. H. (2010). The intracellular dynamic of protein palmitoylation. *The Journal of Cell Biology*, *191*(7), 1229. https://doi.org/10.1083/JCB.201008160

Salaun, C., Takizawa, H., Galindo, A., Munro, K. R., McLellan, J., Sugimoto, I., Okino, T., Tomkinson, N. C. O., & Chamberlain, L. H. (2022). Development of a novel high-throughput screen for the identification of new inhibitors of protein S-acylation. *BioRxiv*, 2022.03.17.484726. https://doi.org/10.1101/2022.03.17.484726

Samant, S. A., Pillai, V. B., Sundaresan, N. R., Shroff, S. G., & Gupta, M. P. (2015). Histone Deacetylase 3 (HDAC3)-dependent Reversible Lysine Acetylation of Cardiac Myosin Heavy Chain Isoforms Modulates Their Enzymatic and Motor Activity *. *Journal of Biological Chemistry*, *290*(25), 15559–15569. https://doi.org/10.1074/JBC.M115.653048

Samavarchi-Tehrani, P., Abdouni, H., Knight, J. D., Astori, A., Samson, R., Lin, Z.-Y., Kim, D.-K., Knapp, J. J., St-Germain, J., Go, C. D., Larsen, B., Wong, C. J., Cassonnet, P., Demeret, C., Jacob, Y., Roth, F. P., Raught, B., & Gingras, A.-C. (2020). A SARS-CoV-2 – host proximity interactome. *BioRxiv*, 2020.09.03.282103. https://doi.org/10.1101/2020.09.03.282103

Sanbe, A., James, J., Tuzcu, V., Nas, S., Martin, L., Gulick, J., Osinska, H., Sakthivel, S., Klevitsky, R., Ginsburg, K. S., Bers, D. M., Zinman, B., Lakatta, E. G., & Robbins, J. (2005). Transgenic rabbit model for human troponin I-based hypertrophic cardiomyopathy. *Circulation*, *111*(18), 2330–2338. https://doi.org/10.1161/01.CIR.0000164234.24957.75

Sarge, K. D., & Park-Sarge, O. K. (2009). Detection of Proteins Sumolyated In Vivo and In Vitro. *Methods in Molecular Biology (Clifton, N.J.)*, *590*, 265. https://doi.org/10.1007/978-1-60327-378-7_17

Sarikas, A., Carrier, L., Schenke, C., Doll, D., Flavigny, J., Lindenberg, K. S., Eschenhagen, T., & Zolk, O. (2005). Impairment of the ubiquitin-proteasome system by truncated cardiac myosin binding protein C mutants. *Cardiovascular Research*, *66*(1), 33–44. https://doi.org/10.1016/J.CARDIORES.2005.01.004

Sarkar, S. S., Trivedi, D. v., Morck, M. M., Adhikari, A. S., Pasha, S. N., Ruppel, K. M., & Spudich, J. A. (2020). The hypertrophic cardiomyopathy mutations R403Q and R663H increase the number of myosin heads available to interact with actin. *Science Advances*, *6*(14). https://doi.org/10.1126/SCIADV.AAX0069

Schianchi, F., Glatz, J. F. C., Gascon, A. N., Nabben, M., Neumann, D., & Luiken, J. J. F. P. (2020). Putative Role of Protein Palmitoylation in Cardiac Lipid-Induced Insulin Resistance. *International Journal of Molecular Sciences*, *21*(24), 1–26. https://doi.org/10.3390/IJMS21249438

Schillinger, W., & Kögler, H. (2003). Altered phosphorylation and Ca2+-sensitivity of myofilaments in human heart failure. *Cardiovascular Research*, *57*(1), 5–7. https://doi.org/10.1016/S0008-6363(02)00743-5

Schlender, K. K., Hegazy, M. G., & Thysseril, T. J. (1987). Dephosphorylation of cardiac myofibril C-protein by protein phosphatase 1 and protein phosphatase 2A. *Biochimica et Biophysica Acta*, *928*(3), 312–319. https://doi.org/10.1016/0167-4889(87)90191-1

Schlesinger, M. J., Magee, A. I., & Schmidt, M. F. G. (1980). Fatty acid acylation of proteins in cultured cells. *Journal of Biological Chemistry*, *255*(21), 10021–10024. https://doi.org/10.1016/S0021-9258(19)70417-7

Schlossarek, S., Mearini, G., & Carrier, L. (2011). Cardiac myosin-binding protein C in hypertrophic cardiomyopathy: Mechanisms and therapeutic opportunities. *Journal of Molecular and Cellular Cardiology*, *50*(4), 613–620. https://doi.org/10.1016/j.yjmcc.2011.01.014

Schmidt, J. W., & Catterall, W. A. (1987). Palmitylation, sulfation, and glycosylation of the alpha subunit of the sodium channel. Role of post-translational modifications in channel assembly. *The Journal of Biological Chemistry*, *262*(28), 13713–13723.

Schober, T., Huke, S., Venkataraman, R., Gryshchenko, O., Kryshtal, D., Hwang, H. S., Baudenbacher, F. J., & Knollmann, B. C. (2012). Myofilament Ca sensitization increases cytosolic Ca binding affinity, alters intracellular Ca homeostasis and causes pause-dependent Ca triggered arrhythmia. *Circulation Research*, *111*(2), 170. https://doi.org/10.1161/CIRCRESAHA.112.270041

Schröder, F., Handrock, R., Beuckelmann, D. J., Hirt, S., Hullin, R., Priebe, L., Schwinger, R. H. G., Weil, J., & Herzig, S. (1998). Increased availability and open probability of single L-type calcium channels from failing compared with nonfailing human ventricle. *Circulation*, *98*(10), 969–976. https://doi.org/10.1161/01.CIR.98.10.969

Schuldt, M., Pei, J., Harakalova, M., Dorsch, L. M., Schlossarek, S., Mokry, M., Knol, J. C., Pham, T. v., Schelfhorst, T., Piersma, S. R., dos Remedios, C., Dalinghaus, M., Michels, M., Asselbergs, F. W., Moutin, M. J., Carrier, L., Jimenez, C. R., van der Velden, J., & Kuster, D. W. D. (2021). Proteomic and Functional Studies Reveal Detyrosinated Tubulin as Treatment Target in Sarcomere Mutation-Induced Hypertrophic Cardiomyopathy. *Circulation*.

Heart Failure, *14*(1), e007022. https://doi.org/10.1161/CIRCHEARTFAILURE.120.007022

Schulz, E. M., Wilder, T., Chowdhury, S. A. K., Sheikh, H. N., Wolska, B. M., Solaro, R. J., & Wieczorek, D. F. (2013). Decreasing Tropomyosin Phosphorylation Rescues Tropomyosin-induced Familial Hypertrophic Cardiomyopathy *. *Journal of Biological Chemistry*, *288*(40), 28925–28935. https://doi.org/10.1074/JBC.M113.466466

Schwamborn, K., Knipscheer, P., van Dijk, E., van Dijk, W. J., Sixma, T. K., Meloen, R. H., & Langedijk, J. P. M. (2008). SUMO assay with peptide arrays on solid support: insights into SUMO target sites. *Journal of Biochemistry*, *144*(1), 39–49. https://doi.org/10.1093/JB/MVN039

Schwinger, R. H. G., Hoischen, S., Reuter, H., & Hullin, R. (1999). Regional expression and functional characterization of the L-type Ca2+-channel in myocardium from patients with end-stage heart failure and in non-failing human hearts. *Journal of Molecular and Cellular Cardiology*, *31*(1), 283–296. https://doi.org/10.1006/JMCC.1998.0869

Schwinger, R. H. G., Wang, J., Frank, K., Müller-Ehmsen, J., Brixius, K., McDonough, A. A., & Erdmann, E. (1999). Reduced sodium pump alpha1, alpha3, and beta1-isoform protein levels and Na+,K+-ATPase activity but unchanged Na+-Ca2+ exchanger protein levels in human heart failure. *Circulation*, *99*(16), 2105–2112. https://doi.org/10.1161/01.CIR.99.16.2105

Scotcher, J., Prysyazhna, O., Boguslavskyi, A., Kistamas, K., Hadgraft, N., Martin, E. D., Worthington, J., Rudyk, O., Rodriguez Cutillas, P., Cuello, F., Shattock, M. J., Marber, M. S., Conte, M. R., Greenstein, A., Greensmith, D. J., Venetucci, L., Timms, J. F., & Eaton, P. (2016). Disulfide-activated protein kinase G Iα regulates cardiac diastolic relaxation and fine-tunes the Frank–Starling response. *Nature Communications 2016 7:1*, *7*(1), 1–11. https://doi.org/10.1038/ncomms13187

Sears, R. M., May, D. G., & Roux, K. J. (2019). BioID as a Tool for Protein-Proximity Labeling in Living Cells. *Methods in Molecular Biology (Clifton, N.J.)*, *2012*, 299. https://doi.org/10.1007/978-1-4939-9546-2_15

Setterberg, I. E., Le, C., Frisk, M., Li, J., & Louch, W. E. (2021). The Physiology and Pathophysiology of T-Tubules in the Heart. *Frontiers in Physiology*, *12*, 1193. https://doi.org/10.3389/FPHYS.2021.718404/BIBTEX

Shaffer, J. F., Kensler, R. W., & Harris, S. P. (2009). The myosin-binding protein C motif binds to F-actin in a phosphorylation-sensitive manner. *Journal of Biological Chemistry*, *284*(18), 12318–12327. https://doi.org/10.1074/jbc.M808850200

Shah, A., Gandhi, D., Srivastava, S., Shah, K. J., & Mansukhani, R. (2017). Heart Failure: A Class Review of Pharmacotherapy. *Pharmacy and Therapeutics*, *42*(7), 464. /pmc/articles/PMC5481297/

Shah, K. S., Xu, H., Matsouaka, R. A., Bhatt, D. L., Heidenreich, P. A., Hernandez, A. F., Devore, A. D., Yancy, C. W., & Fonarow, G. C. (2017). Heart Failure With Preserved, Borderline, and Reduced Ejection Fraction: 5-Year Outcomes. *Journal of the American College of Cardiology*, *70*(20), 2476–2486. https://doi.org/10.1016/J.JACC.2017.08.074

Shao, R., Zhang, F. P., Tian, F., Anders Friberg, P., Wang, X., Sjöland, H., & Billig, H. (2004). Increase of SUMO-1 expression in response to hypoxia: direct interaction with HIF-1alpha in adult mouse brain and heart in vivo. *FEBS Letters*, *569*(1–3), 293–300. https://doi.org/10.1016/J.FEBSLET.2004.05.079

Sharma, K., D'Souza, R. C. J., Tyanova, S., Schaab, C., Wiśniewski, J. R., Cox, J., & Mann, M. (2014). Ultradeep Human Phosphoproteome Reveals a

Distinct Regulatory Nature of Tyr and Ser/Thr-Based Signaling. *Cell Reports*, *8*(5), 1583–1594. https://doi.org/10.1016/J.CELREP.2014.07.036

Sheng, Z., Wang, X., Ma, Y., Zhang, D., Yang, Y., Zhang, P., Zhu, H., Xu, N., & Liang, S. (2019). MS-based strategies for identification of protein SUMOylation modification. *ELECTROPHORESIS*, *40*(21), 2877–2887. https://doi.org/10.1002/ELPS.201900100

Shetty, P. M. V., Rangrez, A. Y., & Frey, N. (2020). SUMO proteins in the cardiovascular system: friend or foe? *Journal of Biomedical Science 2020 27:1*, *27*(1), 1–14. https://doi.org/10.1186/S12929-020-00689-0

Shimizu, Y., Lambert, J. P., Nicholson, C. K., Kim, J. J., Wolfson, D. W., Cho, H. C., Husain, A., Naqvi, N., Chin, L. S., Li, L., & Calvert, J. W. (2016). DJ-1 Protects the Heart Against Ischemia-Reperfusion Injury by Regulating Mitochondrial Fission. *Journal of Molecular and Cellular Cardiology*, *97*, 56. https://doi.org/10.1016/J.YJMCC.2016.04.008

Shipston, M. J. (2014). S-acylation dependent post-translational cross-talk regulates large conductance calcium- and voltage- activated potassium (BK) channels. *Frontiers in Physiology*, *5*. https://doi.org/10.3389/FPHYS.2014.00281

Sichelschmidt, O. J., Hahnefeld, C., Hohlfeld, T., Herberg, F. W., & Schrör, K. (2003). Trapidil protects ischemic hearts from reperfusion injury by stimulating PKAII activity. *Cardiovascular Research*, *58*(3), 602–610. https://doi.org/10.1016/S0008-6363(03)00261-X

Simmonds, S. J., Cuijpers, I., Heymans, S., & Jones, E. A. V. (2020). Cellular and Molecular Differences between HFpEF and HFrEF: A Step Ahead in an Improved Pathological Understanding. *Cells*, *9*(1). https://doi.org/10.3390/CELLS9010242

Singh, R. R., McNamara, J. W., & Sadayappan, S. (2021). Mutations in myosin S2 alter cardiac myosin-binding protein-C interaction in hypertrophic cardiomyopathy in a phosphorylation-dependent manner. *The Journal of Biological Chemistry*, *297*(1). https://doi.org/10.1016/J.JBC.2021.100836

Sipido, K. R., Volders, P. G. A., Vos, M. A., & Verdonck, F. (2002). Altered Na/Ca exchange activity in cardiac hypertrophy and heart failure: A new target for therapy? *Cardiovascular Research*, *53*(4), 782–805. https://doi.org/10.1016/S0008-6363(01)00470-9/2/53-4-782-GR4.GIF

Smotrys, J. E., & Linder, M. E. (2004). Palmitoylation of Intracellular Signaling Proteins: Regulation and Function. *Http://Dx.Doi.Org/10.1146/Annurev.Biochem.73.011303.073954*, *73*, 559–587. https://doi.org/10.1146/ANNUREV.BIOCHEM.73.011303.073954

Soni, S., Raaijmakers, A. J. A., Raaijmakers, L. M., Damen, M. J. A., van Stuijvenberg, L., Vos, M. A., Heck, A. J. R., van Veen, T. A. B., & Scholten, A. (2016). A Proteomics Approach to Identify New Putative Cardiac Intercalated Disk Proteins. *PLOS ONE*, *11*(5), e0152231. https://doi.org/10.1371/JOURNAL.PONE.0152231

Soyombo, A. A., & Hofmann, S. L. (1997). Molecular cloning and expression of palmitoyl-protein thioesterase 2 (PPT2), a homolog of lysosomal palmitoyl-protein thioesterase with a distinct substrate specificity. *The Journal of Biological Chemistry*, *272*(43), 27456–27463. https://doi.org/10.1074/JBC.272.43.27456

Spannbauer, A., Traxler, D., Zlabinger, K., Gugerell, A., Winkler, J., Mester-Tonczar, J., Lukovic, D., Müller, C., Riesenhuber, M., Pavo, N., & Gyöngyösi, M. (2019). Large Animal Models of Heart Failure With Reduced Ejection Fraction (HFrEF). *Frontiers in Cardiovascular Medicine*, *6*. https://doi.org/10.3389/FCVM.2019.00117

Spinelli, M., Fusco, S., Mainardi, M., Scala, F., Natale, F., Lapenta, R., Mattera, A., Rinaudo, M., Li Puma, D. D., Ripoli, C., Grassi, A., D'Ascenzo, M., & Grassi, C. (2017). Brain insulin resistance impairs hippocampal synaptic plasticity and memory by increasing GluA1 palmitoylation through FoxO3a. *Nature Communications*, *8*(1). https://doi.org/10.1038/S41467-017-02221-9

Spudich, J. A. (2015). The myosin mesa and a possible unifying hypothesis for the molecular basis of human hypertrophic cardiomyopathy. *Biochemical Society Transactions*, *43*(1), 64–72. https://doi.org/10.1042/BST20140324

Stanczyk, P. J., Seidel, M., White, J., Viero, C., George, C. H., Zissimopoulos, S., & Lai, F. A. (2018). Association of cardiac myosin-binding protein-C with the ryanodine receptor channel – putative retrograde regulation? *Journal of Cell Science*, *131*(15). https://doi.org/10.1242/JCS.210443

Starr, R., & Offer, G. (1971). Polypeptide chains of intermediate molecular weight in myosin preparations. *FEBS Letters*, *15*(1), 40–44. https://doi.org/10.1016/0014-5793(71)80075-3

Stathopoulou, K., Wittig, I., Heidler, J., Piasecki, A., Richter, F., Diering, S., van Velden, J. der, Buck, F., Donzelli, S., Schröder, E., Wijnker, P. J. M., Voigt, N., Dobrev, D., Sadayappan, S., Eschenhagen, T., Carrier, L., Eaton, P., & Cuello, F. (2016). S-glutathiolation impairs phosphoregulation and function of cardiac myosin-binding protein C in human heart failure. *FASEB Journal*, *30*(5), 1849–1864. https://doi.org/10.1096/FJ.201500048/-/DC1

Steffensen, A. B., Andersen, M. N., Mutsaers, N., Mujezinovic, A., & Schmitt, N. (2018). SUMO co-expression modifies KV11.1 channel activity. *Acta Physiologica*, *222*(3), e12974. https://doi.org/10.1111/APHA.12974

Stehmeier, P., & Muller, S. (2009). Phospho-regulated SUMO interaction modules connect the SUMO system to CK2 signaling. *Molecular Cell*, *33*(3), 400–409. https://doi.org/10.1016/J.MOLCEL.2009.01.013

Steinbusch, L. K. M., Luiken, J. J. F. P., Vlasblom, R., Chabowski, A., Hoebers, N. T. H., Coumans, W. A., Vroegrijk, I. O. C. M., Voshol, P. J., Margriet Ouwens, D., Glatz, J. F. C., & Diamant, M. (2011). Absence of fatty acid transporter CD36 protects against Western-type diet-related cardiac dysfunction following pressure overload in mice. *American Journal of Physiology. Endocrinology and Metabolism*, *301*(4). https://doi.org/10.1152/AJPENDO.00106.2011

Stelzer, J. E., Patel, J. R., & Moss, R. L. (2006). Protein kinase A-mediated acceleration of the stretch activation response in murine skinned myocardium is eliminated by ablation of cMyBP-C. *Circulation Research*, *99*(8), 884–890. https://doi.org/10.1161/01.RES.0000245191.34690.66

Stenson, P. D., Mort, M., Ball, E. v., Shaw, K., Phillips, A. D., & Cooper, D. N. (2014). The Human Gene Mutation Database: building a comprehensive mutation repository for clinical and molecular genetics, diagnostic testing and personalized genomic medicine. *Human Genetics*, *133*(1), 1. https://doi.org/10.1007/S00439-013-1358-4

Strosberg, A. D., Gerhardt, C. C., Gros, J., Jockers, R., & Piétri-Rouxel, F. (1998). On the putative existence of a fourth ß-adrenoceptor: proof is still missing. *Trends in Pharmacological Sciences*, *19*(5), 165–166. https://doi.org/10.1016/S0165-6147(98)01200-0

Suay-Corredera, C., Alegre-Cebollada, J., Suay-Corredera, C., & Alegre-Cebollada, J. (2022). The mechanics of the heart: zooming in on hypertrophic cardiomyopathy and cMyBP-C. *FEBS Letters*, *596*(6), 703–746. https://doi.org/10.1002/1873-3468.14301

SUMOplot™ Analysis Program | Abcepta. (n.d.). Retrieved February 1, 2022, from https://www.abcepta.com/sumoplot

Sun, J., Morgan, M., Shen, R. F., Steenbergen, C., & Murphy, E. (2007). Preconditioning results in S-nitrosylation of proteins involved in regulation of mitochondrial energetics and calcium transport. *Circulation Research*, *101*(11), 1155–1163. https://doi.org/10.1161/CIRCRESAHA.107.155879

Sun, Y. B., & Irving, M. (2010). The molecular basis of the steep force–calcium relation in heart muscle. *Journal of Molecular and Cellular Cardiology*, *48*(5), 859–865. https://doi.org/10.1016/J.YJMCC.2009.11.019

Sung, M. M. Y., Koonen, D. P. Y., Soltys, C. L. M., Jacobs, R. L., Febbraio, M., & Dyck, J. R. B. (2011). Increased CD36 expression in middle-aged mice contributes to obesity-related cardiac hypertrophy in the absence of cardiac dysfunction. *Journal of Molecular Medicine (Berlin, Germany)*, *89*(5), 459–469. https://doi.org/10.1007/S00109-010-0720-4

Takahashi, T., Allen, P. D., Lacro, R. v., Marks, A. R., Dennis, A. R., Schoen, F. J., Grossman, W., Marsh, J. D., & Izumo, S. (1992). Expression of dihydropyridine receptor (Ca2+ channel) and calsequestrin genes in the myocardium of patients with end-stage heart failure. *The Journal of Clinical Investigation*, *90*(3), 927–935. https://doi.org/10.1172/JCI115969

Taniguchi, K., Takeya, R., Suetsugu, S., Kan-o, M., Narusawa, M., Shiose, A., Tominaga, R., & Sumimoto, H. (2009). Mammalian formin fhod3 regulates actin assembly and sarcomere organization in striated muscles. *The Journal of Biological Chemistry*, *284*(43), 29873–29881. https://doi.org/10.1074/JBC.M109.059303

Tanner, B. C. W., Previs, M. J., Wang, Y., Robbins, J., & Palmer, B. M. (2021). Cardiac myosin binding protein-C phosphorylation accelerates ß-cardiac myosin detachment rate in mouse myocardium. *American Journal of Physiology. Heart and Circulatory Physiology*, *320*(5), H1822–H1835. https://doi.org/10.1152/AJPHEART.00673.2020

Tansey, E. A., Montgomery, L. E. A., Quinn, J. G., Roe, S. M., & Johnson, C. D. (2019). Understanding basic vein physiology and venous blood pressure through simple physical assessments. *Advances in Physiology Education*, *43*(3), 423–429. https://doi.org/10.1152/ADVAN.00182.2018/ASSET/IMAGES/LARGE/ZU1003 1933340005.JPEG

Tatham, M. H., Jaffray, E., Vaughan, O. A., Desterro, J. M. P., Botting, C. H., Naismith, J. H., & Hay, R. T. (2001). Polymeric chains of SUMO-2 and SUMO-3 are conjugated to protein substrates by SAE1/SAE2 and Ubc9. *The Journal of Biological Chemistry*, *276*(38), 35368–35374. https://doi.org/10.1074/JBC.M104214200

Tham, Y. K., Bernardo, B. C., Ooi, J. Y. Y., Weeks, K. L., Mcmullen, J. R., Tham, Y. K., Bernardo, · B C, Ooi, J. Y. Y., Mcmullen, · J R, Mcmullen, J. R., & Weeks, K. L. (2015). Pathophysiology of cardiac hypertrophy and heart failure: signaling pathways and novel therapeutic targets. *Archives of Toxicology 2015 89:9*, *89*(9), 1401–1438. https://doi.org/10.1007/S00204-015-1477-X

Tian, L., McClafferty, H., Jeffries, O., & Shipston, M. J. (2010). Multiple palmitoyltransferases are required for palmitoylation-dependent regulation of large conductance calcium- and voltage-activated potassium channels. *Journal of Biological Chemistry*, *285*(31), 23954–23962. https://doi.org/10.1074/jbc.M110.137802

Tian, L., McClafferty, H., Knaus, H. G., Ruth, P., & Shipston, M. J. (2012). Distinct acyl protein transferases and thioesterases control surface expression of calcium-activated potassium channels. *The Journal of*

Biological Chemistry, *287*(18), 14718–14725. https://doi.org/10.1074/JBC.M111.335547

Tilemann, L., Lee, A., Ishikawa, K., Aguero, J., Rapti, K., Santos-Gallego, C., Kohlbrenner, E., Fish, K. M., Kho, C., & Hajjar, R. J. (2013). SUMO-1 Gene Transfer Improves Cardiac Function in a Large-Animal Model of Heart Failure. *Science Translational Medicine*, *5*(211), 211ra159-211ra159. https://doi.org/10.1126/scitranslmed.3006487

Tobushi, T., Nakano, M., Hosokawa, K., Koga, H., & Yamada, A. (2017). Improved diastolic function is associated with higher cardiac output in patients with heart failure irrespective of left ventricular ejection fraction. *Journal of the American Heart Association*, *6*(3). https://doi.org/10.1161/JAHA.116.003389

Toepfer, C., Caorsi, V., Kampourakis, T., Sikkel, M. B., West, T. G., Leung, M. C., Al-Saud, S. A., MacLeod, K. T., Lyon, A. R., Marston, S. B., Sellers, J. R., & Ferenczi, M. A. (2013). Myosin Regulatory Light Chain (RLC) Phosphorylation Change as a Modulator of Cardiac Muscle Contraction in Disease. *The Journal of Biological Chemistry*, *288*(19), 13446. https://doi.org/10.1074/JBC.M113.455444

Tomatis, V. M., Trenchi, A., Gomez, G. A., & Daniotti, J. L. (2010). Acyl-Protein Thioesterase 2 Catalizes the Deacylation of Peripheral Membrane-Associated GAP-43. *PLoS ONE*, *5*(11), 15045. https://doi.org/10.1371/JOURNAL.PONE.0015045

Tong, C., Morrison, A., Mattison, S., Qian, S., Bryniarski, M., Rankin, B., Wang, J., Thomas, D. P., & Li, J. (2013). Impaired SIRT1 nucleocytoplasmic shuttling in the senescent heart during ischemic stress. *The FASEB Journal*, *27*(11), 4332. https://doi.org/10.1096/FJ.12-216473

Tong, C. W., Dusio, G. F., Govindan, S., Johnson, D. W., Kidwell, D. T., de La Rosa, L. M., Rosas, P. C., Liu, Y., Ebert, E., Newell-Rogers, M. K., Michel, J. B., Trzeciakowski, J. P., & Sadayappan, S. (2017). Usefulness of Released Cardiac Myosin Binding Protein-C as a Predictor of Cardiovascular Events. *American Journal of Cardiology*, *120*(9), 1501–1507. https://doi.org/10.1016/j.amjcard.2017.07.042

Tong, C. W., Nair, N. A., Doersch, K. M., Liu, Y., & Rosas, P. C. (2014). Cardiac myosin-binding protein-C is a critical mediator of diastolic function. *Pflugers Archiv European Journal of Physiology*, *466*(3), 451–457. https://doi.org/10.1007/s00424-014-1442-1

Tong, C. W., Stelzer, J. E., Greaser, M. L., Powers, P. A., & Moss, R. L. (2008). Acceleration of Crossbridge Kinetics by Protein Kinase A Phosphorylation of Cardiac Myosin Binding Protein C Modulates Cardiac Function. *Circulation Research*, *103*(9), 974–982. https://doi.org/10.1161/CIRCRESAHA.108.177683

Tong, G., Aponte, A. M., Kohr, M. J., Steenbergen, C., Murphy, E., & Sun, J. (2014). Postconditioning leads to an increase in protein S-nitrosylation. *American Journal of Physiology. Heart and Circulatory Physiology*, *306*(6). https://doi.org/10.1152/AJPHEART.00660.2013

Tonino, P., Kiss, B., Gohlke, J., Smith, J. E., & Granzier, H. (2019). Fine mapping titin's C-zone: Matching cardiac myosin-binding protein C stripes with titin's super-repeats. *Journal of Molecular and Cellular Cardiology*, *133*, 47–56. https://doi.org/10.1016/J.YJMCC.2019.05.026

Touma, A. M., Tang, W., Rasicci, D. v., Vang, D., Rai, A., Previs, S. B., Warshaw, D. M., Yengo, C. M., & Sivaramakrishnan, S. (2022). Nanosurfer assay dissects ß-cardiac myosin and cardiac myosin-binding protein C interactions. *Biophysical Journal*. https://doi.org/10.1016/J.BPJ.2022.05.013

Tulloch, L. B., Howie, J., Wypijewski, K. J., Wilson, C. R., Bernard, W. G., Shattock, M. J., & Fuller, W. (2011). The inhibitory effect of phospholemman on the sodium pump requires its palmitoylation. *The Journal of Biological Chemistry*, *286*(41), 36020–36031. https://doi.org/10.1074/jbc.M111.282145

Ullmann, R., Chien, C. D., Avantaggiati, M. L., & Muller, S. (2012). An acetylation switch regulates SUMO-dependent protein interaction networks. *Molecular Cell*, *46*(6), 759–770. https://doi.org/10.1016/J.MOLCEL.2012.04.006

Ulphani, J. S., Cain, J. H., Inderyas, F., Gordon, D., Gikas, P. v., Shade, G., Mayor, D., Arora, R., Kadish, A. H., & Goldberger, J. J. (2010). Quantitative analysis of parasympathetic innervation of the porcine heart. *Heart Rhythm*, *7*(8), 1113–1119. https://doi.org/10.1016/J.HRTHM.2010.03.043

Valdez-Taubas, J., & Pelham, H. (2005). Swf1-dependent palmitoylation of the SNARE Tlg1 prevents its ubiquitination and degradation. *The EMBO Journal*, *24*(14), 2524–2532. https://doi.org/10.1038/SJ.EMBOJ.7600724

van der Velden, J., Klein, L. J., van der Bijl, M., Huybregts, M. A. J. M., Stooker, W., Witkop, J., Eijsman, L., Visser, C. A., Visser, F. C., & Stienen, G. J. M. (1999). Isometric tension development and its calcium sensitivity in skinned myocyte-sized preparations from different regions of the human heart. *Cardiovascular Research*, *42*(3), 706–719. https://doi.org/10.1016/S0008-6363(98)00337-X/2/42-3-706-FIG8.GIF

van der Velden, J., Papp, Z., Zaremba, R., Boontje, N. M., de Jong, J. W., Owen, V. J., Burton, P. B. J., Goldmann, P., Jaquet, K., & Stienen, G. J. M. (2003). Increased Ca2+-sensitivity of the contractile apparatus in end-stage human heart failure results from altered phosphorylation of contractile proteins. *Cardiovascular Research*, *57*(1), 37–47. https://doi.org/10.1016/S0008-6363(02)00606-5/2/57-1-37-FIG7.GIF

van Dijk, S. J., Dooijes, D., Remedios, C. dos, Michels, M., Lamers, J. M. J., Winegrad, S., Schlossarek, S., Carrier, L., Cate, F. J. T., Stienen, G. J. M., & van Velden, J. der. (2009). Cardiac myosin-binding protein C mutations and hypertrophic cardiomyopathy: haploinsufficiency, deranged phosphorylation, and cardiomyocyte dysfunction. *Circulation*, *119*(11), 1473–1483. https://doi.org/10.1161/CIRCULATIONAHA.108.838672

van Dolah, D. K., Mao, L. M., Shaffer, C., Guo, M. L., Fibuch, E. E., Chu, X. P., Buch, S., & Wang, J. Q. (2011). Reversible Palmitoylation Regulates Surface Stability of AMPA Receptors in the Nucleus Accumbens in Response to Cocaine in vivo. *Biological Psychiatry*, *69*(11), 1035. https://doi.org/10.1016/J.BIOPSYCH.2010.11.025

van Driest, S. L., Ellsworth, E. G., Ommen, S. R., Tajik, A. J., Gersh, B. J., & Ackerman, M. J. (2003). Prevalence and spectrum of thin filament mutations in an outpatient referral population with hypertrophic cardiomyopathy. *Circulation*, *108*(4), 445–451. https://doi.org/10.1161/01.CIR.0000080896.52003.DF

Vartak, N., Papke, B., Grecco, H. E., Rossmannek, L., Waldmann, H., Hedberg, C., & Bastiaens, P. I. H. (2014). The Autodepalmitoylating Activity of APT Maintains the Spatial Organization of Palmitoylated Membrane Proteins. *Biophysical Journal*, *106*(1), 93–105. https://doi.org/10.1016/J.BPJ.2013.11.024

Vignier, N., Schlossarek, S., Fraysse, B., Mearini, G., Krämer, E., Pointu, H., Mougenot, N., Guiard, J., Reimer, R., Hohenberg, H., Schwartz, K., Vernet, M., Eschenhagen, T., & Carrier, L. (2009). Nonsense-mediated mRNA decay and ubiquitin-proteasome system regulate cardiac myosin-binding protein C

mutant levels in cardiomyopathic mice. *Circulation Research*, *105*(3), 239–248. https://doi.org/10.1161/CIRCRESAHA.109.201251

Virani, S. S., Alonso, A., Benjamin, E. J., Bittencourt, M. S., Callaway, C. W., Carson, A. P., Chamberlain, A. M., Chang, A. R., Cheng, S., Delling, F. N., Djousse, L., Elkind, M. S. V., Ferguson, J. F., Fornage, M., Khan, S. S., Kissela, B. M., Knutson, K. L., Kwan, T. W., Lackland, D. T., … Heard, D. G. (2020). Heart Disease and Stroke Statistics-2020 Update: A Report From the American Heart Association. *Circulation*, *141*(9), E139–E596. https://doi.org/10.1161/CIR.0000000000000757

Wages, J. M. (2005). POLYMERASE CHAIN REACTION. *Encyclopedia of Analytical Science: Second Edition*, 243–250. https://doi.org/10.1016/B0-12-369397-7/00475-1

Walcott, S., Docken, S., & Harris, S. P. (2015). Effects of cardiac myosin binding protein-C on actin motility are explained with a drag-activation-competition model. *Biophysical Journal*, *108*(1), 10–13. https://doi.org/10.1016/j.bpj.2014.11.1852

Wang, J., Chen, L., Wen, S., Zhu, H., Yu, W., Moskowitz, I. P., Shaw, G. M., Finnell, R. H., & Schwartz, R. J. (2011). Defective sumoylation pathway directs congenital heart disease. *Birth Defects Research. Part A, Clinical and Molecular Teratology*, *91*(6), 468. https://doi.org/10.1002/BDRA.20816

Wang, L., Ji, X., Barefield, D., Sadayappan, S., & Kawai, M. (2014). Phosphorylation of cMyBP-C Affects Contractile Mechanisms in a Site-specific Manner. *Biophysical Journal*, *106*(5), 1112. https://doi.org/10.1016/J.BPJ.2014.01.029

Wang, L., Wang, P., Xu, S., Li, Z., Duan, D. D., Ye, J., Li, J., Ding, Y., Zhang, W., Lu, J., & Liu, P. (2022). The cross-talk between PARylation and SUMOylation in C/EBPβ at K134 site participates in pathological cardiac hypertrophy. *International Journal of Biological Sciences*, *18*(2), 783. https://doi.org/10.7150/IJBS.65211

Wang, L., Wansleeben, C., Zhao, S., Miao, P., Paschen, W., & Yang, W. (2014). SUMO2 is essential while SUMO3 is dispensable for mouse embryonic development. *EMBO Reports*, *15*(8), 878. https://doi.org/10.15252/EMBR.201438534

Wang, T., Wu, J., Dong, W., Wang, M., Zhong, X., Zhang, W., Dai, L., Xie, Y., Liu, Y., He, X., Liu, W., Madhusudhan, T., Zeng, H., & Wang, H. (2021). The MEK inhibitor U0126 ameliorates diabetic cardiomyopathy by restricting XBP1's phosphorylation dependent SUMOylation. *International Journal of Biological Sciences*, *17*(12), 2984–2999. https://doi.org/10.7150/IJBS.60459

Wang, X., Liu, X., Wang, S., & Luan, K. (2012). Myofibrillogenesis regulator 1 induces hypertrophy by promoting sarcomere organization in neonatal rat cardiomyocytes. *Hypertension Research*, *35*(6), 597. https://doi.org/10.1038/HR.2011.228

Watkins, H., Conner, D., Thierfelder, L., Jarcho, J. A., MacRae, C., McKenna, W. J., Maron, B. J., Seidman, J. G., & Seidman, C. E. (1995). Mutations in the cardiac myosin binding protein-C gene on chromosome 11 cause familial hypertrophic cardiomyopathy. *Nature Genetics*, *11*(4), 434–437. https://doi.org/10.1038/NG1295-434

Weber, F. E., Vaughan, K. T., Reinach, F. C., & Fischman, D. A. (1993). Complete sequence of human fast-type and slow-type muscle myosin-binding-protein C (MyBP-C). Differential expression, conserved domain structure and chromosome assignment. *European Journal of Biochemistry*, *216*(2), 661–669. https://doi.org/10.1111/j.1432-1033.1993.tb18186.x

Weber, S., Meyer-Roxlau, S., Wagner, M., Dobrev, D., & El-Armouche, A. (2015). Counteracting protein kinase activity in the heart: The multiple roles of protein phosphatases. *Frontiers in Pharmacology*, *6*(NOV), 270. https://doi.org/10.3389/FPHAR.2015.00270/BIBTEX

Wedegaertner, P. B., & Bourne, H. R. (1994). Activation and depalmitoylation of Gsα. *Cell*, *77*(7), 1063–1070. https://doi.org/10.1016/0092-8674(94)90445-6

Wei, S. K., Mccurley, J. M., Hanlon, S. U., & Haigney, M. C. P. (2007). Gender differences in Na/Ca exchanger current and beta-adrenergic responsiveness in heart failure in pig myocytes. *Annals of the New York Academy of Sciences*, *1099*, 183–189. https://doi.org/10.1196/ANNALS.1387.026

Wei, X., Schneider, J. G., Shenouda, S. M., Lee, A., Towler, D. A., Chakravarthy, M. v., Vita, J. A., & Semenkovich, C. F. (2011). De Novo lipogenesis maintains vascular homeostasis through endothelial nitric-oxide synthase (eNOS) palmitoylation. *Journal of Biological Chemistry*, *286*(4), 2933–2945. https://doi.org/10.1074/jbc.M110.193037

Wei, X., Yohannan, S., & Richards, J. R. (2021). Physiology, Cardiac Repolarization Dispersion and Reserve. *StatPearls*. https://www.ncbi.nlm.nih.gov/books/NBK537194/

Wijnker, P. J. M., Foster, D. B., Tsao, A. L., Frazier, A. H., dos Remedios, C. G., Murphy, A. M., Stienen, G. J. M., & van der Velden, J. (2013). Impact of site-specific phosphorylation of protein kinase A sites Ser23 and Ser24 of cardiac troponin I in human cardiomyocytes. *American Journal of Physiology. Heart and Circulatory Physiology*, *304*(2). https://doi.org/10.1152/AJPHEART.00498.2012

Willis, M. S., Schisler, J. C., Portbury, A. L., & Patterson, C. (2009). Build it up-Tear it down: protein quality control in the cardiac sarcomere. *Cardiovascular Research*, *81*(3), 439. https://doi.org/10.1093/CVR/CVN289

Wills, L. (2017). *SUMOylation of the B2AR influences receptor internalisation, desensitisation and downstream signalling* [University of Glasgow]. https://eleanor.lib.gla.ac.uk/record=b3289853

Winegrad, S. (1999). Cardiac Myosin Binding Protein C. *Circulation Research*, *84*(10), 1117–1126. https://doi.org/10.1161/01.RES.84.10.1117

Winer, J., Jung, C. K. S., Shackel, I., & Williams, P. M. (1999). Development and validation of real-time quantitative reverse transcriptase-polymerase chain reaction for monitoring gene expression in cardiac myocytes in vitro. *Analytical Biochemistry*, *270*(1), 41–49. https://doi.org/10.1006/ABIO.1999.4085

Witt, C. C., Gerull, B., Davies, M. J., Centner, T., Linke, W. A., & Thierfelder, L. (2001). Hypercontractile Properties of Cardiac Muscle Fibers in a Knock-in Mouse Model of Cardiac Myosin-binding Protein-C *. *Journal of Biological Chemistry*, *276*(7), 5353–5359. https://doi.org/10.1074/JBC.M008691200

Wolhuter, K., Whitwell, H. J., Switzer, C. H., Burgoyne, J. R., Timms, J. F., & Eaton, P. (2018). Evidence against Stable Protein S-Nitrosylation as a Widespread Mechanism of Post-translational Regulation. *Molecular Cell*, *69*(3), 438. https://doi.org/10.1016/J.MOLCEL.2017.12.019

Woodley, K. T., & Collins, M. O. (2019). S-acylated Golga7b stabilises DHHC5 at the plasma membrane to regulate cell adhesion. *EMBO Reports*, *20*(10), e47472. https://doi.org/10.15252/EMBR.201847472

Woodley, K. T., & Collins, M. O. (2021). Regulation and function of the palmitoyl-acyltransferase ZDHHC5. *The FEBS Journal*, *288*(23), 6623–6634. https://doi.org/10.1111/FEBS.15709

Woodman, S. E., Park, D. S., Cohen, A. W., Cheung, M. W. C., Chandra, M., Shirani, J., Tang, B., Jelicks, L. A., Kitsis, R. N., Christ, G. J., Factor, S. M.,

Tanowitz, H. B., & Lisanti, M. P. (2002). Caveolin-3 knock-out mice develop a progressive cardiomyopathy and show hyperactivation of the p42/44 MAPK cascade. *The Journal of Biological Chemistry*, *277*(41), 38988–38997. https://doi.org/10.1074/JBC.M205511200

Wu, H., Li, L., Niu, P., Huang, X., Liu, J., Zhang, F., Shen, W., Tan, W., Wu, Y., & Huo, Y. (2017). The Structure-function remodeling in rabbit hearts of myocardial infarction. *Physiological Reports*, *5*(12), 13311. https://doi.org/10.14814/PHY2.13311

Wypijewski, K. J., Tinti, M., Chen, W., Lamont, D., Ashford, M. L. J., Calaghan, S. C., & Fuller, W. (2015). Identification of caveolar resident proteins in ventricular myocytes using a quantitative proteomic approach: dynamic changes in caveolar composition following adrenoceptor activation. *Molecular & Cellular Proteomics : MCP*, *14*(3), 596–608. https://doi.org/10.1074/MCP.M114.038570

Xie, B., Liu, X., Yang, J., Cheng, J., Gu, J., & Xue, S. (2018). PIAS1 protects against myocardial ischemia-reperfusion injury by stimulating PPARγ SUMOylation. *BMC Cell Biology*, *19*(1). https://doi.org/10.1186/S12860-018-0176-X

Xing, J., Chinnaraj, M., Zhang, Z., Cheung, H. C., & Dong, W. J. (2008). Structural Studies of Interactions between Cardiac Troponin I and Actin in Regulated Thin Filament using Förster Resonance Energy Transfer. *Biochemistry*, *47*(50), 13383. https://doi.org/10.1021/BI801492X

Xiong, D., Li, T., Dai, H., Arena, A. F., Plant, L. D., & Goldstein, S. A. N. (2017). SUMOylation determines the voltage required to activate cardiac IKs channels. *Proceedings of the National Academy of Sciences of the United States of America*, *114*(32), E6686–E6694. https://doi.org/10.1073/PNAS.1706267114/-/DCSUPPLEMENTAL

Xue, Y., Zhou, F., Fu, C., Xu, Y., & Yao, X. (2006). SUMOsp: a web server for sumoylation site prediction. *Nucleic Acids Research*, *34*(suppl_2), W254–W257. https://doi.org/10.1093/NAR/GKL207

Yamamoto, K., & Moos, C. (1983). The C-proteins of rabbit, red, white and cardiac muscles. *J Biol Chem*, *13*, 8395–8401.

Yang, M., Zhang, Y., & Ren, J. (2020). Acetylation in cardiovascular diseases: Molecular mechanisms and clinical implications. *Biochimica et Biophysica Acta (BBA) - Molecular Basis of Disease*, *1866*(10), 165836. https://doi.org/10.1016/J.BBADIS.2020.165836

Yang, Q., Sanbe, A., Osinska, H., Hewett, T. E., Klevitsky, R., & Robbins, J. (1999). In vivo modeling of myosin binding protein C familial hypertrophic cardiomyopathy. *Circulation Research*, *85*(9), 841–847. https://doi.org/10.1161/01.RES.85.9.841

Yao, J., Shao, X. H., Song, G. Y., Zhao, Z. Y., Teng, S. Y., & Wu, Y. J. (2015). The expression of Ubc9 and the intensity of SERCA2a-sumoylation were reduced in diet-induced obese rats and partially restored by trimetazidine. *Journal of Cardiovascular Pharmacology*, *65*(1), 47–53. https://doi.org/10.1097/FJC.0000000000000162

Yogeswaran, A., Troidl, C., McNamara, J. W., Wilhelm, J., Truschel, T., Widmann, L., Aslam, M., Hamm, C. W., Sadayappan, S., & Lipps, C. (2021). The C0-C1f Region of Cardiac Myosin Binding Protein-C Induces Pro-Inflammatory Responses in Fibroblasts via TLR4 Signaling. *Cells*, *10*(6). https://doi.org/10.3390/CELLS10061326

Yoshiyama, M., Takeuchi, K., Hanatani, A., Kim, S., Omura, T., Toda, I., Teragaki, M., Akioka, K., Iwao, H., & Yoshikawa, J. (1997). Differences in expression of sarcoplasmic reticulum Ca2+-ATPase and Na+-Ca2+ exchanger

genes between adjacent and remote noninfarcted myocardium after myocardial infarction. *Journal of Molecular and Cellular Cardiology*, *29*(1), 255–264. https://doi.org/10.1006/JMCC.1996.0270

Yount, J. S., Karssemeijer, R. A., & Hang, H. C. (2012). S-palmitoylation and ubiquitination differentially regulate interferon-induced transmembrane protein 3 (IFITM3)-mediated resistance to influenza virus. *Journal of Biological Chemistry*, *287*(23), 19631–19641. https://doi.org/10.1074/JBC.M112.362095/ATTACHMENT/3DA287E6-2F4D-40D4-8671-63A4D13481F8/MMC1.PDF

Yuan, C., Guo, Y., Ravi, R., Przyklenk, K., Shilkofski, N., Diez, R., Cole, R. N., & Murphy, A. M. (2006). Myosin binding protein C is differentially phosphorylated upon myocardial stunning in canine and rat hearts--evidence for novel phosphorylation sites. *Proteomics*, *6*(14), 4176–4186. https://doi.org/10.1002/PMIC.200500894

Zaccolo, M. (2009). cAMP signal transduction in the heart: understanding spatial control for the development of novel therapeutic strategies. *British Journal of Pharmacology*, *158*(1), 50. https://doi.org/10.1111/J.1476-5381.2009.00185.X

Zhang, R., Zhao, J. J., & Potter, J. D. (1995). Phosphorylation of Both Serine Residues in Cardiac Troponin I Is Required to Decrease the Ca2+ Affinity of Cardiac Troponin C (∗). *Journal of Biological Chemistry*, *270*(51), 30773–30780. https://doi.org/10.1074/JBC.270.51.30773

Zhang, R., Zhao, J., Mandveno, A., & Potter, J. D. (1995). Cardiac Troponin I Phosphorylation Increases the Rate of Cardiac Muscle Relaxation. *Circulation Research*, *76*(6), 1028–1035. https://doi.org/10.1161/01.RES.76.6.1028

Zhang, X., Kampourakis, T., Yan, Z., Sevrieva, I., Irving, M., & Sun, Y. B. (2017). Distinct contributions of the thin and thick filaments to length-dependent activation in heart muscle. *ELife*, *6*. https://doi.org/10.7554/ELIFE.24081

Zhao, L., Zhang, C., Luo, X., Wang, P., Zhou, W., Zhong, S., Xie, Y., Jiang, Y., Yang, P., Tang, R., Pan, Q., Hall, A. R., Luong, T. V., Fan, J., Varghese, Z., Moorhead, J. F., Pinzani, M., Chen, Y., & Ruan, X. Z. (2018). CD36 palmitoylation disrupts free fatty acid metabolism and promotes tissue inflammation in non-alcoholic steatohepatitis. *Journal of Hepatology*, *69*(3), 705–717. https://doi.org/10.1016/J.JHEP.2018.04.006

Zhao Q, Xie Y, Z. Y. (2014). GPS-SUMO: Prediction of SUMOylation Sites & SUMO-interaction Motifs. *Nucleic Acids Research*, *42*, 325–330.

Zhao, Q., Xie, Y., Zheng, Y., Jiang, S., Liu, W., Mu, W., Liu, Z., Zhao, Y., Xue, Y., & Ren, J. (2014). GPS-SUMO: a tool for the prediction of sumoylation sites and SUMO-interaction motifs. *Nucleic Acids Research*, *42*(W1), W325–W330. https://doi.org/10.1093/NAR/GKU383

Zhao, W., Zhao, J., Zhang, X., Fan, N., & Rong, J. (2021). Upregulation of Small Ubiquitin-Like Modifier 2 and Protein SUMOylation as a Cardioprotective Mechanism Against Myocardial Ischemia-Reperfusion Injury. *Frontiers in Pharmacology*, *12*. https://doi.org/10.3389/FPHAR.2021.731980

Zhao, Z. H., Youm, J. B., Wang, Y., Lee, J. H., Sung, J. H., Kim, J. C., Woo, S. H., Leem, C. H., Kim, S. J., Cui, L., & Zhang, Y. H. (2016). Cardiac inotropy, lusitropy, and Ca2+ handling with major metabolic substrates in rat heart. *Pflugers Archiv*, *468*(11), 1995. https://doi.org/10.1007/S00424-016-1892-8

Zhou, B., & Tian, R. (2018). Mitochondrial dysfunction in pathophysiology of heart failure. *The Journal of Clinical Investigation*, *128*(9), 3716–3726. https://doi.org/10.1172/JCI120849

Zhou, P., & Pu, W. T. (2016). Recounting cardiac cellular composition. In *Circulation Research* (Vol. 118, Issue 3, pp. 368–370). Lippincott Williams and Wilkins. https://doi.org/10.1161/CIRCRESAHA.116.308139

Zhou, T., Li, J., Zhao, P., Liu, H., Jia, D., Jia, H., He, L., Cang, Y., Boast, S., Chen, Y. H., Thibault, H., Scherrer-Crosbie, M., Goff, S. P., & Li, B. (2015). Palmitoyl acyltransferase Aph2 in cardiac function and the development of cardiomyopathy. *Proceedings of the National Academy of Sciences of the United States of America*, *112*(51), 15666–15671. https://doi.org/10.1073/PNAS.1518368112/-/DCSUPPLEMENTAL

Zhou, X., Jeong, E., Liu, H., Kaseer, B., Liu, M., Shrestha, S., Imran, H., Kavanagh, K., Jiang, N., Desimone, L., Feng, F., Shi, G., Jeong, G. E., Zhou, A., Stockwell, P., & Dudley, S. C. (2022). Circulating S-Glutathionylated cMyBP-C as a Biomarker for Cardiac Diastolic Dysfunction. *Journal of the American Heart Association*, *11*(11). https://doi.org/10.1161/JAHA.122.025295

Zhou, X., Wulfsen, I., Korth, M., McClafferty, H., Lukowski, R., Shipston, M. J., Ruth, P., Dobrev, D., & Wieland, T. (2012). Palmitoylation and membrane association of the stress axis regulated insert (STREX) controls BK channel regulation by protein kinase C. *The Journal of Biological Chemistry*, *287*(38), 32161–32171. https://doi.org/10.1074/JBC.M112.386359

Zhu, B., Farris, T. R., Milligan, S. L., Chen, H., Zhu, R., Hong, A., Zhou, X., Gao, X., & McBride, J. W. (2016). Rapid identification of ubiquitination and SUMOylation target sites by microfluidic peptide array. *Biochemistry and Biophysics Reports*, *5*, 430. https://doi.org/10.1016/J.BBREP.2016.02.003

Zi, M., Stafford, N., Prehar, S., Baudoin, F., Oceandy, D., Wang, X., Bui, T., Shaheen, M., Neyses, L., & Cartwright, E. J. (2019). Cardiac hypertrophy or failure? - A systematic evaluation of the transverse aortic constriction model in C57BL/6NTac and C57BL/6J substrains. *Current Research in Physiology*, *1*, 1. https://doi.org/10.1016/J.CRPHYS.2019.10.001

Ziman, A. P., Gómez-Viquez, N. L., Bloch, R. J., & Lederer, W. J. (2010). Excitation-Contraction Coupling Changes during Postnatal Cardiac Development. *Journal of Molecular and Cellular Cardiology*, *48*(2), 379. https://doi.org/10.1016/J.YJMCC.2009.09.016

Zoghbi, M. E., Woodhead, J. L., Moss, R. L., & Craig, R. (2008). Three-dimensional structure of vertebrate cardiac muscle myosin filaments. *Proceedings of the National Academy of Sciences of the United States of America*, *105*(7), 2386–2390. https://doi.org/10.1073/PNAS.0708912105